Tropical daylighting: predicting sky types and interior illuminance in north-east Brazil

Ricardo Carvalho Cabús

A thesis submitted for the degree of

Doctor of Philosophy

School of Architectural Studies

September 2002

Light is to architecture
as poetry is to literature,
both provide the means
of seeing things.

Acknowledgements

First, I am very grateful to Prof. Peter Tregenza. Besides his vast theoretical knowledge, his talent to supervise was clearly shown during this period and was crucial for the conclusion of this thesis.

During the fieldwork I could count with the collaboration of the Federal University of Alagoas (UFAL), in particular from Dr. Leonardo Bittencourt, Dr. Gianna Barbirato, Dr. Lindemberg Medeiros and Mr. Jurandir Nicácio for providing equipments and encouragement. I must also show gratitude to Ms. Taísa Cabús for offering her time and ability to take several photographs during measurements that I was involved. The meteorological data was supplied directly or indirectly by Mr. José Lima Filho (Fapeal), Dr. José Leonaldo de Souza (UFAL), Dr. Roberto Lamberts (UFSC), Ms. Solange Goulart, Ms. Ana Lígia Abreu (UFSC) and Ms. Joyce Carlo (UFSC); their help is gratefully acknowledged.

I am thankful to Dr. Paul Littlefair (BRE) and Dr. John Mardaljevic (De Montfort University). The first for authorising and the second for sending and commenting the BRE-IDMP dataset used for validating the computer program developed in this research. I would also like to show gratitude to Mr. Joe Lynes just for being in some of the meetings of the Society of Lighting and Light (SLL) that I could participate. His presence and words were source of inspiration for my research.

I wrote in Portuguese the phrase on page ii of this thesis sometime ago. When translating to English the words only came with the assistance of the poet and friend Prof. Archie Markham (Sheffield Hallam University). I am also indebt to Ms. Ony Bright for revising the manuscript.

I am very grateful to Mr. Ian Ward for inviting me to teach in the Architecture Master Course of the University of Sheffield during the last years of my PhD. I

would also like to express appreciation to Prof. Steve Sharples, who supervised during the firsts two months of this research, and to the technicians and secretaries of the School of Architecture, in particular to Mrs. Hazel Hall.

It is also important to emphasise the importance of my friends and colleagues for their friendship and encouragement during this period. It is also extended to the Sheffield's Brazilian Society and to the Forrobodó For All Brazilian Dancing Group.

This research was funded by CAPES and UFAL, to whom I am very thankful.

Finally, my most heartfelt appreciation goes to my family, which support, in all levels, could not be disregarded at any time.

Summary

Title: Tropical daylighting: predicting sky types and interior illuminance in north-east Brazil

Author: Ricardo Carvalho Cabús

Daylight is present in tropical regions in a considerable intensity throughout the year. The sky characteristics are changeable and sunlight cannot be disregarded. Daylighting techniques are still wanted to answer particular tropical features. The main aim of this thesis is to present a daylighting analysis tool for the tropics developed out of existing procedures. It is structured in three parts.

The first part provides a broad view of climatic aspects related to daylighting studies in a typical tropical city - Maceió, Brazil. A brief climatic description of the city and a study relating climate and building are followed by a literature review of climatic fundamentals. A study is made of meteorological station measurements in relation to the city and a field investigation is described. These lead to a simplified method for sky type selection. It shows that a reasonable assumption about daylight climate can be made from very simple data and that new structure of CIE standard general sky could be applied everywhere.

The second part investigates methods that could be appropriated for calculating daylighting in humid climates and concludes with a methodology based on an adaptation of existing techniques. The Monte Carlo and ray tracing techniques are reviewed, as well as the daylight coefficients concept. These are incorporated in prototype software, TropLux, written in MATLAB code. The development of the method in this thesis can be seen as an extension of the daylight factor concept to the CIE Standard General Sky and reflected sunlight. The software validation is done and results show that the level of prediction is comparable with those produced by Radiance and overall the results appear to be robust. Analysis indicates that it is not essential to have climate-specific calculation technique. Universal lighting software is viable, providing the local climate and architectural characteristics are taken into account.

The last part applies TropLux to ground-reflected light. It is found that the influence of reflected sunlight on interior illuminance can be very large. Among shading devices analysed, overhang has shown the best performance. There is a key zone of ground outside window that provides the majority of the reflected light. A direct design implication can be the reduction of window size.

Table of Contents

Part II - Tropical Daylighting Technique

Chapter 5 Monte Carlo and ray tracing techniques

Chapter 6 Daylight and auxiliary coefficients: definition and equations

Part III - Application and Conclusion

Appendices

List of figures

List of Tables

1 Introduction

1.1 The importance of daylighting in the tropics

Tropical daylighting is important from two differing but not conflicting viewpoints: the technical and the social-economical.

Technically, the first point of note is the quantity of natural light available. In the tropics, where countries are favoured by solar geometry, natural illumination may allow buildings to be totally daylit throughout the year and the use of artificial light confined to twilight and night-time. However, this gift has a price: light carries heat, and extra heat is not required. People in the tropics associate (usually correctly) an excess of light with thermal discomfort. Possibly D H Lawrence makes this point in the following lines of his poem *Tropic* [1]:

Sun, dark sun
Sun of black void heat
Sun of the torrid mid-day's horrific darkness.

Fortunately, with good design these problems can be avoided. The basic passive strategy in the humid tropics is to fight thermal discomfort with shading and natural ventilation. In deep rooms, natural and electric lighting can be used together.

Tropical regions include many countries where a significant part of the population lives in poverty. Here, the need for natural lighting can be more a question of economics rather than of comfort. A considerable number of the buildings do not even have electric light. Taking the example of Brazil, Barbosa et al. [2] report that at the end of the twentieth century nearly 15% of the population had no access to electric power; this represented about 25 million people living in rural areas of the country. The figures for school buildings are even more striking: Bernardes [3], using the Brazilian governmental census of 1999, reported that 34.5% of primary schools had no electric power.

Therefore, research into tropical daylighting can be viewed as a contribution not only to the quality of buildings (and as a consequence the well-being of their users) but also to the regional economy. Furthermore, daylighting technique is an under-explored subject. People generally and most architects in practice use intuition more than any technical framework. A belief that underlies the thesis is that daylighting guidelines could persuade designers that visual comfort is still wanted.

1.2 Aims

Since the advent of the scientific study of daylighting, research has concentrated on the temperate climate. For a long time, almost all calculations were based on uniform or overcast skies. The 'Daylight Factor' was widely spread as a simple and fast assessment tool but variations of sky luminance distribution and in particular of sunlight were usually neglected.

Three dominant factors changed this: the increasing cost of primary energy, the growth of ecological consciousness and the availability of fast computing. For the last three decades, the study of sky luminance patterns has been worldwide. Computers made long calculations possible: ray tracing, Monte Carlo simulation, the recording and statistical analysis of real skies. Typical tropical buildings characteristics, such as shading devices, could now be introduced into computation. New theoretical approaches, such as the concept of daylight coefficients, simplified the simulation of different sky distributions and sunlight patterns and made prediction of daily and annual daylighting practicable.

Although such techniques are now well known, they have generally not been used together, especially in conjunction with measured sky luminance data for warm climates. The aim of this thesis is to present a daylighting analysis tool for the tropics developed out of existing procedures.

The specific goals are:

- A method for sky type selection with incomplete sky luminance data
- A tested framework of algorithms and prototype software focussed on prediction of interior daylight in humid tropical climates, using the CIE Standard General Sky
- An example of this method in use.

During the course of the work it became clear that ground-reflected light is a major component of interior illumination in the tropics. It was found also that the literature on this topic was small. As a consequence the externally reflected component became a special focus of the research and the thesis presents a new approach.

1.3 Structure of the thesis

After this introductory appraisal, the thesis is divided into three parts. Each part encompasses a variable number of chapters and is related to each of the specific aims. At the end of the chapters, there is a conclusion that lists the main points and discusses the implications for the next stages of the work.

Part I gives a comprehensive view of climatic aspects related to daylighting studies in a typical tropical city – Maceió, Brazil – and then develops a method for sky type selection. A brief climatic description of the city and a study relating climate and building are followed by a literature review of climatic fundamentals with particular reference to the tropics. A study is made of meteorological station measurements in relation to the city, then a field investigation is described. These lead to a simplified method for sky type selection.

Part II investigates methods that could be appropriated for calculating daylighting in humid climates and concludes with a methodology based on an adaptation of existing techniques. The Monte Carlo and ray tracing techniques are reviewed, as well as the

daylight coefficients concept. These are incorporated in prototype software written in MATLAB code.

Part III applies this program to ground-reflected light and then proposes some new relationships. In conclusion, it integrates the overall results of this research, considers their limitations and recommends supplementary work.

Appendices list the code of the main programs in the simulation tool, give selected data and describe some additional studies. Figure 1-1 shows this structure.

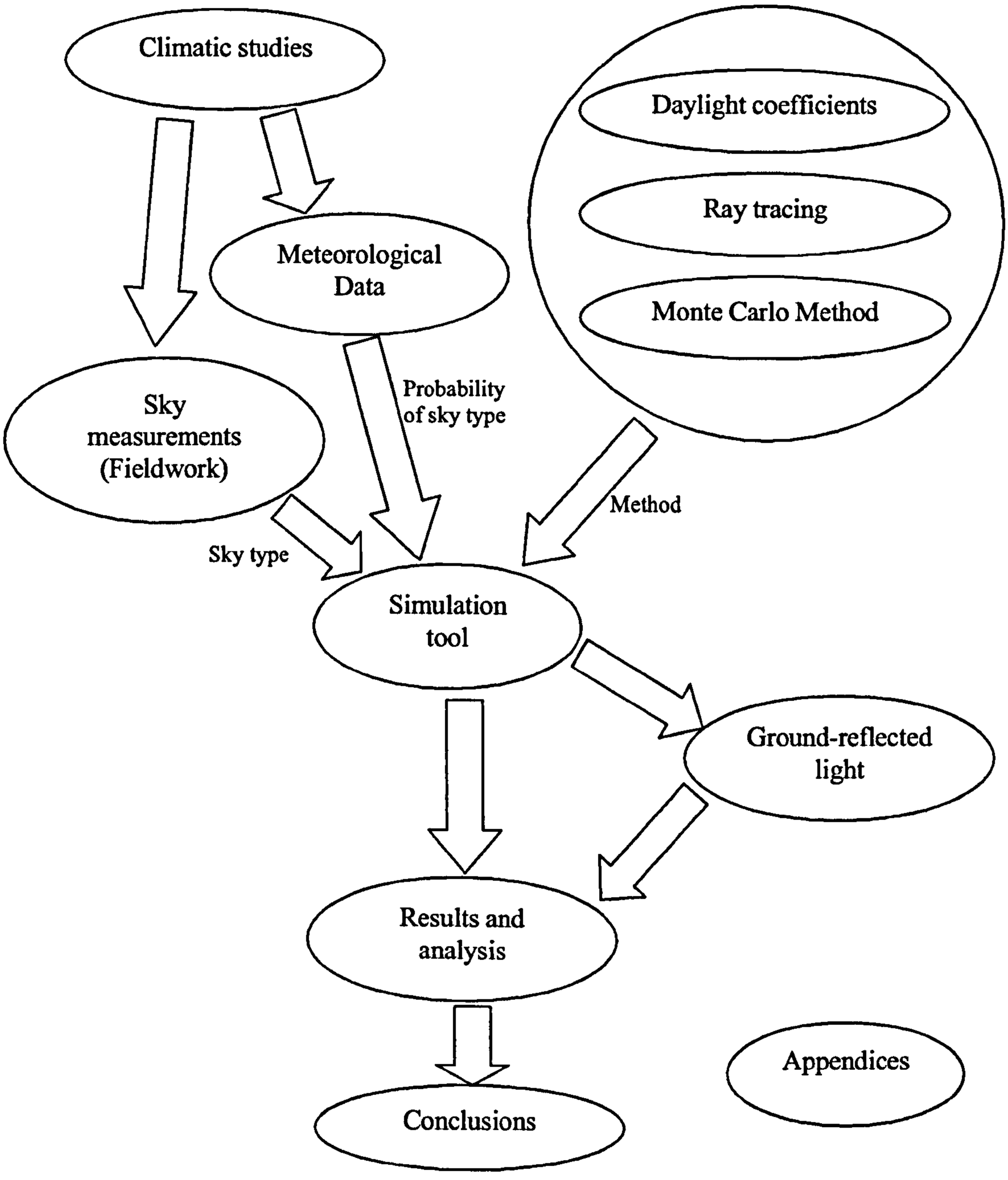

Figure 1-1 - Structure of the thesis

References

1. Lawrence, D. H., *Birds, beasts and flowers*. Santa Rosa, USA: Black Sparrow, 1992.

2. Barbosa, E. M. d. S., *et al.*, *Photovoltaic water pumping systems installer training: a partnership experience between the university and São Francisco hydroelectric power plant.* Renewable Energy, **21**(2): p. 187-205, 2000.

3. Bernardes, B., *Brasil tem 63 mil escolas sem luz [Brazil has 63,000 schools without electric light]*, in *Folha de São Paulo*. São Paulo-Brasil, 01/05/2000.

Part I

Daylight Climate

The first part of the thesis comprises the next three chapters. Chapter 2 introduces the climatic perspective for this research. It describes the general climatic characteristics of the site, investigates the relationship between climate and the built environment, reviews climatic fundamentals, and points out gaps in the tropical daylighting approach.

Chapter 3 and 4 describe the particular daylight climate of the city of Maceió – in north-east Brazil. The first analyses the local meteorological station data, while the later reports an investigation on the local sky luminance distribution. Both suggest a methodology and indicate input for a daylighting analysis by the computer tool developed for this research.

Chapter 2 The climatic context

2.1 Introduction

This Chapter aims to introduce the climatic perspective for this thesis. It starts by describing the general climatic characteristics for the site of the research. There then follows an investigation into the relationship between climate and the built environment, in particular thermal and visual comfort criteria. A review with regards to the fundamentals of climate is produced in order to understand the climatic classification and in which framework the researched city is applied. It leads to a particular analysis for the humid tropics. The conclusion points out how local conditions can be extrapolated and proposes new directions for this research based on the detected gaps.

2.2 Climatic description of the studied city

Maceió, the capital city of the State of Alagoas, Brazil, is a seaboard city with a humid tropical climate located at latitude 9°40'S and longitude 35°42'W, as seen on Figure 2-1. Founded in 1815, in a narrow strip of land between a lagoon and the Atlantic Ocean, Maceio has a population of around 800,000 inhabitants (Census 2000). It is on a sedimentary coastal plateau with four different altitudes related to sea level, between 4 and 80 metres.

The following Sections present an overview of its climatic parameters.

Figure 2-1 - Brazilian map and the city of Maceió

2.2.1 Temperature

The annual mean temperature is 24.8ºC and as a typical humid tropical city Maceió has low thermal variation, as temperatures vary slightly between day and night and also during the year. The highest monthly mean temperature, 26.3ºC, occurs in February, while the lowest comes about in August with 23.5ºC. Figure 2-2 describes the monthly mean temperature, based on the Climatologic Normal, for 30 years, between 1961 and 1990 [1]. All other data shown in Section 2.2 have the same source.

The monthly maximum and minimum temperatures also show only small amplitude, as illustrated in Figure 2-3. The maximum varies from 27.0ºC in July to 30.4ºC in February, while the minimum ranges from 20.2ºC in August to 22.7ºC in March.

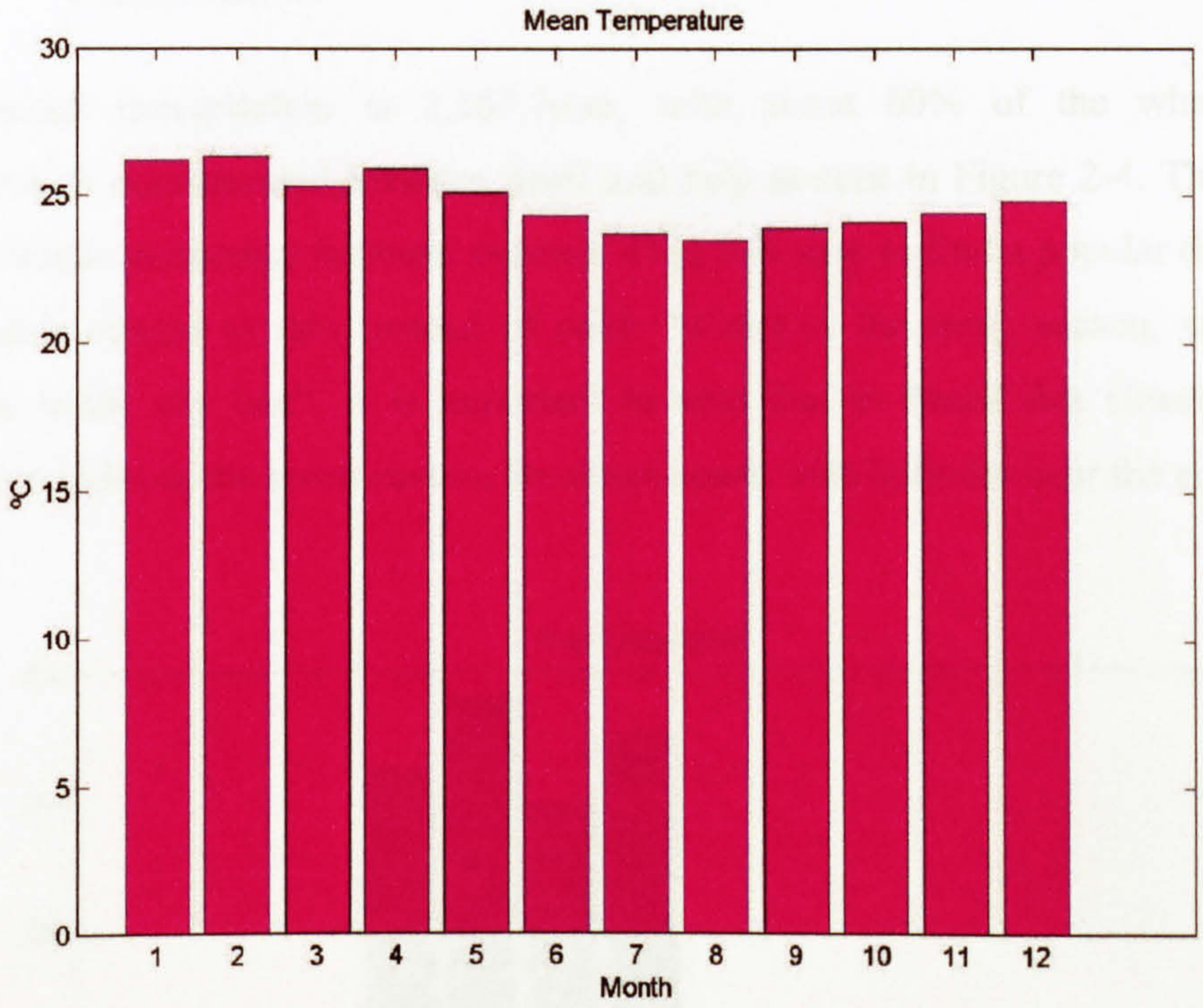

Figure 2-2 - Monthly mean temperature

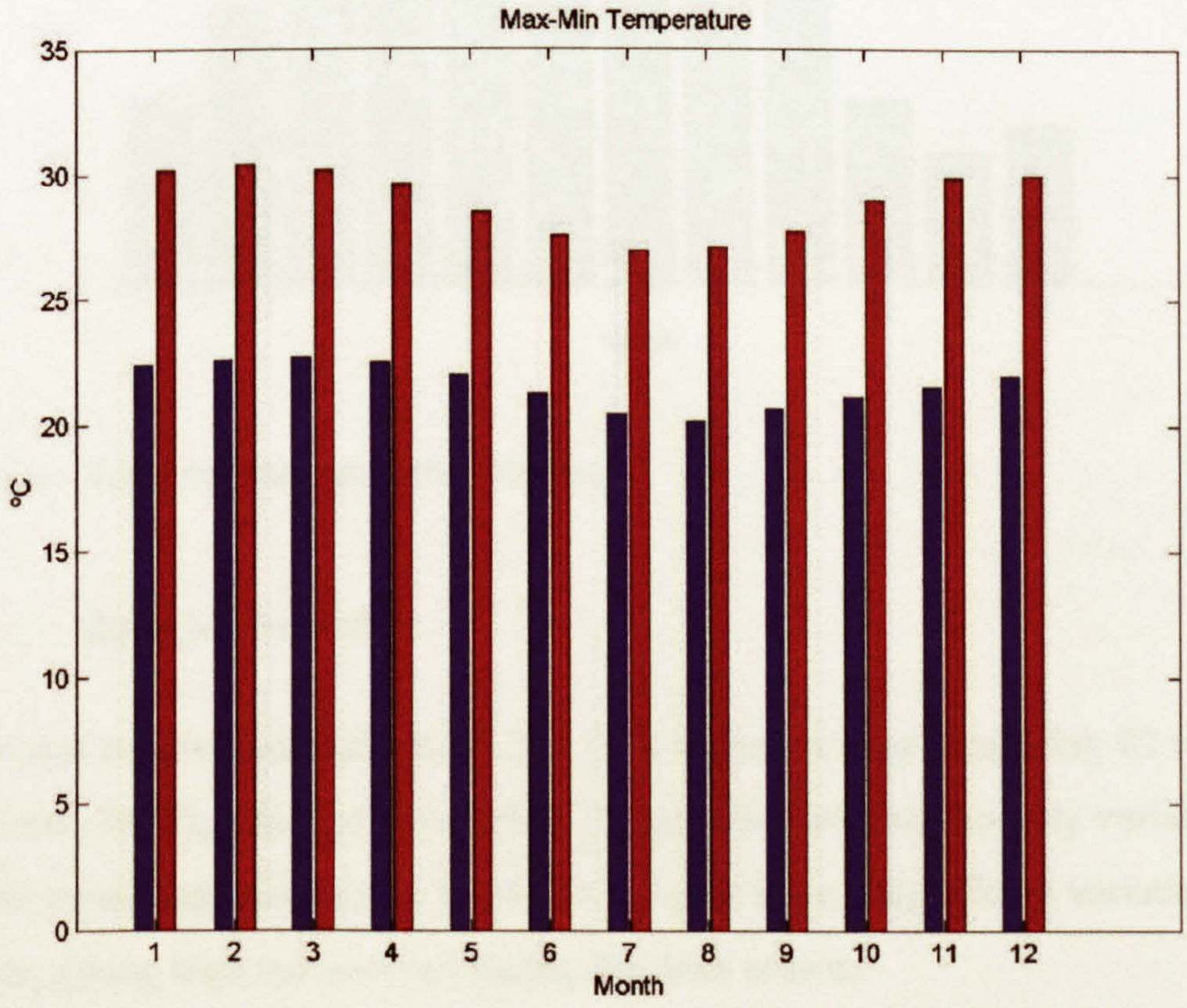

Figure 2-3 - Minimum and maximum monthly temperature

2.2.2 Precipitation

The annual precipitation is 2,167.7mm, with about 60% of the whole year precipitation concentrated between April and July as seen in Figure 2-4. This is the main climatic difference between seasons. Thus it is easy to find a popular definition of seasons related to rain instead of cold: "winter is the rainy season, while the summer is the dry one". It is important to note that in Brazil this situation only applies to cities in the north-eastern Brazilian coast, with latitudes near the equator.

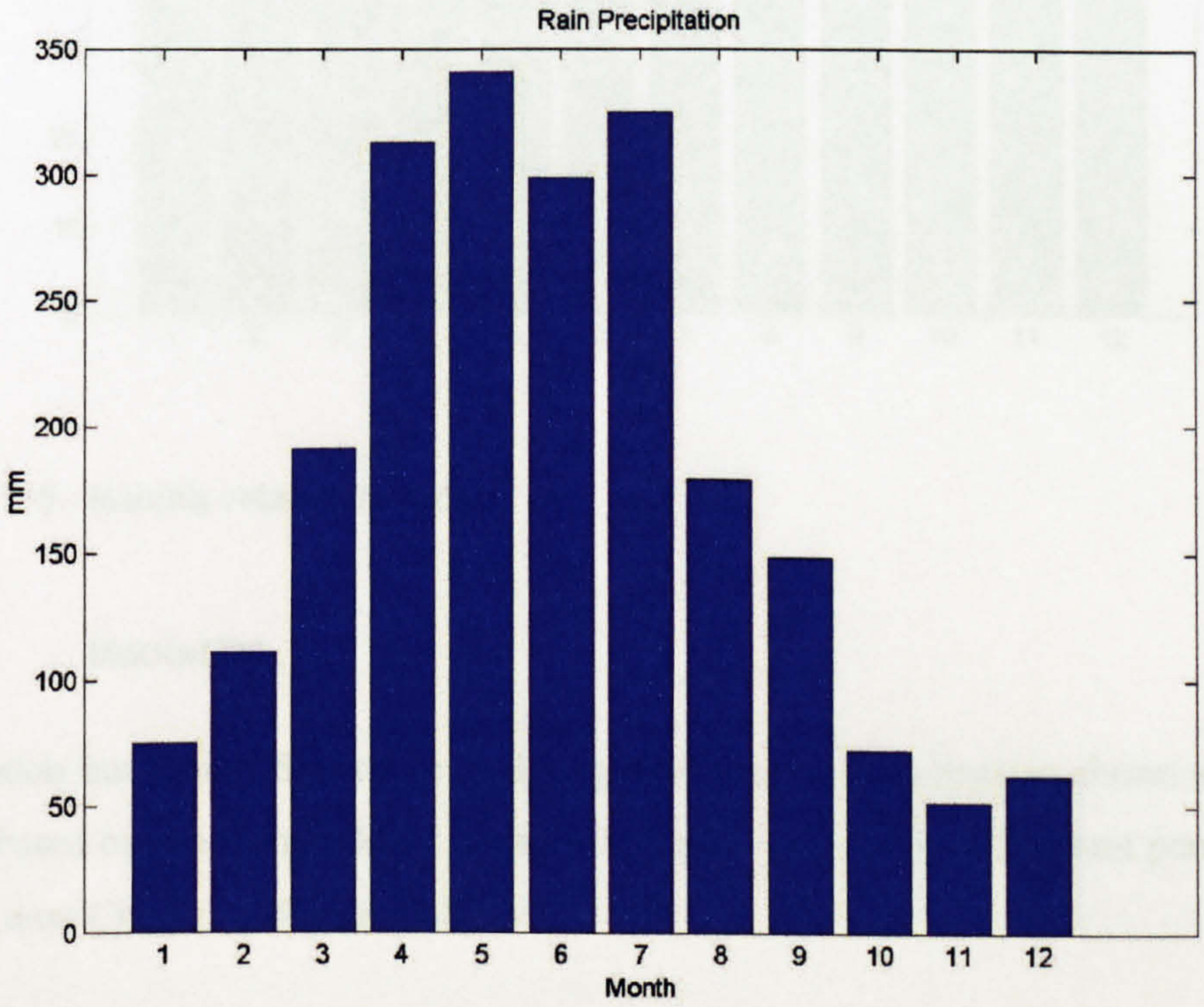

Figure 2-4 - Total monthly rain precipitation

2.2.3 Relative humidity

The annual relative humidity is 78.3%. It is higher in May producing 82.6%, while the lowest, 74.7%, arises in November. Figure 2-5 shows its monthly variation. It is possible to see that the relative humidity does not have a significant variation around the year, giving high values even during the drier season.

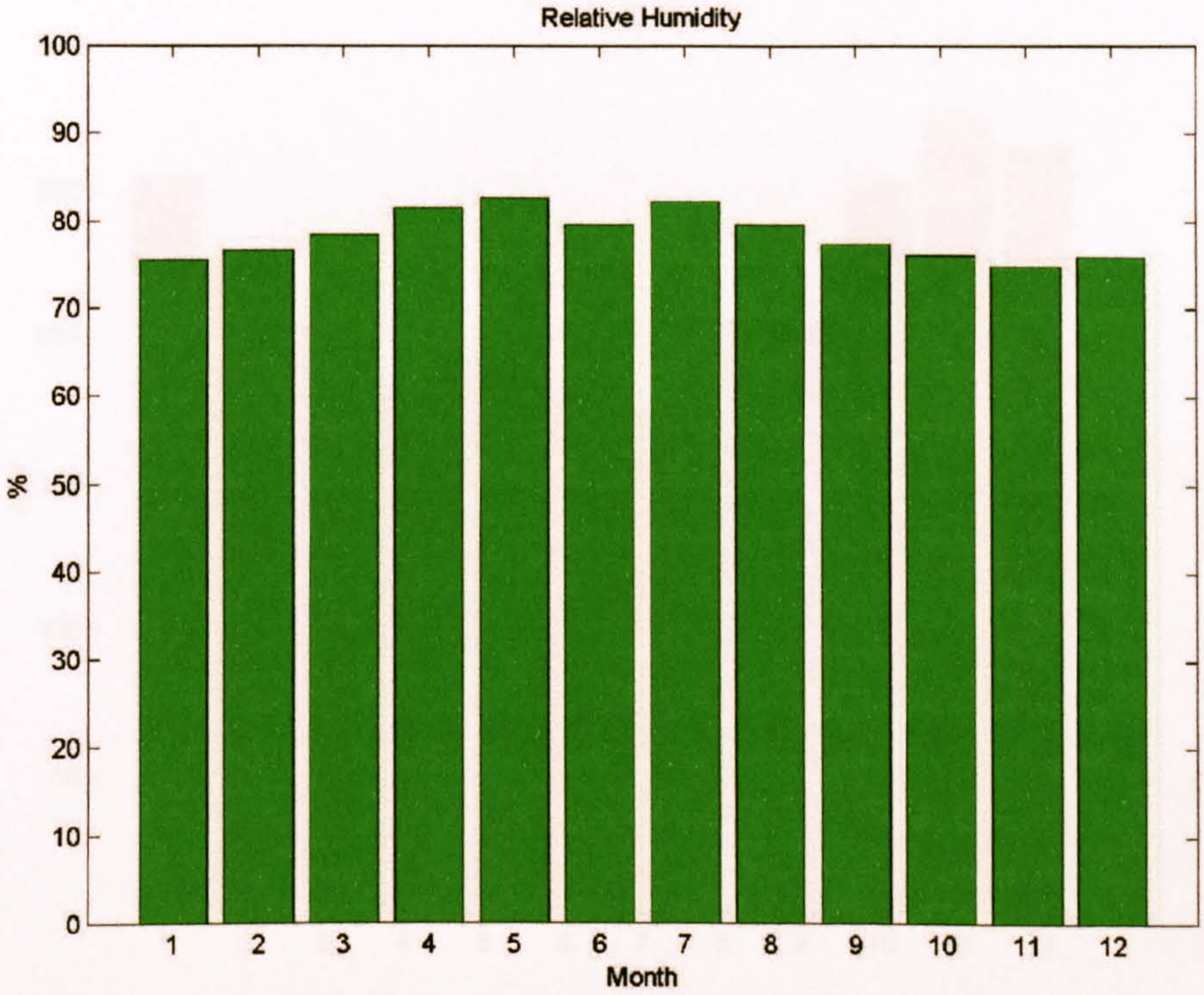

Figure 2-5 - Monthly relative humidity

2.2.4 Insolation

Insolation has a significant role in daylight in tropics. This Section shows a briefly view based on the Climatologic Normal. It is also analysed in a different perspective in the next Chapter in Section 3.2.

From Figure 2-6, it is possible to see that insolation, shown in hours per month, is greater during the drier season than during the wet months. The graph shows an opposite tendency comparing with Figure 2-4, which represents the rain precipitation.

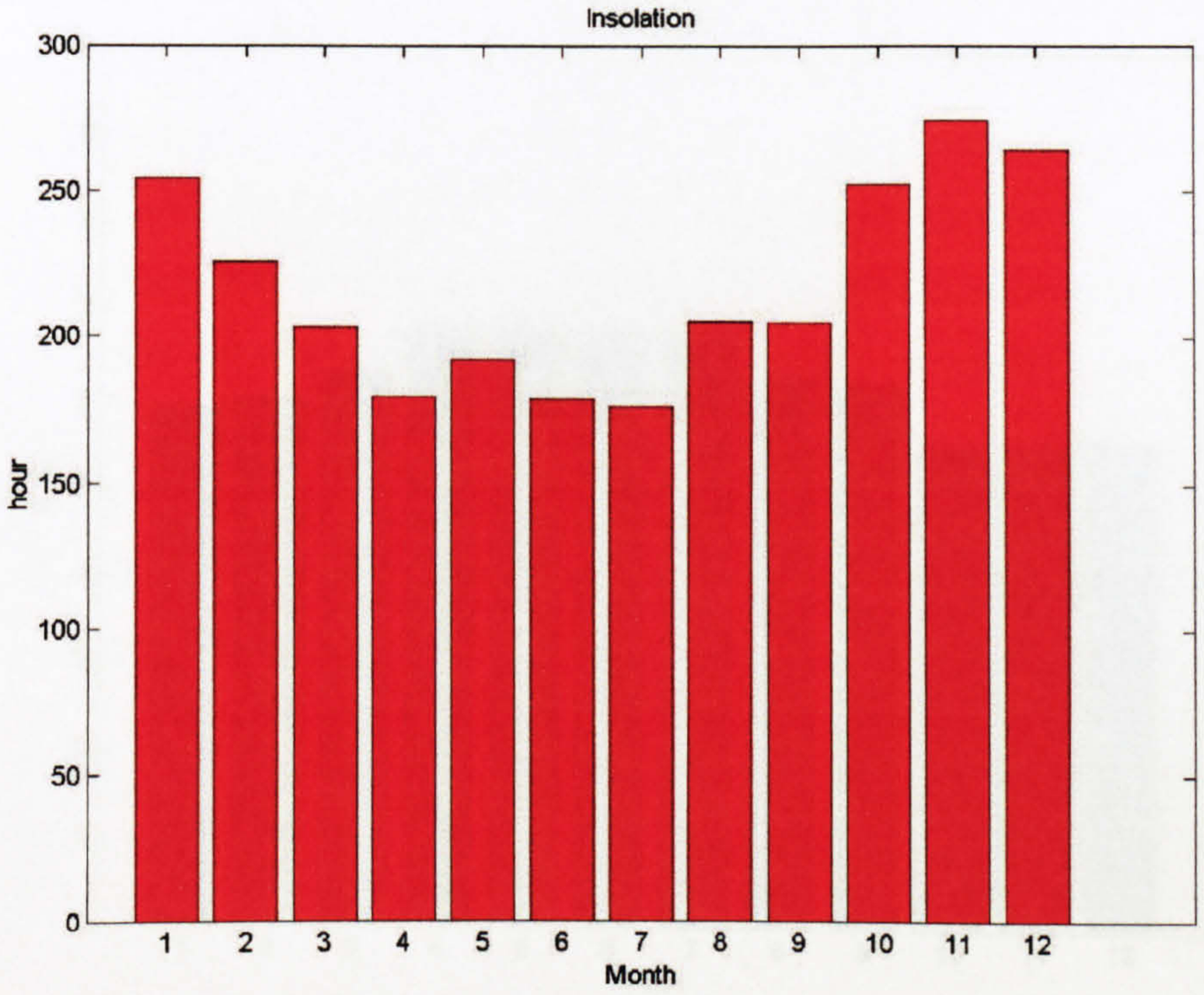

Figure 2-6 - Total monthly insolation

2.2.5 Nebulosity

The nebulosity is shown in Figure 2-7 as monthly average in ratio 1:10. It can be seen that nebulosity is higher in the same period as the rain precipitation, from April to July, but it is also considerable throughout the year. Compared with insolation, nebulosity shows a curve with an inverse tendency.

Nebulosity, as with insolation, has a major role in daylight studies. It is further considered in Section 3.3 in the next Chapter, where raw meteorological data is investigated.

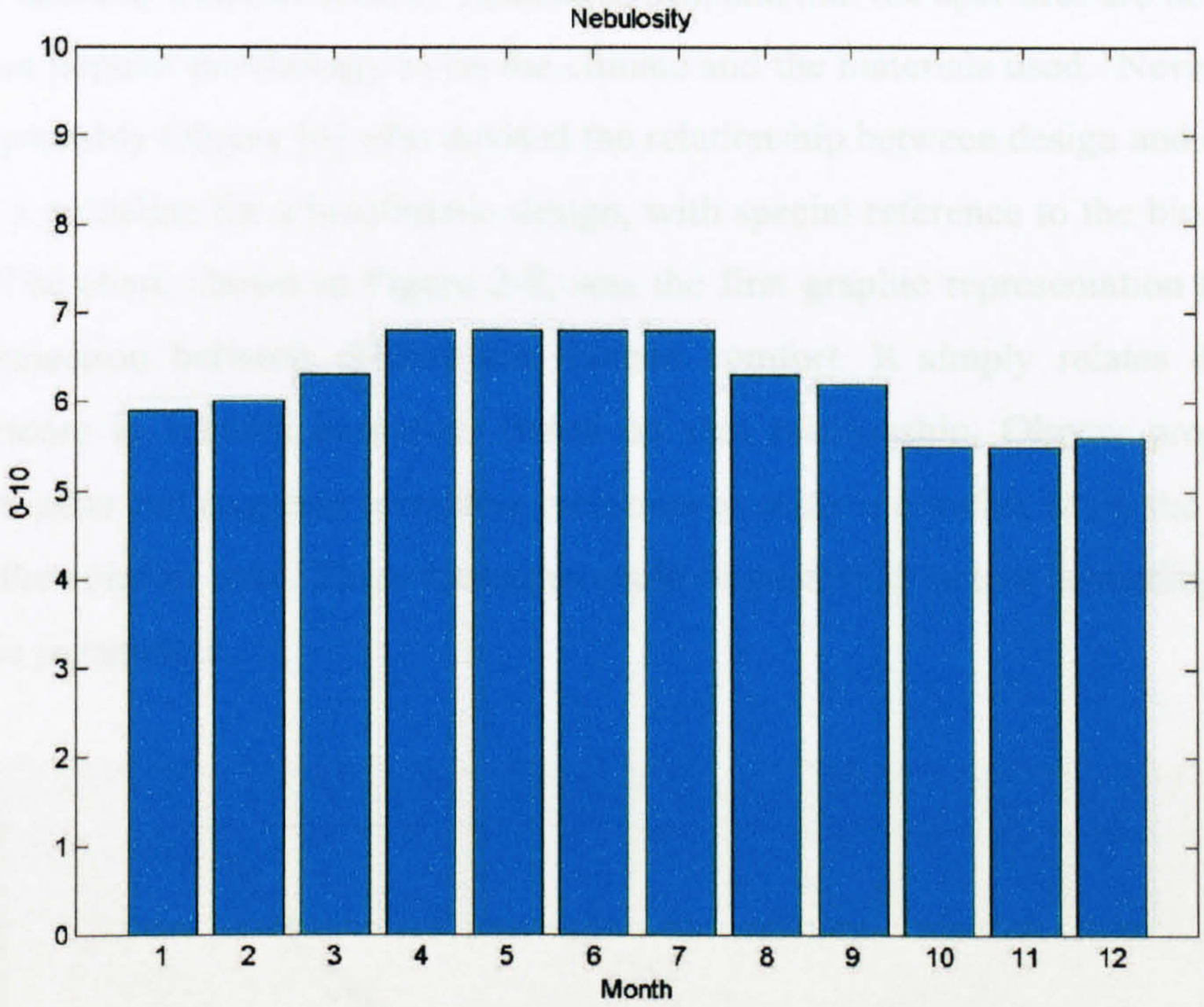

Figure 2-7 - Monthly nebulosity (1-10)

2.3 Climate and buildings

The association between climate and built environment has long been noted in discourse on ancient architecture. Sun and latitude were the basis for first studies. In the first century BC, Vitruvius [2] wrote a remarkable book. He points out the climatic needs commenting that

> *It seems necessary to develop the types of building in one way in Egypt, another way in Hispania, still differently in Pontus, otherwise in Rome, and so on, according to the distinctive properties of other lands and regions. For in one part of the world the earth is overwhelmed by the course of the sun; in another it stands far distant from it, in still another part it is held at a middling distance.*

However more specific studies were carried out during the 20th century. Some earlier research can be detached. It is important to mention the findings of Jean Dollfus [3] survey (also alluded to by Olgyay [4]). He contends that building styles are defined

less by national frontiers than by climatic zones, and that the apertures are defined as much on popular psychology as on the climate and the materials used. Nevertheless it was probably Olgyay [4] who devised the relationship between design and climate, giving a guideline for a bioclimatic design, with special reference to the bioclimatic chart. The chart, shown in Figure 2-8, was the first graphic representation to show the connection between climate and human comfort. It simply relates dry-bulb temperature to relative humidity. Based on that relationship, Olgyay proposes a comfort zone and suggests corrective measures to achieve comfort when the point is out of the comfort zone. These measures could be passive or active depending on the climatic parameters.

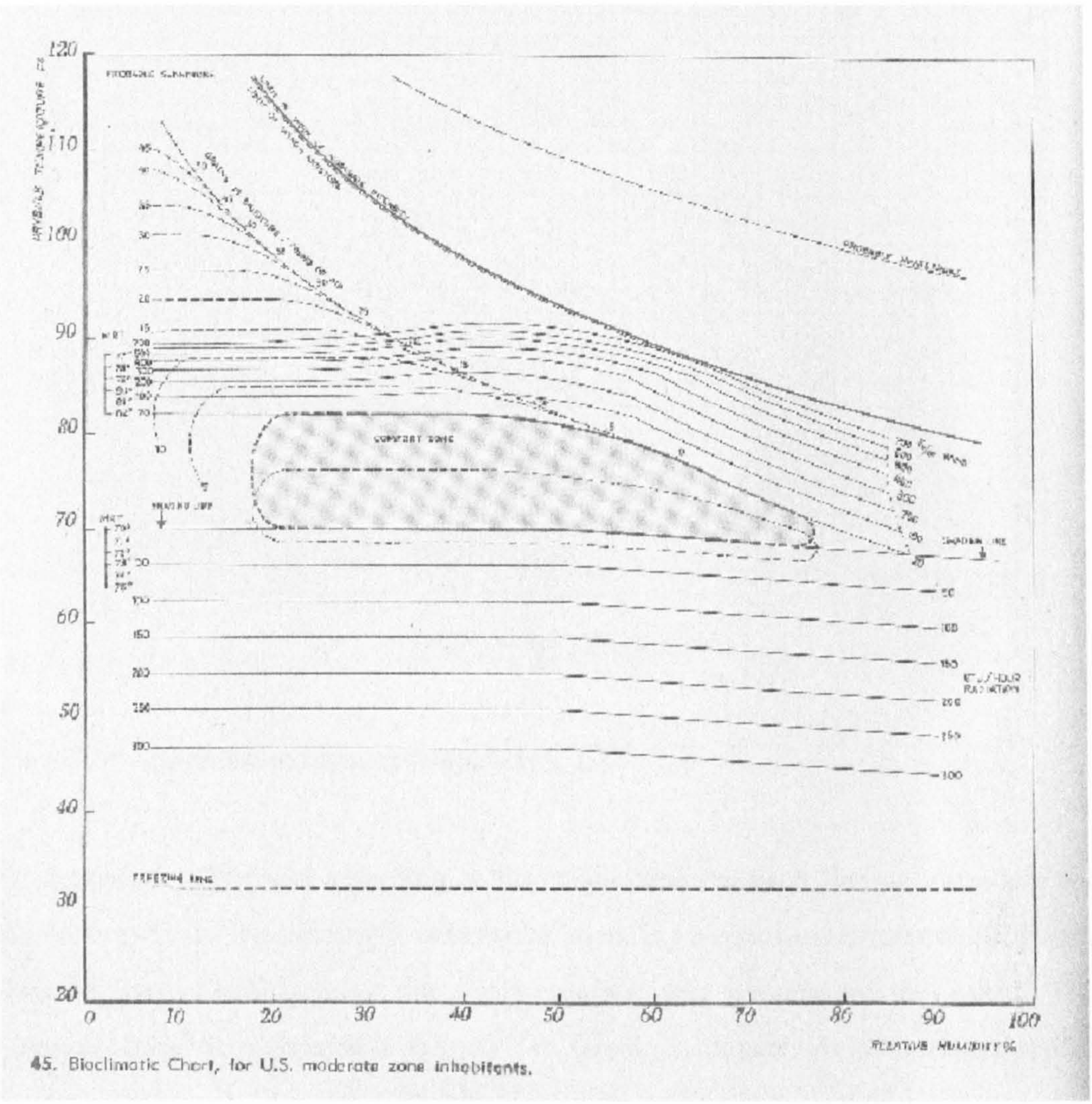

45. Bioclimatic Chart, for U.S. moderate zone inhabitants.

Figure 2-8 - Olgyay's bioclimatic chart. [4]

Five years later, Givoni [5], developing Olgyay's idea, proposes a building bioclimatic chart, based on the psychometric chart, which besides dry bulb temperature and relative humidity, includes vapour pressure and wet bulb temperature. An example of that chart is shown in Figure 2-9. So far it has been used widely, with some enhancement later proposed by several authors, including Givoni himself.

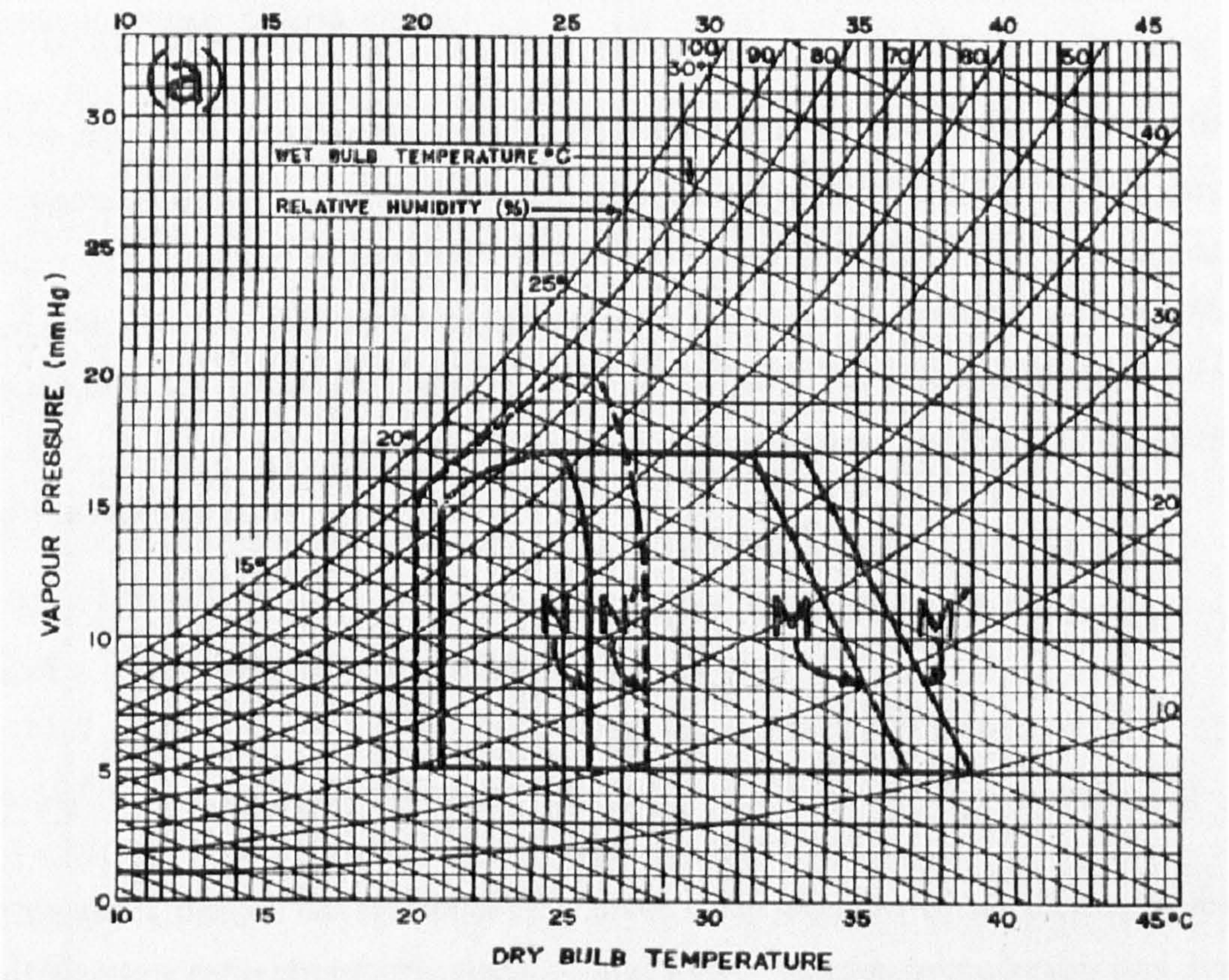

Figure 2-9 - Givoni's building bioclimatic chart. [5]

If studies are advanced regarding to the connection between thermal concepts and climate, as far as daylighting is concerned, there is no conclusive research proposing how to give visual comfort for every specific location around the world. This proposal could be compared to Olgyay's or Givoni's contribution to thermal comfort.

This gap could probably be filled by a daylight climate atlas linked with a corresponding design criteria for every region proposed.

The advent of the CIE (Commission Internationale de l'Eclairage) International Daylight Measurement Program (IDMP), which started in 1990 [6], was an important step forward. It was complemented with the proposal of the CIE standard Skies [7], based on earlier Kittler studies [8, 9]. Tregenza [10] also contributed with his investigation for maritime climates. Working with data generated from IDMP and statistically relating to 15 standard skies proposed by Kittler, he asserts the possibility of using standard skies in daylighting design for even the chaotic sky patterns present in those regions.

With regards to visual design criteria, although studies are in an advanced stage for temperate climates, it is not possible to affirm the same for any other climatic region. For tropical region, in particular, it can be boosted with the advent of computer programs that can cope with complex geometry in aperture systems and with variable sky luminance distribution. Also those codes should be fed with realistic local data, which includes sky luminance, building geometry and materials photometric characteristics.

2.4 The Climatic fundamentals

2.4.1 Introduction

Climate is one of the identities of a place. It is the sum of all meteorological occurrences in the atmosphere synthesised at a given location over a long period. It is possible to say that no two locations on earth's surface have identical climates. The combination of characteristics like latitude, height above sea level, nearness to sea or other large body of water, and to hills or mountains, wetness of the ground and the nature of its vegetation can create countless climatic types [11-14].

On the other hand, climate is continuously changing, either by slow geomorphological transformations, or by the interference of man, which is generally fast, by cutting down forests, damming rivers, and polluting the skies.

Climate can be divided into macro, meso and microclimates. The first is concerned with larger spaces such as continents, countries, and oceans; the second is concerned with relatively small areas of between 10 and 100 km across (e.g. study of urban climate). Microclimate, in turn, relates to a limited area such as room, street, town, or small landscape, dependent upon the frame of reference [11, 12].

Despite the fact that no two locations are the same climatically, it is possible to define areas where the climate is broadly uniform from place to place. This is generally referred to as a climatic region. To facilitate their mapping, different climates must be classified using suitable criteria. Hence, climatic classification comes out from the need to synthesise and group similar climatic elements into climatic types from which climatic regions are mapped [12].

2.4.2 Climatic classification

According to Ayoade [12], the purpose of climatic classification is to provide an efficient framework for organising climatic data and learning about the complex variations in world climate. Through climatic classification, the details and complexities of monthly or seasonal climatic statistics are compressed into simpler forms which are more easily understood.

2.4.2.1 Importance

Regarding building science, perhaps the overarching purpose of climatic classification is to allow the extrapolation of techniques developed for one region to a similar one in a different part of the world, as well as keeping the correspondence between the key climatic parameters. The choice of those parameters varies according to the field of study.

Through observation, a prudent designer will become acquainted with the detailed climate of the place and site where work is taking place. However he may be called on to build in an unfamiliar place. In this case, an appropriate climatic classification can be quite helpful to the project [13].

2.4.2.2 *Difficulties*

Although climatic classification is desirable, it is a hard task. The classification of climate cannot be observed, it is a mental construction composed of statistical abstractions of measured elements and observable occurrences of weather episodes. Allied to that, it is necessary to identify the crucial climatic parameters that constitute characteristic climatic types. Another problem arises from the inadequacy of available climatic data both in terms of coverage of the earth and in terms of duration and reliability, although it tends to be solved along time. Nevertheless, the chief difficulty lies in the fact that actual climatic conditions usually change very gradually, with one type merging into another over long distances. Moreover, climate is not static it fluctuates and varies over time. As a result there are no real boundaries between climatic types, but broad transition zones instead [12, 14-19].

Numerous schemes, proposed by climatologists, geomorphologists, biologists, and even by building designer researchers have been used to classify the tropical region. There are inherent difficulties of delimiting the outer boundaries of the tropics and defining different types of 'tropics' are particularly pronounced, especially across continental areas. Each scientific discipline also has different requirements of a classification system. While botanists will analyse vegetation assemblages, climatologists will pay more attention on atmospheric conditions and geomorphologists will prefer to observe where physical processes take place. Thus, one cannot suppose that at some point the boundaries of the various systems will correspond exactly.

2.4.2.3 *Approaches*

There are two basic approaches to climate classification: *genetic*, based on causes behind the observed facts; and *empirical* or *generic*, based on the observed climatic elements themselves or their effects on other phenomena, such as vegetation or man. Since the genetic scheme incorporates features that cannot be precisely measured - such as air circulation patterns and air moisture fluxes - and therefore must be handled subjectively, most climatic classification schemes have therefore adopted the empirical approach for which data are more readily [12, 15].

Ptolomy, the astronomer, developed the most basic classification during the 2nd century AD. He believed that as the solar altitude induces air temperature, the earth was divided into three zones: (i) the tropics or torrid zones, where the sun can be on zenith at least one time a year; (ii) the temperate zones, north and south, with intermediate incident angles at solar noon; and (iii) the frigid or cold zones, around the poles, with low solar angles and even an absence of sun for part of the year [20].

In 1900 Wladimir Köppen [21], however, devised the most distinguished scheme. It was based on vegetation zones but in 1918 it was revised and temperature and rainfall became its basis [12]. Despite some criticism regarding its simplicity, Köppen's scheme, shown in Figure 2-10, continues to be used to the present day. A recent study [22] used Köppen's original scheme. Furthermore, several schemes, such as those of Trewartha [23] and Miller [24], appeared based on Köppen's approach, attempting to correct some points or adapt to different fields of science. With reference to building science, Olgyay [4] also used Köppen's scheme to propose his climatic zones, as shown in Figure 2-11, simplifying it to just four types: hot and humid, hot and arid, temperate and cool.

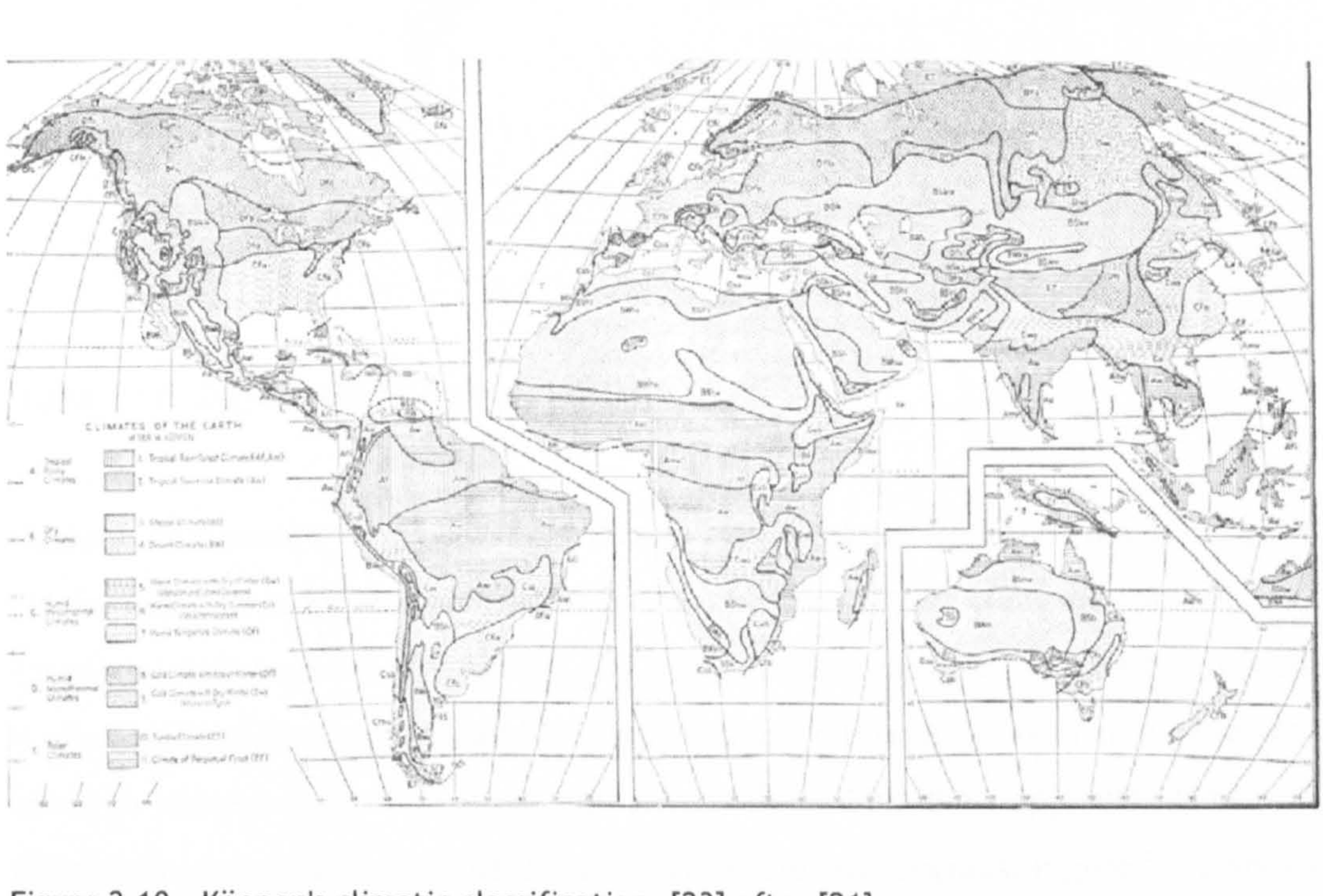

Figure 2-10 - Köppen's climatic classification. [23] after [21]

Mofidi [22] contends, quoting Trewartha [25], that Köppen's scheme is an empirical-genetic one. However Ayoade [12] asserts that it is an empirical scheme and Barry [26] expresses the same view stressing that Köppen's scheme is the prime example of generic classification related to plant growth or vegetation. Moreover Lydolph [15] affirms that one must decide whether the classification system is to be an empirical scheme, based on observations of such elements as temperature and precipitation - as was shown that Köppen's scheme is based - or genetic, based on causes behind the observed facts.

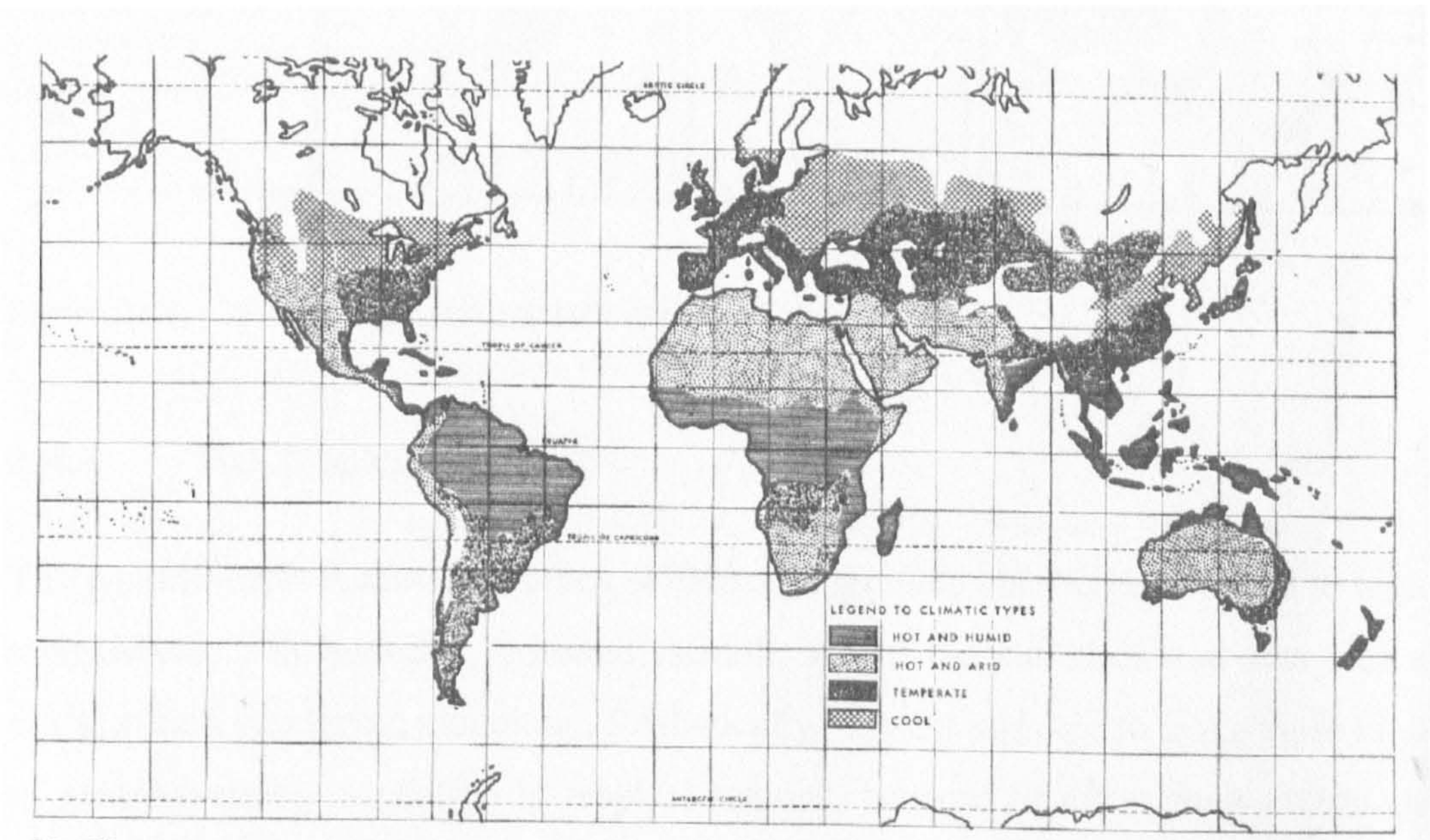

16. Climatic zones.

17. Typical occurrence of indigenous roof types.

Figure 2-11 - Olgyay's climatic zones. [4]

Strahler, conversely, proposes one effective genetic classification of the world [27]. He divides the world into three major groups: (i) low-latitude climates, controlled by equatorial and tropical air masses; (ii) mid-latitudes climates, controlled by both tropical and polar air masses; and (iii) high-latitude climates, controlled by polar and arctic air masses. It shows a slight similarity with the Ptolomy's approach. However, these main groups are subdivided into fourteen climatic regions. Figure 2-12 shows Strahler's classification.

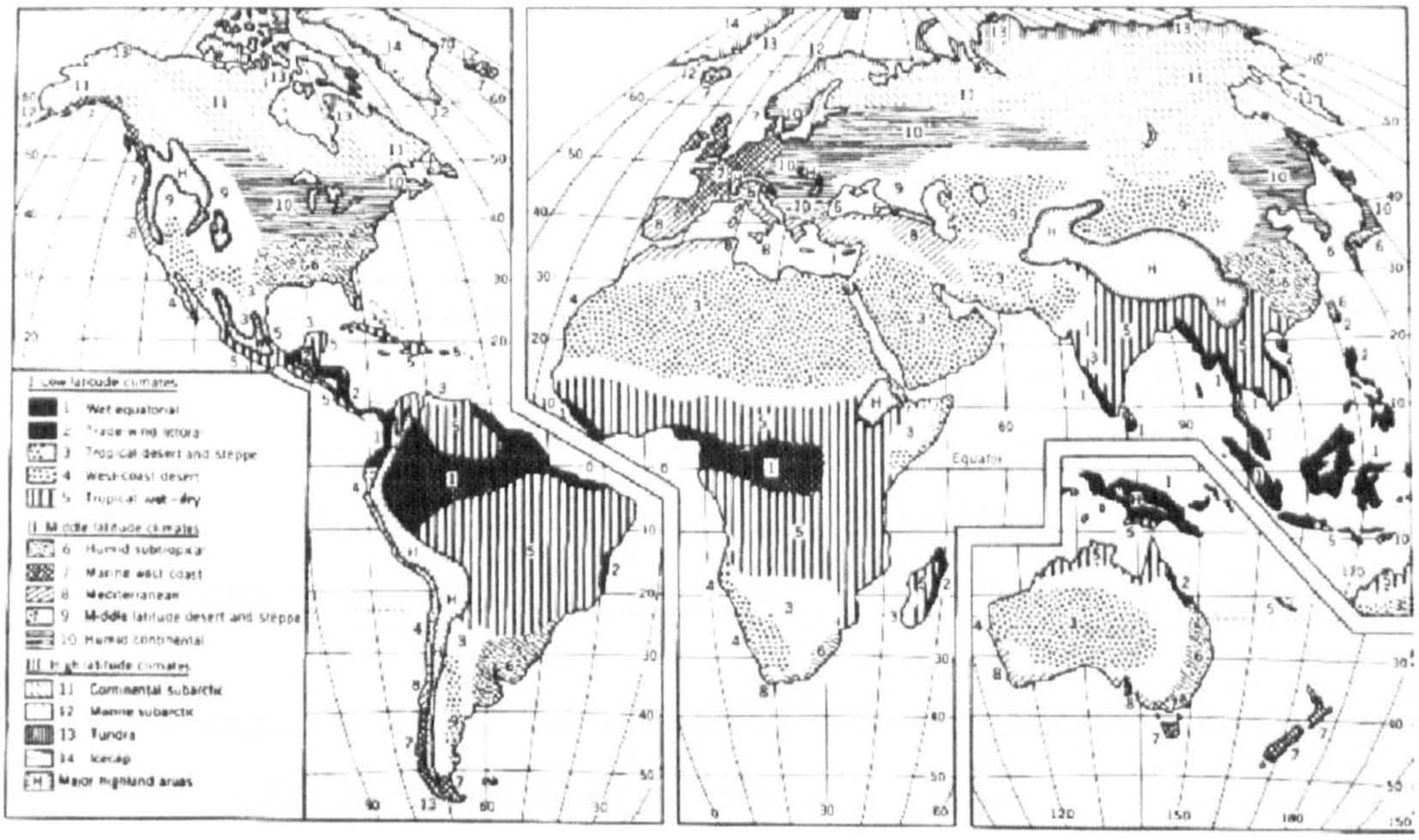

Figure 2-12 - Strahler's genetic climatic regions. [27]

2.4.3 The Tropics

The popular myth is that the tropics, within a geographic context, are related to high temperatures and humidity, constant rainfall, where the sun rises and sets like a clock, a kind unrelieved monotony. Realistically, it is not possible to make these kind of generalisations in relation to tropical regions, because of either their enormous area, or their unequal distribution of land and sea [28, 29].

2.4.3.1 Definition and boundaries

In ancient Greek, the word '*Tropikos*' signified the Tropics of Cancer and Capricorn. Nowadays, sensu stricto, the 'tropics' refer to parts of the earth that lie between the Tropic of Cancer (23º27'N) and the Tropic of Capricorn (23º27'S). These latitudinal boundaries correspond to the outer limits of the areas where the sun can lie at zenith. The tropical zone therefore receives large amounts of solar radiation throughout the year; as a result, seasonal fluctuations in temperature are minimal and there is no distinct winter season. It covers about 40 per cent of the earth's total surface area, or about 36 per cent of its land area [11, 12, 17, 30, 31].

Another astronomical definition would be the latitudes 30° north and south, which divide the global surface into two halves, tropics and extratropics [12, 26, 32, 33].

However, these astronomical definitions are too rigid and cannot properly delimit a region with particular physical or biological characteristics. In this sense, several authors have been tried to redefine the tropics based on others criteria. Thus, the tropics has been classified in different ways, according to the fields of science, like climatology [15, 18, 19, 21], agriculture [34, 35], botany [36, 37], human geography [16], geomorphology [38], and even in relation to building needs [11, 13, 29, 39-44].

Usually the tropics as a whole are delimited by thermal criteria, while the degree of moisture or rainfall determines the subdivision.

Köppen [21] delimits an average mean temperature for coldest month of 18°C as the thermal requirement for tropical climate. Szokolay [41] proposes the same figures, but observes that there is at least one month of the year with a mean temperature higher than 20°C and a mean relative humidity around 80 per cent. Lippsmeier [11] and Sperling [43], using another thermal approach, define the tropics as the area situated between 20°C isotherms of the northern and southern hemispheres, based on an annual mean temperature. Miller [24] also developed an empirical classification based on temperature and rainfall, which is rather similar to Köppen's scheme, and the hot climates occupy areas with the mean annual temperature is greater than 21.1°C, and no month has mean temperature less than 18°C.

However, according to Nieuwolt [18, 19], a better approach to determine climatic boundaries is to define a major common feature, and the most important on the low latitudes is the absence of a cold season, as illustrated by the old adage '*where the winter never comes*'. This point is concordant with several studies about tropical climate [12, 13, 17, 33].

Moreover Nieuwolt [18, 19] noting that the Köppen scheme excludes the tropical highlands - where there is no winter, but temperatures are frequently well below the limit of 18°C – proposes a new temperature criterion. In this, temperatures are reduced to sea level, based upon a 5-6°C per thousand metre elevation relationship.

He also admits that it is a fictitious figure in many continental areas, because the actual decline varies greatly both with season and location. However, on a world scale these errors are relatively minor. Figure 2-13 shows the result of this approach.

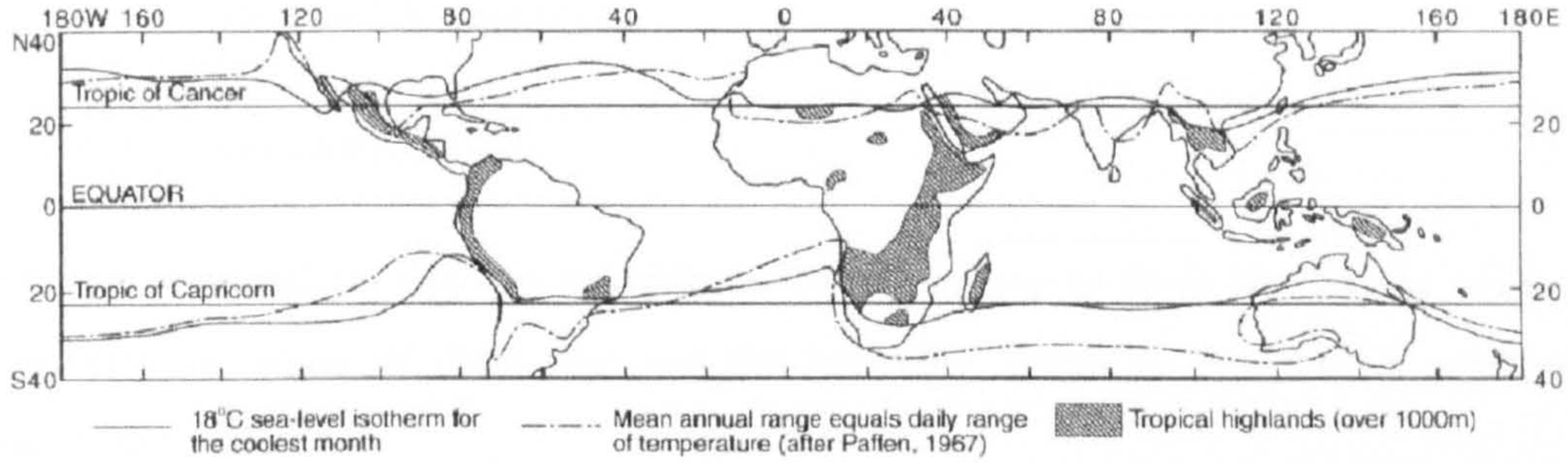

Figure 2-13 - Two boundaries of the tropics and tropical highlands. [18, 19]

In contrast, Barrow (1987) [35], quoted by Reading et al. [17], points out that high and low altitude tropical areas are not directly comparable in botanical terms. Tricart [38], who has also based his approach on temperature levels, likewise excludes from the tropics the cooler highlands and also the cool, foggy littoral deserts.

The tropics can also be defined as the area of the world where the annual range of temperature is equal or less than the mean daily ranges [12]. Nevertheless, Nieuwolt [18, 19] says that it is valid only over land surfaces.

2.4.3.2 Classification

There are many methods to classify the tropics, like climatic elements or by the effects of climate on vegetation. However, as temperature and insolation are relatively uniform in the tropics, moisture is currently used as a criterion to distinguish between different types of tropics.

The most widespread and elementary classification separates the tropics into humid and dry regions. In this way, Hopkinson [45] affirms regarding daylighting purposes it can be considered a good figure. In contrast, Atkinson [13], former head of the Tropical Building Section of BRS, says that separating the tropics into warm-humid

and hot-dry regions hides features of significance and on occasion can mislead inexperienced designers. There are several approaches that comprise other divisions, but for the aims of this work, only those regarding humid tropics will be treated.

2.4.4 The Humid Tropics

2.4.4.1 Boundaries

Most of the authors use the rainfall as the parameter to limit the humid tropics. Furthermore, some of them also use the humidity, either as first, or as auxiliary parameter.

There is no consensus as to the amount of rainfall. Köppen [21] proposes figures of 450-600mm per year to divide the tropics into dry and humid. Nieuwolt and McGregor [18, 19] follow Köppen. On the other hand, Gourou [46] first sets 700mm as the limit but after reduces to 500mm[1], while Tricart [38] defends an interval of 700-800mm[2] and Szokolay [41] a 750mm limit[3]. At the other extreme, Garnier [47]

---

[1] Faniran and Jeje in 1983 [30], and Reading et al. in 1995 [17], quoting Gourou, say that this limit is 400mm. But Gourou asserts on the 4th Ed. of the Tropical World, in 1966 [46]:

> *(...) As for rainfall, it is impossible to name a precise isohyet beyond which agriculture demands irrigation; in earlier editions of this book a figure of 27.5 inches was proposed, but now it seems that 20 inches might be more appropriate (...)*

And Gourou confirms on the 5th edition, in 1980 [34], when says:

> *(...) in earlier editions of this book a figure of 700mm was proposed, but now it seems that 500mm might be more appropriate (...)*

Maybe the mistake occurred because Gourou also says:

> *(...) Professor W. B. Morgan, in 'The distribution of food-crop storage methods in Nigeria' (Journ. Tropical Geog. 13, 1959, 58-64) suggest that a rainfall of 400 mm annually 'may be considered as the minimum normally necessary for agriculture'.*

But Gourou is explicit putting figure of 500 mm as his point of view for this limit.

[2] Again Faniran and Jeje in 1983 [30], and Reading et al. in 1995 [17] put different figures of 750-800mm, while Tricart [38] says on pages 44-46, about the limits of the humid tropics with the dry zone, that

> *'There is, of course, no sharp limit between the two as changes are gradual. There is however a more rapid change in the neighbourhood of 750mm (30in) isohyet. In West Africa (...). In other areas also a critical annual rainfall not higher than 750 to 800mm (30 to 32in) seems to correspond to a change in plant formations. (...). In Australia, too, it is near the 700mm (28in) isohyet that the more humid vegetation of the north, with Indonesian affinities, disappears to make room for xerophytic formations (...). Similar changes occur in the north of Peru (...) and in Venezuela (...).*

defends a mean annual rainfall total of at least 1000mm, and for at least 6 months precipitation in 75mm each month, while Sperling [43] less precisely says that annual rainfall is usually over 1270mm, and monthly usually over 51mm.

When the parameter is humidity, Givoni [40] does not specify a limit but characterises the hot-humid climate with specific humidity of about 20gr/kg, sometimes rising to about 25gr/kg, with relative humidity often around and above 90 per cent. Szokolay [41] says that mean relative humidity should be around 80 per cent.

2.4.4.2 Classification

As illustrated earlier, there are several approaches to classify the climate and the most significant, regarding the humid tropics, are explained below.

Köppen defines the humid tropics as 'A' climate, and divides into several groups, which can also be mixed. It is possible to detach and rearrange into 3 groups:

(i) *Tropical wet* (Af,), where the rainfall of the driest month is at least 60mm.

(ii) *Tropical wet and dry* (Aw or As), where there is a distinct dry season in low-sun period or winter and at least one month must have less than 60mm. If the dry season occurs during low-sun period or winter it is Aw, otherwise, if it occurs during high-sun period[4], it is As.

The Brazilian caatinga and the African Sahel are therefore included with the dry regions, whereas the Sudanese savannas and the campos cerrados and their equivalents are included with the humid tropics. The transition between these two large groups of plant formation-types corresponds to a mean annual rainfall of 700 to 800mm (28 to 32in).'

Thus, it is possible to say that Tricart puts figures of 700-800mm to this limit.

[3] Szokolay also says that the monthly rainfall is often over 2000mm, but apparently it might be a misprint.
[4] It occurs on the Brazilian north-eastern coastal zone, from 5°S to 13°S [17].

(iii) *Tropical monsoon* (Am), with short dry season, but with total rainfall so great that ground remains sufficiently wet throughout the year to support rainforest.

Based on a subjective evaluation, Atkinson classifies climate from the standpoint of building design. Firstly in 1953 [39] and after, with some adjustments, in 1960 [13], he divides the humid tropics into warm-humid, intermediate and upland. Koenigsberger et al. [14] and Evans [42] also proposed some developments on Atkinson's scheme, while Fry and Drew [29], using first Atkinson's approach, maps the tropics as shown in Figure 2-14.

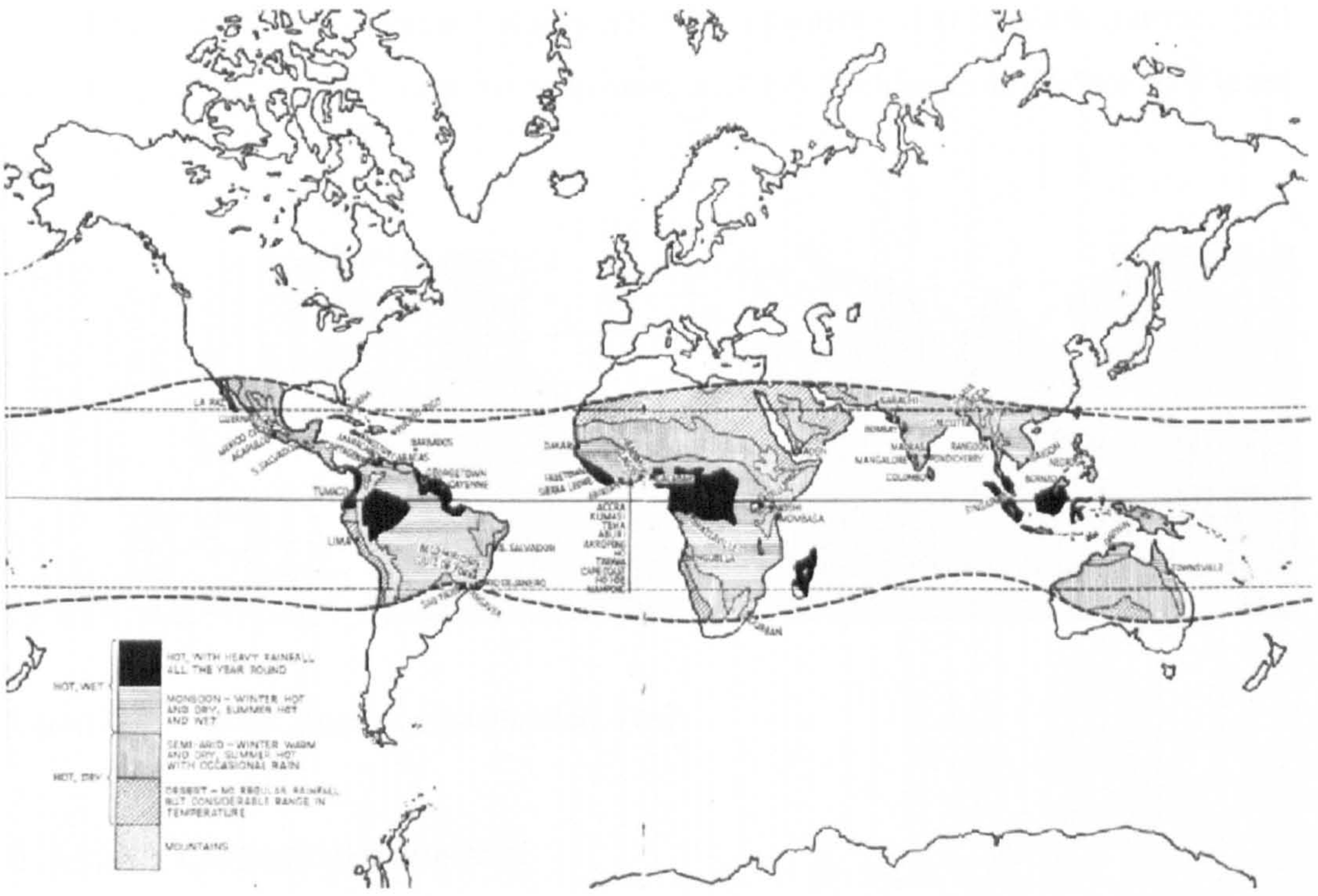

Figure 2-14 - Fry and Drew climatic classification [29]

Lippsmeier [11] division of the humid tropics is quite similar Köppen's approach. However, subsidiary zones - which can occur within humid and dry tropics and usually results in a moderation of the negative characteristics of the respective climate - are also analysed. They are divided into (i) tropical upland zones, which

cover altitudes of over 1500m; and (ii) maritime zones, whose weather is influenced by the ocean.

Analysing building and urban design, Givoni [40] divides the hot-humid regions into (i) equatorial and tropical-marine regions, which are warm during all year, and (ii) regions with hot-humid summers but cool or cold winters.

Hodder [28], following Köppen's scheme, contends that tropics can be broadly divided into 3 groups: (i) equatorial lowland, (ii) tropical monsoon, and (iii) tropical savanna.

Senior [16] divides the humid tropics into (i) equatorial, (ii) tropical marine, (iii) tropical continental, (iv) tropical monsoon, and (v) highland, as shown in Figure 2-15.

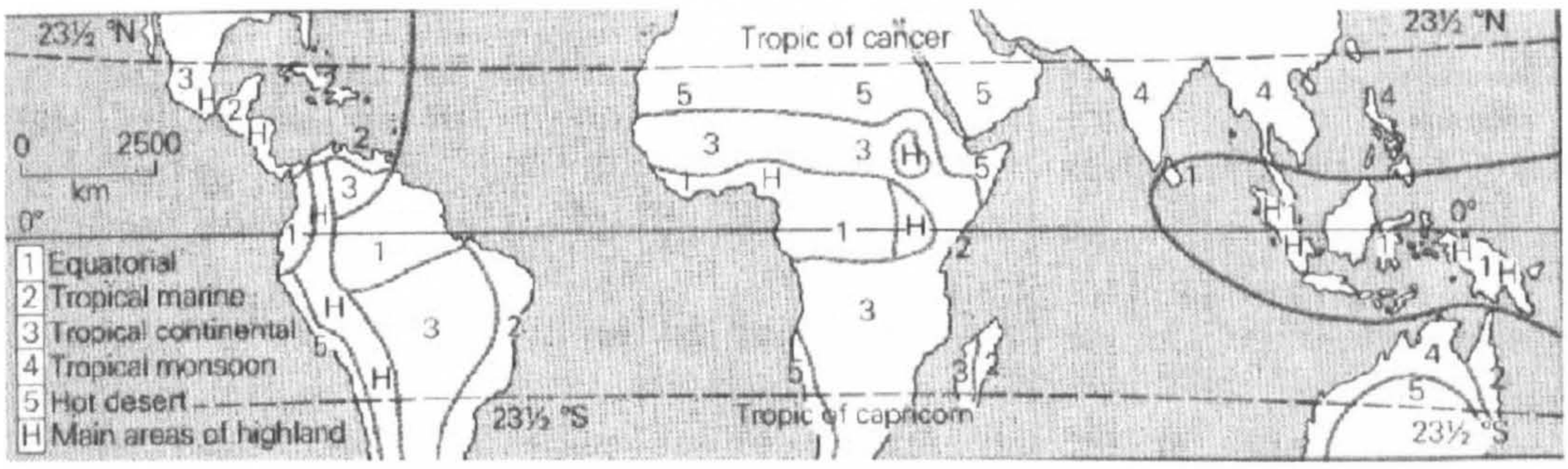

Figure 2-15 - Senior tropical classification. [16]

2.4.4.3 Climatic parameters

The most important climatic parameters are generally temperature and rainfall. With regards to building science, humidity, cloudiness, and wind may also be taken into account.

- Temperature

Although temperatures in the humid tropics are high at all times, they are less extreme than is sometimes believed, compared to dry tropics or sub-tropics. [31]

Since tropical climates are defined by the absence of a cold season, temperature differences between seasons are generally insignificant. The same occurs within the diurnal temperature range. In general, the range is lowest near the equator, but continentality, elevation and cloudiness can alter significantly this range. [17, 19, 30]

Moreover, temperature differences within places are not significant, because there are only very small differences in the amount of net radiation received, and most of the tropics consist of ocean surfaces, great heat storage reservoirs. However, elevation often causes large temperature differences over short distances, since temperature decreasing upward at an average rate of about 1°C per 150 metres high. [16, 17, 19]

- Rainfall

Since the temperatures are quite similar during the year, rainfall becomes the determinant of season. [17]

The rainfall in humid tropics generally has a great intensity, although the highest intensity is only normal over short periods of time. This heavy precipitation tends to occur in areas near the equator and seacoast, which also receive rainfall throughout the year.

Furthermore, the humid tropics experience significant rainfall variations from year to year. It is naturally an important point to agriculture and meteorology. [16, 31, 32]

- Humidity

In most parts of the humid tropics, humidity is near saturation point at night, but decreases rapidly during the day. Seasonal variation is equally marked, being highest in the wet season and lowest in the dry season [30]. The vapour pressures normally exceed 25mb and relative humidity levels are always high, generally above 80 per cent [17].

According to Jarrett [31], the consistently high relative humidity can produce very uncomfortable living conditions and considerably reduce the output of human energy.

Evapotranspiration in the humid tropics is connected to the relative humidity and the capacity of the air to absorb water vapour [30].

- Cloudiness

Clouds in the tropics occur in a range of sizes, extending from small isolated cumuli to large cloud ensembles [48]. Although the humid tropics are famously cloudy areas, there are seasonal variation associated with the changing location and intensity of the intertropical convergence zone (ITCZ), a wide belt characterised by relatively low surface pressure, rising air movements and convergence of air masses [18, 19]. Figure 2-16 shows the seasonal shift of the intertropical convergence zone.

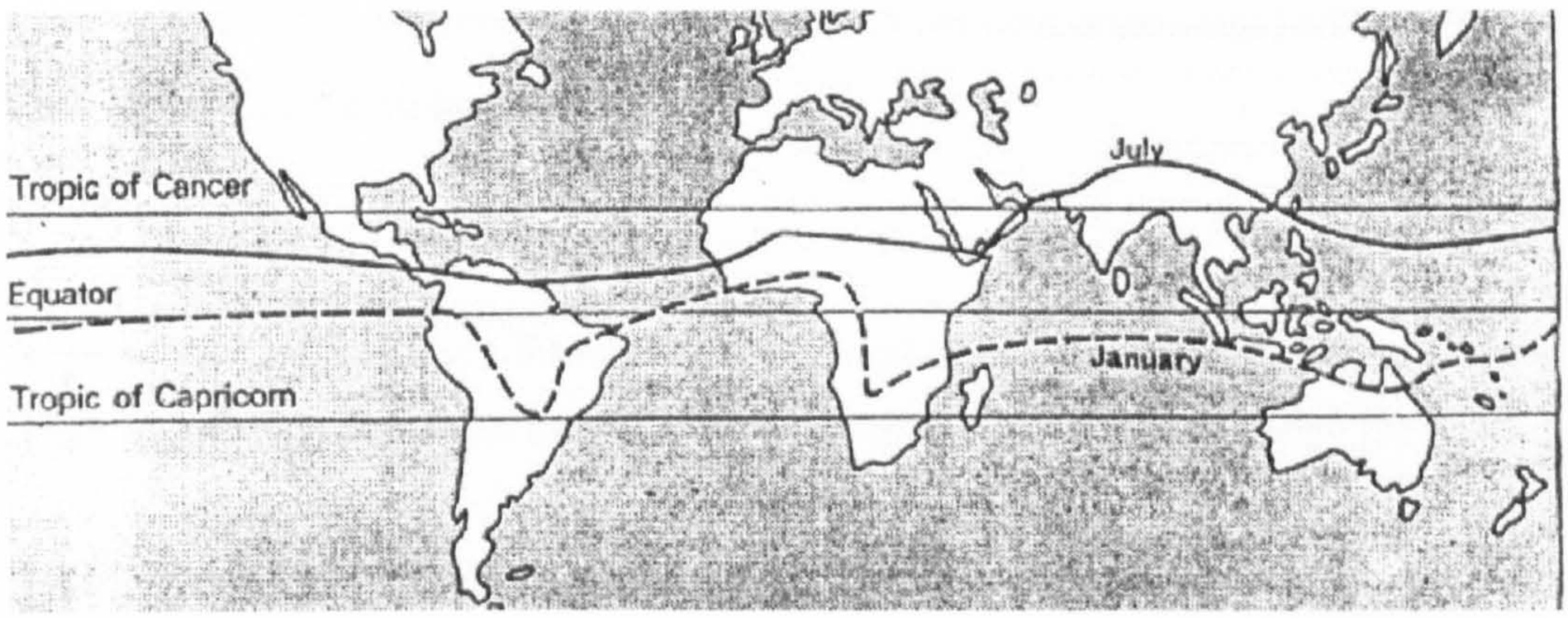

Figure 2-16 - Seasonal shift of the intertropical convergence zone. [14]

There are also diurnal changes varying in terms of coastal versus inland location. While shore stations encounter maximum cloud cover during the early morning and clearer conditions in the early afternoon, inland stations experience maximum cloud cover in the late afternoon [17].

Hopkinson in 1966 [45] wrote that the hot humid climate is characterised by a sky that is frequently overcast. In the same way, Koenigsberger [14] says that in warm-

humid climates the sky is typically overcast, with a luminance often exceeding 7000 cd/m^2. The proportion of diffused or skylight is predominant and the very bright sky viewed from a moderately lit room can cause discomfort glare. However in 1972, Hopkinson [49] affirmed that the hot-humid tropical climate is one with a high variability of cloudiness together with frequent seasonal sunshine. It is also characterised by skies of very high brightness.

According to Oakley [50], since the atmosphere contains a lot of water vapour, skies are generally cloudy. When not shielding the rays of the sun, large clouds may increase the intensity of radiation by reflection of bright sunshine. Under overcast conditions, the sky and not the sun is the main source of heat and, when thinly overcast, the intensity of radiation from the sky is high.

On the other hand, Bittencourt [51], researching the Brazilian north-eastern coast climate, affirms that the typical sky condition in warm humid climates is partially cloudy. Clear sky occurrences are rare (about 4.5 per cent on average) while overcast skies are just above 15 per cent.

- Wind

In general, winds are light throughout the humid tropics, although strong winds can occur in specific areas from time to time, in a violent and destructive way [31].

During the rain time wind is associated with driving rains [51].

2.5 Conclusion

Climatic classification is presented as a challenging task. There is no concurrence among most of the authors, and there is a tendency to specify a field of science as the object for the approach. This is also the case with classification of the tropics.

Nevertheless, the annual thermal amplitude is not significant in the whole tropical region. Also, humidity is intrinsically linked to cloudiness as well as to daily thermal amplitude. In this way, a basic classification for the tropics between dry and humid

seems adequate for daylighting proposes, since the sky characteristics is the most important climatic parameter. It will define the luminance distribution of the main source of light, giving also the possibility of sunshine.

The hot-dry tropics have as basic characteristics clear sky and significant daily thermal amplitude. On the other hand the humid tropics present a slight temperature variation and partly cloudy skies most of the time.

However those sky patterns are still not sufficient investigated. The number of IDMP stations in the tropical world is still limited. In this way the present study proposes in Chapter 4 a simplified methodology to measure the sky luminance and correlates results with the CIE standards to propose a set of typical skies for a specific location. Results are shown for the city of Maceió in the Brazilian north-east.

An important observation is that climatic conditions found in the north-eastern Brazilian coast are typical of a large tropical area. Thus results can be extrapolated when the main parameters are not significantly contrasting.

Furthermore, the requests for thermal comfort are also imperative and should be allied to daylighting design. They can delineate the apertures characteristics, including glazing, shading, size and sill width. For the humid tropics, the traditional and efficient passive approach uses natural ventilation and shading, with a particular reference to orientation. Although useful for hot-dry tropics, thermal mass is not required in the humid tropics, since temperature amplitude is insignificant between night and day. It leads to thin walls and consequently small sill width.

Natural ventilation studies have a connected role with daylighting design as both works with apertures. A slat used to redirect the wind, can make a room underlit or improve the daylighting quality, depending on its design.

A basic daylighting design criteria for the humid tropics could shade the direct sun and reduce the direct sky view, without losing the ventilation net area and keeping lighting levels greater than the minimum required. Combining wind direction with

shading cut-angles for shading devices can be a target to be achieved in an integrated environmental design for the humid tropics.

Rain is another problem to be dealt with. During the rainy season, skies are commonly overcast, which means lower light level. Apertures not properly designed to deal with rain can force users to close windows and consequently reduce the illuminance level inside the building when the glazing area is diminished. It should be borne in mind that glazing is not a good approach for the tropics due to thermal concepts. Thus reduced glazed areas should be expected. In this way, shading devices can also be designed taking into account the rain angles to allow open windows most of the time, improving both thermal and visual comfort.

However, those techniques can induce apertures with complex geometries, which require an appropriate methodology for assessing daylight levels. In addition, proper assessment of reflected sunshine contribution to internal daylight levels requires specific techniques. Part II of the present study proposes a method to achieve these goals.

References

1. Departamento Nacional de Meteorologia, *Normais climatológicas*: Brasília, 1992.

2. Vitruvius, *Ten books on architecture*. Cambridge: Cambridge University, 1999.

3. Dollfus, J., *Aspects de l'architecture populaire dans le monde*. Paris: Morance, 1954.

4. Olgyay, V. and A. Olgyay, *Design with climate: bioclimatic approach to architectural regionalism*. Princeton: Princeton University Press, 1963.

5. Givoni, B., *Man, climate and architecture*. 1st ed. London: Elsevier, 1969.

6. CIE - Commission Internationale de l'Eclairage, *Guide to recommended practice of daylight measurement*, CIE - Commission Internationale de L'Eclairage: Wien, 1994.

7. CIE - Commission Internationale de l'Eclairage, *Spatial distribution of daylight - CIE general sky*, CIE: Wien, 2001.

8. Kittler, R., R. Perez, and S. Darula. *A new generation of sky standards*. in *Lux Europe*. p. 359-373, 1997.

9. Kittler, R., *Universal modelling of daylight climates for design purposes*. Architectural Science Review, **40**(June 1999): p. 75-78, 1999.

10. Tregenza, P. R., *Standard skies for maritime climates*. Lighting Research and Technology, **31**(3): p. 97-106, 1999.

11. Lippsmeier, G., *Tropenbau - Building in the tropics*. München: Callwey, 1980.

12. Ayoade, J. O., *Introduction to climatology for the tropics*. Chichester: John Wiley & Sons, 1983.

13. Atkinson, G. A., *Principles of tropical design*. Architectural review, **128**(761 - July 1960): p. 81-83, 1960.

14. Koenigsberger, O. H., *et al.*, *Manual of tropical housing and building.* Vol. I: Climatic design. London: Longman, 1974.

15. Lydolph, P. E., *The climate of the earth.* Totowa: Rowman & Allanheld, 1985.

16. Senior, M., *Tropical lands: A human geography.* London: Longman, 1979.

17. Reading, A. J., R. D. Thompson, and A. C. Millington, *Humid tropical environments.* Oxford: Blackwell, 1995.

18. Nieuwolt, S., *Tropical climatology: An introduction to the climates of the low latitudes.* London: John Wiley & Sons, 1977.

19. McGregor, G. R. and S. Nieuwolt, *Tropical climatology: An introduction to the climates of the low latitudes.* 2nd ed. Chichester: John Wiley & Sons, 1998.

20. Oliver, P., ed. *Encyclopedia of vernacular architecture of the world.* Cambridge University: Cambridge, 1997

21. Köppen, W., *Das Geographische System der Klimate*, in *Handbuch der Klimatologie.* Kraus-Thomson: Berlin, 1936.

22. Mofidi, S. M., *Climatic Urban Design*, PhD, in *School of Architecture*, University of Sheffield: Sheffield, 1998.

23. Trewartha, G. T. and L. H. Horn, *An introduction to climate.* 5th ed. New York: McGraw-Hill, 1980.

24. Miller, A. A., *Climatology*. London: Methuen, 1965.

25. Trewartha, G. T., *An introduction to climate.* 4th ed. McGraw-Hill Series in Geography, ed. J.C. Weaver. New York: McGraw-Hill, 1968.

26. Barry, R. G. and R. J. Chorley, *Atmosphere, weather & climate.* 7th ed. London: Routledge, 1998.

27. Strahler, A. N., *Physical geography*. 3rd ed. New York: Wiley, 1969.

28. Hodder, B. W., *Economic development in the tropics*. 2nd ed. London: Methuen, 1973.

29. Fry, M. and J. Drew, *Tropical architecture in the dry and humid zones*. New York: Robert E Krieger, 1964.

30. Faniran, A. and L. K. Jeje, *Humid tropical geomorphology*. London: Longman, 1983.

31. Jarrett, H. R., *Tropical geography*. "Aspect" geographies, ed. H. Robinson. Plymouth: MacDonald & Evans, 1977.

32. Riehl, H., *Climate and weather in the tropics*. London: Academic Press, 1979.

33. Henderson-Sellers, A. and P. J. Robinson, *Contemporary climatology*. Essex: Longman Scientific & Technical, 1986.

34. Gourou, P., *The tropical world: Its social and economic conditions and its future status*. 5th ed. London: Longman, 1980.

35. Barrow, C., *Water resources and agricultural development in the tropics*. Harlow: Longman, 1987.

36. Fosberg, F. R., B. J. Garnier, and A. W. Küchler, *Delimitation of the humid tropics*. The Geographical Review, **51**(3): p. 333-347, 1961.

37. Küchler, A. W., *Mapping the humid tropics: vegetation criteria*. Geographical Review, **51**(3): p. 346-347, 1961.

38. Tricart, J., *The landforms of the humid tropics, forests and savannas*. Geographies for advanced study, ed. S.H. Beaver. London: Longman, 1972.

39. Atkinson, G. A., *An introduction to tropical building design*. Architectural Design, **23**(oct 1953): p. 268-271, 1953.

40. Givoni, B., *Climate considerations in building and urban design*. New York: Van Nostrand Reinhold, 1998.

41. Szokolay, S. V., *Environmental science handbook*. Lancaster: The Construction Press, 1980.

42. Evans, M., *Housing, climate and comfort*. London: The Architectural Press, 1980.

43. Sperling, R., *Non-traditional building for warm climates: A guide to good design and practice*. Overseas Building Notes, **117**(April 1967): p. 1-20, 1967.

44. Konya, A., *Design primer for hot climates*. London: The Architectural Press, 1980.

45. Hopkinson, R. G., P. Petherbridge, and J. Longmore, *Daylighting*. London: Heinemann, 1966.

46. Gourou, P., *The tropical world: Its social and economic conditions and its future status*. 4th ed. London: Longmans, 1966.

47. Garnier, B. J., *Mapping the humid tropics: climatic criteria.* Geographical Review, **51**(3): p. 333-338, 1961.

48. Hastenrath, S., *Climate and circulation of the tropics*. Atmospheric science library. Dordrecht: D. Reidel, 1985.

49. Hopkinson, R. G. and J. D. Kay, *The lighting of buildings*. 2nd ed. London: Faber and Faber, 1972.

50. Oakley, D., *Tropical Houses. A guide to their design*. London: B.T. Batsford, 1961.

51. Bittencourt, L. S., *Ventilation as a cooling resource for warm-humid climates: An investigation on perforated block wall geometry to improve ventilation inside low-rise buildings*, PhD, in *Environment and Energy Studies Programme*, Architectural Association Graduate School: London. 314 p., 1993.

Chapter 3 Meteorological Station Data and Analysis

3.1 Introduction

This Chapter investigates records from meteorological stations in Maceió, Brazil. Among the available data, only insolation and nebulosity were valuable to analyse. There was no workable data for solar radiation which could give global and diffuse figures. Also at that time no sky luminance data had been collected. As regards insolation there was no raw data available and work was done based on the climatologic normal, which gives only monthly averages of insolation in hours. Nebulosity, on the other hand, was accessible in raw data and results could be arranged to produce suitable analysis for the proposals of this thesis.

3.2 Insolation

The aim for working with insolation data is to propose a table of probability of sunshine specific for daylighting calculation. A very simple methodology is used to assess the probability of sunshine, based on the available climatologic normal.

As data are provided on a monthly basis, the probability should also be proposed on the same basis. Probability is assessed relating the total monthly insolation in hours with the equivalent total monthly daytime hours.

Daytime hours are calculated based on the astronomical day length. The increment due to sunlight refraction in the atmosphere, known as apparent sunrise and sunset, has not been taken into account since it is not significant. Figure 3-1 shows the astronomical day length for Maceió. The Y-Axis shows the length in decimal hours, and the X-Axis shows the Julian day. As a city located near the equator, the graph reveals that the difference between the smallest day in winter solstice and the biggest in summer solstice is not expressive, a bit more than one hour.

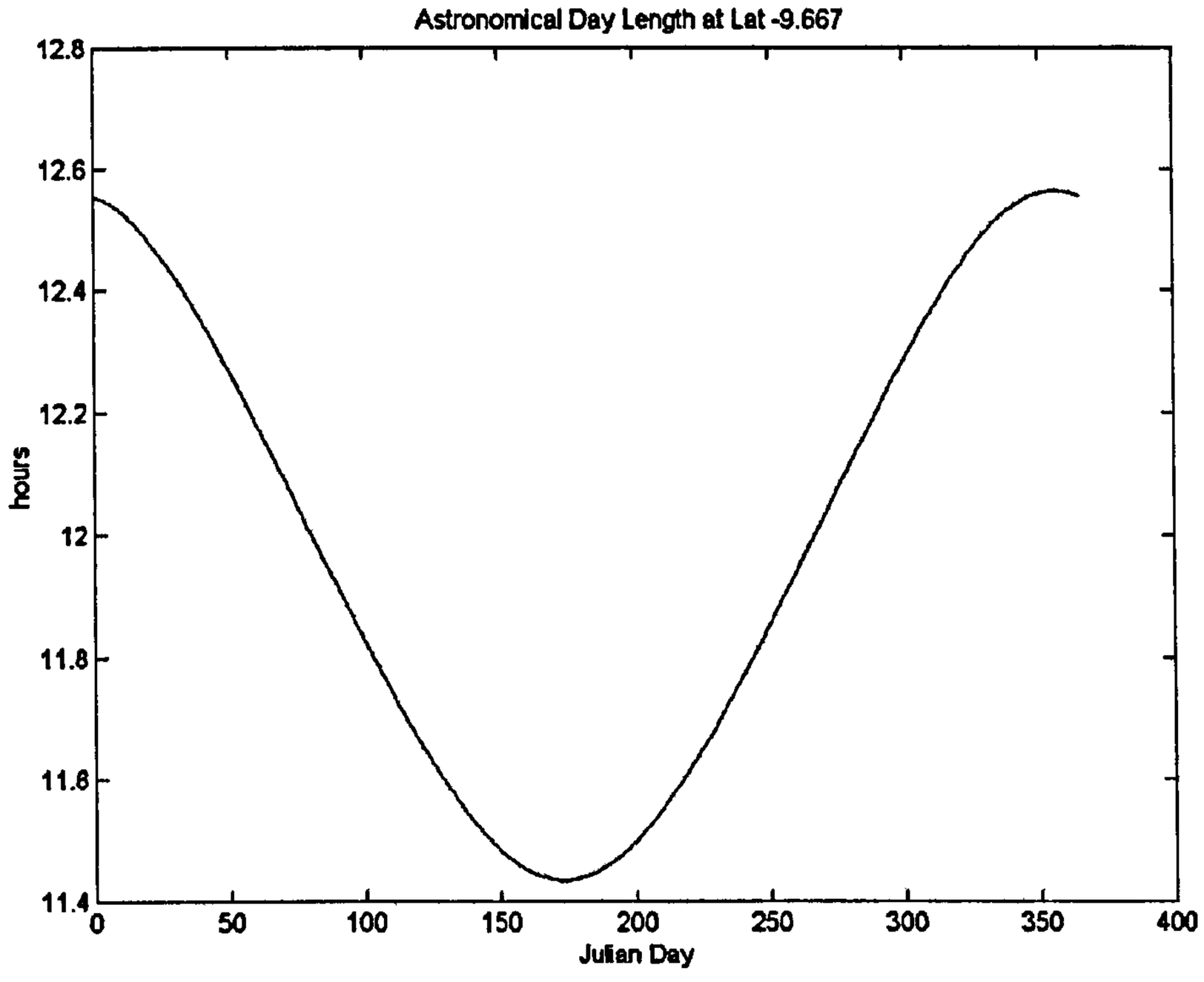

Figure 3-1 - Astronomical day length

The suggested method relates insolation and day length as simple as shown in Equation (3.1).

$$P(I) = \frac{I}{L} \times 100\ (\%) \tag{3.1}$$

where I is the monthly time of insolation, L is the monthly daytime length, and $P(I)$ is the probability of sunshine in percentage.

This makes possible to propose a monthly probability of insolation, which can be used in the model proposed in this thesis. Table 3-1 shows the probability of insolation for every month, based in the monthly insolation previously presented in Figure 2-6, and the astronomical day length shown in Figure 3-1.

Table 3-1 - Monthly probability of insolation in Maceio

Month	Day length (h)	Insolation (h)	Insolation (%)
01	387.4	254.2	65.6
02	344.4	225.7	65.5
03	373.4	203.0	54.4
04	353.4	179.4	50.8
05	358.3	191.8	53.5
06	343.4	178.6	52.0
07	356.3	176.0	49.4
08	362.0	205.2	56.7
09	357.9	204.6	57.2
10	378.1	252.4	66.8
11	372.9	274.7	73.7
12	389.1	264.2	67.9

Based on those results it is possible to assert the importance of sunshine in daylighting design for this region. The scenario where insolation has less importance represents about 50% of daytime. On the top, figures go to about three quarters during the driest month.

Insolation data are also arranged as function, shown in Equation (3.2), that allow being used in a Monte Carlo method based computer program.

$$ins = f(m) \tag{3.2}$$

where m is the month of year and *ins* is a binary number giving 1 when sunlight is available and 0 when obstructed.

In the case of the availability of raw data of insolation or solar radiation, another methodology would be proposed, in function of the data format.

3.3 Nebulosity

The analysis of nebulosity in Maceió was based on data collected by the station located at *Zumbi dos Palmares Airport*, latitude 09º31'S and Longitude 35º47'W. Original data format was the International Surface Weather Observations Data

Format. Only some fields were extracted, those related to date and time – year, month, day, hour and minute – and the Total Sky Cover (SKC), which represents the fraction of the celestial dome covered by clouds according to Table 3-2.

Table 3-2 - Total Sky Cover (TSC) description

Value	Amount in Eighths	Amount in Tenths
0	0	0
1	1 okta or less, but not zero	1/10 or less but not zero
2	2 oktas	2/10 3/10
3	3 oktas	4/10
4	4 oktas	5/10
5	5 oktas	6/10
6	6 oktas	7/10 8/10
7	7 oktas or more, but not 8 oktas	9/10 or more, but not 10/10
8	8 oktas	10/10
9	Sky obscured, or cloud cannot be estimated	

There was available information from 1982 to 1997, with values for every 3 hours, for most of the years.

The first tackled aspect was the selection of the data series, as the raw data displayed several gaps of information.

A MATLAB code was written as part of the software developed as a simulation tool for this thesis. The program converts original data into MATLAB matrix, analyses and generates tables and graphics shown in this Section.

The analysis for the integrity of nebulosity data files was based only in daytime hours, since only those values were necessary for the thesis. As available times were every 3 hours, the selected times were: 6:00, 9:00, 12:00, 15:00 and 18:00. Although Maceió has its sunset before 18:00 (legal time) every day of the year, due to its longitudinal position related to the legal time meridian, this time was selected to be used in graphics and interpolation, and also to give a balance between morning and afternoon values.

After analysis of data integrity, a series of 10 years, from 1982 to 1991, was selected. Then data were analysed in two ways, first nebulosity was calculated taking into account variations during the year and throughout the day, and second a proposal of sky type probability was presented.

3.3.1 Nebulosity analysis

The analysis of the nebulosity starts with an overview of cloud cover variation during the year and through the day. Data are grouped in two ways, monthly and hourly as shown in Figure 3-2 and Figure 3-3, respectively. All graphs in this Section are bar charts where the Y-Axis represents the nebulosity in percentage. In order to simplify the visual analysis, each graph shows a horizontal line which corresponds to the average nebulosity.

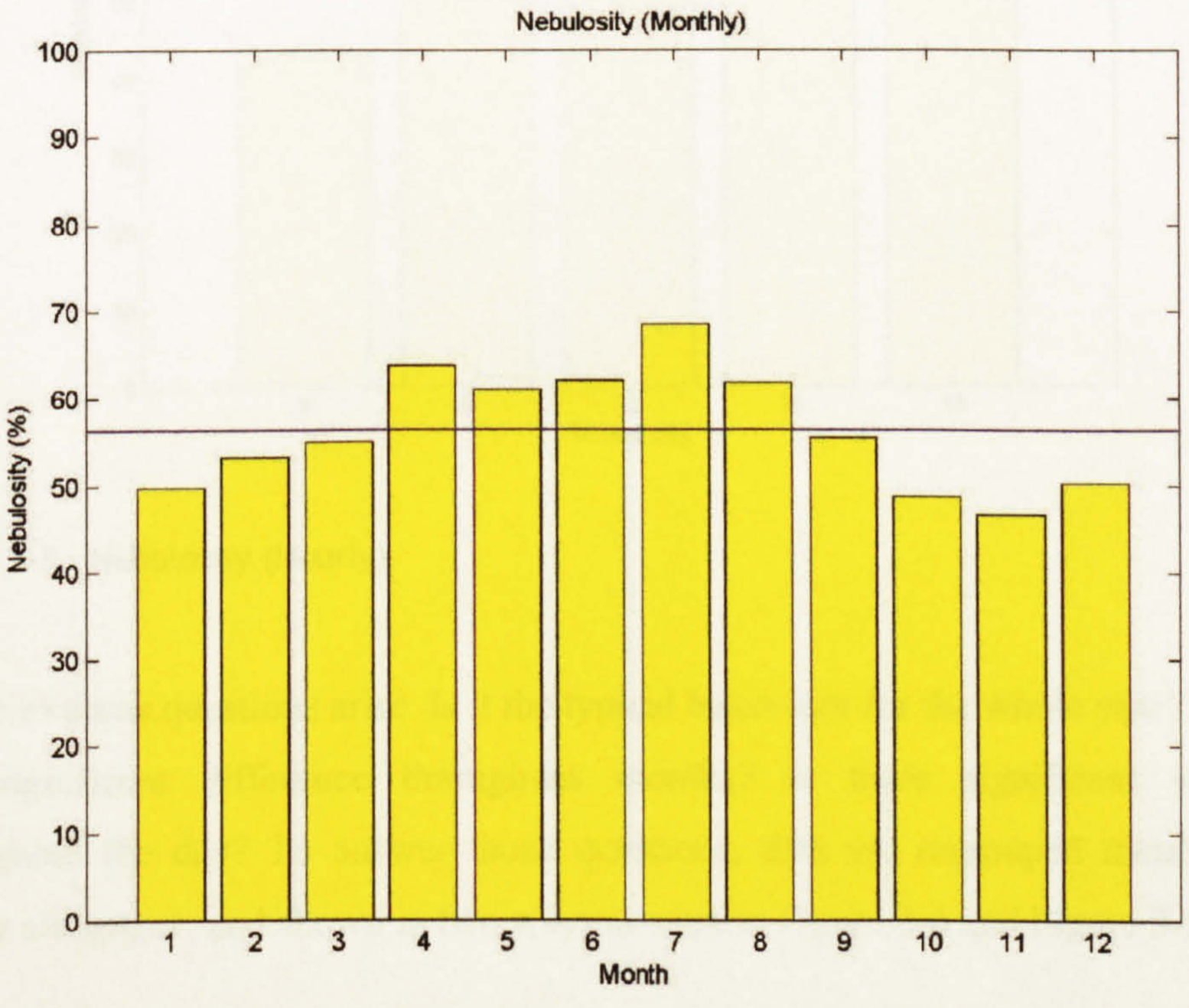

Figure 3-2 - Nebulosity (Monthly)

Figure 3-2 can be compared with Figure 2-7, previously shown. Both show similar shape, although Figure 2-7 presents a smoother variation. This could occur due to

difference in data source and in the sample interval, as Figure 2-7 represents 30 years average, while Figure 3-2 encompasses only 10 year. However it does not represent any incompatibility.

Although significant, the graph does not show cloudiness variation during the day. It is shown in Figure 3-3. Nebulosity is lower early morning, increases during the day with a top in early afternoon and reducing until sunset.

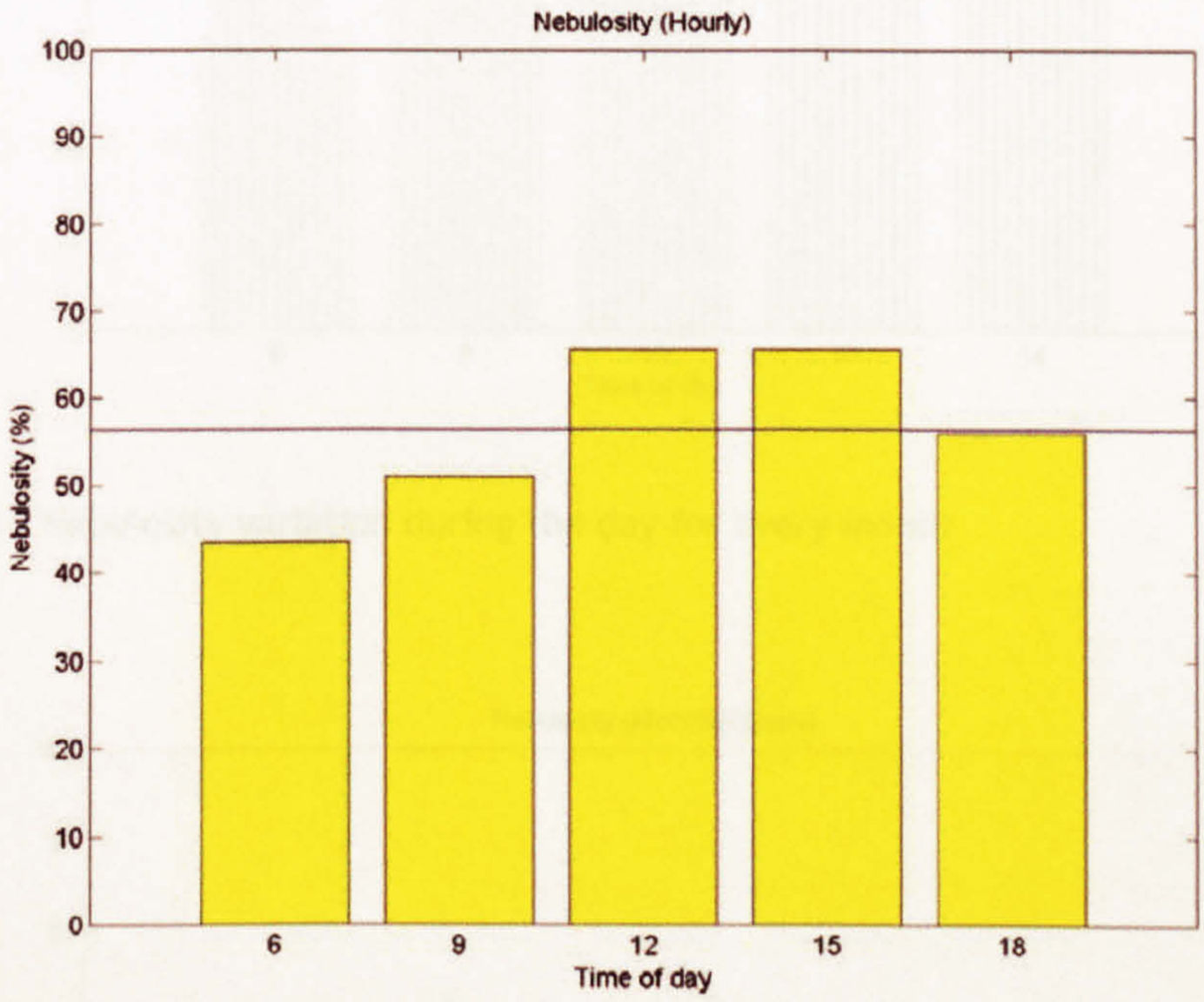

Figure 3-3 - Nebulosity (Hourly)

However some questions arise. Is it the typical behaviour for the whole year? Is there any significant difference throughout months? Is there significant variation throughout the day? To answer those questions, data are regrouped monthly and hourly altogether, and shown in two ways as seen in Figure 3-4 and Figure 3-5.

The results, shown graphically, reveal that the nebulosity variation through months is significant during morning and sunset, when dry and wet season can be easily located. On the other hand, during early afternoon, and midday in particular, nebulosity is less vulnerable to seasonal variation.

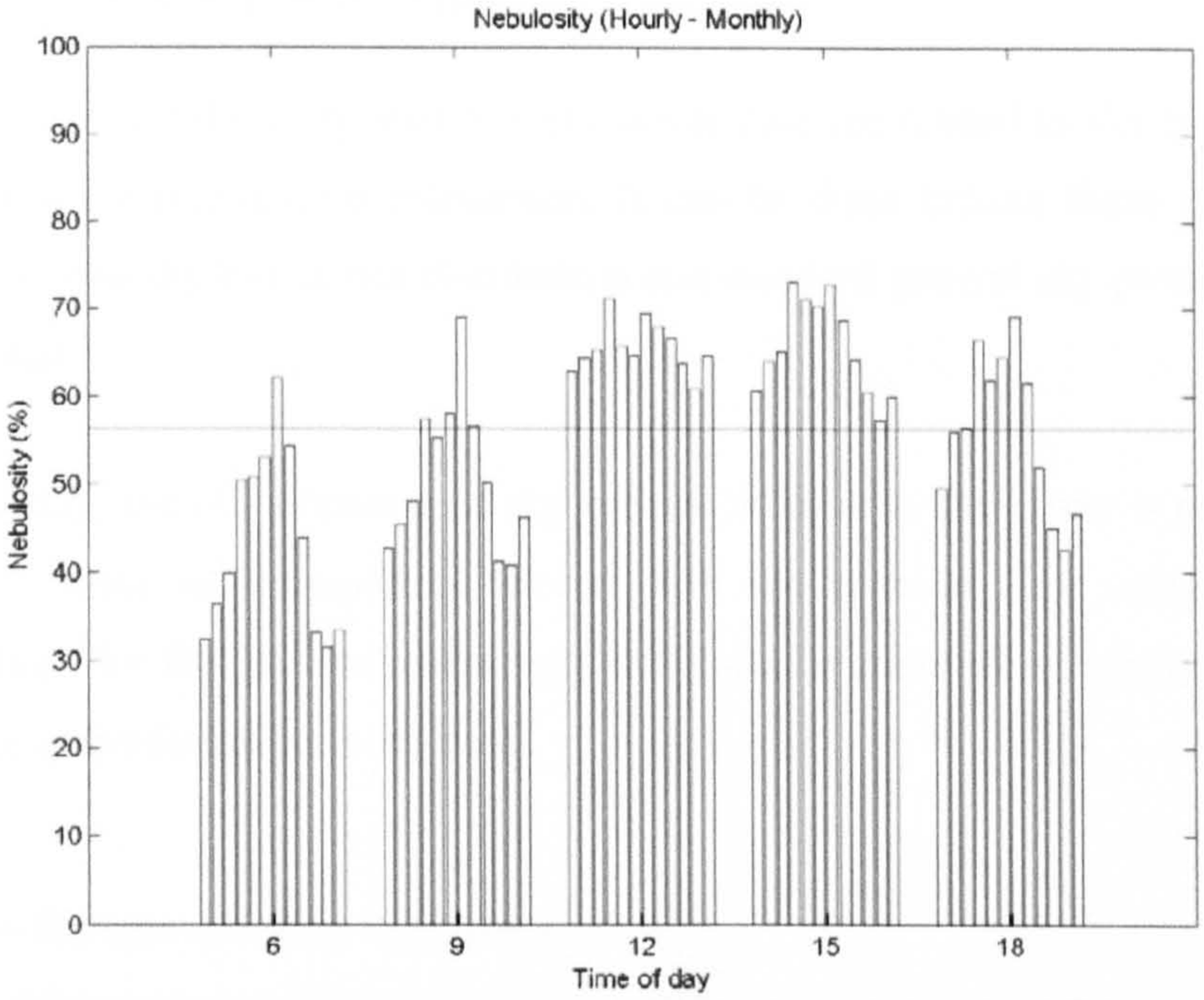

Figure 3-4 - Nebulosity variation during the day for every month

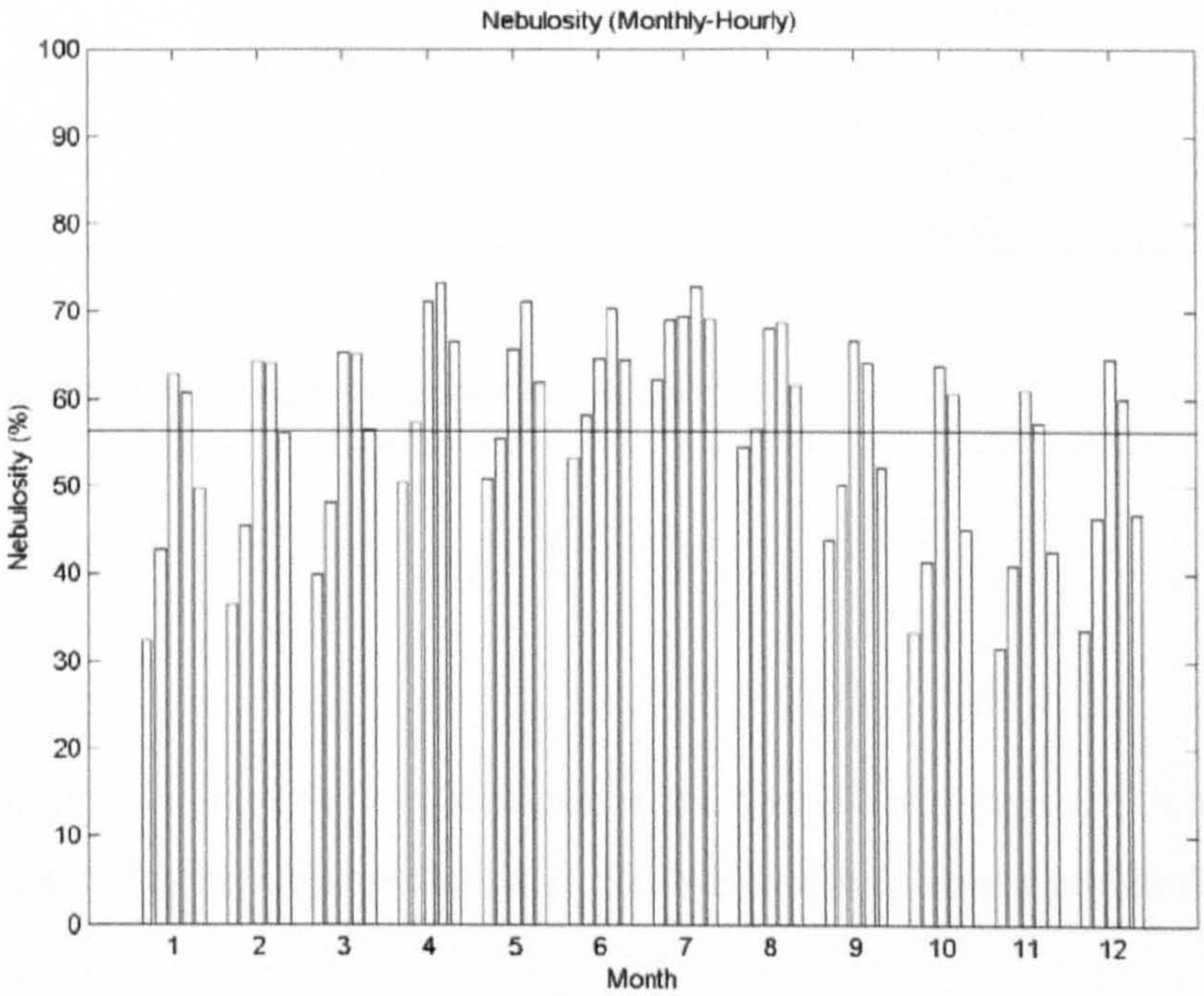

Figure 3-5 - Nebulosity variation during the year for 5 hours of the day

3.3.2 Probability of sky type

After the generic nebulosity analysis, sky cover data are related to sky type in order to be useful for daylighting calculation. It can be done linking these results with those relative to sky luminance distribution and standard general sky presented in the next Chapter.

For this study, the classification of sky type in relation to sky cover is presented in Table 3-3. Data are grouped in accord with the specific aim, using the same methodology for the previous nebulosity analysis, i.e. monthly or hourly, searching further for interrelation between them.

Table 3-3 - Sky type and Total Sky Cover (TSC)

TSC in Eighths	Sky Type
0	Clear
1 okta	Clear
2 oktas	Partly Cloudy
3 oktas	Partly Cloudy
4 oktas	Partly Cloudy
5 oktas	Partly Cloudy
6 oktas	Partly Cloudy
7 oktas	Overcast
8 oktas	Overcast

The probability proposed is based on equation (3.3).

$$P(i) = \frac{T(i)}{T} \tag{3.3}$$

where *T(i)* is the number of occurrences of the specific sky type *i*, *T* is the total of occurrences in the particular period, and *P(i)* is the correspondent probability.

It is important to affirm that the probability proposed here is based on 10 years frequency. Although representative, these results can express bias, which can only be identified with a more representative data sample and an appropriate statistical approach.

Nevertheless the results can serve as a primary reference and generally illustrate the local sky behaviour for daylighting purposes.

The most general outcome is presented in Figure 3-6. It groups the whole data set and results show that the partly cloudy sky, as expected for the region, is the most common one, with about 61.8% of the occurrences. Overcast skies follows with 25.8%, while clear skies occurs 12.4%.

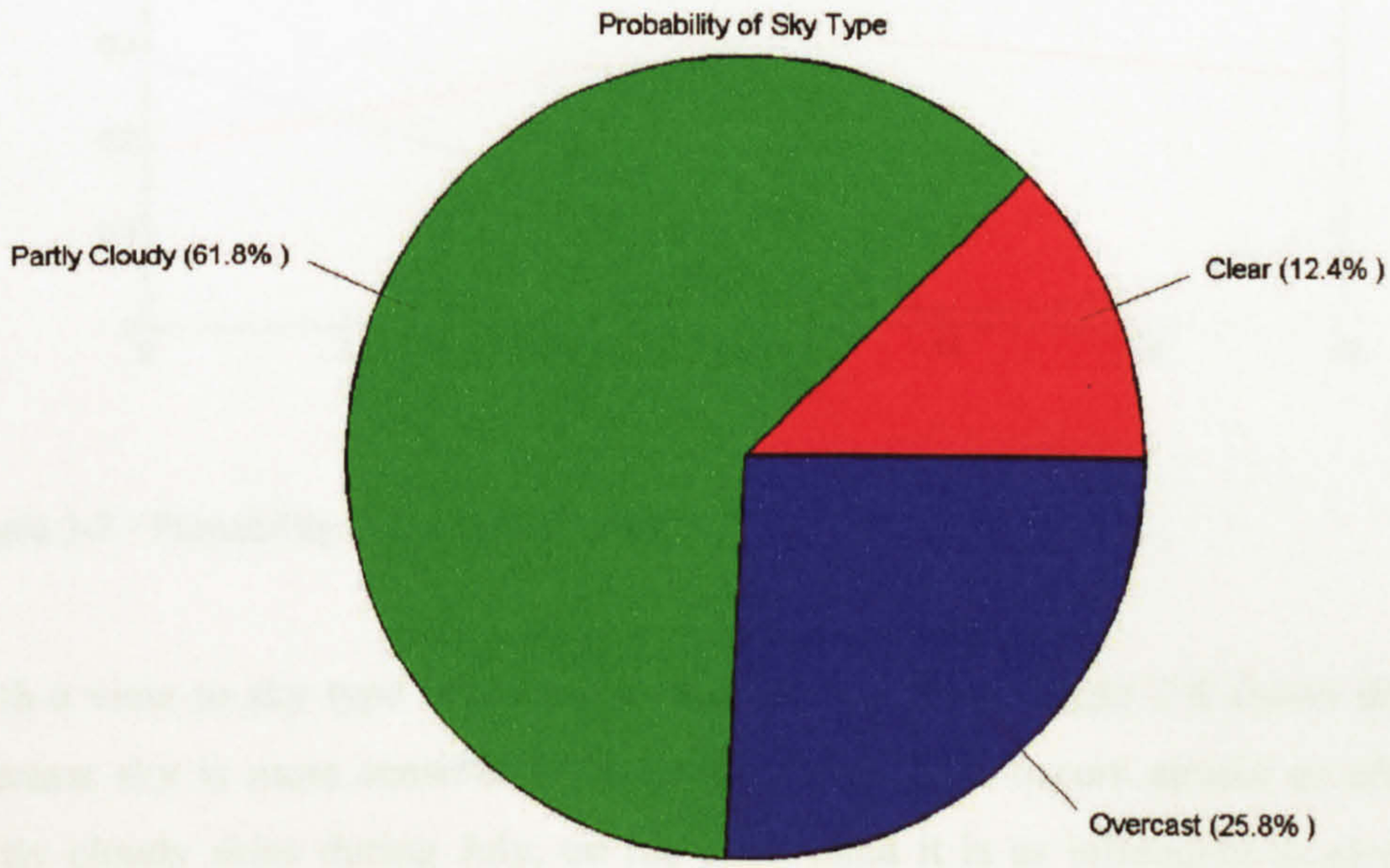

Figure 3-6 - Probability of sky type

The next stage is grouping the whole set hourly and monthly, as shown in Figure 3-7 and Figure 3-8, respectively.

Regarding the time of the day, it is possible to see from Figure 3-7 that the clear sky is the most affected one. It is more frequent when the sun altitude is lower, mainly during morning, being rare midday and early afternoon. Overcast sky, conversely is less frequent during sunset, but varies slightly afterwards. Partly cloudy sky is always the most common, with a top during afternoon.

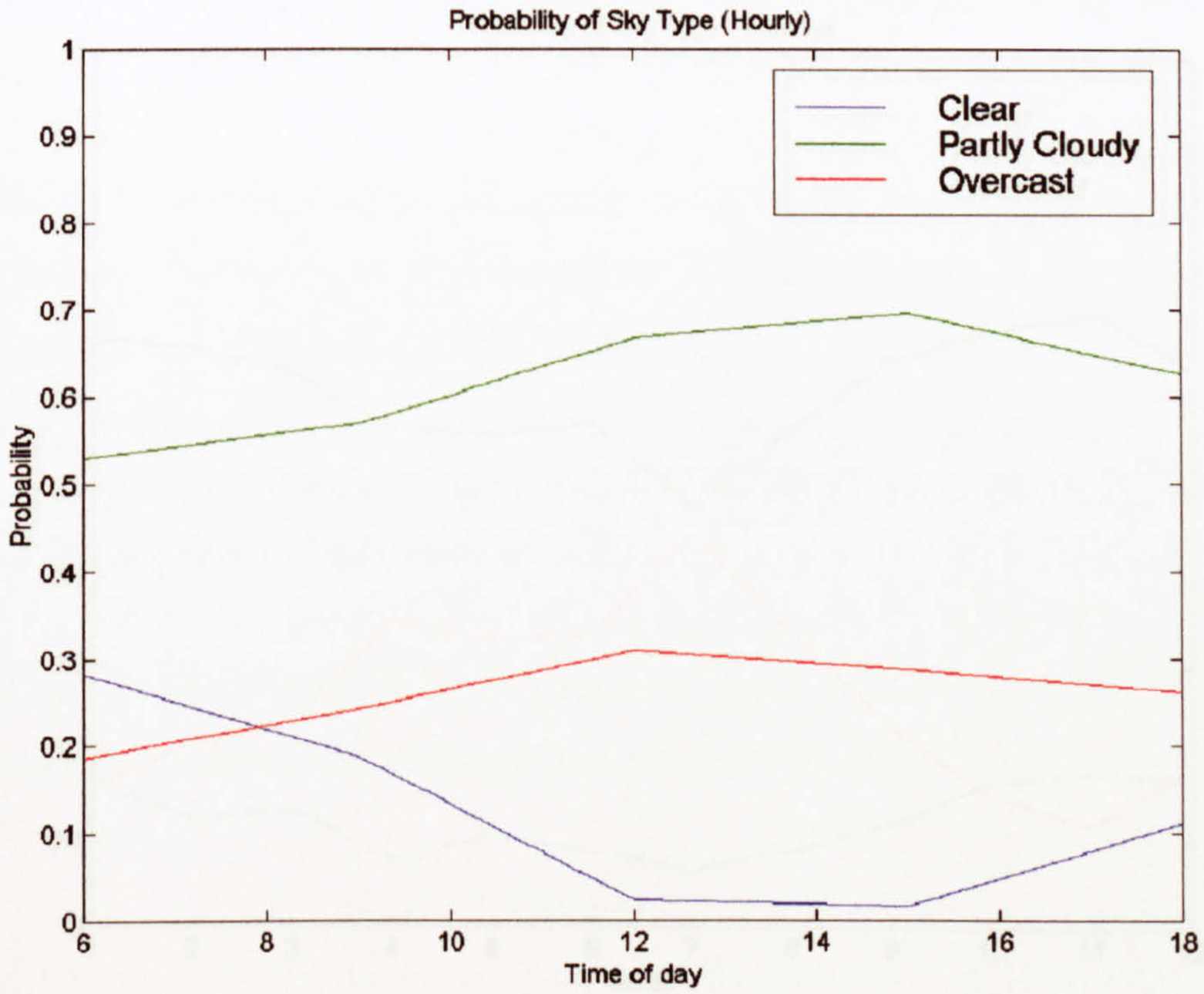

Figure 3-7 - Probability of sky type (Hourly)

With a view to sky type behaviour throughout the year, Figure 3-8 shows that the overcast sky is more sensible for seasonal variation. It occurs almost as often as partly cloudy skies during July, on the other hand it is as infrequent as clear sky during the drier months and even less so in October and November, in particular.

Results are crossed between time of the day and month of the year. Firstly, every five different studied time are analysed and results shown in Appendix A from Figure A-13 to Figure A-17. From those graphs is possible to observe the significance of the crossed influence. Sunrise has always a most common partly cloudy sky, keeping above 50% except in July when overcast sky has its apex and gets closer. Overcast sky is seldom at this time between October and March, when clear sky appears more often.

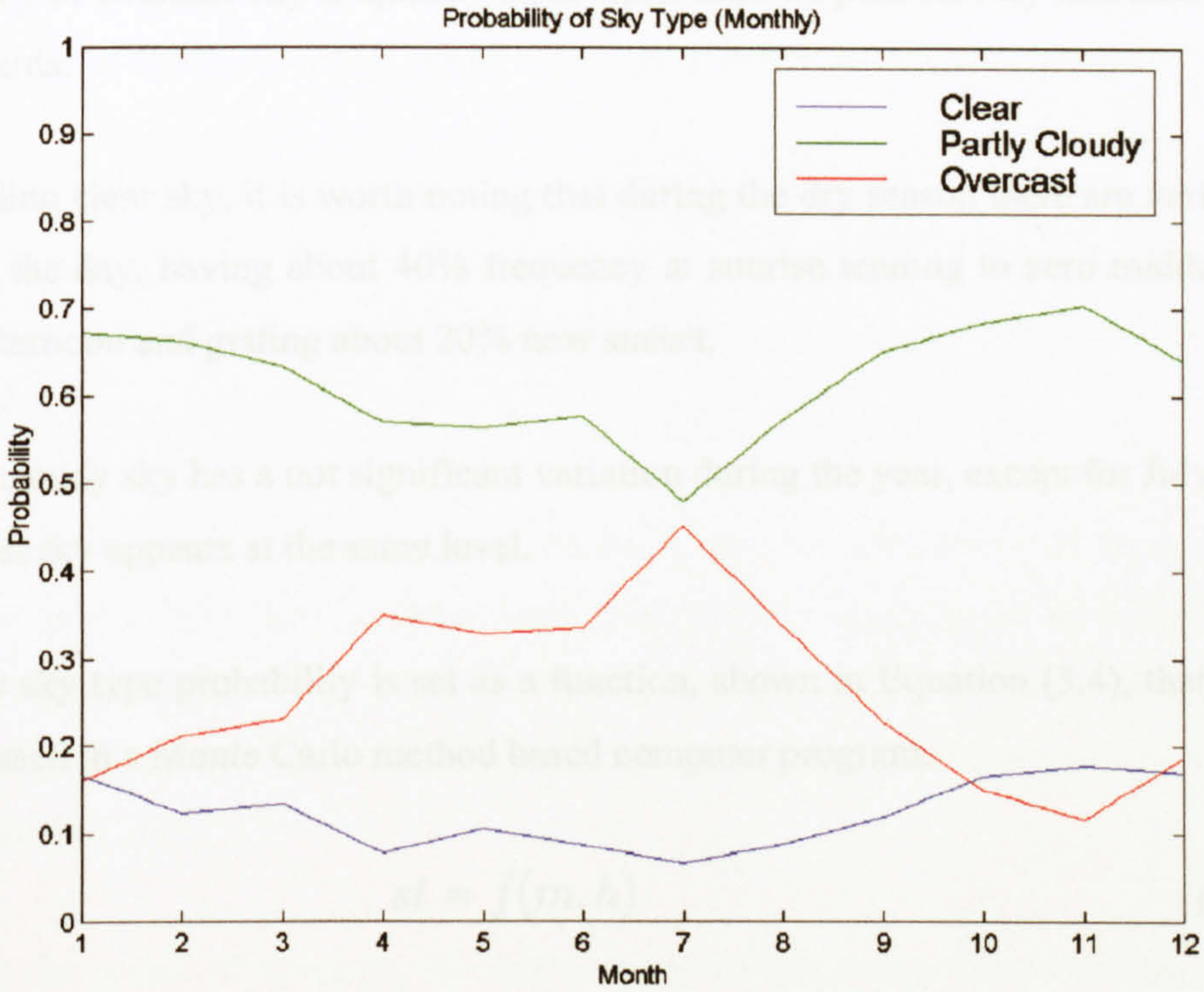

Figure 3-8 - Probability of sky type (Monthly)

Mid-morning, curves change slightly. Clear sky reduces and overcast sky increases, being even more frequent than partly cloudy in July.

Midday, clear sky is very rare, and surprisingly has only a slight occurrence during the wet season, at this time of the day. Partly cloudy is more often, mainly in the dry season, with a peak in November.

Mid-afternoon has slight difference from midday. Now clear sky is statistically not significant.

Near sundown however, clear sky happens again, reducing partly cloudy occurrence. Now it is even more often than overcast sky in October and November.

Another way to see previous data is grouping them monthly as illustrated in Appendix A from Figure A-1 to Figure A-12. Then it is possible to see the similarity among dry season month's curves. Also it is valuable to perceive the crescent

tendency of overcast sky frequency from April until its pick on July and decreasing afterwards.

Regarding clear sky, it is worth noting that during the dry season there are variations during the day, having about 40% frequency at sunrise tending to zero midday and mid-afternoon and getting about 20% near sunset.

Partly cloudy sky has a not significant variation during the year, except for July when overcast sky appears at the same level.

Finally sky type probability is set as a function, shown in Equation (3.4), that allow being used in a Monte Carlo method based computer program.

$$st = f(m, h) \tag{3.4}$$

where *st* is the chosen sky type, *m* is the month, and *h* is the hour of day.

3.4 Conclusion

This chapter has worked with meteorological station data in order to propose elements for a daylight climate analysis for Maceió, Brazil.

It was found that insolation has a significant role as a daylight source. Sunlight is available no less the 50% of the month daytime period even during the rain season. In the driest month, it gets a peak of almost three quarters of daylight time.

Nebulosity was analysed in two ways. First the Total Sky Cover (TSC) was studied for 10 years raw data. Results showed an average of 58% of sky cover for a whole year. It increases with the rain season, between April and August, reaching a peak of about 70% in July. In November, the driest month, nebulosity is about 48%. During the day, nebulosity is higher around mid-day and mid-afternoon, being the sky clearer on sunrise. This tendency is reduced during the rain season, when nebulosity

is about the average throughout the day. Results also showed that all over the year nebulosity varies more during sunrise and sunset than during the rest of the day.

Second, nebulosity was analysed as a probability of sky type. TSC is related to clear, partly cloudy and overcast sky. Partly cloudy skies are the most common, appearing more than 60% of the year during daytime. Clear skies are rare showing up about 12% of the same period.

Nebulosity data were also processed monthly and for five times of the day in a suitable format to be used as input data in computer program based on Monte Carlo method (see Chapter 5). Results for sunlight availability are also suitable for computer simulation, however daily variation is not evaluated due to restriction on available raw data.

During the period of research, no luminance or radiance data were available for the studied city. The meteorological data therefore only allow a broad categorisation of sky types. This is not sufficient for daylighting modelling of the rooms in details. So further data were collected in the field study.

The next chapter complements the daylight climate approach reporting the fieldwork that investigated the local sky luminance distribution. Measurements are related to CIE standard skies, suggesting a set of sky models for the site.

The functions for probabilities of sky types and sunlight availability proposed here can be used integrated with the sky models proposed in the following chapter in a daylighting simulation program.

Chapter 4 Fieldwork data and analysis

4.1 Introduction

This chapter continues the daylight climate study for Maceió. As shown in previous chapters, there is a lack of information on sky luminance distribution for the region. Therefore a simplified method for the collection of local sky luminance is presented. Collected data are analysed in two ways, stratified and as a whole. Results are investigated and a set of three standard skies is suggested as the best choice for daylighting calculation for the site.

4.2 The Survey

4.2.1 Choosing the equipment

Any equipment used in the fieldwork had to be easily transportable – both from Sheffield to Maceió and for systematic site visit. Rainy weather is common at the time the research was done (June-August), and this also had to be taken into account. In this way, the sky scanner was put aside and a luminance meter with a tripod was used to carry out sky luminance measurements. A photographic camera with fish-eye lens was used to take several pictures of the sky, and to register some aspects of the fieldwork, shown in this chapter. The whole set of equipment used during fieldwork is described in Appendix B.

4.2.2 Choosing the site

The selection of the site was based in two main criteria: i) open view of the sky vault and ii) easy access. Based on these points, a site at the higher part of the Federal University of Alagoas Campus was chosen. The location of the site enables sky luminance measurements at altitude even lower the 5°. Figure 4-1 shows a 360° view, while Figure 4-2 shows a fish-eye view of the site in a partly cloudy day with an obstructed sun.

Figure 4-1 - 360º view of the site at Federal University of Alagoas

Figure 4-2 - Fish-eye view of the site in a partly cloudy day

4.2.3 Site characterisation

After the site selection, a GPS (Figure 4-3) collected the geographical parameters: latitude of 9º33'07.2''S, longitude of 35º46'13.3''W and altitude of 101m above sea level. The place where the tripod would be put was sited in a part of the terrain as plain as possible with an easy access.

Although the sun would be a more precise reference point in the sky, it was decided to choose a fixed starting point, since it is not possible to locate the sun in cloudy days. A starting point for measurements was defined at the North and located by a compass (Figure 4-6). The magnetic declination at the site in 2001, when measurements were done, was 23°11' anti-clockwise, thus north given by compass (magnetic north - MN) was adjusted to the true geographic north (TN), as shown in Figure 4-4.

Figure 4-3 - Site location by GPS

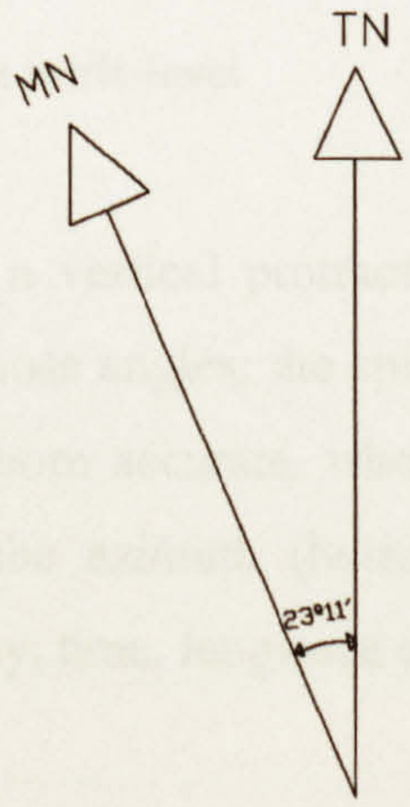

Figure 4-4 - Magnetic declination

4.2.4 Sky luminance measurements

4.2.4.1 Settling the tripod

Before starting luminance measurements, the tripod base was levelled with a spirit-level (Figure 4-5), in order to reduce the error in altitude angle when the instrument was moved around the sky, shooting at the same altitude. Subsequently, with the instrument locked, the horizontal protractor provided by the tripod was matched with the true north (Figure 4-6).

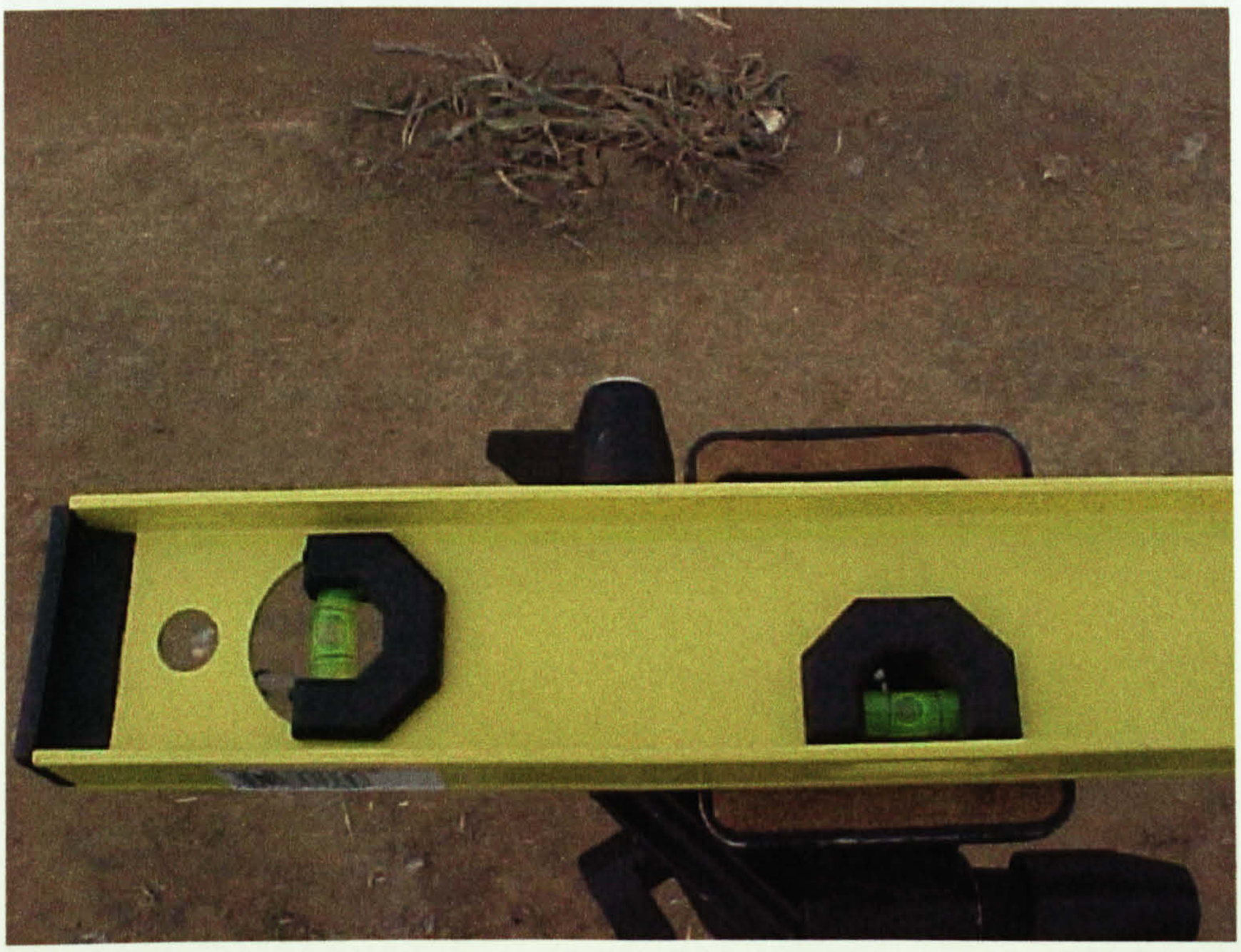

Figure 4-5 - Levelling tripod with a spirit-level

Since the tripod did not have a vertical protractor, an ordinary plastic protractor (Figure 4-7) was used to find those angles; the spirit-level was used again to get the horizontal line. Figures were more accurate, when the sun altitude was measured, since the vertical angle and the azimuth (horizontal angle) were calculated by algorithms [1], in function of day, time, longitude and latitude of site.

Figure 4-6 - Setting compass with tripod's horizontal protractor

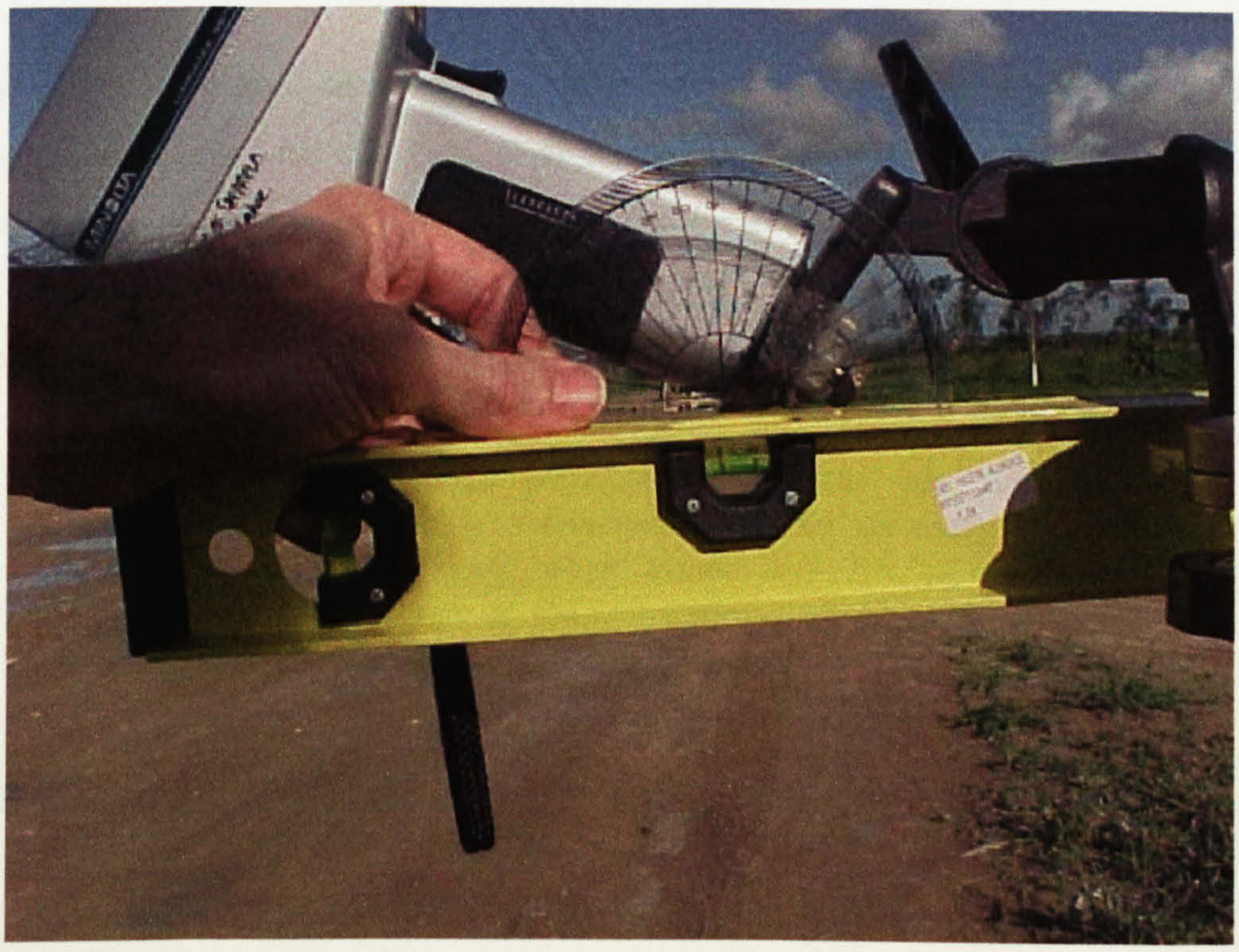

Figure 4-7 - measuring vertical angle with a protractor

4.2.4.2 *Selecting sky measurement points*

Sky luminance measurements were done for the zenith and in almucantar lines – circumferences on the celestial sphere parallel to the horizon – based on Kittler [2]. The set holds 25 sky luminance values, 1 for the zenith and 24 for the almucantar, where measurements were done every 15°. It is illustrated in Figure 4-8.

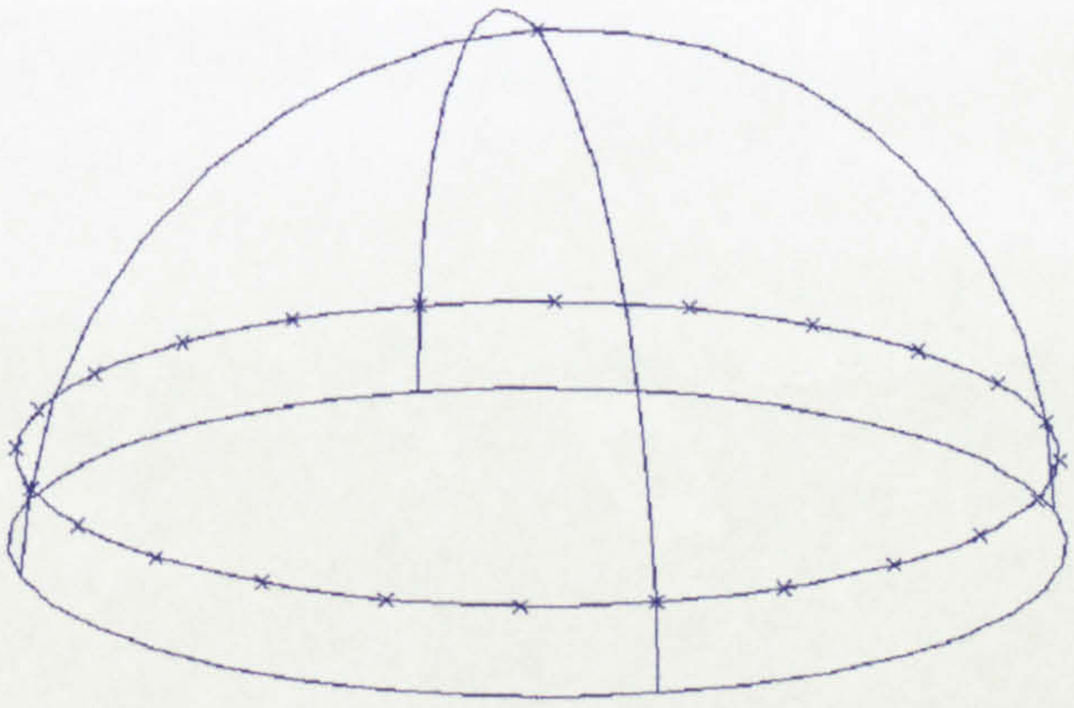

Figure 4-8 - Sky measurement points

The tripod had a horizontal protractor that making it possible to assess those angles easily. The choice for the vertical angle of measurements was done in order to accomplish two situations: (i) the greater sky circumference, i.e. as near as possible of the horizon, which was at 5° altitude and (ii) the solar almucantar. Whenever possible, both previous situation were merged, following Kittler observation that

> *"in equatorial and tropical regions the sky luminance measurements have to concentrate rather on early morning and evening periods when under low sun positions the diffusion properties of the atmosphere can be more fully and precisely investigated. "* **[2]**

4.2.4.3 *Measuring at solar almucantar*

To make measurements at solar altitude, firstly was necessary to 'view' the sun by the luminance meter viewfinder and fix the tripod at that vertical angle. Those measurements could only be made when the sun was uncovered, or when the covering clouds were not thick enough to forbid locating the sun. Since it is not safe

to view the sun directly, its location was done, either using a sun filter (Figure 4-9), or – when it was not available – a white paper put about 50 cm far from the luminance meter viewfinder. For the later, the position was found when the sun image was clear on the white paper. After the exact point was located, the vertical angle of tripod was fixed and measurements were taken around the solar almucantar, every 15°.

Figure 4-9 - Using a solar filter to localise the sun

4.2.4.4 Measuring at general almucantar

For measurements at general almucantar, the desired vertical angle was fixed using the transparent protractor (Figure 4-7). Afterwards measurements were done every 15° at the almucantar.

4.2.4.5 Measuring auxiliary points

Sequentially, the luminance was measured on the zenith (Figure 4-10), giving 25 sky measurements for every set of data. In succession, luminance was measured on a white paper (diffuse surface) on the floor (horizontal plane) (Figure 4-11). This value

allows assessing the external horizontal diffuse illuminance (E_h) by the equation (4-1).

$$E_h = \frac{L_{wp}\,\pi}{\rho_{wp}} \qquad (4\text{-}1)$$

where L_{wp} is the luminance on the white paper in cd/m^2, ρ_{wp} is the white paper reflectance and E_h is the external horizontal diffuse illuminance in lux.

Figure 4-10 - measuring luminance on zenith

When the sun was uncovered, it was blocked in order to measurement on white paper reflecting only the diffuse component, i.e. the sky contribution. Then it was possible to use the same instrument, the luminance meter, to measure both sky luminance and horizontal illuminance. On the other hand, the sky obstruction by the instrument operator reduced the sky view from the paper and consequently underestimating the results. Also, the white paper was supposed to be a Lambertian surface, and variation due to different view angles from the luminance meter viewfinder to the white paper was not taken into account.

4.2.4.6 Recording collected data

Since a data logger was not available, all readings were voice recorded in a handy tape recorder (Figure 4-12). Afterwards tapes were transcribed into a worksheet, which model is shown in Appendix C. Then those figures were input and processed by a program.

During the period of field research, 46 sets of data were collected. Each set contains information to localise the site in time and space, plus sun and sky conditions, geometric position and values for sky luminance measurements, and luminance in a white paper.

Figure 4-11 - Measuring luminance on white paper

Figure 4-12 - Recording luminance values

4.2.4.7 Disclaimer

During sky measurement and data transcription, some error could arise. Sometimes the sky changed significantly during the set of measurement. In addition, there was the possibility of error in sky angles reading, moving the tripod, reading luminance data at luminance meter, transcribing and typing data errors.

The systematic error from instrument calibration was avoided as sky luminance are analysed in relation to the external horizontal illuminance, which was measured with the same instrument. However, the time gap due to that procedure can produce an error if sky changes considerably at this point. The use of more than one instrument at the same time was not possible, since only one person did all measurements.

One way to reduce the influence of those errors is to extract the outliers. this will be described in the next section.

4.3 Data Analysis

Data were analysed by the program in order to find the best choices of sky model from the set of 15 described by CIE. Sky models are presented in Appendix D. The method used was similar the one applied by Tregenza [3]. The main difference comes from the number of sky measurements, as a set of data here has only 25 luminance values, while Tregenza followed the CIE scanning pattern, which subdivides the sky hemisphere into 145 zones of about 11° angular diameter.

Each set of data, corresponding to a specific observed sky situation, was analysed independently and compared with the sky model distributions in order to find the closest fit for the real data. The steps were the following:

1. Calculation of solar altitude and azimuth for the time of measurements;

2. Removal of measurements within 12° of the sun from the set, eliminating errors or dummy reading from the luminance meter;

3. Calculation of the horizontal illuminance from the luminance of a white paper on the floor, as shown in Figure 4-11, by equation (4-1).

4. Division of the whole set of 25 sky luminance by the horizontal illuminance, giving a relative luminance with respect to a horizontal illuminance of unity.

5. Calculation of the luminance for each measured sky point for all of the 15 standard sky distributions. Again, these values were normalised to horizontal illuminances of unity.

6. Computation of the root-mean-square (RMS) difference between the measured luminance for each point and the correlated luminance for every sky model distribution.

Thus the best-fit sky model was that with the lowest RMS error based on the relative luminances.

After the first results were obtained, a subset of data looked suspicious. The treatment was done in two stages. First, data that appeared to be inconsistent with the remainder set of data were reanalysed looking for non-statistical factors. Some misprints were found and the data were then reprocessed. Yet, a cloudy of data still looks suspicious. Coincidently those values were collected on the same period and the input form reported a considerable changing on sky during data collection. Since those outliers should have arisen for purely deterministic reasons, the considered offending sample values were removed from the sample, as it was not possible to replace or correct them [4, 5].

Figure 4-13 to Figure 4-18 compare data distribution before and after outliers' removal, regarding to sky type, sun covering and time of measurements.

As it is shown, after the removal of outliers, data distribution regarding sky type and sun covering remains representative. Moreover, its distribution per hour of day is emphasised in the end of day, when solar almucantar represents the greater sky circumference.

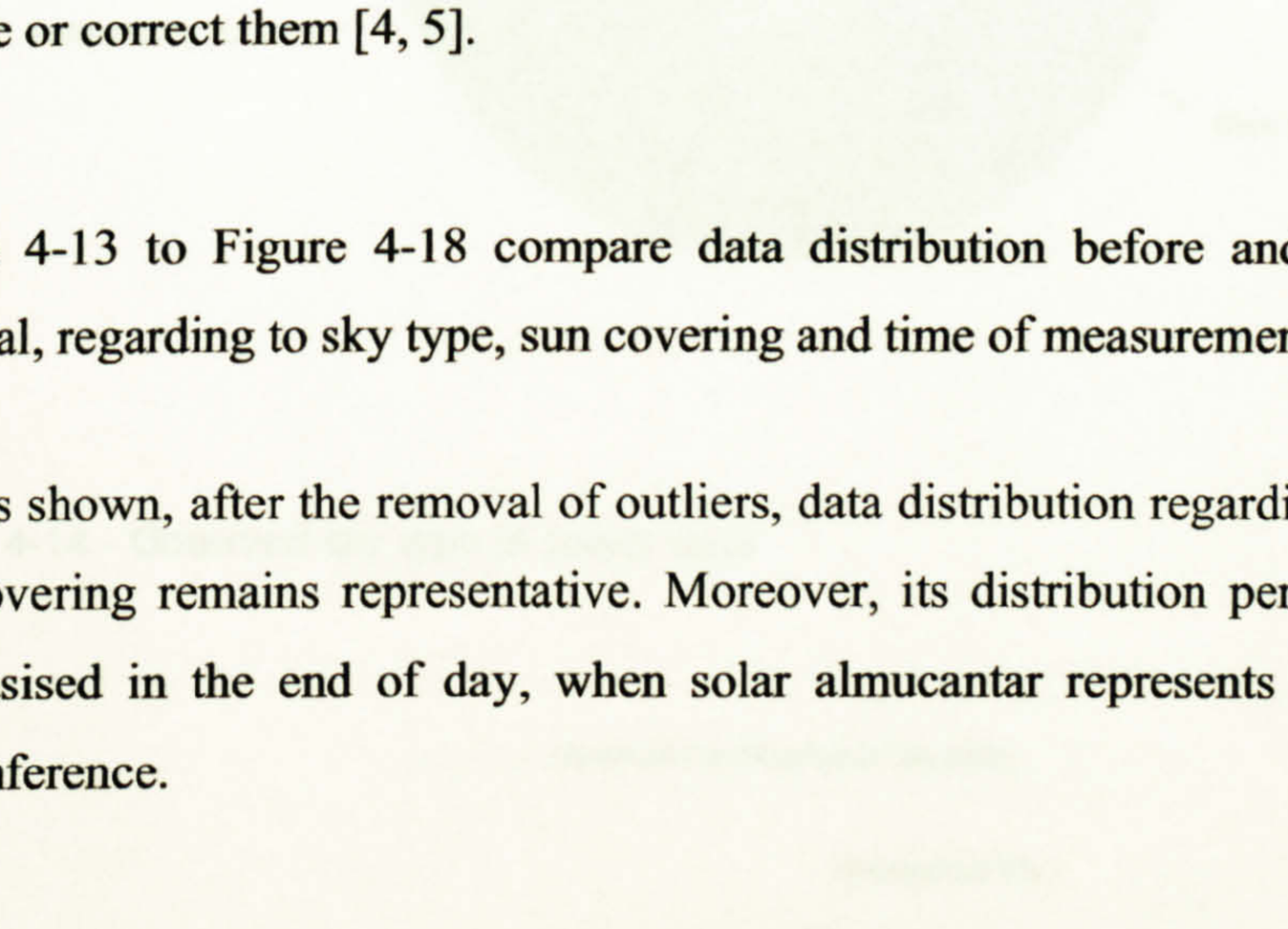

Figure 4-13 - Observed sky type in raw data

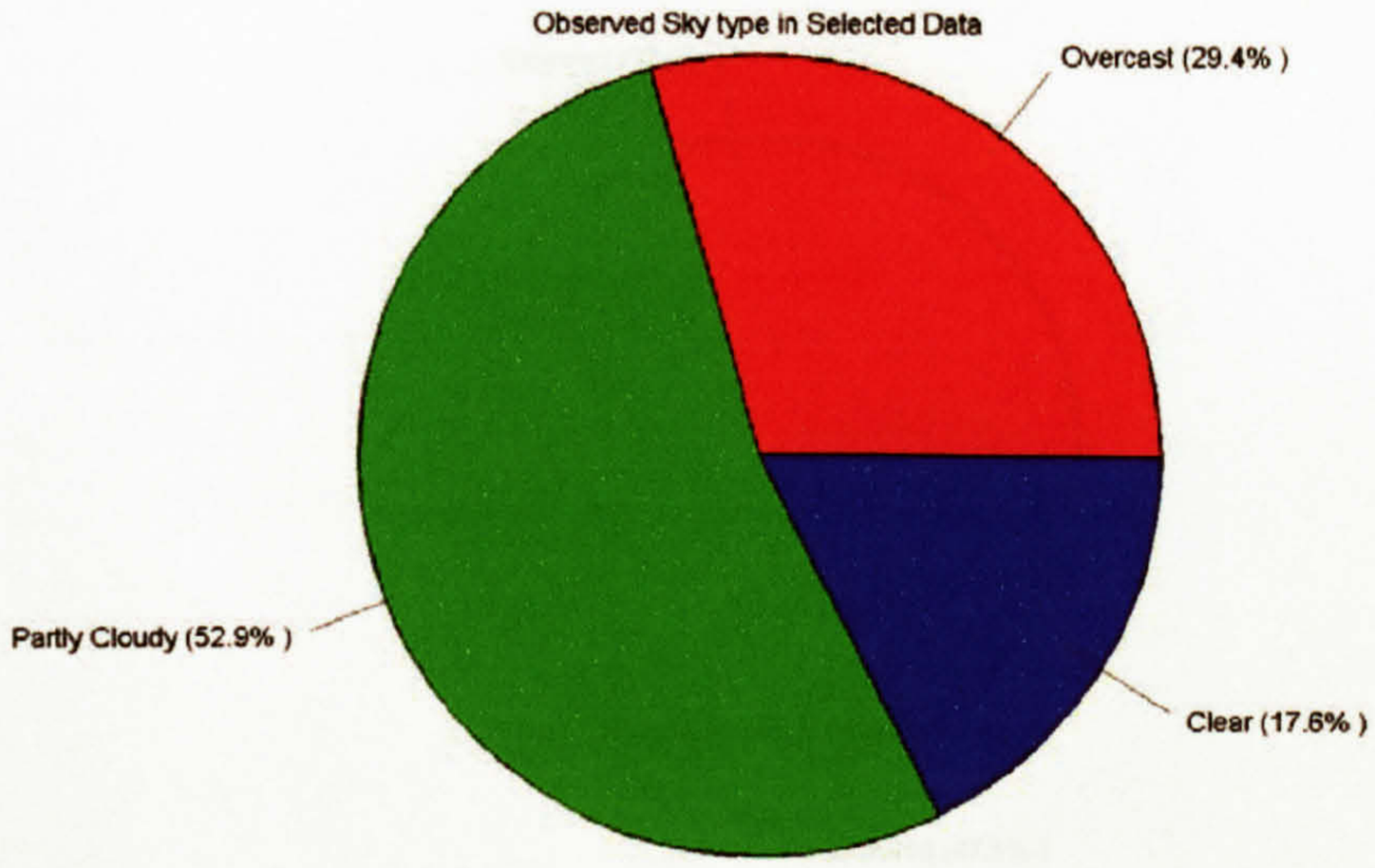

Figure 4-14 - Observed sky type in select data

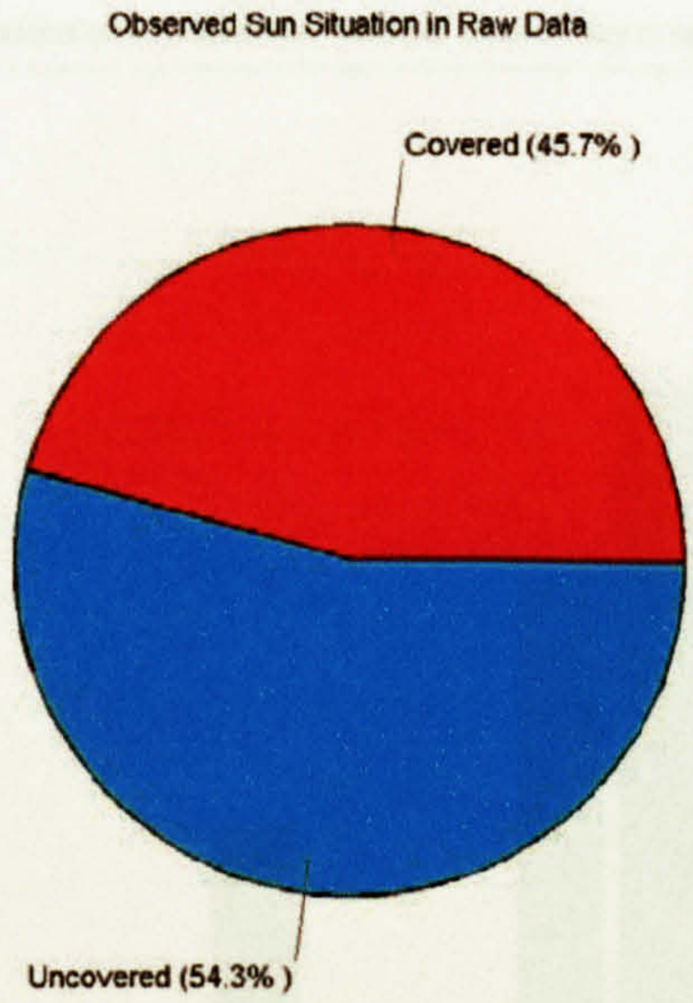

Figure 4-15 - Observed sun situation in raw data

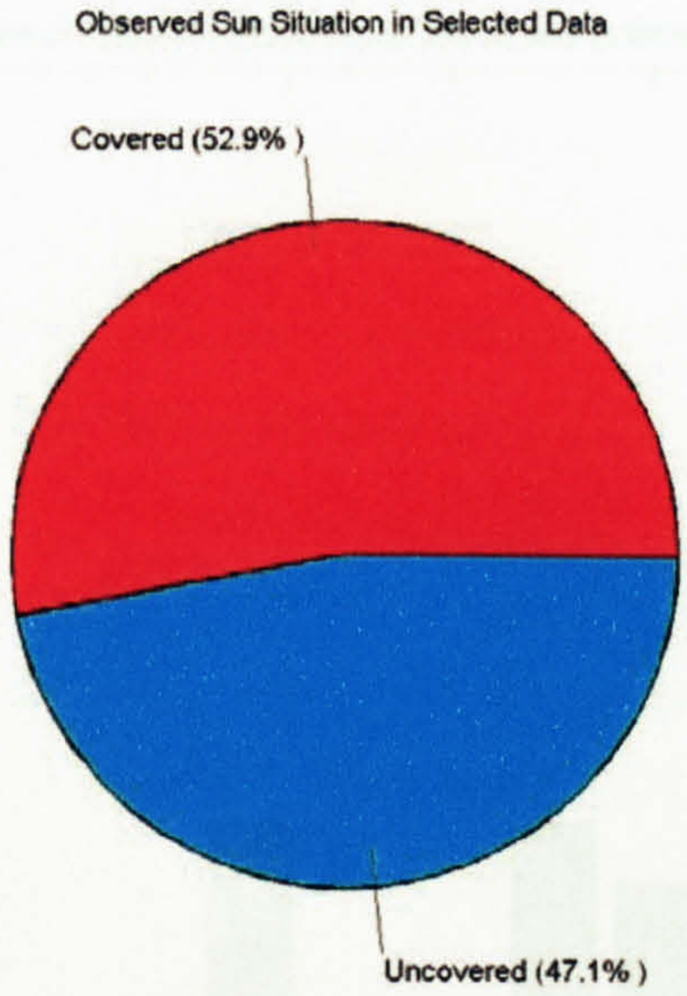

Figure 4-16 - Observed sun situation in select data

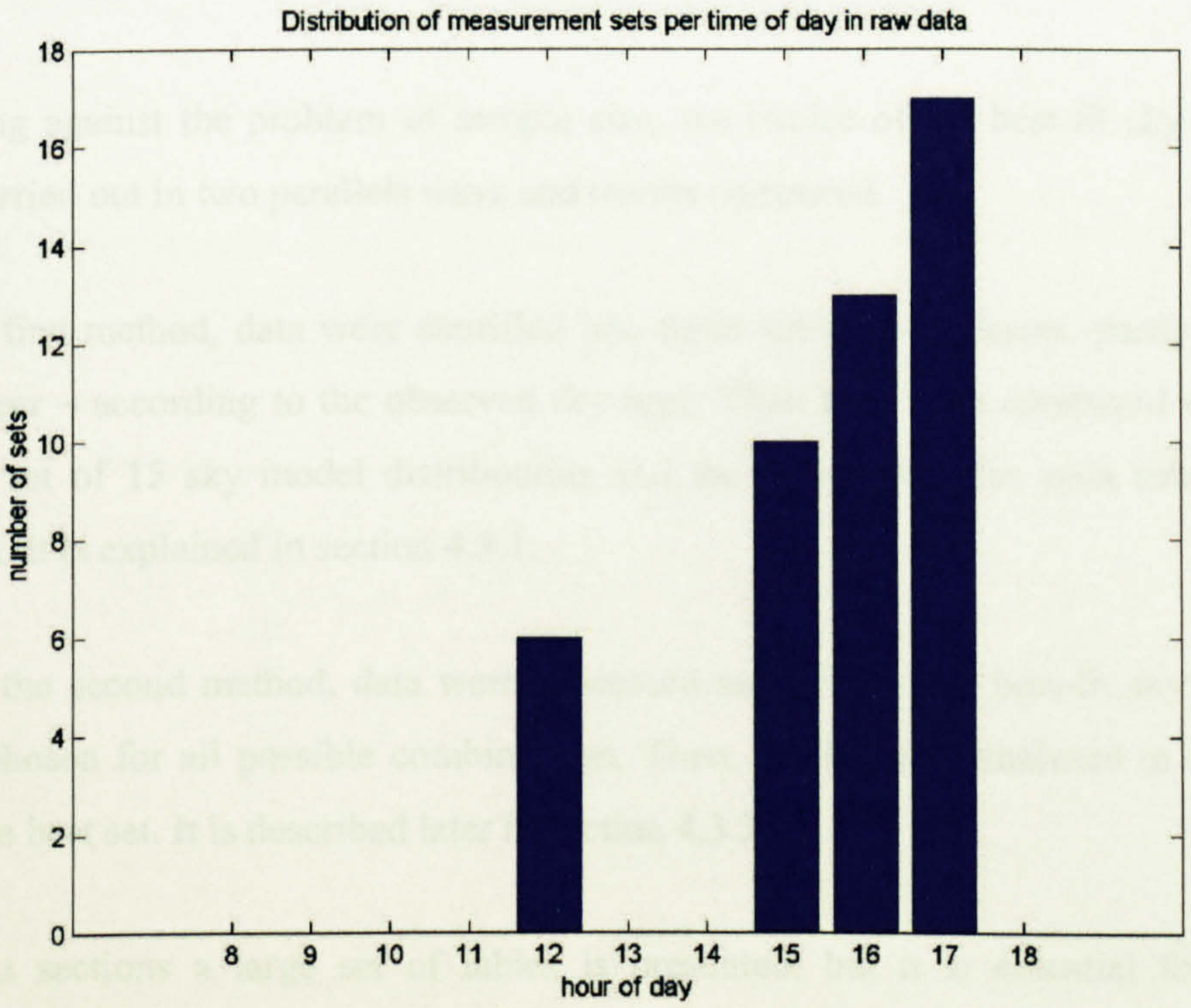

Figure 4-17 - Distribution of measurement sets per time of day in raw data

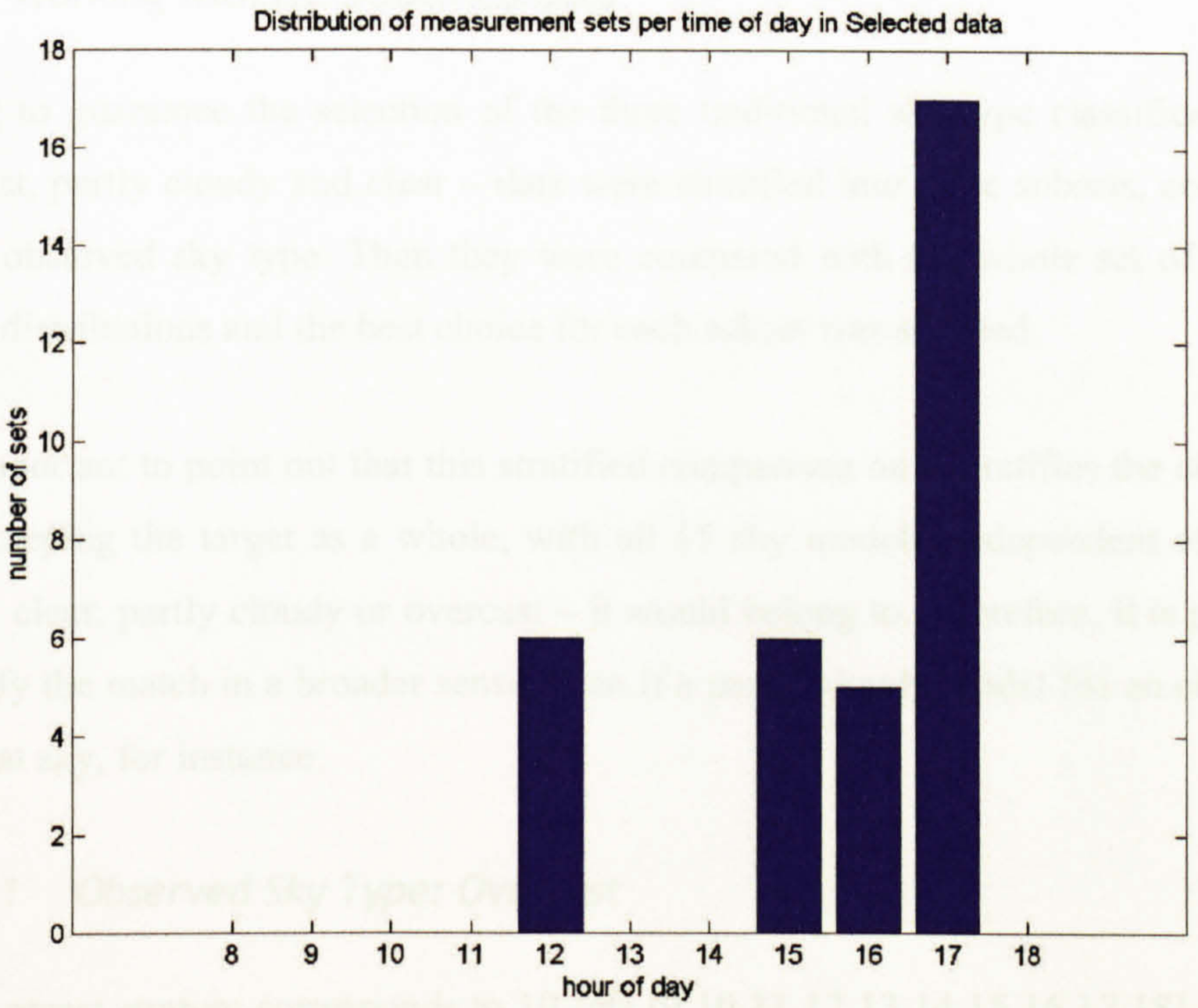

Figure 4-18 - Distribution of measurement sets per time of day in selected data

Fighting against the problem of sample size, the choice of the best-fit sky models was carried out in two parallels ways and results compared.

In the first method, data were stratified into three subsets – overcast, partly cloudy and clear – according to the observed sky type. Then they were compared with the whole set of 15 sky model distributions and the best choice for each subset was chosen. It is explained in section 4.3.1.

Using the second method, data were processed as a whole and best-fit sky models were chosen for all possible combinations. Then, results were analysed in order to find the best set. It is described later in section 4.3.2.

In next sections a large set of tables is presented, but it is essential for better comprehension.

4.3.1 Working with the stratified data

Trying to guarantee the selection of the three traditional sky type classifications – overcast, partly cloudy and clear – data were stratified into three subsets, according to the observed sky type. Then they were compared with the whole set of 15 sky model distributions and the best choice for each subset was selected.

It is important to point out that this stratified comparison only stratifies the observed data, keeping the target as a whole, with all 15 sky models, independent of which class – clear, partly cloudy or overcast – it would belong to. Therefore, it is possible to verify the match in a broader sense, even if a partly cloudy model fits an observed overcast sky, for instance.

4.3.1.1 Observed Sky Type: Overcast

The overcast stratum corresponds to 10 sets [9 10 11 12 13 14 15 16 17 18] of data. First each set was analysed for the whole 15 sky models and results of the best fit is shown in Table 4-1. The number of sky model is described in Table D-1 in Appendix D.

Table 4-1 - Sky Chosen in each set. Stratum: overcast

Set	Sky Chosen	RMS error (cd/m^2)
7	5	0.248
8	5	0.203
9	5	0.214
10	3	0.165
11	8	1.315
12	2	0.888
13	1	0.095
14	5	0.927
15	5	0.749
16	5	1.020

Following, data were summarised, in Table 4-2, giving number of choices, cumulative and weighted RMS error calculated for every sky model type.

Table 4-2 - Sky Choice Summary by number of choices - stratum: overcast

Sky	Number of Choices	Cumulative RMS error for chosen set (cd/m²)	Weighted RMS error (cd/m²)
1	1	0.095	0.095
2	1	0.888	0.888
3	1	0.165	0.165
4	0	0.000	0.000
5	6	3.363	0.560
6	0	0.000	0.000
7	0	0.000	0.000
8	1	1.315	1.315
9	0	0.000	0.000
10	0	0.000	0.000
11	0	0.000	0.000
12	0	0.000	0.000
13	0	0.000	0.000
14	0	0.000	0.000
15	0	0.000	0.000

Results shown in Table 4-2 suggest the sky model 5, the Uniform Sky, would be the best choice for overcast stratum, since it was chosen 60% of sets. Another information given by that table is that only one set (number 8) has selected a sky model outside the overcast options (sky models 1 to 5).

Although this summary may express a positive view of the data, one question arises, what if one sky model has not been so accepted, but on the other hand has a good performance in most of the sets? Also, it was possible to see that sky model 1 was chosen just once but had the best weighted RMS error. In this case, since sky 5 was chosen six times, it would be easy to choose, but again a question: what if the number of choices was not that different?

To answer the questions above, another analysis was done. The summary, shown in Table 4-3, accumulates the RMS error for the whole 15 skies for each set of data, then when the best choice given before on Table 4-1 was in a very close situation it will be reflect now in the results. Also, it would be possible to see the performance for every sky type, even between those that was never chosen.

Table 4-3 - Sky Choice Summary by cumulative RMS error - stratum: overcast

Sky	Cumulative RMS error (cd/m²)	Weighted RMS error (cd/m²)
1	14.567	1.457
2	14.095	1.410
3	9.028	0.903
4	9.280	0.928
5	7.270	0.727
6	8.238	0.824
7	10.779	1.078
8	15.815	1.582
9	16.787	1.679
10	24.787	2.479
11	37.279	3.728
12	73.032	7.303
13	99.574	9.957
14	214.326	21.433
15	277.473	27.747

For the overcast stratum, coincidently the previous best choice, sky 5, was confirmed. However, the difference between sky model 5 and sky model 6, which is a partly cloudy sky, was only about 13%. Now it would be patent that clear sky models (11-15) cannot best fit for the overcast stratum, as difference between sky 5 and sky 11, the best clear sky model, goes to 412%.

4.3.1.2 Observed Sky Type: Partly Cloudy

The partly cloudy stratum corresponds to 18 sets of data [3:8 19:30]. The analysis was done with the same method previously described for overcast stratum. Table 4-4 shows the results of the best-fit sky model for each set. The number of sky model is described in Table D-1 in Appendix D.

Table 4-5 summarises data by number of choices for partly cloudy stratum. Now, the best choice is between skies type 1 and 5, with three choices per each. The final choice can be decided by the weighted RMS error, which leads again to sky model 5. It is important to indicate that both skies are in sub-set of overcast skies models, while the stratum analysed represents the observed partly cloudy skies.

Table 4-4 - Sky Chosen in each set. Stratum: Partly cloudy

Set	Sky Chosen	RMS error (cd/m²)
1	10	1.429
2	5	1.471
3	9	0.760
4	2	0.091
5	13	1.434
6	2	0.914
17	5	0.334
18	3	0.206
19	5	0.364
20	1	0.891
21	1	1.066
22	1	3.083
23	15	2.392
24	15	1.298
25	14	1.887
26	13	4.627
27	11	3.697
28	9	4.302

Table 4-5 - Sky Choice Summary by number of choices - stratum: partly cloudy

Sky	Number of Choices	Cumulative RMS error for chosen set (cd/m²)	Weighted RMS error (cd/m²)
1	3	5.040	1.680
2	2	1.005	0.502
3	1	0.206	0.206
4	0	0.000	0.000
5	3	2.169	0.723
6	0	0.000	0.000
7	0	0.000	0.000
8	0	0.000	0.000
9	2	5.062	2.531
10	1	1.429	1.429
11	1	3.697	3.697
12	0	0.000	0.000
13	2	6.061	3.031
14	1	1.887	1.887
15	2	3.690	1.845

When data are analysed by the cumulative RMS error, as shown in Table 4-6, the best choice goes to sky type 10, which sub-set, partly cloudy, matches with the stratum analysed. However it is possible to observe that difference between the best-

fit sky and the others are not so significant as in others strata (see Table 4-3 and Table 4-9).

Table 4-6 - Sky Choice Summary by cumulative RMS error - stratum: partly cloudy

Sky	Cumulative RMS error (cd/m²)	Weighted RMS error (cd/m²)
1	49.881	2.771
2	46.490	2.583
3	46.339	2.574
4	42.266	2.348
5	45.274	2.515
6	40.094	2.227
7	39.252	2.181
8	40.981	2.277
9	41.175	2.288
10	38.594	2.144
11	39.253	2.181
12	43.588	2.422
13	45.065	2.504
14	58.358	3.242
15	61.188	3.399

4.3.1.3 Observed Sky Type: Clear

The clear stratum corresponds to six sets of data [31:36]. The analysis was done with the same method previously described for overcast stratum. Table 4-7 shows the results of the best-fit sky model for each set. The number of sky model is described in Table D-1 in Appendix D.

Table 4-7 - Sky Chosen in each set. Stratum: Clear

Set	Sky Chosen	RMS error (cd/m²)
29	10	2.808
30	15	1.100
31	13	1.068
32	14	7.941
33	14	6.850
34	14	5.389

Table 4-8 summarises data by number of choices for clear stratum. Now, the best choice is sky 14, with 50% of choices; of note is the fact that the weighted RMS

error is higher than the others. It is important to indicate that only one set have a best-fit sky out of clear skies subset of sky models. Also, no overcast sky was pointed out.

Table 4-8 - Sky Choice Summary by number of choices - stratum: clear

Sky	Number of Choices	Cumulative RMS error for chosen set (cd/m^2)	Weighted RMS error (cd/m^2)
1	0	0.000	0.000
2	0	0.000	0.000
3	0	0.000	0.000
4	0	0.000	0.000
5	0	0.000	0.000
6	0	0.000	0.000
7	0	0.000	0.000
8	0	0.000	0.000
9	0	0.000	0.000
10	1	2.808	2.808
11	0	0.000	0.000
12	0	0.000	0.000
13	1	1.068	1.068
14	3	20.179	6.726
15	1	1.100	1.100

Table 4-9 - Sky Choice Summary by cumulative RMS error - stratum: clear

Sky	Cumulative RMS error (cd/m^2)	Weighted RMS error (cd/m^2)
1	79.756	13.293
2	73.916	12.319
3	71.965	11.994
4	64.639	10.773
5	65.940	10.990
6	57.364	9.561
7	51.468	8.578
8	47.202	7.867
9	42.914	7.152
10	36.336	6.056
11	32.244	5.374
12	28.711	4.785
13	27.515	4.586
14	25.542	4.257
15	26.170	4.362

On Table 4-9 – which summarises by cumulative RMS error – the best choice goes again to sky model type 14. Here it is possible to denote that the difference between most clear sky models is not significant, however others subsets – overcast and partly cloudy – are quite far from the best fit.

4.3.1.4 Summary

Results achieved with this method lead to the choice of three standard skies: sky 5 (uniform sky), sky 10 (partly cloudy, brighter circumsolar) and sky 14 (cloudless turbid with broader solar corona).

Moreover it was detected that observed overcast skies are more suitable to standardization than partly cloudy or clear skies. It is illustrated in Table 4-10, which condenses the weighted RMS error per stratum. It shows that overcast sky stratum has the smallest weighted RMS error and consequently could be a better fit than the others.

Table 4-10 - Weighted RMS error per stratum

Stratum	Cumulative RMS error (cd/m^2)	Number of sets	Weighted RMS error (cd/m^2)
Overcast	5.826	10	0.583
Partly cloudy	30.245	18	1.680
Clear	25.156	6	4.193

However, the data stratification needs more studies to confirm its strength, as it can be seen as an induction to favourable results. This will be done in the following section, where a new approach is proposed.

4.3.2 Working with the whole set of data

Following the analysis done in the previous section, here data are considered not stratified. Then results achieved from both methods can be compared afterwards.

Firstly data are regrouped in Table 4-11. It is an amalgamation of Table 4-1, Table 4-4 and Table 4-7.

Table 4-11 - Best-fit sky model in each set

Set	Sky	Sun	Sky Chosen	RMS error (cd/m^2)
1	II	U	10	1.429
2	II	U	5	1.471
3	II	U	9	0.760
4	II	C	2	0.091
5	II	C	13	1.434
6	II	U	2	0.914
7	I	C	5	0.248
8	I	C	5	0.203
9	I	C	5	0.214
10	I	C	3	0.165
11	I	C	8	1.315
12	I	C	2	0.888
13	I	C	1	0.095
14	I	C	5	0.927
15	I	C	5	0.749
16	I	C	5	1.020
17	II	U	5	0.334
18	II	U	3	0.206
19	II	U	5	0.364
20	II	U	1	0.891
21	II	U	1	1.066
22	II	U	1	3.083
23	II	U	15	2.392
24	II	U	15	1.298
25	II	C	14	1.887
26	II	C	13	4.627
27	II	C	11	3.697
28	II	C	9	4.302
29	III	U	10	2.808
30	III	U	15	1.100
31	III	U	13	1.068
32	III	U	14	7.941
33	III	U	14	6.850
34	III	U	14	5.389
Cumulative RMS error				61.227

This table shows the results of the best-fit sky model for each set, with its respective RMS error, which represents the smallest error among the 15 sky models tested for the set. The second column shows the observed sky type stratum, where I is overcast, II corresponds to partly cloudy and III means clear sky. The third column shows if sun is covered (C) or uncovered (U). It is important again to stress that several sets do not match the observed sky type stratum with the subset for the best-fit sky

model, like set number 2, with an observed party cloudy sky and best-fit sky model number 5, Uniform Sky.

Table 4-12 summarises sky choice by number of choices. It is possible to see that sky model 5 is the most accepted with nine choices. But, as was explained before, this table does not take into account the situation created by a hypothetical runner-up with small difference to the best choice for most of the sets. One sky can fit several sets very well and still be quite far from the others, while another has an average performance.

Table 4-12 - Sky Choice Summary by number of choices

Sky	Number of Choices	Cumulative RMS error for chosen set (cd/m^2)	Weighted RMS error (cd/m^2)
1	4	5.135	1.284
2	3	1.893	0.631
3	2	0.371	0.186
4	0	0.000	0.000
5	9	5.531	0.615
6	0	0.000	0.000
7	0	0.000	0.000
8	1	1.315	1.315
9	2	5.062	2.531
10	2	4.237	2.118
11	1	3.697	3.697
12	0	0.000	0.000
13	3	7.129	2.376
14	4	22.067	5.517
15	3	4.790	1.597

To deal with this issue, data are analysed in Table 4-13 by the Weighted RMS error for the whole 15 skies for each set of data. Now it is possible to see the performance for every sky type, even those that were never chosen in Table 4-12.

Table 4-13 - Sky Choice Summary by cumulative RMS error

Sky	Cumulative RMS error (cd/m^2)	Weighted RMS error (cd/m^2)
1	144.205	4.241
2	134.501	3.956
3	127.331	3.745
4	116.185	3.417
5	118.484	3.485
6	105.696	3.109
7	101.498	2.985
8	103.999	3.059
9	100.876	2.967
10	99.717	2.933
11	108.776	3.199
12	145.332	4.274
13	172.154	5.063
14	298.226	8.771
15	364.832	10.730

Then Table 4-13 is sorted in function of the weighted RMS error in Table 4-14, which gives a better view of the results. In this table, it is possible to see the sky model number 10 as the best choice for the whole set of data in the experimental research, if only one sky should be chosen. However it is also worth noting that the difference between the first and the second choice is little more than 1%. This fact points to finding a better form of analysis. However, before that can be done, some other comments should be made with reference to the fact of the best five choices being in partly cloudy sky subset. This probably occurs because the partly cloudy sky models reflect an average sky between clear and overcast, and consequently the difference between the whole set of data to a partly cloudy model would be smaller than to one type from an extreme subset, either overcast or clear sky subset. In addition clear sky models seem less compatible to be chosen as the best choice for the whole set, as 80% of them came to the last four position, and the best of them, sky number 11, get only the sixth position. Moreover, sky number 5, which occurred more frequently with more than 26% of the preferences, as seen on Table 4-12, now has been put as the eighth option. This is predictable because, although it can fit most of the overcast and some of the partly cloudy skies, it is extremely far from a clear sky luminance distribution generating a greater error.

Then, one key question is still looking for an answer: what is the best representation for the real sky in Maceió? From Table 4-14, it was possible to observe that the difference between the first choices is not significant, as was commented at the beginning of the previous paragraph. It suggests that choosing only one sky is not the best method to answer the question. The obvious next approach is just increasing the number of skies chosen. But then two new questions arise: the first one is 'How many skies should be selected?' and the second one, 'After choosing one best sky model, how to choose the others?'

Table 4-14- Sky Choice Summary by weighted RMS error - in order of error

Order	Sky	Weighted RMS error (cd/m^2)
1st	10	2.933
2nd	9	2.967
3rd	7	2.985
4th	8	3.059
5th	6	3.109
6th	11	3.199
7th	4	3.417
8th	5	3.485
9th	3	3.745
10th	2	3.956
11th	1	4.241
12th	12	4.274
13th	13	5.063
14th	14	8.771
15th	15	10.730

Table 4-15 is a primary attempt at answering those questions. From Table 4-14, it was selected in a sequence, one more sky and the weighted RMS error was assessed. It was done until the whole set of 15 skies was used. Two more columns were aggregated to express the reduction of error after increasing the number of skies chosen. The fourth column shows the percentage of error reduced with this addition, in relation to the best choice, sky number 10; and the fifth column shows the reduction in relation to the previous choice of skies. To have another view of the error reduction after this method is applied, results are also shown in Figure 4-19, as a line graph. There the Y-axis represents de weighted RMS error and the X-axis the number of skies chosen.

Table 4-15 - Weighted RMS error after increment of chosen skies by method 1

Qt	Chosen Skies	Weighted RMS error (cd/m^2)	% error reduction from best one	% error reduction from previous
01	10	2.933		
02	10 9	2.639	10.0	10.0
03	10 9 7	2.388	18.6	9.5
04	10 9 7 8	2.348	19.9	1.7
05	10 9 7 8 6	2.264	22.8	3.6
06	10 9 7 8 6 11	2.134	27.2	5.7
07	10 9 7 8 6 11 4	2.122	27.7	0.6
08	10 9 7 8 6 11 4 5	2.045	30.3	3.6
09	10 9 7 8 6 11 4 5 3	2.038	30.5	0.3
10	10 9 7 8 6 11 4 5 3 2	2.029	30.8	0.4
11	10 9 7 8 6 11 4 5 3 2 1	2.025	31.0	0.2
12	10 9 7 8 6 11 4 5 3 2 1 12	1.920	34.5	5.2
13	10 9 7 8 6 11 4 5 3 2 1 12 13	1.866	36.4	2.8
14	10 9 7 8 6 11 4 5 3 2 1 12 13 14	1.805	38.5	3.3
15	10 9 7 8 6 11 4 5 3 2 1 12 13 14 15	1.801	38.6	0.2

Although the previous method seems an advance in relation to choosing just one sky, it does not give the impression of answering both questions put forward. From Figure 4-19 it is not likely to establish how many skies would be a good choice, as error reduction with the increment in the number of skies chosen is not significant in any step. Moreover, as seen in the fifth column of Table 4-15, the reduction factor does not decrease as the number of skies chosen increase, as would be expected. It should occur due to one reason that was pointed out previously. Since the first five skies models chosen are from the same subset, i.e. partly cloudy, it seems that has no difference increasing the number of skies chosen with another from the same subset, as different observed skies would not be best fit, with the exclusion of the others subset.

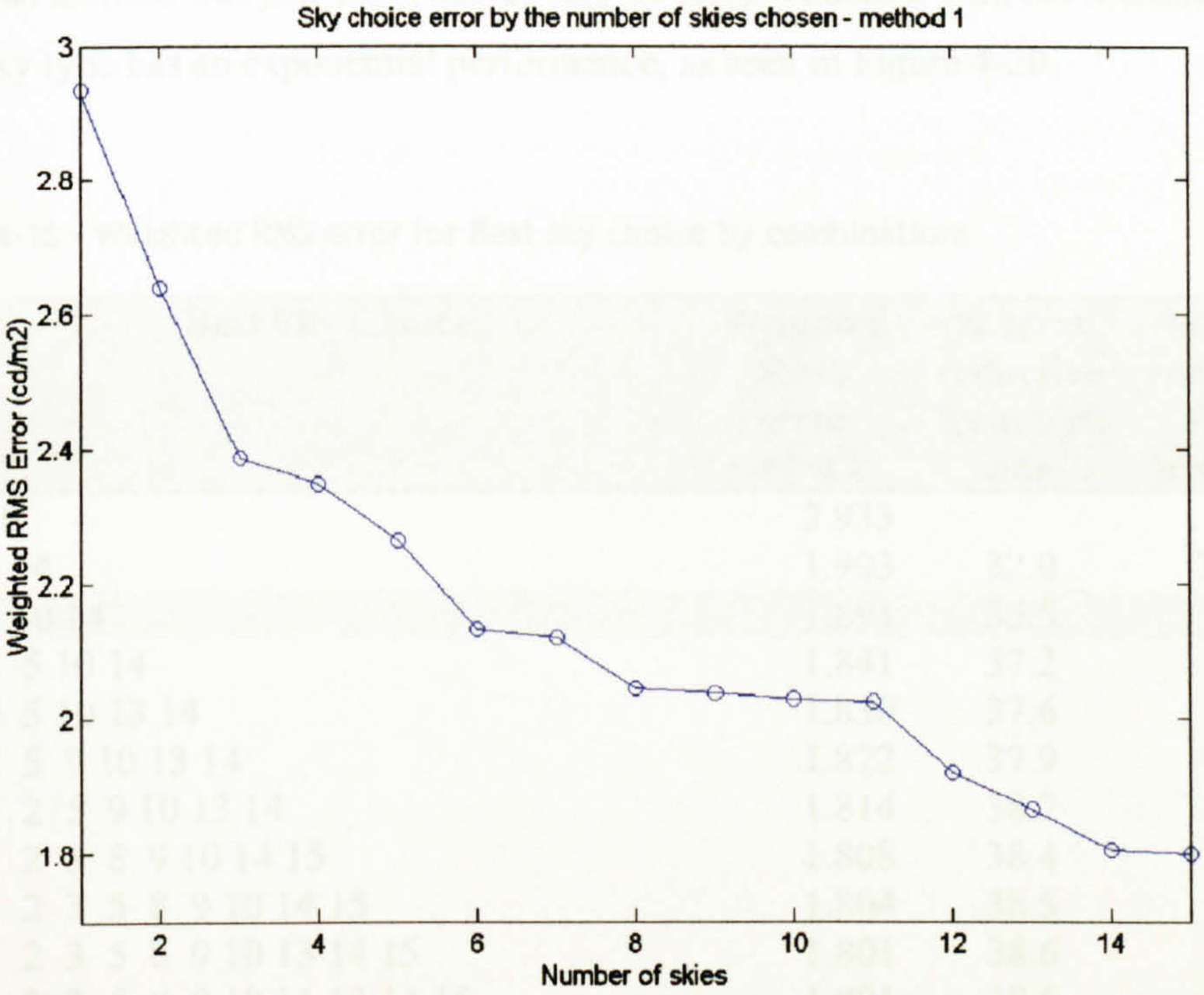

Figure 4-19 - Sky choice error by the number of skies chosen - method 1

Therefore, if the previous method cannot answer the question, what could be the solution? First it is important to clarify that if only one sky is chosen as the best fit for the whole sets of data, this sky would be one in the sub-set of partly cloudy skies, and for the available data, the sky number 10 is the best-fit, although difference for the second choice, sky 9, is only about 1%.

Then, how to choose the next sky? The answer can be found by doing the calculations of RMS error for the whole combination of 15 skies by the number of skies that would be tested. For instance, for two skies, there would be 105 combinations. Using the computer program developed for this thesis, results were found for the complete possibility of combinations of sky choices.

Table 4-16 shows that this new method can answer how many skies should be chosen. Now, the error reduction with the second sky addition is 32%, while with the

previous method was just 10%. Moreover, the error reduction with the increment of a new sky type has an exponential performance, as seen in Figure 4-20.

Table 4-16 - Weighted RMS error for Best sky choice by combinations

Qt	Best Sky Choice	Weighted RMS error (cd/m^2)	% error reduction from best one	% error reduction from previous
01	10	2.933		
02	5 14	1.993	32.0	32.0
03	5 10 14	1.891	35.5	5.1
04	2 5 10 14	1.841	37.2	2.6
05	2 5 10 13 14	1.830	37.6	0.6
06	2 5 9 10 13 14	1.822	37.9	0.4
07	1 2 5 9 10 13 14	1.814	38.2	0.4
08	1 2 5 8 9 10 14 15	1.808	38.4	0.3
09	1 2 3 5 8 9 10 14 15	1.804	38.5	0.2
10	1 2 3 5 8 9 10 13 14 15	1.801	38.6	0.2
11	1 2 3 5 8 9 10 11 13 14 15	1.801	38.6	0.0
12	1 2 3 4 5 8 9 10 11 13 14 15	1.801	38.6	0.0
13	1 2 3 4 5 6 8 9 10 11 13 14 15	1.801	38.6	0.0
14	1 2 3 4 5 6 7 8 9 10 11 13 14 15	1.801	38.6	0.0
15	1 2 3 4 5 6 7 8 9 10 11 12 13 14 15	1.801	38.6	0.0

Then the reduction factor decreases after increasing the number of skies chosen. The possibility of an answer to the question of how many skies should be chosen now emerges. It is clear that two skies are better than one for best fit to the real sky with the 15 sky models proposed by CIE. But is it necessary to have three, four or more skies? Defining 5% as a significant reduction for increment the number of skies, then the choice of three skies is the answer. However, more arguments can be put forward. The best choice of one sky is sky number 10, from partly cloudy subset. When combination of two skies is done, the best choice goes to skies 5 and 14, from overcast and clear skies subsets, respectively. The sky 10 is taken out. Why? For the same reason a partly cloudy sky fits better for the choice of one. Now the clear and the overcast skies are closer to their pairs, and one observed partly cloudy sky could be fitted either with overcast or clear sky configuration. However, when the third sky is introduced, the situation improves. The set of three skies – 5, 10 and 14 – represents all three subsets of overcast, partly cloudy and clear skies.

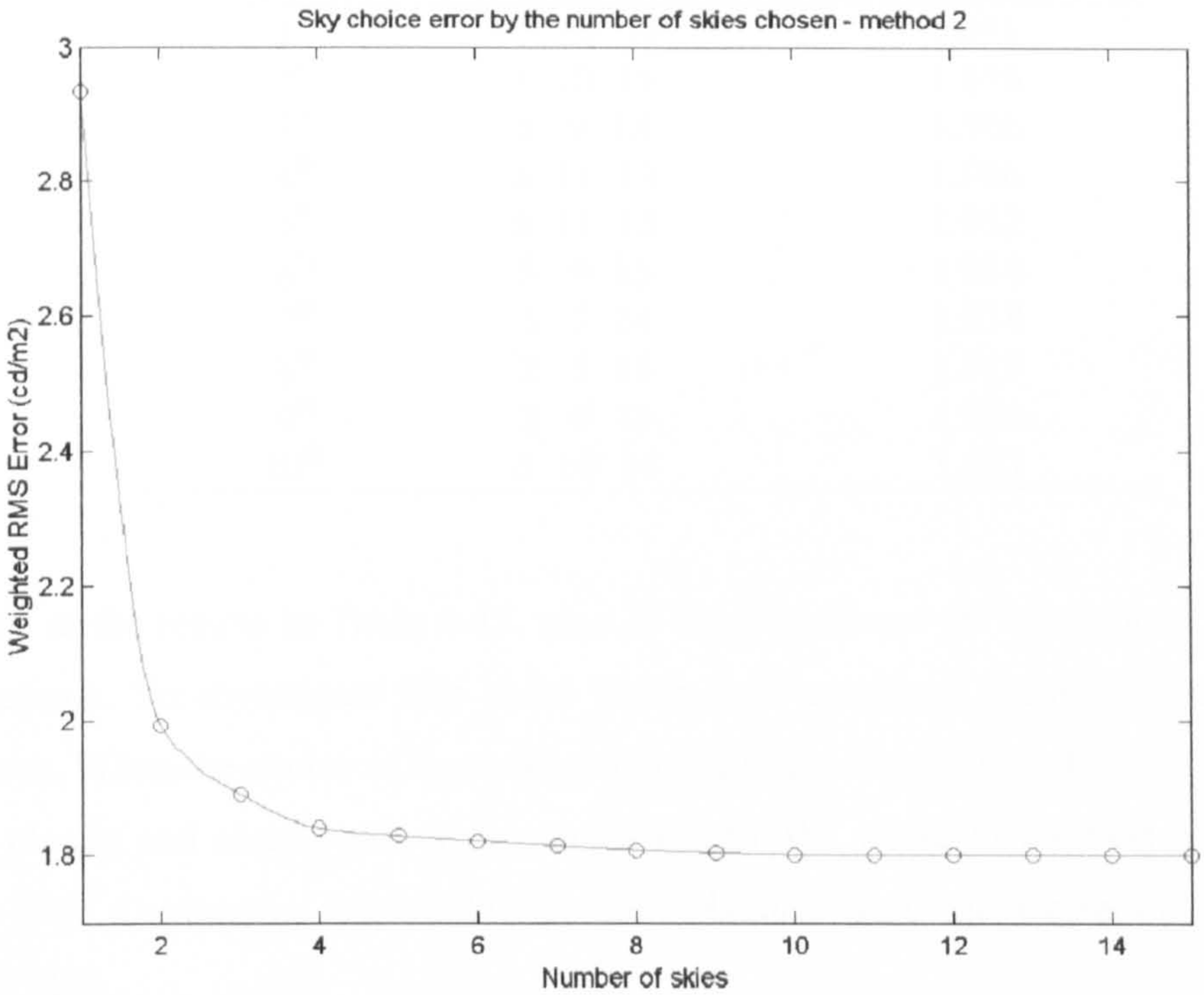

Figure 4-20 - Sky choice error by the number of skies chosen - method 2

If a fourth sky is chosen, sky number 2, the improvement is not significant. The error reduction is only 2.6% and does not compensate. Sky number 5 already represents its subset. When the increment continues, as expected, its implication reduces still more.

So far, the question of how many skies best-fit Maceió sky behaviour can be answered with three skies. However the question of which ones, that was answered with skies 5, 10 and 14, can arise another issue: Are those skies chosen significantly better than any other combination of three skies? The solution can be found in Table 4-17, which shows the 10 best choices of three skies.

As shown there, the difference between the first and the fourth choice is less than 1%, which can generate doubt in the previous choice. It is possible to say that choosing sky 14 or 15 in the previous selected group has no significant difference. The same as change sky 10 by sky 9 or 11.

Table 4-17 - Best sky choice of three skies

Order	Best Sky Choice - 3 skies	Weighted RMS error (cd/m^2)
1st	5 10 14	1.891
2nd	5 10 15	1.896
3rd	5 9 14	1.906
4th	5 11 14	1.906
5th	5 11 15	1.912
6th	5 9 15	1.914
7th	5 7 14	1.918
8th	2 5 14	1.919
9th	3 9 14	1.923
10th	3 10 14	1.927

Looking at the results in Table 4-17, nine of them represent all three subset of sky distributions. To investigate this point Table 4-18 compares results for extreme situations. When the choice of three skies represents one from each subset – overcast, partly cloudy and clear – the error reduction from the worse to the best choice is about 17%. Comparing the whole set, the reduction from the worse to the best reaches 62%.

Table 4-18 - Typical error values for combinations of three skies

	Sky numbers	Weighted RMS error (cd/m^2)
Overall best choice	5 10 14	1.9
Worse of 3 skies from different subsets	2 8 11	2.3
Overall worse choice	13 14 15	5.0

4.4 Conclusion

This survey was made with a small sample of skies taken over a short period. The purpose was to get realistic data for the model. However, two clear conclusions emerge; they are based on similar outcomes from the two different methods and are also strongly supported by the literature for other warm-humid climates [3, 6, 7].

Firstly, little reduction in RMS error was found when the number of skies selected to fit the data was increased beyond three. Comparison with published results suggests that a set of about three skies may be generally sufficient to define a daylight climate.

Secondly the three best-fit skies were a combination of the uniform sky (CIE Sky 5), the partly cloudy with brighter circumsolar (CIE Sky 10) and the cloudless turbid with broader solar corona (CIE Sky 14). However, provided that the selection consisted of one sky from each subset – an overcast, a partly cloudy and a clear distribution – it was found that the actual choice of sky had only small effect on the error level. There may therefore be a general result: the set of standard skies that best characterise a climate consists of three sky types from distinct subset.

It is also important to point out that the choice of those three sky models – 5 , 10 and 14 – was based only on restricted data, and cannot necessarily represent the definitive choice for the site. For that, data sample should be more significant, be collected in different months of the year, time of the day and gather more sky luminance measurements at the same time.

References

1. Tregenza, P. and S. Sharples, *Daylight algorithms*, University of Sheffield: Sheffield, 1993.

2. Kittler, R., *Luminance distribution characteristics of homogeneous skies: a measurement and prediction strategy*. Lighting Research and Technology, **17**(4): p. 183-188, 1985.

3. Tregenza, P. R., *Standard skies for maritime climates*. Lighting Research and Technology, **31**(3): p. 97-106, 1999.

4. Barnett, V. and T. Lewis, *Outliers in statistical data*. 3rd ed. Chichester: John Wiley & Sons, 1994.

5. Neuilly, M., *Modelling and Estimation of Measurement Errors*. Paris: Intercept, 1999.

6. Lam, K. P., *et al.*, *Mapping of the sky luminance distribution and computational prediction of daylighting performance in Singapore*. Singapore: National University of Singapore, 1997.

7. Ullah, M. B. and J. K. Tan. *Daylight models - Singapore sky*. in *Tropical daylight and buildings 2002*. Singapore: NUS - National University of Singapore, 2002.

Part II

Tropical Daylighting Technique

The second part of the thesis has an introductory consideration about possible approaches to suitable techniques for tropical daylighting and why a new computer code was developed. Following it is divided into three chapters. Chapter 5 presents a review of the Monte Carlo method with ray tracing and how it is employed in this thesis. Chapter 6 discusses the daylight coefficients concept, presents equations suitable for use in a daylighting simulation program, and shows how it interrelates with ray tracing and Monte Carlo methods. Finally Chapter 7 introduces the computer simulation tool developed for this thesis.

Introduction

It was clear from the outset of the project that predictions of daylight illuminance and luminance would be required, possibly for complex building geometries. Four approaches were considered: (i) measurements in physical scale models; (ii) the use of standard software such as Lightscape or Radiance; (iii) specifically written software using primarily ray-tracing and Monte Carlo procedures; (iv) specifically written software based primarily on radiosity algorithms.

Four main criteria were used in making the choice: (i) the need to calculate with non-standard skies; (ii) flexibility in modifying building form and materials, in particular with complex geometries that may extend to the surrounding of the building; (iii) the possibility of developing and testing new algorithms; and (iv) the time required for learning or writing programs, and for entering and computing experimental cases.

Table II-I summarises the analysis. It was concluded that the most appropriate technique was the use of purpose-written software based on MC/ray-tracing algorithms but using a standard scientific package rather than generating code in a general programming language. This decision was reinforced by the fact that other researchers in the department had already produced some applicable code in MATLAB and that further work on lighting in this software environment would be mutually beneficial.

Table II-1 - Comparing possible approaches with tropical daylighting requirements

Requirements	Possible approaches			
	Physical Model	Standard software	Monte Carlo and Ray tracing	Radiosity
Non-standard skies	*	*	+	*
Numerical methods	-	+	+	+
Test of different algorithms	-	-	+	-
Speed	+	+	-	*

where (+) means a strong match, (*) partial match, and (-) weak or no match.

Chapter 5 Monte Carlo and ray tracing techniques

5.1 Introduction

The Monte Carlo method and ray tracing technique have been considered important components in interior lighting calculation. This chapter discusses the statistical principles of the Monte Carlo method and its relation with daylighting calculation. The ray tracing approach is also considered, being interrelated with the Monte Carlo method. Finally, the chapter presents the procedures proposed in this thesis for using the Monte Carlo method and ray tracing in a lighting simulation program that would be suitable for tropical daylighting.

5.2 The Monte Carlo method concept

The Monte Carlo method is a statistical numerical approach to the solution of multiple integrals as expressed, in a general way, in Equation (5.1).

$$I(\xi_1,\xi_2,\ldots,\xi_n) = \int_0^1\int_0^1\ldots\int_0^1 w(\xi_1,\xi_2,\ldots,\xi_n)dP_1(\xi_1)dP_2(\xi_2)\ldots dP_k(\xi_k) \qquad (5.1)$$

where $\xi_1,\xi_2,\ldots,\xi_k$ are related to random variables and $P_1(\xi_1)$, $P_2(\xi_2),\ldots,$ $P_k(\xi_k)$ are the corresponding cumulative distribution or probability distribution functions. If η_k is a random variable, then the probability is expressed by Equation (5.2).

$$P_k(\xi_k) = probability(\eta_k < \xi_k) \qquad (5.2)$$

The Monte Carlo method obtains approximate solutions by using random numbers after the conversion of a problem under determinism to a stochastic matter. It is based on the following premise: if the probability of occurrence of each separate event in a sequence of events is known, then it is possible to determine the probability with which the entire sequence of events will occur.

The classical utilisation of this method is *the random walk*, which is based on a *Markov chain*. This is a series of events in sequence where the probability of each following event has no influence by previous events [1].

As it evolved in several ways, satisfying different objectives, it is possible to say that the term Monte Carlo method embodies a series of loosely related techniques.

5.2.1 Strengths and drawbacks

The Monte Carlo approach provides a means of calculation when analytical methods are impossible or computationally expensive. It is particularly effective – when compared to deterministic methods – to treat multi-dimensional problems such as radiation exchange in a complex geometry [2].

However, the disadvantage is that the required computation time can be excessive. In general, the statistical uncertainty is inversely proportional to the square root of the sample size. Therefore, the method depends on the finding of efficient algorithms that optimise the use of loops and exclude superfluous processing [3].

5.2.2 Random numbers and pseudo-random numbers

The numerical evaluation of probability functions – fundamental to Monte Carlo solutions – requires substitution of random variables by numerical quantities, termed random numbers. Although the production of true random numbers is possible, this process is not convenient for computer-based numerical computation, as it requires storage space proportional to the quantity of random numbers required. The pseudo-random numbers concept solves this problem.

There are several ways of generating them. Two of them are described here. One that was commonly used is based on equation (5.3).

$$X_k = (aX_{k-1} + c)(\mathrm{mod}\, b) \tag{5.3}$$

where *a*, *b* and *c* are three selected integers, and X_0 is the seed number. Another method is to take the low-order 36 bits of the product $R_{n-1}K$, where $K=5^{15}$ and R_{n-1} is the previously computed random number.

Pseudo-random numbers routines are easy to generate by computers. However, they are not real random numbers. It is necessary to evaluate if the sequence repeats itself and, if so, after how many numbers. The program developed in this thesis is written in Matlab, a well-known computer language for scientific proposals. The pseudo-random numbers produced by Matlab have the sequence of numbers produced by the state of the generator. This generator can create all the floating-point numbers in the closed interval $[2^{-53}, 1-2^{-53}]$. Theoretically it can generate over 2^{1492} values before repeating itself [4].

A random number is usually given as a value in the closed interval [0;1], and there is an even probability that it will lie within the interval. However, variables do not necessarily drop within this range nor are they necessarily uniformly distributed. In this way, random numbers should be scaled to process calculation by the probability distribution that expresses the physical process.

5.2.3 Weighted particle values

A simple way to process the method is by giving weight for particles. Each particle starts with weight equals to one, and every time it finds a surface, the weighting number of the particle is reduced by multiplying the previous value by the appropriate reflectance or transmittance. It happens repeatedly until the particle leaves the building (see section 5.5.4.4) or is considered absorbed by surface, as discussed in section 5.5.4.3. Then the simulation re-starts with a new particle.

5.2.4 Evaluation of error

As a statistical approach, the Monte Carlo method requires a probability-based inference for its results. Results achieved from this approach will vary around a mean value which accuracy will increase with the number of calculated values.

To establish the accuracy of the solutions one of several tests can be applied. Siegel [3] discusses this point using the central limit theorem and the relations governing normal probability distribution. When the samples do not originate from a single source, as in most daylighting calculation, Siegel suggests subdividing the calculation of the desired statistical mean result into a group of N submeans, and then applying the central limit theorem. Thus error, δ, can be assessed by standard deviation of the mean, σ, as shown in equation (5.4).

$$\delta = \frac{f\sigma}{\sqrt{N}} \tag{5.4}$$

where, f is a factor related to the confidence level (cl), being 1 for 68%, 2 for about 95% and 3 for 99.7% of confidence level.

5.3 Ray tracing technique

The ray tracing technique follows the path of a ray between surfaces. Initially the approach was developed in the field of computer graphics, as it can deal with complex scenes. Later, it was widespread and lighting calculation has become a field where it can be properly applied.

The ray tracing method can be classified regarding its direction, as forward or backward (see Section 5.3.2), and regarding its mathematical approach, as deterministic or stochastic (see Section 5.3.3).

5.3.1 Strengths and drawbacks

The main advantage of the ray tracing approach is the possibility of giving simple theoretical solutions for complex geometries, this is in contrast to most other techniques that can generally assess only simple room geometry.

Another strength is that collision events, such as reflection and transmission, cannot be restricted to diffuse phenomenon. Specular reflection and regular transmission

simulation are straightforward, diffuse and composite events have no restriction to be simulated.

However, for diffuse and composite phenomenon ray tracing computation time can be expensive. To improve performance a more sophisticated numerical algorithm should be considered to work together. The Monte Carlo method can fill this gap.

As seen above, ray tracing can simulate the natural behaviour of light with significant accuracy. However, this accuracy varies in relation to the chosen approach. Moreover, ray tracing actually does not take into account light diffracted around corners when object details are very small and near the wavelength of light. However this is not significant for general daylighting calculations.

5.3.2 Forward and backward ray tracing

Ward [5], introducing ray tracing as a lighting calculation technique, says "ray-tracing is a method for computing luminance by following light backwards from the point of measurement to the source(s)", however lighting calculations can be done, by reciprocity, with either backward or forward ray tracing system.

Forward and backward are opposite ways of ray tracing. While the forward approach follows the ray from its source to the target, as in nature, the backward method makes it in reverse, i.e. from target to source.

The forward approach can be view-independent, whereas backward ray tracing is always view-dependent. This is the major disadvantage of backward ray tracing, as new computation should be done for each point of view.

Even though the backward approach seems outlandish, it carries some improvements in comparison to forward ray tracing with regard to computational time. When the incident light source is a surface (as most direct and indirect natural light sources are considered, excepting the sun) and the target is a point, the backward method can be much more economical, in comparison to the forward approach.

5.3.3 Deterministic and stochastic ray tracing

The difference between deterministic and stochastic ray tracing is that while the deterministic algorithm can get the same result every time it is repeated, stochastic ray tracing gives slightly different outputs for each processing. Although this can be frustrating, it is the way that light performs in nature. If necessary – for debugging the process, for instance – the state of the pseudo random numbers generator can be reset every run spawning the same sequence of random numbers and consequently the same result.

When the aim is to assess direct illuminance at a point, i.e. there is no diffuse reflected light, and consequently the ray path is straightforward, the deterministic method is more suitable.

These topics are considered in detail in the next Chapter in Section 6.5.1, where they are related to the daylight coefficients approach.

5.4 Monte Carlo method in lighting calculation

Widely used in flux transfer calculation, the Monte Carlo method was rarely used in interior lighting calculation until about twenty years ago. In the 1980's, the advent of specific techniques [6, 7] and the availability of faster computers changed that. Several papers have been published since [8-13]. In architectural lighting, the major application of the Monte Carlo method is the calculation of the interreflected component in complex room geometry and when surface reflectances are not necessarily perfectly diffuse (non-Lambertian). In these cases, it can be considered more efficient than flux transfer approach.

On the other hand, since this is a stochastic algorithm when repeated it will normally give somewhat different results. Nonetheless, it is the way light exists in the natural world, where photons are bouncing about randomly. It is only their vast number that gives light the appearance of stability at any given point [14].

5.5 How the Monte Carlo method is used in this thesis

This Section describes the specific techniques used in this work to adapt the general principles of the Monte Carlo method into a daylighting analysis computer program with particular reference to the tropics.

5.5.1 Choosing between backward and forward ray tracing

If the source of light is considered a point source, the forward ray tracing approach may be applied properly. On the other hand if the goal is to assess illuminance at a point forward technique needs to have an approximation by creating a surface around the point to get particles falling in, since the probability of a ray reaching a point is zero. However, even with this trick it can be extremely inefficient computationally since most of the particles emitted will never reach the target. There are some techniques to reduce this weakness, such as restricting the direction of rays emitted from source, however complexities arise when the source is not a point but a surface, for example the sky, walls and ground.

Viewed in this way, the backward ray tracing approach appears more suitable, mainly when view independence is not required. It is straightforward to assess illuminance at a point. When the goal is a mean illuminance surface, a grid of random points may be used efficiently. It is also important to point out that there is no significant waste of particles, in comparison with forward method. All particles 'emitted from the target' will reach a source of light, either directly or indirectly. Thus, the backward method appears more efficient computationally than the forward approach for the purposes of this work.

5.5.2 Inter-reflected and direct components

The Monte Carlo method is quite suitable for inter-reflected light, however to assess the direct component it requires a great number of particles to be reasonably accurate. This occurs as the particles emitted are largely wasted. A solution could be found restricting the direction of rays toward the target. However, in this case a deterministic ray tracing is more convenient, as discussed in Section 5.3.3.

5.5.3 The geometric framework

This work uses three axis systems to specify the location of a point in space: general coordinates, local surface coordinates and sky coordinates, as proposed by Tregenza and Sharples [15].

5.5.3.1 General coordinates

- Point

A point, A, may be described by the Cartesian form (x,y,z) or with spherical coordinates (r,ϕ,θ), described in Figure 5-1.

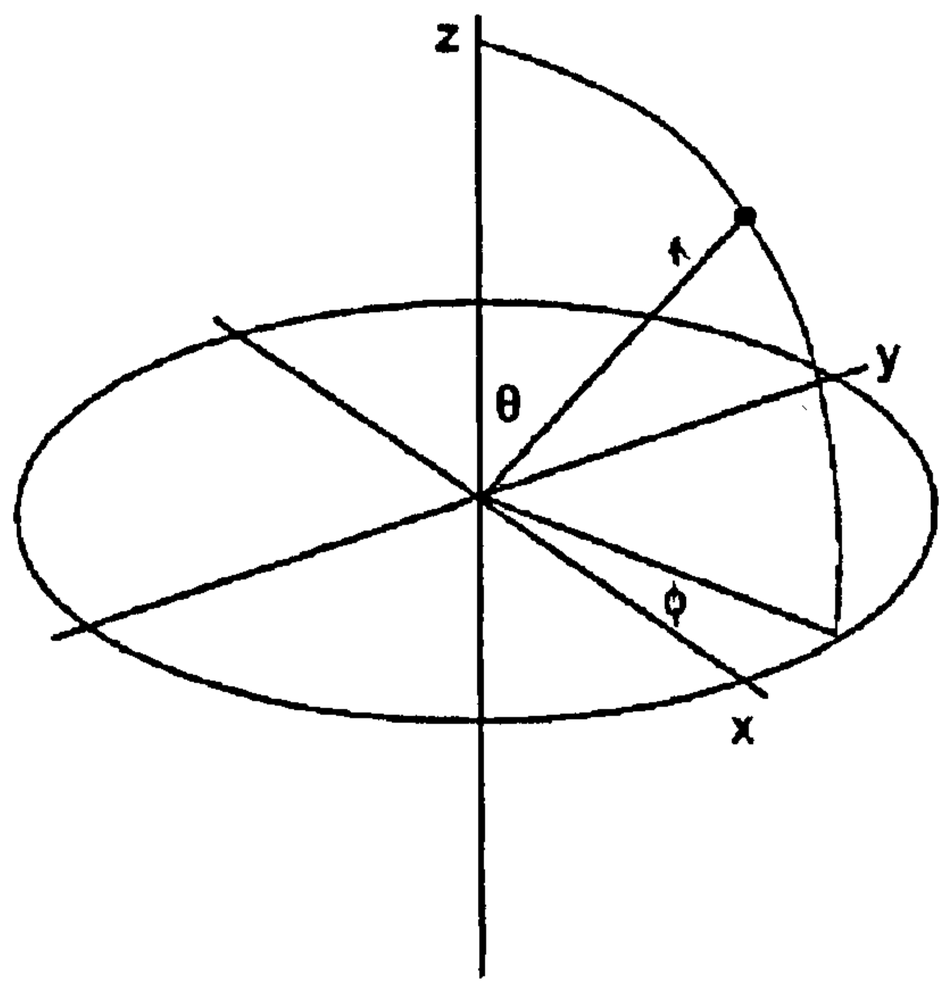

Figure 5-1- General coordinates. [15]

The relation between the two systems is expressed by equations (5.5), (5.6) and (5.7), where $(-\pi < \phi \leq \pi)$ and $(0 \leq \theta \leq \pi)$.

$$x = r\cos\phi\sin\theta \tag{5.5}$$

$$y = r\sin\phi\sin\theta \tag{5.6}$$

$$z = r\cos\theta \tag{5.7}$$

- Straight Line

The path of a ray or the direction of a straight line in space may be described by its direction cosines (c_x, c_y, c_z), which relate this line with each axis (X,Y,Z). They are assessed by equations (5.8), (5.9) and (5.10).

$$c_x = \cos\phi \sin\theta \tag{5.8}$$

$$c_y = \sin\phi \sin\theta \tag{5.9}$$

$$c_x = \cos\theta \tag{5.10}$$

so

$$c_x^2 + c_y^2 + c_z^2 = 1 \tag{5.11}$$

- Plane surfaces

Plane surfaces may be defined by the direction cosines of its normal, n_x, n_y, n_z, and its perpendicular distance, P, from the general origin. P is positive when the normal faces away from the general origin.

Equations (5.12), (5.13), (5.14), (5.15) assess n_x, n_y, n_z and P from three non-collinear ($r \neq 0$) given points (x_1,y_1,z_1), (x_2,y_2,z_2) *and* (x_3,y_3,z_3) of this surface. Points should be anticlockwise when viewed from the general origin.

$$n_x = w_1 / r \tag{5.12}$$

$$n_y = w_2 / r \tag{5.13}$$

$$n_z = w_3 / r \tag{5.14}$$

$$P = x_1 n_1 + y_1 n_2 + z_1 n_3 \tag{5.15}$$

where

$$w_1 = (y_2 - y_1)(z_3 - z_1) - (y_3 - y_1)(z_2 - z_1) \tag{5.16}$$

$$w_2 = (x_3 - x_1)(z_2 - z_1) - (x_2 - x_1)(z_3 - z_1) \tag{5.17}$$

$$w_1 = (x_2 - x_1)(y_3 - y_1) - (x_3 - x_1)(y_2 - y_1) \tag{5.18}$$

$$r = \sqrt{w_1^2 + w_2^2 + w_3^2} \tag{5.19}$$

5.5.3.2 *Local surface coordinates*

To simplify calculation, the concept of a local surface coordinate is introduced. As shown in Figure 5-2, it creates new coordinates in just two dimensions. The origin of the new system is located at the point on the surface where the z' axis would pass through the general origin. In his turn, the y' axis is always parallel with the general x-y plane.

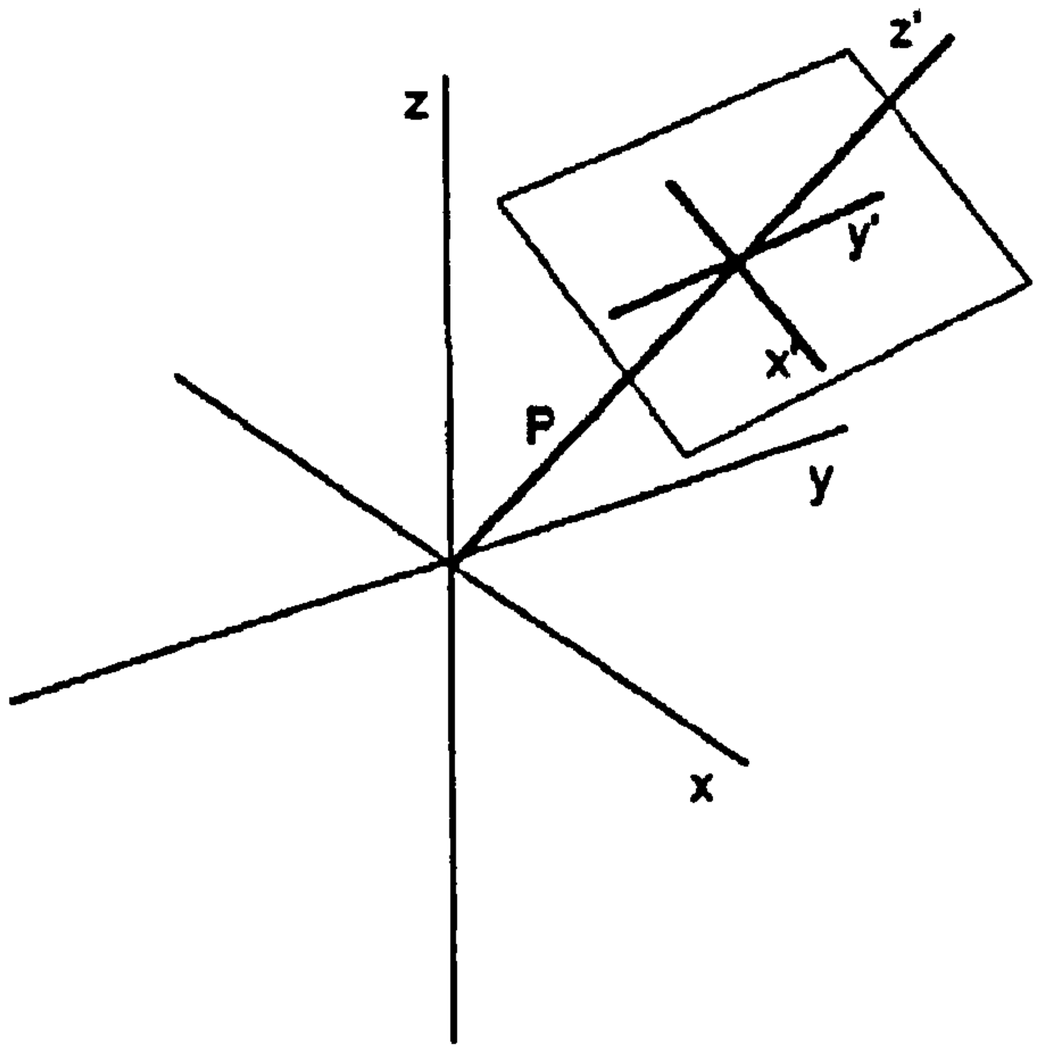

Figure 5-2 - Local coordinates. Source [15]

5.5.3.3 *Sky coordinates*

Sky coordinates are used to localise a point in the sky. It is described by azimuth, α, ($0 \leq \alpha \leq 2\pi$), an angle in the horizontal plane, measured clockwise from geographical north, and altitude, γ, ($0 \leq \gamma \leq \pi/2$), a vertical angle, measured from the astronomical horizon. Figure 5-3 illustrates those angles.

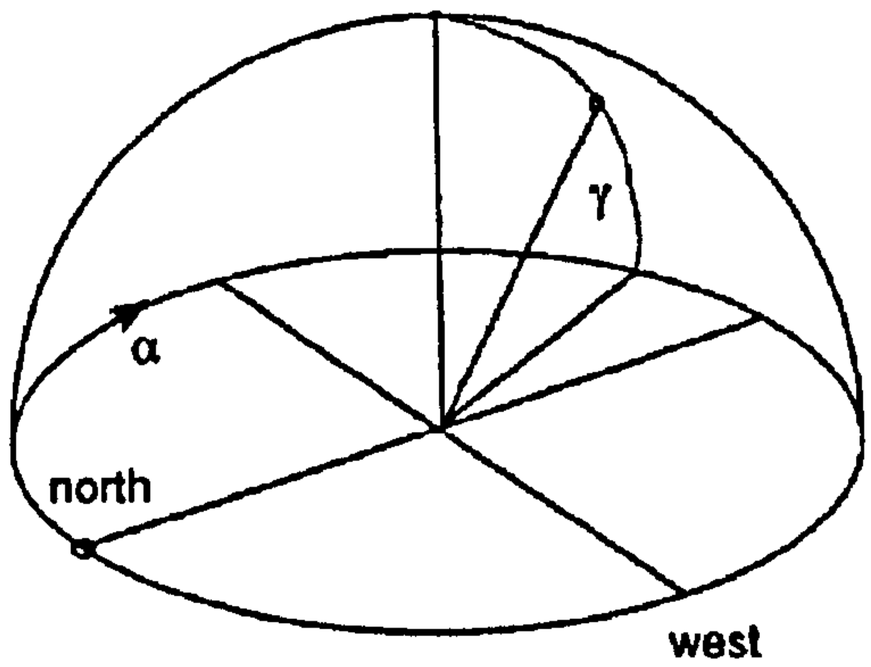

Figure 5-3 - Sky coordinates. Source [15]

As well as for general coordinates, a point may also be described by its direction cosines (c') with respect to sky coordinates by equations (5.20), (5.21) and (5.22).

$$c_x' = \cos\alpha \cos\gamma \tag{5.20}$$

$$c_y' = \sin\alpha \cos\gamma \tag{5.21}$$

$$c_z' = \sin\gamma \tag{5.22}$$

5.5.3.4 Axis system conversion

Axis system conversion is necessary to properly identify points created in different systems. It is done by matrix operations, based on the general theory of analytic geometry. Four conversions can be performed [15]:

(i) Local surface coordinates to general coordinates, based on the direction cosines of surface normal, the perpendicular distance of the surface from general origin and the coordinates of a point with respect to local surface axes;

(ii) General coordinates to local surface coordinates, similar to the previous conversion, but with the coordinates of a point with respect to the general axes;

(iii) Sky coordinates to general coordinates, based on the azimuth of X-axis and the direction cosines of a vector or a sky point with respect to sky coordinates;

(iv) General coordinates to sky coordinates, similar to the previous conversion, but with respect to general coordinates.

5.5.3.5 Room Geometry

The room is defined by a set of surfaces. For simplification, surfaces are based on planes. If a curved surface is required, a set of planes can be used to simulate it. Each surface has (i) sequential number, for identification; (ii) type, to classify its material, valuing 0 for clear opening, positive for surfaces described by reflectance and transmittance index, and negative if glass type; (iii) coordinates (x,y,z) for the vertices of planes; infinite values are allowed, and are used for ground surface. From those points, the system assesses the surface's direction cosines by equations (5.12), (5.13), (5.14) and (5.15).

The external surfaces are defined in the same way. Figure 5-4 describes the geometry for basic room and external surfaces.

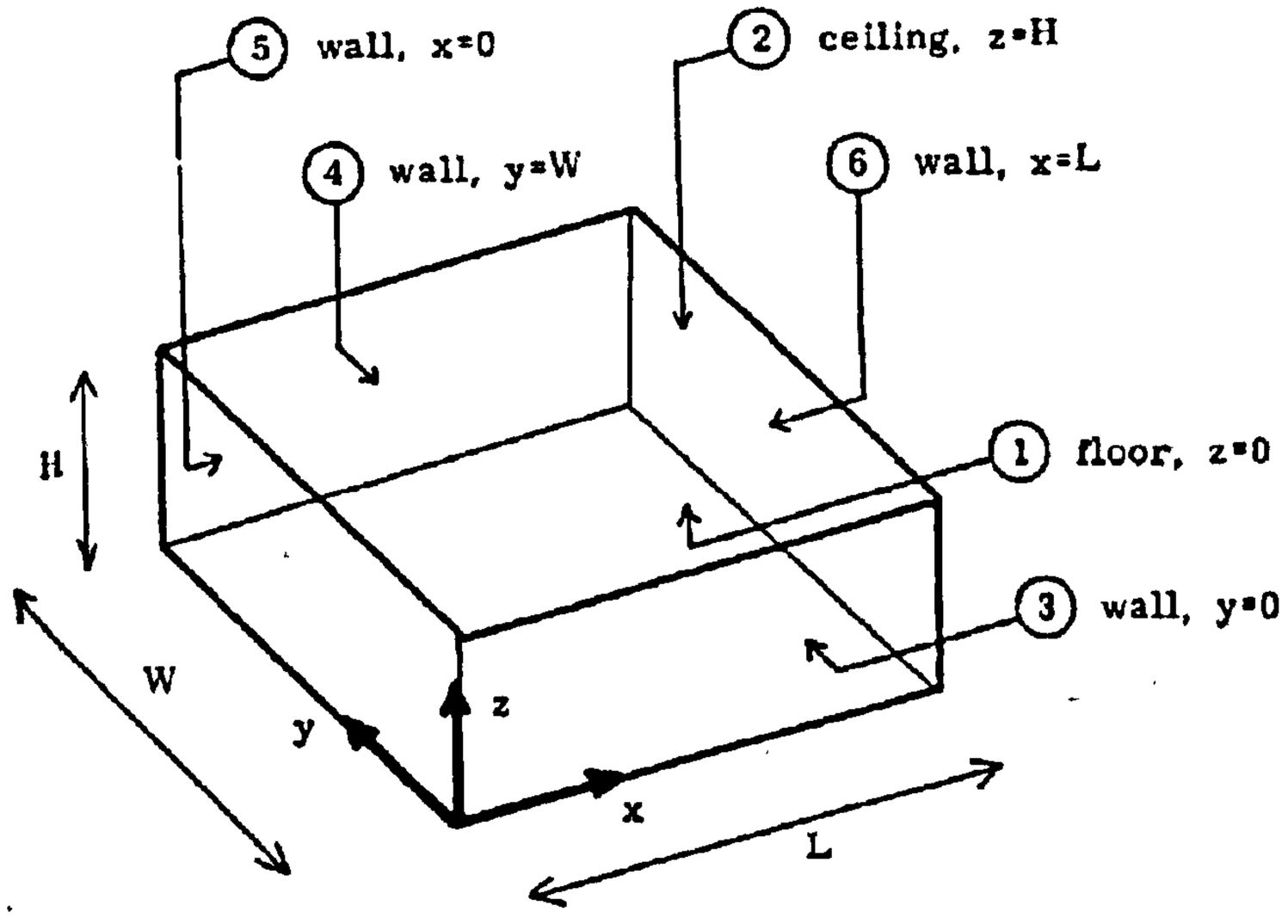

Figure 5-4 - Room Geometry. [6]

5.5.4 The backward ray tracing way

If the aim is assessing illuminance (or daylight coefficients) in a specific point on a surface, get the point coordinates (x,y,z) and generate *N* rays from this point. On the other hand, when the goal is the mean illuminance (or daylight coefficients) on a surface, a random grid of *N* points on this surface should be generated, and from each of them just one particle be emitted. The number *N* should follow instructions of section 5.5.4.1.

Each ray emitted has its direction according to the rules defined on section 5.5.4.2. Moreover, section 5.5.4.3 explains what happen when ray reaches a new surface. Then section 5.5.4.4 describes the process when ray leaves the building.

A flowchart summarising how to assess daylight coefficients using the Monte Carlo method can be seen in Figure 7-7 in Chapter 7. In his turn daylight coefficients are discussed in Chapter 6.

5.5.4.1 The number of rays emitted

To optimise calculation performance, it is important to carefully define the number of particles taken in function of a stochastic error. It can be estimated using the following steps [15]:

(i) divide the run of repetitions into successive shorter runs of fixed length;

(ii) calculate the illuminance (or daylight coefficients) of each short run on completing it;

(iii) calculate cumulatively the standard error, based on Section 5.2.4;

(iv) stop when the standard error falls below a preset value.

However, the difference in the number of rays to achieve the preset error for every daylight coefficient and for the overall illuminance is quite significant. Therefore, the choice of method should relate to the influence of each illuminance component. For

instance, a particular daylight coefficient error can be important to the final daylighting results when the sun is available and located in that patch. This point is analysed in depth in Section 7.5.1 in Chapter 7.

5.5.4.2 Characterisation of the source

A basic step is to set up the independent variables that form the particle. Basically these are the emission point position in general coordinates (x,y,z), the direction cosines for the ray, and the weight of the particle. Particles have weight set up to one. Direction cosines are assessed from angles θ and ϕ, calculated by equations (5.23) and (5.24). The point is defined either by the user, if just one, or by a random grid.

- The first emitted ray (uniform diffuse)

The emission direction of a single particle from a point on a surface may take any vertical (or cone) angle, θ, between 0 and π, and any horizontal (or circumferential) angle, ϕ, in the closed interval from 0 to 2π, in relation to the surface's axes. With regard to the vertical angle θ, the probability of any particle angle is proportional to *sin* θ, as explained in equations (5.23) and (5.24).

$$P_\theta = \int_0^\theta 2\pi \cos\theta \sin\theta \quad d\theta = 2\pi \left[\frac{\sin^2\theta}{2} \right]_0^\theta = 2\pi \left(\frac{\sin^2\theta}{2} - 0 \right) = \pi \sin^2\theta \qquad (5.23)$$

$$\xi = \frac{\int_0^\theta P_\theta d\theta}{\int_0^{\pi/2} P_\theta d\theta} = \frac{\pi \sin^2\theta}{\pi} = \sin^2\theta \qquad (5.24)$$

Equations (5.25) and (5.26) show the relation between angles θ and ϕ, and independent random numbers ξ_1 and ξ_2.

$$\theta = \arcsin\sqrt{\zeta_1} \qquad (5.25)$$

$$\phi = 2\pi\xi_2 \qquad (5.26)$$

5.5.4.3 When ray reaches a new surface

Each time a ray reaches a new surface, it is necessary to evaluate if the ray was absorbed, reflected or transmitted. The absorption phenomenon is treated later in this Section.

If the ray is not absorbed, cumulative probability is used to find what happened to the ray afterwards. The technique is also called the 'top hat' method, which says that the probability of an object being pulled out of a hat is proportional to the number of objects of that sort lying in the hat. For each surface an array, $aMat_i$, of 4 elements is created to represent the cumulative probability. Let ρ_d, ρ_s, τ_d and τ_s, be respectively the diffuse reflectance, specular reflectance, diffuse transmittance and specular (or regular) transmittance of surface, i; then the array $aMat_i$ is shown in equation (5.27).

$$aMat_i = \left[\rho_d, (\rho_d + \rho_s), (\rho_d + \rho_s + \tau_d), (\rho_d + \rho_s + \tau_d + \tau_s)\right] \qquad (5.27)$$

Normalising array $aMat_i$ in function of the not absorbed fraction, the new array $aMat_n$ gets 1 as the last element, as shown in equation (5.28), and consequently a random number $\xi[0:1]$ can be used.

$$aMat_n = \left[\frac{\rho_d}{\rho_d + \rho_s + \tau_d + \tau_s}, \frac{(\rho_d + \rho_s)}{\rho_d + \rho_s + \tau_d + \tau_s}, \frac{(\rho_d + \rho_s + \tau_d)}{\rho_d + \rho_s + \tau_d + \tau_s}, 1\right] \qquad (5.28)$$

Then taking into account just the not absorbed fraction, for a random number $\xi[0:1]$, if $\xi < aMat_n(1)$, the ray is diffused reflected, else if $\xi < aMat_n(2)$ it is specular reflected, else if $\xi < aMat_n(3)$ it is diffused transmitted, otherwise it is specular transmitted.

Depending on ξ, the particle gets a new weight and direction. The new weight is calculated multiplying the old weight by the surface reflectance or transmittance. The new directions are explained later in this Section.

This approach also allows for surfaces with composite material characteristics, where reflection and/or transmission are/is not simply diffuse or specular.

- **Diffuse reflection**

The rules for diffuse reflection from a plane surface are similar to the random emission from a diffusing surface source, as shown in Section 5.5.4.2

- **Specular reflection**

The reflected angle is equal to the incident angle after a specular reflection. The cosines of the reflected ray (c_i') are expressed in equations (5.29), (5.30) and (5.31).

$$c_x' = (-n_x^2 + n_y^2 + n_z^2)c_x + (-2n_x n_y)c_y + (-2n_x n_x)c_z \quad (5.29)$$

$$c_y' = (-2n_x n_y)c_x + \left(n_x^2 - n_y^2 + n_z^2\right)c_y + (-2n_y n_z)c_z \quad (5.30)$$

$$c_z' = (-2n_x n_z)c_x + (-2n_y n_z)c_y + (1 - 2n_z^2)c_z \quad (5.31)$$

provided

$$-(c_x n_x + c_y n_y + c_z n_z) > 0 \quad (5.32)$$

where c_x, c_y, c_z are the direction cosines of the original ray, and n_x, n_y, n_z are the direction cosines of surface normal.

Therefore when the surface is horizontal, $c_x' = c_x$; $c_y' = c_y$ and $c_z' = -c_z$.

- **Diffuse transmission**

The rules for diffuse transmission from a plane surface are similar to the random emission from a diffusing surface source, as shown in Section 5.5.4.2

- **Regular transmission**

There is no shifting in ray angle direction after a regular transmission. The 'leap' due to refraction is not taken into account, since transparent surfaces thickness is insignificant relating to building dimensions.

- Absorption

The absorption phenomenon is simulated by a Monte Carlo technique as well. If the weighting number of the particle reaches a value less than a threshold, a random number, ξ [0;1], is used in a stopping rule .

If ξ is less than 0.5, the weight is set to zero and consequently the ray is considered absorbed. Then, the simulation continues with a new particle, until the number of particles is less than the preset in Section 5.5.4.1.

Otherwise, if ξ is more or equal to 0.5, weight is multiplied by 2 and ray goes on.

5.5.4.4 When ray leaves the building

When ray leaves the building it can go in direction to three different goals: sky, ground or obstruction. Every time a ray reaches the target, its weight is added to a target's weight counter. These counters can be used to assess daylight coefficients, if ray goes to sky; or auxiliary coefficients, otherwise. Daylight and auxiliary coefficients are discussed in Chapter 6.

5.6 Conclusion

This chapter has reviewed the principles of the Monte Carlo and ray tracing techniques. Specific routines for daylighting calculation were discussed and presented in a suitable way for computer processing. The method has been appropriated for use in tropical daylighting, since it allows for complexity in room geometry and variation in sky luminance patterns.

Questions discussed in this chapter are addressed in Chapter 6, which discusses the daylight coefficients. They are the theoretical foundation of the computer program presented in Chapter 7.

References

1. Minkowycz, W. J., *et al.*, eds. *Handbook of numerical heat transfer*. John Wiley & Sons: New York, 1988

2. Kalos, M. H. and P. A. Whitlock, *Monte Carlo methods*. Vol. 1, 1986.

3. Siegel, R. and J. R. Howell, *Thermal radiation heat transfer*. 3rd ed. Washington: Hemisphere, 1992.

4. The Math Works, *MATLAB - Using MATLAB - Version 5*. Natick: The Math Works, 1998.

5. Ward, G. J. and F. M. Rubinstein, *A new technique for computer simulation of illuminated spaces.* Journal of the Illuminating Engineering Society, **17**(1): p. 80-91, 1988.

6. Tregenza, P., *The Monte Carlo method in lighting calculations.* Lighting Research & Technology, **15**(4): p. 163-170, 1983.

7. Stanger, D., *Monte Carlo procedures in lighting design.* Journal of the Illuminating Engineering Society, **13**(4): p. 368-371, 1984.

8. Ohtani, Y., *et al.*, *Illuminance calculation using Monte Carlo method.* Journal of Light and Visual Environment, **24**(1): p. 42-49, 2000.

9. Uchida, A. and Y. Ohtani, *Fundamental study of shadow characteristics under task ambient lighting.* Journal of Light and Visual Environment, **24**(1): p. 50-58, 2000.

10. Tregenza, P. R., *The sensitivity of room daylight to sky brightness.* Architectural Science Review, **42**(june 1999): p. 129-132, 1999.

11. Chen, L., *et al.*, *Luminous intensity characteristics of luminaries: Monte Carlo simulation.* Lighting Research and Technology, **30**(4): p. 159-164, 1998.

12. Chen, L., *et al.*, *Louvre lighting performance: Monte Carlo assessment.* Lighting Research and Technology, **30**(4): p. 165-168, 1998.

13. Sever, S. *Uncertainties in indirect lighting calculations*. in *CIBSE - National Lighting Conference*. Bath - UK: CIBSE. p. 344-348, 1996.

14. Ward, G. and R. Shakespeare, *Rendering with radiance: the art and science of lighting visualization*. San Francisco: Morgan Kaufmann, 1998.

15. Tregenza, P. and S. Sharples, *Daylight algorithms*, University of Sheffield: Sheffield, 1993.

Chapter 6 Daylight and auxiliary coefficients: definition and equations

6.1 Introduction

Daylight coefficients were proposed about two decades ago and have being considered as a fundamental approach in daylighting calculations. As a new technique, it needs being tested for different situations and some enhancement may be necessary in order to generalise its use. This chapter discusses the concept and presents equations suitable for use in a daylighting simulation program. In addition, ground and obstruction coefficients are introduced as auxiliary to the daylight coefficients method, allowing specific tropical daylighting characteristics to be assessed. The coefficients interact with the Monte Carlo method, discussed in Chapter 5. New schemes for sky, ground and external obstruction subdivision are also proposed.

6.2 Definition of daylight coefficients

The daylight coefficient approach, created by Tregenza and Waters in 1983 [1], relates the illuminance on a given surface, *i*, from a given patch, *j*, of sky and the normal illuminance (E_n) from that sky patch on an unobstructed plane, as shown on Equation (6.1).

$$d(i,j) = \frac{E_i(j)}{E_n(j)} = \frac{E_{i(j)}}{L_j \omega_j} \tag{6.1}$$

where L_j and ω_j are respectively the luminance and the subtended area in steradians of the sky patch, *j*.

Thus, the daylight coefficients are dependent on the geometry of the room, ground and obstructions, and their surface reflectance. On the other hand, they are independent of sky luminance distribution and consequently of the room orientation, the time of the day and the day of the year.

In this approach, the sky is considered as an array of small sources. Its subdivision is discussed in the section 6.3.

6.3 Sky subdivision

The implementation of daylight coefficients is dependent on the subdivision of the sky into a defined number of patches. Each sky patch has its own daylight coefficient for a specific point or surface.

The general principles for sky subdivision are symmetry, geometry and constant zone size. Symmetry is useful but not essential. At least it is important to get the basic geographic orientations. Geometry for scanning pattern should lead to identical shape and allow measurements being done in an efficient manner. In this way, Tregenza [2] suggests circular patches orientated in bands parallel with the horizon. For computation, geometry is related to how to cover the whole hemisphere, which makes circular patches inadequate. A geometry which could be linked with the one used for scanner is useful, as results can be compared. In addition, tidy geometry can generate a simple computer code.

Constant zone size is essential for scanner measurements, but not for computation. In order to simplify calculation, the zone size for scanner should be neither so small that produces an excessive number of measurements creating difficult or even making scanning not feasible, nor so big that can not be treated as a point source. The accepted limit for a surface being considered as point source is when the relation dimension to distance is about 1:5, as discussed in greater depth in Appendix E. In this way, it leads to a zone angle of 11.3°. With reference to computation, size should take into account the method of calculation and which components are analysed. For the Monte Carlo method the size should be as big as possible since its error is as large as smaller the zone size is. However, size should also be on the limits of being treated as a point source. For direct calculation, size should be as small as possible to reduce error due to solar location in patch. Refinement should be done with care, as an increment in number of zones creates a large amount of coefficients, increasing calculation time and memory storage.

Several proposals for sky subdivision have been done. The shape of patches and its number have been varied in function of the goals. Earlier sky subdivision aimed at helping sky scanner measurements, and then patches were in circular shapes. Tregenza [2] proposed a 151 circular patches subdivision, with cone opening angles varying by altitude of band, from 11.13° to 12.47°. It covered 71% of the sky vault (See Figure 6-1). In the same paper he also proposed two alternatives, one that covered 75% of sky vault, using a 12° acceptance angle, but removing symmetry across one vertical angle, and another changing the number of zones in some bands, which gives a 3-way symmetry overall, but reducing coverage to 68%. All sky subdivision proposed divided the sky into bands, parallel with the horizon.

Afterwards, Tregenza's third proposal was recommended by the CIE [3]. Its sky subdivision has 145 patches and matches with the sky scanner sensors, used in IDMP stations [4] (See Figure 6-2).

However, as circular patches can never cover the whole sky hemisphere, an inherited uncertainty in daylight computer simulation is created. ESP-r program tried to overcome this problem increasing the open cone of the 145 patches to 13.39° [5]. This led to an overlap and several regions were double counted, generating some miscalculation.

Then circular patches were adapted to a 'rectangular' shape to fill the whole sky vault. This is seen in Figure 6-3, which follows the CIE 145 sky subdivision, but centred on north.

Although CIE 145 sky subdivision can be useful for diffuse daylight calculation, being largely adopted [5-8], it can create significant errors when direct sunlight is taken into account. This happens due to the small solar angular size together with its significant higher luminance, compared to sky patch figures. In this way, a finer discretisation is more suitable.

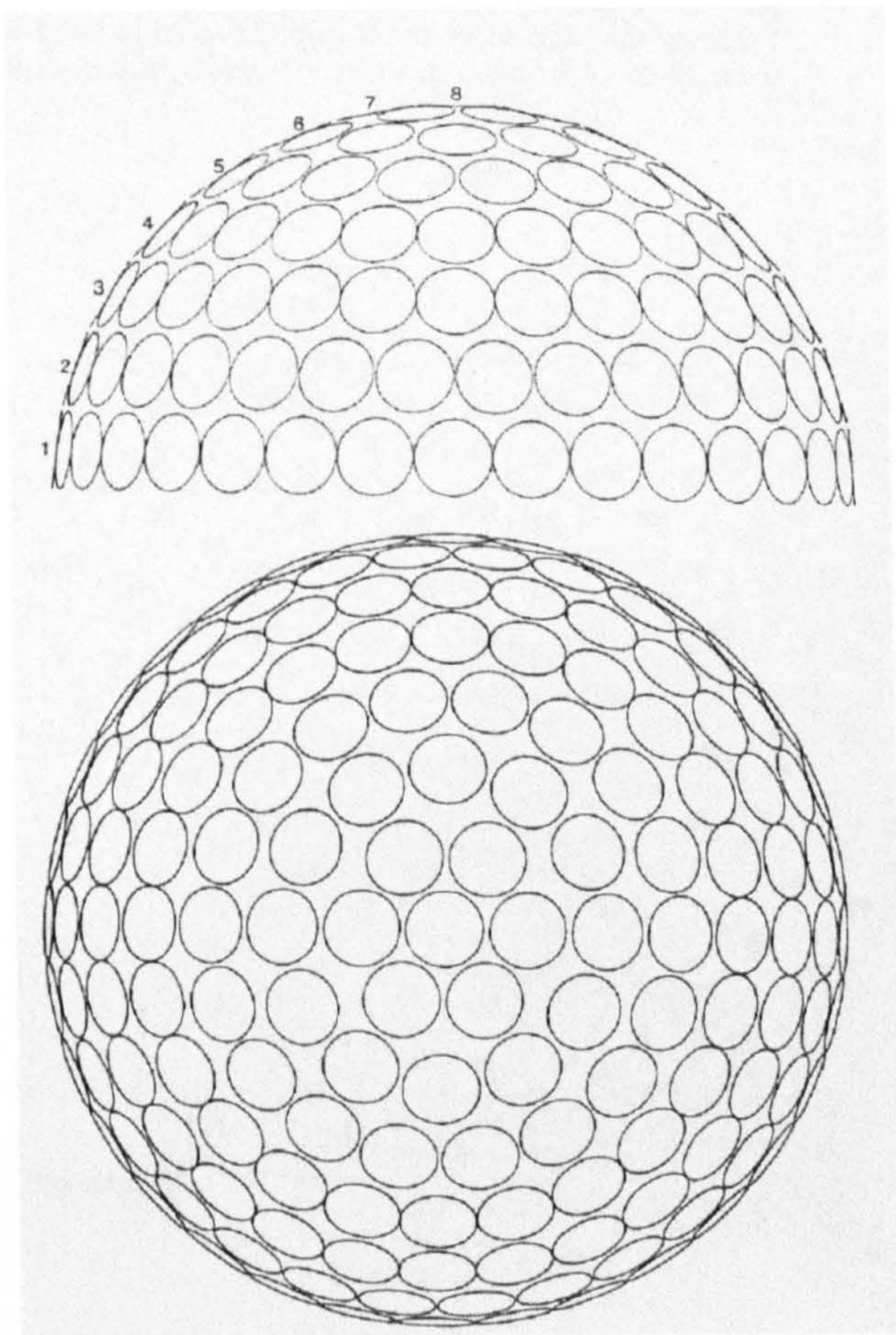

Figure 6-1 - Sky subdivision - 151 circular patches. [2]

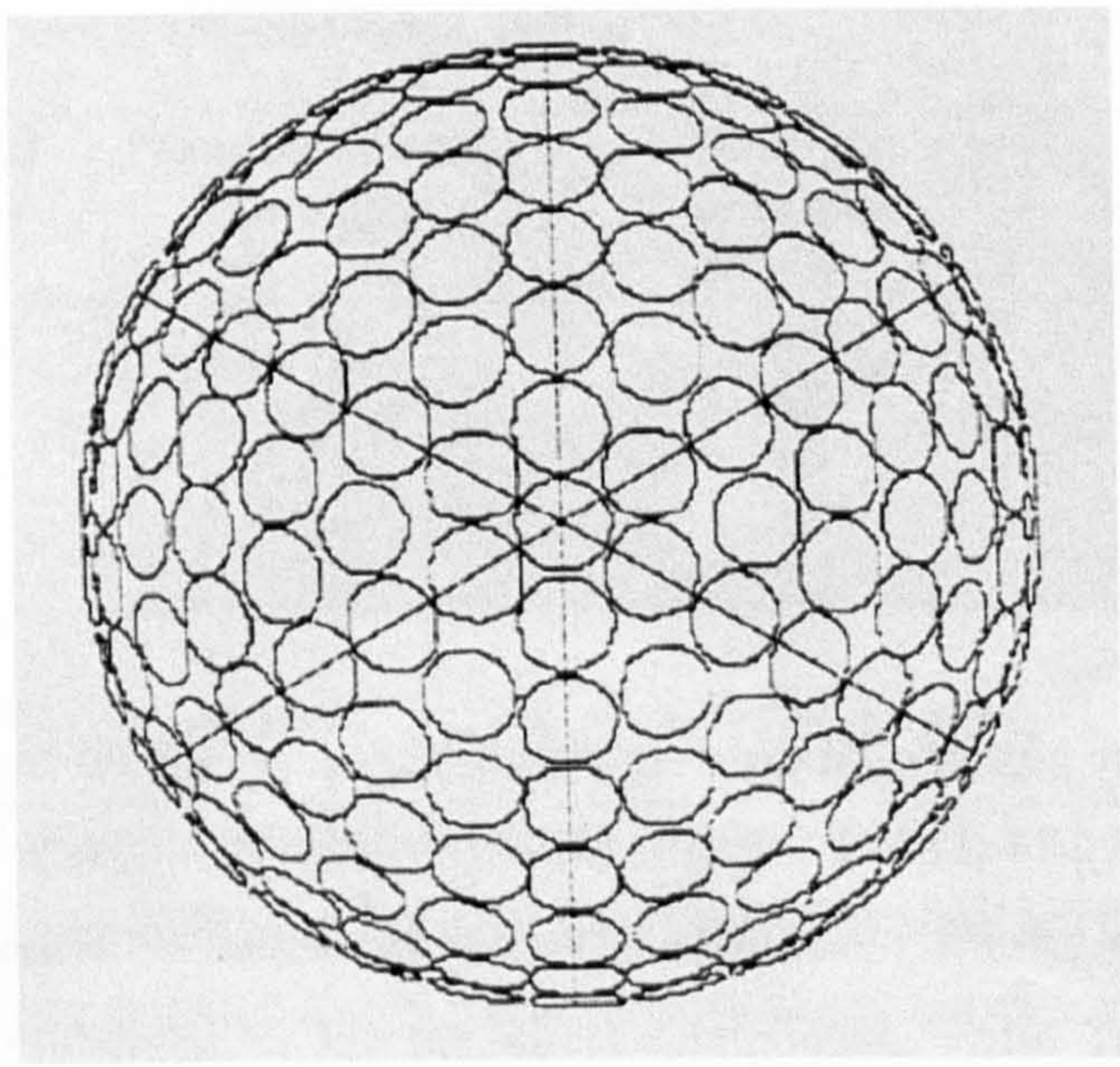

Figure 6-2 - Sky subdivision CIE 145 circular patches. [9]

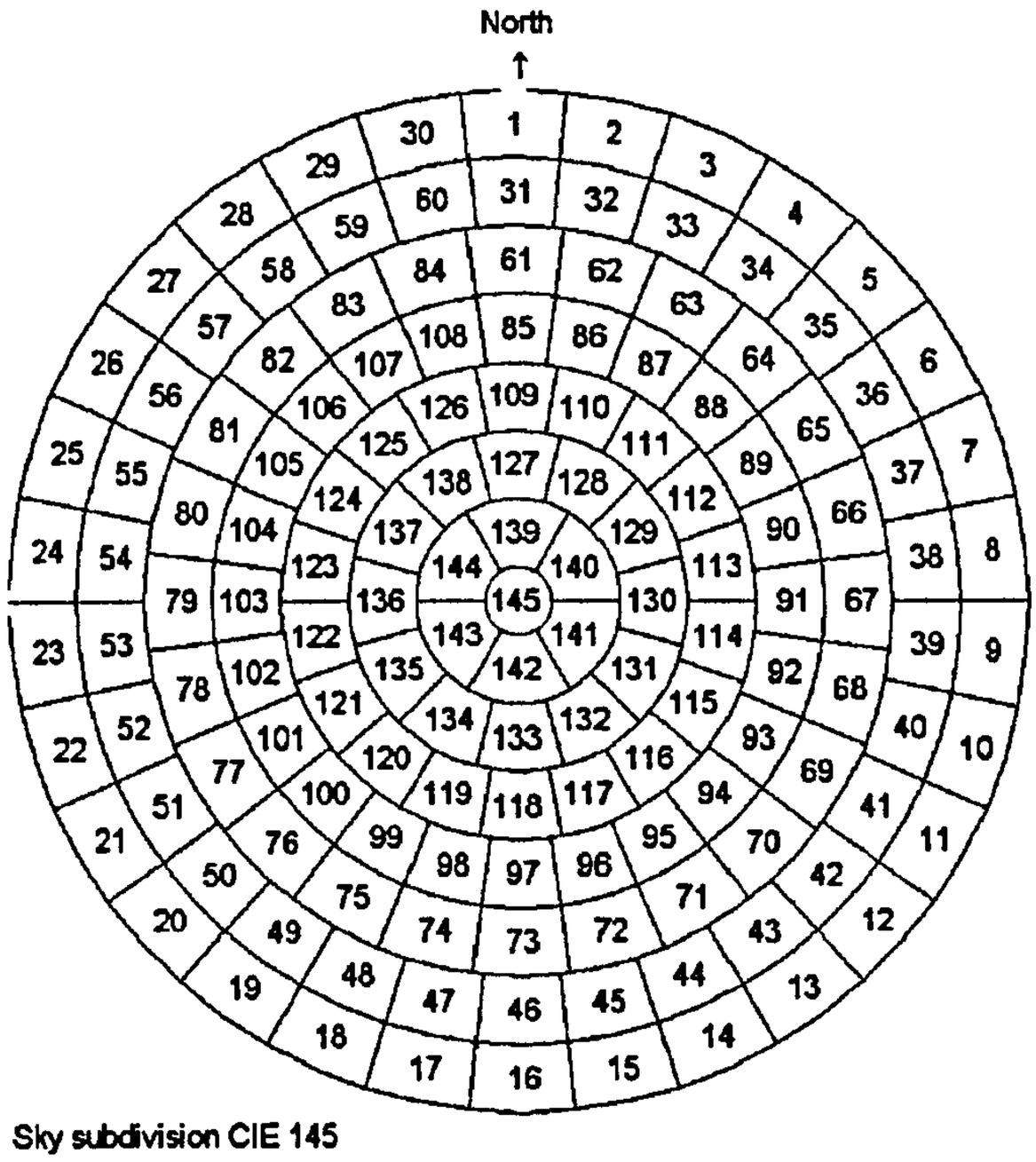

Sky subdivision CIE 145

Figure 6-3 - Sky subdivision CIE 145

Table 6-1 - Angles for CIE 145 subdivision. [10]

Altitude of band centre (degree)	Number of zones in band	Azimuth increment (degree)	Solid angle subtended by zone (steradian)
6	30	12	0.0435
18	30	12	0.0416
30	24	15	0.0474
42	24	15	0.0407
54	18	20	0.0429
66	12	30	0.0445
78	6	60	0.0455
90	1	360	0.0344

Nevertheless, there is no consensus about that refinement. Mardaljevic [7] proposed a 5010 patches subdivision, for the direct component, while Tsangrassoulis [8] divided every 145 sky patches in 144 sub-patches, giving 20880 coefficients.

Reinhart and Herkel [5], on the other hand, suggested no sub-patch but 58 representative sun positions.

For computer simulation, a good approach would be to have a refined symmetrical subdivision. In this way, a very simple subdivision is proposed. Patches have angular sizes with 2 degrees in both vertical and horizontal directions, as shown in Figure 6-4. This gives a neat arrangement and an easy computer implementation.

However, as seen in Figure 6-5, it does not match with CIE 145 subdivision which has been widely accepted because of IDMP data compatibility. Therefore, this work also proposes another subdivision, but keeps its compatibility with the CIE 145. In this subdivision, each CIE 145 patch is divided in 36, except the zenith, to keep the central circular patch, which has 37 sub-patches. It provides a 5221 subdivision, as shown in Figure 6-6. Figure 6-7 shows its match with the CIE 145 subdivision.

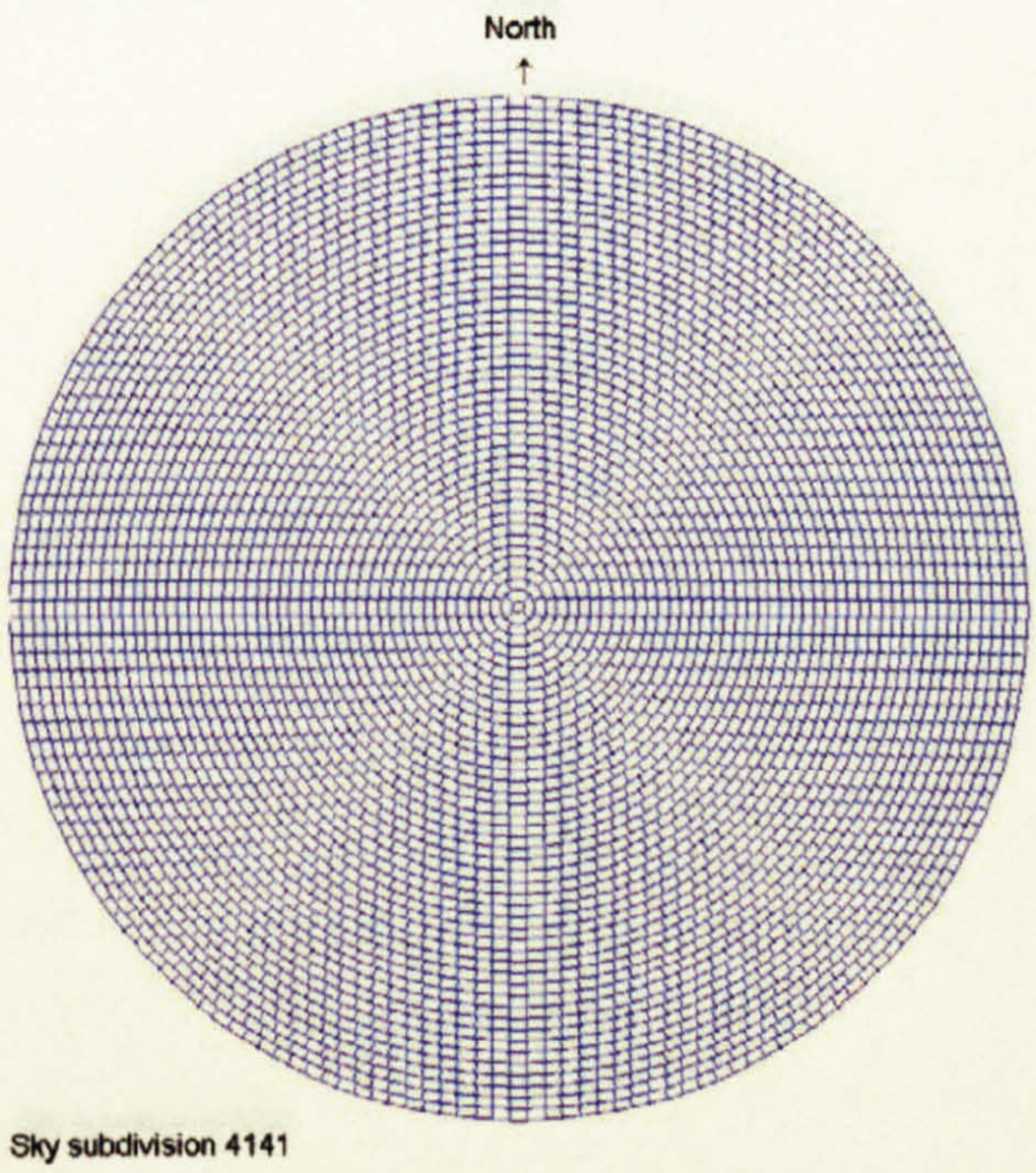

Figure 6-4 - Sky subdivision 4141

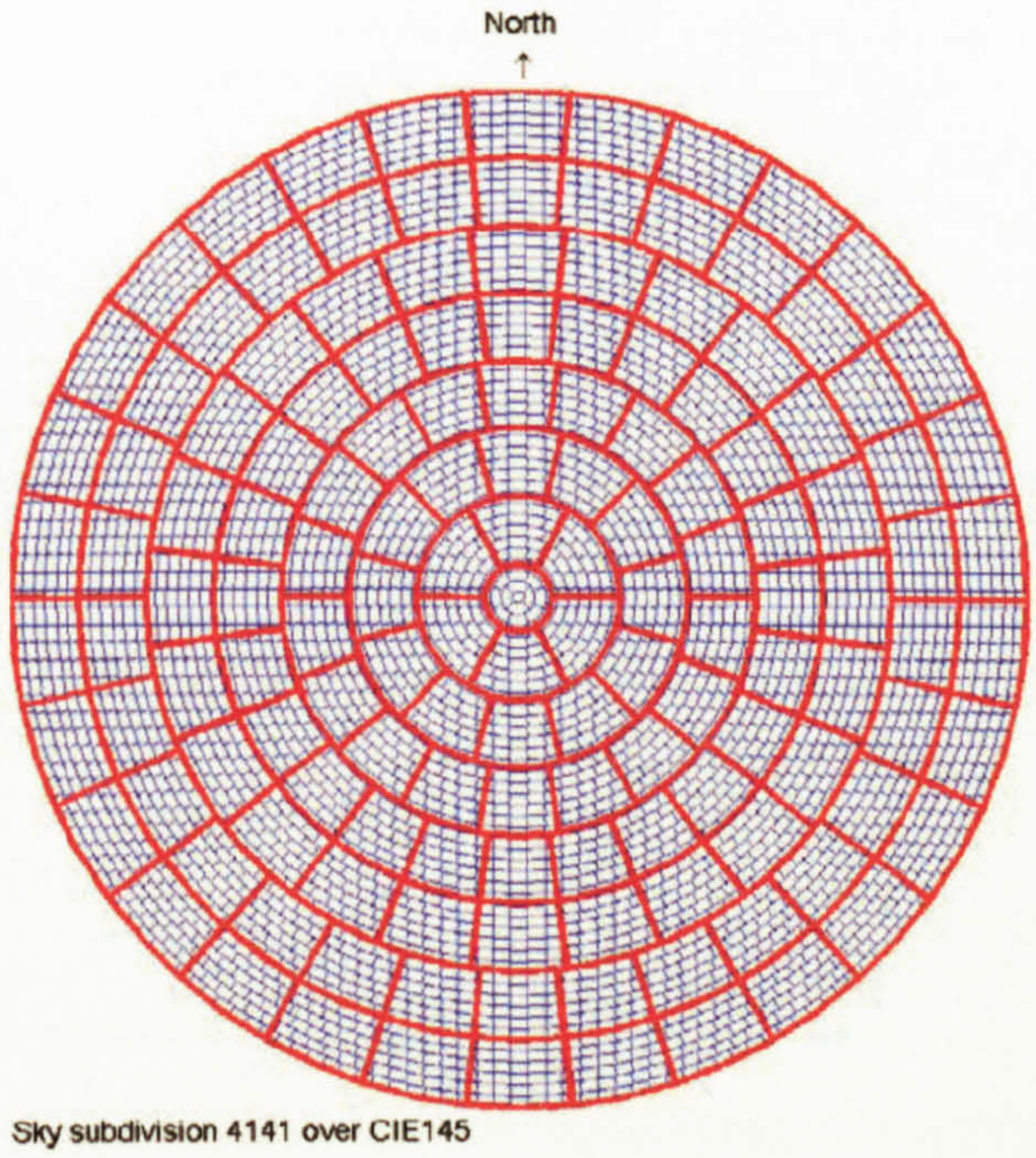

Sky subdivision 4141 over CIE145

Figure 6-5 - Sky subdivision 4141 over CIE 145

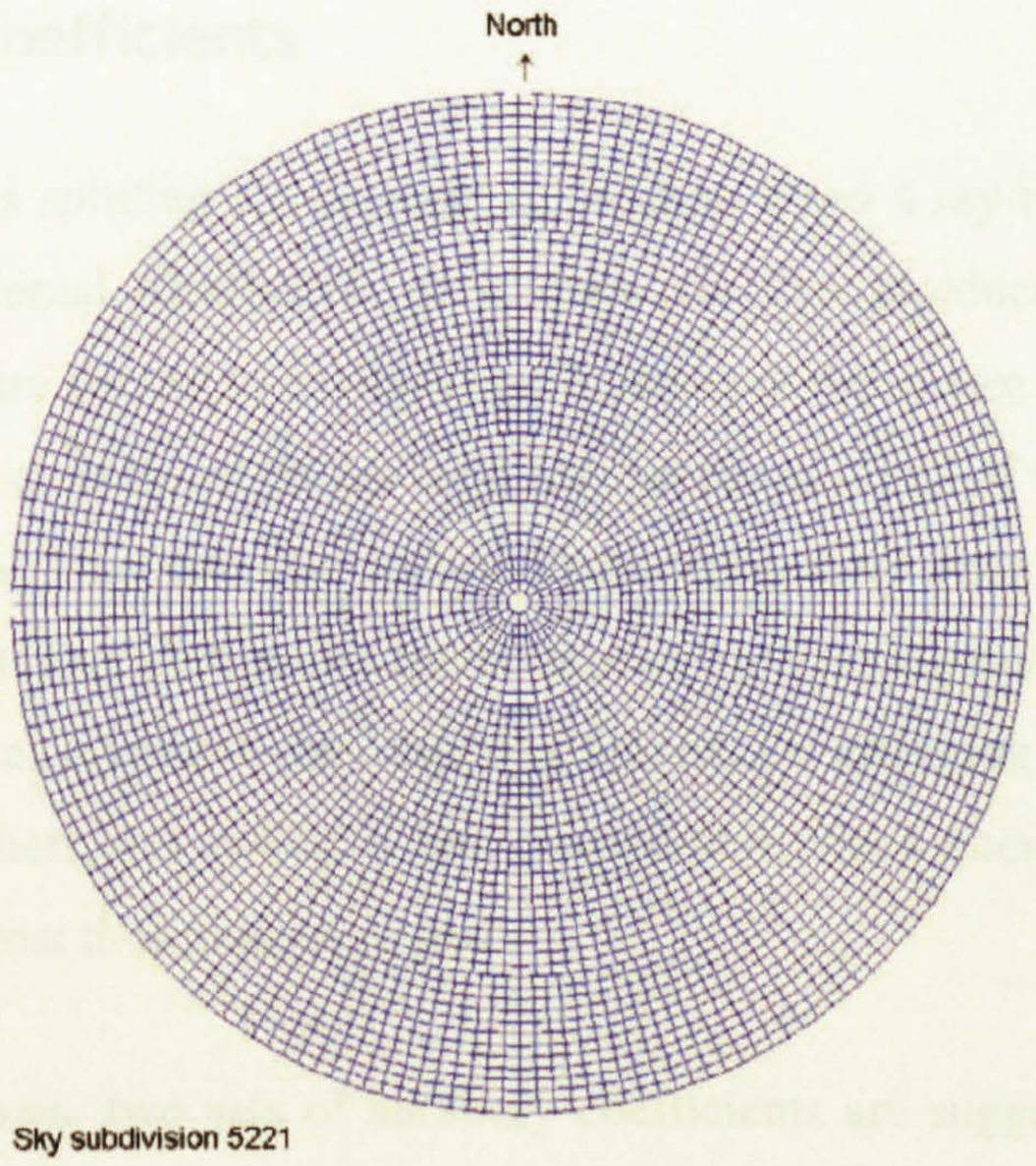

Sky subdivision 5221

Figure 6-6 - Sky subdivision 5221

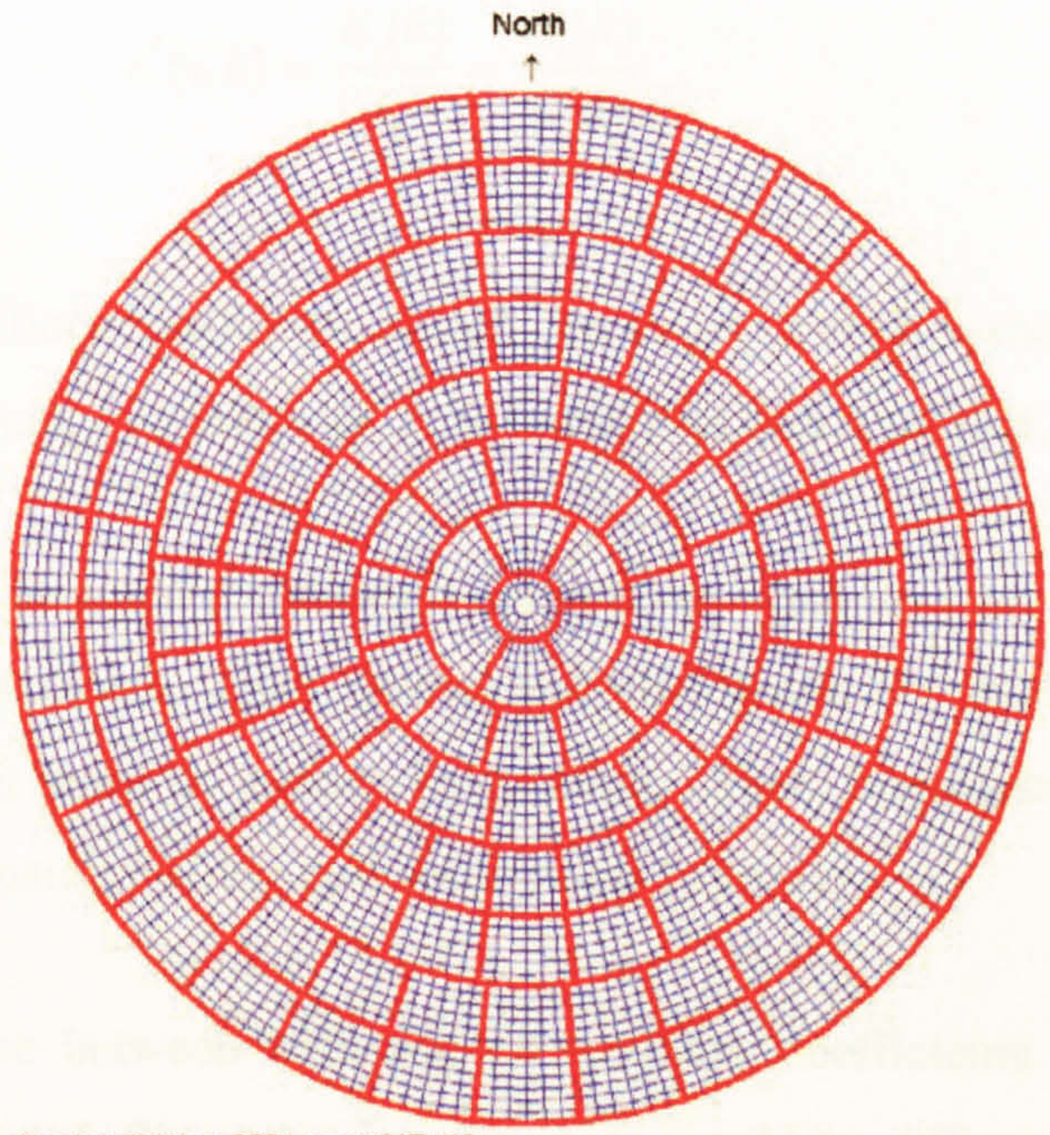

Figure 6-7 - Sky subdivision 5221 over CIE 145

6.4 Auxiliary coefficients

This study proposes splitting the daylight calculation when a ray reaches either the ground or any external obstruction. It is done via the introduction of auxiliary coefficients; these are similar to daylight coefficients but the source of light is not the sky. Their importance is based on the need for specific analysis of those elements in daylight calculation. They can also reduce computation time when changing should be done in ground and/or obstruction characteristics but keeping the room parameters unchangeable. It is also valid in the other way around, i.e. changing room parameters and keeping the others, but saving is less considerable, since internal interreflected component is the most time expensive part.

For practical proposes, two sets of auxiliary coefficients are suggested, the ground coefficients (*gc*) and the obstruction coefficients (*oc*). Both are based on the same theoretical background that leads them being calculated by Equation (6.2).

$$c^*(i,k) = \frac{E_i(k)}{I_k} = \frac{E_i(k)}{L_k A_k} \tag{6.2}$$

where c^* is the auxiliary coefficient, which can be *gc* or *oc*, k is the patch of ground or external obstruction, *I* its intensity, *L* its luminance and *A* its area.

In this method, the reflected components are split up when rays get either the ground or any external obstruction. Then ground and obstruction are treated as sources of light for an internal point or surface calculation. Their luminances are calculated independently also using the daylight coefficients approach.

The basic difference between both sets of auxiliary coefficients is the way their surfaces are subdivided. Since the data structure would be different for ground and obstruction coefficients they are considered independent. The surface subdivision will be discussed in the next Sections.

6.4.1 Ground subdivision

The subdivision of the ground depends on the given importance for ground reflected light in daylighting performance.

Tregenza and Sharples [10] suggested the ground be treated as a single zone or having 145 patches, as a mirror image of the sky subdivision. Littlefair [11] endorses this point of view, emphasising that the second one requires a detailed knowledge of ground reflectance distribution which is not usually available. Two other papers go for a simplified option, Tsangrassoulis and Santamouris [8] choose a single zone, while Reinhart and Herkel [5] opt for three ground daylight coefficients for zenith angles greater than 90°. The three ground segments, S_{g1} … S_{g3}, correspond to zenith angles 90° – 100°, 100° – 120° and 120° – 180°, as shown in Figure 6-8.

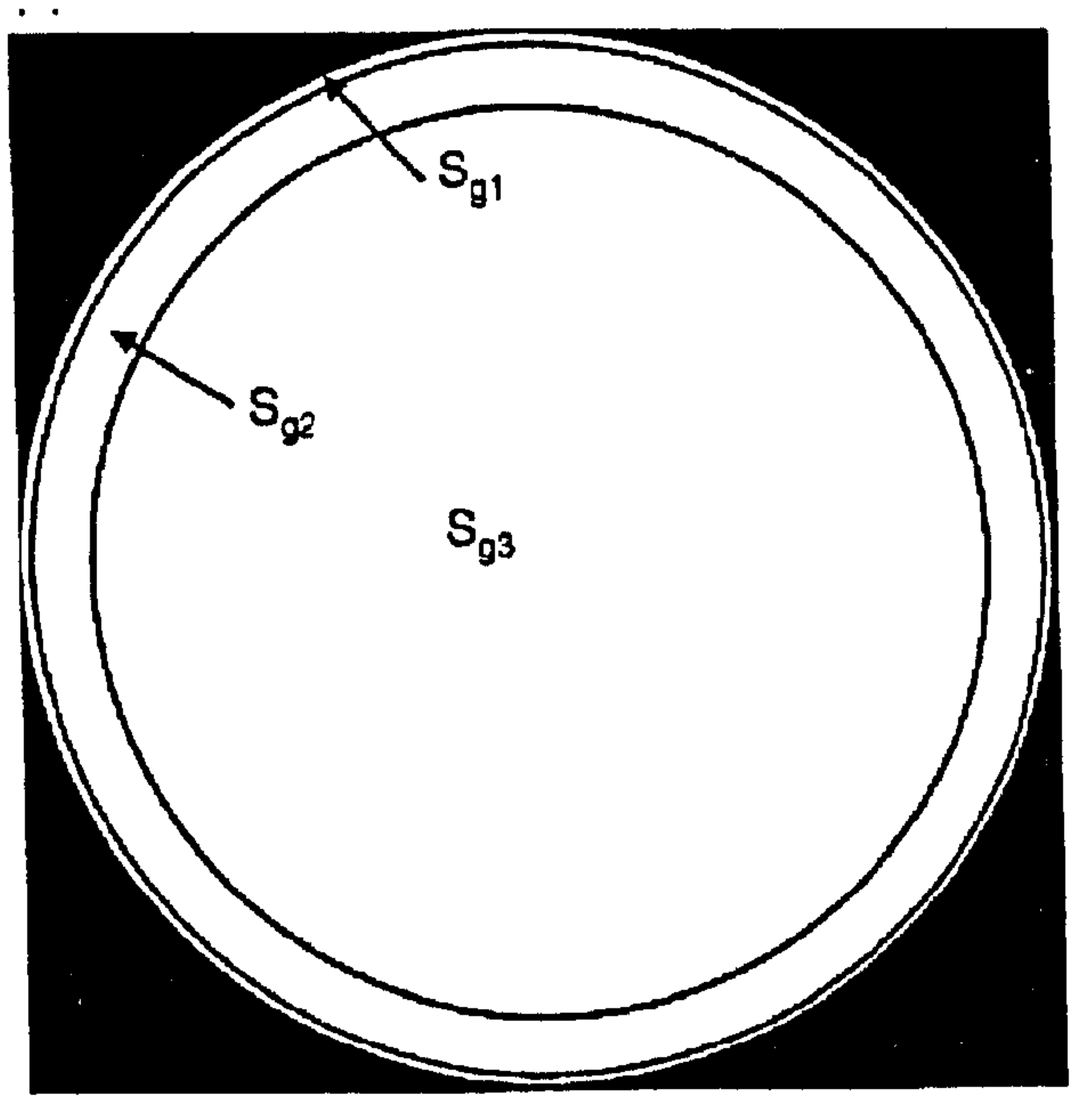

Figure 6-8 - Division of the ground hemisphere into three disjoint segments. [5]

This work detected that dividing the ground using the same approach used for sky, i.e. locating patches in a hypothetical ground hemisphere can mislead results. It occurs due to the significant difference between the distance from an analysed point to sky and to the ground. The distance from an analysed point to sky is virtually infinitum, giving no difference between angles from different points. Relating to the ground, distances are considerably smaller. This point is analysed theoretically in Appendix E.

Thus two different points emitting rays with same directional angles should find the same ground patch in an hemispherical ground, but not in a real ground surface. The case is illustrated on Figure 6-9. If the hemispherical approach was used both rays, A and B, would reach the same patch, but it does not occur in the real situation, when the ground is treated as a plan.

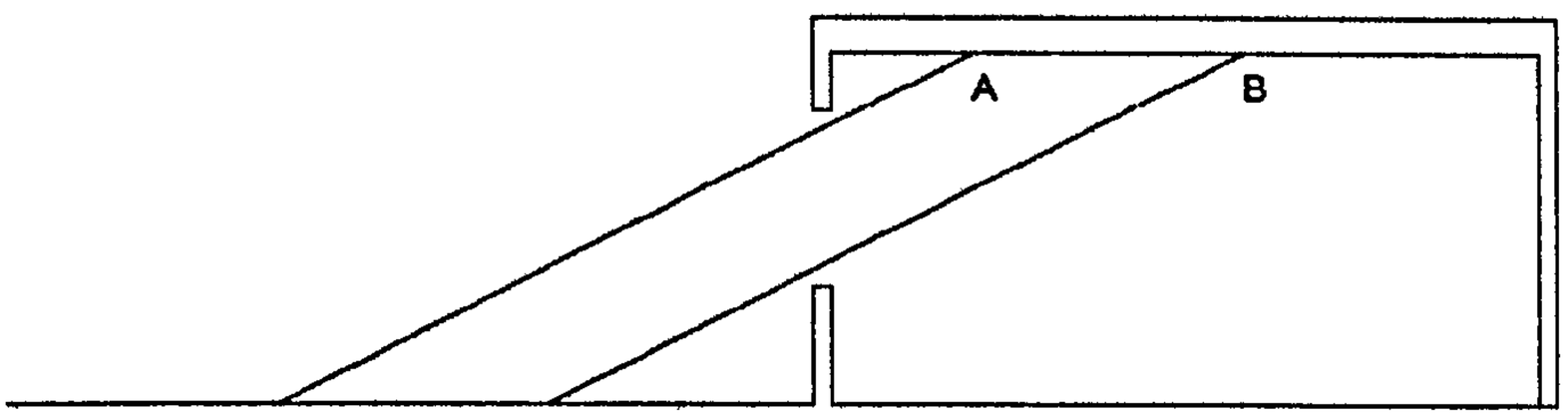

Figure 6-9 - Parallel rays reaching different ground patch

The problem is accentuated when external shading devices are incorporated to the analysed building, as shown in Figure 6-10. In this case, with the hemispherical method the ray would reach a ground patch in the other side of the building, even though it has no window, which is illogical.

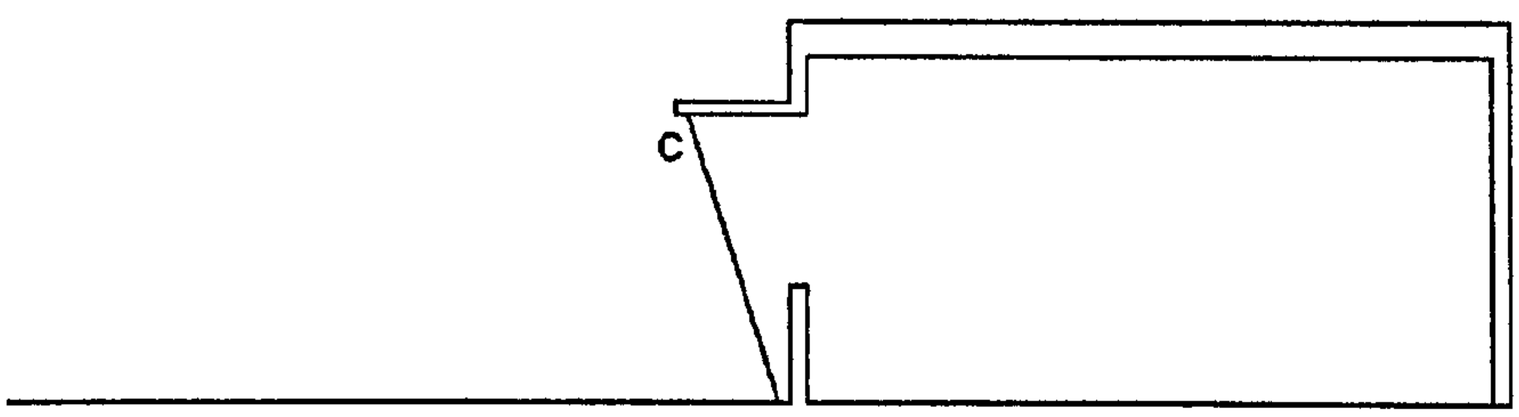

Figure 6-10 - Ray projected from overhang

Therefore, this work proposes working with the ground as a plane, having a subdivision in function of the necessity of ground analysis. Three options of ground subdivision are given. The first is based on rectangular patches with configurable dimensions. It has more accuracy, but needs more information with regard to ground reflectance, normally unavailable. The two others approaches divide the ground in strips parallels to the window façade. The strip width is fixed by distance from window façade in one proposal and fixed to an angle with vertex in the top of the window façade. The last method allows accurate results near the façade. This is more convenient for internal daylighting analysis, as ground far from window does not have a significant role in daylight contribution. The case study proposed in this

thesis uses the last approach. Angles varies from 0° to 90°, each 10°, giving 9 ground strips parallel to window façade as shown in Figure 6-11.

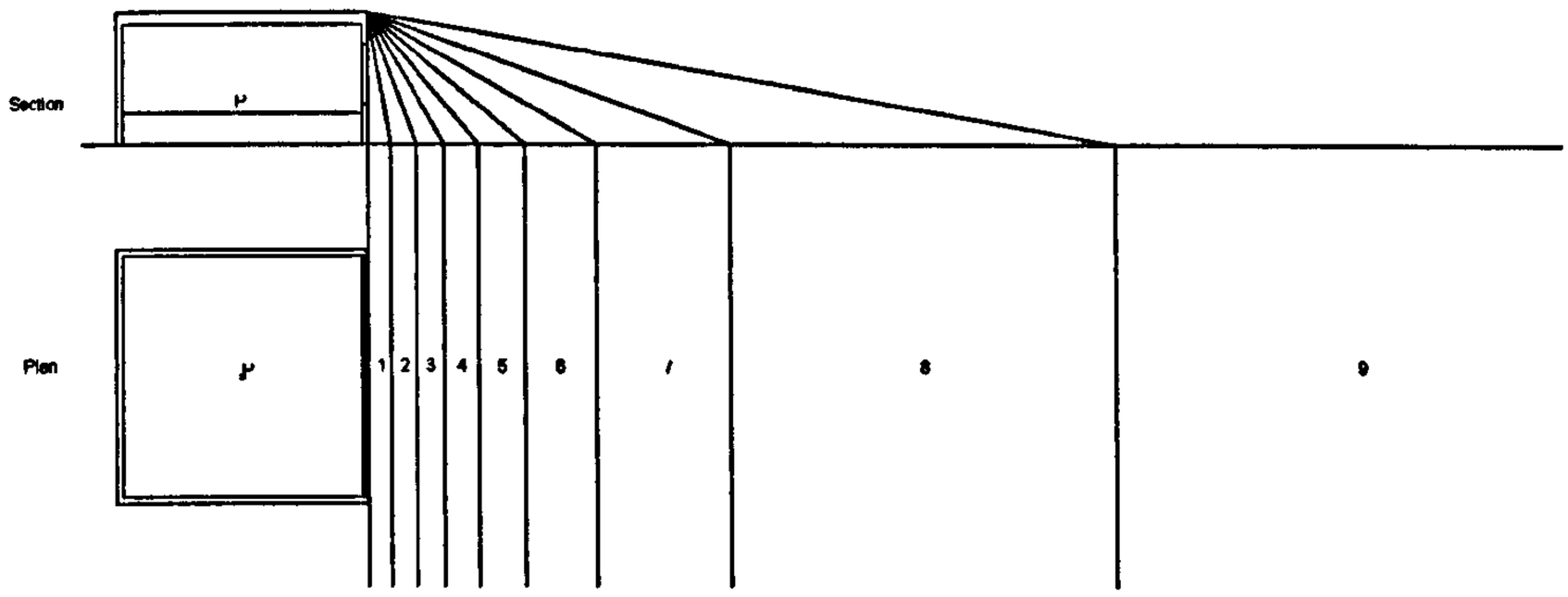

Figure 6-11 - Ground subdivision - strips parallel to window facade defined by angle

6.4.2 Obstruction subdivision

Generally, obstruction can be considered as one entire patch. When size or surface reflectance disparity justify it, a refined subdivision can be utilised, taking into account the fact that each patch will be treated as a point source. In this case, rectangular or strip shaped patches can be more convenient. Then a set of obstruction coefficients will be generated for each patch using the same calculation methods for the ground.

6.5 Calculation of daylight and auxiliary coefficients

In order to accelerate the computation of the daylight and auxiliary coefficients, this work splits the calculation into direct and internally reflected components. This is because the direct component can be calculated very quickly using simple equations. Interreflection simulation requires a more complex and time expensive procedure. For that, the Monte Carlo method was chosen, as observed in Chapter 5.

For the daylight coefficients the sky subdivision is different for direct and diffuse components, as seen in Section 6.3, resulting in a different number of calculations.

Since direct component requires more refined subdivision, the optimisation of its calculation can be significant for time spent on the whole process.

6.5.1 Approaches

There are two approaches to assess coefficients, deterministic and stochastic. The first is more convenient for direct components and the other for interreflected components. However, both can achieve results for all components. The choice will depend on accuracy and available time for computation.

6.5.1.1 Deterministic

A ray is emitted directed from the studied point to the centre of each patch. For daylight coefficients, d_d is calculated by Equation (6.3).

$$d_d = \sin\gamma.\tau_{\alpha j} \tag{6.3}$$

where, j is the sky patch index, γ is the solar altitude and α is the angle between ray and normal to window.

For auxiliary coefficients, c^*_d is calculated by Equation (6.4).

$$c^*_d = \cos\varepsilon_k.\tau_{\alpha k} \tag{6.4}$$

where ε_k is the angle between the ray and the normal to ground or obstruction, τ is the window transmittance, α is the angle between the ray and the normal to ground or obstruction, and k is the ground or obstruction patch index.

6.5.1.2 Stochastic

Rays are emitted following a statistical approach, the Monte Carlo method, discussed in Chapter 5. For daylight coefficients, the method is expresses in Equation (6.5).

$$d_i = \frac{\pi w_{ij}}{nP.\omega_j} \tag{6.5}$$

where w_{ij} is the weight of particles index i (see Table 6-2) on sky patch index j, nP is the number of emitted particles and ω_j is the angular area of sky patch j in steradian.

For auxiliary coefficients, it is calculated by Equation (6.6).

$$d_i = \frac{\pi w_{ik}}{nP.A_k} \tag{6.6}$$

where w_{ik} is the weight of particles index i (see Table 6-2) on ground or obstruction patch index k, nP is the number of emitted particles and A_k is the area of ground or obstruction patch k in m^2.

6.5.2 Daylight Coefficients

Daylight coefficients calculation is split into direct and interreflected components, discussed in sections 6.5.2.1 and 6.5.2.2.

6.5.2.1 Direct component

The direct component can be calculated using deterministic or stochastic procedures. The first, using Equation (6.3), is more convenient as it gives a more accurate result in less time. However since stochastic calculation would be used for the internally reflected component, and there is an insignificant cost for doing the direct calculation together, results can also be achieved using Equation (6.5). Although less precise, those results when compared to the deterministic method can lead to an evaluation of error on the statistical method, and to optimise the number of rays to be emitted by Monte Carlo simulation.

For external points, on ground or obstructions, daylight coefficients are calculated using Equations (6.7) and (6.8), respectively.

$$d_g = \sin\gamma_s \tag{6.7}$$

where γ_s is the sky elevation.

$$d_o = \cos\theta \tag{6.8}$$

where θ is the angle between ray from sky patch and normal to ground or obstruction. θ is calculated by Equation (6.9).

$$\cos\theta = c_1 d_1 + c_2 d_2 + c_3 d_3 \tag{6.9}$$

where c_1, c_2 and c_3, are direction cosines of ray from sky patch, and d_1, d_2 and d_3 are direction cosines of normal to ground or obstruction.

6.5.2.2 Internally reflected component

The internally reflected component of daylight coefficients is calculated using the stochastic approach considered in Section 6.5.1.2. It also uses Equation (6.5), but now the weight (w_{ij}) is based only on rays that come from the point to a sky patch, but necessarily reflecting on an internal wall. If the ray also reaches an external obstruction or the ground, it will be considered separately by auxiliary coefficients.

6.5.3 Auxiliary Coefficients

Auxiliary coefficients encompasses both ground and obstruction coefficients. They have similarities to daylight coefficients, but instead of being related to sky patches, auxiliary coefficients are related to ground or obstruction patches.

6.5.3.1 Direct component

The direct component is very rare for ground coefficients since generally a point in the workplane cannot 'see' the ground. For obstructions, it occurs more often; when sunshine is not considered it represents the ERC in daylight factor calculation. It can

be deterministically assessed by Equation (6.4), or stochastically using Equation (6.6), taking into account observations that arose in section 6.5.2.1.

6.5.3.2 Internally reflected component

The internally reflected component of the auxiliary coefficients is also calculated using the stochastic approach using Equation (6.6), but with weight (w_{ik}) based only on rays that come from the analysed point to a ground or obstruction patch and necessarily reflect on an internal wall.

6.6 Equations for illuminance calculation

This section describes illuminance equations to be used in the program created for this thesis (Chapter 7). Equations are based on the concept of the luminance/illuminance ratio (N) described on section 6.6.1.

6.6.1 N: the luminance/illuminance ratio

To generalise daylighting calculations, sky luminance is often normalised with respect to zenith luminance. This is suitable for temperate region, but in tropical latitudes, where the sun is often near the zenith, this can be a source of significant error. Tregenza [6] proposes an alternative approach using horizontal diffuse illuminance as the reference. It solves the problem of solar position and has the advantage of using the most common daylight measurement. Moreover, results can be related to measured data, daylight factors or ground coefficients.

Thus, the luminance (L) of a sky patch, j, is divided by the illuminance on a horizontal surface from the unobstructed sky, as shown in Equation (6.10).

$$N_j = \frac{L_j}{\sum_j L_j \omega_j \sin(\gamma_j)} = \frac{L_j}{E_h} \qquad (6.10)$$

where j is the sky patch index, γ_j is the sky patch altitude, ω_j is the angular area of sky patch in steradian. The sky should have a defined luminance distribution, for instance one of the CIE's standard skies.

6.6.2 Illuminance from the sun

For solar components, illuminance is calculated by Equation (6.11).

$$E_i = d(i, j_s) \times E_{sn} \tag{6.11}$$

where, E_{sn} is the solar normal illuminance in lux and $d(i,j_s)$ is the daylight coefficient for surface i and the sky patch where the sun is located (j_s).

6.6.3 Illuminance from the whole sky

The illuminance on a given surface, i, from the whole sky, can be calculated rearranging Equation (6.1), as shown in Equation (6.12).

$$E_i = \sum_j L_j d(i, j) \omega_j \tag{6.12}$$

where L_j is the Luminance of sky patch j; $d(i,j)$ is the daylight coefficient for surface i and sky patch j; ω_j is the subtended area of the sky patch in steradian.

Including the concept of luminance/illuminance ratio (Section 6.6.1), joining Equations (6.10) and (6.12), previous equation can be expressed by Equation (6.13).

$$E_i = E_h \sum_j N_j d(i, j) \omega_j \tag{6.13}$$

where E_h is the horizontal illuminance; and N_j is the luminance/illuminance ratio for sky patch j (see Section 6.6.1).

6.6.4 Illuminance from an indirect source of natural light

The illuminance on a given surface, *i*, from another surface, *k*, considered perfectly diffusing, is given by Equation (6.14).

$$E_i(k) = \frac{E_k \rho_k}{\pi} \times c^*(i,k) A_k \qquad (6.14)$$

where E_k is the horizontal illuminance on surface *k*; ρ_k is its reflectance; $c^*(i,k)$ is the auxiliary coefficient at surface *i* from surface patch *k*; A_k is the area of surface patch *k* in m^2.

But since the horizontal illuminance on surface k is expressed by Equation (6.15).

$$E_k = \sum_j L_j d(k,j) \omega_j \qquad (6.15)$$

where L_j is the luminance of sky patch *j*; *d(k,j)* is the daylight coefficient at surface patch *k* from sky patch *j*; ω_j is the subtended area of the sky patch in steradian.

Then, Equation (6.14) can be rearranged as Equation (6.16).

$$E_i(k) = \left[\sum_j L_j d(k,j) \omega_j \right] \times \frac{\rho_k}{\pi} \times c^*(i,k) A_k \qquad (6.16)$$

Moreover, adding all surfaces on Equation (6.16) gives the total illuminance due to an external indirect source of natural light (E_i^r), as expressed by Equation (6.17).

$$E_i^r = \sum_k \sum_j L_j d(k,j) c^*(i,k) \omega_j A_k \frac{\rho_k}{\pi} \qquad (6.17)$$

Including the concept of luminance/illuminance ratio, E_i^r can be calculated by Equation (6.18).

$$E_i^r = \sum_k \sum_j N_j E_h d(k,j)\, c^*(i,k)\, \omega_j A_k \frac{\rho_k}{\pi} \tag{6.18}$$

When the primary source is the sun, illuminance is calculated by Equation (6.19).

$$E_i = \sum_k d(k,j) E_{sn} c^*(i,k) A_k \frac{\rho_k}{\pi} \tag{6.19}$$

6.6.5 Global Illuminance

In the method proposed in this thesis, the global illuminance is calculated as the sum of twelve elements, which are defined in function of their source of light and track of ray, as described in Table 6-2. It is expressed by Equation (6.20).

$$E = \sum_{i=1}^{12} E_i \tag{6.20}$$

where, E is the illuminance and i is the illuminance index according to Table 6-2, which indicates the path of ray and the primary source of light.

Table 6-2 - Illuminance index by ray track and primary source of light

	Ray			
Index	**From**	**To**	**Way**	**Source**
1	Internal Point	Sky Patch	Direct	Sky
2	Internal Point	Sky Patch	Internally reflected	Sky
3	Internal Point	Ground	Internally reflected	Sky
4	Internal Point	Obstruction	Internally reflected	Sky
5	Internal Point	Obstruction	Direct	Sky
6	Internal Point	Ground	Direct	Sky
7	Internal Point	Sky Patch	Direct	Sun
8	Internal Point	Sky Patch	Internally reflected	Sun
9	Internal Point	Ground	Internally reflected	Sun
10	Internal Point	Obstruction	Internally reflected	Sun
11	Internal Point	Obstruction	Direct	Sun
12	Internal Point	Ground	Direct	Sun

Each component of the global illuminance is calculated using equations according to Table 6-3. Same general equations for different illuminance component are discriminated by different daylight or auxiliary coefficients, as discussed in section 6.5.

Table 6-3 - Equations for calculation of illuminance components

Index	Component description	Equation
1	Direct, source sky	(6.13)
2	Internally reflected, source sky	(6.13)
3	Internally reflected from ground, source sky	(6.18)
4	Internally reflected from obstruction, source sky	(6.18)
5	Direct from obstruction, source sky	(6.18)
6	Direct from ground, source sky	(6.18)
7	Direct, source sun	(6.11)
8	Internally reflected, source sun	(6.11)
9	Internally reflected from ground, source sun	(6.19)
10	Internally reflected from obstruction, source sun	(6.19)
11	Direct from obstruction, source sun	(6.19)
12	Direct from ground, source sun	(6.19)

6.7 Conclusion

This chapter has presented the daylight coefficients concept, proposing a set of equations for using in a daylight simulation program. It has detected some limitation in the method for ground reflected light studies and proposes a new approach to generalise its use. It also suggests some improvements in sky subdivision and the introduction of the auxiliary coefficients to deal with obstructions and ground reflected light. The daylight coefficients concept together with ray tracing and the Monte Carlo techniques, discussed in Chapter 5, are the theoretical basis of the computer program presented in Chapter 7.

References

1. Tregenza, P. and I. M. Waters, *Daylight coefficients.* Lighting Research & Technology, **15**(2): p. 65-71, 1983.

2. Tregenza, P. R., *Subdivision of sky hemisphere for luminance measurements.* Lighting Research and Technology, **19**(1987): p. 13-14, 1987.

3. CIE - Commission Internationale de l'Eclairage, *Guide to recommended practice of daylight measurement*, CIE - Commission Internationale de L'Eclairage: Wien, 1994.

4. CIE - Commission Internationale de l'Eclairage, *The IDMP Network.* CIE. http://idmp.entpe.fr/, 1997.

5. Reinhart, C. F. and S. Herkel, *The simulation of annual daylight illuminance distributions - a state-of-the-art comparison of six Radiance-based methods.* Energy and Buildings, **32**: p. 167-187, 2000.

6. Tregenza, P. R., *Standard skies for maritime climates.* Lighting Research and Technology, **31**(3): p. 97-106, 1999.

7. Mardaljevic, J., *Daylight simulation: validation, sky models and daylight coefficients*, PhD, in *Institute of Energy and Sustainable Development*, De Montfort University. 313 p., 1999.

8. Tsangrassoulis, A. and M. Santamouris, *Daylight modelling with passport-light.* 1997.

9. Tregenza, P. R., *The sensitivity of room daylight to sky brightness.* Architectural Science Review, **42**(june 1999): p. 129-132, 1999.

10. Tregenza, P. and S. Sharples, *Daylight algorithms*, University of Sheffield: Sheffield, 1993.

11. Littlefair, P. J., *Daylight coefficients for practical computation of internal illuminances.* Lighting Research and Technology, **24**(3): p. 127-135, 1992.

Chapter 7 The computer simulation tool

7.1 Introduction

One of the bases of this research is the creation of a computer program that is able to simulate daylight performance in a typical tropical environment. This chapter introduces the general principles of the program. Its methodology is based on the concepts of the Monte Carlo method, ray tracing and daylight coefficients, discussed in the two previous chapters. The code validation was carried out by assessing the stochastic and the deterministic error. First evaluates the scattering of results due to Monte Carlo method and a procedure is suggested to improve performance. Second appraises the systematic error due to bugs or limitation on the chosen techniques. It uses three different approaches: simplified methods, recognised lighting software, and real data. In addition, the feasibility of the method was tested assessing the time expended for a regular situation. The program has been shown as a suitable research daylighting tool.

7.2 Aims

The objective for the development of the computer program was to evaluate different algorithms and test different approaches, allowing varying parameters in accord to the specific requirements for daylighting in the humid tropics. It should give a general picture of the internal illuminance in single rooms, allow different window systems, look of the aspects of outside conditions and cope with any sky luminance distribution, including sunlight.

The program was treated as a piece of laboratory tool instead of a finished package. However, the code developed during this research has attained some goals that may be considered as the foundation of a computer tool for daylighting researchers, in particular for the tropics, to be finished in the future.

The program started with some procedures developed in the department using MATLAB environment running on a PC. They were rewritten in order to achieve the

specific goals and connected to the new developed code to form an integrated tool. Basic GUI techniques were used to facilitate its use and batches were allowed to automate repeated running.

The code development and testing took about nine months to achieve the primary goals. Although new codes – mainly in the output module – as well as adjustments and bug correction were still done later on. The whole commented source code encompasses more than 12,000 lines. The Appendix F gives the code for the core part of the software.

To simplify reference, the program is referred to herein as TropLux.

7.3 Overview of the software

TropLux was developed in five modules: Input, Set up, Run, Output and Utility. Table 7-1 concisely describe the main codes of each section, while Figure 7-1 to Figure 7-5 show the module menus. The core procedures are in the Run Module. They are described in flowcharts shown from Figure 7-6 to Figure 7-8.

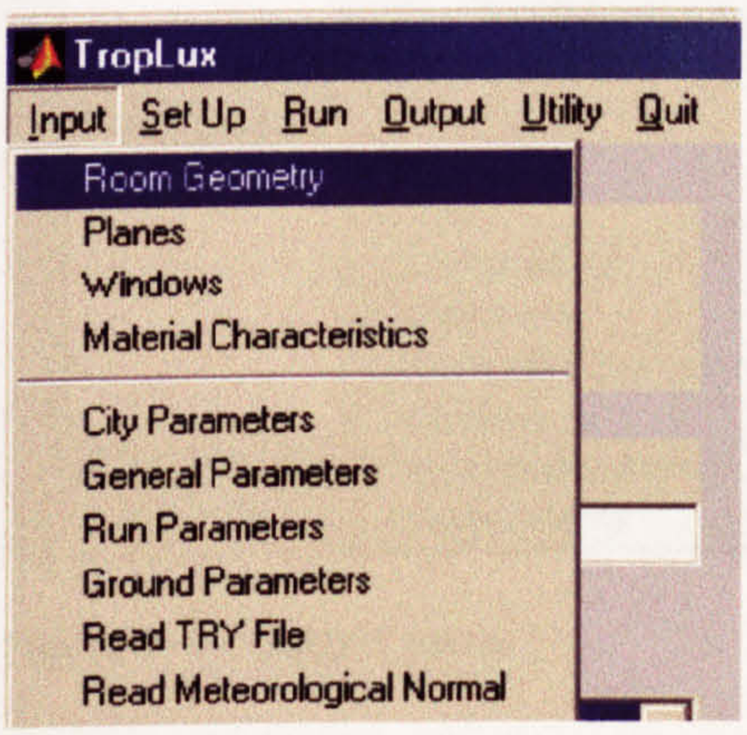

Figure 7-1 - Input menu

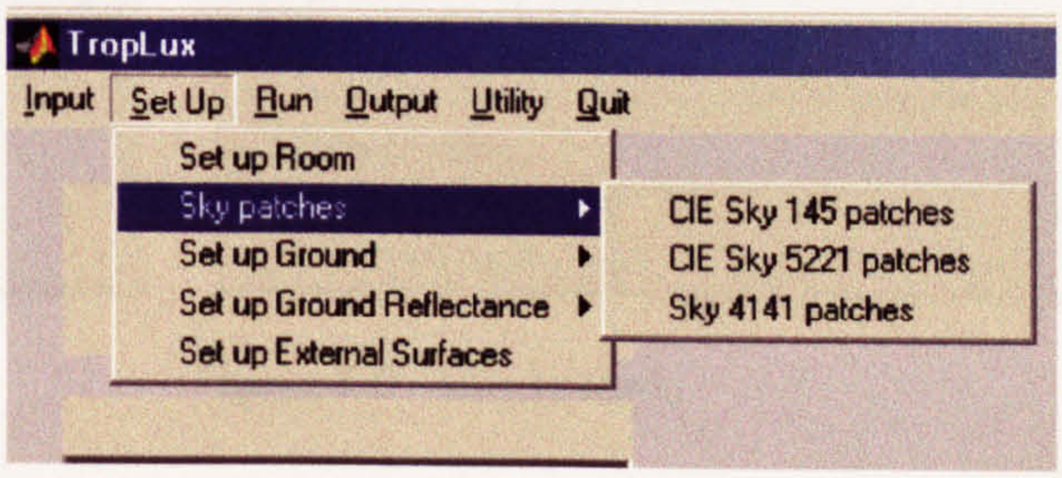

Figure 7-2 - Set up menu

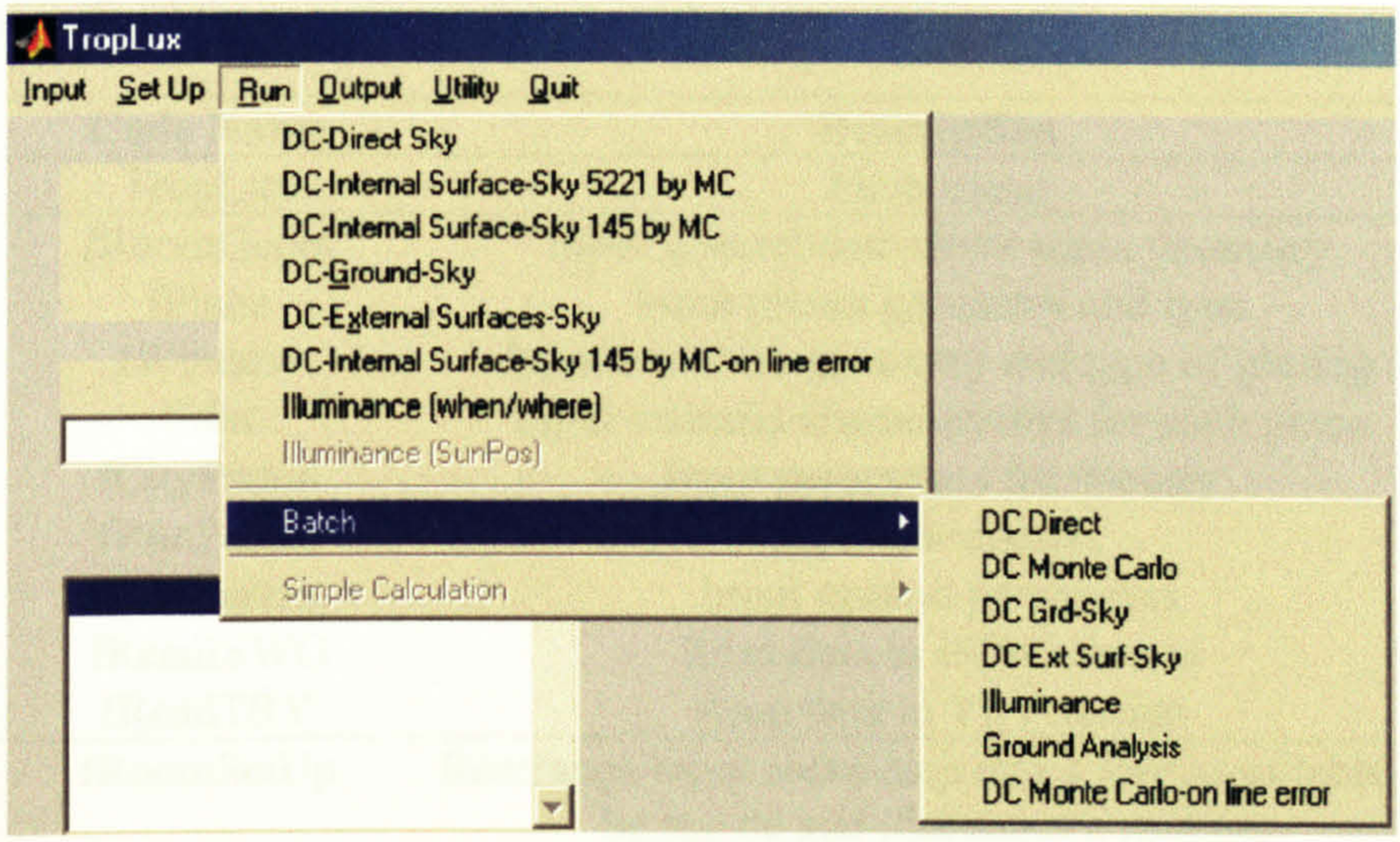

Figure 7-3 - Run menu

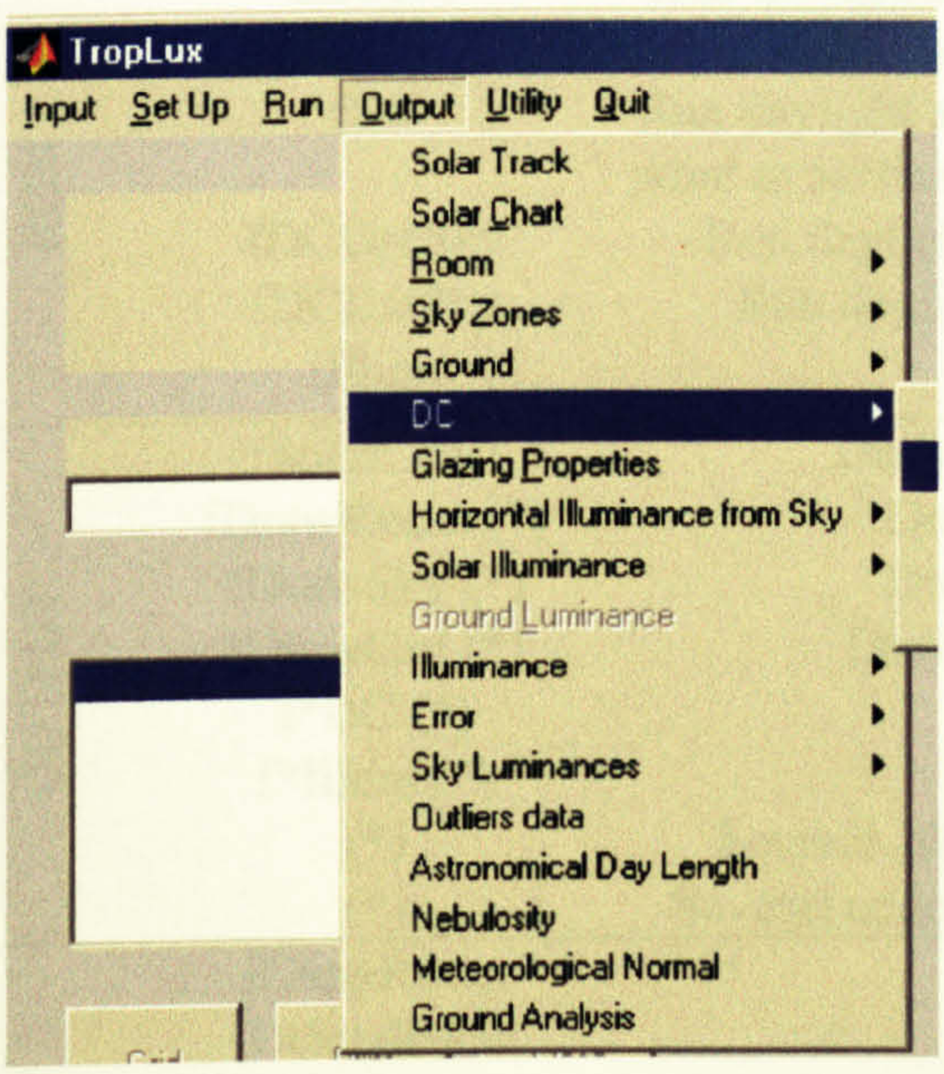

Figure 7-4 - Output menu

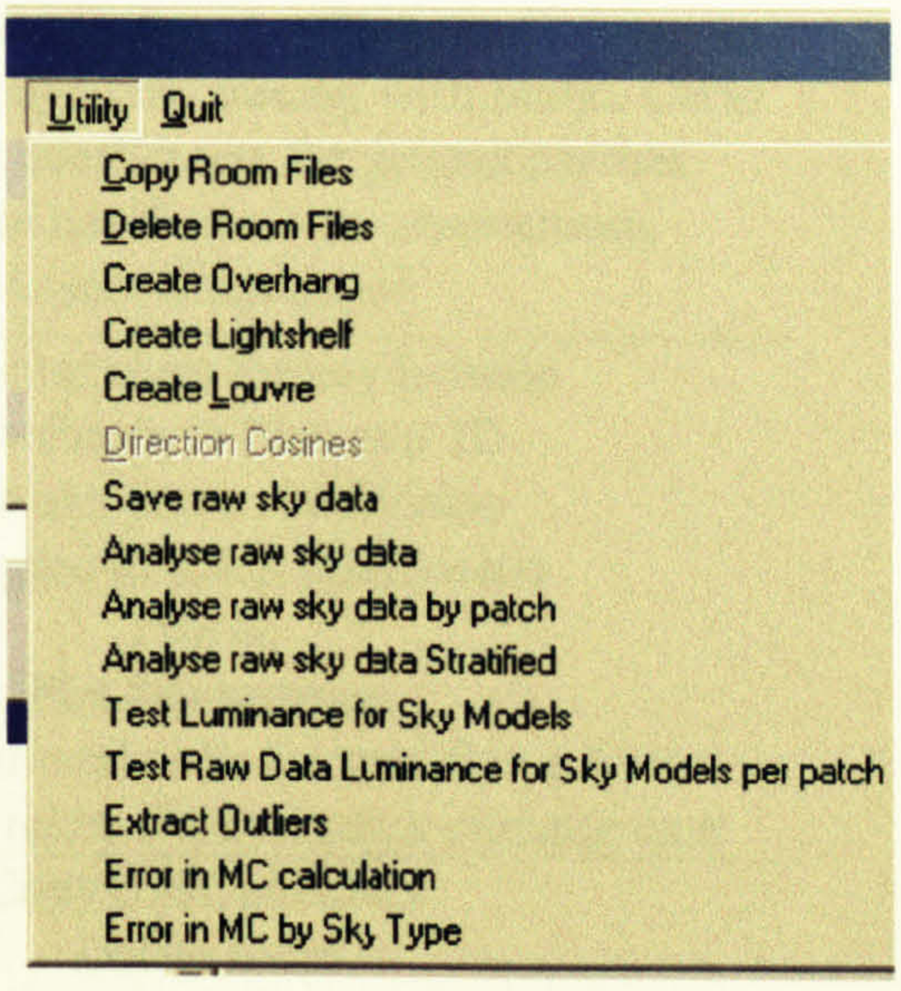

Figure 7-5 - Utility Menu

Table 7-1 - List of main subroutines

Mod	Code Name	Description
	TropLux	Main menu
INPUT	fRoomGeom	Input general data about room geometry
	fPlane	Input planes geometry and type
	fWindow	Input windows geometry and type of glazing
	fMat	Input material characteristics for each plane
	fCityParam	Input parameters for the city
	fRunParam	Input parameters
	fGrdParam	Input ground parameters
	fReadISWO	Read data in ISWO format
	fReadTRY	Read data in TRY format
SETUP	fRoomSetUp	Rearrange input room data into a format suitable to be run dc and illuminance routines
	fSetSky	Set up sky patch subdivision
	fSetGrd	Set up ground patches
	fSetGrd2Ref	Set up reflectance for ground patches
	fSetExt	Set up obstruction data
RUN	dDCDir	Run the direct component of daylight coefficients for internal point using direct ray tracing
	fDC	Run daylight and auxiliary coefficients for internal point or surface using ray tracing with Monte Carlo
	fDCGrdSky	Run daylight coefficients for ground patches
	fDCExtSky	Run daylight coefficients for obstructions
	fIllum	Assess illuminance
OUTPUT	fSolarChart	Draw solar chart for any latitude
	fDrawRoom (*)	Draw Room in Plan and 3D
	fDrawSky (*)	Draw sky patch subdivision
	fDrawGrd (*)	Draw ground patch subdivision
	f*DC (*)	Plot dc
	f*Illum (*)	Plot Illuminance
	(*)	Several additional code for specifics output
	(*)	Several codes relate field research climatic data
UTILITY	fCopyRoom	Copy room structure
	fDeleteRoom	Delete room
	fCreateOvehang	Generate overhang
	fCreateLightshelf	Generate lightshelf
	fCreateLouvre	Generate louvre
	(*)	Several codes relate to analysis of field research climatic data

(*) several codes

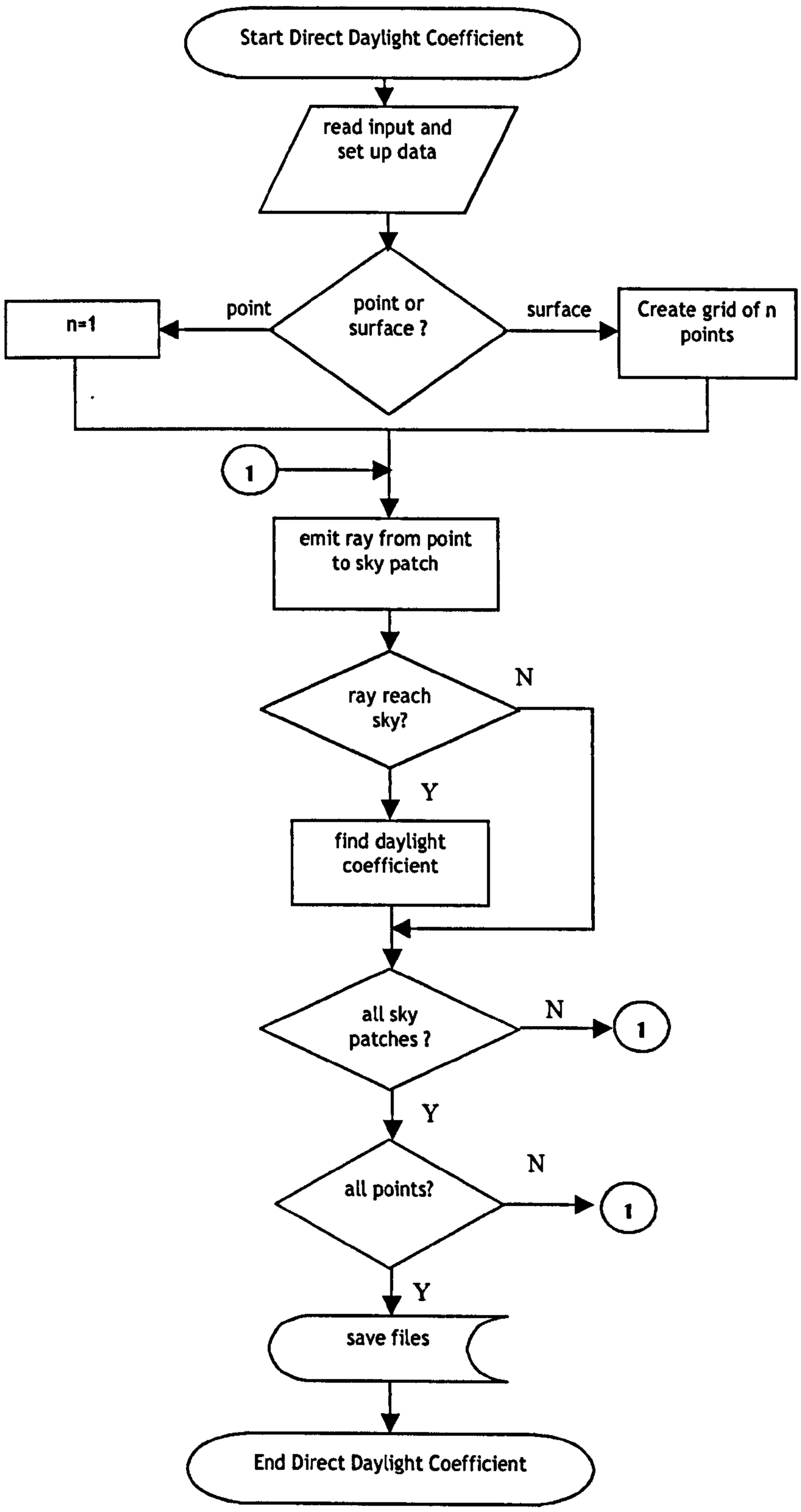

Figure 7-6 - Flowchart for fDCDir

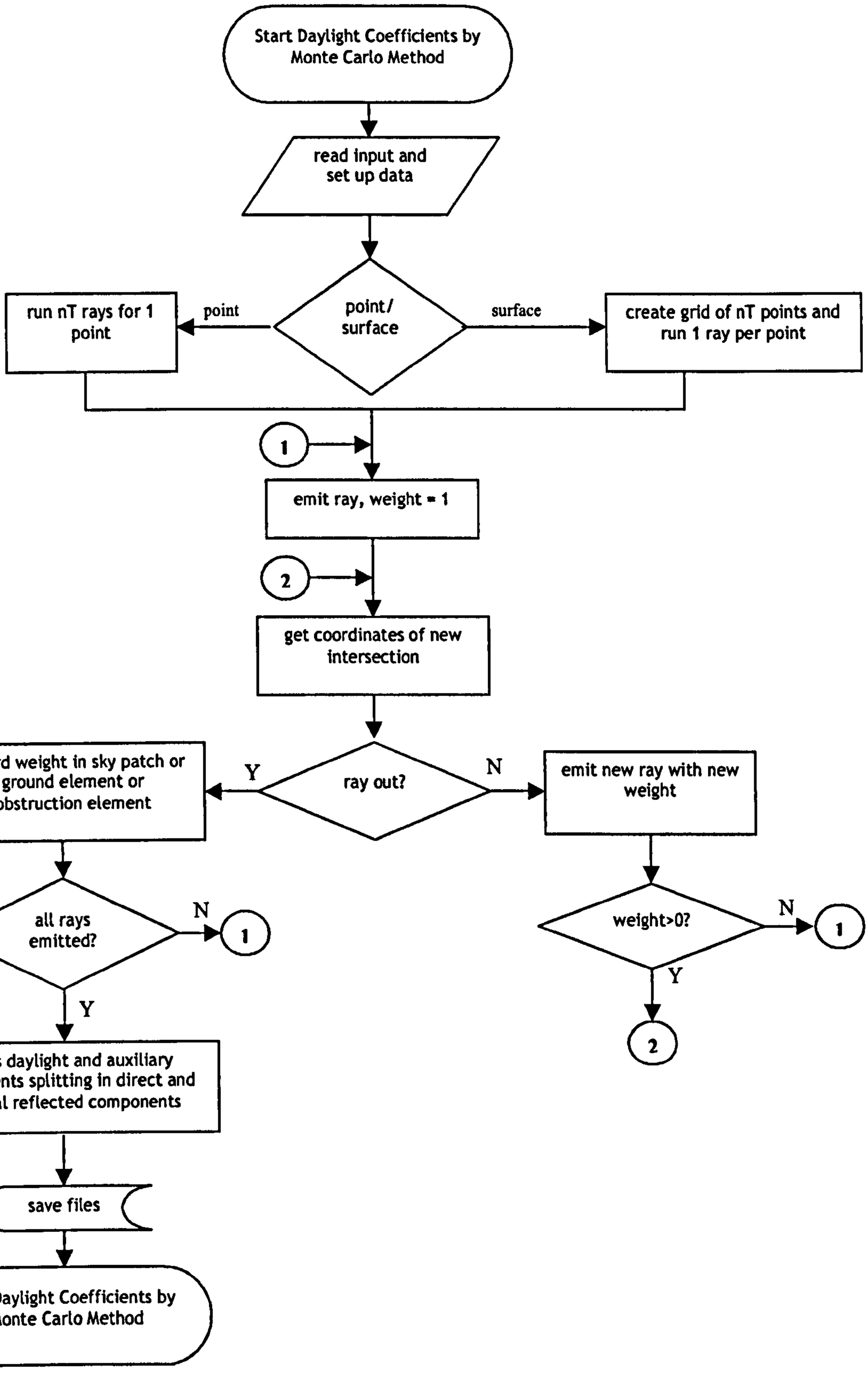

Figure 7-7 - Flowchart for fDC

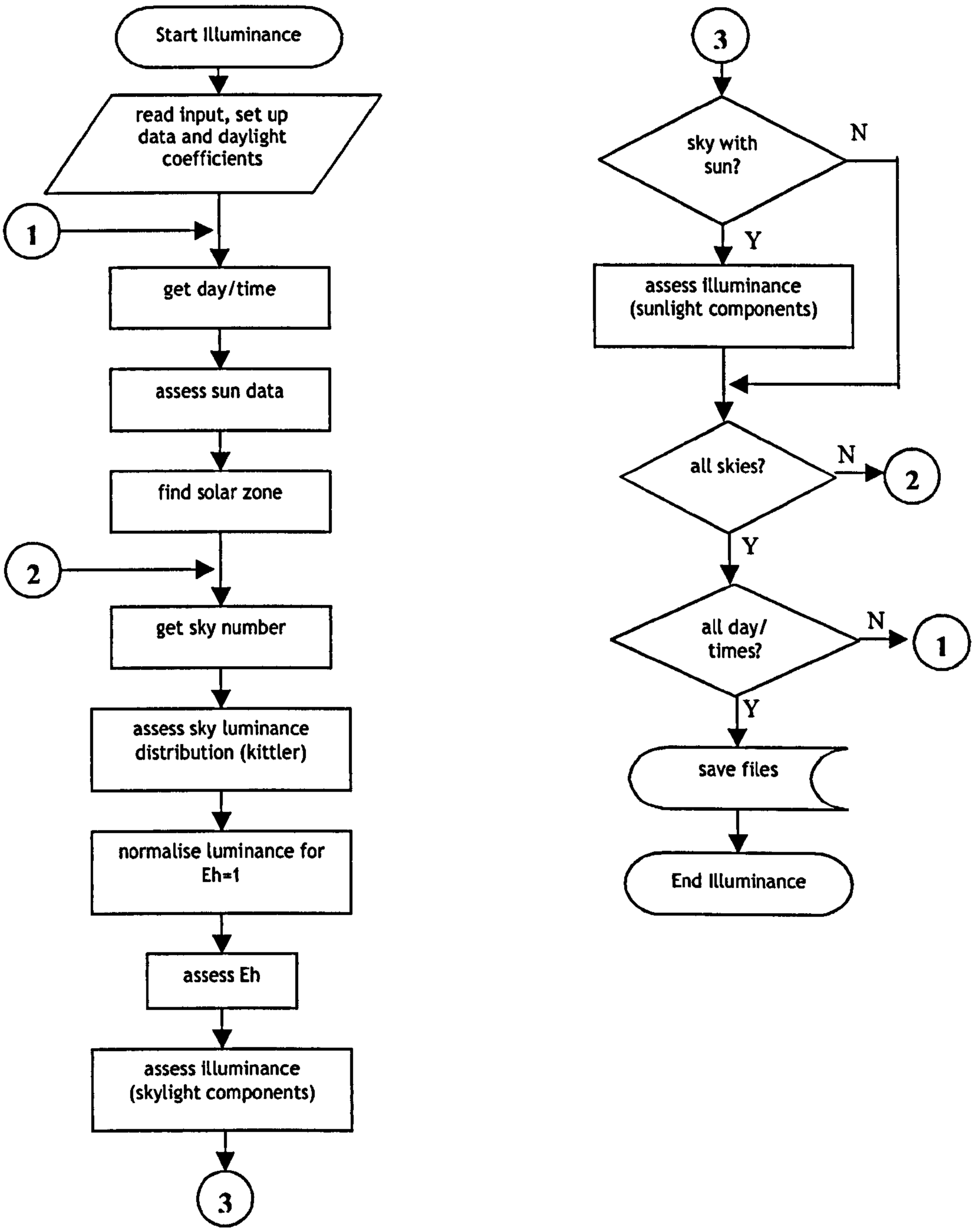

Figure 7-8 - Flowchart for fIllum

The adopted methodology allows illuminance to be split into 12 components as per to Table 7-2.

Table 7-2 - Illuminance components

Order	Component description and source of light	
1	Direct	Sky
2	Internally reflected (only)	Sky
3	Ground and int. reflected	Sky
4	Obstruction and int. reflected	Sky
5	Obstruction direct	Sky
6	Ground direct	Sky
7	Direct	Sun
8	Internally reflected (only)	Sun
9	Ground and int. reflected	Sun
10	Obstruction and int. reflected	Sun
11	Obstruction direct	Sun
12	Ground direct	Sun

Using the concepts of ground and obstruction coefficients (see Section 6.4), TropLux split the internal reflected component in order to assess ground and obstruction contribution. When a ray bounces both in an obstruction and ground the code counts its contribution to where it last bounced.

When the absolute sky luminance is not provided for each patch (by IDMP data, for instance), TropLux calculates the diffuse illuminance (components 1 to 6) based on CIE sky models and on the exterior horizontal illuminance. The horizontal illuminance can be defined by the user or automatically calculated based on IES equations [1], as seen in Figure 7-9.

The same approach is adopted for the sun's contribution. When not available, the solar illuminance is based on the CIE proposal [2], that takes into account the optical air mass, the luminous extinction under a clean and dry (Rayleigh) atmosphere and the luminous/illuminance turbidity factor. It can be calculated for every CIE standard sky, when the sun is present.

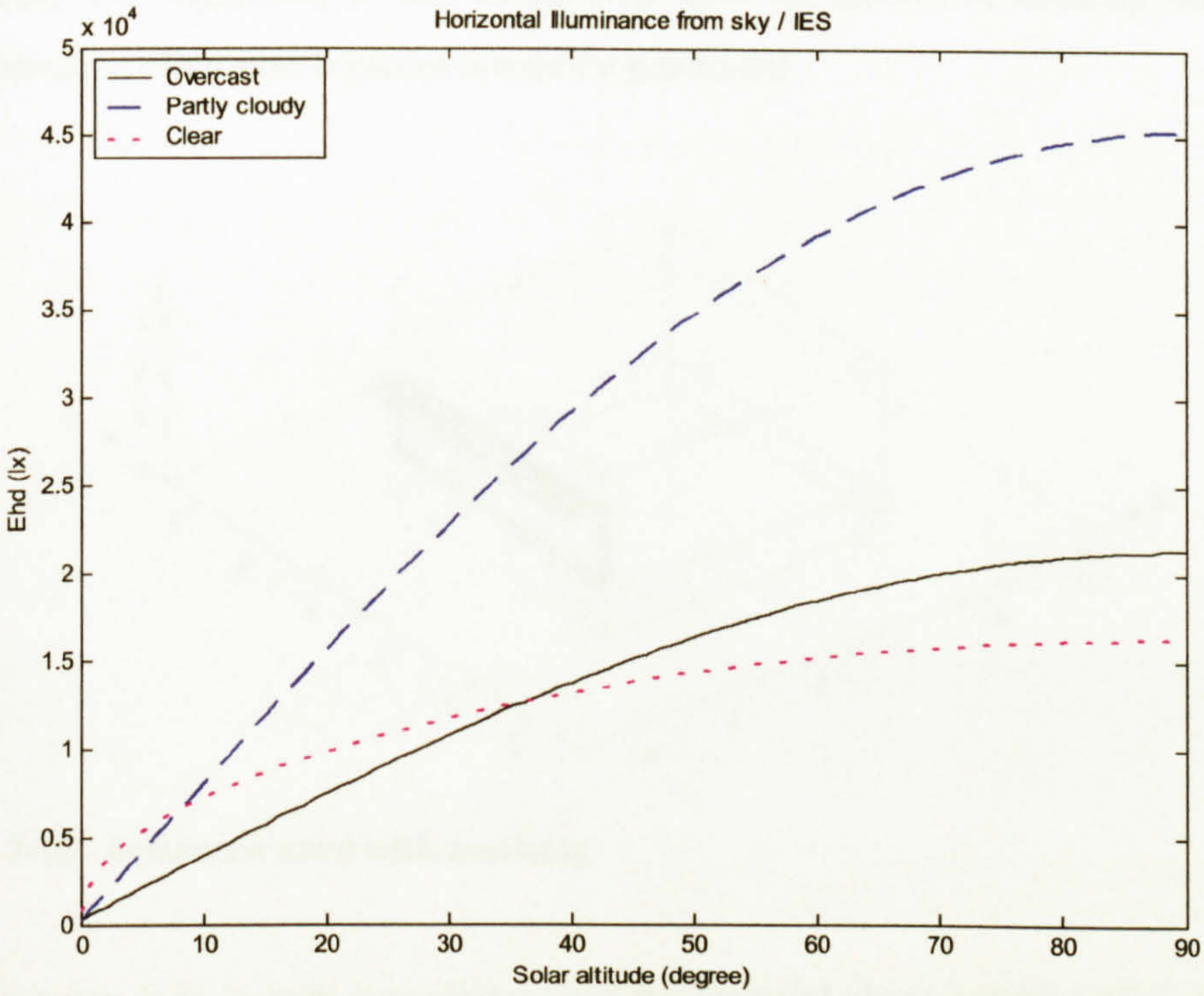

Figure 7-9 - Horizontal illuminance from sky - based on IES equation

7.4 Example of using the program

A reference room with an overhang as shown in Figure 7-10 is used to demonstrate how TropLux works.

The first step is to input room geometry data. Figure 7-11 shows the sample values in its fields in the input window. Then the planes should be generated using the 'Planes' option on the input menu. After typing the room number, if its room geometry has been input, it will generate 15 basic planes for the rectangular room, including workplane, internal and external walls, plus ground. Then new planes can be input manually using fields shown in Figure 7-12. If the geometry is not rectangular, all planes should be input independently. Four points are used to limit the plane and they have to be input in anticlockwise order, in relation to the axis origin view. Since shading devices are basic elements in tropical daylighting, three codes were developed to automate the creation of overhangs, lightshelves and louvres. These options are in the Utility Menu. In this example, one overhang with 1.00 m was

generated. For simplicity it was considered with no thickness, creating only two more planes – otherwise 6 planes would be generated.

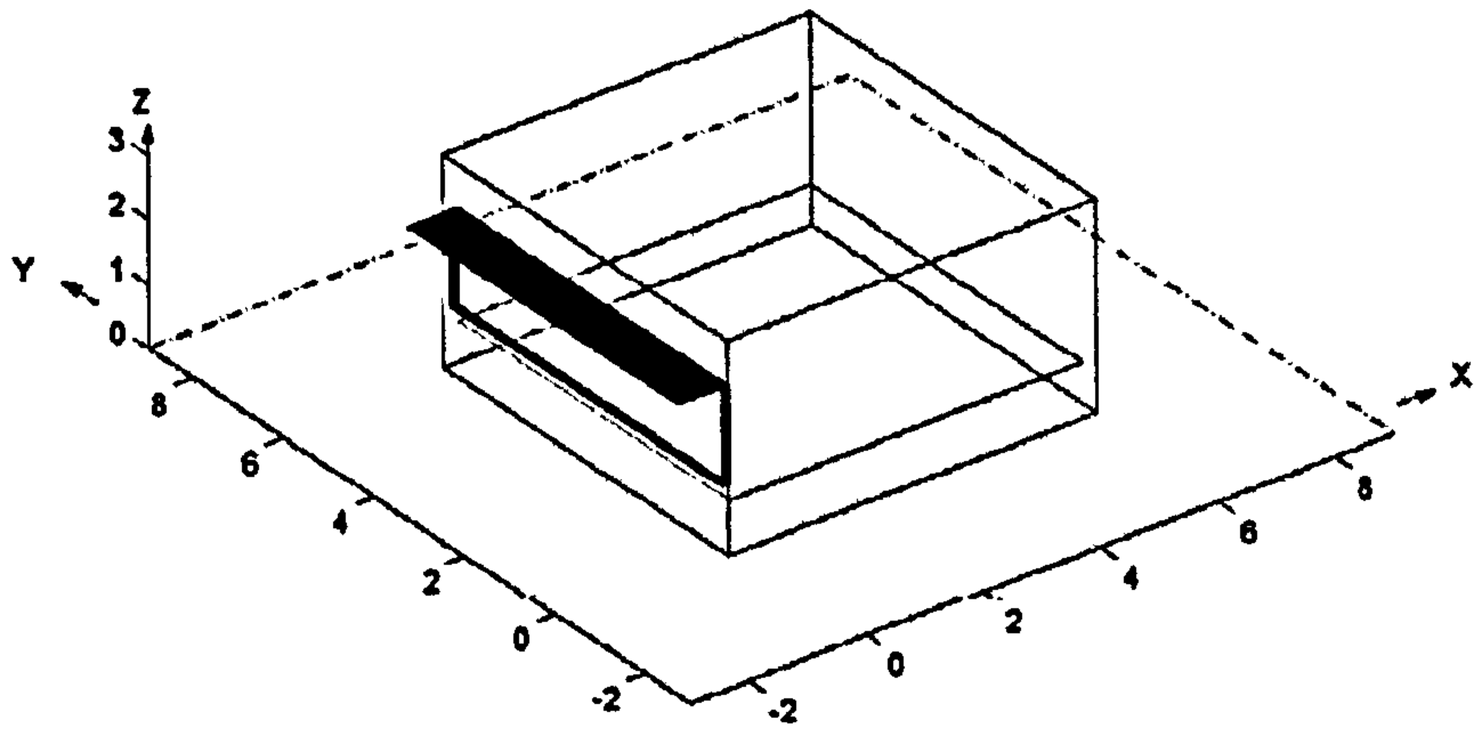

Figure 7-10 - Reference room with overhang

The next step is to include the window and the material characteristics of each plane. Windows should be defined in the same manner as a plane, with four points anticlockwise, including in which plane it is located and, if it is the case, what is the next window in the same plane (see Figure 7-13). When a window is input, the program generates automatically the frame planes with width based on the wall thickness previously input in Room Geometry option. The program actually creates two windows, one in the internal wall and another in the external wall for compatibility. Material characteristics are input for each plane as seen in Figure 7-14. Reflectance and transmittance can have both diffuse and specular components. For this example, only diffuse reflectance is defined for every plane. Default window has clear glass. Transmittance is function of the angle of incidence, and the input transmittance is assumed to be that for light incident onto the glass perpendicularly.

In addition, several parameters are necessary. Figure 7-15 shows how to input city parameters. Ground parameters are input as shown in Figure 7-16. The ground subdivision should be chosen among three preset types: type 1 as a set of squared patches; type 2 as a set of stripes parallel to the window façade and spaced with an even angle (vertex in the top of façade, being 0° at the bottom and 90° at the horizon); and type 3 as a set of stripes parallel from window façade with constant

width. All of the ground subdivisions can be customised by the user. If the ground is considered as a whole with single reflectance, any of the preset types can be used, providing just one reflectance is input for every ground patch. If just one patch is used, the accuracy in the reflected component may decrease significantly. Even when just one reflectance is provided, the ground should be split in a reasonable number of patches. As a standard, nine patches for the ground type 2 is recommended.

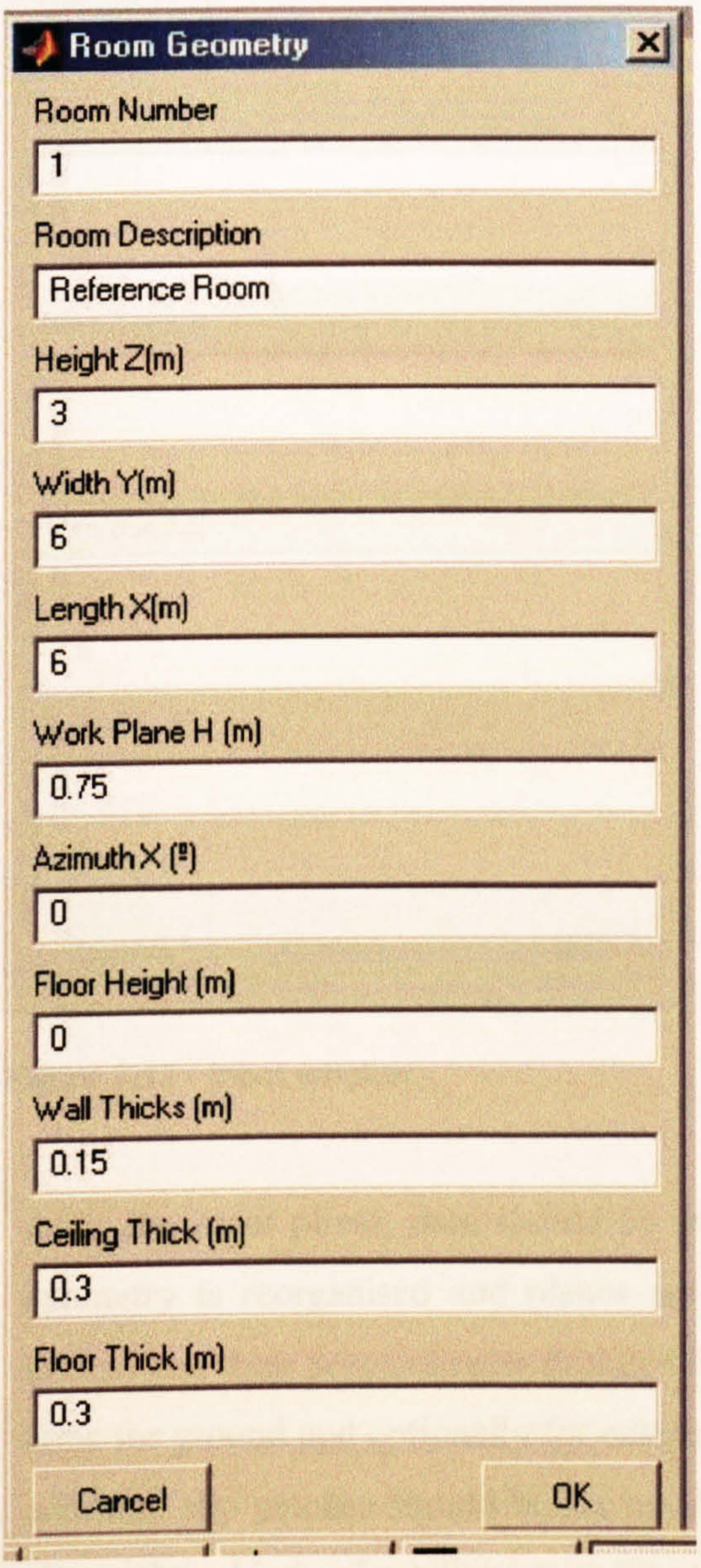

Figure 7-11 - Input room geometry details

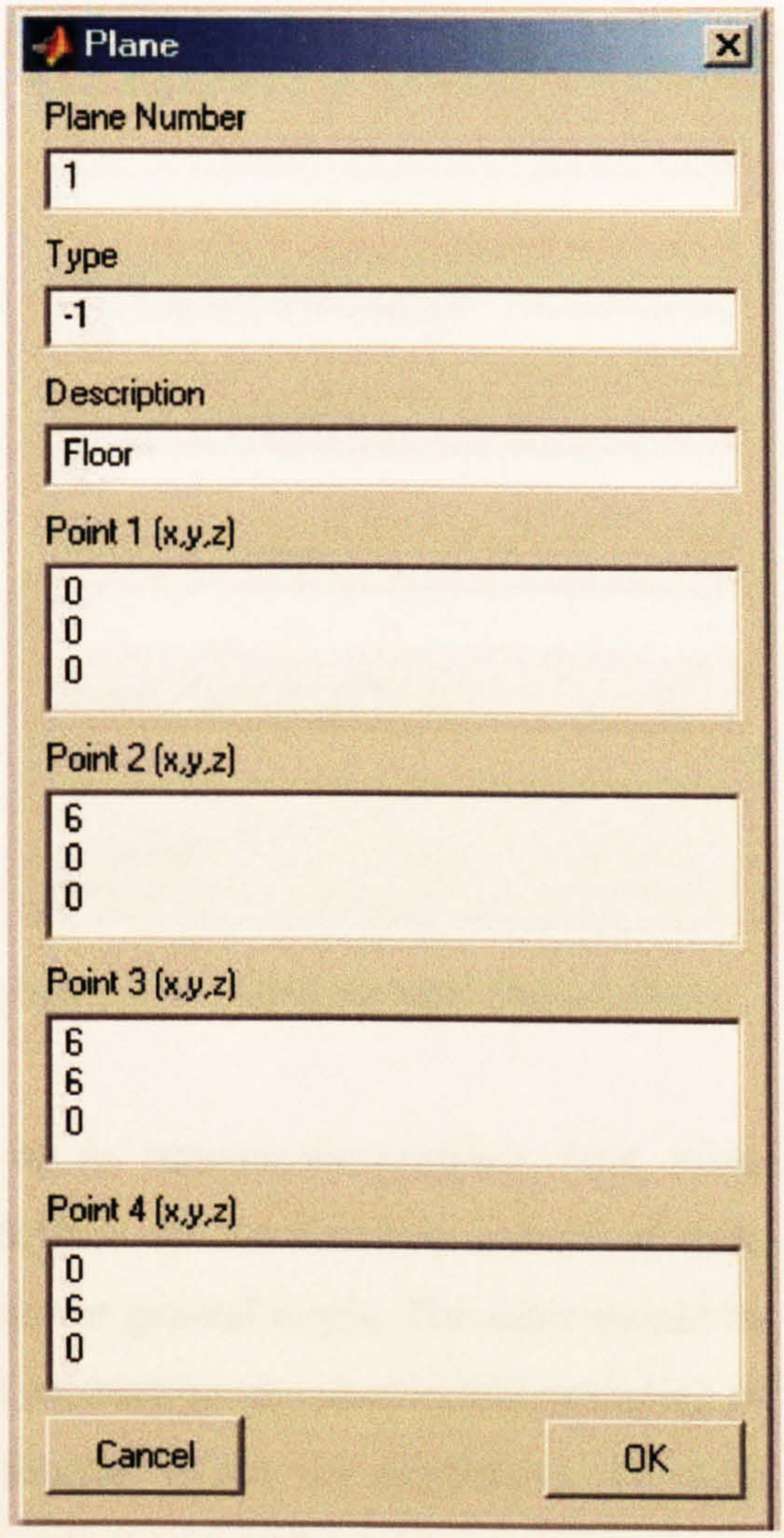

Figure 7-12 - Input plane

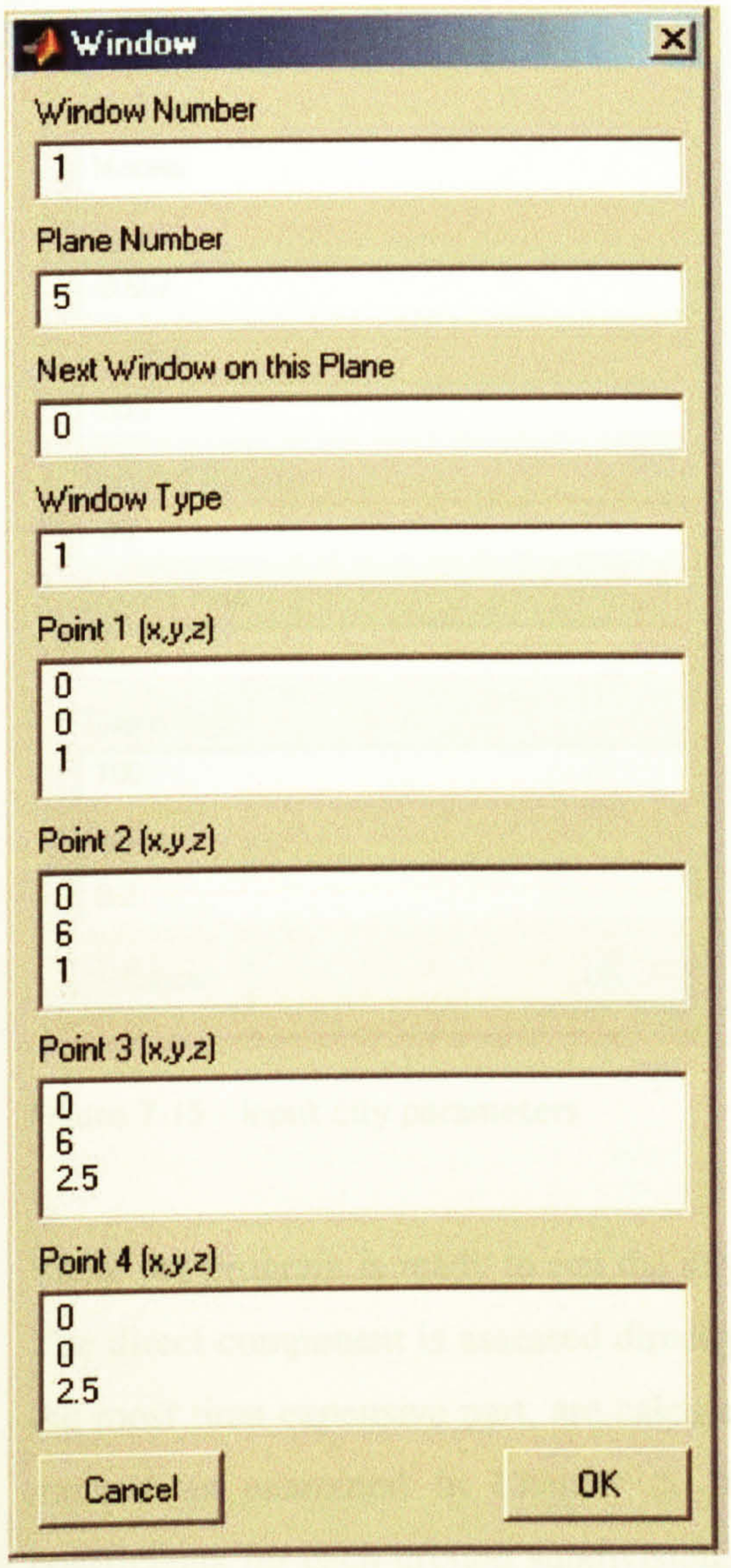

Figure 7-13 - Input window

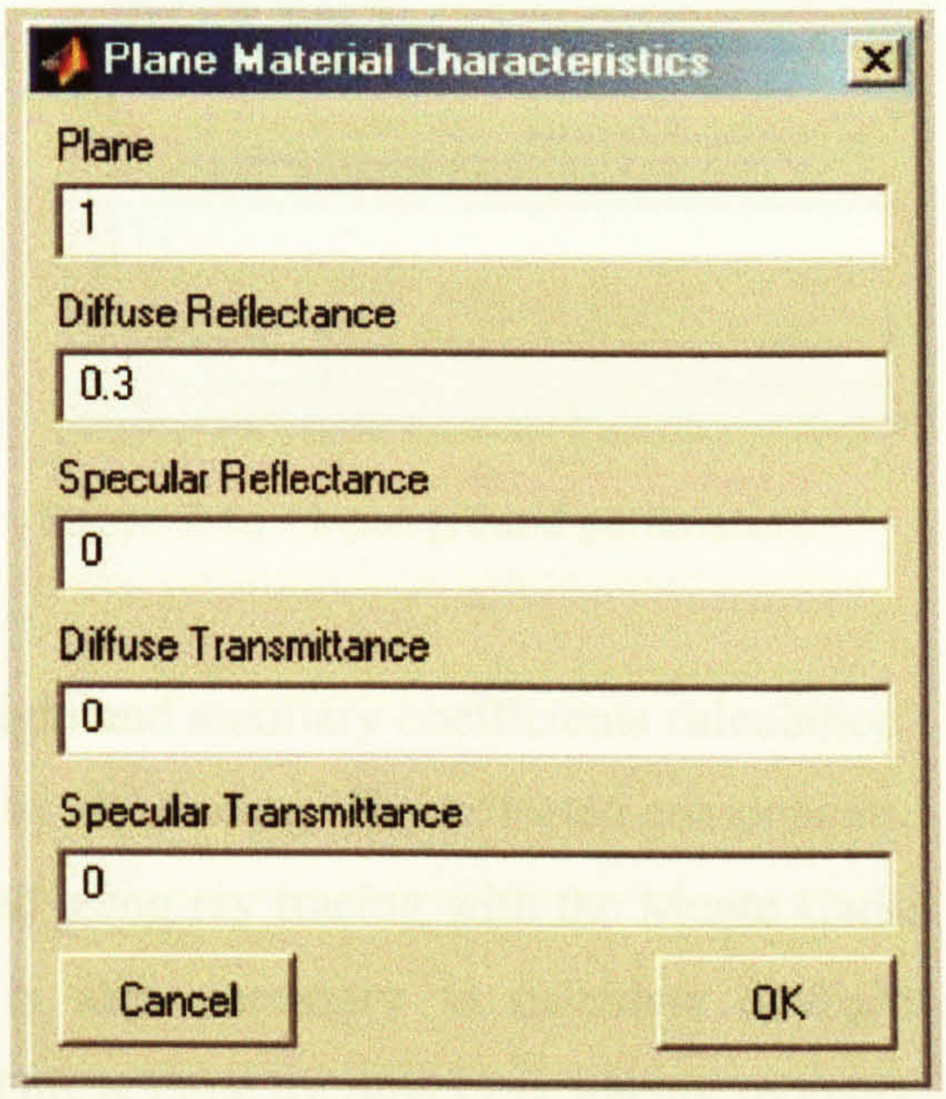

Figure 7-14 - Input material characteristics

After the input phase, data should be set up for running the program. First, room geometry is reorganised and planes are defined by the direction cosines of their normal and their perpendicular distance from the general origin. The same should be done for ground and optionally for external obstruction (not used in this example). In addition, sky patches should be set up in function of the sky subdivision. TropLux allows three kinds of subdivision as discussed in Section 6.3.

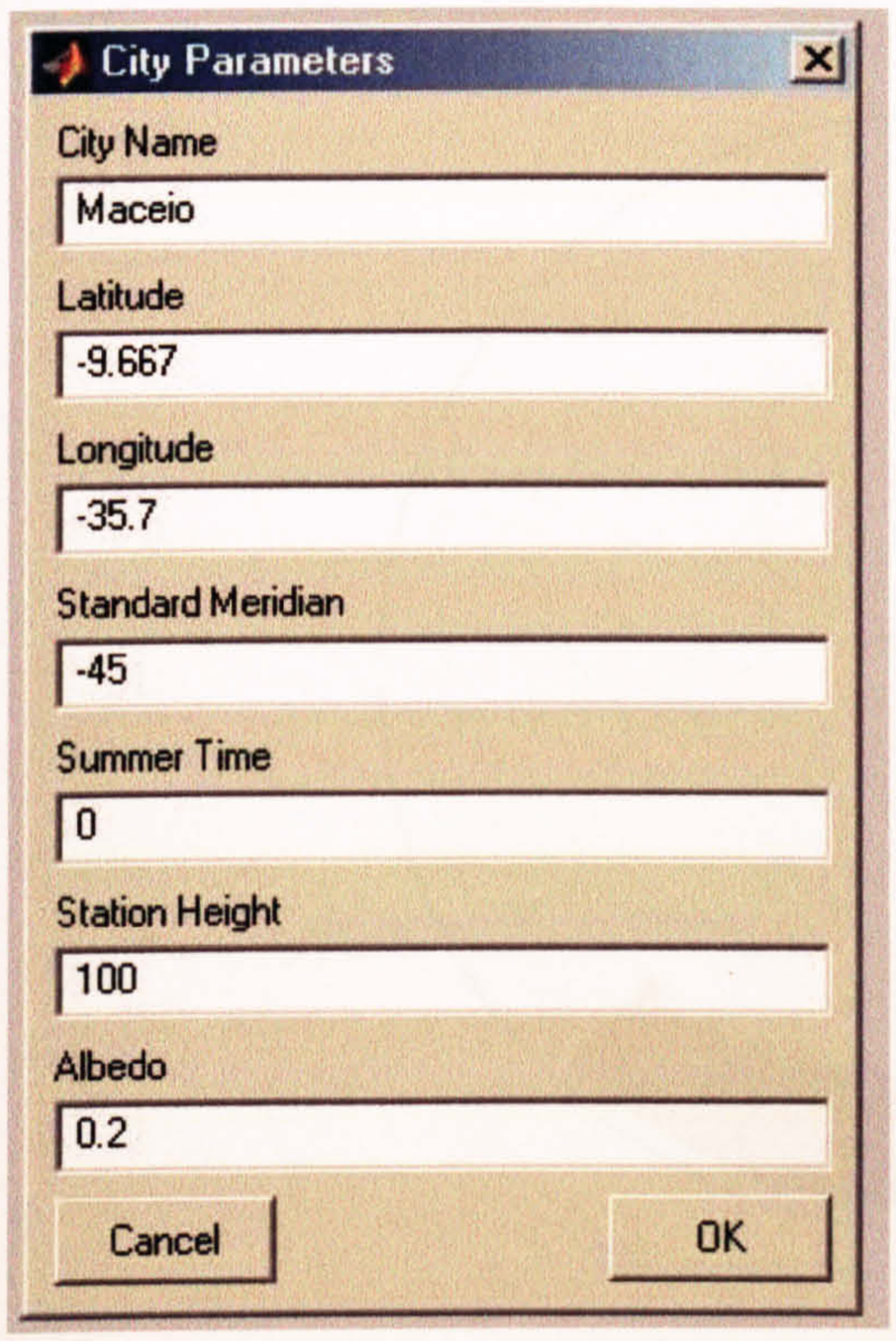

Figure 7-15 - Input city parameters

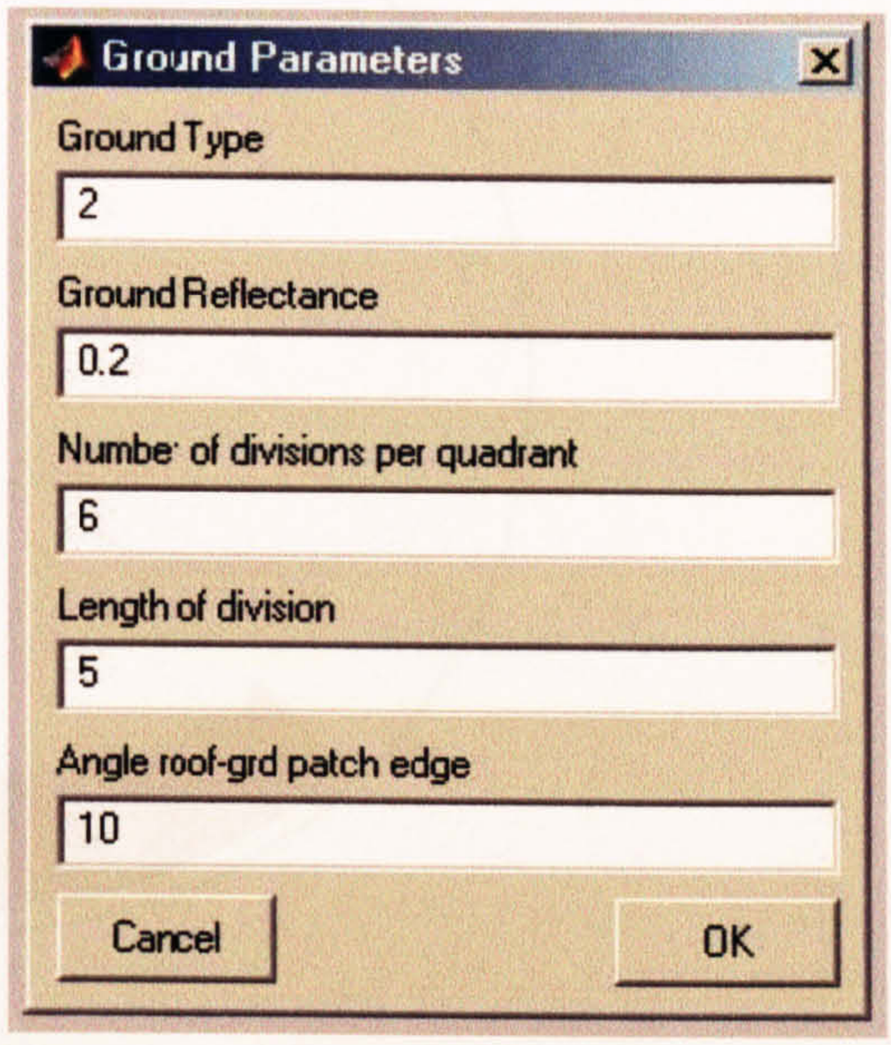

Figure 7-16 - Input ground parameters

Then, the program is ready to run the daylight and auxiliary coefficients calculation. The direct component is assessed directly by ray tracing. The reflected components, the most time expensive part, are calculated using ray tracing with the Monte Carlo method as examined in Chapter 5. It is also necessary to calculate daylight coefficients for each ground subdivision. This is done by direct ray tracing to every sky patch. If there were obstructions, they should also have their own daylight coefficients.

Results for daylight and ground coefficients are shown in the next three figures. Figure 7-17 shows in gray-scale the direct component of daylight coefficients for the studied point in a sky 5221 subdivision. The interreflected component is shown in Figure 7-18 with absolute values of dc (multiplied by 10,000 and rounded to get an integer) in a sky 145 subdivision. Results for ground coefficients are presented in Figure 7-19 in gray-scale in ground type 2 subdivision.

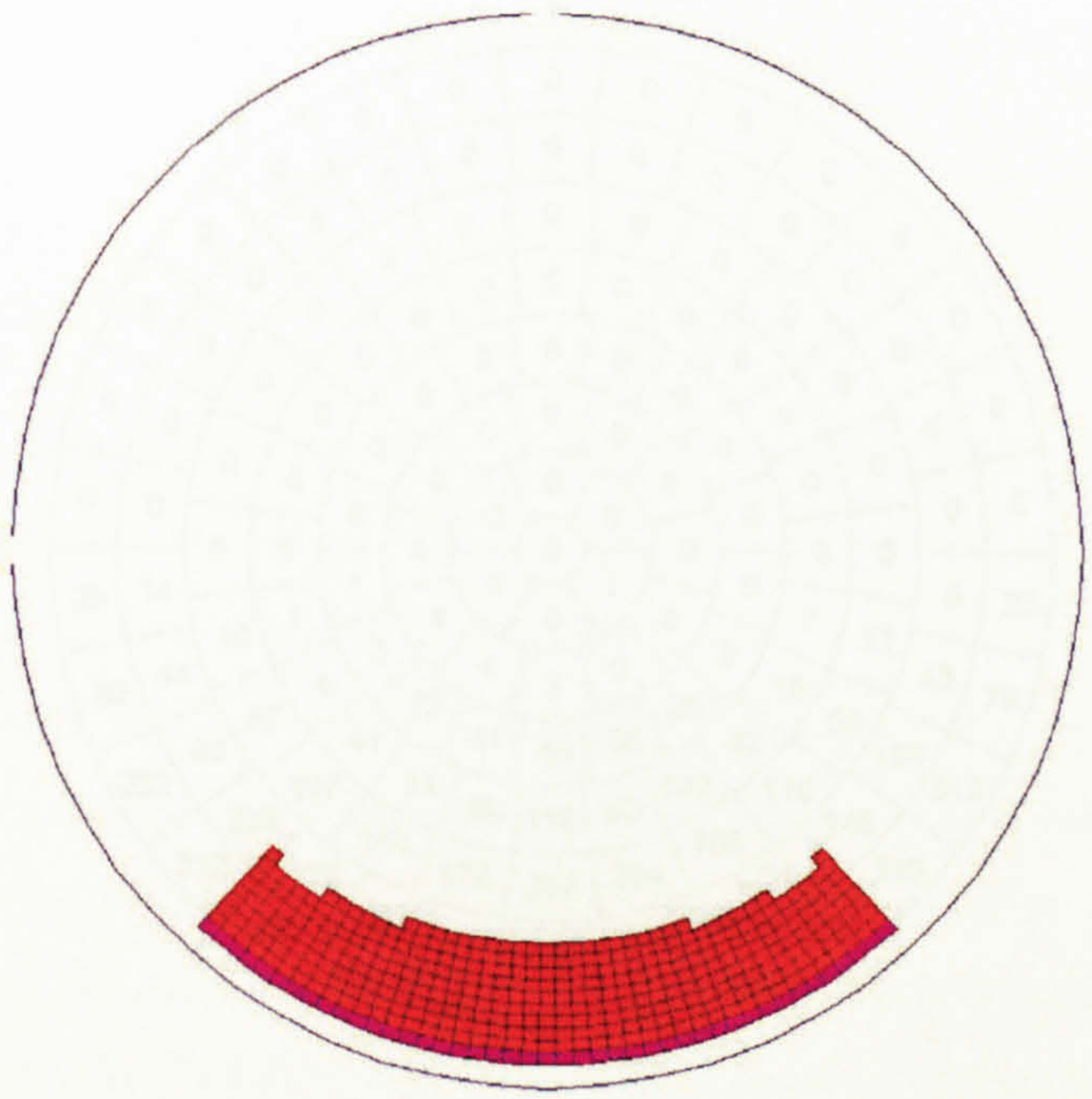

Figure 7-17 - Daylight coefficients - direct component - colour-scale in sky 5221 subdivision. North pointing to top.

At this stage, TropLux can assess the internal illuminance. In this example, illuminance is calculated for a point on the workplane in the centre of the room (X=3.00m, Y=3.00m, Z=0.75m) on summer solstice (22/dec) at midday. The window is 6.00x1.50 m^2 and faces south. The results are shown on Table 7-3, for three sky types. Four components presented not null results.

Table 7-3 - Illuminance (lx) for sample room at summer solstice midday

	Sky		
Component	**Overcast**	**Partly Cloudy**	**Clear**
Sky-Direct	621	1373	524
Sky-Internally Reflected	265	581	251
Sky-Ground Reflected	180	402	151
Sun-Ground Reflected		510	856
Global	1066	2866	1782

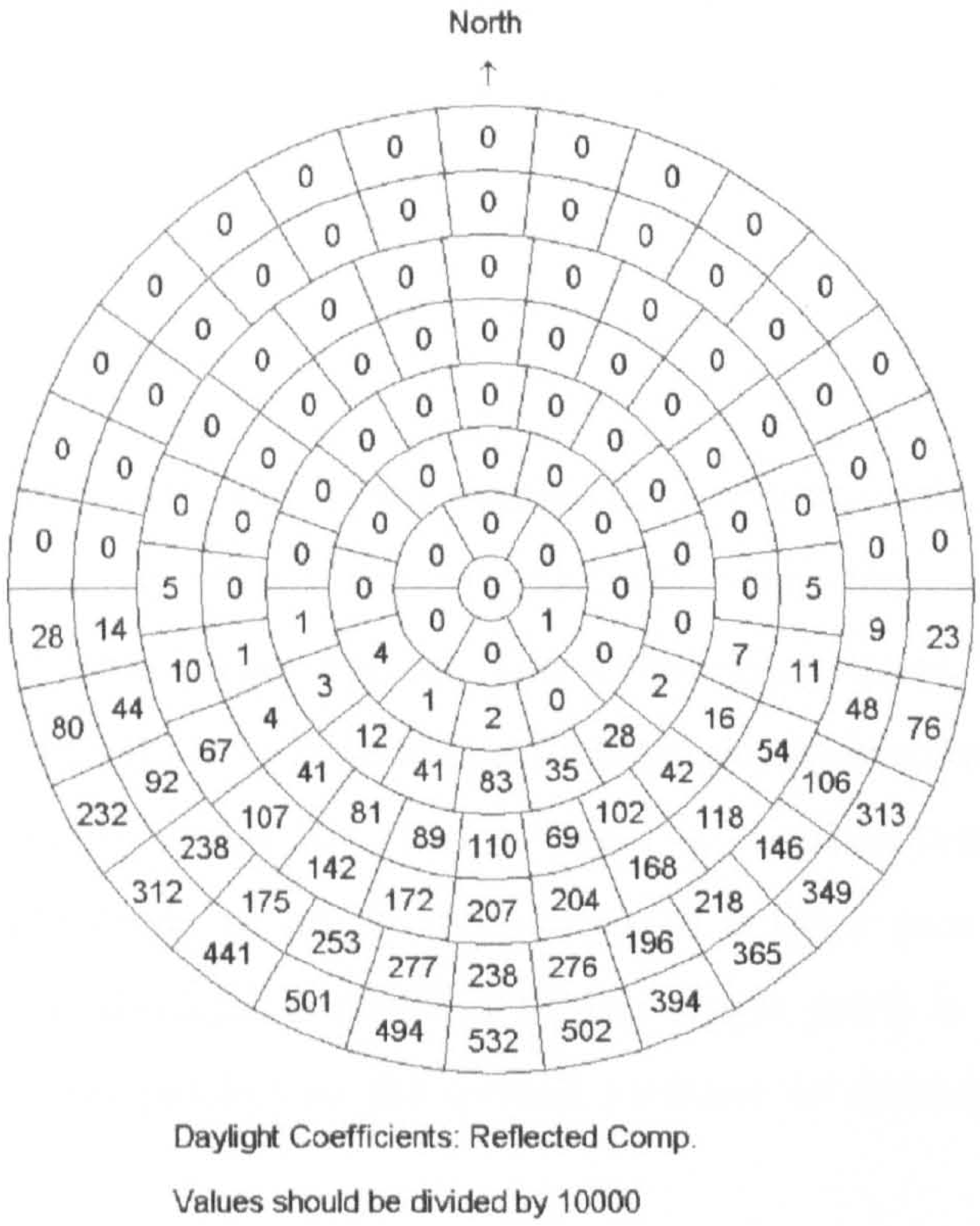

Figure 7-18 - Daylight coefficients - reflected component - absolute values in sky 145 subdivision

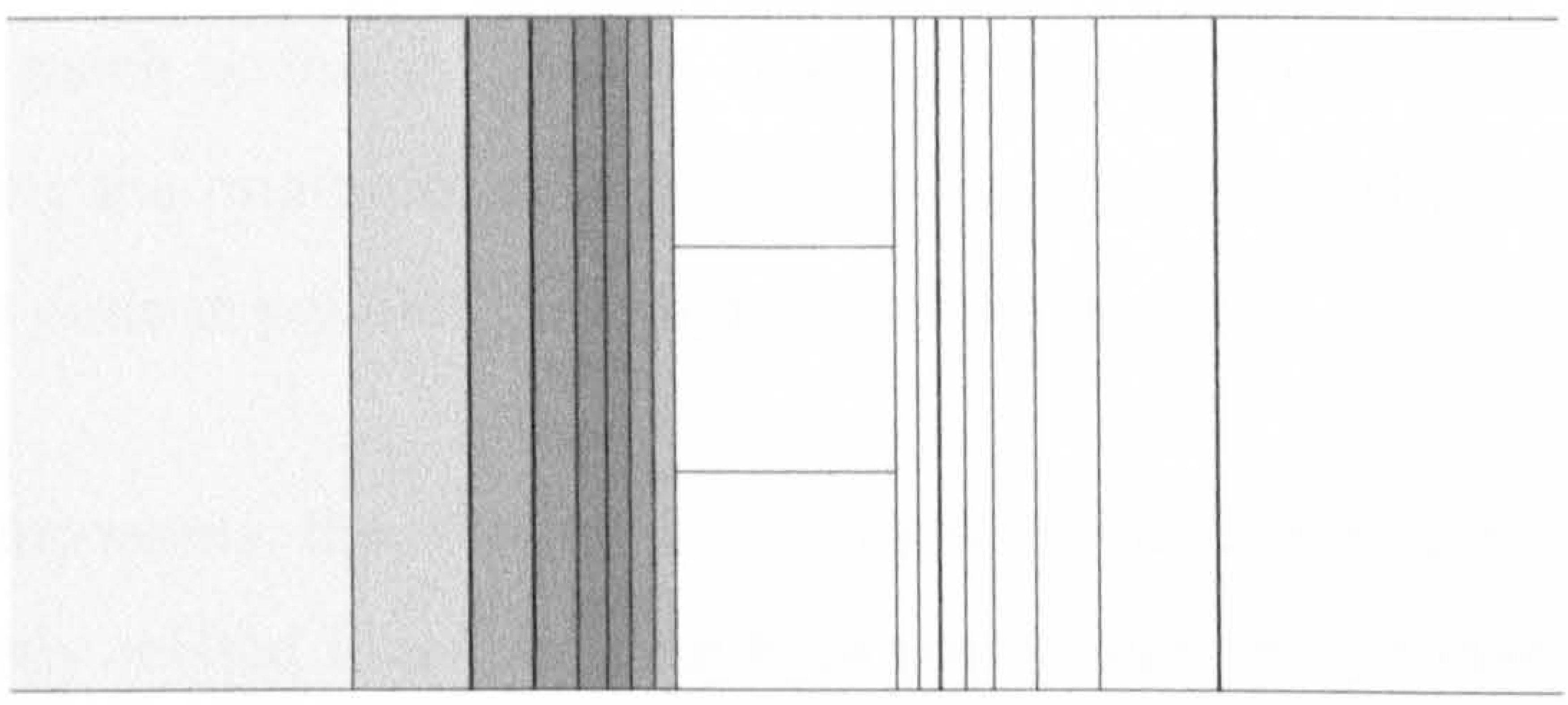

Figure 7-19 - Ground coefficients in gray-scale in ground type 2 subdivision. North pointing to rigth.

7.5 Validation

The TropLux validation is done in three stages, two related to error, for the credibility of its results, and one linked to the time expended to evaluate its feasibility. Firstly, Section 7.5.1 assesses the stochastic error originated by the Monte

Carlo approach. It applies the method discussed in Section 5.2.4. Secondly, Section 7.5.2 analyses the systematic error in three ways. In addition, the running time is discussed in Section 7.5.3.

7.5.1 Stochastic error

Uncertainty due to stochastic error in the computation was minimised by calculating the initial illuminance by direct ray tracing and computing the interreflected components by the Monte Carlo method. The initial illuminance, especially when this is due to direct sunlight, can depend significantly on the brightness of one small sky patch and uncertainty in this has a major effect on the final results. Conversely, interreflected daylight tends to be an integration of a large area of sky and the estimation error in the daylight coefficient of any single patch is compensated by opposite errors for other patches so the overall variance of computed illuminances can be small.

In the program, the calculation of sunlight reflected from the ground and external obstruction is therefore separated into two stages: the ground (or obstruction) coefficients are assessed using the Monte Carlo approach and the sun's contribution to each ground patch is found directly. Since the ground is only split into a few patches, achieving the minimum stochastic error for ground coefficients is not time-expensive and is done in parallel to daylight coefficients.

Amongst all components, the weakest link is light internally reflected from the sun. Its error is directly related to a single daylight coefficient. In this case, the program allows a pre-set threshold for this specific patch. If results are required for different times or azimuths, a calculation is done for any specific patch where the sun is located. However, in the most typical tropical window design, directed sunlight is not allowed into the room thereby eliminating above procedures. If sunshine only goes into the room few times during the year and not to the main region of the workplane, its contribution can be disregarded for design proposes.

7.5.1.1 How the program assesses the stochastic error

Users can define the error that should be achieved when calculating the coefficients. The program is pre-set to a 5% error with 95% confidence level. The routine is run *n* times for a small number of particles, 100 for instance. For each run, an illuminance value for a typical day/time/sky is calculated for the specific room and its value is used to achieve the error. The minimum number *n* of running should be 25 in order to consider illuminance data as a normal distribution.

7.5.1.2 Error by room geometry

Figure 7-20 shows an example of stochastic error for four different rooms, used in calculations presented in Chapter 8. The results are assessed for uniform sky. Since each run emitted 100 particles, error is only considered after 2500 particles.

It is possible to see that error is related to the geometry of the building. In this example, to achieve a 5% error a room with plain windows needed 24500 particles, while with overhang figures went to 33000, an increased ratio of about 35%. Lightshelf and louvre needed about 15 % more particles than a plain window room.

Those differences seem directly related to the possibility of a ray emitted from the assessed point reaches the sky internally reflecting but without reaching the ground or any obstruction. Thus, the overhang had the poorest performance as it can only reflect to the ground (or obstruction in few cases).

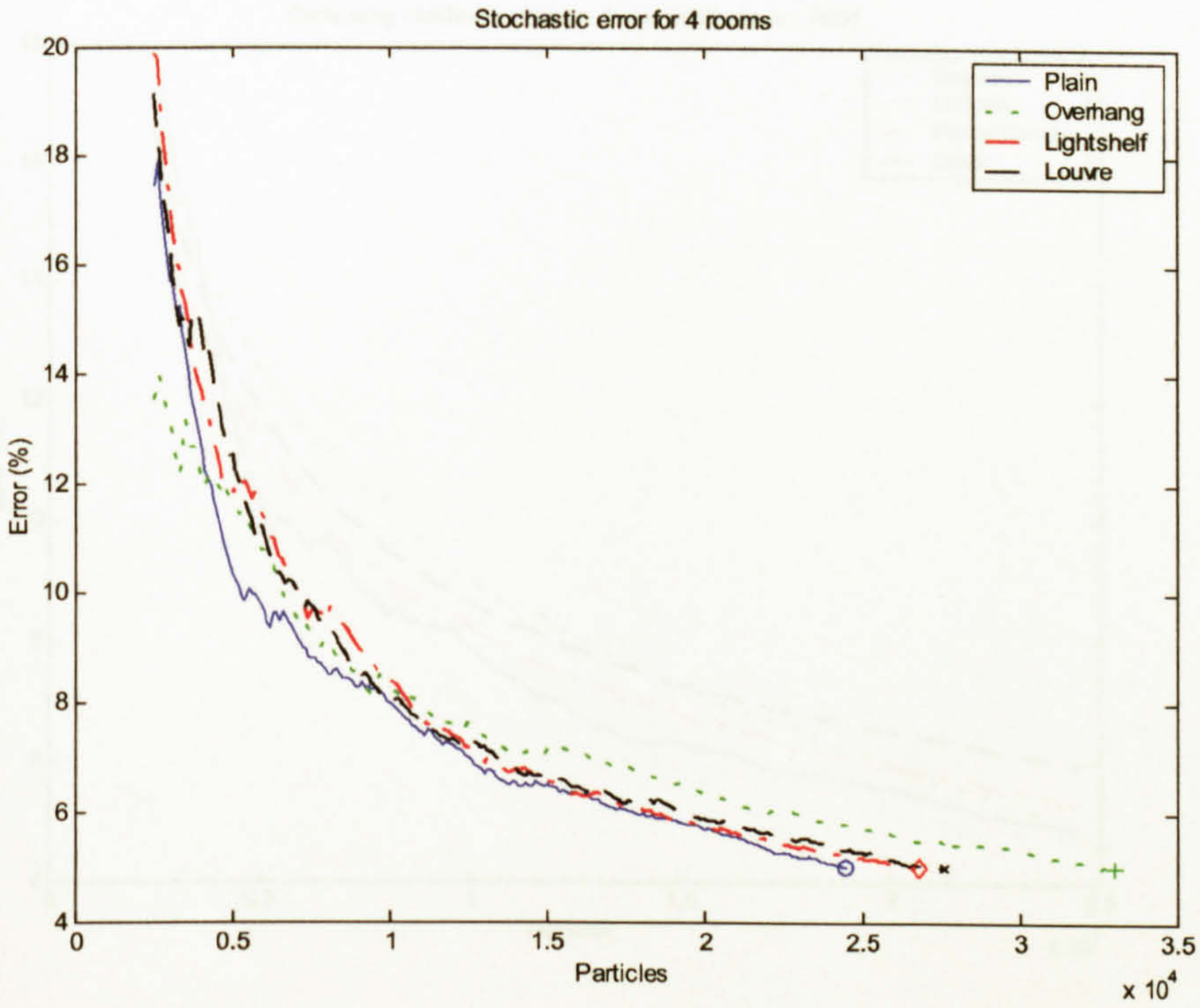

Figure 7-20 -Comparing stochastic error for 4 rooms

7.5.1.3 Error by sky type

To analyse the influence of sky type in stochastic error the same set of coefficients was used to calculate illuminance for four different CIE sky luminance distributions: overcast (CIE 1), uniform (CIE 5), partly cloudy (CIE 10) and clear sky (CIE 14). Figure 7-24 to Figure 7-24 show the results for the same four rooms previously analysed.

Results show that until a 5% error the overcast sky has the smaller error for the same number of emitted particles, but the curves for the uniform sky show a faster tendency to decrease error as the number of emitted particles increases. The tendency is the opposite for clear skies, as they present the smaller ratio for reducing error among the four sky distributions analysed. Although differences between sky types exist, they are not significant overall.

With regard to stochastic error, the results obtained show no relationship between sky type and room geometry.

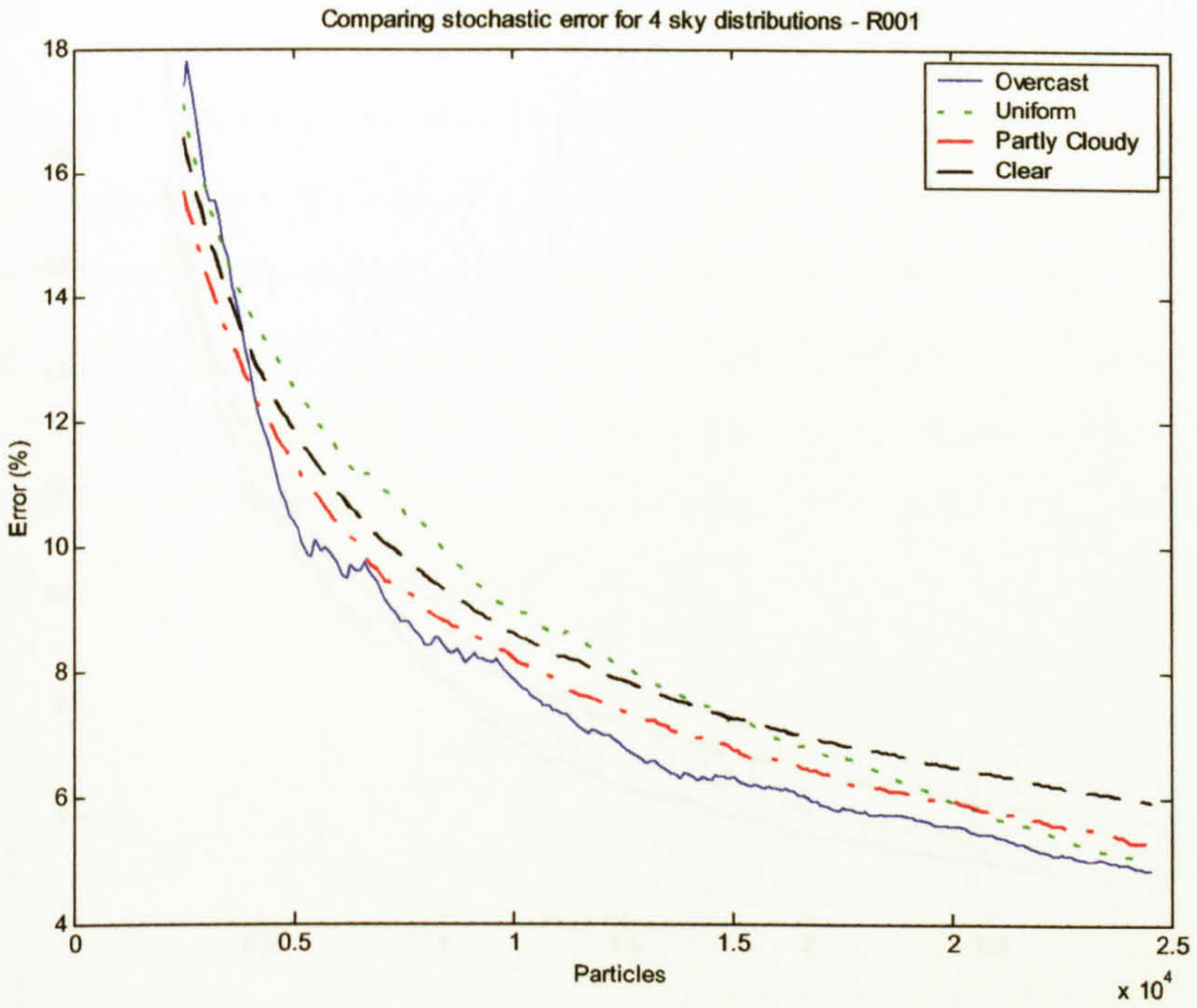

Figure 7-21 - Comparing stochastic error for 4 sky distributions in Room 1

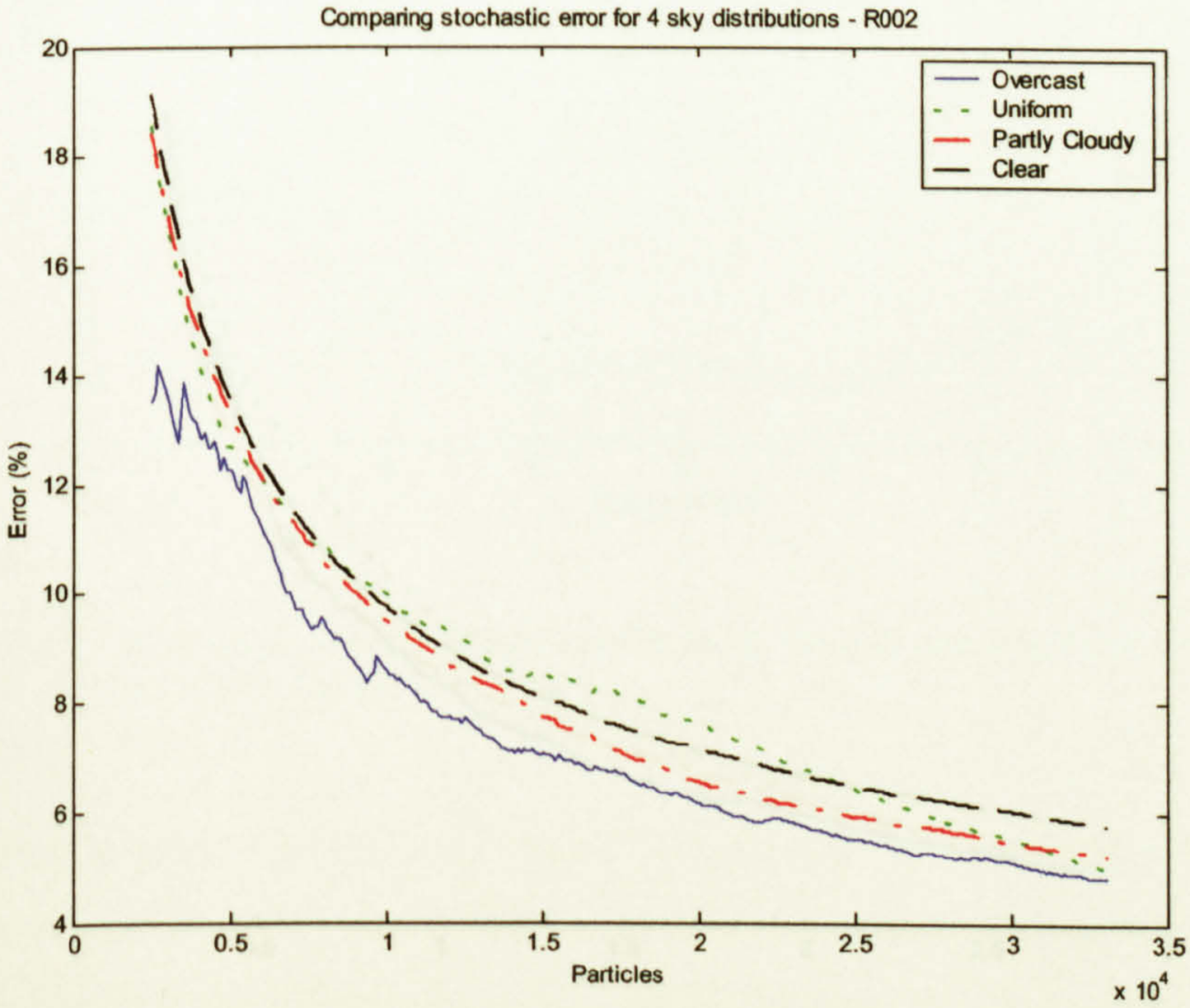

Figure 7-22 - Comparing stochastic error for 4 sky distributions in Room 2

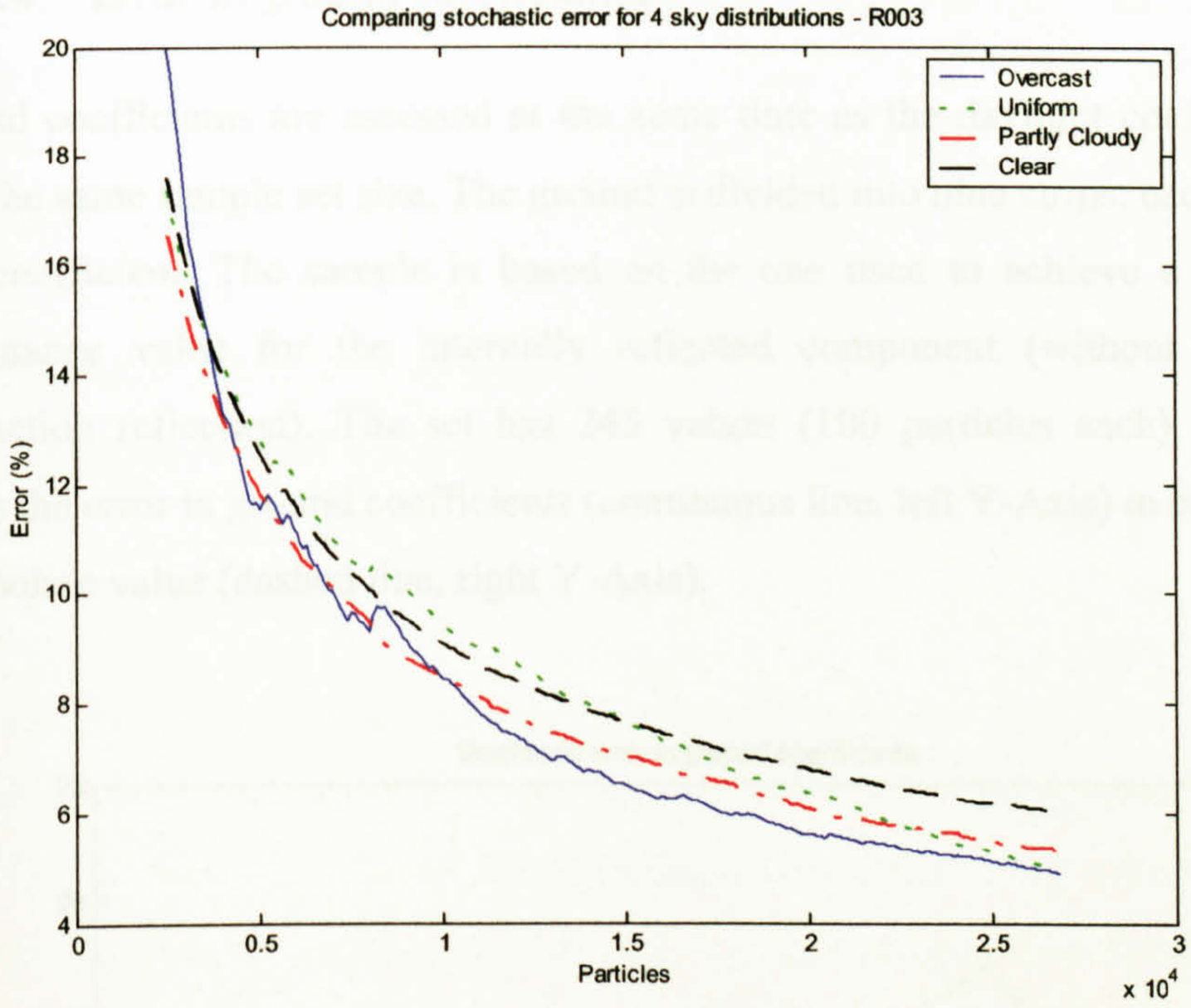

Figure 7-23 - Comparing stochastic error for 4 sky distributions in Room 3

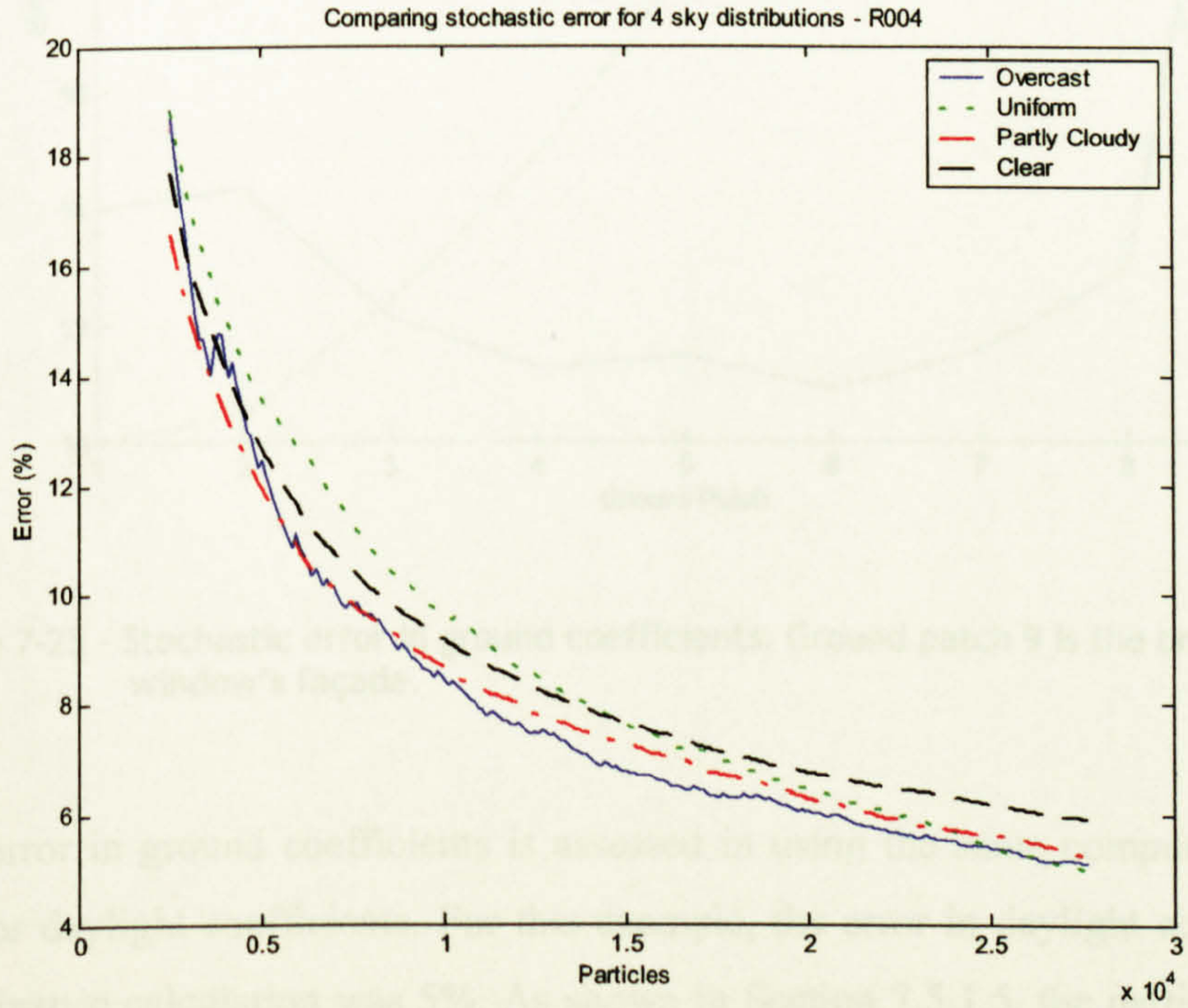

Figure 7-24 - Comparing stochastic error for 4 sky distributions in Room 4

7.5.1.4 Error in ground coefficients

Ground coefficients are assessed at the same time as the daylight coefficients, and have the same sample set size. The ground is divided into nine strips; each one has its own coefficient. The sample is based on the one used to achieve a 5% error in illuminance value for the internally reflected component (without ground and obstruction reflection). The set has 245 values (100 particles each). Figure 7-25 shows the error in ground coefficients (continuous line, left Y-Axis) in comparison to its absolute value (dashed line, right Y-Axis).

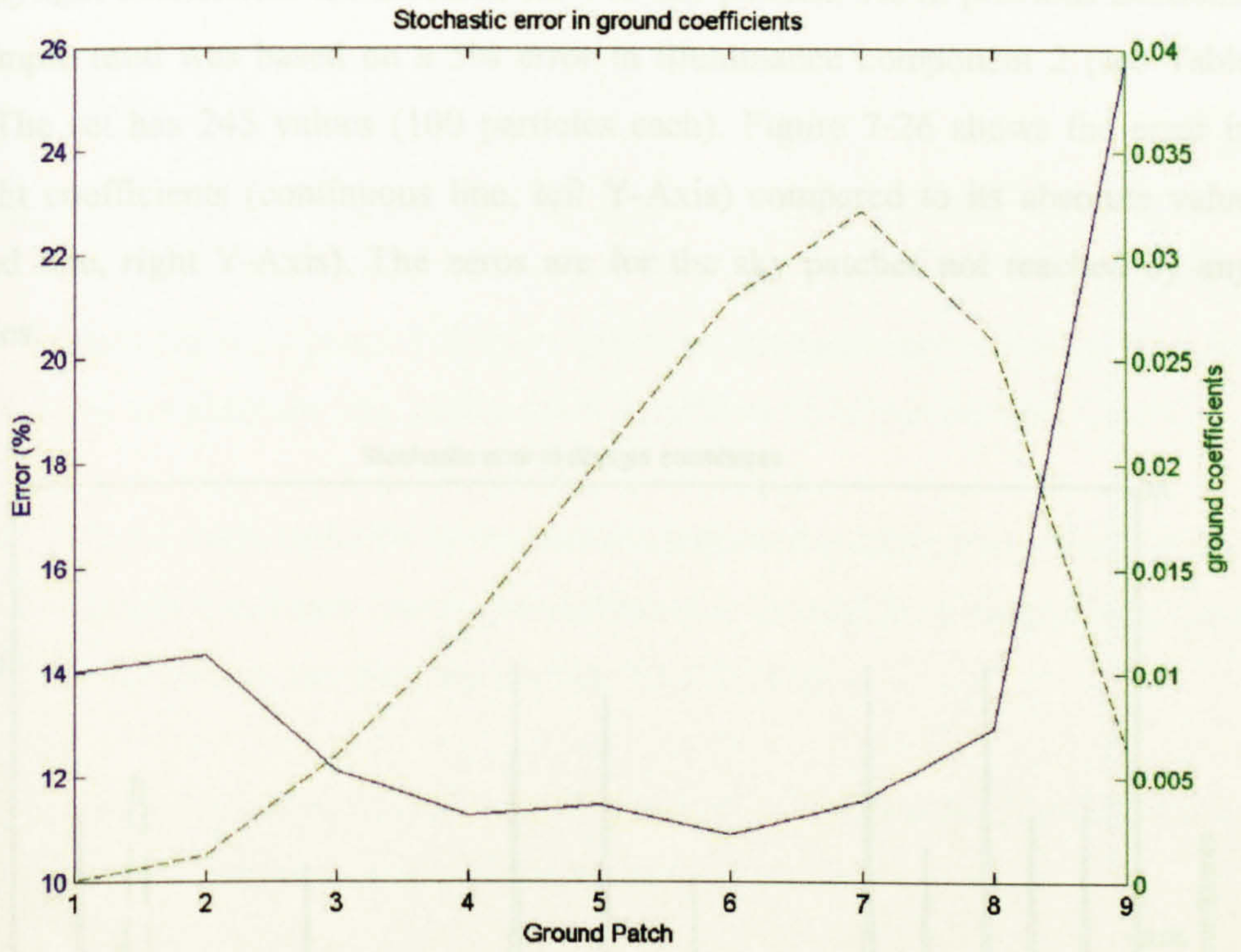

Figure 7-25 - Stochastic error in ground coefficients. Ground patch 9 is the one closest to window's façade.

The error in ground coefficients is assessed in using the same computation carried out for daylight coefficients. For this example, the error in daylight coefficients by illuminance calculation was 5%. As shown in Section 7.5.1.5, the particular error in every daylight coefficients is significantly greater compared to 5% overall error.

Thus, the contribution of ground coefficients to the global error has shown inferior to the daylight coefficients.

Another observation from Figure 7-25 is that the error is inversely proportional to ground coefficients. This implies that the final illuminance/luminance results should have a smaller error. This is because larger errors are in patches with a smaller contribution to the general illuminance.

7.5.1.5 Error in daylight coefficients

The daylight coefficients are assessed for 145 sky patches. As in previous Sections, the sample used was based on a 5% error in illuminance component 2 (see Table 7-2). The set has 245 values (100 particles each). Figure 7-26 shows the error in daylight coefficients (continuous line, left Y-Axis) compared to its absolute value (dashed line, right Y-Axis). The zeros are for the sky patches not reached by any particles.

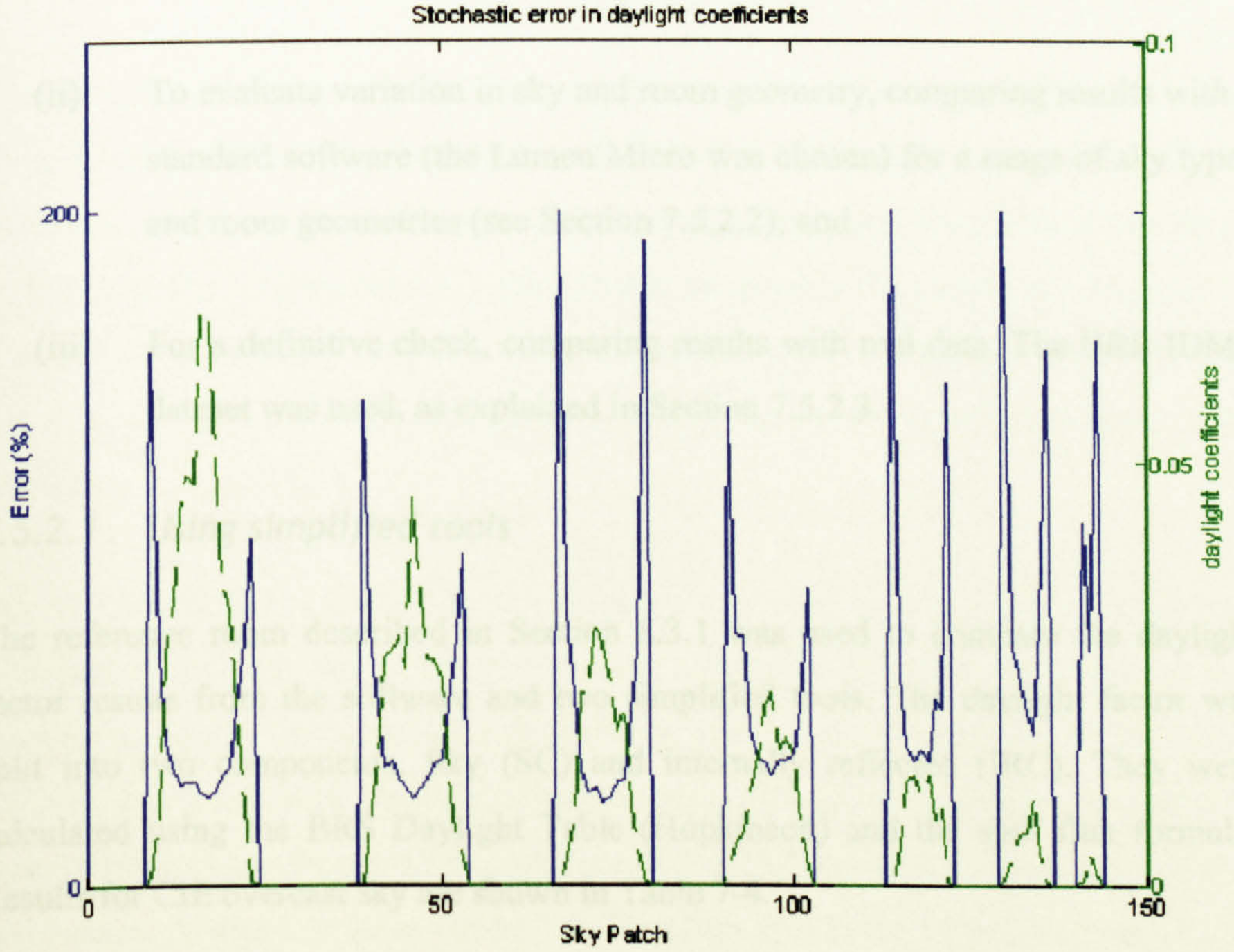

Figure 7-26 - Stochastic error in daylight coefficients

As happened with ground coefficients, the error is inversely proportional to daylight coefficients. Here the error is greater within the limits of a bunch of sky patches reached by backward ray tracing. However, its values are not statistically significant as the number of rays that reaches them is very small.

It is important to note that the error for a specific daylight coefficient, between 24% and more than 100% is quite significant, comparing to the error achieved based on the sum of every coefficient contribution to the illuminance value, which is 5 % for the studied example. It occurs due to compensation between coefficients that go up and down of the average (best estimation).

7.5.2 Deterministic error

The deterministic error is assessed in three ways:

(i) To find discrepancies at early stages, comparing some outcomes assessed by the program with results from simplified tools (see Section 7.5.2.1);

(ii) To evaluate variation in sky and room geometry, comparing results with a standard software (the Lumen Micro was chosen) for a range of sky types and room geometries (see Section 7.5.2.2); and

(iii) For a definitive check, comparing results with real data. The BRE-IDMP dataset was used, as explained in Section 7.5.2.3.

7.5.2.1 Using simplified tools

The reference room described in Section 8.3.1 was used to compare the daylight factor results from the software and two simplified tools. The daylight factor was split into two components, Sky (SC) and internally reflected (IRC). They were calculated using the BRS Daylight Table (Hopkinson) and the split flux formula. Results for CIE overcast sky are shown in Table 7-4.

Table 7-4 - Comparing results with simplified tool

Component	Software	Simplified tool	Relative error
SC	2.57	2.98	16.14%
IRC	1.97	1.96	0.61%
DF	4.54	4.94	8.81%

Results have shown a relative error of less the 10% for the daylight factor. This can be considered acceptable, as the intention was just to find out discrepancies in results as assessed by the program and used to draw the conclusion in Chapter 8.

7.5.2.2 Using a standard software

Lumen Micro 7, by Lighting Technologies, was chosen for validating TropLux for different geometries. The software is based on the radiosity method. Using the IES equations, it can assess illuminance results for three different sky types – clear, partly cloudy and cloudy. It is also able to simulate room geometry with some degree of complexity, enough to evaluate the four kinds of window patterns, studied in the next chapter.

Results were achieved in both programs for a point in the centre of the reference room 6.00 x 6.00 x 3.00, described in Section 8.3.1. TropLux assessed the diffuse horizontal illuminance by IES equations, but sky luminance distribution was based on the CIE. The CIE overcast sky (sky 1) was matched to the cloudy sky assessed by Lumen Micro. TropLux used CIE 10 (partly cloudy with brighter circumsolar effect) and CIE 12 (CIE clear sky with low turbidity), for partly cloudy and clear skies, respectively.

Due to limitations in Lumen Micro, results were compared only grouped as the total illuminance and the direct component. The internally reflected component is not shown, but results can be easily calculated by subtraction of previous values. Table 7-5 and Table 7-6 show the illuminance at the centre of the workplane assessed by Lumen Micro and TropLux, respectively. Table 7-7 shows the relative error as a percentage. A negative value means that TropLux estimation is smaller than Lumen Micro.

Table 7-5 - Illuminance (lx) at the centre of the workplane assessed by Lumen Micro

	Total			Direct		
	Clear	**PC**	**Cloudy**	**Clear**	**PC**	**Cloudy**
Room 1	2321	3444	991	676	1725	578
Room 2	1830	2653	736	579	1321	411
Room 3	1922	2752	793	574	1304	420
Room 4	1500	2461	725	574	1404	459

Table 7-6 - Illuminance (lx) at the centre of the workplane assessed by TropLux

	Total			Direct		
	Clear	**PC**	**Cloudy**	**Clear**	**PC**	**Cloudy**
Room 1	2546	3724	949	682	1888	531
Room 2	1991	2869	692	503	1373	351
Room 3	2324	3143	763	534	1468	406
Room 4	2222	3159	789	569	1576	444

Table 7-7 - Relative error (%) for illuminance estimation by Lumen Micro and TropLux

	Total			Direct		
	Clear	**PC**	**Cloudy**	**Clear**	**PC**	**Cloudy**
Room 1	8.84	7.52	-4.43	0.88	8.63	-8.85
Room 2	8.09	7.53	-6.36	-15.11	3.79	-17.09
Room 3	17.30	12.44	-3.93	-7.49	11.17	-3.45
Room 4	32.49	22.10	8.11	-0.88	10.91	-3.38

Results show that for the room with basic geometry (Room 1, plain window) the relative error between both programs is not significant, being less than 10% for any sky type and for direct or interreflected component. A significant relative error (RER>24%) was found for the reflected component with clear sky in Room 3 (with light shelf) and Room 4 (with horizontal louvres). It may occur because of different approach to sky luminance distribution between softwares, as TropLux takes into account reflected sunlight in both clear and partly cloudy skies. Due to complexity in geometry, the interreflected light in louvre's surfaces can be a source of relative error between both programs.

7.5.2.3 Using real data

As a final check, TropLux was tested with real data. The BRE-IDMP dataset [3] was used as there was no possibility of carrying out a fieldwork of this magnitude within

the scope of this research. The dataset has been used previously for software validation and its performance is considered very satisfactory [4]. The geometry of the test-room is relatively simple although frames and bars work as shading device on a small scale.

Briefly, the room – 3.00m x 9.00m x 2.70m – has six illuminance sensors that access results simultaneously with the IDMP station, set up on the roof of the same building, in Garston, UK.

Mardaljevic [5] thoroughly analysed the BRE-IDMP dataset. He validated a program using the Radiance system. The internal illuminance is accessed based on the luminance values for 145 sky patches and results compared with the dataset.

This thesis has a different approach. Instead of the sky luminances, the validation is based on the horizontal diffuse illuminance in conjunction with the CIE Standard General Sky [6]. There are two basic reasons for that. First, in TropLux the computer code to assess internal luminance from sky luminances is different to the one that calculates from the horizontal diffuse illuminance. Therefore one validation does not work necessarily to the other. Second, if the main input in TropLux were based on sky luminance measurements, its use would be restricted to cities with an IDMP station. That is not the aim of this research. Thus, only the horizontal diffuse illuminance (E_{dh}) would be necessary for a reliable performance of the software. Since E_{dh} is a primary daylighting measurement, it is anticipated that the program will be used more often in this way.

Results for the six points are shown in Appendix G. In this Section, only one of them is chosen to exemplify how data were analysed.

At the first stage, the program assessed the illuminance, based on the 15 CIE Standard General Sky. Results for point 2 are shown in Figure 7-27. The axis Y represents the illuminance in lux, and the axis X the sequential number of measurement/simulation. For each X value, there are 15 black dots for each CIE sky, and one red circle for the measured value. Thus, it is possible to have an overview of the whole analysis.

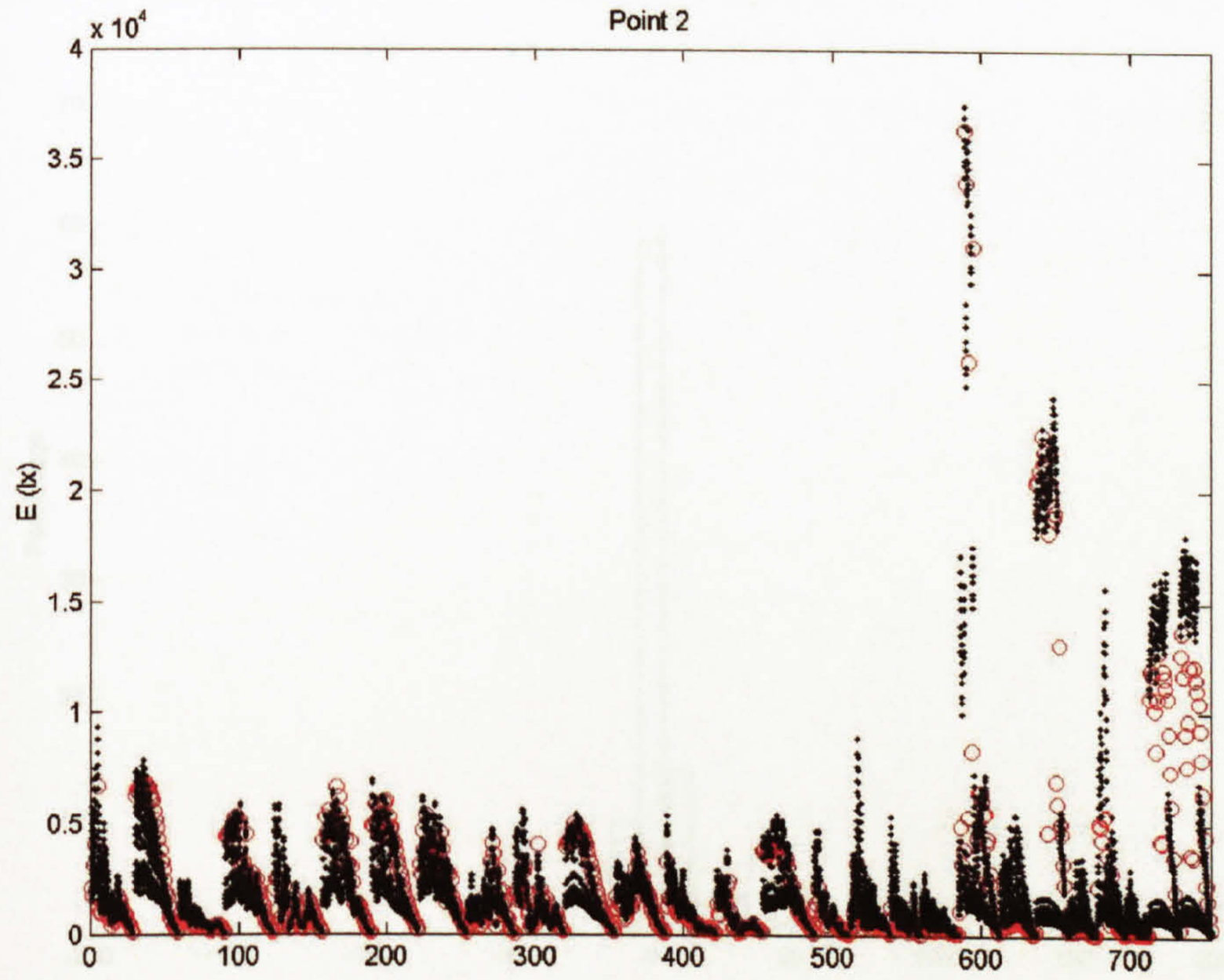

Figure 7-27 - Comparing measured results by BRE-IDMP dataset and by TropLux with 15 CIE standard skies for point P2. Axis X represents the sequential number of measurement/simulation

The program found the best choice, originated from the 15 CIE skies, for each 754 condition, and results were compared using the relative error (RER), calculated by equation (7.1).

$$RER = \frac{E_{pred} - E_{meas}}{E_{meas}} \times 100\% \qquad (7.1)$$

Appendix G shows the results for each condition for the six points. Results were grouped in a histogram for each point as shown for Point 2 in Figure 7-28.

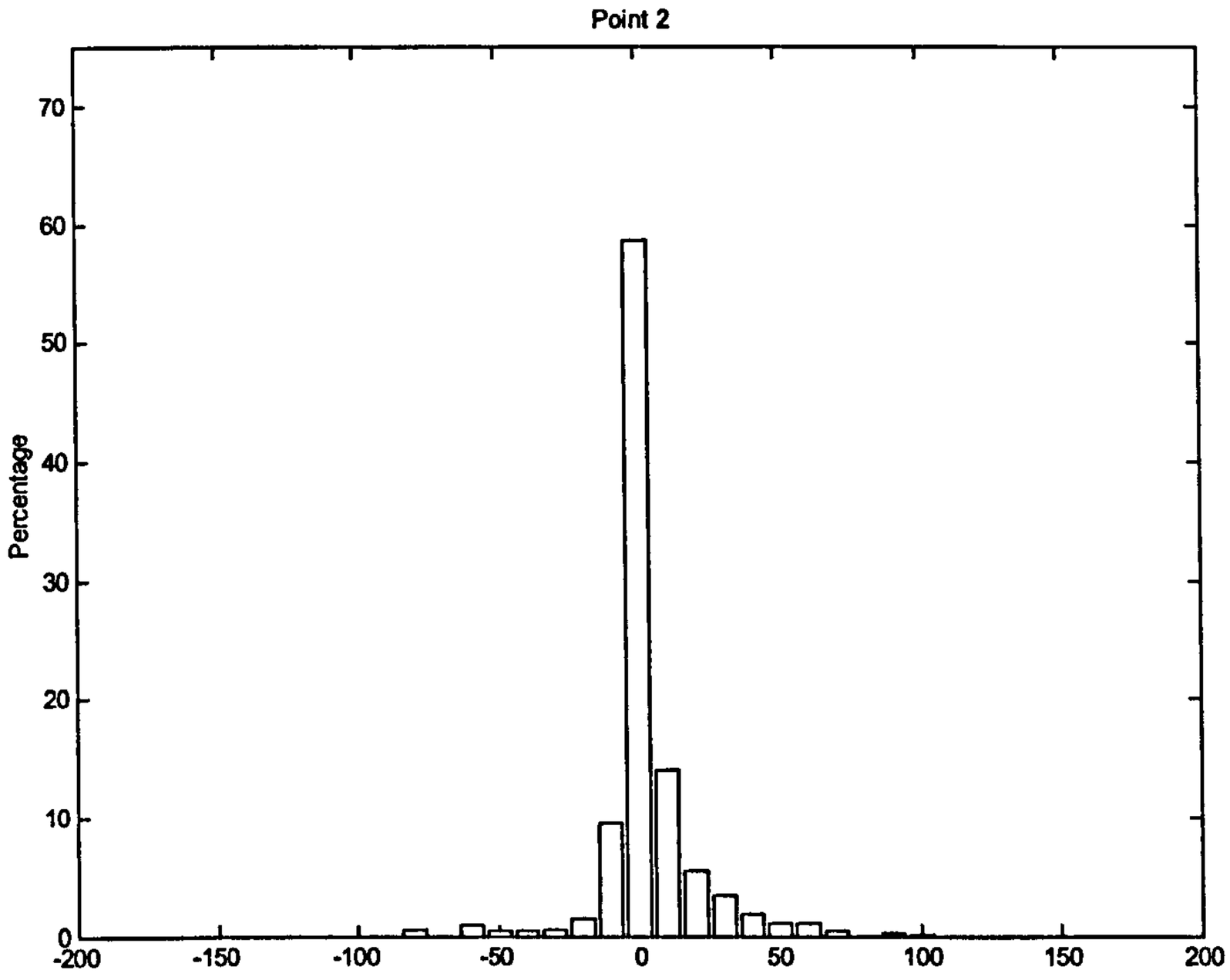

Figure 7-28 - Histogram for the RER (%) between measured and best prediction internal illuminance for point P2

Data were also evaluated by the correlation coefficient. Table 7-8 shows the results for the whole data and after extracting outliers. Values were considered outliers when their deviations from the average were more than three times the standard deviation.

Table 7-8 - Correlation coefficients for predicted and measured illuminance value in six points using the data with and without outliers

	Correlation coefficient	
Point	**Whole data**	**Without outliers**
1	0.900	0.957
2	0.953	0.989
3	0.831	0.955
4	0.921	0.982
5	0.740	0.978
6	0.993	0.998

Only Points 3 and 5 presented a lower correlation, however after the extraction of the outliers the results became more significant. For visualisation, Figure 7-29 shows the

correlation between measured and predicted values. Outliers are plotted in red circles.

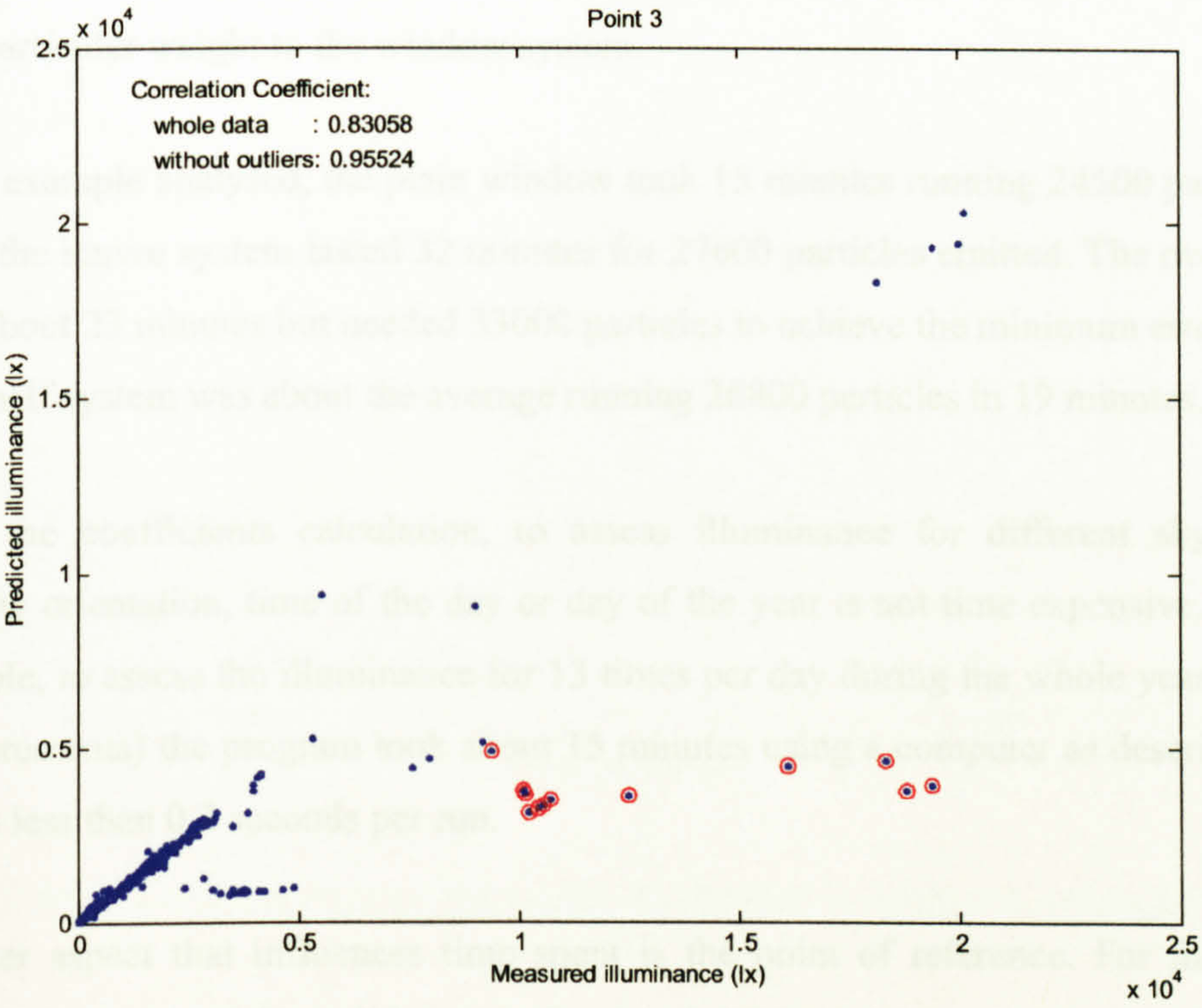

Figure 7-29 - Correlation between measured and predicted illuminance for Point 3

A correlation coefficient of over 0.95 for every six studied points was found. It is a good indication that the validation by real data can be considered satisfactory. The main source of inaccuracy in the model occurs when sunshine is available. The reasons follow the Mardaljevic's 'source visibility related errors'. The lack of precision in the geometrical specification of the building appears to be the main reason. Mardaljevic points out three other reasons that can also be considered: the point source representation of photocell in model, single-ray light source sampling of sun and uncertainty in the sky luminance distribution about the solar position. However, their influence seems to be smaller than the geometrical specification.

7.5.3 Time expended

The time spent with estimated 5% error is about 20 minutes on a PC with Pentium III 666MHz and 128Mb RAM. It varies in function of the room geometry and materials, with particular weight to the window system.

In the example analysed, the plain window took 15 minutes running 24500 particles, while the louvre system lasted 32 minutes for 27600 particles emitted. The overhang took about 23 minutes but needed 33000 particles to achieve the minimum error. The lightshelf system was about the average running 26800 particles in 19 minutes.

After the coefficients calculation, to assess illuminance for different sky type, window orientation, time of the day or day of the year is not time expensive. As an example, to assess the illuminance for 13 times per day during the whole year (4745 measurements) the program took about 15 minutes using a computer as described. It means less than 0.2 seconds per run.

Another aspect that influences time spent is the point of reference. For the BRE reference room used for validation in Section 7.5.2.3, six points were assessed with different distances to window. Figure 7-30 shows the relation between this distance and the time expended for that situation using the computer previously described in this Section.

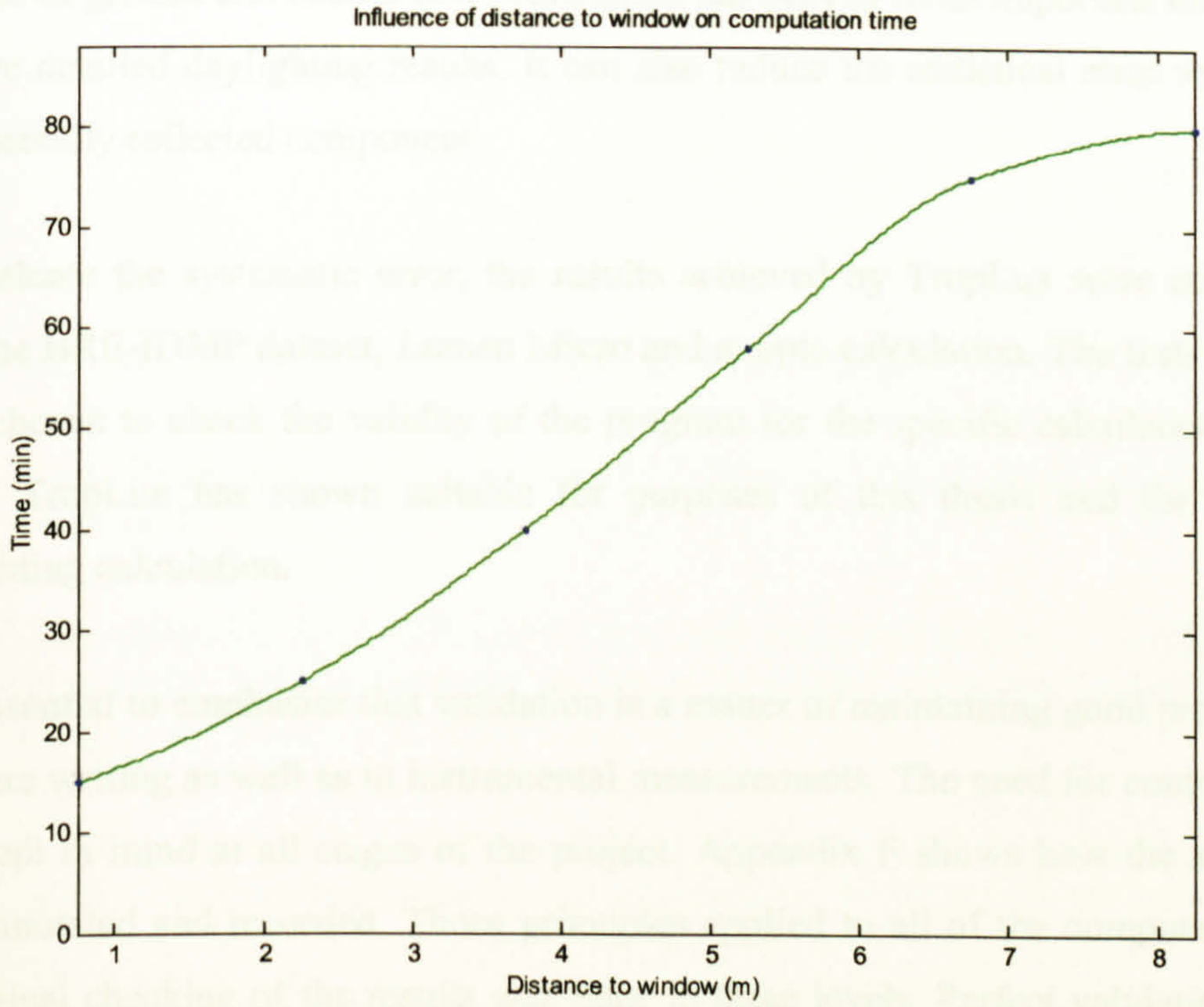

Figure 7-30 - Influence of distance from point of reference to window on computation time

7.6 Conclusion

This chapter has concluded that the program can evaluate specific daylighting characteristics for the tropical environment. The program TropLux, using backward ray tracing with Monte Carlo method, can attain an acceptable standard error within a reasonable time. The use of daylight coefficients allows very fast illuminance calculation for different types of sky distribution, time of the day, day of the year and for changing windows façade orientation.

Using the sky internally reflect component (component 2, Table 7-2) as the basis for statistical error has proved appropriate as it can achieve fast and accurate results. When the reflected sunlight goes into a room without bouncing on the ground or an obstruction (component 8, Table 7-2), attention should be given to the error on the specific daylight coefficient associated to the sun's position.

The use of ground and obstruction coefficients has proved as an important method to achieve detailed daylighting results. It can also reduce the statistical error related to the internally reflected component.

To evaluate the systematic error, the results achieved by TropLux were compared with the BRE-IDMP dataset, Lumen Micro and simple calculation. The tests applied were chosen to check the validity of the program for the specific calculation of the thesis. TropLux has shown suitable for purposes of this thesis and for general daylighting calculation.

It is essential to emphasise that validation is a matter of maintaining good practice in software writing as well as in instrumental measurements. The need for control error was kept in mind at all stages of the project. Appendix F shows how the software was annotated and recorded. Those principles applied to all of the computer work. Numerical checking of the results was done in three levels. Perfect validation is an impossibility. However, the results show that the level of prediction is comparable with those produced by Radiance, as studied by Mardaljevic [5], and overall the results appear to be robust.

In the next Chapter, this methodology is used to assess the influence of the ground-reflected light, a specific tropical daylighting element.

References

1. IES, ed. *Lighting Handbook.* 8th ed., ed. M.S. Rea, IES, 1993

2. CIE - Commission Internationale de l'Eclairage, *TC3-15 Draft Standard - June 1999*, 1999.

3. Aizlewood, M. E., S. Hill, and G. K. Cook. *The development of a reference data set for lighting computer programs.* in *CIBSE - National Lighting Conference.* Bath - UK: CIBSE. p. 172-177, 1996.

4. Mardaljevic, J., *Validation of a lighting simulation program under real sky conditions.* Lighting Research and Technology, **27**(4): p. 181-188, 1995.

5. Mardaljevic, J., *Daylight simulation: validation, sky models and daylight coefficients*, PhD, in *Institute of Energy and Sustainable Development*, De Montfort University. 313 p., 1999.

6. CIE - Commission Internationale de l'Eclairage, *Spatial distribution of daylight - CIE standard general sky*, CIE: Wien, 2002.

Part III

Application and Conclusion

The final part of the thesis consists of two Chapters. Chapter 8 presents an example of how to use the recommended method. It gives some guidelines relating to the use of the ground-reflected light in the humid tropics. Chapter 9 synthesises the relevant conclusions of this thesis, presents the limitations and suggests further studies.

Chapter 8 The influence of ground-reflected light in tropical daylighting

8.1 Introduction

This chapter shows an application of the methodology proposed in this thesis. Tropical regions offer large amounts of natural light. Direct sunlight must usually be screened from entering the window to prevent glare and thermal discomfort; but this also reduces the admittance of skylight. Sunlight reflected diffusely from external surfaces then becomes an important source of illumination, and the amount reflected by the ground surface can be significant. This Chapter analyses the influence of daylight reflected on ground surfaces in relation to internal daylighting performance in tropical region. Three specific goals are investigated: how far from window's façade the ground can be important as a source of natural light; how a shading device's pattern can influence daylighting performance, in relation to ground-reflected component; and what is the sunlight and skylight contribution in function of sky type.

8.2 Brief review on ground-reflected light

In the mid of 20th Century, two papers, one by Hopkinson and Petherbridge [1] and another by Griffith et al. [2], point out the influence of ground as an important source of natural lighting for buildings located in regions where sun is often unobstructed. While Griffith et al. [2] explore the point in a broad way, Hopkinson and Petherbridge [1] indicate a method of attack on the subject, based on measurements using a model-scale and a heliodon to reproduce the relative motions of the earth and sun.

Lam [3] also emphasises the importance of the use of the ground to reflect sunlight into buildings, mainly during summer and at low latitudes.

Afterwards, a study of Tregenza [4] allows the assessment of the ground-reflected component in the mean illuminance on the working plane and on other room surfaces

using a simplified method. It applies a split-flux technique and uses as data, solar normal illuminance and diffuse horizontal illuminance.

8.3 Study Method

This study observes the influence of ground-reflected light for buildings located in the tropical region, with particular reference to the impact of shading devices and ground distance to window façade.

In order to simplify the study, illuminance levels are found for a single observation point in one reference room. The same room is tested for a plain window alone and with three different shading device patterns: overhang, light shelf and louvre.

The building is assumed to be orientated East-West at Maceió-Brazil, latitude 9°40'S and Longitude 35°42'W, with the window facing south. Analysis is based on summer solstice, 22nd of December, midday.

All illuminance results are based on computer simulation. The software presented in Chapter 7 was developed in MATLAB and uses ray tracing technique with Monte Carlo Method and daylight coefficients, previously discussed in Chapters 5 and 6.

8.3.1 The reference room

The reference room, as shown in Figure 8-1, is 6.00 x 6.00 m^2 and 3.00 m height. Those dimensions were chosen following previous studies done for daylighting and natural ventilation for the tropical climate [5, 6]. Internal reflectances are as follow: walls 0.6, ceiling 0.7 and floor 0.3. Shading devices have reflectance equal to 0.5 for every surface. Windows are 6.00 x 1.50 m^2 and its sill is 1.00m height. Wall thickness is 0.15m, typical for light walls in the tropics.

The observation point (P) is located in the centre of the room – 3.00m from the window and others walls – and on the workplane, 0.75m height.

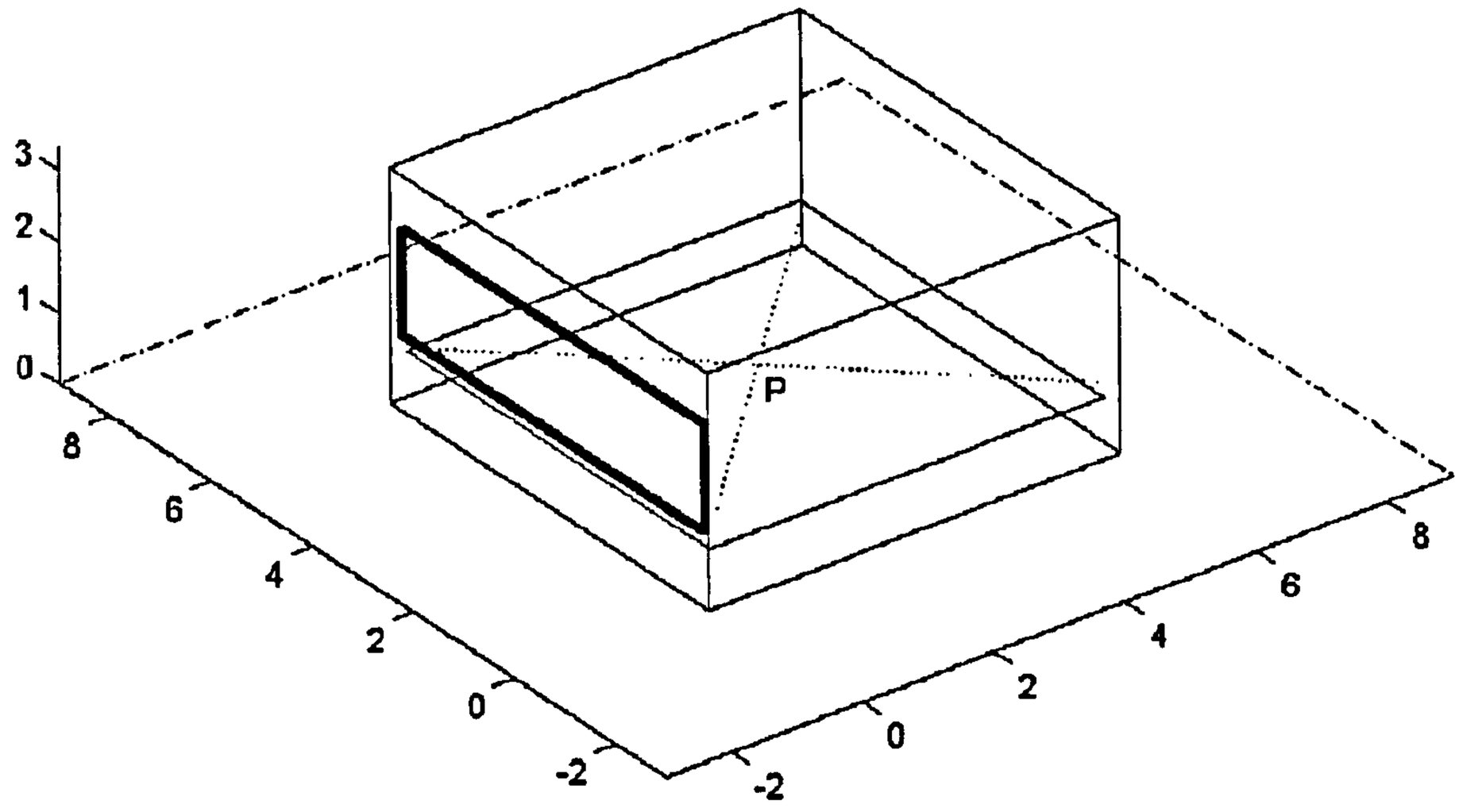

Figure 8-1 - Reference Room

Shading devices, as seen in Figure 8-2, were designed to protect the workplane from direct sun, but allowing a maximum view of the sky.

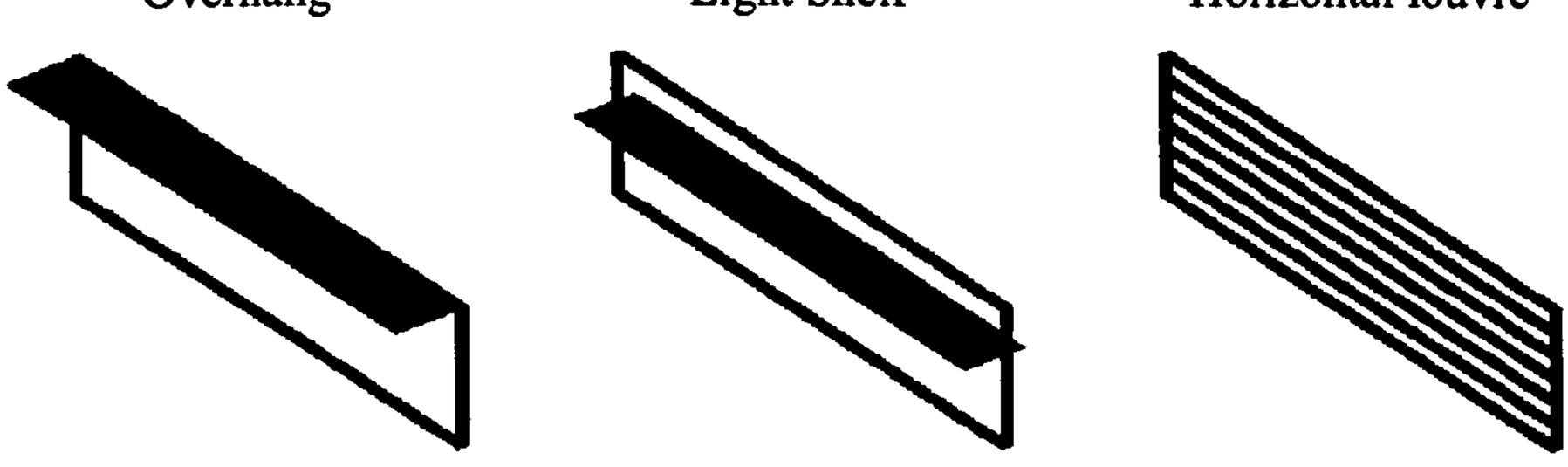

Figure 8-2 - Shading devices

8.3.2 The ground

The ground is split into nine striped regions, parallel to the window façade. Since the zone near the window façade is supposed to be more significant, the subdivision should be not even, but narrower near the window and widening as it goes away from façade. In this way, the time spent in calculation is considerably lessened, without important loss in accuracy. Based on this assumption, the boundaries of each patch are related to an angle formed by imaginary planes from the roofline, on the

window façade wall, to the ground. The angles are defined each 10°, from 0°, on the window façade to 90°, in the infinite (see Figure 8-3).

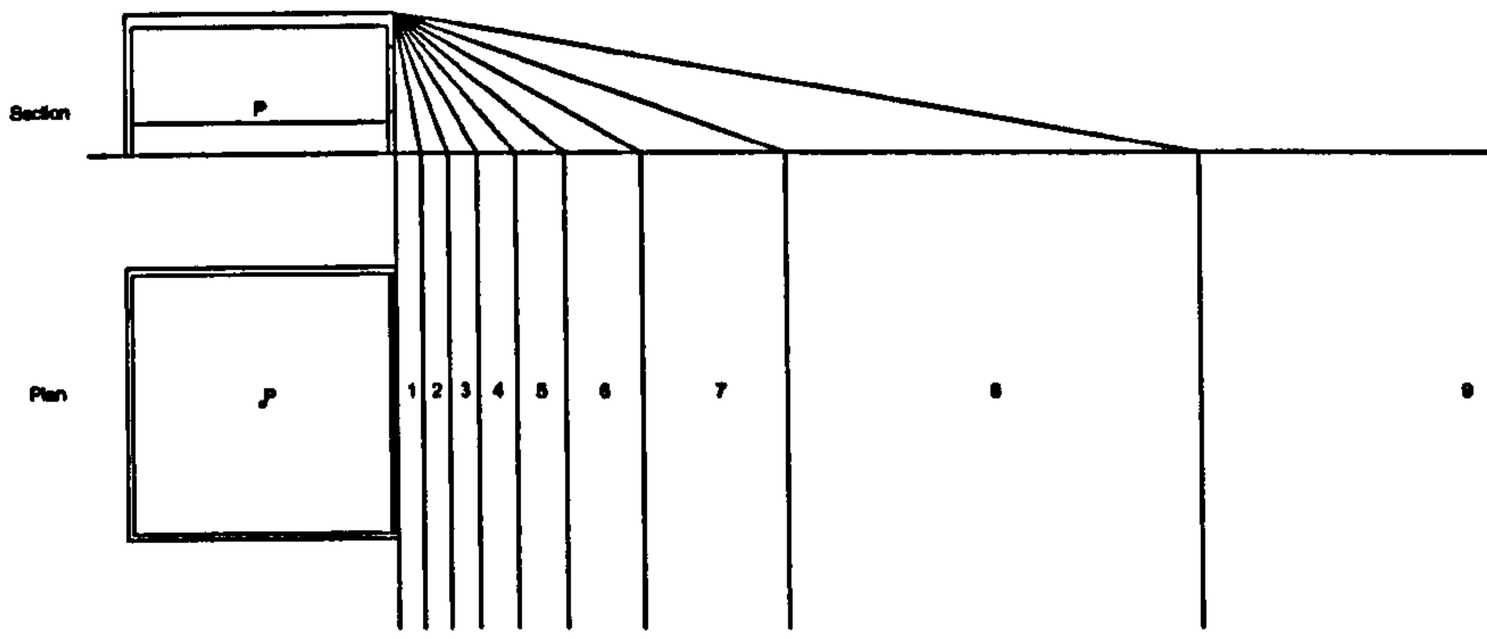

Figure 8-3 - Ground patches and Reference Room - Section and Plan

Table 8-1 - Ground patch configuration

Patch	Distance from Window Façade (m) Limit 1	Mid	Limit 2	Patch width (m)
1	0.00	0.29	0.58	0.58
2	0.58	0.89	1.20	0.61
3	1.20	1.56	1.91	0.70
4	1.91	2.34	2.77	0.86
5	2.77	3.35	3.93	1.16
6	3.93	4.82	5.71	1.78
7	5.71	7.39	9.06	3.35
8	9.06	13.89	18.72	9.65
9	18.72	∞	∞	∞

Table 8-1 shows the limits of each patch, as well as the midpoint and the width. The strip length is considered infinity.

In order to assess the influence of each patch, ground reflectance is set up to zero for all strips, except the one to get results, which has reflectance equal to 0.2. After the independent calculation for every strip, results are concatenated.

8.3.3 The choice of sky distribution

Sky distributions were chosen based on the fieldwork described in Chapter 4. The best choice went to three sky distributions: an overcast sky, represented by CIE Sky number 5 (uniform sky); a partly cloudy sky, CIE Sky 10 (Partly cloudy, brighter circumsolar) and a clear sky, CIE Sky 14 (Cloudless turbid with broader solar corona).

8.4 Ground coefficients

The concept of ground coefficients, discussed in depth in Section 6.4, relates the illuminance (E) on a given surface, i, from a given patch, j, of ground and the ground patch luminance (L) and the subtended area in steradians (ω) of the ground patch, j, as described in equation (8.1).

$$gc(i,j) = \frac{E_i(j)}{L_j \omega_j} \tag{8.1}$$

This concept deals with the geometry of building and ground and with the reflectance of surfaces. Ground coefficients are not dependent on sky distribution or sun position, however the ground luminance (L_{gr}) is.

8.5 Ground-reflected ratio (gr)

Some results in this Chapter are given in the form of the ground-reflected ratio (gr). In this way, the ground-reflected component is related to the total internal illuminance for the same point or surface. This relation is expressed by the equation (8.2)

$$gr = \frac{E_{gr}}{E_i} \times 100\% \tag{8.2}$$

where E_i is the internal horizontal illuminance and E_{gr} is its ground-reflected component.

The advantage of using *gr*, instead of the absolute illuminance value (E_{gr}), is that it makes it possible to compare the influence of different variables, for example sky type or latitude, using the same reference.

8.6 How far from window's façade the ground can be important as a source of natural light

The ground coefficients concept is used in order to assess the influence of ground distance to window's façade in its daylighting performance. It is calculated for every ground patch and results are plotted in Figure 8-4 for the four room patterns.

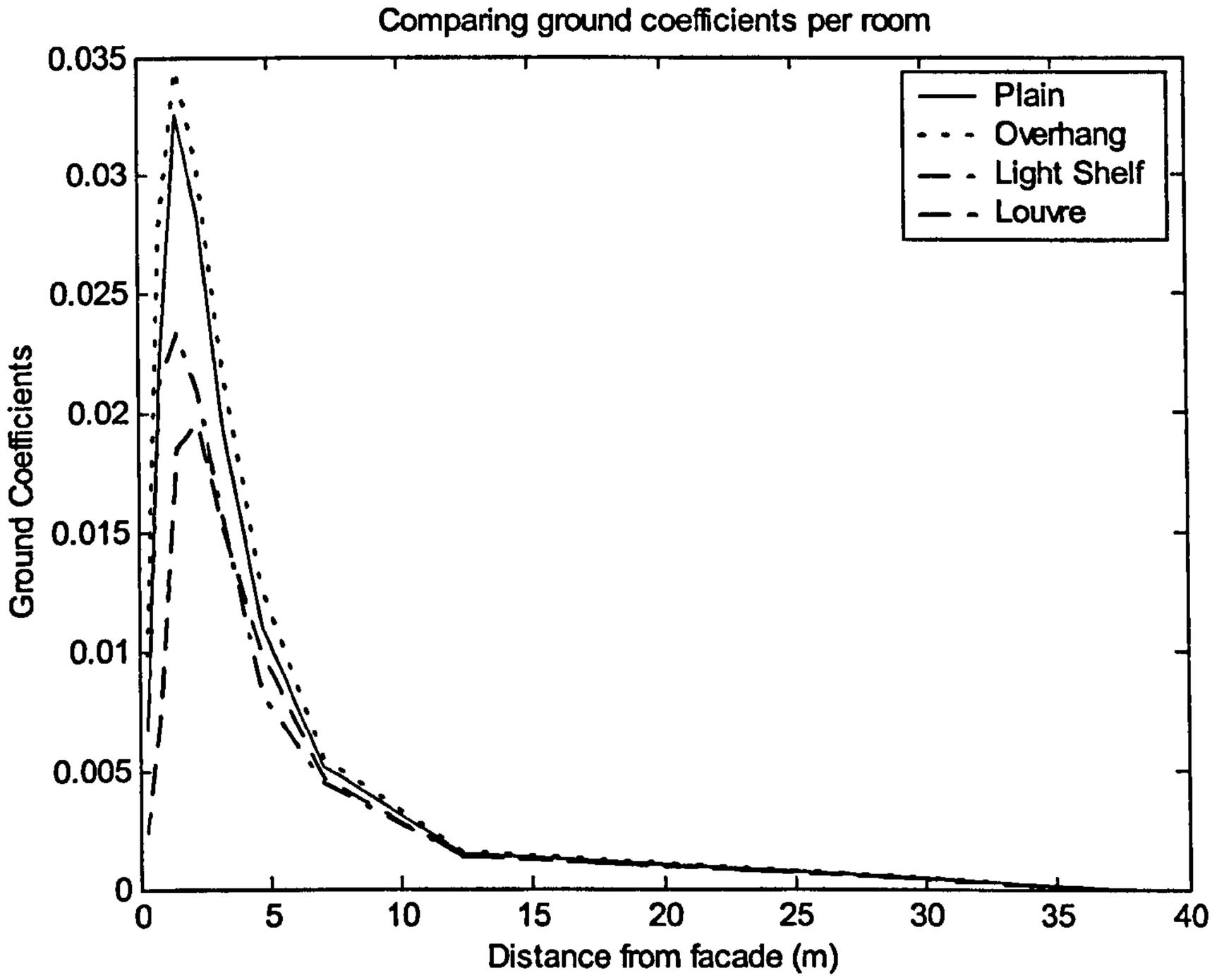

Figure 8-4 - Comparing ground coefficients (gc) by room pattern in function of distance from window

Aside from room pattern, it can be observed that there is a peak next to window façade which shows the most important ground region, regarding to its daylighting performance. For every pattern, *gc* is greater than 0.005 between 0.50m and 7.00m

from façade. It means that if the direct normal illuminance generated by this patch is for instance 10,000 lux, the ground component will be 50 lux.

The influence of shading devices will be better analysed in the next section, however with reference to ground location it is possible to note that the difference between patterns can only be detected within the peak region. There, overhang appears as the best choice to take advantage of ground-reflected light.

8.7 How a shading device's pattern can influence daylighting performance, relating to ground-reflected component

The type of shading device chosen can alter the influence of ground in internal daylighting performance. Comparing three different patterns: overhang (room 2), light shelf (room 3) and horizontal louvre (room 4), with a plain window (room 1), as shown in Figure 8-5, it can be seen that an overhang can increase the ground-reflected component in relation to a plain window.

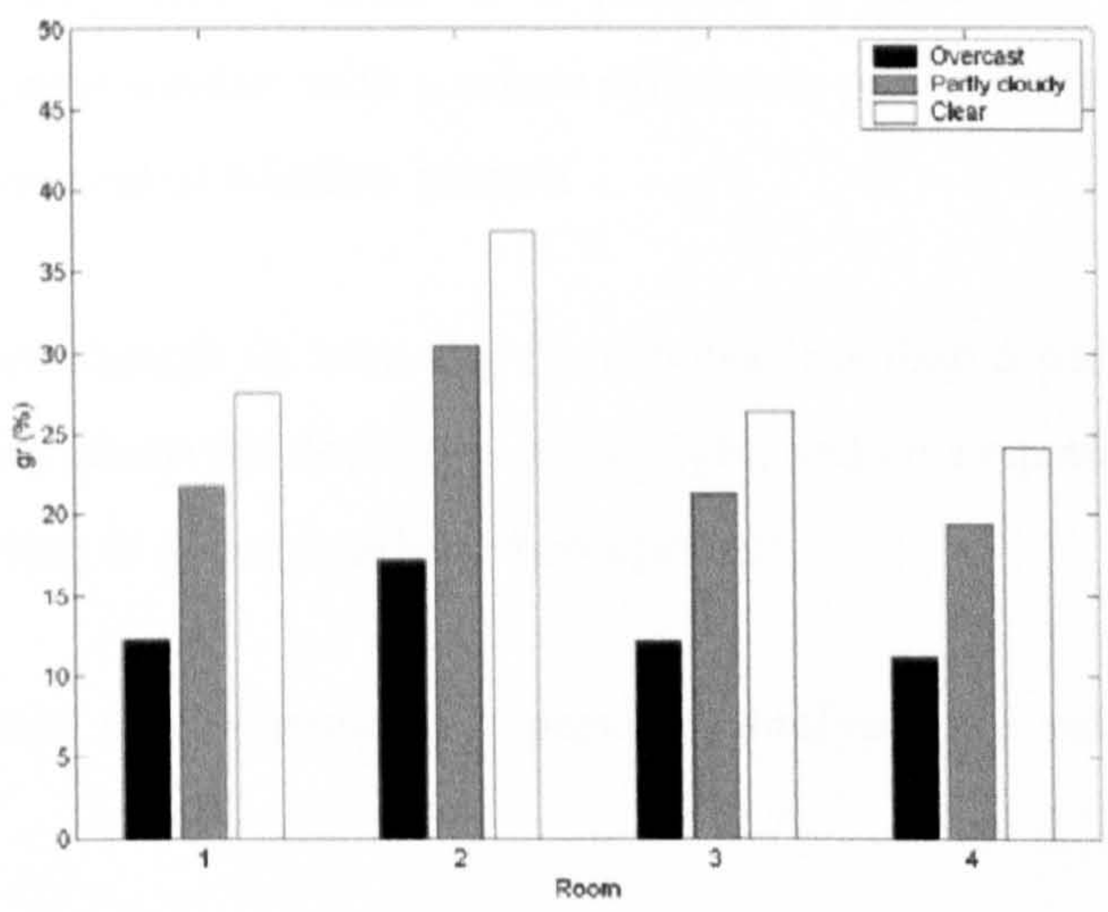

Figure 8-5 - Illuminance from ground-reflected light as a percentage of total daylight illuminance, at the mid-point of the reference room at working-plane (gr) by window pattern and sky type

As regards the other patterns, either light shelf or louvre produce only a slight reduction in the ground-reflected component, having the first a better performance.

It is worth noting that as regards the above points, there is no evidence of sky type influence altogether. Although, as discussed in next section, sky type can influence ground component, independent of window pattern.

8.8 What is the sunlight and skylight contribution, in function of sky type

The relative influence of sunlight and skylight in the ground-reflected component varies with sky type.

Obviously, the overcast sky has no sunshine. For the studied patterns the *gr*, as shown in Figure 8-6, is within the interval from 12% to 18%. However, it is notable that the *gr* due to skylight contribution in overcast sky is larger than partly cloudy and clear skies. Although in absolute figures results show that skylight contribution for partly cloudy and clear skies is higher, because of bigger external horizontal illuminance.

In relation to partly cloudy skies it is possible to note that the sun and sky contribution is almost similar, with a minor difference pro sunlight, as can be seen in Figure 8-6, independent of window pattern.

For clear sky, even though its blue sky contributes less than a partly cloudy sky, its sunlight can supply about the double as its skylight, and consequently giving the best performance relating to ground-reflected component

It is also important to emphasise that previous analyses are valid independent of room pattern.

Overcast sky (sky 1)

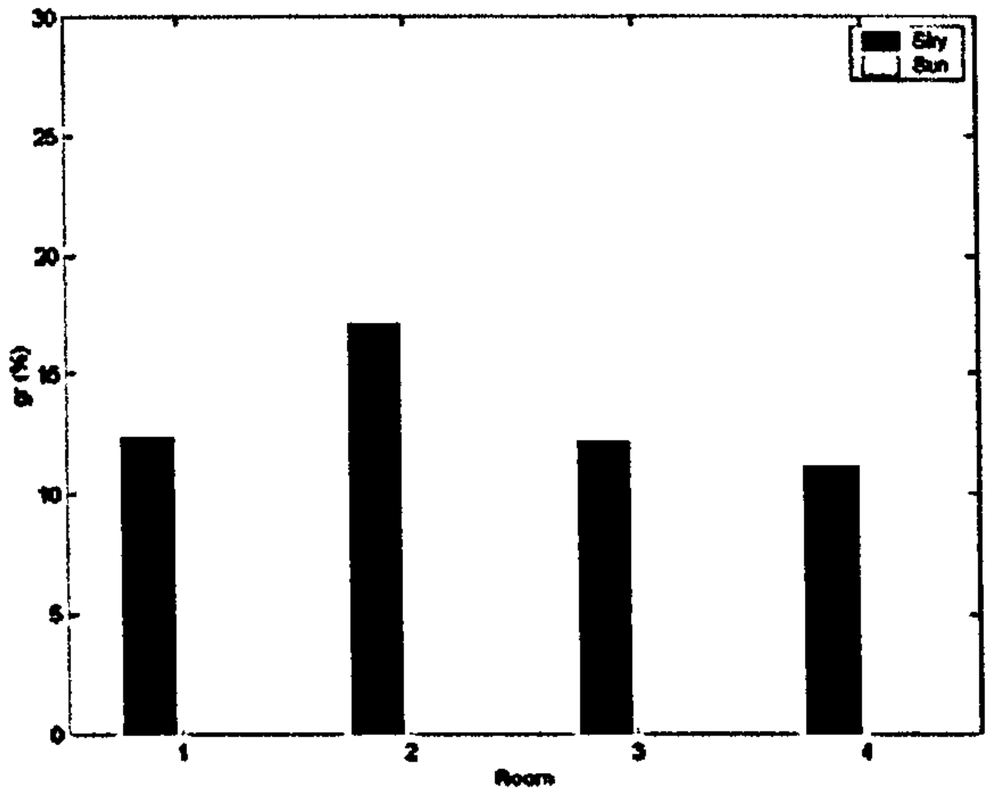

Partly cloudy sky (sky 2)

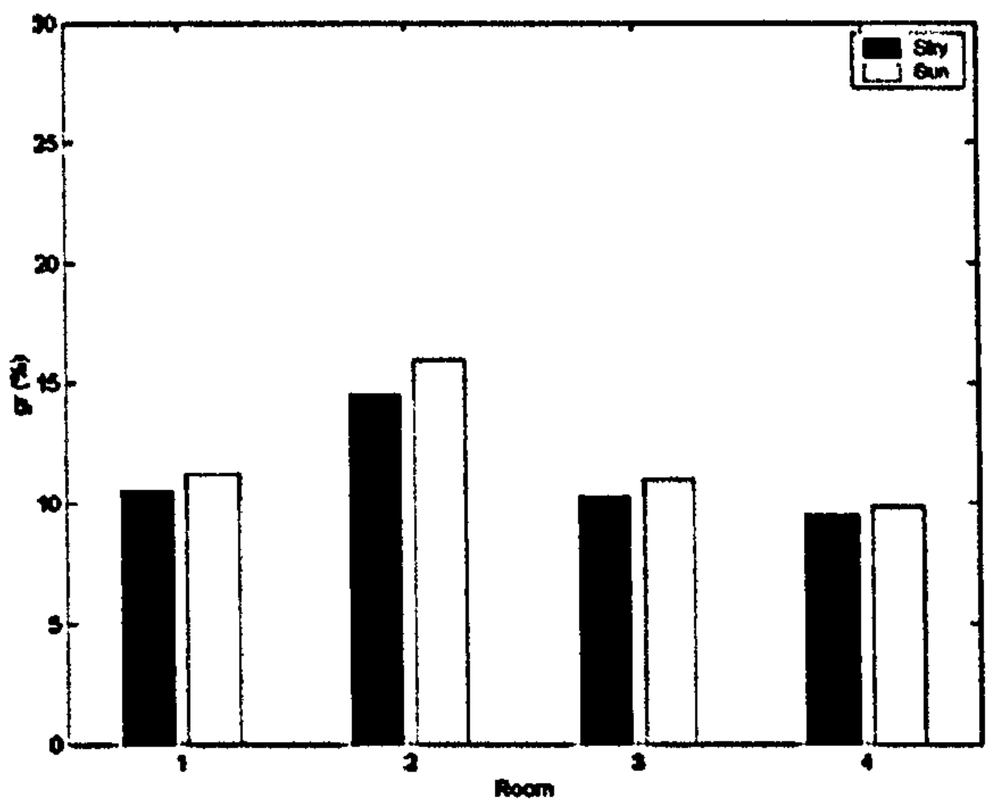

Clear sky (sky 3)

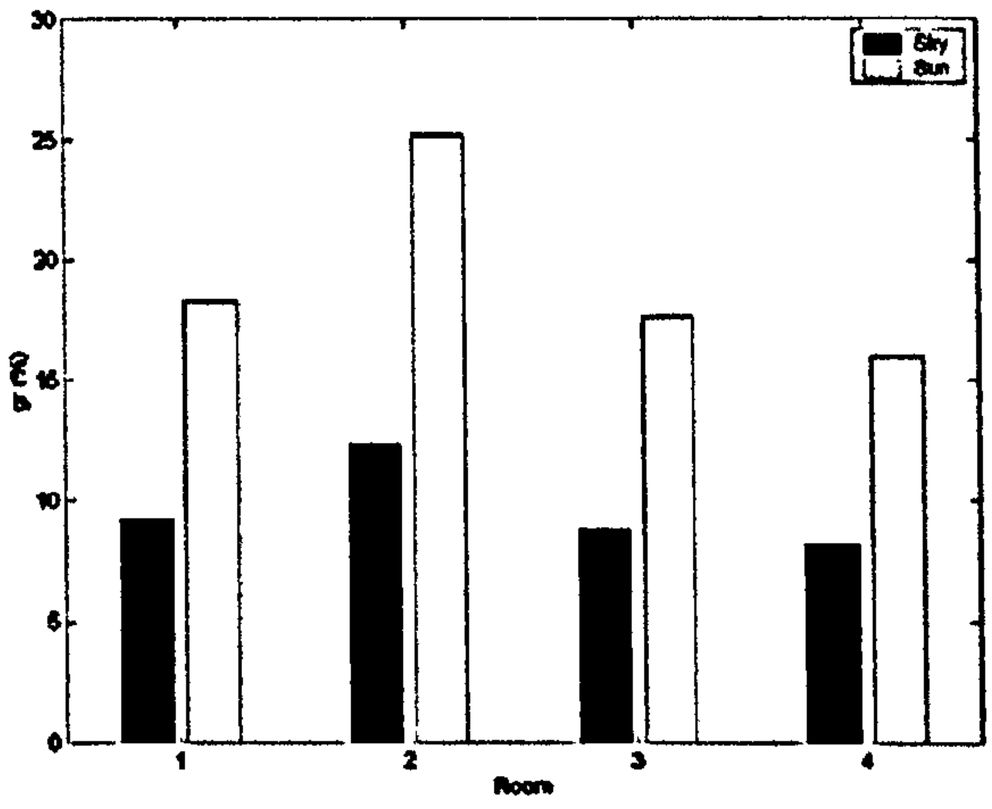

Figure 8-6 - Illuminance from ground-reflected light as a percentage of total daylight illuminance, at the mid-point of the reference room at working-plane (gr) by window pattern and component

8.9 Conclusions

The work has shown that for this reference room the light reflected from the ground (*gr*) is a significant part of the total working-plane daylight. In the examples analysed, *gr* ranges from 10 to 40%. The highest values occur when there is sunshine on the ground. Diffusely reflected sunlight is clearly a significant source of illuminance in tropical buildings, but it can also be said that ground-reflected skylight should be taken into account, as its contribution is almost the same as the ground-reflected sunshine for partly cloudy skies.

It is up to the designer to weight up the importance of each kind of sky, in function of the building location. For instance, a designer in a hot-dry city may emphasise the clear sky characteristics, while a fellow in the humid-warm Brazilian northeastern coast may call more attention to the partly cloudy sky aspects.

Another point to highlight is the ground distance to the window façade. Results have revealed that there is a peak region where the ground can be more important to the internal daylighting. The designer can take the advantage of this point by increasing reflectance in this area. This region is not dependent on the latitude, but on the material characteristics and geometry of building and surrounding. Figure 8-7 shows the location of the peak region (AB) in a section of the reference room.

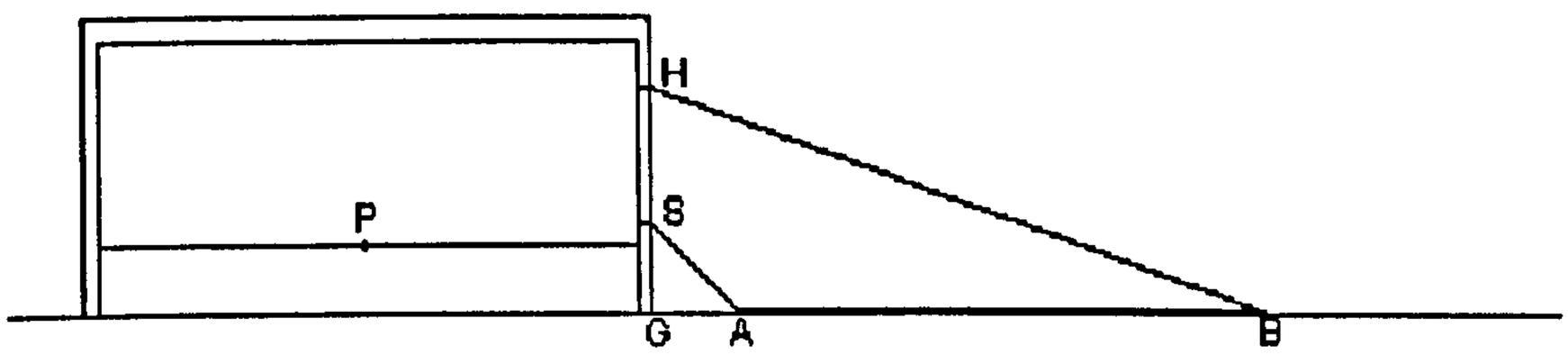

Figure 8-7 - Ground peak region (AB), regarding the ground influence in internal daylighting performance

As a rule of thumb, for a similar one-storey building, the boundaries of the peak region, A and B, can be found by the angles GSA=45° and GHB=70°, where G is the base of façade, S is the sill and H is the head of the window.

Between the shading device patterns analysed, overhang has shown the best results for every sky type. Light shelf and horizontal louvre has achieved results near the plain window. However, it is important to note that both can contribute to reducing glare and insolation, keeping the performance of a plain window, which has tendency to produce glare and thermal discomfort in tropics.

In addition, it is worth noting that any change in the shading device surfaces reflectance has a direct effect which results in a shift in the ground-reflected component. In this way the designer can increase or decrease its value in order to achieve the goal.

Since results were calculated for the room mid-point, it is expected that the ground-reflected ratio can be smaller near the window and greater in the rear of the room. This is due to the decreasing of direct sky component as the observation point (P) is far from the window.

In this study, all surfaces considered are perfect diffusers, and any specular reflection is not taken into account. Inter-reflection between the building and the ground was found to be insignificant with the geometry adopted for this example. Conclusions presented in this Chapter are related to the ground-reflected component of daylight, and do not take into account every aspects of the quality of daylight.

References

1. Hopkinson, R. G. and P. Petherbridge. *The natural lighting of buildings in sunny climates by sunlight reflected from the ground and from opposing facades.* in *Conference on Tropical Architecture.* London, 1953.

2. Griffith, J. W., O. F. Wenzler, and G. W. Conover, *The importance of ground reflection in daylighting.* Illuminating Engineering (New York), **48**: p. 35-38, 1953.

3. Lam, W. M. C., *Sunlighting as formgiver for architecture.* New York: Van Nostrand Reinhold, 1986.

4. Tregenza, P. R., *Mean daylight illuminance in rooms facing sunlit streets.* Building and Environment, **30**(1): p. 83-89, 1995.

5. Bittencourt, L., G. Bianna, and J. M. Cruz. *Efeito de protetores solares verticais e horizontais na ventilação natural de salas de aula do 2° grau.* in *I Encontro latino Americano e III Encontro Nacional de Conforto no Ambiente Construído.* Gramado: ANTAC. p. 383-388, 1995.

6. Bittencourt, L., *et al. Influência da localização, dimensão e forma das janelas nos níveis de iluminação natural produzidos por céus encobertos.* in *I Encontro latino Americano e III Encontro Nacional de Conforto no Ambiente Construído.* Gramado: ANTAC. p. 571-576, 1995.

Chapter 9 Conclusions

9.1 Results and goals

The three specific goals of the thesis are embodied in the three parts of the dissertation. The aim of this chapter is to give a concise summary of the outcomes of the project and their implications for later research and practice.

A The first goal was a method for sky type selection with incomplete sky luminance data. Chapter 4 shows that *a reasonable assumption about the daylight climate of a place in the humid tropics can be made from very simple data*. This suggests that, provided a small network of research-class measuring stations is available to provide calibrated comparisons, the new structure of CIE Standard General Sky, which requires appraisal of the local daylight climate, could be applied everywhere.

B The second goal was to assemble a framework of algorithms and prototype software (TropLux) focussed on prediction of interior daylight in humid tropical climates. This is developed in Part II, chapters 5 – 7. It is shown that *existing techniques, largely originating from researchers working in temperate climates can be successfully used for predicting daylight illumination in the tropics*. The basis of the new calculation can be seen as an extension of the daylight factor concept to the CIE Standard General Sky and sunlight. Also from the results, it may be concluded that it is not essential to have climate-specific calculation techniques and that universal lighting software is practicable.

C A special focus of the research was ground-reflected light; this constitutes the worked example, the third of the goals. Part III shows that *in the tropics, even in cloudy regions, the influence of reflected light on interior illuminance can be very large*. It is shown that there is a key zone of ground outside a window that provides the majority of the reflected light. This has important implication for design, especially in that window sizes could be reduced by making better

use of diffused sunlight. Chapter 5 introduces the idea of a ground coefficient; chapter 8 summarises the results and describes an approach to calculation.

9.2 Results and the current literature

A Chapter 2 shows that climate classification can be approached in various ways but it was found that the current literature does not give clear guidance on the best choice of classification type for daylighting research [1]. From the present study it appears that *a subdivision based on humidity is the most appropriate and therefore a 'hot-dry : warm-humid' classification should be adopted for tropical daylight research.* Humidity has a direct relationship with cloud formation and therefore on both daylight availability and sky luminance distribution. The results of this research can thus be extended to tropical regions that are similar in climate to north-east Brazil, based on Section 2.4.4 discussion.

B The small sample of site measurements produced daylight data which was entirely consistent with published results from other sites (see Section 4.4). The selection of three skies – Uniform Sky (CIE Sky 5), partly cloudy with brighter circumsolar (CIE Sky 10) and cloudless turbid with broader solar corona (CIE Sky 14) – supports the proposals made by earlier research [2]. As a general result: the set of standard skies that best characterising a climate consists of three sky types from distinct subset – overcast, partly cloudy and clear distributions.

C It was found in the research that *backward ray tracing with Monte Carlo simulation can deal satisfactorily with the variation in tropical skies and the complexities of apertures* required for sunlight control (Chapter 5). This gives weight to the assumptions behind programs such as RADIANCE [3]. In general, the project offers support to the application to tropical climates of software and algorithms that were originally developed for temperate and high-latitude climates.

D The project makes *a contribution to daylight prediction theory with the ideas of ground and obstruction coefficients*, complementing the concept of daylight coefficients [4]. In addition, new sky grids with smaller subdivisions are proposed for sunlight calculation. One is related to the existing CIE sky subdivision and is useful if related to IDMP station data. The other is a very neat symmetrical subdivision, capable of being implemented in computer simulation of sky models, such as the CIE standard general skies. This work also suggests a pattern of ground subdivisions that can optimise the calculation of the daylight and ground coefficients.

9.3 Implications for primary school building design

The results found for ground-reflected light are independent of the building. There is however a particular implication for primary schools design, which was an early interest of the research:

A Considering the typical building material of the Brazilian north-east, it is clear that interior lighting could be enhanced by the use of beach sand, instead of grass or clay in the critical ground area near the window (Chapter 8, Figure 8-7). There is scope for further study, however, to examine the consequent thermal effects.

B Perforated block is a typical element of primary schools window apertures. Its use was thoroughly studied by Bittencourt [5] and when correctly applied represents a cheap and efficient way to deal with local climate. The daylighting performance of perforated block could be boosted by increasing the ground-reflected light.

C Orientation of the building is important. Although this is not specifically analysed in the research, the results have implications for the choice of orientation. Direct sunlight is not welcome in school classroom. East and West orientations should be avoided since they need more complex shading devices comparing to North and South orientations. As the place becomes closer to the equator, the daylighting differences between North and South façades become

insignificant. Both can be protected from the direct sunshine with simple overhangs.

When the site's latitude moves southwards from the equator, the North façade receives longer periods of sunlight then the South. The difference between orientations intensifies with latitude and it is important to note that increasing hours of sunshine are associated with lower solar altitudes. Although higher solar altitudes give more light and heat, they are easier to protect with shading devices.

Thus for the tropics in South hemisphere, orientation for classrooms should be chosen in this order of preference: South, North, East and West. Naturally, for northern latitudes the order should be North, South, East and West. These conclusions are not valid for high latitude regions where sunshine is welcome in winter due to thermal requirements.

9.4 Limitations of the results and suggestions for future research

The focus of the project and the limited time scale of PhD research necessarily restrict the scope of results. The following limitations should be noted:

A The proposal for insolation and sky type probability is intended as guidance for daylighting design; it does not necessarily have significance for meteorological forecasting.

B The choice of sky types for Maceió, presented in this thesis, can only be regarded as an initial proposal. Due to the nature of the fieldwork, it was based on a restricted period of time and a limited number of measurements.

C The prototype software for daylighting calculation, although has been shown suitable for daylighting research, has limited use for designers. This is because an unacceptable amount of time can be spent testing different designs,

comparing against software currently available for design offices. The interface developed in this work is not suitable for non-expert users.

D During the TropLux validation using BRE-IDMP dataset, the building and surrounding geometry were simplified, based on the available data.

These lead to suggesting for future research:

E Further climatic studies are to be welcomed, as they increase the body of knowledge with regard to the comprehension of the tropical daylight climate. The occurrence of sunshine needs more data to feed a detailed annual daylighting analysis. A relation between sky cover and availability of sunshine could also be interesting for general daylighting simulation.

F The use of the sky luminance measurement methodology proposed for a longer period and assessed for a larger number of sky points could give a better conclusion about the choice of sky type.

G Some similarities in results between different sky models (see Chapter 4) suggest more research with regard to the influence of different sky standards in internal illuminance. The effect of reflected sunshine should also be taken into account.

H The link between tropical daylighting and thermal issues should bring about researches with regard to suggestions of upper illuminance levels for specific room situations, in addition to the usually proposed lower illuminance level in official standards.

I Daylighting studies are usually simplified due to: (i) difficulties to get the real characteristics of the building and surrounding; (ii) lack of a daylighting tool to assess specific features; or (iii) time limitation. TropLux can deal with very complex room geometry and allow detailed definition for material characteristics. It can point to an analysis on the consequences of simplification on daylighting simulation.

J This work has presented an approach to ground-reflected light. More generalisations could be done for multi-storey buildings, for variation in windows orientation and period of the day/year. In the research, all surfaces were considered perfect diffusers and specular reflection not taken into account. Work is required to test the validity of this and to examine the effects of complex obstruction.

K Generally, guidelines and rules of thumb are still needed in tropical daylighting. This work has produced a reliable tool for daylighting researchers. It is expected that TropLux can be used as an impetus for new developments in this area.

9.5 Epilogue

In the introduction, a distinction was made between the technical and the socio-economics arguments for improving the utilisation of daylight. The results have been concentrated on the technical analyses. It is clear, however, that there are economic consequences.

Although a good daylighting design may increase the initial building costs, the reduction on window size for daylighting purposes, achieved by using ground-reflected light, proposed in Chapter 8, may also reduce building costs, keeping the cutback on long-term electricity costs.

The simplified method for sky type selection, proposed in Chapter 4 can significantly reduce the equipments costs, when compared with the IDMP research station. It may facilitate the creation of daylight research centres in regions that cannot afford a complete set of daylighting instruments.

As a consequence, the dissemination of daylighting research in tropical countries, based against a theoretical background plus regional information, may produce better solutions for the use of natural light in buildings, which could in turn lead to reduce energy costs and improve the quality of life of the people.

Reference

1. Köppen, W., *Das Geographische System der Klimate*, in *Handbuch der Klimatologie*. Kraus-Thomson: Berlin, 1936.

2. Tregenza, P. R., *Standard skies for maritime climates.* Lighting Research and Technology, **31**(3): p. 97-106, 1999.

3. Ward, G. and R. Shakespeare, *Rendering with radiance: the art and science of lighting visualization.* San Francisco: Morgan Kaufmann, 1998.

4. Tregenza, P. and I. M. Waters, *Daylight coefficients.* Lighting Research & Technology, **15**(2): p. 65-71, 1983.

5. Bittencourt, L. S., *Ventilation as a cooling resource for warm-humid climates: An investigation on perforated block wall geometry to improve ventilation inside low-rise buildings*, PhD, in *Environment and Energy Studies Programme*, Architectural Association Graduate School: London. 314 p., 1993.

Appendices

Eight appendices are presented as supplementary information for the full comprehension of some points presented in the body of the thesis. Appendix A shows 34 figures for monthly and daily nebulosity variations and the probability of sky type, discussed in Chapter 3. The equipment and accessories used in fieldwork, reported in Chapter 4, are listed in Appendix B. Appendix C describes the input table used during the sky luminance measurement, explained in Chapter 4. Also referred to in Chapter 4, Appendix D reviews the CIE standard general sky and presents images of the relative luminance distribution for the 15 sky types, for a visual comparison. As a theoretical complement, Appendix E analyses when a surface can be considered a point source in lighting calculation. It is referred to in Chapter 6. A selection of the main codes of TropLux, studied in Chapter 7, is aggregated in Appendix F, while graphs reported on in the validation (Section 7.5.2.3) are shown in Appendix G. Finally, Appendix H shows the poster and the paper presented in PLEA 2002, based on the research developed in this thesis.

Appendix A - Monthly and daily nebulosity variation and probability of sky type

A.1 Nebulosity variation during the day for each month

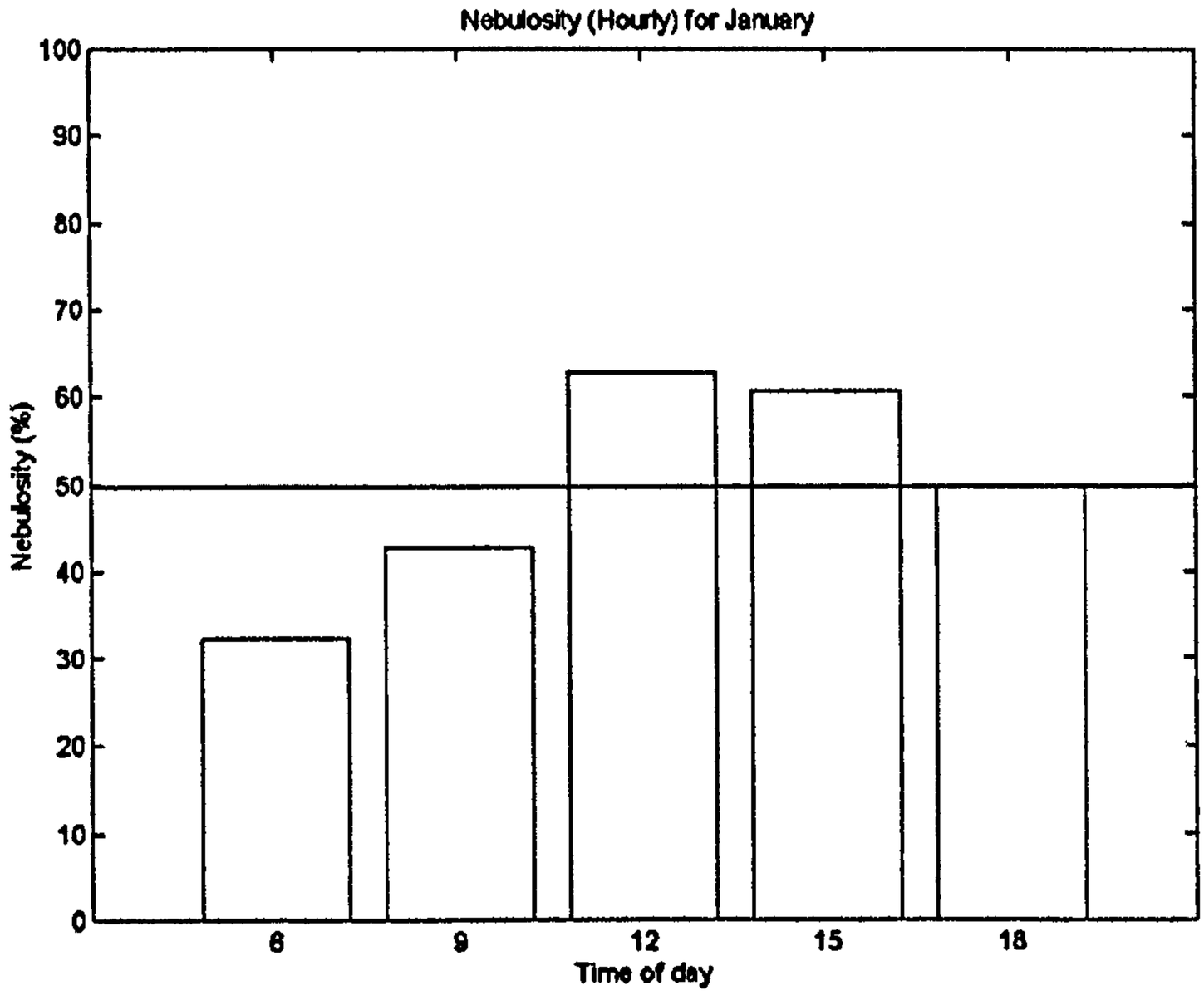

Figure A-1 - Nebulosity (Hourly) for January

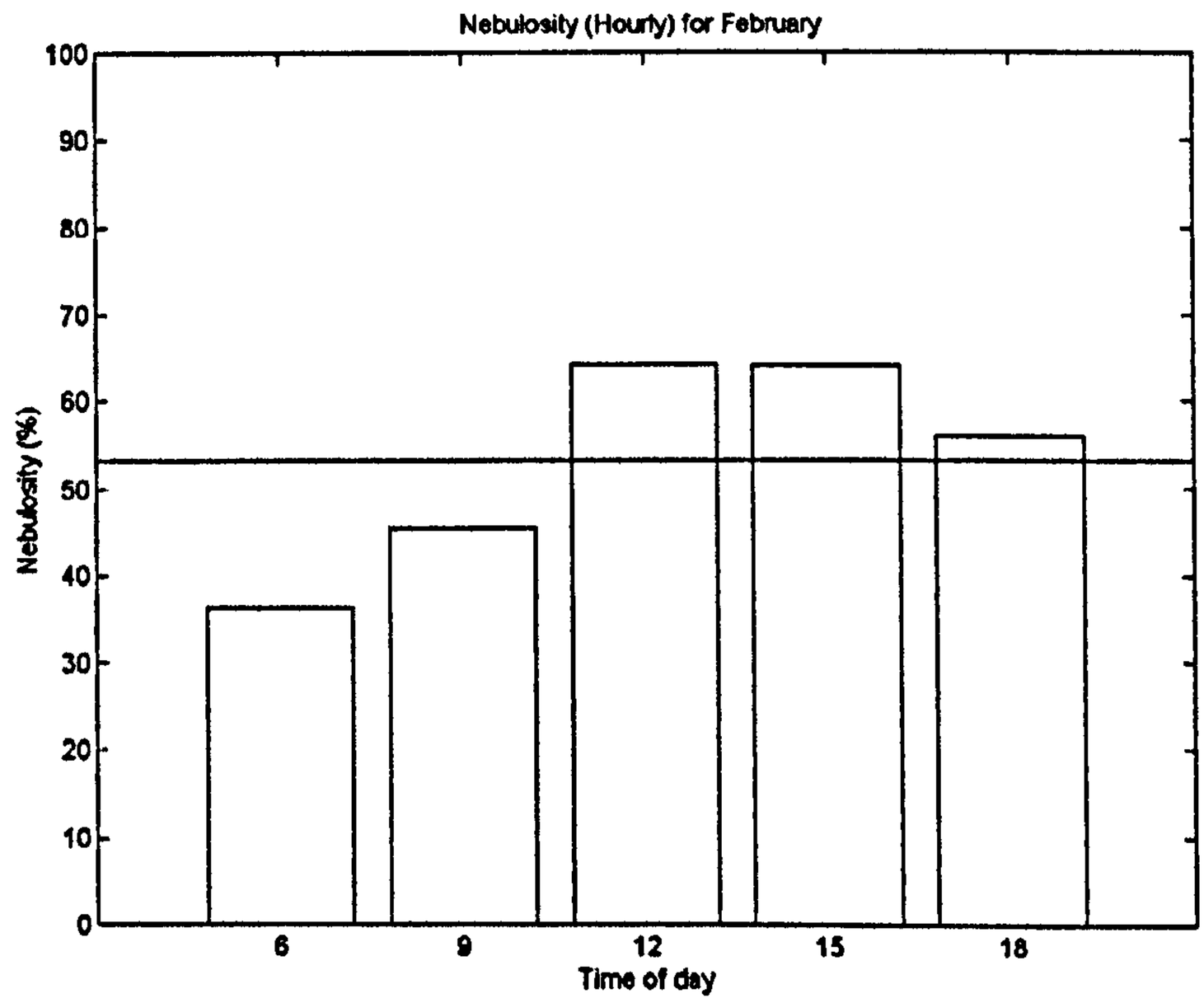

Figure A-2 - Nebulosity (Hourly) for February

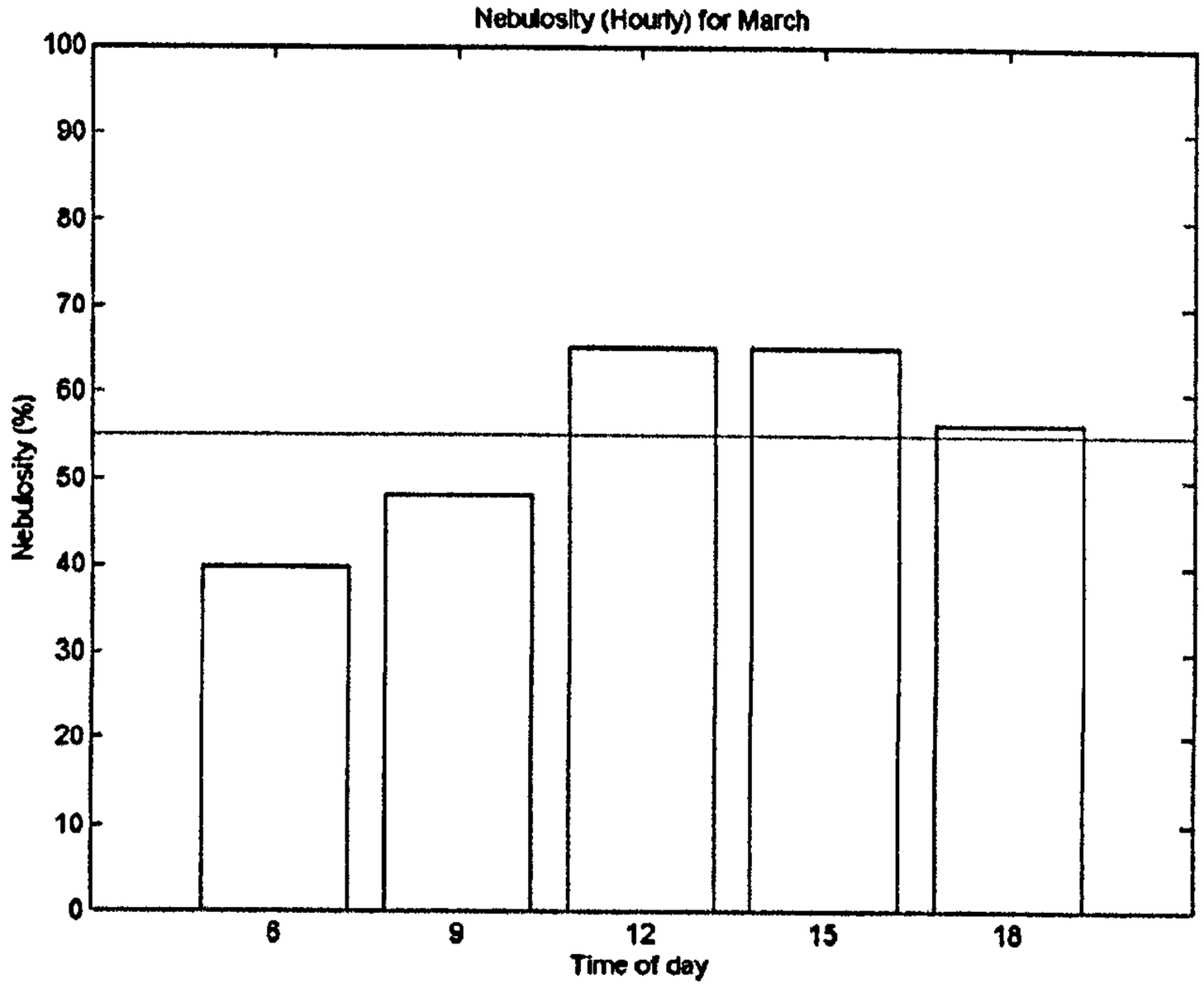

Figure A-3 - Nebulosity (Hourly) for March

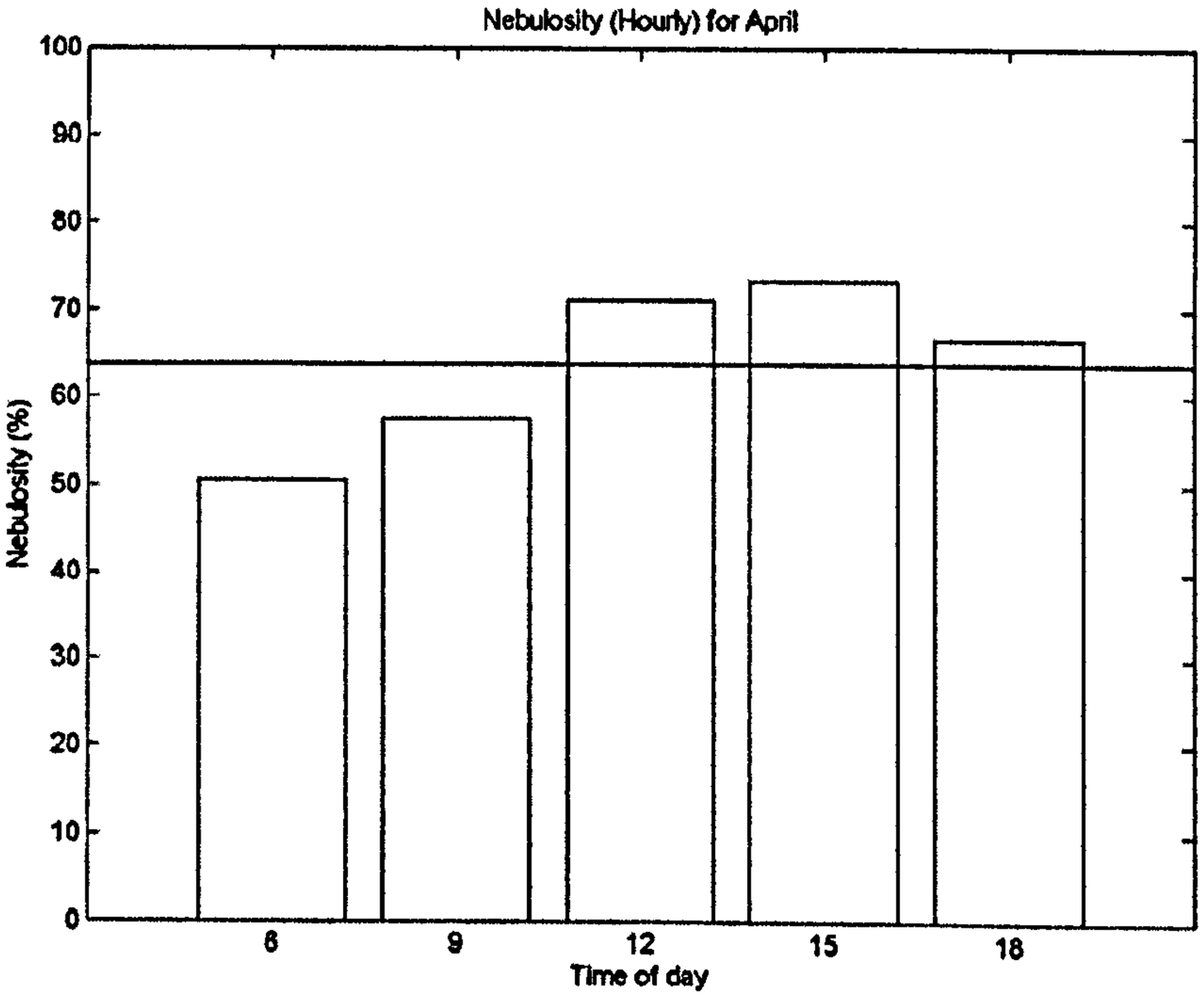

Figure A-4 - Nebulosity (Hourly) for April

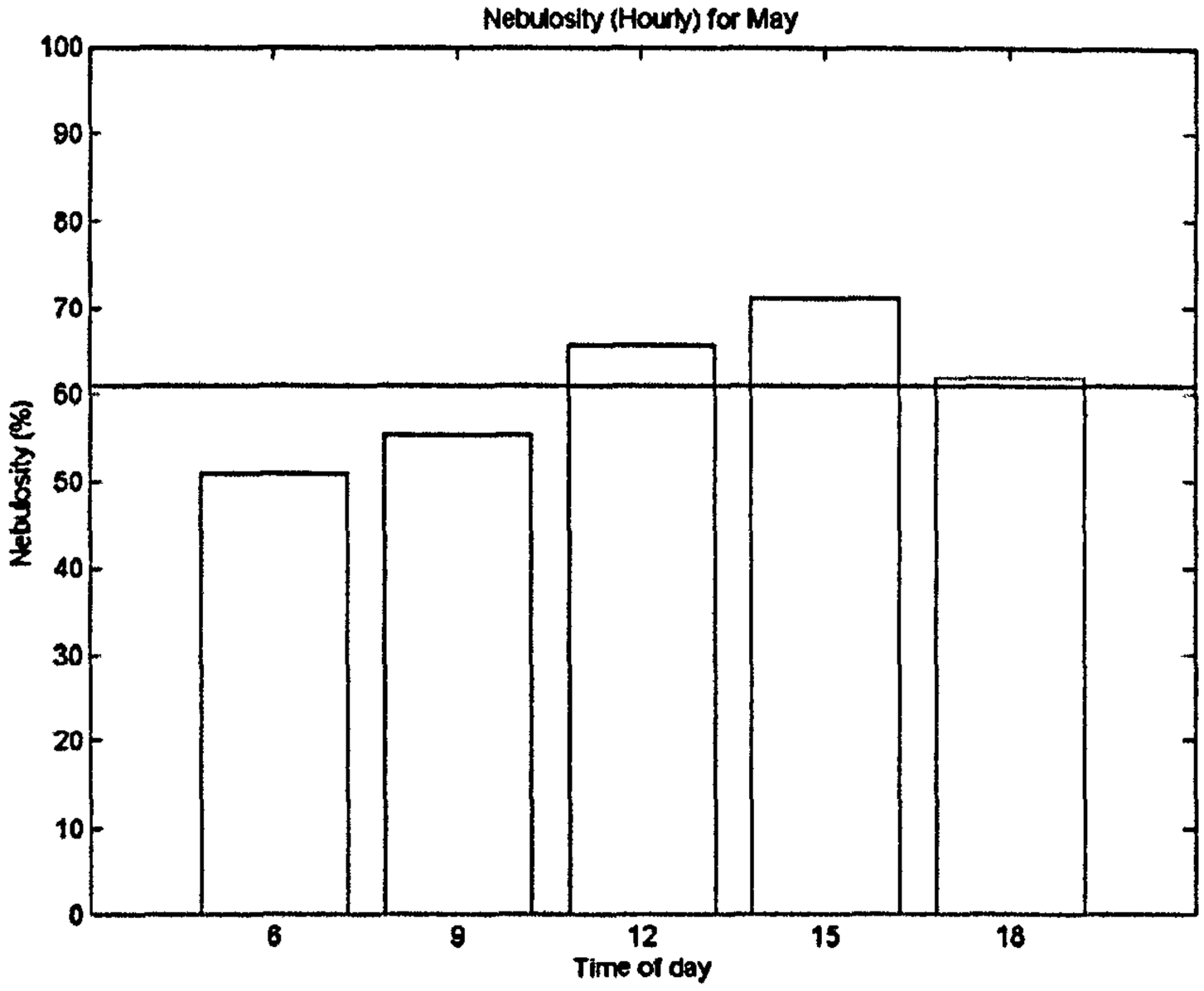

Figure A-5 - Nebulosity (Hourly) for May

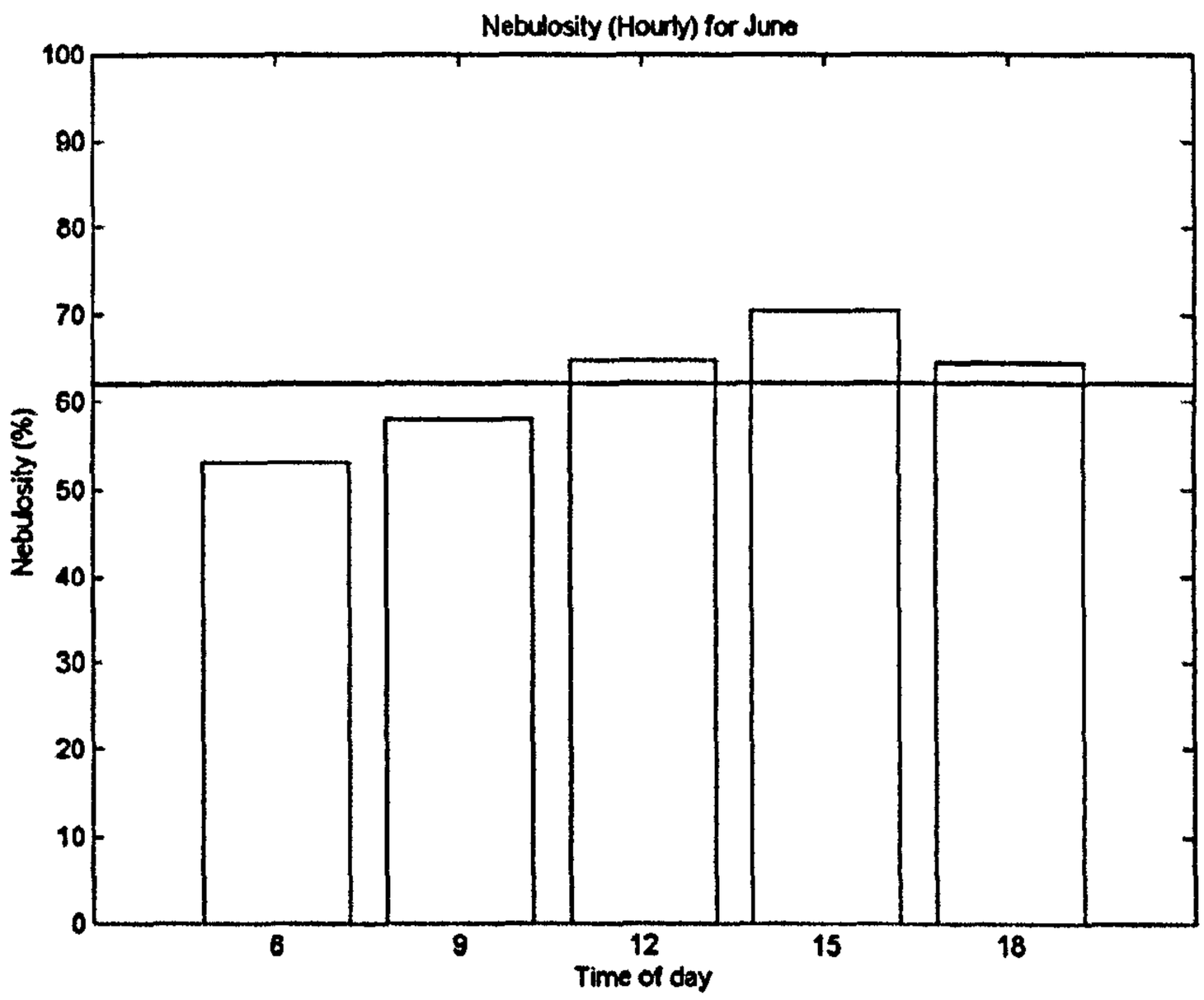

Figure A-6 - Nebulosity (Hourly) for June

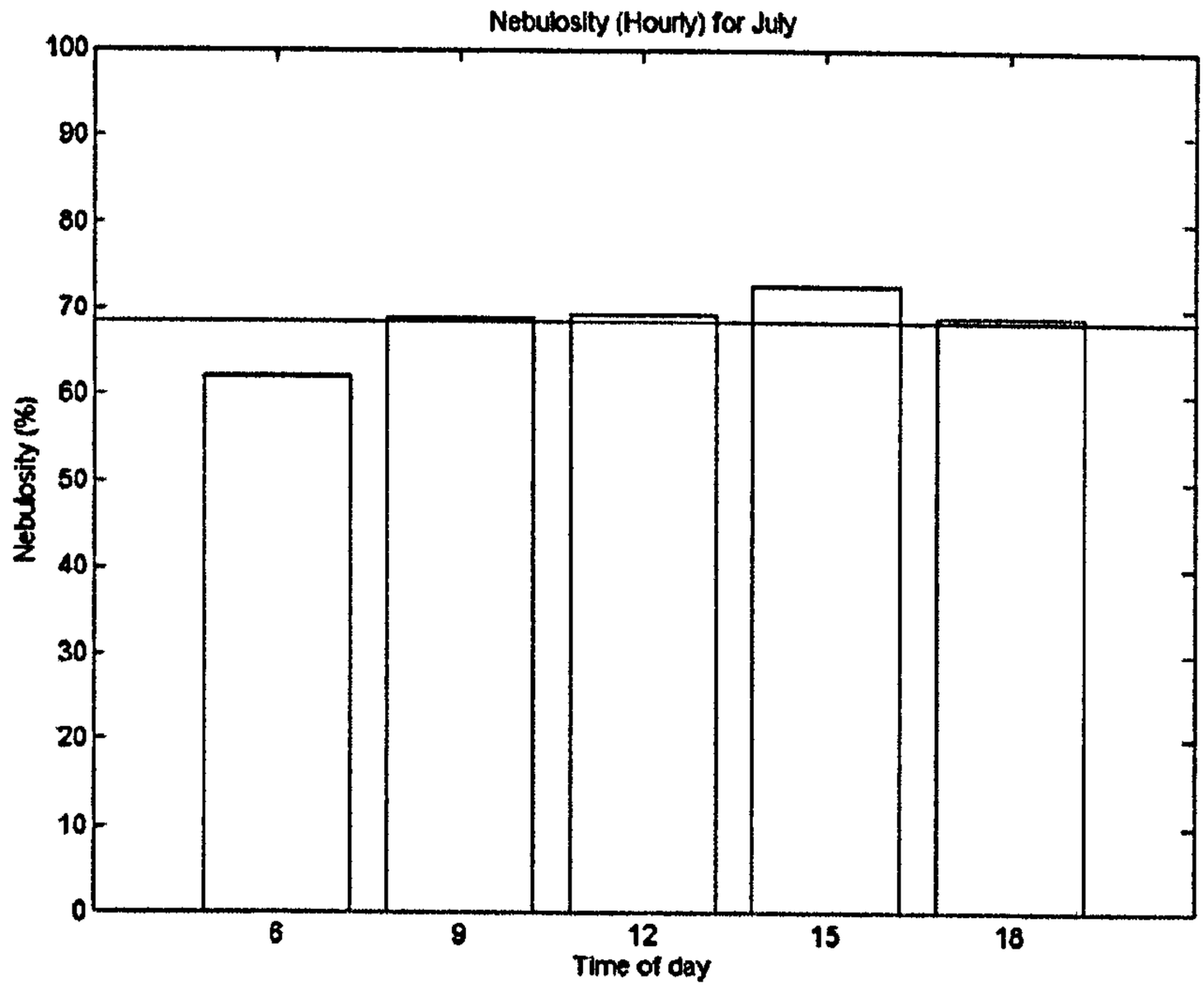

Figure A-7 - Nebulosity (Hourly) for July

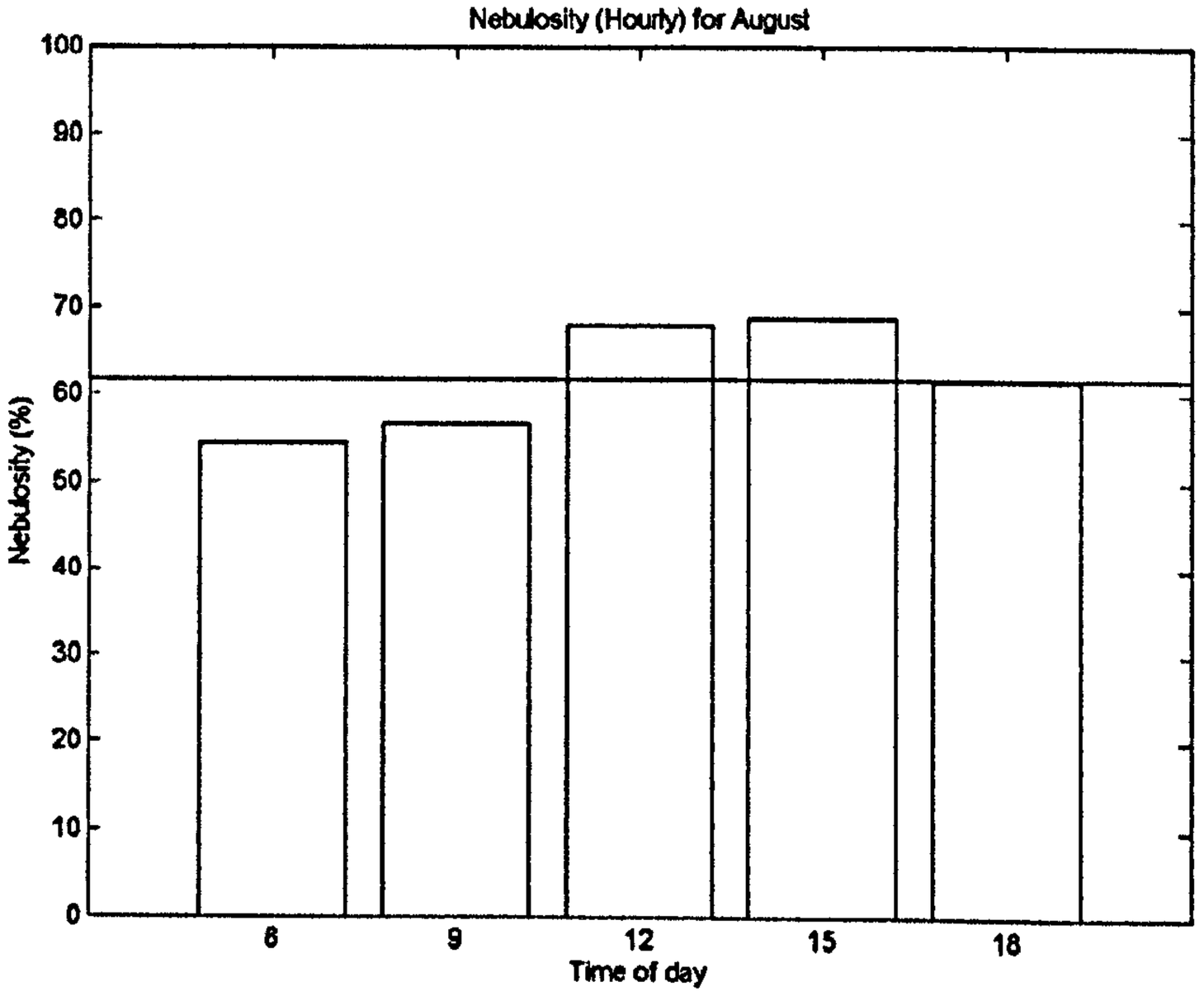

Figure A-8 - Nebulosity (Hourly) for August

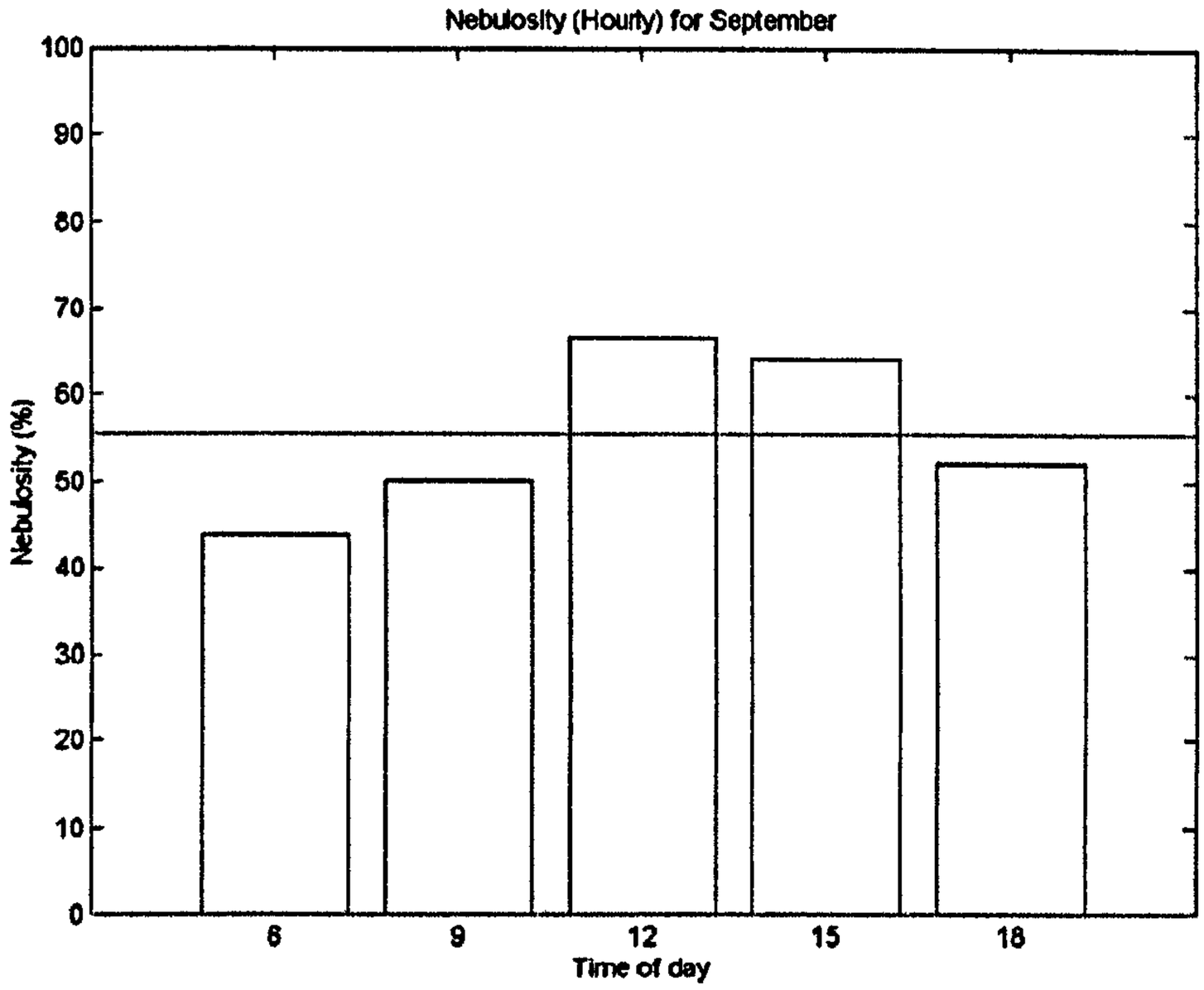

Figure A-9 - Nebulosity (Hourly) for September

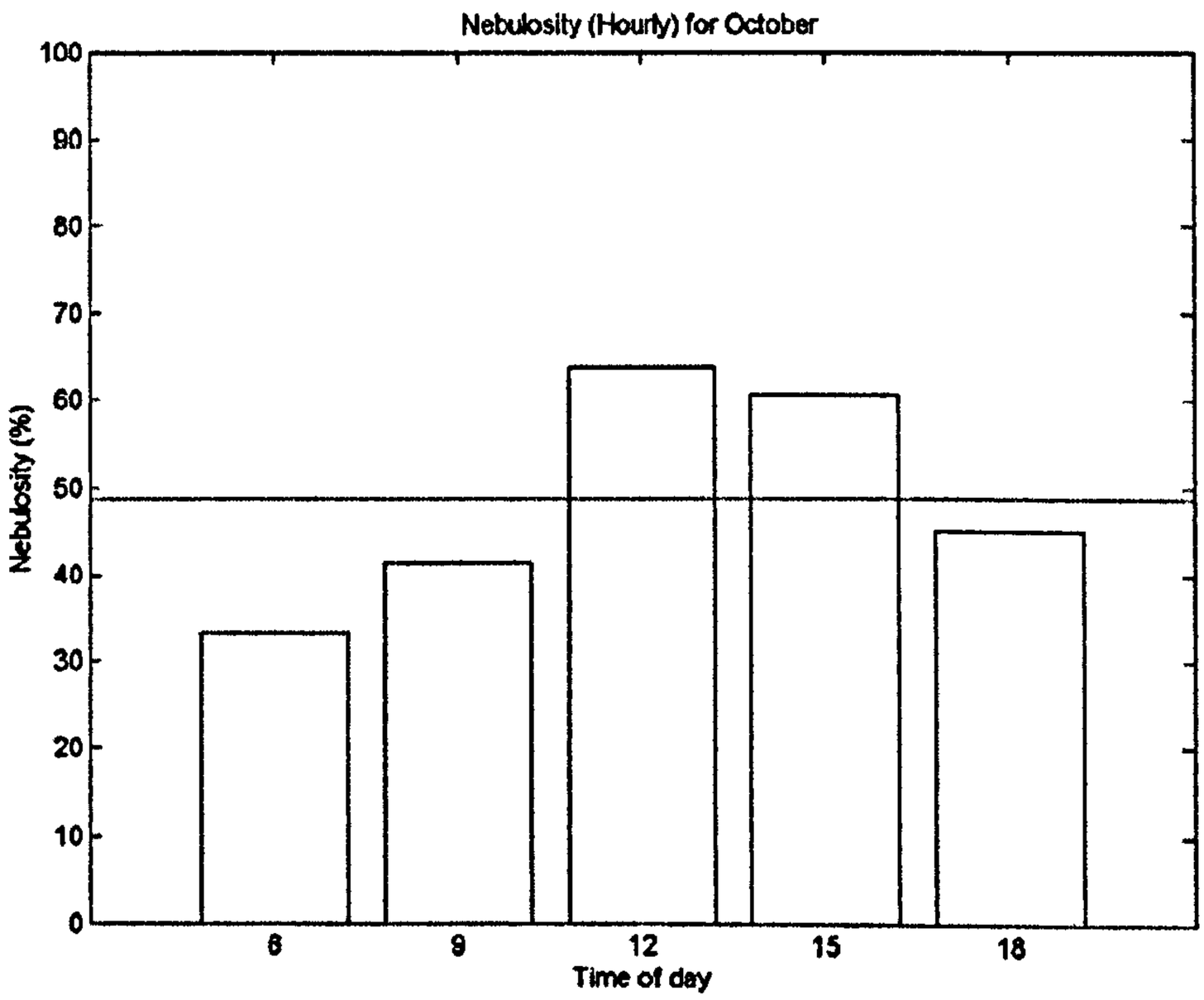

Figure A-10 - Nebulosity (Hourly) for October

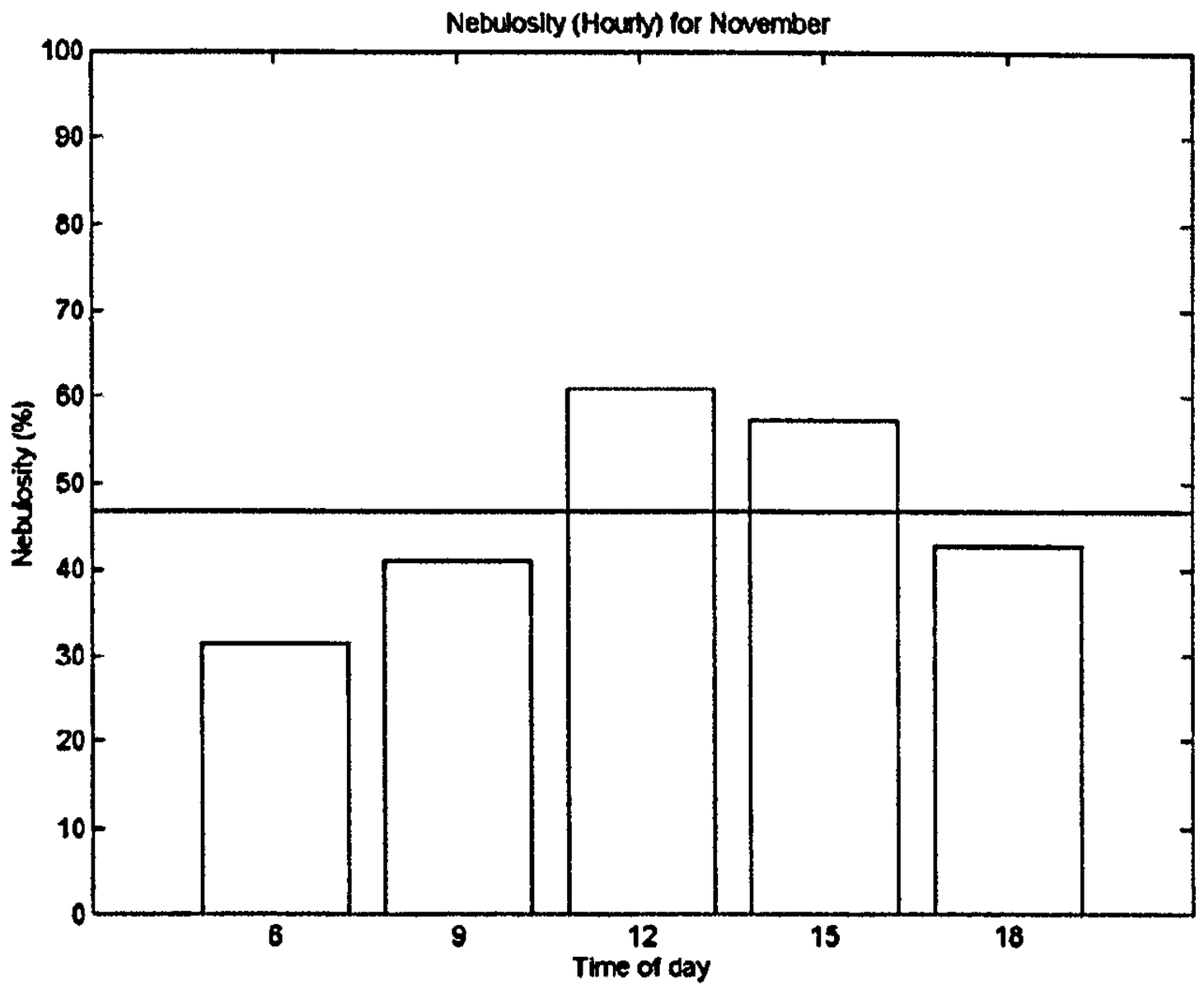

Figure A-11 - Nebulosity (Hourly) for November

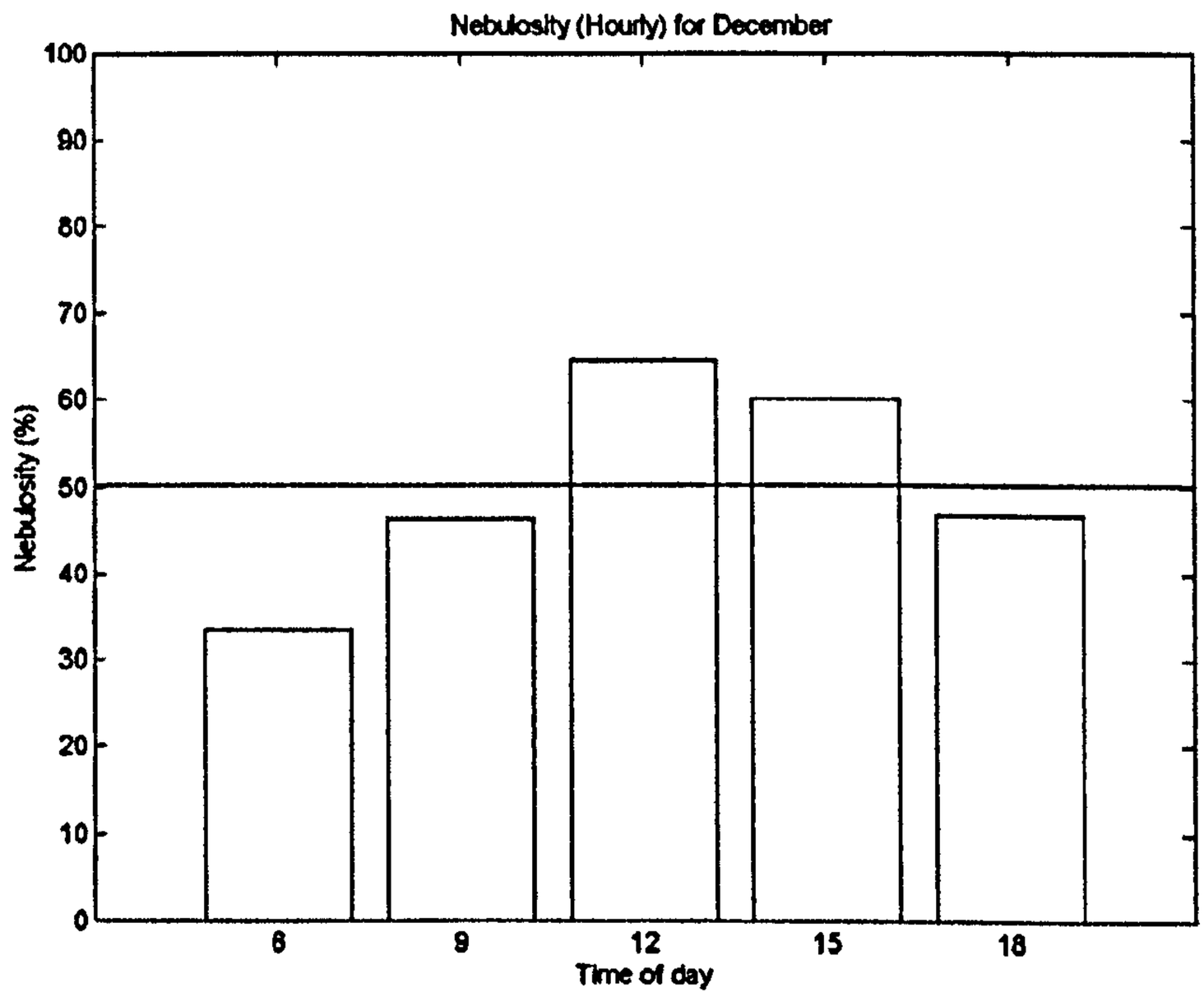

Figure A-12 - Nebulosity (Hourly) for December

A.2 Nebulosity variation during the year for 5 times of the day

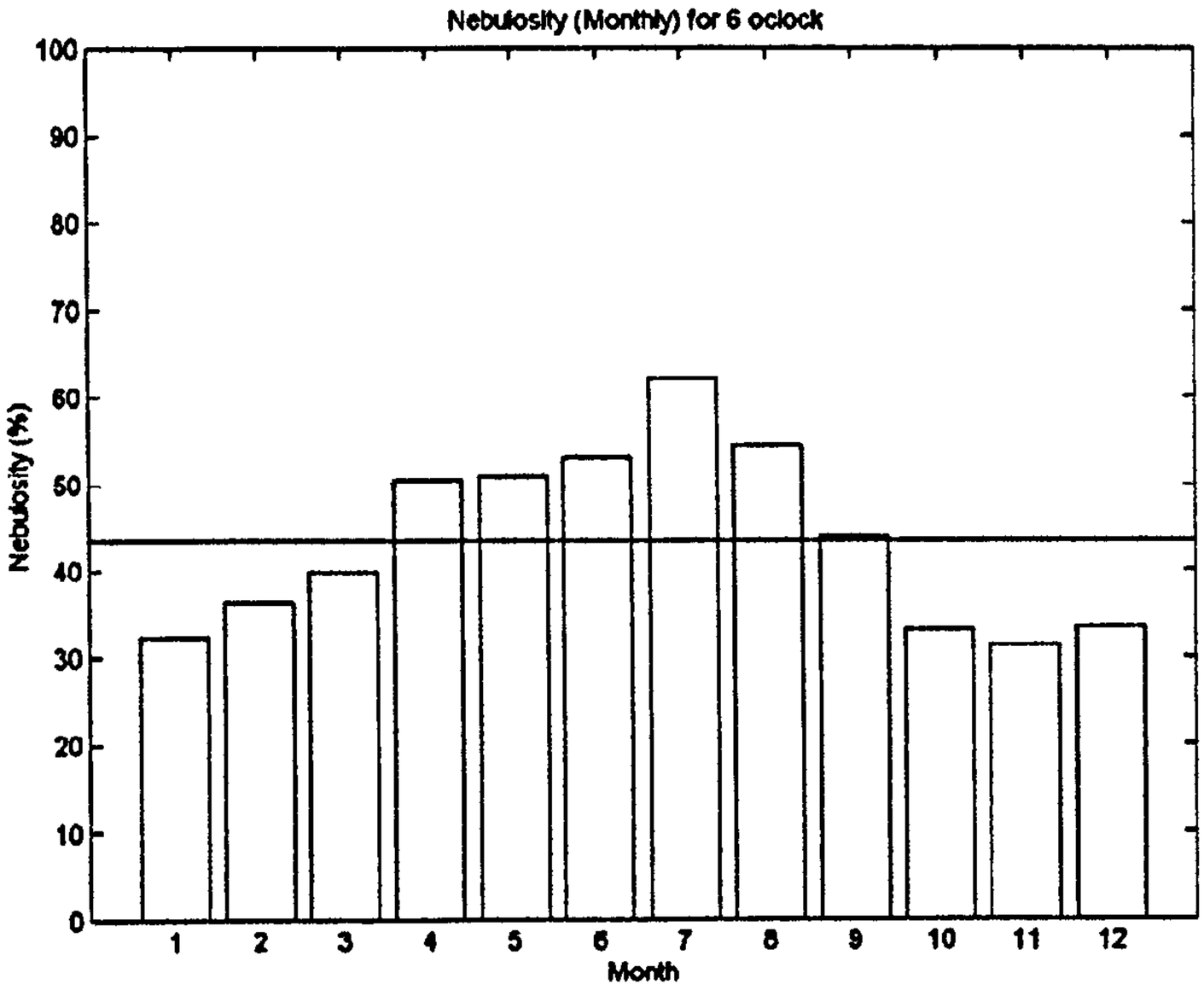

Figure A-13 - Nebulosity (Monthly) for 6 o'clock

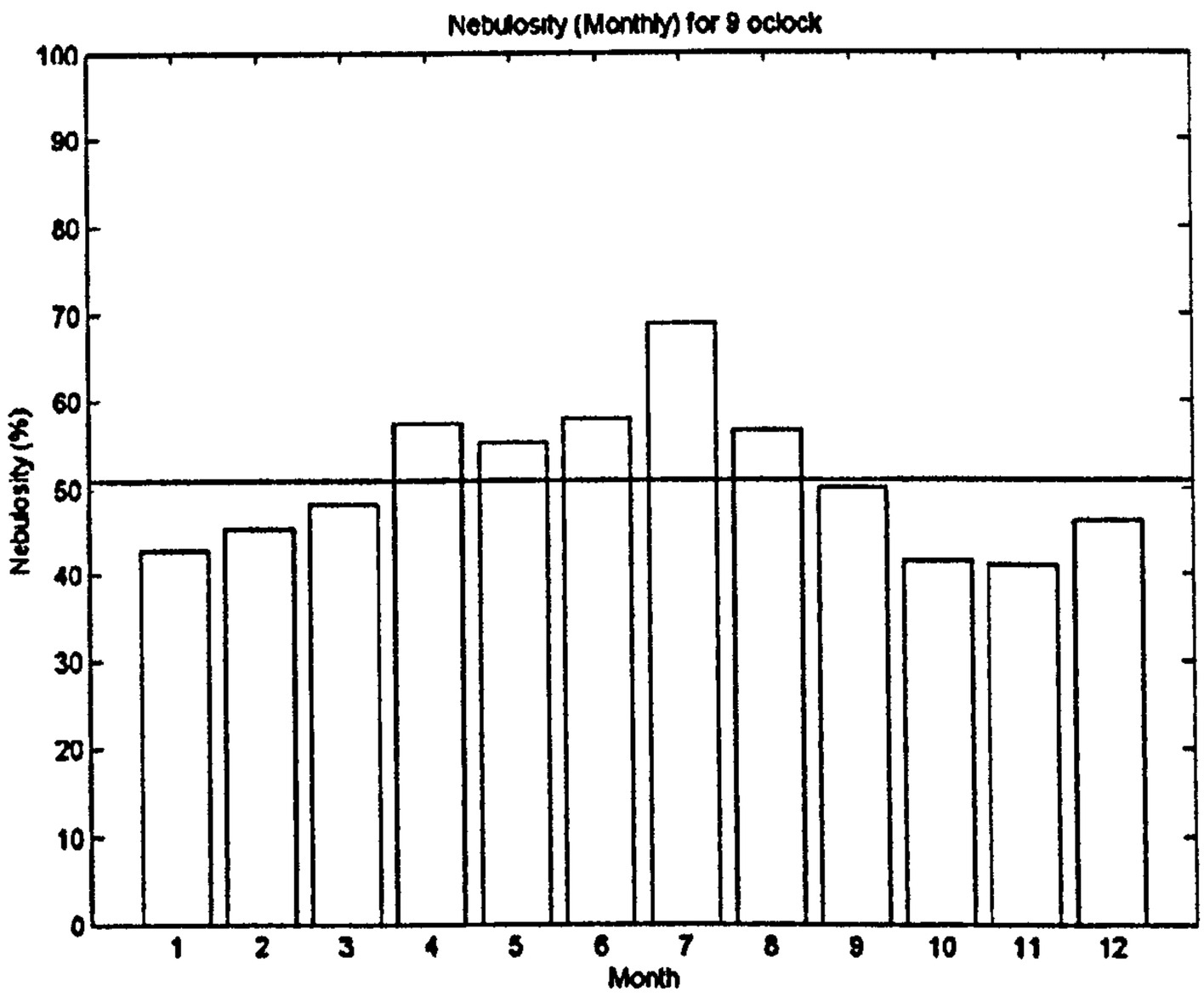

Figure A-14 - Nebulosity (Monthly) for 9 o'clock

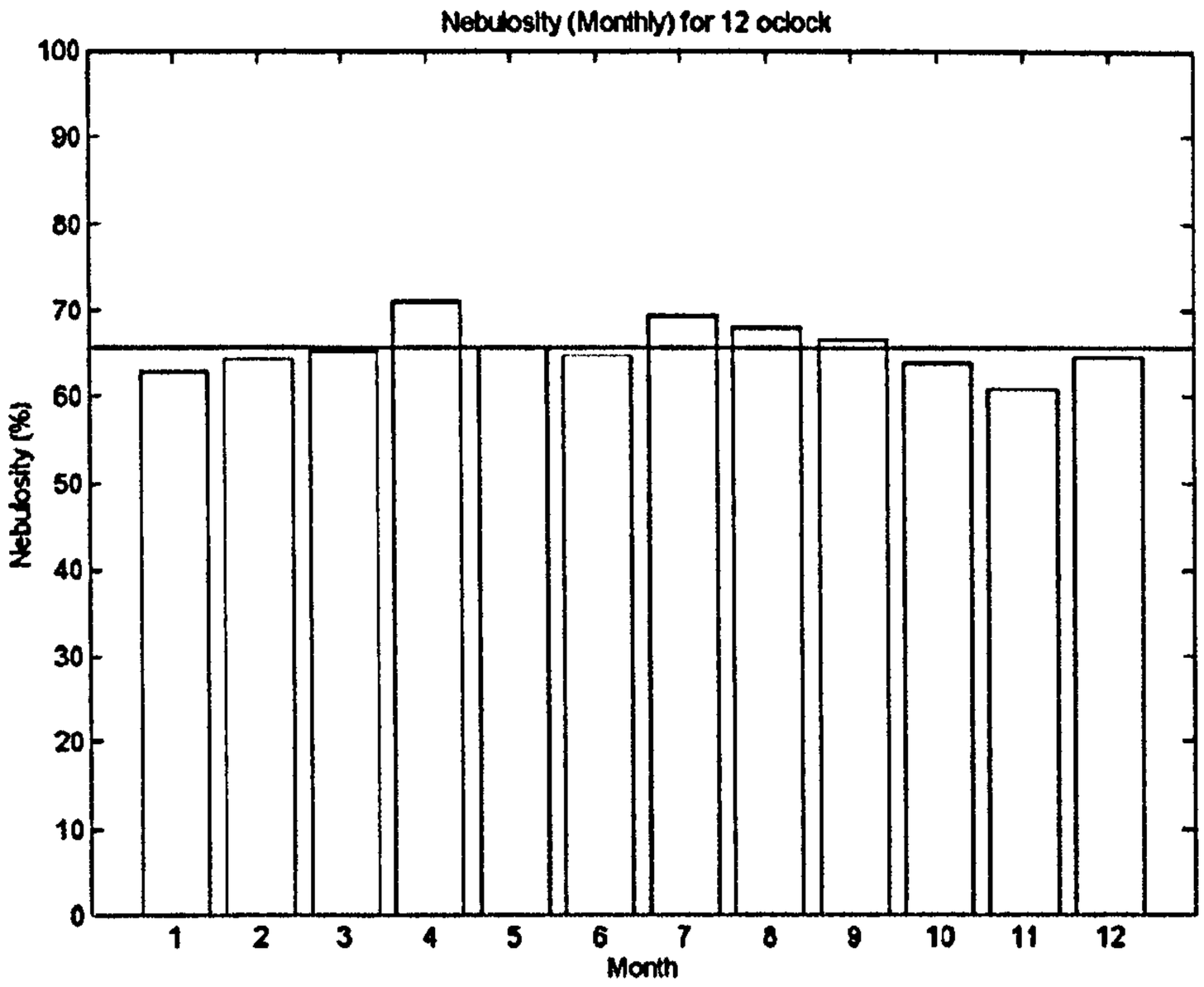

Figure A-15 - Nebulosity (Monthly) for 12 o'clock

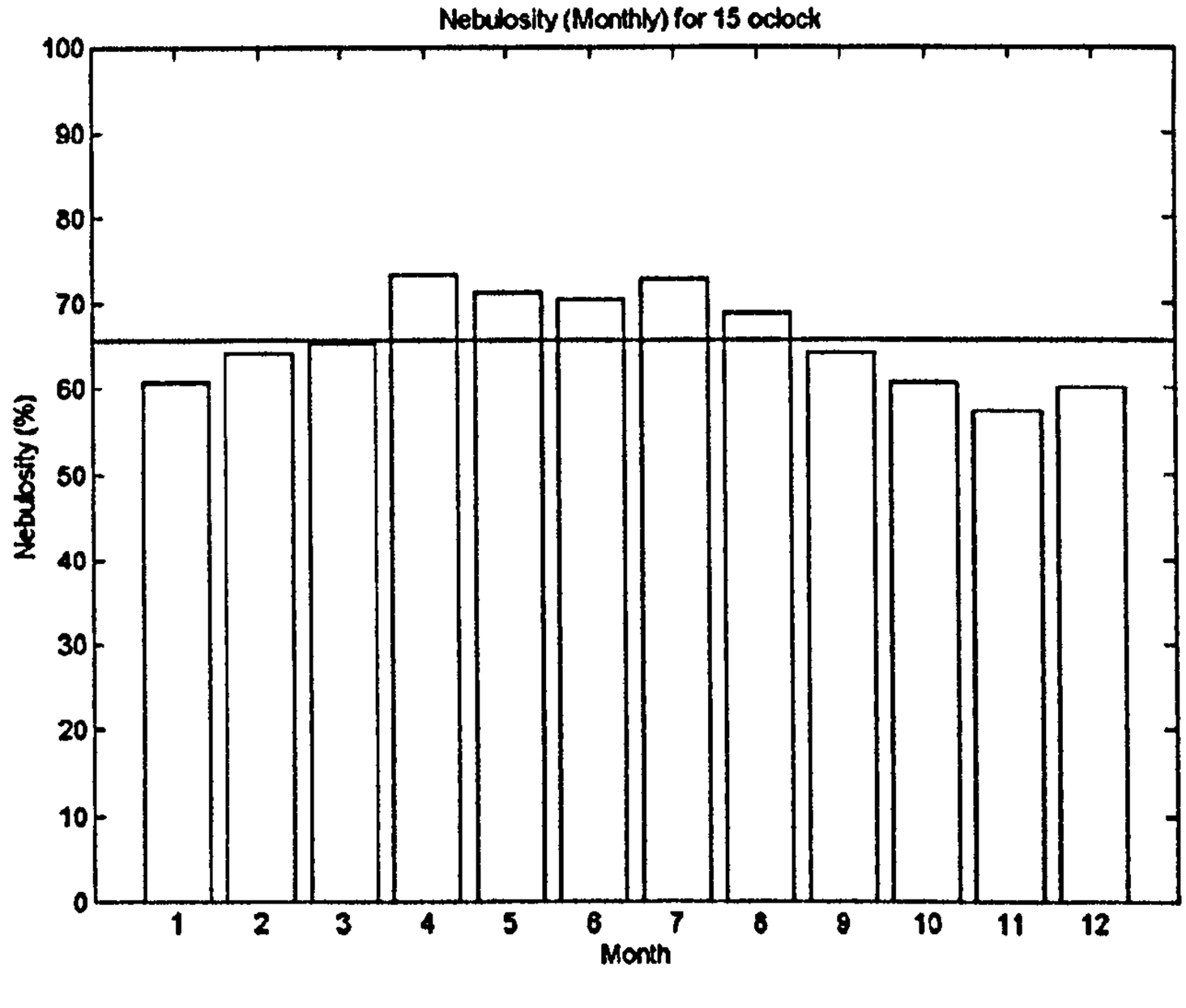

Figure A-16 - Nebulosity (Monthly) for 15 o'clock

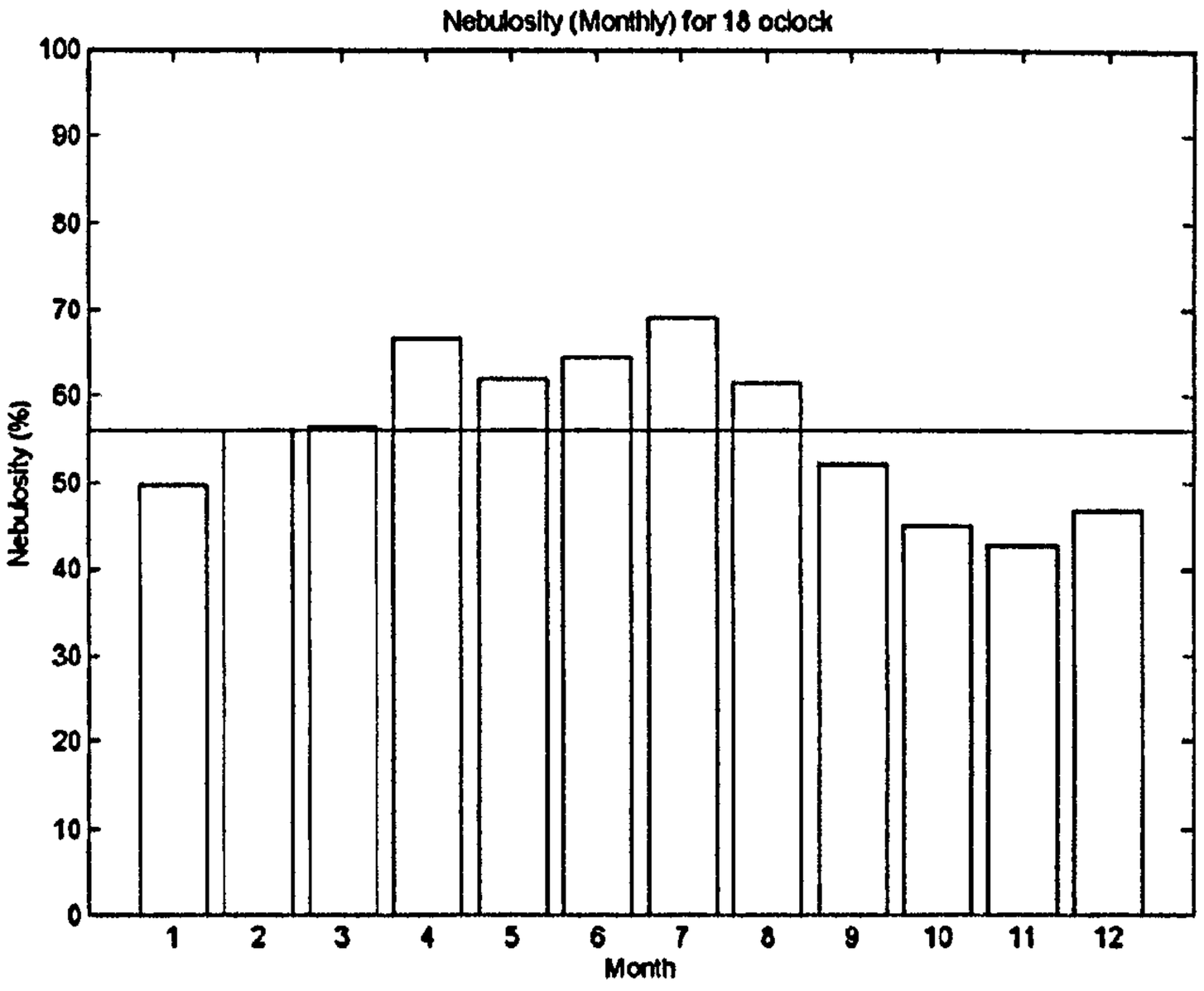

Figure A-17 - Nebulosity (Monthly) for 18 o'clock

A.3 Probability of sky type during the day for each month

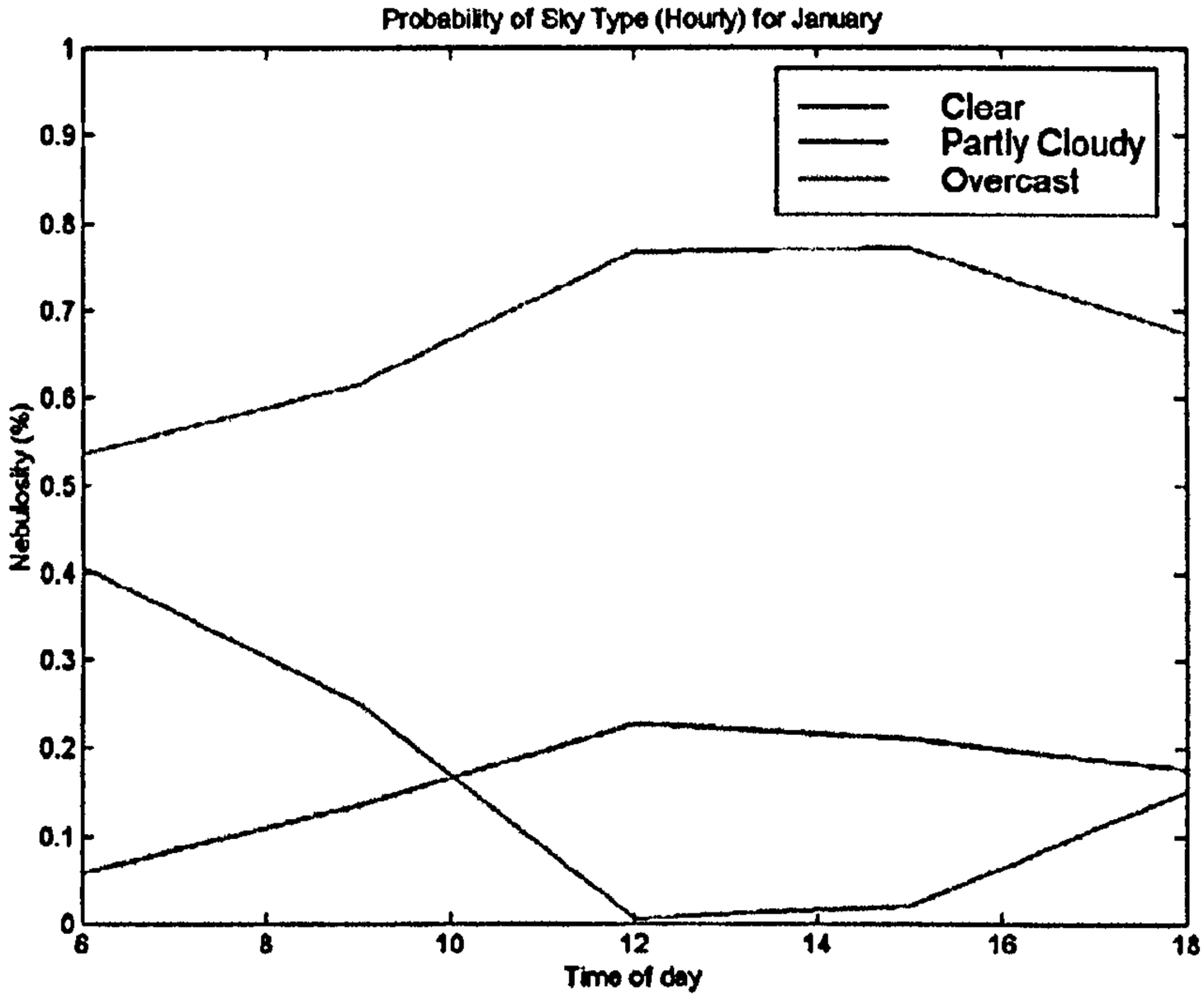

Figure A-18 - Probability of sky type (Hourly) for January

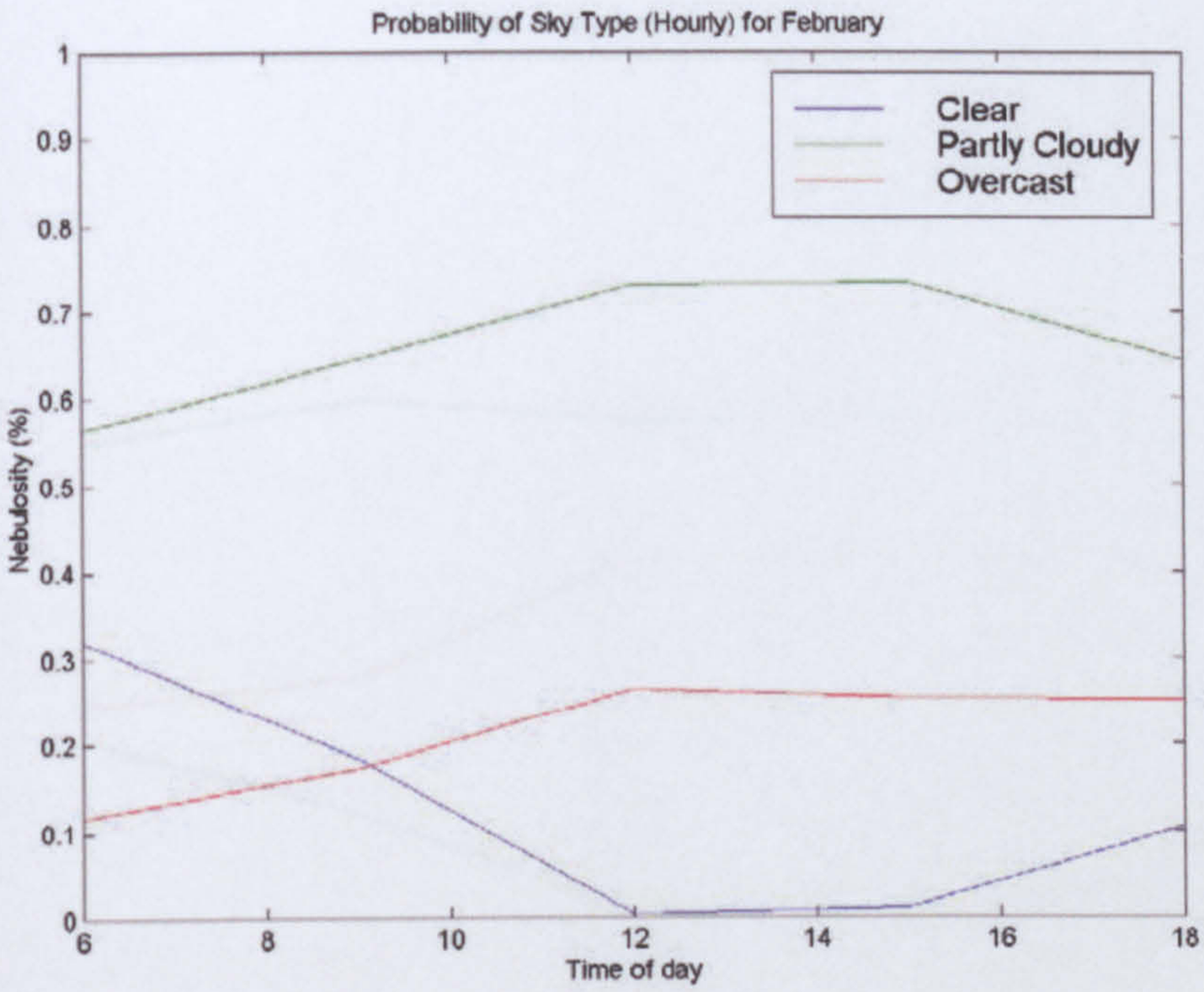

Figure A-19 - Probability of sky type (Hourly) for February

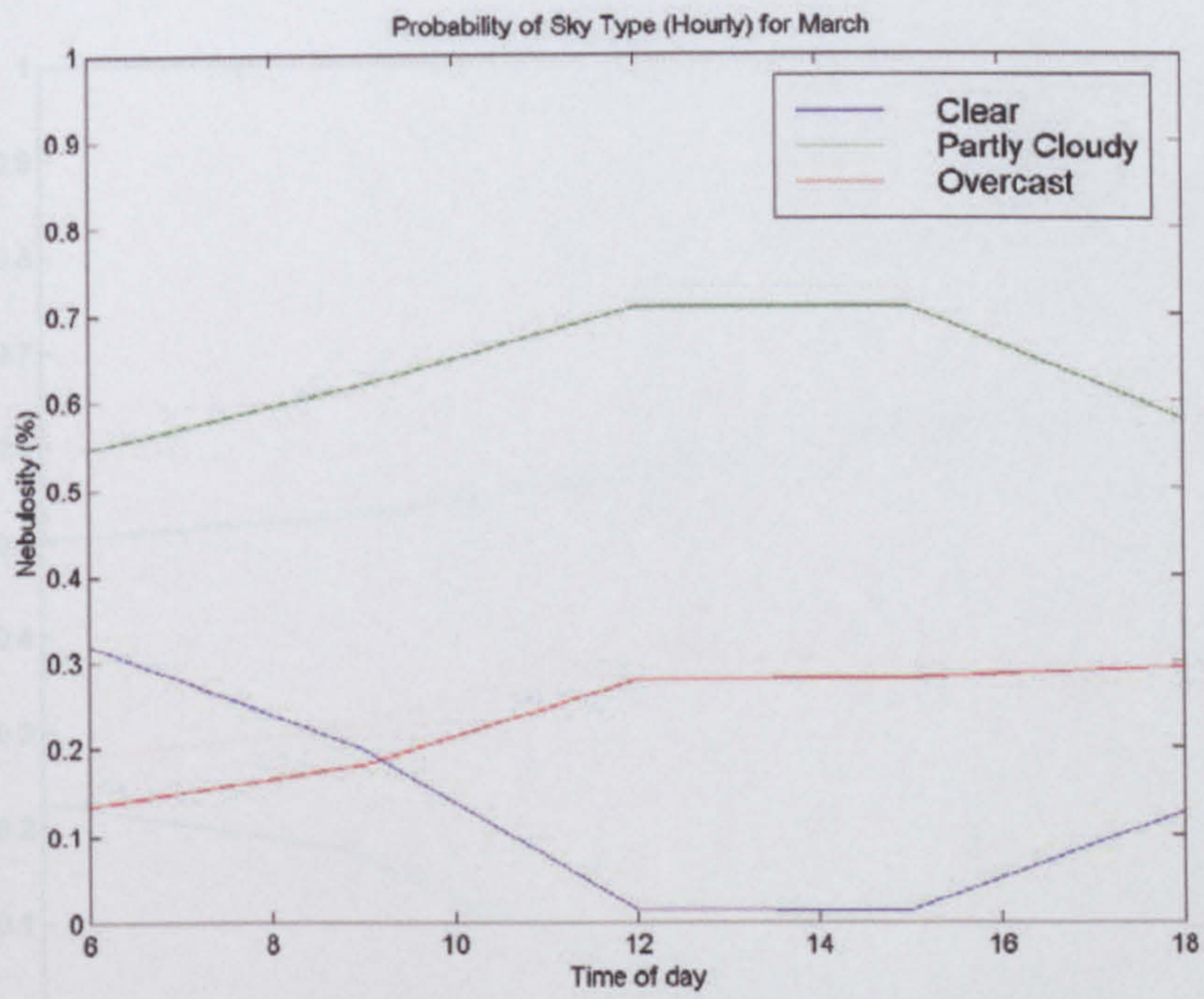

Figure A-20 - Probability of sky type (Hourly) for March

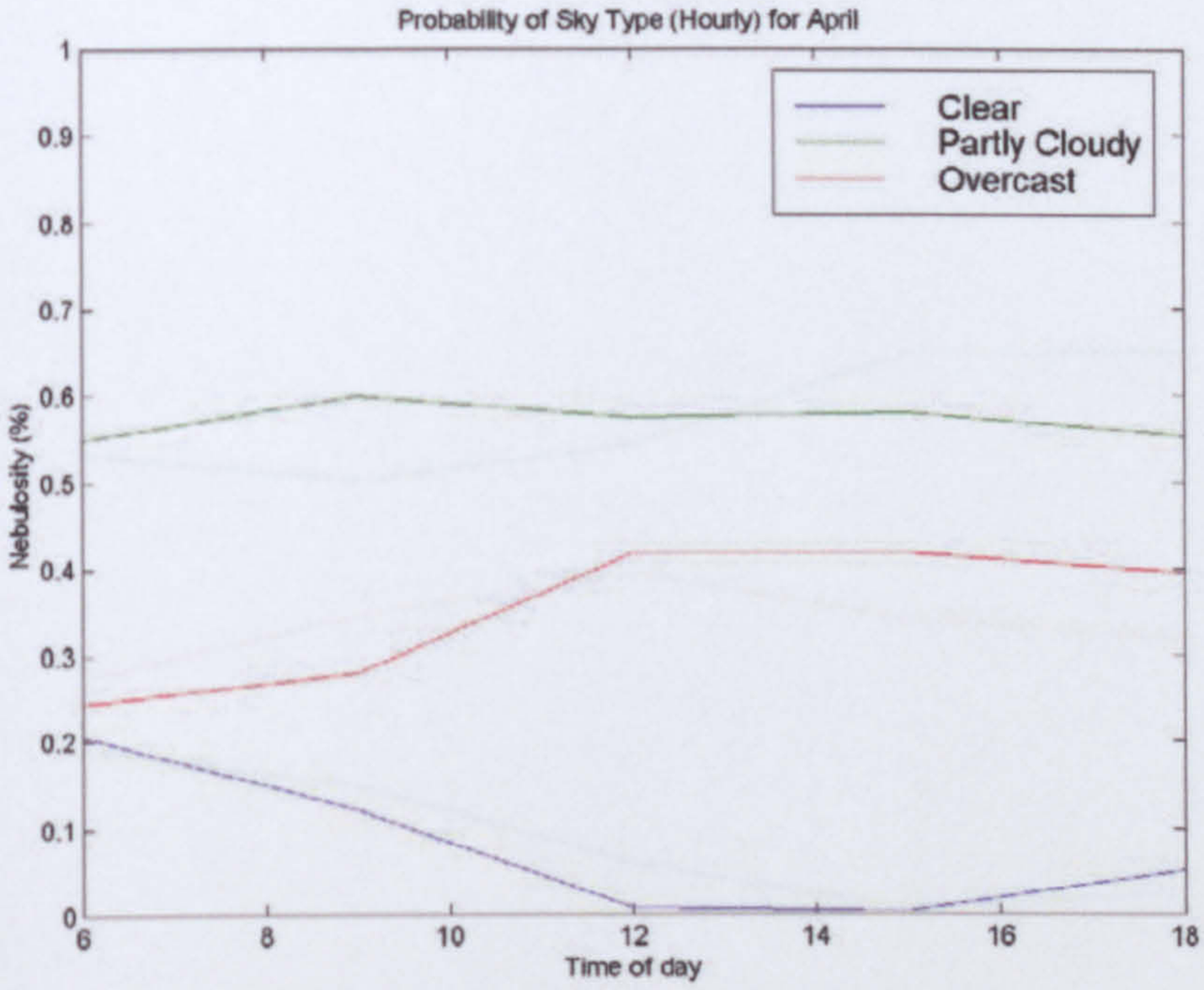

Figure A-21 - Probability of sky type (Hourly) for April

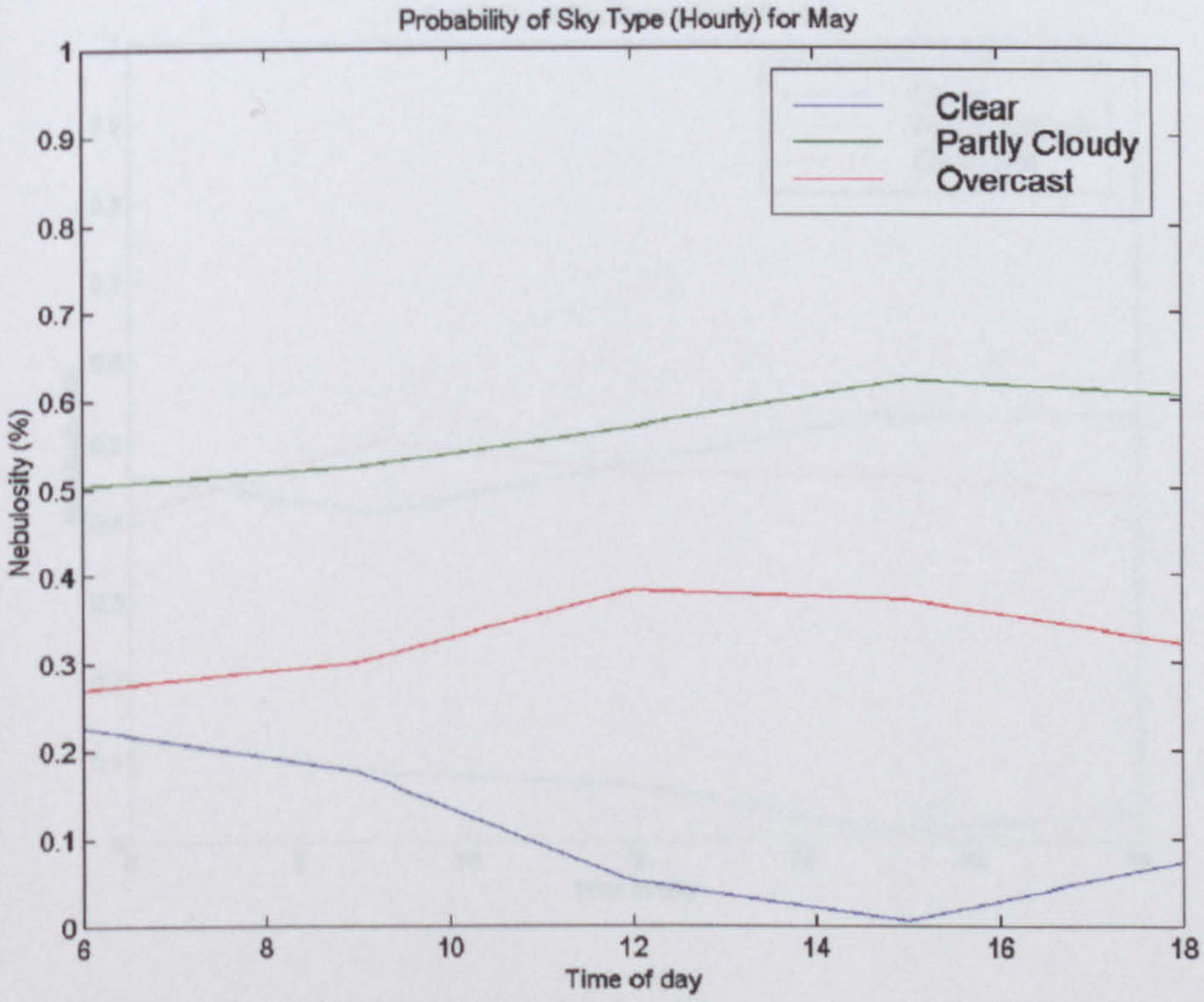

Figure A-22 - Probability of sky type (Hourly) for May

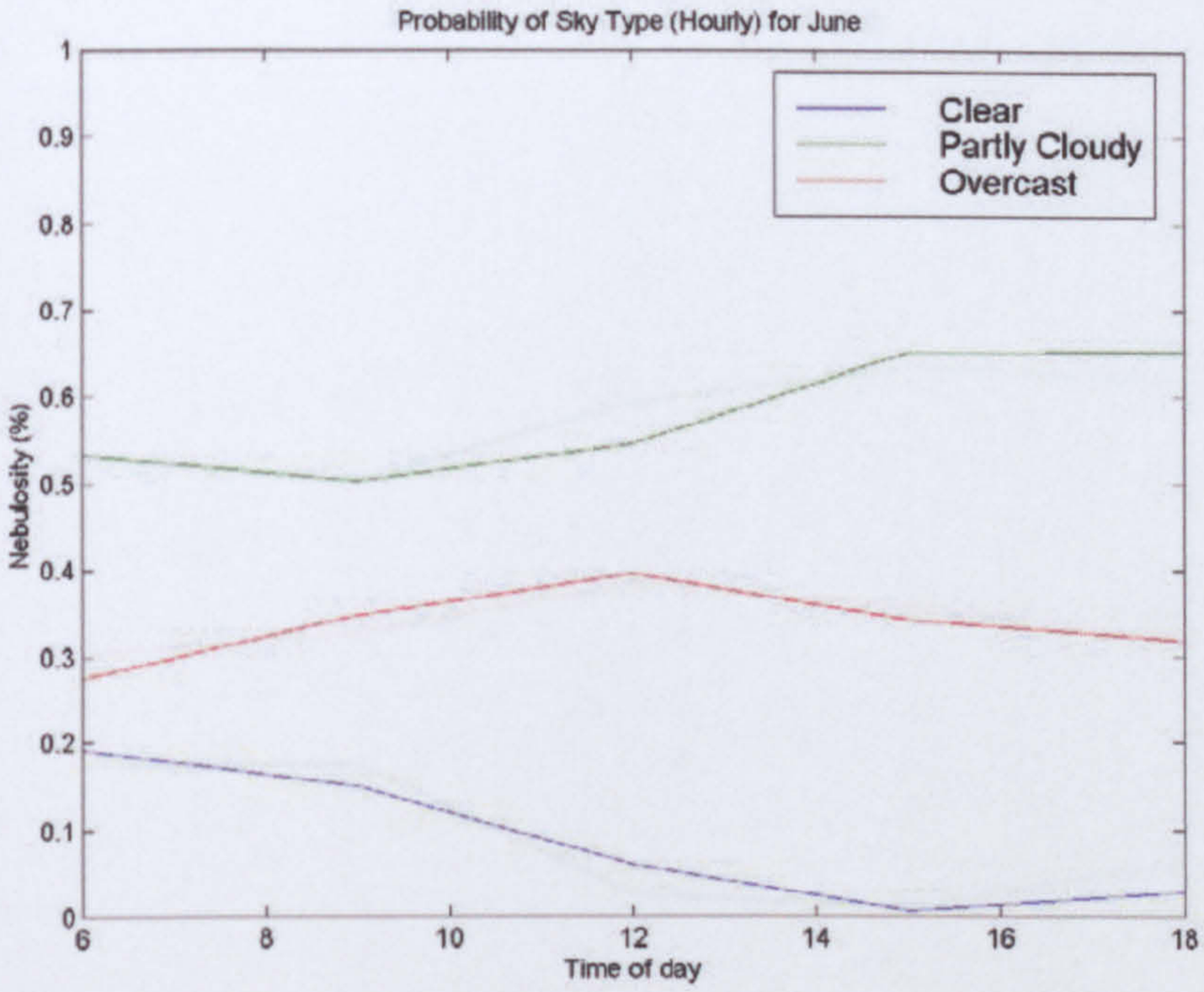

Figure A-23 - Probability of sky type (Hourly) for June

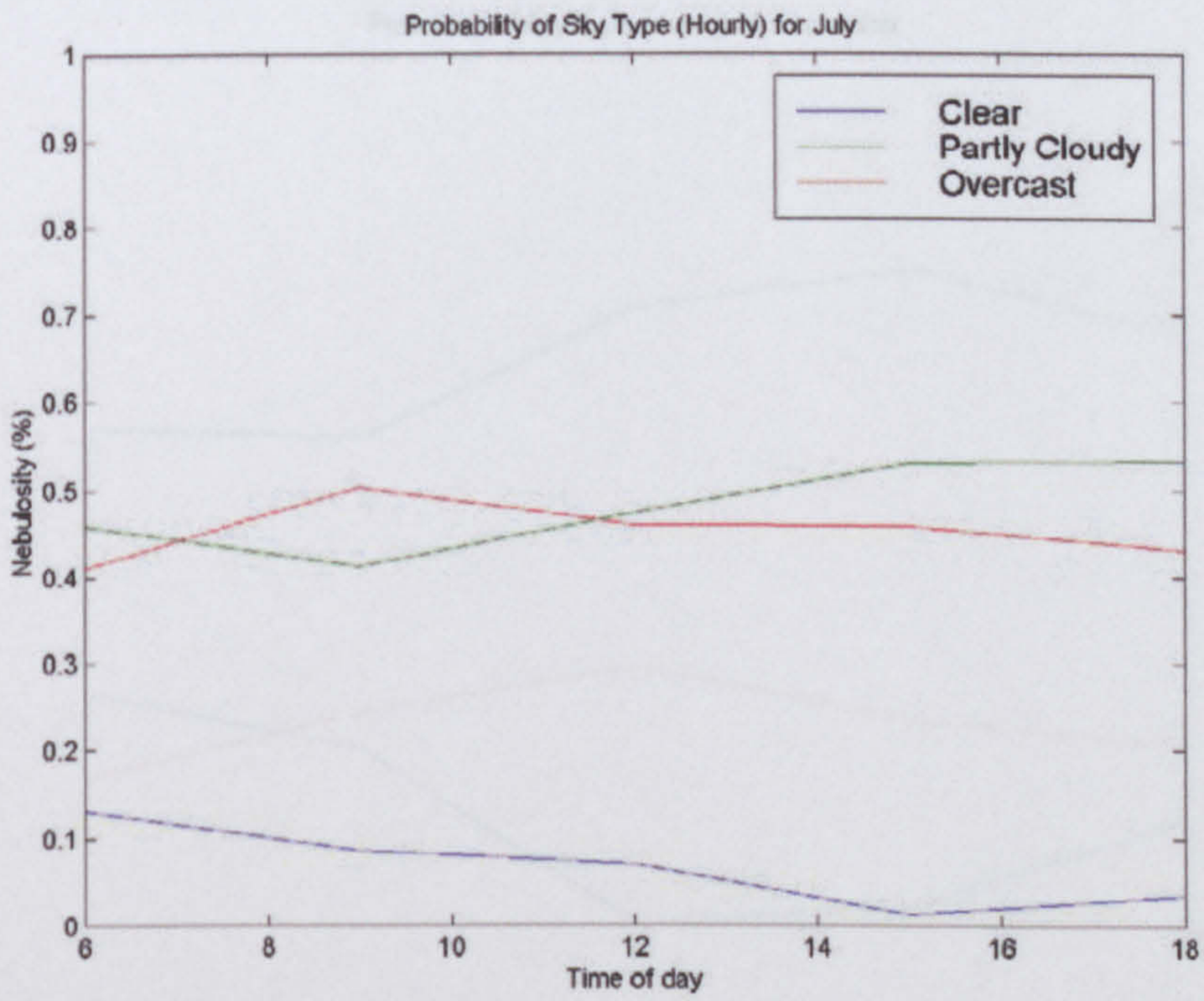

Figure A-24 - Probability of sky type (Hourly) for July

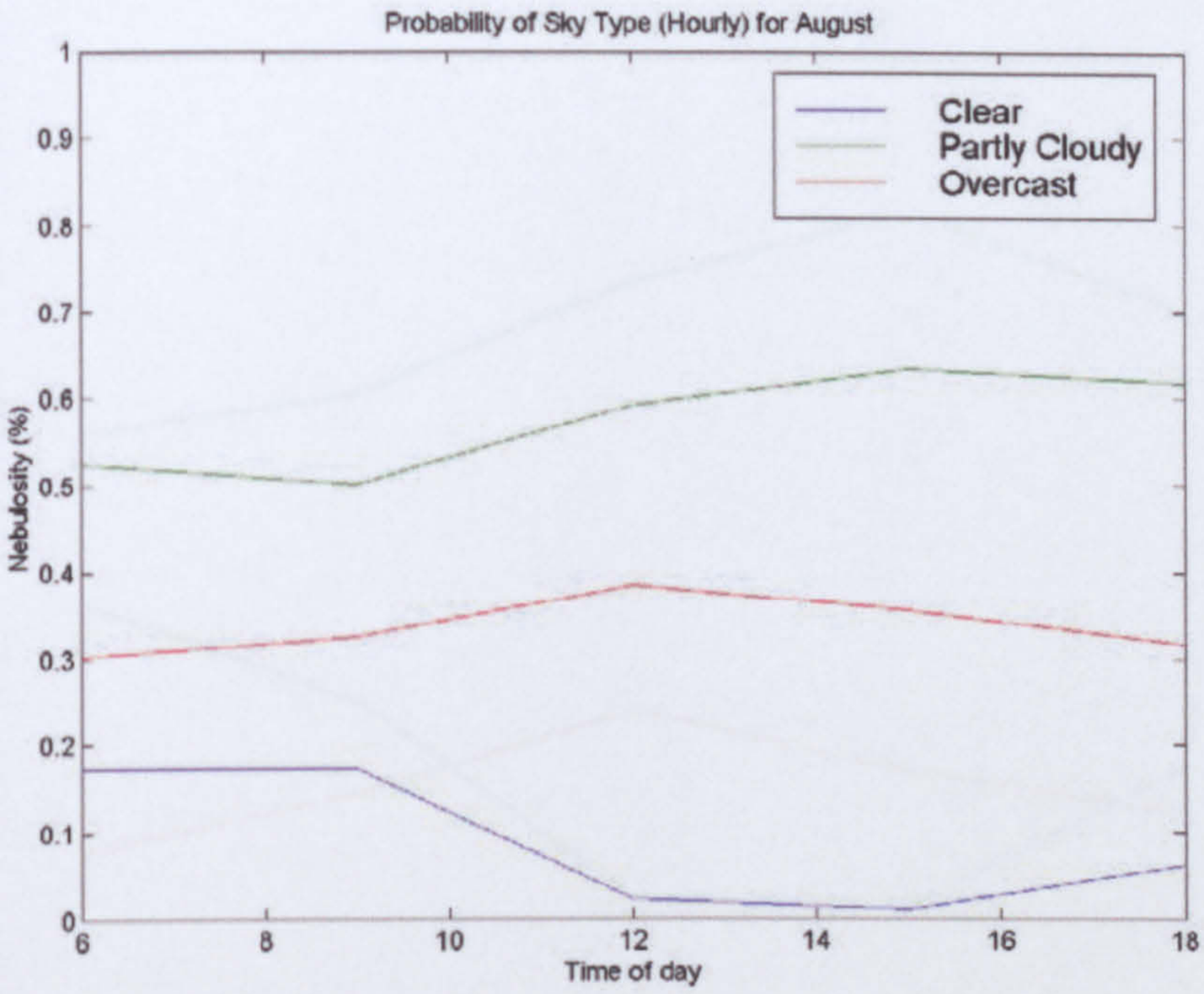

Figure A-25 - Probability of sky type (Hourly) for August

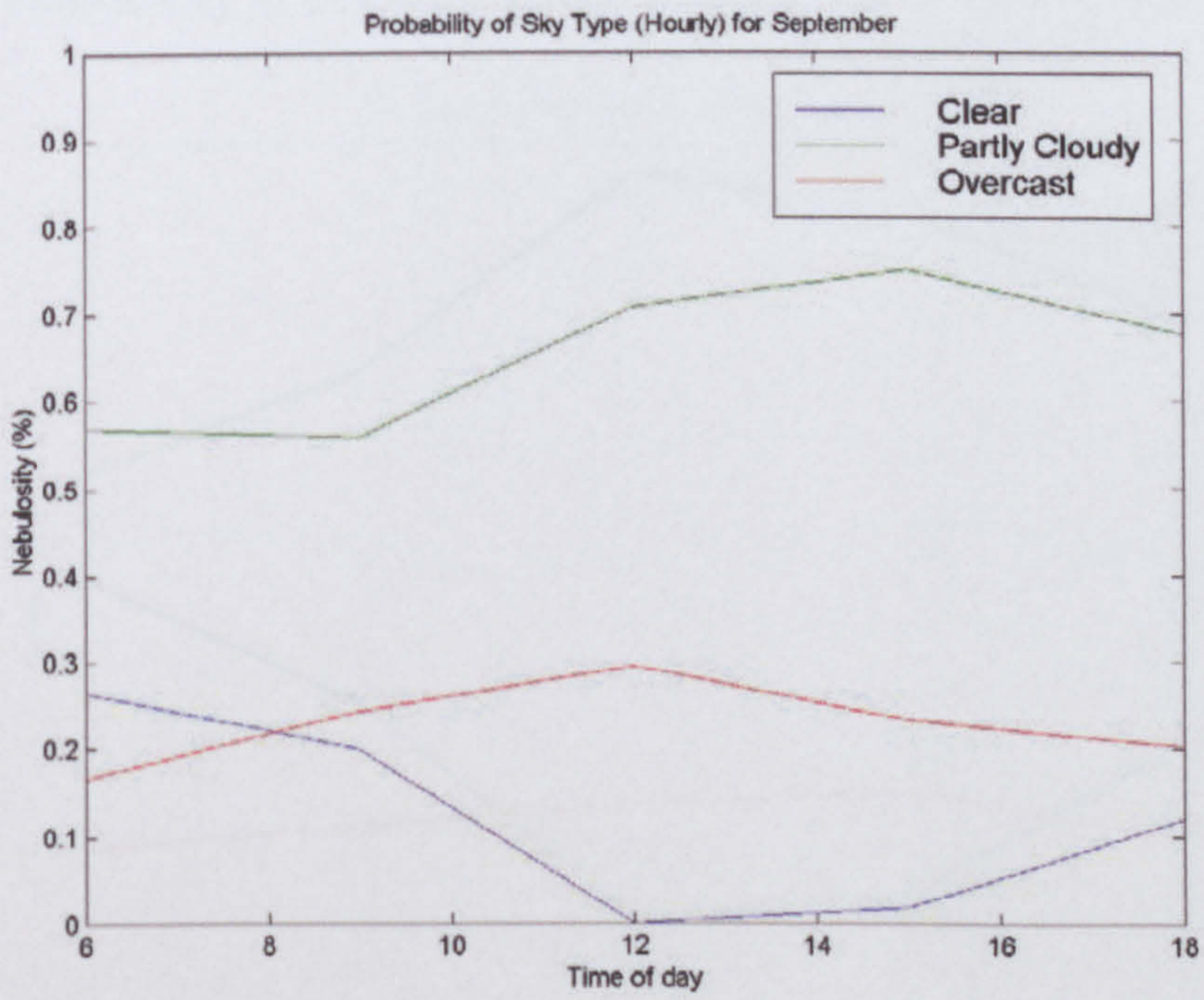

Figure A-26 - Probability of sky type (Hourly) for September

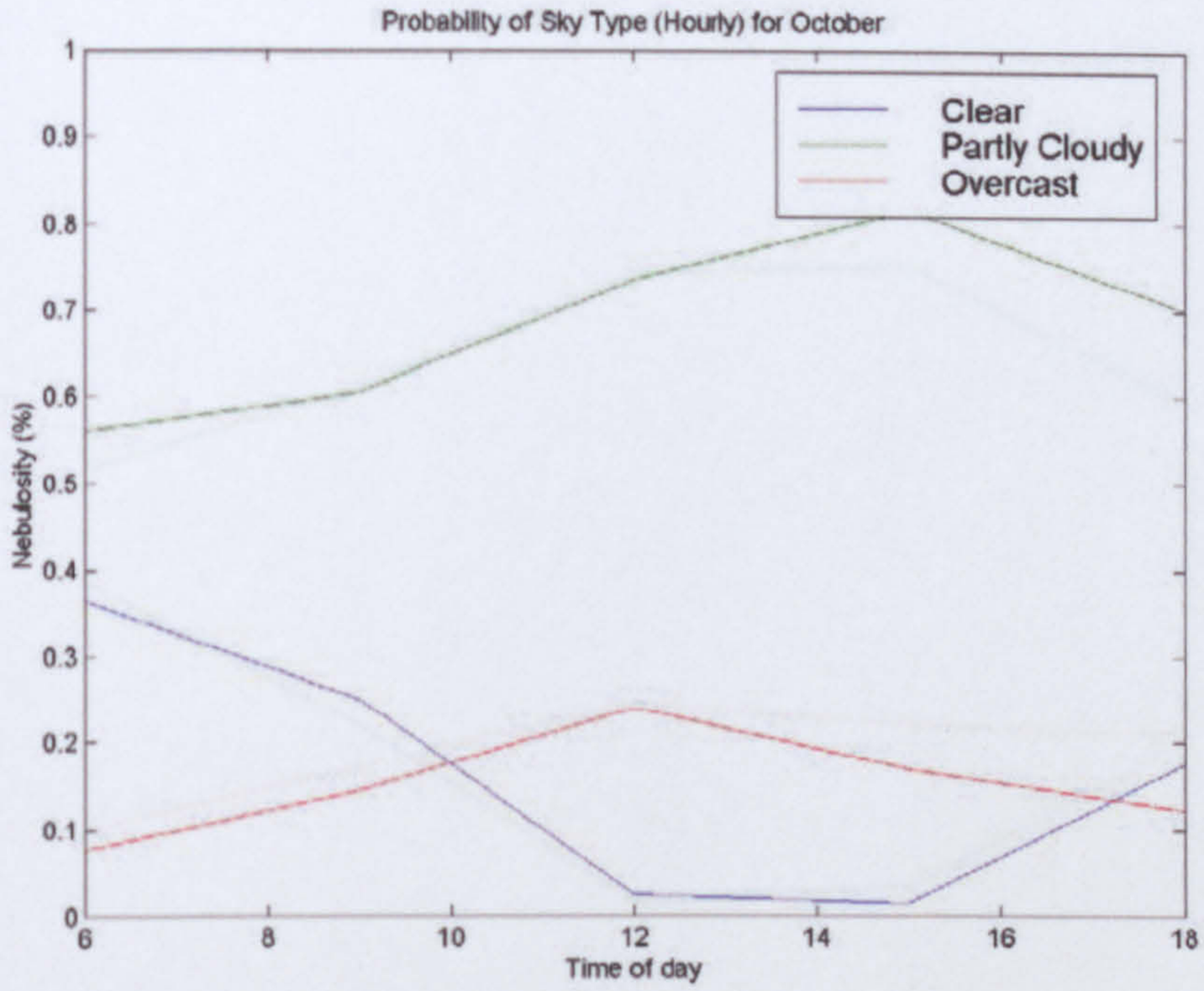

Figure A-27 - Probability of sky type (Hourly) for October

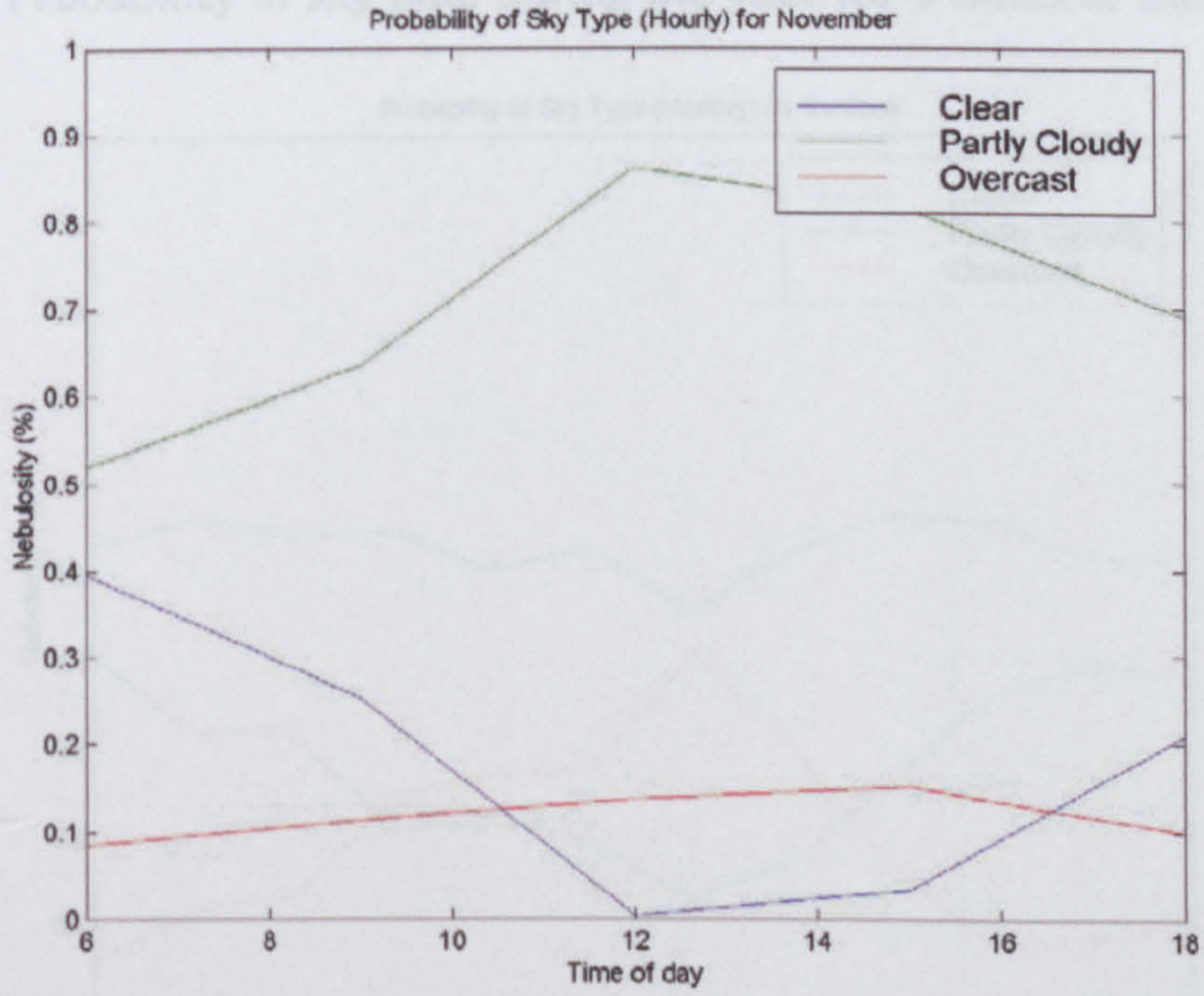

Figure A-28 - Probability of sky type (Hourly) for November

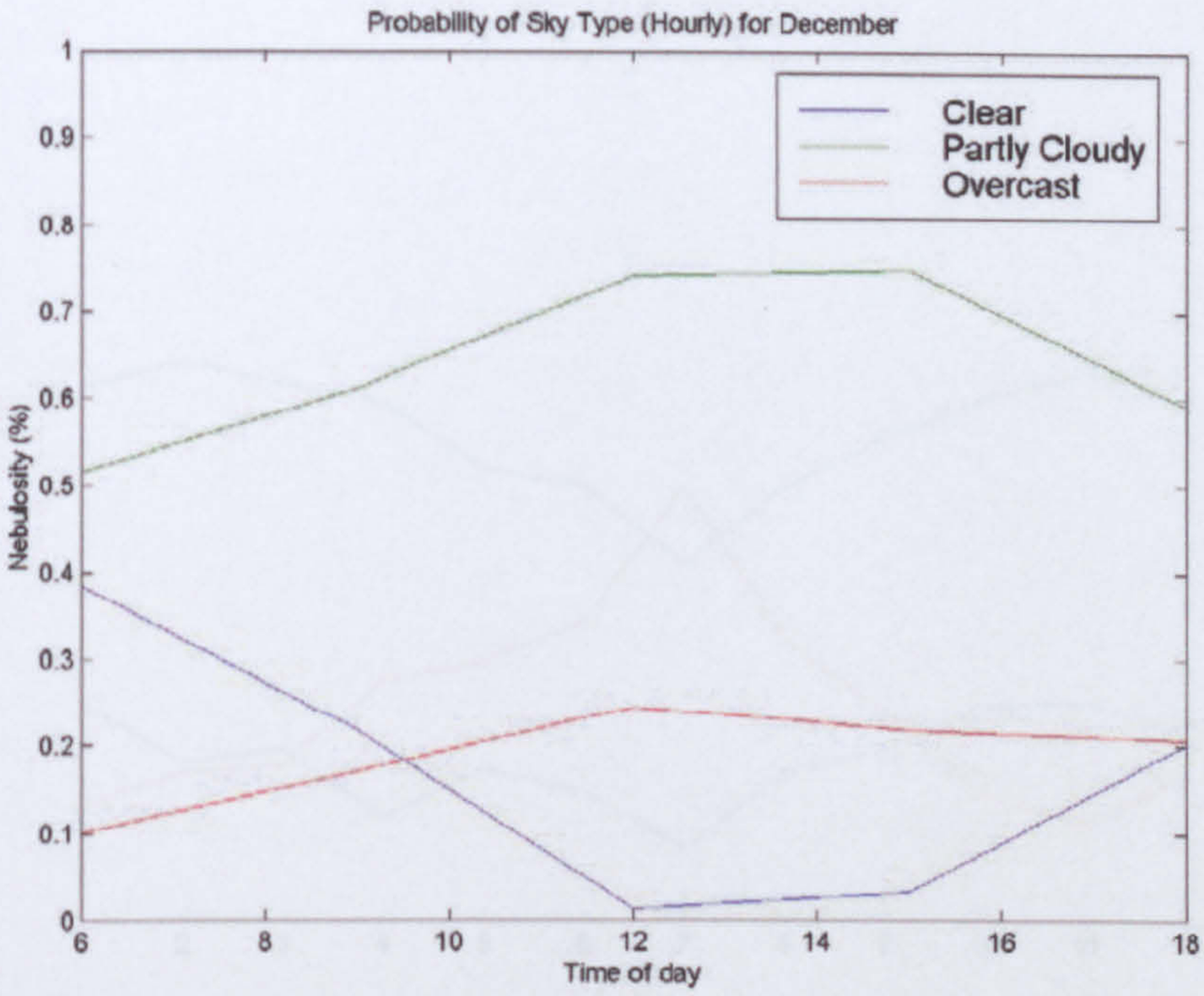

Figure A-29 - Probability of sky type (Hourly) for December

A.4 Probability of sky type during the year for 5 times of the day

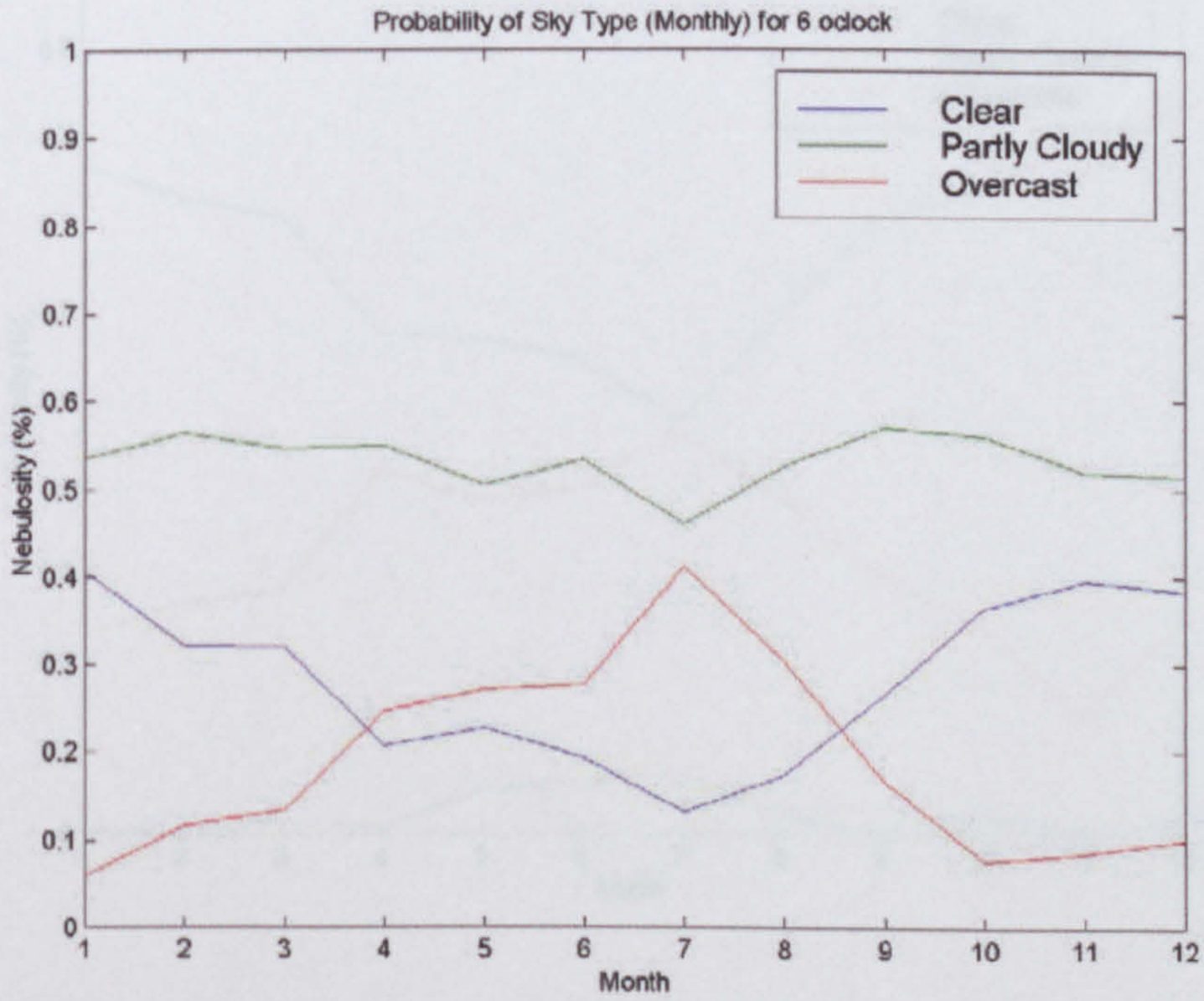

Figure A-30 - Probability of sky type (Monthly) for 6 o'clock

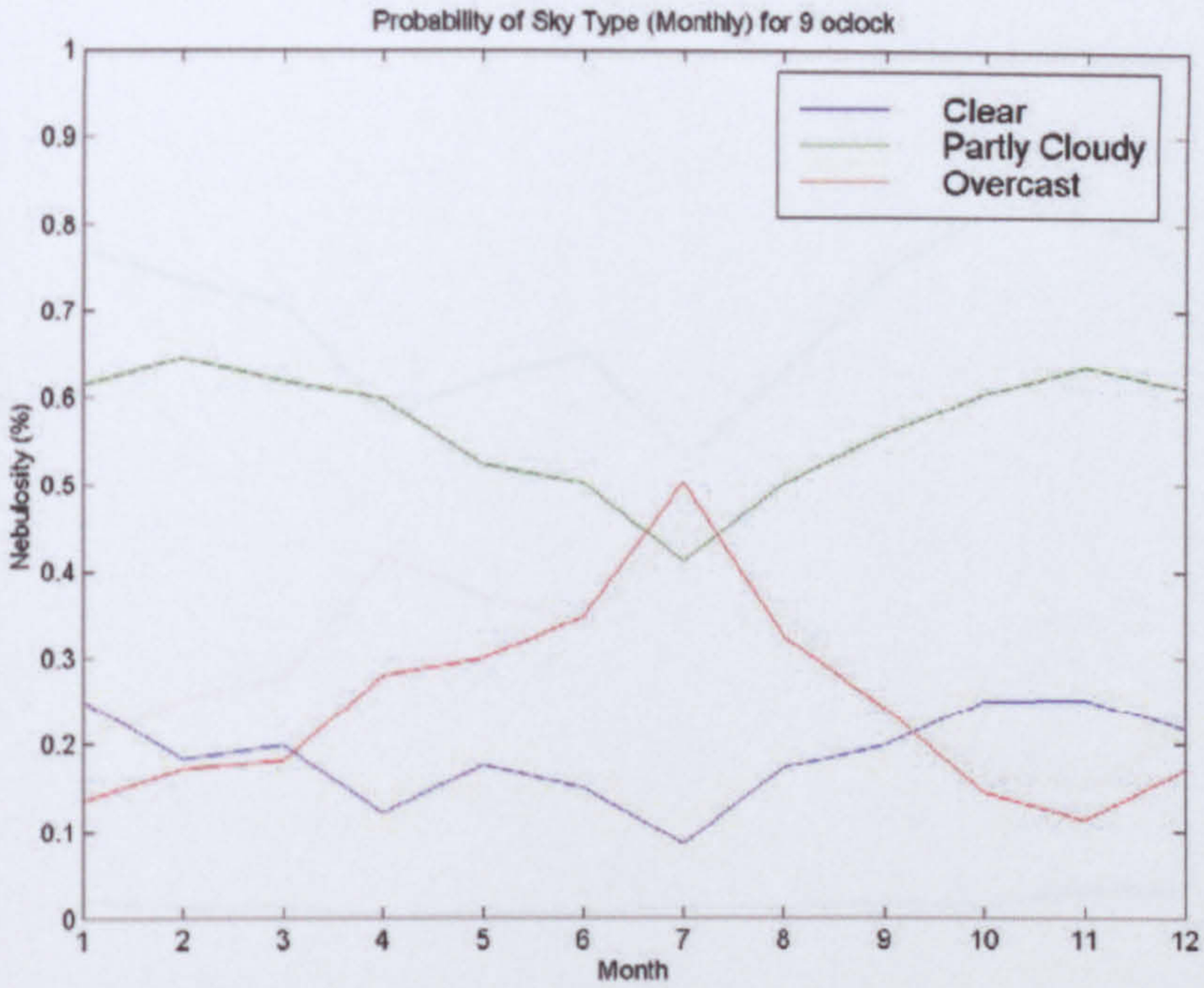

Figure A-31 - Probability of sky type (Monthly) for 9 o'clock

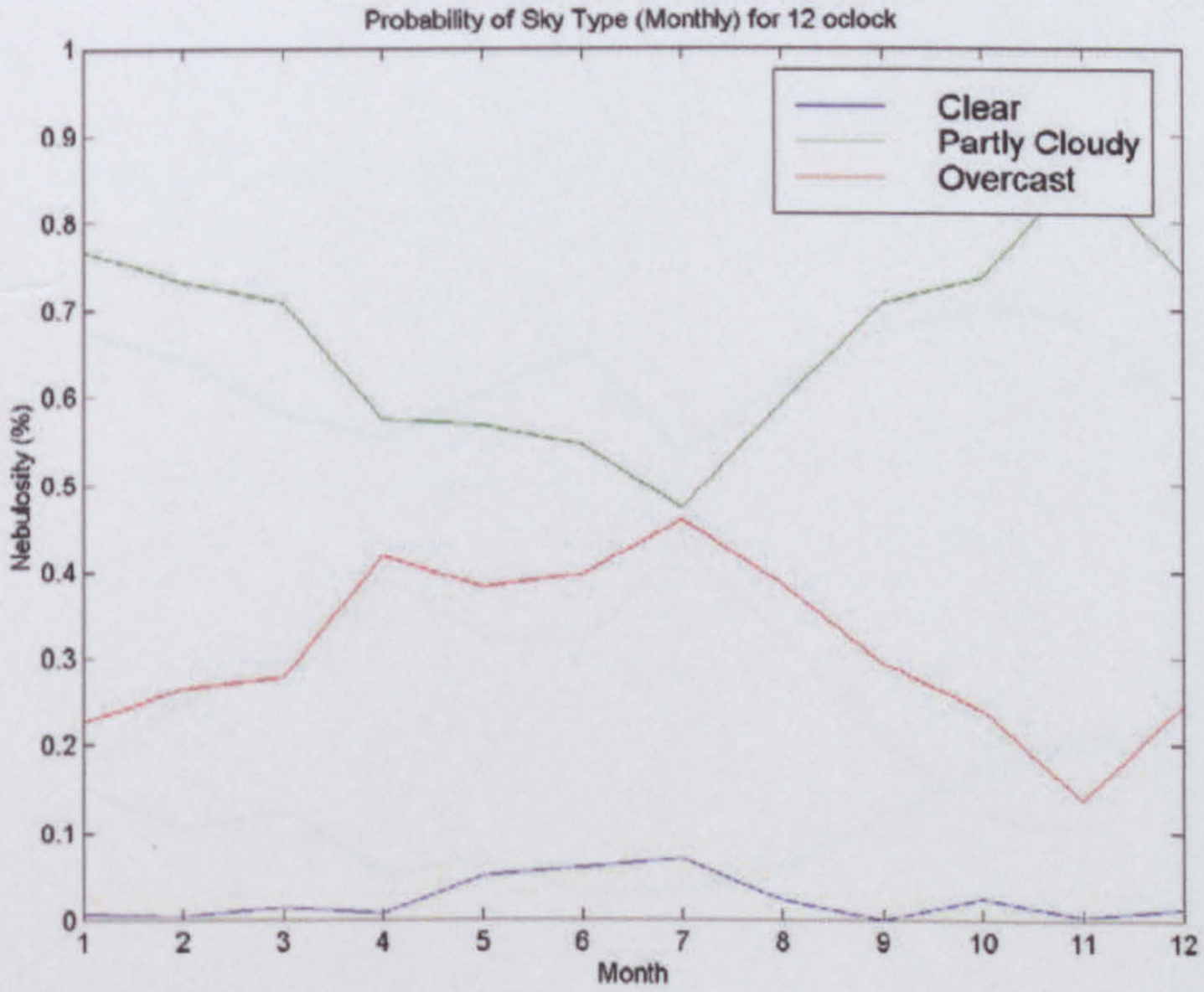

Figure A-32 - Probability of sky type (Monthly) for 12 o'clock

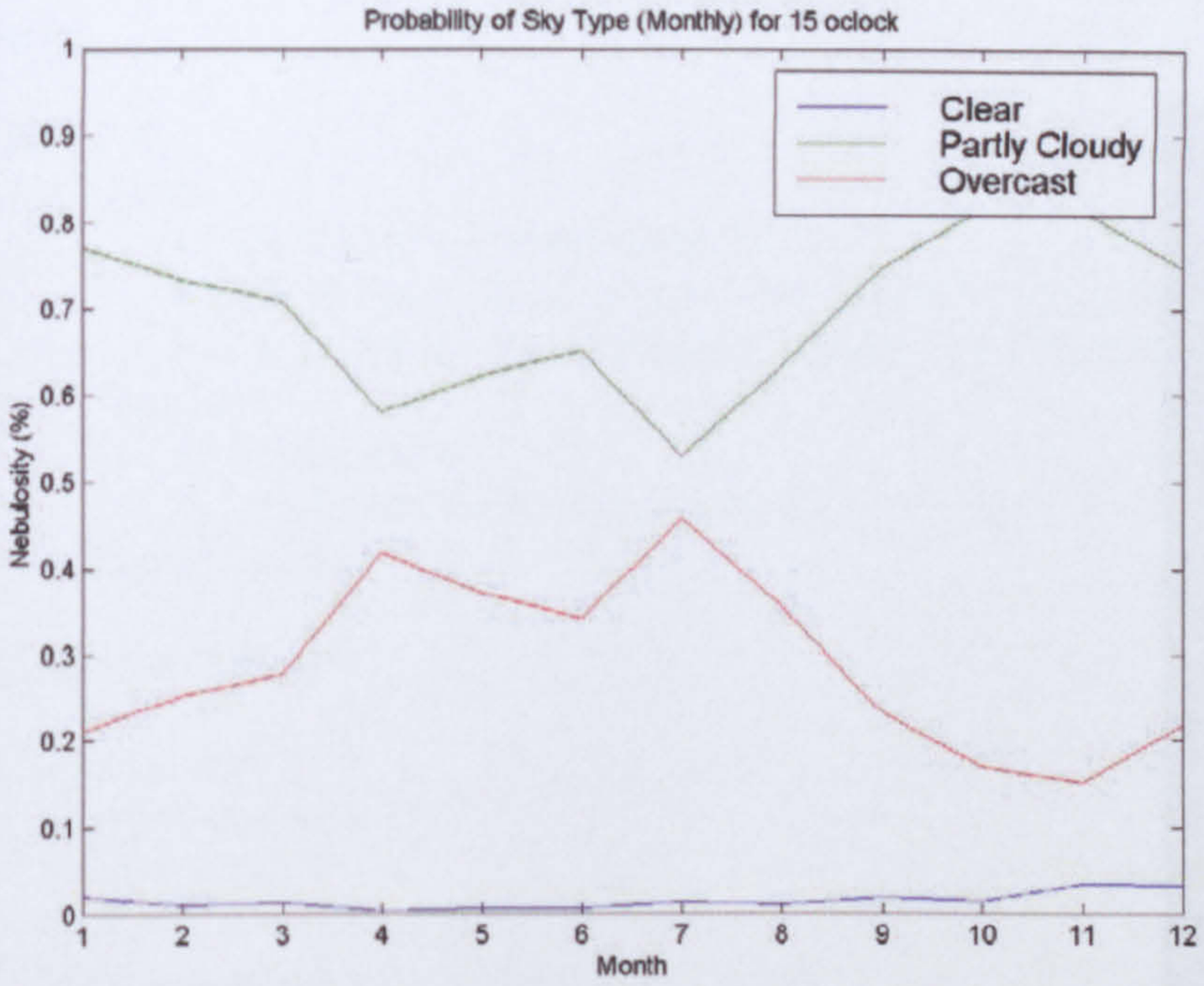

Figure A-33 - Probability of sky type (Monthly) for 15 o'clock

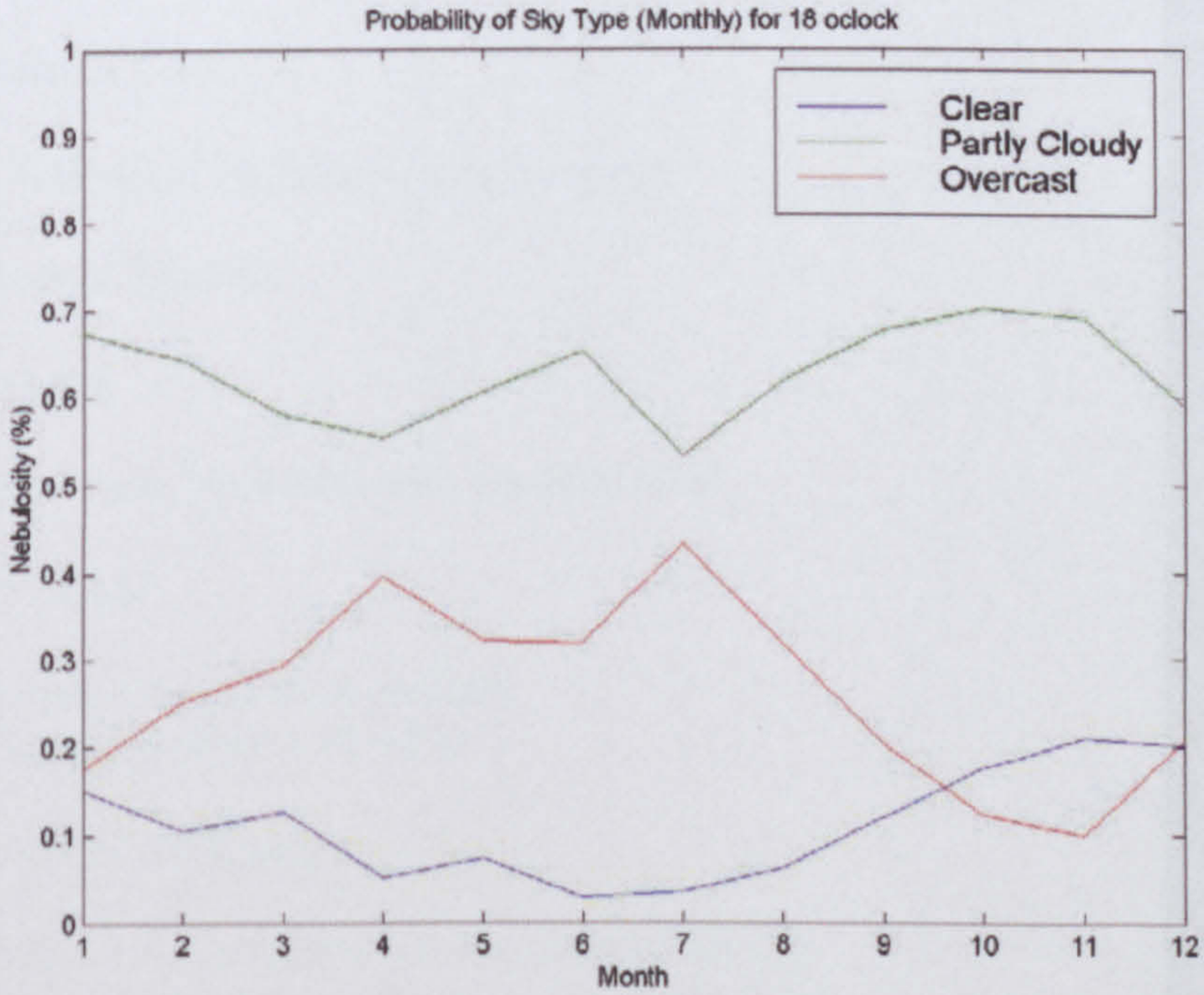

Figure A-34 - Probability of sky type (Monthly) for 18 o'clock

Appendix B - Equipment and accessories used in fieldwork

- **Camera**
  - Nikon F70
    - Lens:
      - (i) Nikkor – Fisheye-8mm 1:2.8
      - (ii) Nikkor – Zoom 35mm – 80mm.1:4.5-5.6 (∞ -0.3m)
      - (iii) Nikkor – Zoom 80mm – 200mm. 1:4.5-5.6 (∞ -1.5m)
    - Tripod
      - Brand name:
      - Horizontal protractor provided
  - Sony Digital Camera

- **Luminance Meter**
  - Minolta LS-100
    - Acceptance angle: 1°
    - Field of view: 9°
    - Focusing distance: 1014mm to infinity
    - Minimum target area: ϕ14.4mm at 1014mm
    - Measuring range: 0.001 to 49990 cd/m^2 (slow);
      0.001 to 299990 cd/m^2 (fast)
    - Accuracy: 0.001 to 0.9999 cd/m^2: ± 2% ± 1 digit of measured value

- **Illuminance Meter (Luxmeter)**
  - Minolta T-10

- **GPS - Global Positioning System**
  - Garmin. Mod 48.

- **Compass**
  - Rosenhain, Mod 206, with a bubble level

- **Protractor**
  - Horizontal protractor (0-360°)
  - Vertical protractor (0-90°)

- **Reflectance Card**
  - Grey Card – reflectance 0.18; size (cm) 20x25
  - White Card – reflectance 0.90; size (cm) 20x25

Appendix C - Sky luminance measurement - input table

Table C-1 - Sky Luminance Measurements - Input Table

Sky luminance measurements – input table				
Set Number				
Latitude				
Longitude				
Standard Meridian				
Summer Time				
Year				
Month				
Day				
Hour				
Minute				
Second				
Sky (1-overcast 2-partly cloudy 3-clear)				
Sun (1-clear 2-covered)				
Vertical Angle (º)				
Luminance in almucantar (cd/m^2)	1			
Luminance in almucantar (cd/m^2)	2			
Luminance in almucantar (cd/m^2)	3			
Luminance in almucantar (cd/m^2)	4			
Luminance in almucantar (cd/m^2)	5			
Luminance in almucantar (cd/m^2)	6			
Luminance in almucantar (cd/m^2)	7			
Luminance in almucantar (cd/m^2)	8			
Luminance in almucantar (cd/m^2)	9			
Luminance in almucantar (cd/m^2)	10			
Luminance in almucantar (cd/m^2)	11			
Luminance in almucantar (cd/m^2)	12			
Luminance in almucantar (cd/m^2)	13			
Luminance in almucantar (cd/m^2)	14			
Luminance in almucantar (cd/m^2)	15			
Luminance in almucantar (cd/m^2)	16			
Luminance in almucantar (cd/m^2)	17			
Luminance in almucantar (cd/m^2)	18			
Luminance in almucantar (cd/m^2)	19			
Luminance in almucantar (cd/m^2)	20			
Luminance in almucantar (cd/m^2)	21			
Luminance in almucantar (cd/m^2)	22			
Luminance in almucantar (cd/m^2)	23			
Luminance in almucantar (cd/m^2)	24			
Zenith Luminance (cd/m^2)				
Luminance - White Paper (cd/m^2)				
Azimuth 1st Measurement (º)				

Appendix D - CIE standard general sky

The CIE, Commission Internationale de l'Eclairage, proposes a set of luminance distribution, which could model the sky under a wide range conditions. It aims to be a universal basis for the classification of measured sky luminance distributions and to give a method for calculating sky luminance in daylighting design procedures. [1]

Table D-1 describes the 15 sky models proposed by the CIE. It also includes one column dividing the group into 3 sub-sets, which correspond to the 3 traditional sky classification, overcast skies (I), partly cloudy skies (II) and clear skies (III).

Table D-1 - CIE Sky Models

Sky Number	Sky Description	Sub-set
1	Overcast, steep gradation (approx CIE overcast)	I
2	Overcast, steep gradation, brightening towards sun	I
3	Overcast, moderate gradation, uniform in azimuth	I
4	Overcast, moderate gradation, brightening towards sun	I
5	Uniform sky	I
6	Partly cloudy, moderately graded, brightening towards sun	II
7	Partly cloudy, moderately graded, brighter circumsolar	II
8	Partly cloudy, rather uniform, clear solar corona	II
9	Partly cloudy, shaded sun position	II
10	Partly cloudy, brighter circumsolar	II
11	White-blue sky with clear solar corona	III
12	CIE clear sky with low turbidity	III
13	CIE clear sky with higher turbidity	III
14	Cloudless turbid with broader solar corona	III
15	White-blue turbid sky with wide solar corona	III

In order to visualise the effects of those models, images were generated for each of them for a specific day and time, for instance 16th August at 3.30pm. They are grouped by sub-set from Figure D-1 to Figure D-3. They show the relative luminance for 145 sky patches. A grey scale is used and a whiter patch means a brighter luminance. The letter 'S' represents the sun position. The scale is the same for every 15 model for better comparison among the whole set. However it makes it more difficult to visualise difference in the same sub-set.

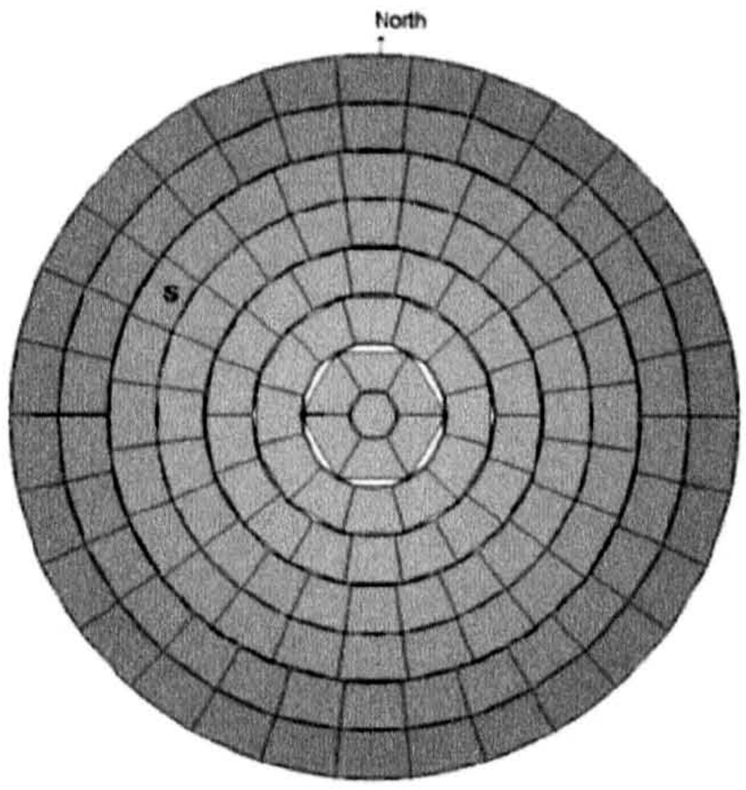

Sky Luminances - Sky 1 Day 16-08-2001 Time 15:30:00

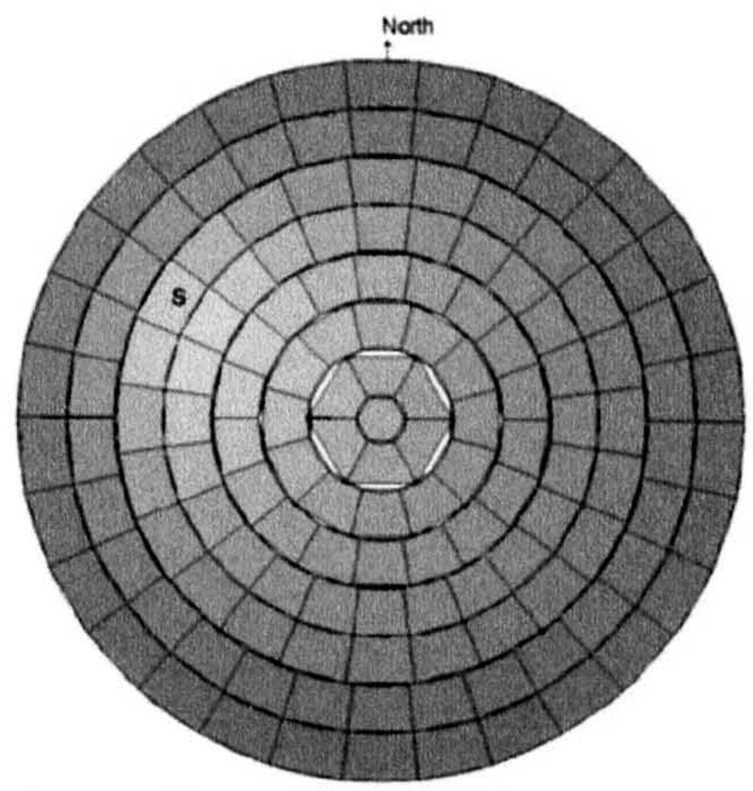

Sky Luminances - Sky 2 Day 16-08-2001 Time 15:30:00

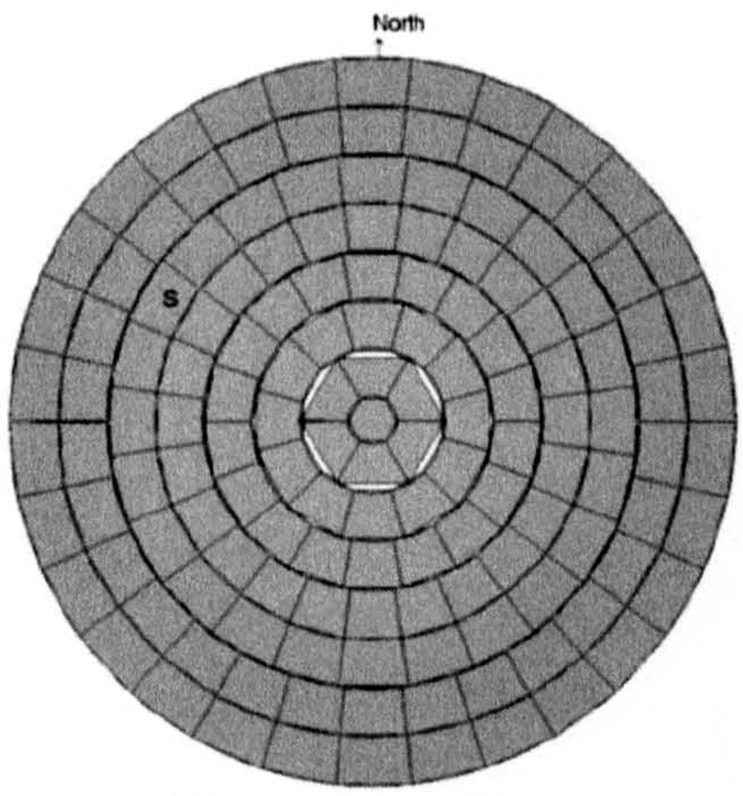

Sky Luminances - Sky 3 Day 16-08-2001 Time 15:30:00

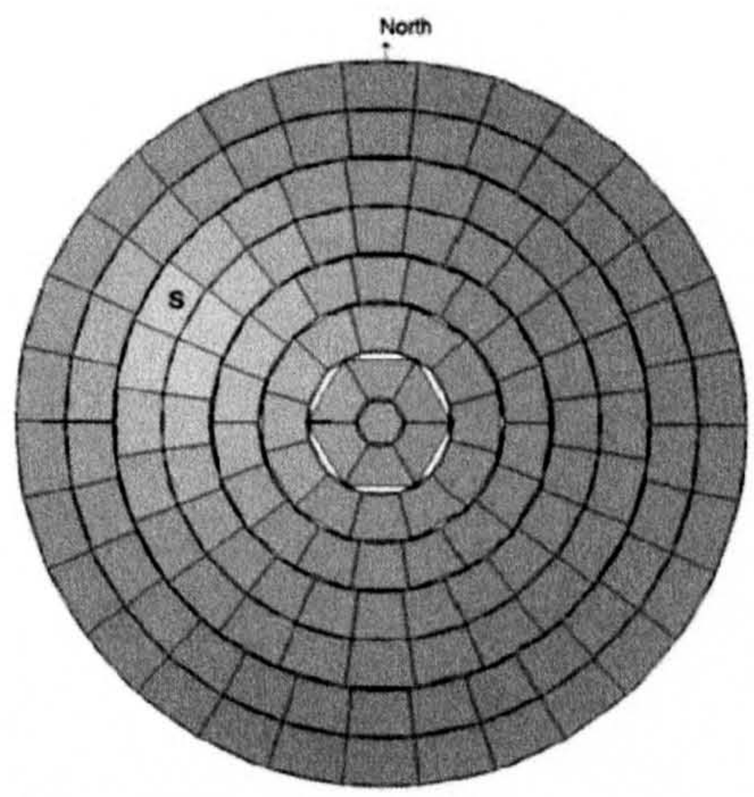

Sky Luminances - Sky 4 Day 16-08-2001 Time 15:30:00

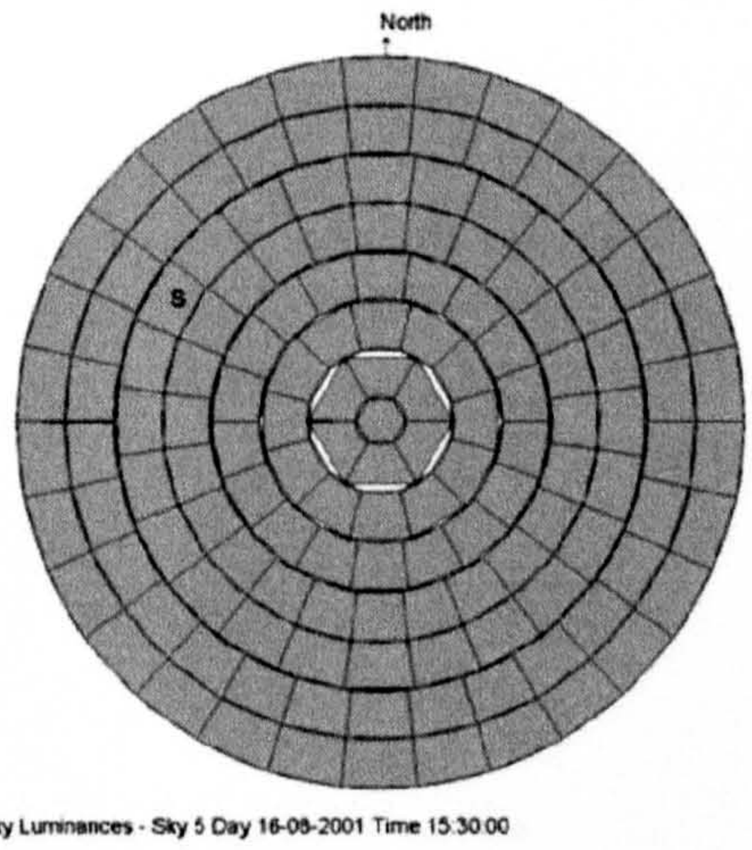

Sky Luminances - Sky 5 Day 16-08-2001 Time 15:30:00

Figure D-1 - Relative luminance distribution for overcast sky models (1-5)

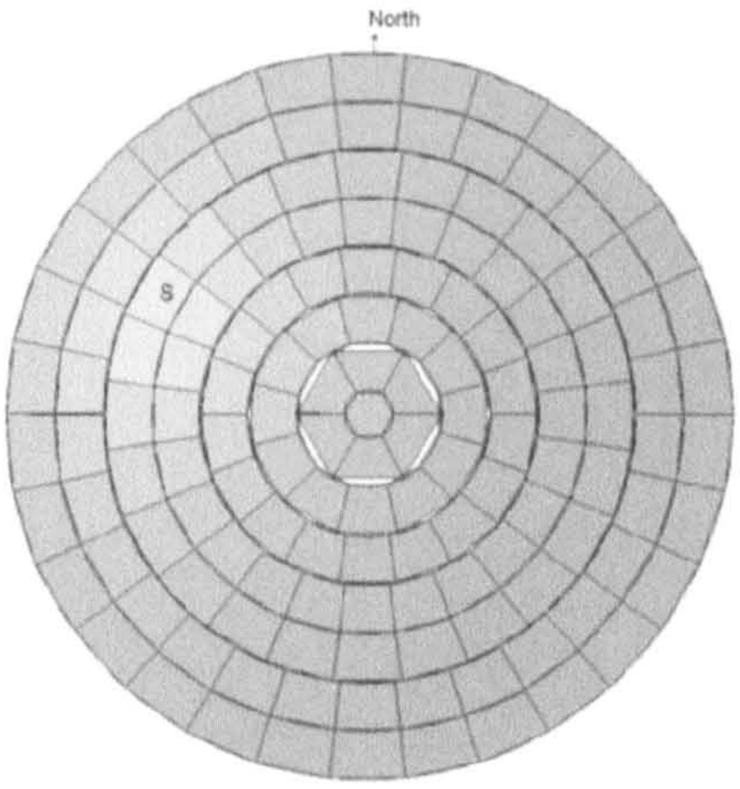

Sky Luminances - Sky 6 Day 16-08-2001 Time 15:30:00

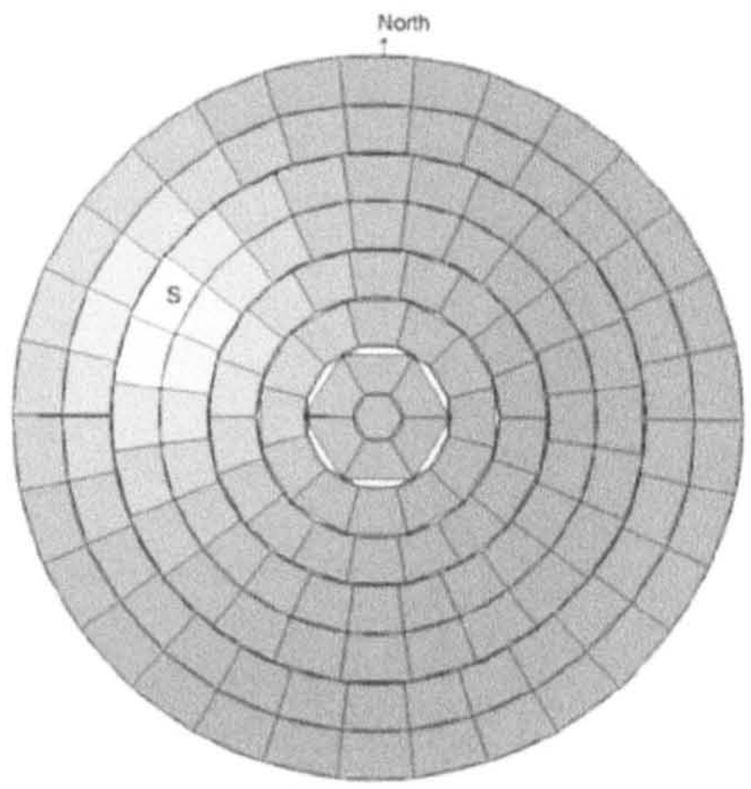

Sky Luminances - Sky 7 Day 16-08-2001 Time 15:30:00

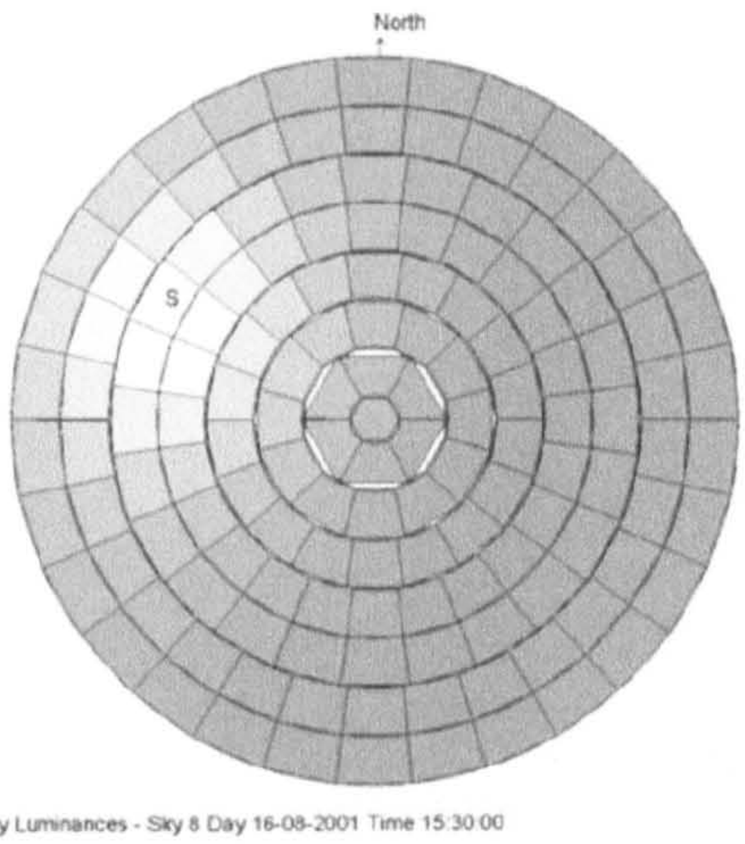

Sky Luminances - Sky 8 Day 16-08-2001 Time 15:30:00

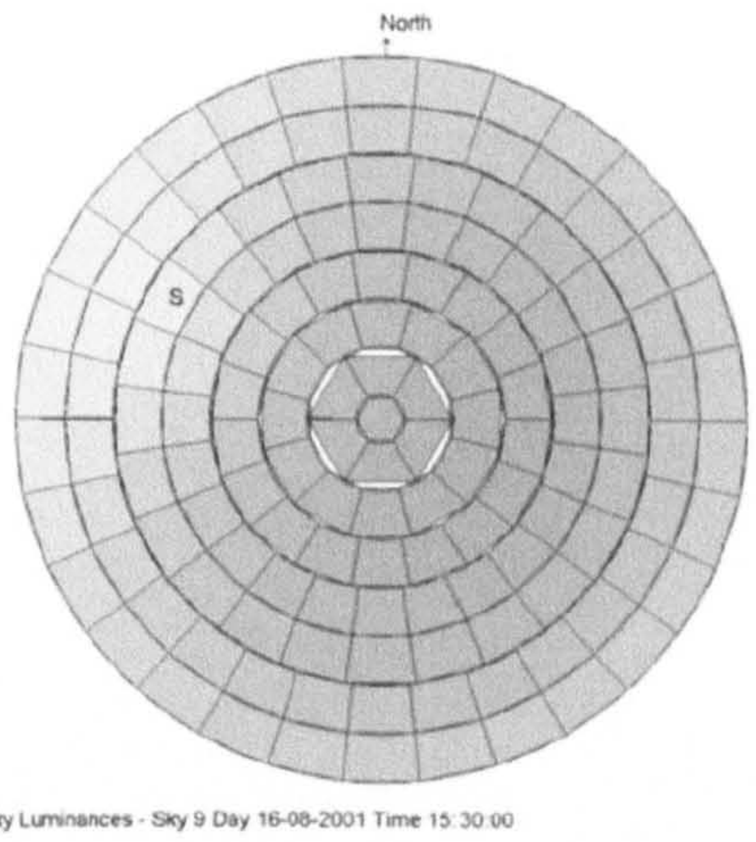

Sky Luminances - Sky 9 Day 16-08-2001 Time 15:30:00

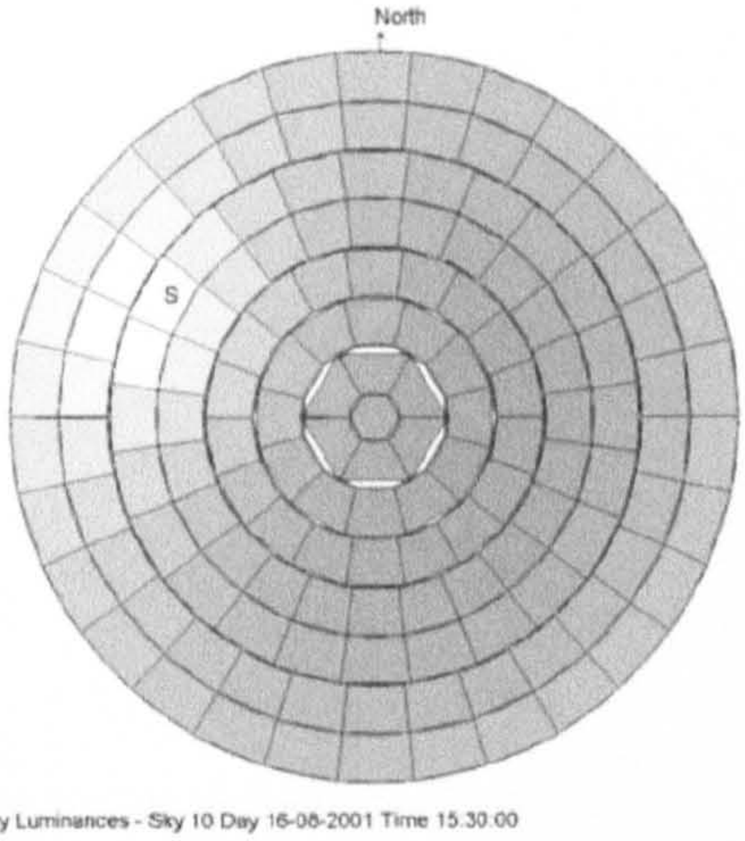

Sky Luminances - Sky 10 Day 16-08-2001 Time 15:30:00

Figure D-2 - Relative luminance distribution for partly cloudy sky models (6-10)

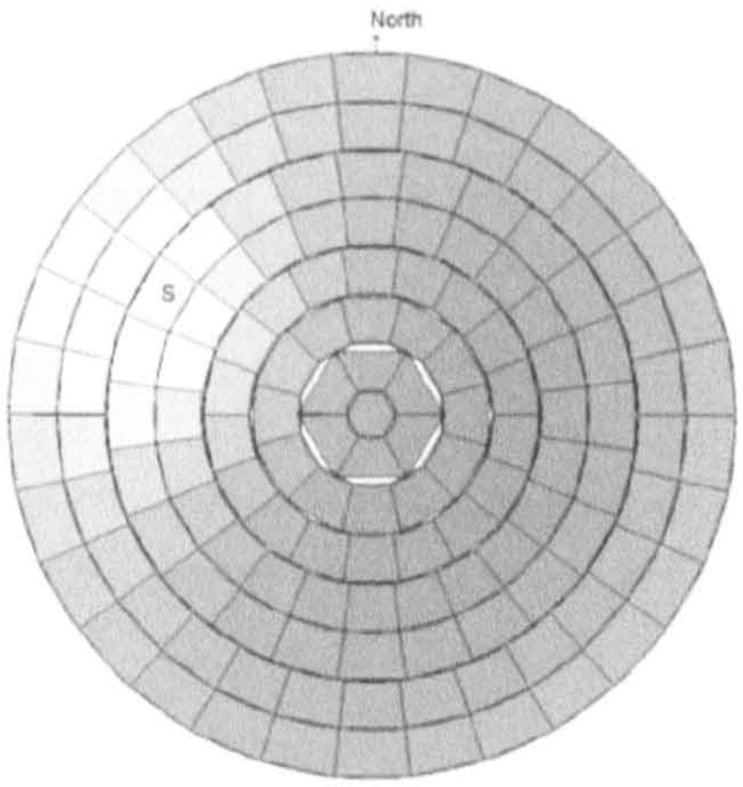

Sky Luminances - Sky 11 Day 16-08-2001 Time 15:30:00

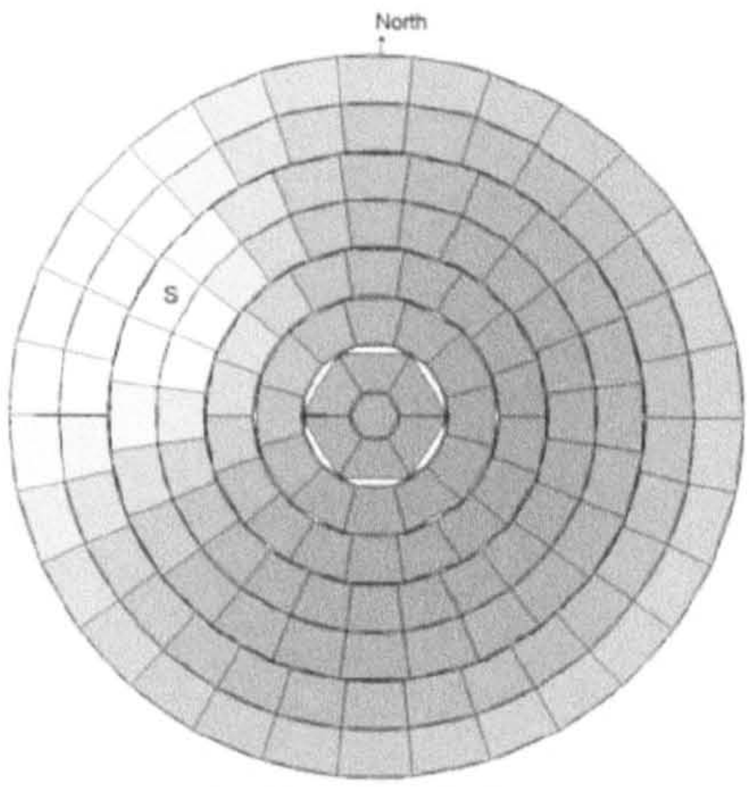

Sky Luminances - Sky 12 Day 16-08-2001 Time 15:30:00

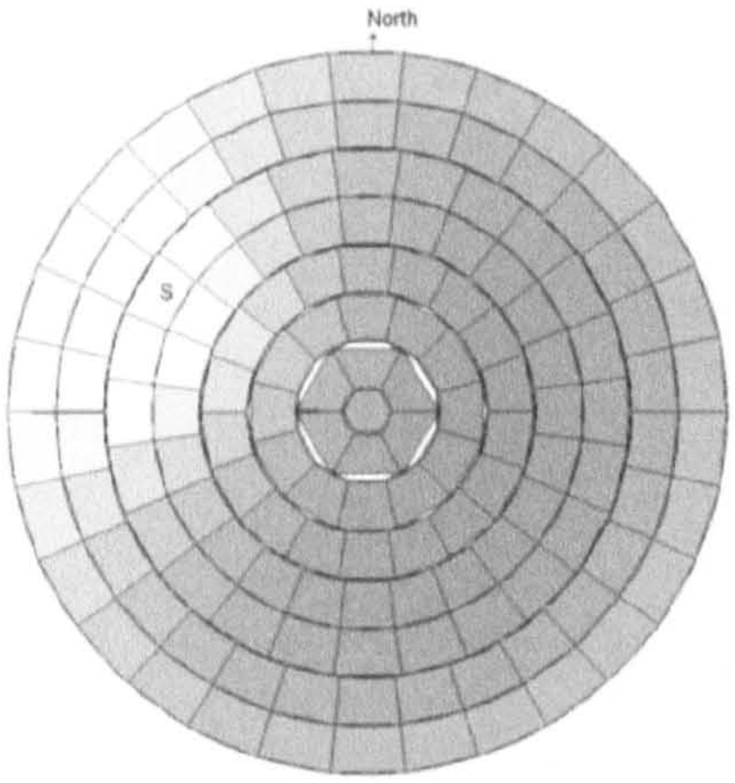

Sky Luminances - Sky 13 Day 16-08-2001 Time 15:30:00

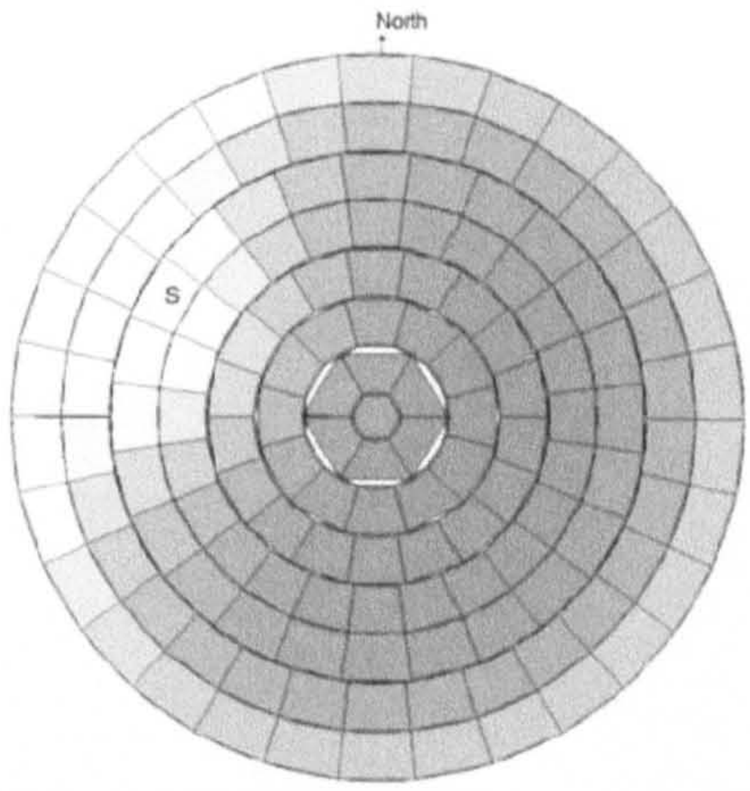

Sky Luminances - Sky 14 Day 16-08-2001 Time 15:30:00

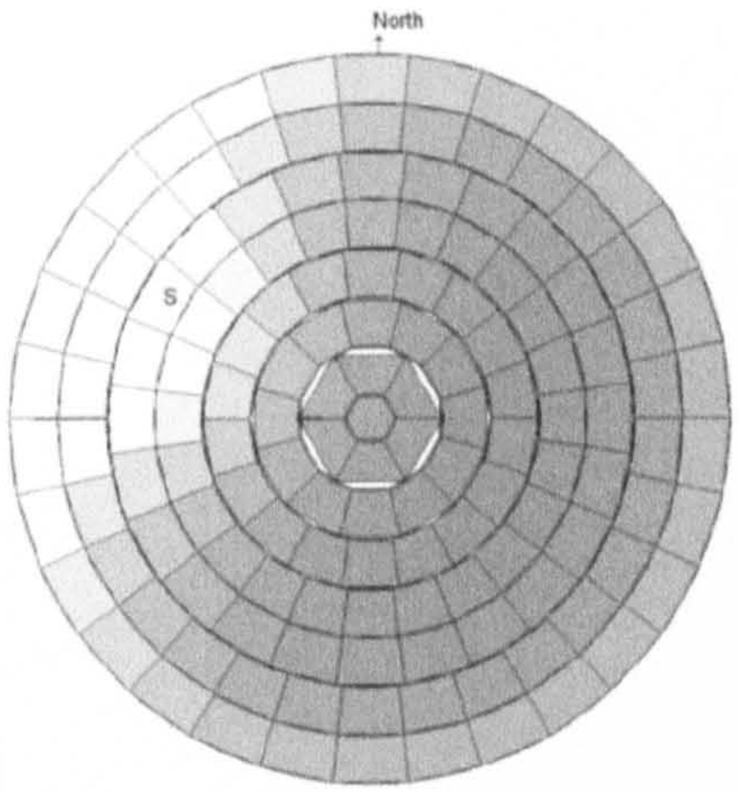

Sky Luminances - Sky 15 Day 16-08-2001 Time 15:30:00

Figure D-3 - Relative luminance distribution for clear sky models (11-15)

Reference

1. CIE - Commission Internationale de l'Eclairage, *Spatial distribution of daylight - CIE standard general sky*, CIE: Wien, 2002.

Appendix E - Comparing point and surface sources

In lighting calculation, some procedures can be simplified when a non-point source (B) can be treated as a point source (A). It occurs when illuminance in a point P at distance *d* from both sources, A and B, with same Intensity (*I*) can achieve results with no significant disparity.

The aim of this appendix is to:

(i) decide in the computer model when to treat a surface as a point source;

(ii) support the proposal of a new method for ground subdivision;

(iii) give a check to the size of sky zones in the CIE 145 sky subdivision and

(iv) give a check to the well-known rule-of-thumb, which asserts the relation distance/diagonal as 5:1 for a surface being treated as a point source.

Thus, this work compares illuminance results from a point source and a circular-disk source. It is based on the relation between the diameter of the disk and its distance to the observation point.

Illuminance from the disk source is based on equation (E.1) proposed by Moon [1].

$$\frac{E}{L} = \frac{R^2}{R^2 + D^2} \qquad \text{(E.1)}$$

where, E is the illuminance on a plane parallel to the source, L is its luminance, R is the radius of source and D is the distance between source and observation point (projected on the centre of the disk).

The illuminance on a plane parallel to a point source (E) is calculated by the Equation (E.2), based on the inverse squared law, where the intensity I is changed by the relation L/π allowing comparison with results achieved by the Equation (E.1). D is the distance from the point source to the observation point P.

$$\frac{E}{L} = \frac{1}{\pi D^2} \tag{E.2}$$

Results shown in the next figures are calculated for a point source and a circular-disk source with the same Intensity (I), varying the value D/d, where d is the disk diameter and D is its distance to the observation point. First, results are expressed as the relation E/L in Figure E-1, and as angular size in degree in Figure E-2.

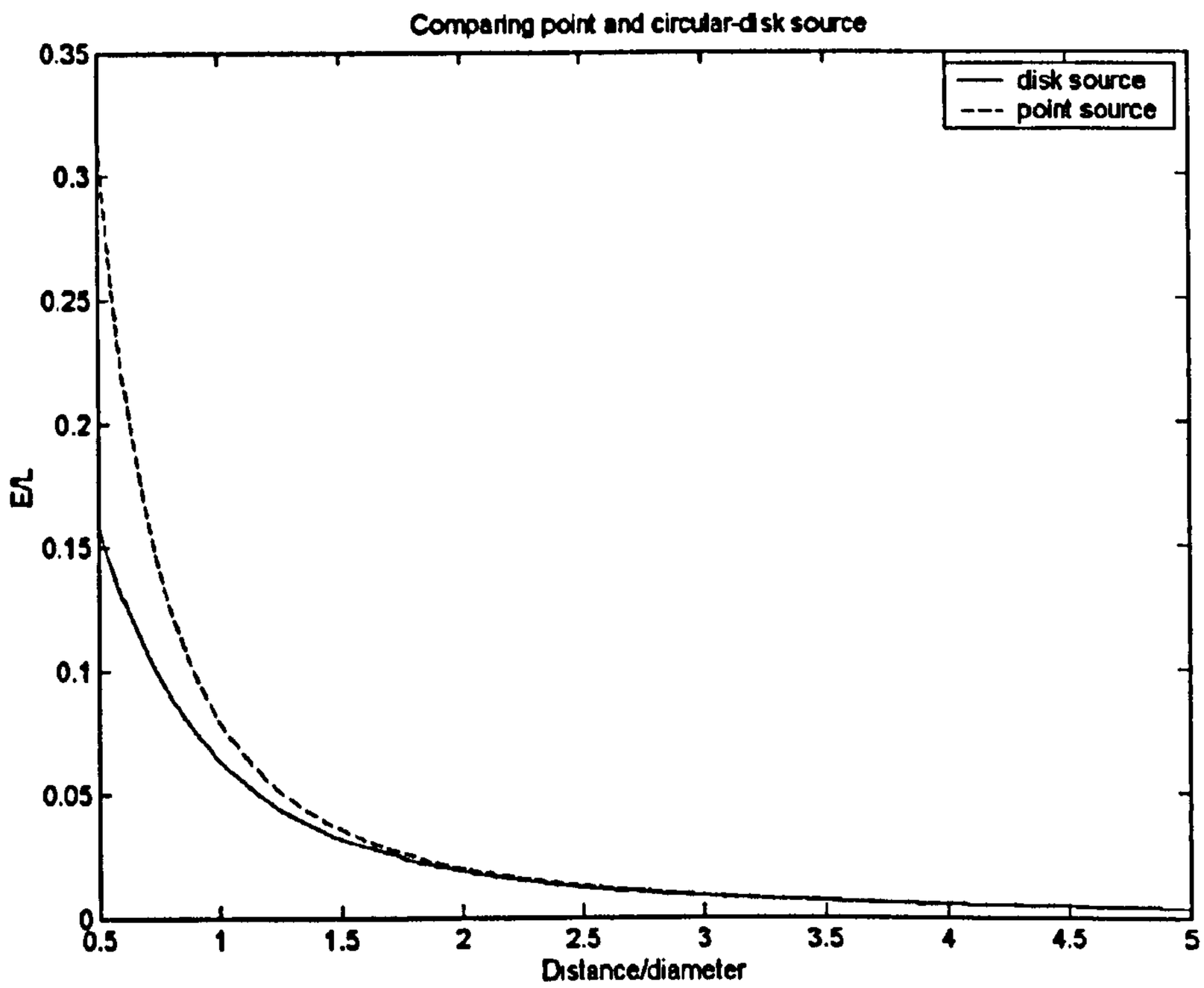

Figure E-1 - Comparing point and circular-disk sources, by distance/diameter

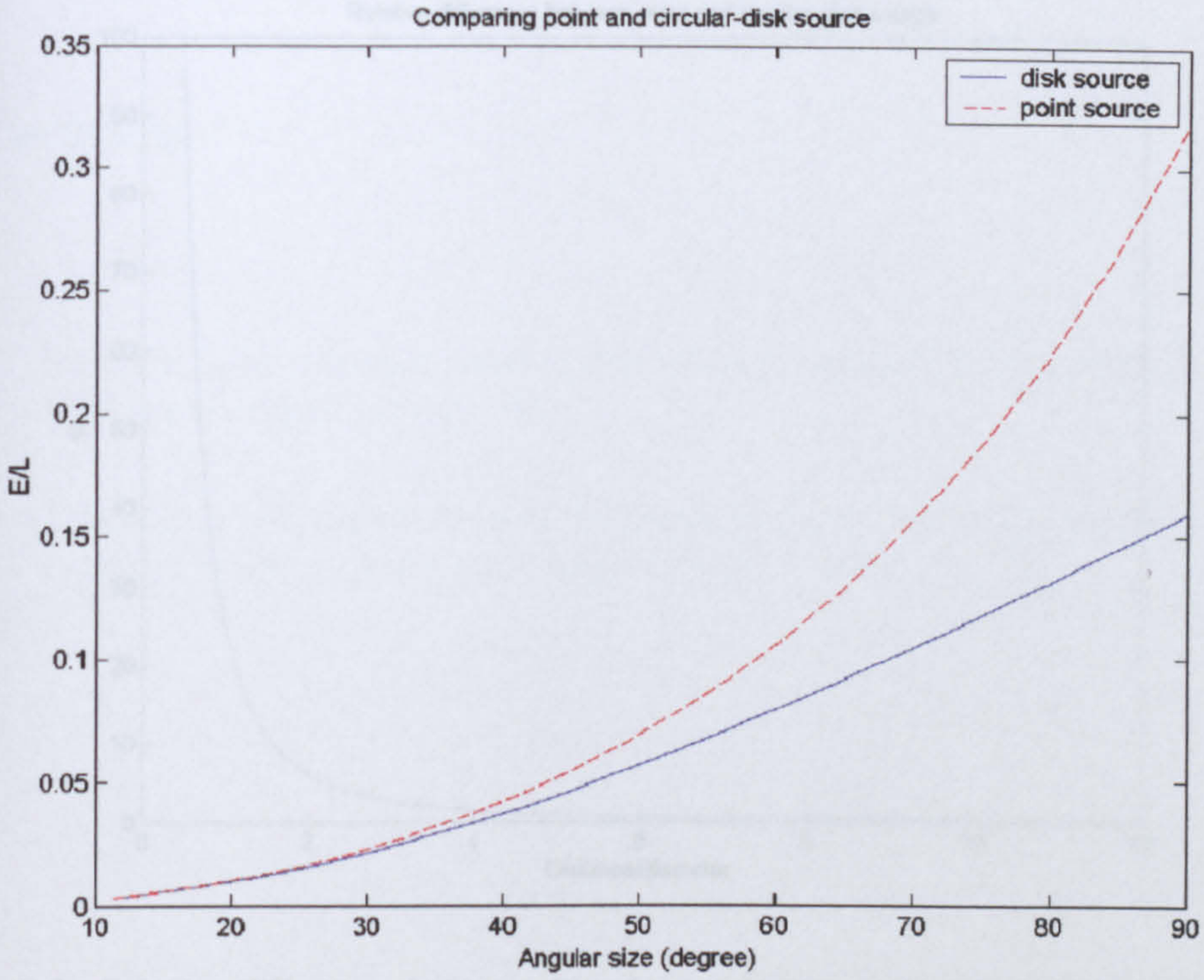

Figure E-2 - Comparing point and circular-disk sources, by angular size

The relative difference between a point source and a circular-disk source is shown in Figure E-3. A well-known rule of thumb defines the relation distance(D)/diameter(d) as 5, for a surface being treated as a point source. At this point, the relative error is 1%.

Results are also shown as angular sizes in degree in Figure E-4. Making a correlation with the rule of thumb, 5 D/d gives an angular size of 11.42° which is around the angular sizes proposed by Tregenza [2] for sky subdivision, later adopted by CIE. There, the sky patch angular size varies from 11.41° to 12.47°, which can give an error between 1.0% and 1.2%, if those surfaces are treated as a point source.

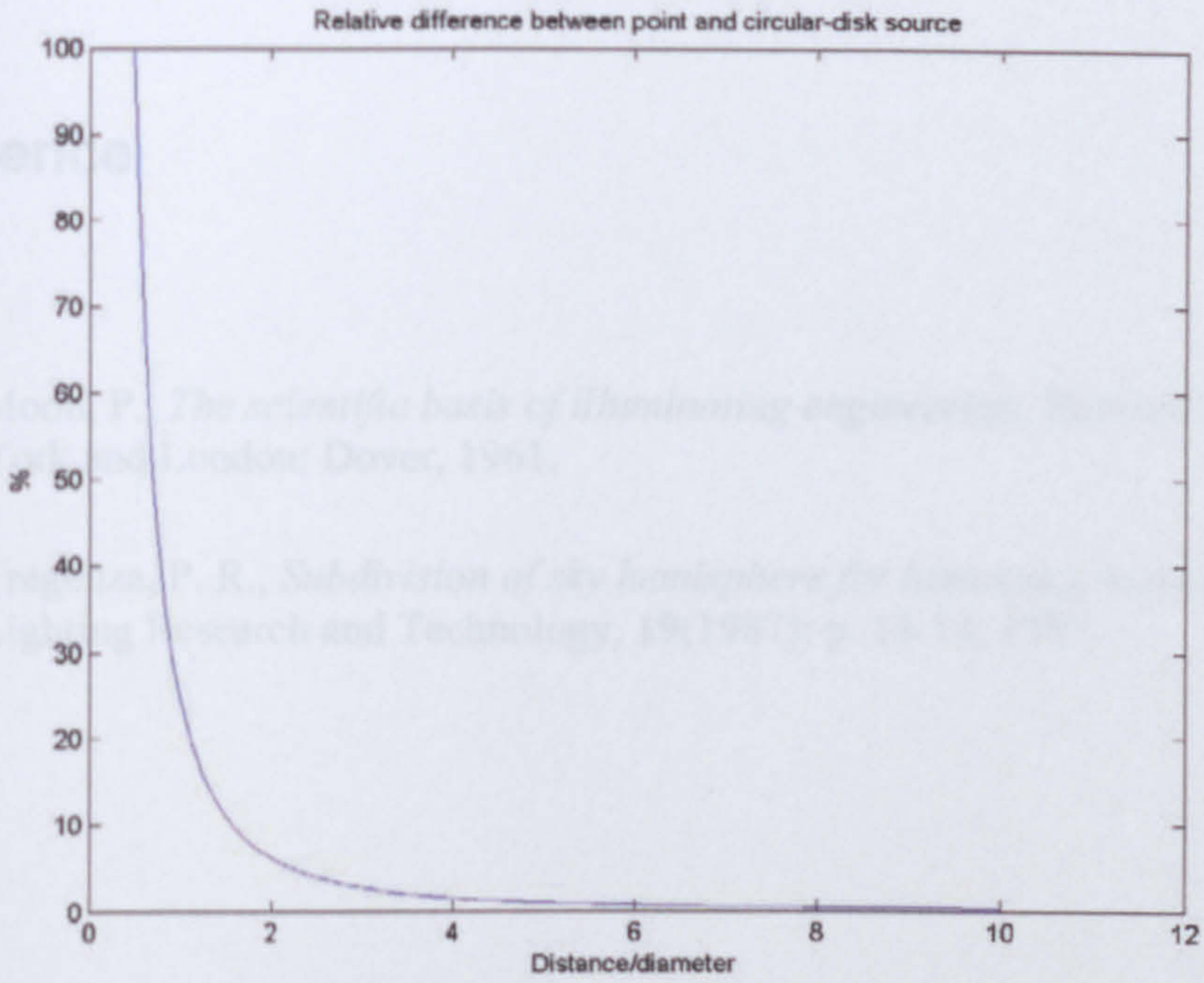

Figure E-3 - Relative difference between illuminance from a point and a circular-disk sources, by distance/diameter

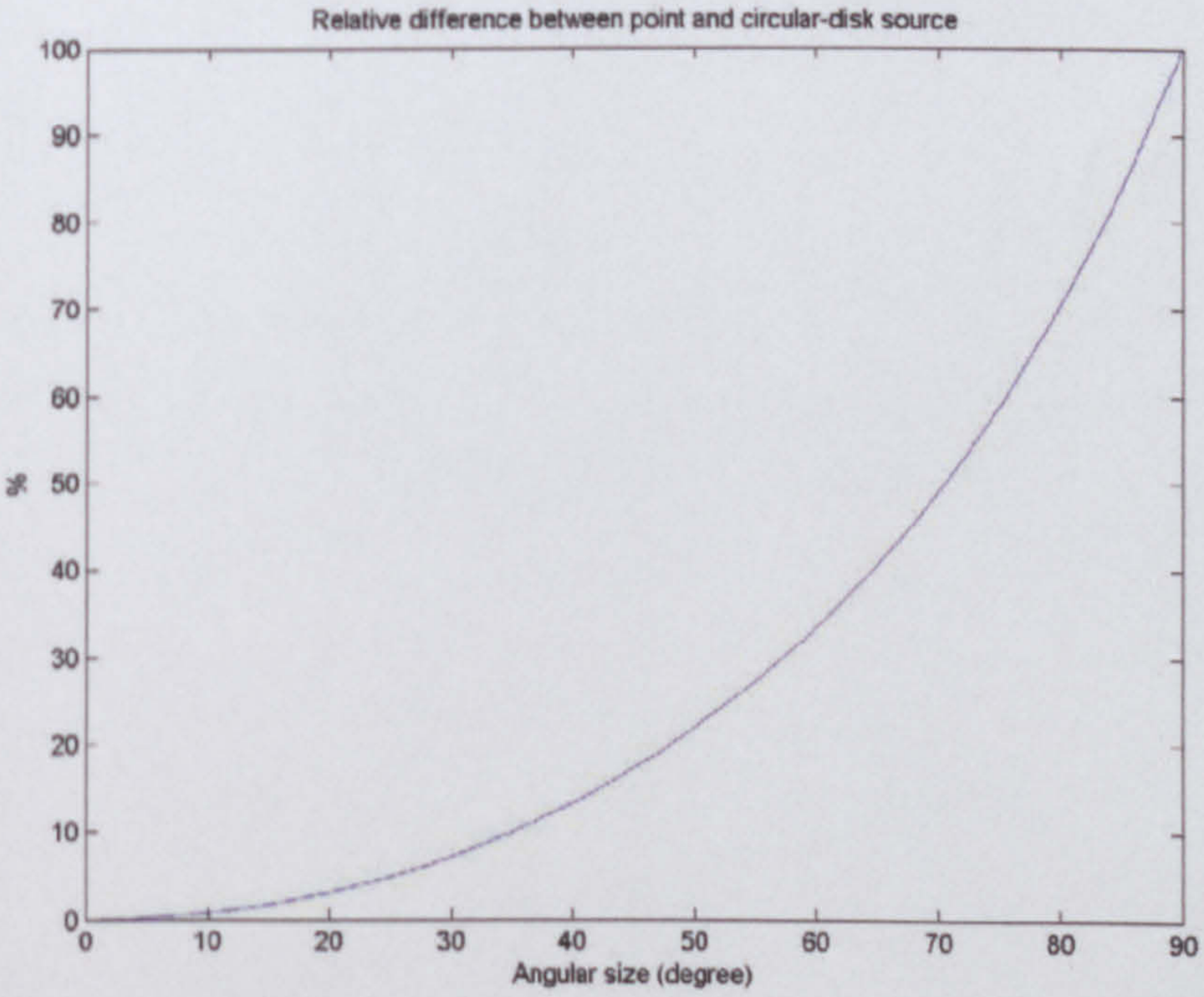

Figure E-4 - Relative difference between illuminance from a point and a circular-disk sources, by angular size

Reference

1. Moon, P., *The scientific basis of illuminating engineering*. Revised ed. New York and London: Dover, 1961.

2. Tregenza, P. R., *Subdivision of sky hemisphere for luminance measurements.* Lighting Research and Technology, **19**(1987): p. 13-14, 1987.

Appendix F - Main codes of the computer simulation tool

F.1 Daylight and auxiliary coefficients (internal point)

```
%%%%%%%%%%%%%%%%%%%%%%%%%%%%%%%%%%%%%%
function aDC=fDC(nRoom,nTimes,nErrorLim,nPla,aPt)
%%%%%%%%%%%%%%%%%%%%%%%%%%%%%%%%%%%%%%
% function aDC=fDC(nRoom,nTimes,nPla,aPt)
% function fDC computes daylight coefficients(DC) using Monte Carlo simulation
%   of particle tracks from window at a chosen Plane or point
% Author: Ricardo Cabus
% Begin 04.10.1999
% call: fEmit,fNewSurf,fNewMat,fHit,fBounce,fRaySky,fRayGrd,fRayExt,fIllumBasic
%
% Input: nRoom  - number of room to process
%       nTimes - number of times (particles or points) to process monte carlo simulation
%       nErrorLim - limit of error (default=0.05)
%       nPla   - number of plane to assess DC. if
%       aPt    - [nX nY nZ] point to assess DC, if empty process whole plane
%
% Output: aDC(aSkyZone,aComponent)
%          aSkyZone=[1:145] aComponent=[1:6]
%           1=direct(from sky patch), 2= internal reflected(from sky)
%           3=int refl(from ground) 4= int refl (from Ext surf)
%           5=External Reflected (no int. ref.) 6= Direct from ground
%       Saved in bDC

%%%%%%%%%%%%
% alt:
% 08.11.1999
% 01.12.1999 defines surfaces (planes), material and patches.
% 02.01.2000 Analyse SC and IRC
% 23.01.2000 transformed from script to function
% 27.04.2000 transformed in gDC
% 15.05.2000 new input aRoomNum, allows multi room calculation and stores
%         at the same array all DC, for every room, point, zone and component.
%         grid points are processed here instead of passed by parameter,
%         which is just how many points per row/col
% 02.06.2000 create gDCMean allowing mean DC for a surface (in a different function)
% 19.06.2000 include aNRay to count number of rays reaching nSkyZone
% 19.07.2000 allows grid half or whole surface (see fGrid)
%         saves elapse time (again)
% 01.08.2000 rename file when save to include more details and avoid overwriting
%         allow half grid
% 04.08.2000 correct bug
% 15.08.2000 aSkyWei is introduced to get information for sky graph
% 17.08.2000 correct a bug introduced by a mistake during copy-paste
% 23.08.2000 allows process or not aSkyWei, since it takes time and disk space
% 24.08.2000 allow split ground in more planes with different reflectances
% 07.09.2000 New Version. unify gDC and gDCMean into fDC.
%         create just a 2 dim matrix (sky patch, component).
%         Multi-rooms and grid are processed in a different function, which calls
%           this one
%         ground is treated separated. Assess DC for External surfaces.
% 14.09.2000 pi is removed for DC and put in fIllum calculation.
% 20.09.2000 allow parameters being passed by file
% 09.10.2000 adjusts
% 18.10.2000 comments
```

```
% 07.11.2000 pi is put again
% 12.05.2001 adjust position of  waitforbuttonpress command (at the end)
% 13.05.2001 adjust cd(sInputDir)
% 14.05.2001 adjust (specify which file is load each time)
% 16.05.2001 include message of elepsed time
%          block running direct. Only from batch menu !
% 28.07.2002 error is defined by parameters (5% is the default), then
%          the number of particles is not pre-defined. Program will run until
%          error is below the pre-set value. It is linked to fIllum using
%          basic parameters in order to assess error for Illuminance value
%          instead of dc. program will run in modules of 1000 particles,
%          cumulative.

%%%%%%%%%%%%%%%%%%%%%%%%%%%%%%%%%%%%%%%%%%%%%%%%%%%%%%%%%%%%%%%%%%%%%%%%%%%%%%%%
%%%%%%%%%%%%%%%%%%%%%%%%%%%%%%%%%%%%%%%%%%%%%%%%%%%%%%

global cRot aSkyZ aSkyWei aGrdZ aGrdWei aExtWei aNRaySky aSkyWei2 lDebug sInputDir

cd(sInputDir) %% save files in sInputDir directory
sTextBas='Running Daylight Coefficients';
nTFig=findobj(gcbf,'Tag','tText1');
set(nTFig,'String',sTextBas)

lDebug=logical(0); %% 1==debug on  //  0==debug off
%global iPart %% just to debug
aPlGrd=13; % ground plane, internally defined
if nargin==0
  errordlg('Missing Parameters, Run Batch DC')
  set(nTFig,'String','')
  return
end
if nargin==4;aPt=[];end
if isempty(aPt);lGrid=logical(1); % process grid
else;lGrid=logical(0);end; % process just one point

sFile='bGrdParam.mat';
if exist(sFile)==2;load(sFile,'nGrdType');
else errordlg([sFile ' not found']);set(nTFig,'String','');return;end

nTC=6; % total number of components processed
nSkyX=1;%1:process aSkyWei | 2:(aSkyWei+aNRaySky+aSkyWei2)
sRoom=fPut0(nRoom,3); % number of room with 3 digits (string)

lSky=logical(0); % logical variable to get ray reaching the sky
lGrd=logical(0); % logical variable to get ray bounced on the ground
lExt=logical(0); % logical variable to get ray bounced on external surfaces
lRef=logical(0); % logical variable to get reflected ray
if nSkyX==2
  aNRaySky=zeros(145,nTC);% aNRaySky(nSkyZone,nComp)=number of rays reaching nZone
  aSkyWei2=zeros(90,360,nTC); % similar aSkyWei, but more acurate (32400 patches)
end
sFile=['bSkyZone.mat'];
if exist(sFile)==2;load(sFile,'aSkyZ');
else errordlg([sFile ' not found']);set(nTFig,'String','');return;end; %% aSkyZ
nLenSkyZ=length(aSkyZ);
if isempty(nLenSkyZ);errordlg([sFile ' damaged']);set(nTFig,'String','');return;end
%
if nGrdType==1;  sFile=['bGrdZone' num2str(nGrdType) '.mat'];
else ;  sFile=['bGrdZone' num2str(nGrdType) '-r' num2str(sRoom) '.mat'];end
if exist(sFile)==2;load(sFile,'aGrdZ');
```

```
else errordlg([sFile ' not found']);set(nTFig,'String',");return;end; %% aGrdZ
nLenGrdZ=length(aGrdZ);
if isempty(nLenGrdZ);errordlg([sFile ' damaged']);set(nTFig,'String',");return;end
%
sFile=['bPlExt' sRoom '.mat'];
if exist(sFile)==2;  load(sFile,'aPlExt'); %% get external planes
else;  errordlg([sFile ' not found']);set(nTFig,'String',");return;end
nLenExt=length(aPlExt);
if isempty(nLenExt);errordlg([sFile ' damaged']);set(nTFig,'String',");return;end
%
aSkyWei=zeros(nLenSkyZ,2);% aSkyWei(nSkyZone,nComp)=nWeight
aGrdWei=zeros(nLenGrdZ,2);%
aExtWei=zeros(nLenExt,2);
% get room parameters and test file
sFile=['bRoom' sRoom '.mat'];
if exist(sFile)==2
  load(sFile,'cRoom','cRot') %% % gets room parameters
  if exist('cRoom')==0;
    errordlg(['cRoom not found in ' sFile]);set(nTFig,'String',");return;end
  if exist('cRot')==0;
    errordlg(['cRot not found in ' sFile]);set(nTFig,'String',");return;end
else;errordlg([sFile ' not found']);set(nTFig,'String',");return;end
nAzX=cRoom{5}(5); % azimuth Axis X
if lGrid;aPtGrid=fRandGrid(nPla,nTimes,cRoom,0);end %% create grid
tic % Start a stopwatch timer

iSmp=0; % counter for number of samples (to assess error)
nError=1; % start value for assessed error
aSkyWeiT=0;aGrdWeiT=0;aExtWeiT=0;
while nError>nErrorLim
  iSmp=iSmp+1; %%
% set up weight values:
aSkyWei=zeros(nLenSkyZ,2);% aSkyWei(nSkyZone,nComp)=nWeight
aGrdWei=zeros(nLenGrdZ,2);%
aExtWei=zeros(nLenExt,2);
for iT=1:nTimes
  %if mod(iT,100)==0;sMens=['Particle ' num2str(iT) '/' num2str(nTimes)];disp(sMens);end
  if mod(iT,100)==0
    sText=['Sample ' num2str(iSmp) '  Error ' num2str(fRound(nError*100,1)) ' %'];
    set(nTFig,'String',{sTextBas;sText})
  end
  lRef=0;lSky=0;lGrd=0;lExt=0;  % clear logical variables
  if lGrid;aPhot=fEmit(aPtGrid(iT,:),nPla); % initial vector of ray
  else aPhot=fEmit(aPt,nPla);end % initial vector of ray
  while aPhot(8)>0
    aXYZPla=fNewSurf(cRoom,aPhot);  % coordinates of new intersection
    if ismember(aXYZPla(4),aPlGrd);lGrd=1;break; %% hit ground plane
    elseif ismember(aXYZPla(4),aPlExt);lExt=1;break;%% hit External surface
    elseif aXYZPla(4)==0;lSky=1;break;end;     %% hit sky
    aWinPatMat=fNewMat(cRoom,aXYZPla); % window, patch, material type of new surface
    if (aWinPatMat(1)==0 & ~lGrd);lRef=1;end; %% not window % lRef=1 =>reflected %
    aNewPhot=fHit(aPhot,aXYZPla); % record intersection
    aPhot=fBounce(cRoom,aNewPhot,aWinPatMat); % new vector and weight
  end % of single particle
  if ~lRef; nC=1; % direct
  else; nC=2;end;      % internally reflected
  if lSky %% Ray hits sky
    fRaySky(aPhot(1:3),aPhot(8),nAzX,nC,nSkyX);  %aPhot(8)=weight
  elseif lGrd % ray hits ground
    fRayGrd(aXYZPla(1:3),aPhot(8),nC);
```

```
  elseif lExt % ray hits external surface
   fRayExt(aXYZPla,aPhot(8),nC,sRoom);
  end
  % obs: ray bouncing both ground and ext. surf. is counted for which one bounces last
  % before enter the room.
end % particle loop
%% get DCs:
for iC=[1:2] % sky
 aDCt(:,iC)=pi.*aSkyWei(:,iC)./(nTimes.*aSkyZ(:,9)); % dc for later average
 if nSkyX==2
  aNRay(:,iC)=aNRaySky(:,iC);
  aSkyWei(:,:,iC)=aSkyWei2(:,:,iC);
 end
end
% ground
% aDC[ 3=IRC(from ground) 6=direct from ground]
% aDC(:,3)=aDCGrd(:,1)// aDC(:,6)=aDCGrd(:,2)
aDCGrdt(:,1)=pi.*aGrdWei(:,1)./(nTimes.*aGrdZ(:,5)); % aGrdZ(5)=area
aDCGrdt(:,2)=pi.*aGrdWei(:,2)./(nTimes.*aGrdZ(:,5)); % aGrdZ(5)=area
% external surface
% aDC [4=IRC(from Ext.Surf) 5=ERC (Ext Ref. Comp)]
% aDC(:,4)=aDCExt(:,1)// aDC(:,5)=aDCExt(:,2)
for i=1:nLenExt
 nArea=cRoom{2}(nPla,14);
 aDCExtt(:,1)=pi.*aExtWei(:,1)./(nTimes.*nArea); %
 aDCExtt(:,2)=pi.*aExtWei(:,2)./(nTimes.*nArea); %
end
%%% assess dc error (by illuminance) % does not include ground or obtruction coefficients
aSky=[5];aAzX=[0];aDay=[22;12;2001];aTime=[12;00;00]; %dummy values
aIllum(iSmp)=fIllumBasic(aSky,aAzX,aDay,aTime,aDCt);
%    error (only assessed after n>=25 to get a normal distribution)
 if iSmp==1
  nError=1; %dummy value
 else
  nSTD=std(aIllum); % standard deviation of illuminances
  nMean=mean(aIllum); % mean of illuminances
  nError=(2*nSTD/sqrt(iSmp))/nMean; % error with 95%confidence level
 end
 aError(iSmp,:)=[nTimes*iSmp,nError]; %% save for printing
 aDCSmp(iSmp,:,:)=aDCt;       % save for re-run with diferent skies and compare error %
 aDCGrdSmp(iSmp,:,:)=aDCGrdt;  %  used only for validation
 %% totalise weights to process final coefficients
 aSkyWeiT=aSkyWeiT+aSkyWei;
 aGrdWeiT=aGrdWeiT+aGrdWei;
 if nLenExt>0
  aExtWeiT=aExtWeiT+aExtWei;
 end
end
%% assess coefficients mean
nTimesT=nTimes*iSmp; % total number of particles
for iC=[1:2] % sky
 aDC(:,iC)=pi.*aSkyWeiT(:,iC)./(nTimesT.*aSkyZ(:,9));
 aDCGrd(:,iC)=pi.*aGrdWeiT(:,iC)./(nTimesT.*aGrdZ(:,5));
 if nLenExt>0
  aDCExt(:,iC)=pi.*aExtWeiT(:,iC)./(nTimesT.*nArea);
 end
end
%

nETime=toc; %Read the stopwatch timer.
```

```
%% save files:
sFile='bDC';
sFile=[sFile '-r' sRoom]; % room number
sFile=[sFile '-g' num2str(nGrdType)]; % ground type
if lGrid
  sFile=[sFile '-pl' num2str(nPla) '-'] ;
else
  sFile=[sFile '-pt'];
  for iPt=1:3
    sFile=[sFile fDec2Str(aPt(iPt),2) '-'];
  end
end
sFile=[sFile  't' num2str(nTimesT)];% number of times processed (total):

sExt='';
i=1;
while exist([sFile sExt '.mat'])==2 %% avoid overwrite sFile
   i=i+1;  sExt=['v' fPut0(i,2)];
end
sFile1=[sFile sExt '.mat'];
nTimes=nTimesT; % just for compatibility when save/load paramenters
if exist('aDCExt')==1
  save(sFile1,'aDC','aDCGrd','aDCExt','sRoom','nPla','aPt','nETime','nGrdType',...
    'nTimes','aError','aDCSmp','aDCGrdSmp');
else
  save(sFile1,'aDC','aDCGrd','sRoom','nPla','aPt','nETime','nGrdType','nTimes',...
    'aError','aDCSmp','aDCGrdSmp');
end
if nSkyX==2
  sFile2=[sFile sExt 'Sky.mat'];
  save(sFile2,'aNRay','aSkyWei');
end
if nargin==0
  sText=['Daylight coefficients stored in file ' sFile];
  sText2=[num2str(fRound((nETime/60),1)) ' min elapsed'];
  set(nTFig,'String',{sText;sText2})
  waitforbuttonpress
end
set(nTFig,'String','')

return
%%%%%%%%%%%%%%%%%%%%%%%%%%%%%%%%%%%%%%%%%%%%%%%%%%%%%%%%%%%%%%%%%%%%%%%%%%%%
%% end function aDC=fDC(nRoom,nTimes,nPla,aPt)
%%%%%%%%%%%%%%%%%%%%%%%%%%%%%%%%%%%%%%%%%%%%%%%%%%%%%%%%%%%%%%%%%%%%%%%%%%%%
%

%%%%%%%%%%%%%%%%%%%%%%%%%%%%%%%%%%%%%%%%%%%%%%%%%%%%%%%%%%%%%%%%%%%%%%%%%%%%
function aPhot=fEmit(aPoint,nPla)
%%%%%%%%%%%%%%%%%%%%%%%%%%%%%%%%%%%%%%%%%%%%%%%%%%%%%%%%%%%%%%%%%%%%%%%%%%%%
% fEmit gives random starting angle of particle in Monte Carlo
%       simulation from point
% Author: RCC based on Peter Tregenza, June 1998
% begin: 19.10.99
% called by fDC
% Input : aPoint(X,Y,X), nPla (plane)
% Output: aPhot=[c1 c2 c3 nX nY nZ nPla nWeight]
%                       direct cosines; point coordinates; plane; weight of particle
% Algorithms from 'Daylighting algorithms' ETSU S 1350 1993
% alt:
% 15.12.1999 - Allows Point in all planes
```

```
% 01.01.2000 - allows point without a 'supporting' plane
% 07.09.2000 - adapt new version

%%%%% just to debug
global lDebug
global aDebugEmit
global iPart
%%%%%
global cRot
nRand1=rand;nRand2=rand;          % random numbers
nPhi=2.*pi.*nRand2;
nCosPhi=cos(nPhi);
nSinPhi=sin(nPhi);
if nPla==0
 nTheta=(pi.*nRand1);
 nCosT=cos(nTheta);
 nSinT=sin(nTheta);
else
 nCosT=sqrt(1-nRand1);
 nSinT=sqrt(nRand1);
end
%% cosines relative to plane:
aCosPla(1)=nCosPhi.*nSinT;
aCosPla(2)=nSinPhi.*nSinT;
aCosPla(3)=nCosT;
if nPla==0;aCosRay=aCosPla;
else;aCosRay=aCosPla*cRot{nPla,1}; % cosines in general coordinates
end
nWeight=1; %% default
aPhot=[aCosRay aPoint nPla nWeight];
%%%%%% just to debug - save all variables into bNewSurf
if lDebug
 if exist('aDebugXYZ')==0;aDebugXYZ=[];end
 aDebugEmit=[aDebugEmit; iPart aPhot];
 save bDebugEmit aDebugEmit
end
%%%%%%%%%%%%%%%%%%%%%%%%%%%%%%%%%%%%%%%%%%%%%%%%%%%%%%%%%%%%%%%%%%%%%%%%%%%%
% end function aPhot=fEmit(aPoint,nPla)
%%%%%%%%%%%%%%%%%%%%%%%%%%%%%%%%%%%%%%%%%%%%%%%%%%%%%%%%%%%%%%%%%%%%%%%%%%%%

%%%%%%%%%%%%%%%%%%%%%%%%%%%%%%%%%%%%%%%%%%%%%%%%%%%%%%%%%%%%%%%%%%%%%%%%%%%%
function aXYZPla=fNewSurf(cRoom,aPhot)
%%%%%%%%%%%%%%%%%%%%%%%%%%%%%%%%%%%%%%%%%%%%%%%%%%%%%%%%%%%%%%%%%%%%%%%%%%%%
% fNewSurf assess nearest intersection of ray and plane
% Author: RCC based on Peter Tregenza, May 1998
% Algorithms from 'Daylighting algorithms' ETSU S 1350 1993
% begin : 19.10.99
% called by fDC
% Input: cRoom={aRoomMat aPlane aWindow aPatch aPtPl aPtWin};%room parameters
%          aPtPl(iPl,jPl-3,kPl)=cPlane{iPl,jPl}(kPl);
%      aPhot=[c1 c2 c3 nX nY nZ nStartPlan nWeight]
% Output: aXYZPla=[x y z plane]

%%%%%%%%%%
% alt:
% 23.11.1999
% 15.12.1999
% 03.05.2000 local coordinates and allows all kind of polygons
% 13.05.2000 correct bug
% 08.06.2000 compare performance (using profile) between fIsInPoly and inpolygon
```

```
% 15.06.2000 correct bug: when nPl==0 (rarely occurs) an error was created in the
%              function who had called fNewSurf.
% 07.09.2000 adapt new version
%%%%%%%%%%%%
global cRot
%%%%%%%  debug
global lDebug
if lDebug
 global iPart aDebugXYZ aDebugNewSurf
 if exist('aDebugNewSurf')==0;aDebugNewSurf=[];end
end
%%%%%%%  debug
aPlEdge=cRoom{2}(:,8:13); % Plane edges: xmin,xmax,ymin,ymax,zmin,zmax
aPtPl=cRoom{6}; %% Plane vertices
aCosPla=cRoom{2}(:,1:3); % cosines of planes [old: n]
aP=cRoom{2}(:,4); % origin distance of planes [old:p]
[nCount nPar]=size(aCosPla);
aCount=1:nCount; % plane numbers in aCosPla
aType=cRoom{2}(:,5); % type
[aType0 iPar]=find(aType==0);
if aPhot(7)==0 %% no starting plane
 aDiscardPl=[aType0]; %% discarding planes: type==0
else
 aDiscardPl=[aPhot(7); aType0]; %% discarding planes: current(starting) and type==0
end
aCosPla(aDiscardPl,:)=[];
aP(aDiscardPl,:)=[];
aCount(aDiscardPl)=[];
aCosRay=aPhot(1:3); % cosines of ray [old: c]
aXYZ=aPhot(4:6); % start position of ray
aCosT=aCosPla*aCosRay'; % cos angle of incidence
aNeg=find(aCosT<0);
aCosTNeg=aCosT(aNeg);
aCosPlaNeg=aCosPla(aNeg,:);
aPNeg=aP(aNeg);
aCountNeg=aCount(aNeg); % planes facing ray
aR=(aCosPlaNeg*aXYZ'-aPNeg)./aCosTNeg; % distances from point to planes
%% discarding planes with aR>0 => the ray never reach them
aNeg2=find(aR<0);
aRNeg2=aR(aNeg2);
aCountNeg2=aCountNeg(aNeg2); % planes where ray cannot reach -%
[aSortR aIndexR]=sort(abs(aRNeg2)); % distance sorted
[nPl nPar]=size(aRNeg2);
iPl=1;
lRayOut=1;
while iPl<=nPl
 nNewPl=aCountNeg2(aIndexR(iPl)); % Plane number
 aNewXYZ=aXYZ+aSortR(iPl).*aCosRay; % New XYZ (intercept)
 %%%%%%% just to debug
 if lDebug;aDebugNewSurf=[aDebugNewSurf; iPart aNewXYZ nNewPl];end;
 %%%%%%%
 aNewXYZL=aNewXYZ*cRot{nNewPl,2};%% local cordinates (point to test)
 nU=aNewXYZL(1);nV=aNewXYZL(2); % point to test
 aPtPlL=squeeze(aPtPl(nNewPl,:,:))*cRot{nNewPl,2}; %% local cordinates (points of polygon)
 aU=aPtPlL(:,1);aV=aPtPlL(:,2);
 if fIsInPoly(nU,nV,aPtPlL)
  lRayOut=0;%%intercept surface
  break %% exit
 else %% out of surface - look next surface
  iPl=iPl+1;
```

```
  end
 end
 if lRayOut | nPl==0  % ray out
  aNewXYZ=[0 0 0];   %% not used
  nNewPl=0; %% Plane =0 => ray out
 end
 aXYZPla=[aNewXYZ nNewPl]; % intercept & plane number & ground reflection
 %%%%%%%% just to debug
 if lDebug
  if exist('aDebugXYZ')==0;aDebugXYZ=[];end
  aDebugXYZ=[aDebugXYZ; iPart aXYZPla];
  save bDebugNewSurf aDebugXYZ aDebugNewSurf
 end
 %%%%%%% debug^
 return
 %%%%%%%%%%%%%%%%%%%%%%%%%%%%%%%%%%%%%%%%%%%%%%%%%%%%%%%%%%%%%%%%%%%%%%%%%%%%
 % end function aXYZPla=fNewSurf(cRoom,aPhot)
 %%%%%%%%%%%%%%%%%%%%%%%%%%%%%%%%%%%%%%%%%%%%%%%%%%%%%%%%%%%%%%%%%%%%%%%%%%%%


 %%%%%%%%%%%%%%%%%%%%%%%%%%%%%%%%%%%%%%%%%%%%%%%%%%%%%%%%%%%%%%%%%%%%%%%%%%%%
 function aWinPatMat=fNewMat(cRoom,aXYZPla)
 %%%%%%%%%%%%%%%%%%%%%%%%%%%%%%%%%%%%%%%%%%%%%%%%%%%%%%%%%%%%%%%%%%%%%%%%%%%%
 % fNewMat finds material at intersection of ray & surface
 % Author: RCC based on Peter Tregenza, May 1998
 % begin : 19.10.99
 % called by fDC
 % Input : cRoom={aRoomMat aPlane aWindow aPatch ...}; %%room parameters
 %        aXYZPla=[nX nY nZ nPla] intercept & plane number%
 %         aPlane=[n1 n2 n3 p type win pat axref]
 %             cosines of normal, origin distance, material
 %                        first window, first patch (0 if no window or patch), axes reference
 %          aWindow=[xmin xmax ymin ymax zmin zmax reve type pla next]
 %          type=0 is unglazed, otherwise glass type
 % Output: aWinPatMat=[nWin nPat nType] where nType=-mat,0 or glazing type

 % alt
 % 15.12.1999
 % 07.09.2000 adapt new version

 %% just to debug
 global lDebug iPart aDebugWM %% to debug
 %%
 nX=aXYZPla(1);nY=aXYZPla(2);nZ=aXYZPla(3); nPla=aXYZPla(4);
 % defaults:
 nWin=0; nPat=0; nType=cRoom{2}(nPla,5);
 % test for windows in plane
 % iWin is row number in wins of the window on the plane
 % if plane has more than 1 window 'iWin' must be the first with
 % minimum next<>0
 iWin=cRoom{2}(nPla,6);
 while iWin>0
   if nX+eps*10>=cRoom{3}(iWin,1) & nX-eps*10<=cRoom{3}(iWin,2) &...
       nY+eps*10>=cRoom{3}(iWin,3) & nY-eps*10<=cRoom{3}(iWin,4) & ...
       nZ+eps*10>=cRoom{3}(iWin,5) & nZ-eps*10<=cRoom{3}(iWin,6)
     nWin=iWin;
     nType=cRoom{3}(iWin,8);
     break;
   else
     iWin=cRoom{3}(iWin,10); % next window
```

```
  end
end
aWinPatMat=[nWin nPat nType];
%% just to debug
if lDebug
  if exist('aDebugWM')==0; aDebugWM=[];end
  aDebugWM=[aDebugWM; iPart aWinPatMat];
  save bDebugNewMat aDebugWM
end
%%%%%%%%%%%%%%%%%%%%%%%%%%%%%%%%%%%%%%%%%%%%%%%%%%%%%%%%%%%%%%%%%%%%%%%%%%%%
% end function aWinPatMat=fNewMat(cRoom,aXYZPla)
%%%%%%%%%%%%%%%%%%%%%%%%%%%%%%%%%%%%%%%%%%%%%%%%%%%%%%%%%%%%%%%%%%%%%%%%%%%%
%%%%%%%%%%%%%%%%%%%%%%%%%%%%%%%%%%%%%%%%%%%%%%%%%%%%%%%%%%%%%%%%%%%%%%%%%%%%
function aNewPhot=fHit(aPhot,aXYZPla)
% fHit records intersection of particle and surface
%%%%%%%%%%%%%%%%%%%%%%%%%%%%%%%%%%%%%%%%%%%%%%%%%%%%%%%%%%%%%%%%%%%%%%%%%%%%
% Author: RCC based on Peter Tregenza, June 1998
% Begin: 19.10.99
% called by fDC
% Input: aPhot=[c1 c2 c3 nX nY nZ nStartPlan nWeight]
%              aXYZPla=[nX nY nZ nPla]
% Output: aNewPhot=[c1 c2 c3 nX nY nZ nPlane nWeight]
%
% Obs: this routine is kept just for compatibility with old versions and to allow
%       new implementation in the future.
%%%%%%%%%%
% alt
% 15.12.1999
% 07.09.2000 adapt new version
%%%%%%%%%%
aNewPhot=aPhot;
aNewPhot(4:6)=aXYZPla(1:3); % new xyz
aNewPhot(7)=aXYZPla(4); % new plane number

%%%%%%%%%%%%%%%%%%%%%%%%%%%%%%%%%%%%%%%%%%%%%%%%%%%%%%%%%%%%%%%%%%%%%%%%%%%%
% end function aNewPhot=fHit(aPhot,aXYZPla)
%%%%%%%%%%%%%%%%%%%%%%%%%%%%%%%%%%%%%%%%%%%%%%%%%%%%%%%%%%%%%%%%%%%%%%%%%%%%



%%%%%%%%%%%%%%%%%%%%%%%%%%%%%%%%%%%%%%%%%%%%%%%%%%%%%%%%%%%%%%%%%%%%%%%%%%%%
function aNewPhot2=fBounce(cRoom,aNewPhot,aWinPatMat)
%%%%%%%%%%%%%%%%%%%%%%%%%%%%%%%%%%%%%%%%%%%%%%%%%%%%%%%%%%%%%%%%%%%%%%%%%%%%
% fBounce gives new direction and weight of ray after transmission
% Author: RCC Based on Peter Tregenza, June 1998
%       Algorithms from 'Daylighting algorithms' ETSU S 1350 1993
% Begin: 19.10.99
% called by: fDC
% call: fGlazing fDifEmit fSpecRef fDifTran
% Input: cRoom={aRoomMat aPlane aWindow aPatch}
%              aRoomMat=[rhod rhos+rhod taud+rhos+rhod taus+taud+rhos+rhod]
%       aNewPhot=[nCos1 nCos2 nCos3 nX nY nZ nStartPlan nWeight]
%       aWinPatMat=[nWin nPat nType] where nType=-mat,0 or glazing type
%
% Output: aNewPhot2=[nCos1 nCos2 nCos3 nX nY nZ nPlane nWeight]
%       obs: aNewPhot2 == aPhot In pDC
%
```

```
%%%%%%
% alt:
% 15.12.1999 when ray is out of window it will continue and will be tested on fNewSurf
% 07.09.2000 adapt new version

%% just to debug
global lDebug
if lDebug
  global iPart aDebugBounce aDebugBounce2
  if exist('aDebugBounce')==0;aDebugBounce=[];end
end
%%%%%%
aNewPhot2(4:7)=aNewPhot(4:7); % update location
nPl=aNewPhot(7); % plane number
nWeight=aNewPhot(8);

%DOES RAY TERMINATE?
nThreshold=0.001;
if nWeight<nThreshold
  if rand<0.5       % 0.5 probability of stopping if below threshold
    aNewPhot2=zeros(1,8);return;
  else;nWeight=nWeight*2;end; % compensate for stopped rays
end
nType=aWinPatMat(3);
if nType==0       % test for clear opening
  aNewPhot2(1:3)=aNewPhot(1:3);
  aNewPhot2(8)=nWeight;% direction & weight unchanged
  aNewCos=aNewPhot(1:3);
  %   aDebugBounce=[aDebugBounce; iPart 0];
else % interaction with material
  aCosRay=aNewPhot(1:3);          % cosines of ray
  aCosNor=cRoom{2}(nPl,1:3); % cosines of surface normal
  nCosT=aCosRay*aCosNor'; % angle of incidence
  if nType>0       %  test for glazing
    aGlazProp=fGlazing(nCosT,nType); % glazing transmittance
    nNotAbs=sum(aGlazProp); % fraction not absorbed
    if nNotAbs<eps          % total absorption
      aNewPhot2=zeros(1,8);
      return
    end
    nW=aGlazProp(2)/nNotAbs;
    aCumRT=[0 nW nW 1];           % cumulative reflect & trans of glazing (
  else % use material code(=-nType)
    nNotAbs=cRoom{1}(-nType,4);
    if nNotAbs<eps          % black material
      aNewPhot2=zeros(1,8);
      return
    end
    aCumRT=cRoom{1}(-nType,1:4)./nNotAbs; % scaled cumulative reflect & trans of material
  end
  aNewPhot2(8)=nWeight.*nNotAbs; % new weight
  %Select Reflection or transmission
  nRand=rand; % random number
  if nRand<aCumRT(1)     % diffuse reflection
    aNewCos=fDifEmit(nPl);
    if lDebug; aDebugBounce=[aDebugBounce; iPart 1]; end
  elseif nRand<aCumRT(2)          % specular reflection
    aNewCos=fSpecRef(aCosRay,nPl);
    if lDebug; aDebugBounce=[aDebugBounce; iPart 2]; end
  elseif nRand<aCumRT(3)          % diffuse transmittance
```

```
   aNewCos=fDifTran(nPl);
   if lDebug; aDebugBounce=[aDebugBounce; iPart 3]; end
  else % regular transmittance
   aNewCos=aCosRay;
   if lDebug; aDebugBounce=[aDebugBounce; iPart 4]; end
  end
end
aNewPhot2(1:3)=aNewCos; % new direction cosines
%% just to debug - save all variables into bNewSurf
if lDebug
 if exist('aDebugBounce2')==0; aDebugBounce2=[]; end
 [nDebSize nPar]=size(aDebugBounce2);
 aDebugBounce2=[aDebugBounce2; iPart aNewPhot2];
 save bDebugBounce aDebugBounce aDebugBounce2
end
%%
%%%%%%%%%%%%%%%%%%%%%%%%%%%%%%%%%%%%%%%%%%%%%%%%%%%%%
% end function aNewPhot2=fBounce(cRoom,aNewPhot,aWinPatMat)
%%%%%%%%%%%%%%%%%%%%%%%%%%%%%%%%%%%%%%%%%%%%%%%%%%%%%


%%%%%%%%%%%%%%%%%%%%%%%%%%%%%%%%%%%%%%%%%%%%%%%%%%%%%
function fRaySky(aNewCos,nWeight,nAzX,nC,nSkyX)
%%%%%%%%%%%%%%%%%%%%%%%%%%%%%%%%%%%%%%%%%%%%%%%%%%%%%
% fRaySky gives the sky zone 'reached' by the ray and its weight
% Author: RCC (based in rayout (by P Tregenza))
% Begin: 19.10.99
% called by fDC
% call fRound
% Input: aNewCos=[c1,c2,c3],
%       nWeight % weight of particle
%       nAzX : Azimuth from N to Axis X
%       nC:component (vide
%       nSkyX: if 1:process just aSkyWei
%             2:process (aSkyWei+aNRaySky+aSkyWei)
%
%       [global]: aSkyZ=[1:9 nGamma1 nGamma2 nAlpha1 nAlpha2]
%               nGamma1-2: elevation of sky patch limits
%               nAlpha1-2: azimuth of sky patch limits
%
% Output: [global]: aSkyWei(nSkyZ,:)=[nWeightC1 nWeightC2];
%

%%%%%%%%%%%%
% alt:
% 17.12.1999
% 02.01.2000
% 16.05.2000 nC renumbered
% 19.06.2000 saves number of rays that reach each sky patch
% 03.08.2000 besides aSkyZ of 145 sky patches, sky is divided into 90x360 patches.
% 23.08.2000 allows process or not aSkyWei, since it takes time and disk space
% 08.09.2000 renamed from fRayOut to fRaySky, since ware created fRayGrd and fRayExt
%           to lead with ray that bounces ground or a external surface before
%           enter the room
%%%%%%%%%%%%


%% just to debug -
global lDebug iPart aDebugRayOut %% to debug
%%%%%%%
```

```
global aSkyZ aSkyWei aNRaySky aSkyWei2

nSkyZ=0;
% angles of ray
nThetaRd=acos(aNewCos(3));
nTheta=nThetaRd*180/pi;
nGamma=90-nTheta;
nPhiRdS1=asin(aNewCos(2)/sin(nThetaRd));
if nPhiRdS1 >= 0
 nPhiRdS2=pi-nPhiRdS1; % (positive)
else
 nPhiRdS1=2*pi+nPhiRdS1; % (positive)
 nPhiRdS2=3*pi-nPhiRdS1; % (positive)
end
nPhiRdC1=acos(aNewCos(1)/sin(nThetaRd)); % (positive)
nPhiRdC2=2*pi-nPhiRdC1;              % (positive)

if fRound(abs(nPhiRdS1-nPhiRdC1),4)==0
 nPhi=nPhiRdS1*180/pi;
elseif fRound(abs(nPhiRdS1-nPhiRdC2),4)==0
 nPhi=nPhiRdS1*180/pi;
elseif fRound(abs(nPhiRdS2-nPhiRdC1),4)==0
 nPhi=nPhiRdS2*180/pi;
elseif fRound(abs(nPhiRdS2-nPhiRdC2),4)==0
 nPhi=nPhiRdS2*180/pi;
else
 disp('Matlab round error - var nPhi');
 return
end
nAlpha=nAzX-nPhi;
if nAlpha<0
 nAlpha=360+nAlpha;
end
nG=ceil(nGamma); % rounded gamma
nA=ceil(nAlpha); % rounded alpha
if nSkyX==2
 aSkyWei2(nG,nA,nC)=nWeight+aSkyWei2(nG,nA,nC);
end
for iZ=[1:145]
 if nGamma+eps*100>=aSkyZ(iZ,10) & nGamma-eps*100<=aSkyZ(iZ,11) & ...
    ((nAlpha+eps*100>=aSkyZ(iZ,12) & nAlpha-eps*100<=aSkyZ(iZ,13))|...
    (nAlpha+eps*100>=aSkyZ(iZ,14) & nAlpha-eps*100<=aSkyZ(iZ,15)))
  nSkyZ=iZ;
  break;
 end
end
if nSkyZ~=0
 aSkyWei(nSkyZ,nC)=nWeight+aSkyWei(nSkyZ,nC); %% new weight / nC
 if nSkyX==2
  aNRaySky(nSkyZ,nC)=1+aNRaySky(nSkyZ,nC); %% number of rays reaching nSkyZ / nC
 end
else
 errordlg('Ray could not reach sky (nSkyZ=0)','Run Error')
end
%%%%%%%%%%%%%%%%%%%%%%%%%%%%%%%%%%%%%%%%%%%%%%
% end function fRaySky
%%%%%%%%%%%%%%%%%%%%%%%%%%%%%%%%%%%%%%%%%%%%%%
```

```
%%%%%%%%%%%%%%%%%%%%%%%%%%%%%%%%%%%%%%%%%%%%%%%%
function fRayGrd(aXYZ,nWeight,nC)
%%%%%%%%%%%%%%%%%%%%%%%%%%%%%%%%%%%%%%%%%%%%%%%%
% fRayGrd gives the ground zone 'reached' by the ray and its weight
% Author: RCC (based in fRaySky)
% Begin: 08.09.2000
% called by fDC
% Input: aXYZ=[nX,nY,nZ], % point hit on Ground plane
%       nWeight % weight of particle
%       nC:component
%       [global]: aGrdZ=[nX1 nX2 nY1 nY2 nRef nLum]
%
% Output: [global]: aGrdWei(nGrdZ,:)=[nWeightC3 nWeightC6];
%

%%%%%%%%%%%%
% alt:
% 12.09.2000
%%%%%%%%%%%%

global aGrdZ aGrdWei
nGrdZ=0;
nLenZ=length(aGrdZ);

%%% ^ needs improvement ^ (speed)
for iZ=[1:nLenZ]
  if aXYZ(1)>=aGrdZ(iZ,1) & aXYZ(1)<=aGrdZ(iZ,2) & ...
     aXYZ(2)>=aGrdZ(iZ,3) & aXYZ(2)<=aGrdZ(iZ,4)
   nGrdZ=iZ;
   break;
  end
end
%%% ^ needs improvement ^

if nGrdZ~=0
  aGrdWei(nGrdZ,nC)=nWeight+aGrdWei(nGrdZ,nC); %% new weight / nC
% else % out of ground definition, weigth=0
end;
%%%%%%%%
% end function fRayGrd
%%%%%%%%


%%%%%%%%%%%%%%%%%%%%%%%%%%%%%%%%%%%%%%%%%%%%%%%%
function fRayExt(aXYZPla,nWeight,nC,sRoom)
%%%%%%%%%%%%%%%%%%%%%%%%%%%%%%%%%%%%%%%%%%%%%%%%
% fRayExt gives the External surface plane 'reached' by the ray and its weight
% Author: RCC (based in fRaySky)
% Begin: 08.09.2000
% called by fDC
% Input: aXYZ=[nX,nY,nZ, nPla], % point and plane
%       nWeight % weight of particle
%       nC:component
%       sRoom: room number
%       [global]: aGrdZ=[nX1 nX2 nY1 nY2 nRef nLum]
%
% Output: [global]: aGrdWei(nGrdZ,:)=[nWeightC4 nWeightC5];
%

%%%%%%%%%%%%
```

```
% alt:
% 20.09.2000
%%%%%%%%%%%%%

%%%%%%%
global aExtWei
sFile=['bPlExt' sRoom '.mat'];
if exist(sFile)==2
  load(sFile,'aPlExt'); %% get external planes
else;  errordlg([sFile ' not found']);  return; end
nPla=aXYZPla(4);
nLenExt=length(aPlExt); %% number of external planes
iExt=find(aPlExt==nPla);
if ~isempty(iExt)
  aExtWei(iExt,nC)=nWeight+aExtWei(iExt,nC); %% accum.
else
  errordlg('Ray could not reach External Surface','Run Error')
end
%%%%%%%%%%%%%%%%%%%%%%%%%%%%%%%%%%%%%%%%%%%%%%%%%%%%%%%%%%%%%%%%%%%%%%%%%%%%
% end function fRayExt
%%%%%%%%%%%%%%%%%%%%%%%%%%%%%%%%%%%%%%%%%%%%%%%%%%%%%%%%%%%%%%%%%%%%%%%%%%%%



%%%%%%%%%%%%%%%%%%%%%%%%%%%%%%%%%%%%%%%%%%%%%%%%%%%%%%%%%%%%%%%%%%%%%%%%%%%%
function nIllum=fIllumBasic(aSky,aAzX,aDay,aTime,aDC1)
%%%%%%%%%%%%%%%%%%%%%%%%%%%%%%%%%%%%%%%%%%%%%%%%%%%%%%%%%%%%%%%%%%%%%%%%%%%%
%% assess illuminance for error calculation (just the reflected component (excluding ground and obst)
%% based on fIllum
% 28.07.2002: return parameter: aIllum (to be used in fDC for assessing error in runtime)
%
global aSkyZ aGrdZ
%% coefficients for adjusting sky:
nCoefKit145s1= 0.99299; % coef. adjust based on sky 1 for sky subdivision 145(CIE)
nCoefKit145s5= 0.99455; % coef. adjust based on sky 5 for sky subdivision 145(CIE)
nCoefKit145= 0.99377; % average coef. adjust based on sky 1&5 for sky 145(CIE)
%%
if exist('aWhere')==0
  sFile='bCityParam.mat';
  if exist(sFile)==2;load(sFile);
  else errordlg([sFile ' not found']);set(nTFig,'String','');return;end; %% sCity
  aWhere=[sCity.nLat sCity.nLon sCity.nStanMeridian sCity.nSummerTime];
end

aPlGrd=13; % ground plane, internally defined
nLenSkyZ=length(aSkyZ);% number of sky zones
nLenGrdZ=length(aGrdZ);% number of ground zones
nTSky=length(aSky); % number of skies processed
nTAzX=length(aAzX); % number of Azimuth processed
[nPar nTDay]=size(aDay); % number of days of year processed
[nPar nTTime]=size(aTime); % number of times of day processed
nUnit=1;%%1= relative (E/Eh% =Daylight factor)/2= Absolute (lux)
if nUnit==1;nTComp=6;else nTComp=12;end;%% components processed
aIllum1=zeros(nTComp,nTSky,nTAzX,nTDay,nTTime); % %MC 145

aWhen=[aDay(:,1);aTime(:,1)]; % [yyyy mm dd hh mm ss]
aSunData=fSunData(aWhen,aWhere);
%Generate standard skies & find illuminances(E):
```

```
nAzX=aAzX(1);
nSky=aSky(1);
%sText=['Day ' fPut0(aDay(3,1),2) '/' fPut0(aDay(2,1),2)...
%    ' Time ' fPut0(aTime(1,1),2) ':' fPut0(aTime(2,1),2)  ...
%    ' Sky ' fPut0(nSky,2) '  Az ' num2str(nAzX) '°' ];
%set(nTFig,'String',{sTextBas;sText})

nSunZon145=fSunZone(aSunData,aSkyZ);%% Find solar zone sky 145:

aSkyLum=fKitLum(aSunData,nSky);%lum distribution of standard (cie sky)
if nSky==1
  aSkyLum=aSkyLum*nCoefKit145s1;      % adjust for geometrical approximation
elseif nSky==5
  aSkyLum=aSkyLum*nCoefKit145s5;      % adjust for geometrical approximation
else
  aSkyLum=aSkyLum*nCoefKit145;      % adjust for geometrical approximation
end

nIllumStanDif=sum(aSkyLum.*aSkyZ(:,3).*aSkyZ(:,9)); %Ehd (diffuse, sky)
%    aSkyLumN=aSkyLum./(nIllumStanDif*pi); %normalise luminances to Eh=1
aSkyLumN=aSkyLum./nIllumStanDif; %normalise luminances to Eh=1

%% Change Sun and Sky position in funciton of Azimuth nAzX - sky 145
aSkyLumN=fMovSky145(aSkyLumN,nAzX);
nSunZon145=fMovSun145(nSunZon145,nAzX);
%
nESky=fSkyLight(nUnit,nSky,aSunData(7)); %  horizontal illuminance Ehdif (diffuse)

% skylight components :
%%%% sky (for cie 145):
if ~isempty(aDC1)
  aIllum1(1)=0; %% direct component is assessed with no MC
  aIllum1(2)=sum(aSkyLumN.*aDC1(:,2).*aSkyZ(:,9))*nESky;
end
%%%% ground:
%for iGr=1:nLenGrdZ
%  aLGrd(iGr)=sum(aSkyLumN.*aDCGrdSky(iGr,:)'.*aSkyZ(:,9))*nESky*aGrdZ(iGr,6)/pi;
%end
%if ~isempty(aDC1)
%  %  aIllum1(6)=0; %% direct component is assessed with no MC
%  aIllum1(3)=sum(aDCGrd1(:,2).*aGrdZ(:,5).*aLGrd');
%end
%%%% ext. surf:
%if lExt
%  for iEx=1:nLenExt
%    aLExt(iEx)=sum(aSkyLumN.*aDCExtSky(iEx,:)'.*aSkyZ(:,9))*aExtM(iEx,1)*nESky/pi;
%  end
%  % sky 145
%  if ~isempty(aDC1)
%    %   aIllum1(5)=0;%% direct component is assessed with no MC
%    aIllum1(4)=sum(aDCExt1(:,2).*aExtA(:,1).*aLExt');
%  end
%end
nIllum=sum(aIllum1);
return
%%%%%%%%%%%%%%%%%%%%%%%%%%%%%%%%%%%%%%%%%%%%%%%%%%%%%%%%%%%%%%%%%%%%%%%%%%%%
%% end function aIllum=fIllumBasic(aSky,aAzX,aDay,aTime,aDC1,aDCGrd1,aDCGrdSky,cExt)
%%%%%%%%%%%%%%%%%%%%%%%%%%%%%%%%%%%%%%%%%%%%%%%%%%%%%%%%%%%%%%%%%%%%%%%%%%%%
```

F.2 Illuminance

```
%%%%%%%%%%%%%%%%%%%%%%%%%%%%%%%%%%%%%%%%
function fIllum(cDCFile,sGrdFile,aSky,aAzX,aDay,aTime)
%%%%%%%%%%%%%%%%%%%%%%%%%%%%%%%%%%%%%%%%
% fIllum function to calculate internal illuminance from standard skies
%   and daylight coefficients
% Author: Ricardo Cabus
% Begin 02.11.1999
% Input:
%   by parameter:
%      cDCFile{iR}={sFileDCDir,sFileDC,sFileDC2,sFileGr,sFileEx};
%        sFileDCDir[aDCDirSky, aDCDirGrd, aDCDirExt]
%        sFileDC: for sky 145
%           [aDC    % daylight coefficients (point-sky)
%            aDCGrd % daylight coefficients (point-ground)
%            aDCExt % daylight coefficients (point-external surfaces)
%            sRoom,nTimes,nPla,aPt]
%        sFileDC2: == sFileDC, but for sky 5221
%        sFileGr [aDCGrdSky % daylight coefficients (direct ground-sky)]
%        sFileEx [aDCExtSky % daylight coefficients (External Surface-sky)]]
%      sGrdFile  % bGrdZone*.mat
%      aSky      % Types of skies   [1:15 by kittler]
%      aDay      % Days of the year [yyyy;mm;dd]
%      aTime     % Times of the day [hh;mm;ss] (24h)
%      aAzX      % Azimuth for Sky North related to Axis X
%   by file:
%      bCityParam [parameters of location]
%      bSkyZone   [aSkyZ]     % sky zones
%      bGrdZone   [aGrdZ]     % ground zones
%      bGParam    [aPlGrd,aPlExt]   % ground plane,plane of external surfaces
%
% call: fSunData,fKitLum,fSkyLight,fSunlight
%
% Output: aIllum1
%          aIllum1(1:15,...)  => MC Sky 145
%          aIllum2(1:15,...)  => MC Sky 5221
%          aIllumDir(1:2,...) => Direct Component for Sky and Sun
%   Components for aIllum1 & aIllum2
%          ' 1 Sky - Direct Component '
%          ' 2 Sky - Internal Reflected '
%          ' 3 Sky - Internal Reflected by Ground '
%          ' 4 Sky - Internal Reflected by Obstruction '
%          ' 5 Sky - Obstruction Reflected (No Internal Reflection) '
%          ' 6 Sky - Ground Reflected (No Internal Reflection) '
%          ' 7 Sun - Direct Component '
%          ' 8 Sun - Internal Reflected '
%          ' 9 Sun - Internal Reflected by Ground '
%          '10 Sun - Internal Reflected by Obstruction '
%          '11 Sun - Obstruction Reflected (No Internal Reflection) '
%          '12 Sun - Ground Reflected (No Internal Reflection) '

%%%%%%
% alt:
% 01.01.2000
% 13.01.2000
% 13.05.2000
% 15.05.2000 new output and passing parameter to gDC. Allows multi-rooms, multipoints
%          no needs to use cell of array, aIllum is double array
```

```
% 16.05.2000 rename to gIllum (includ gui functions)
%           renumber components( first sky (2:5) after sun (6:9))
% 02.06.2000 allows input from fDCMean (n Points, 1 particle for point)
% 11.06.2000 script converted in funtion to get input arguments for .mat file
% 15.06.2000 adapted for passes parameters
% 16.06.2000 output aIllum
% 01.08.2000 copy ro gIllumMean to separate from gIllum. this gets results from
%            aDCMean (points ramdomly distributed)
% 21.08.2000 reprocessing sun-components
% 22.08.2000 includes nUnit to get DF(1) or lux(2)
% 24.08.2000 upgrade aIllum
% 11.09.2000 new version. treat ground and external surface independently
% 20.09.2000 adapt to gui version
% 28.09.2000 change equation (put rho in L, instead of E (the results are the same
%              but it follows the definition
%           change fSunLight for fEsn (horizontal for normal illuminance)
% 31.10.2000 fSunZone2 merged with fSunZone
%           correct calculation aIllum2
% 07.11.2000 adjust equations (pi)
% 12.11.2000 avoid input file for PlExt when not need
% 13.11.2000
% 18.02.2001 - include option of different ground zone file
%           - coef. to adjust sky subdivision to sky1 and sky5 are split and mean
%             is only used for others;
% 20.02.2001 allow calculating without DCDir files
%           also saves 'aSky','aDay','aTime'
% 08.04.2001: -exclude sun for sky 9
%            -Allows (correct) changing Azimuth for same DC calculation (before, DC was
%              linked to Azimuth)
% 02.05.2001: save Ehdif and Esn
% 20.05.2001: rename aAzS to aAzX (to not create confusion with solar azimuth (aAzS)
%           allow batch imput in a separated function
% 21.05.2001: allow batch for rooms (in fBatIllum
% 23.05.2001: redefine Components and matrices to save Illum
% 03.06.2001: adjust comments
%
% 05.06.2001: define aIllum, the merge between aIllum1 and aIllumDir as default
%              illuminance matrix
%
% 14.11.2001: fix error in array size (just to save memory, no error in results)
% 30.11.2001: no more summarise comp 13:15 to save disk memory
% 06.08.2002: allow Ehd being calculated by different equations
%             (introduces the IES proposal)
%
global sInputDir sOutputDir

nTypeEhd=1; % 1=IES ; 2='empirical, based on Treg measurements in Nottingham

nCoefKit145s1= 0.99299; % coef. adjust based on sky 1 for sky subdivision 145(CIE)
nCoefKit145s5= 0.99455; % coef. adjust based on sky 5 for sky subdivision 145(CIE)
nCoefKit145= 0.99377; % average coef. adjust based on sky 1&5 for sky 145(CIE)
nCoefKit5221s1= 0.99741;% coef. adjust based on sky 1 for sky subdivision 5221
nCoefKit5221s5= 0.99984;% coef. adjust based on sky 5 for sky subdivision 5221
nCoefKit5221= 0.99863;% average coef. adjust based on sky 1 & 5 for sky subdiv 5221

sTextBas='Running Illuminances';
nTFig=findobj(gcbf,'Tag','tText1');
set(nTFig,'String',sTextBas)
if nargin==0
  errordlg('Missing Parameters, Run Batch DC')
```

```
 set(nTFig,'String',")
 return
end

%% get files and parameters
[lError,aDCDirSky,aDC1,aDCGrd1,aDCExt1,aDC2,aDCGrd2,aDCExt2,aDCGrdSky,aDCExtSky,...
  sRoom,aPt,nPla,nGrdType,lExt,nTimes1,nTimes2,nTimes3]=fGetDCFiles(cDCFile);

if lError
 errordlg('Error getting files and parameters')
 set(nTFig,'String',")
 return
end

%%
sFile=['bRoom' sRoom '.mat'];
if exist(sFile)==2;load(sFile,'cRoom');
else errordlg([sFile ' not found']);set(nTFig,'String',");return;end; %% cRoom
sFile=['bSkyZone.mat'];
if exist(sFile)==2;load(sFile,'aSkyZ');
else errordlg([sFile ' not found']);set(nTFig,'String',");return;end; %% aSkyZ
sFile=['bSkyCIE5221.mat']; % sky subdivision for sun direct component
if exist(sFile)==2;load(sFile,'aSkyZ2');
else errordlg([sFile ' not found']);set(nTFig,'String',");return;end; %% aSkyZ2
%% ground file (aGrdZ)
if exist(sGrdFile)==2;load(sGrdFile,'aGrdZ');
else errordlg([sGrdFile ' not found']);set(nTFig,'String',");return;end; %% aGrdZ

sFile='bCityParam.mat';
if exist(sFile)==2;load(sFile);
else errordlg([sFile ' not found']);set(nTFig,'String',");return;end; %% sCity
if lExt
 nLenExt=length(aPlExt);% number of external planes
 aMat=cRoom{1}; % material characteristics (ref & transm)
 aPlane=cRoom{2}; % all planes
 aExtA=aPlane(aPlExt,14);% area of external planes
 aExtM=aMat(aPlExt,1);%reflectance of external planes
end
aWhere=[sCity.nLat sCity.nLon sCity.nStanMeridian sCity.nSummerTime];
aPlGrd=13; % ground plane, internally defined
nLenSkyZ=length(aSkyZ);% number of sky zones
nLenGrdZ=length(aGrdZ);% number of ground zones
nTSky=length(aSky); % number of skies processed
aSkyWithSun=[7:8 10:15]; %Sky types Associated With Sun
nTAzX=length(aAzX); % number of Azimuth processed
[nPar nTDay]=size(aDay); % number of days of year processed
[nPar nTTime]=size(aTime); % number of times of day processed
nUnit=2;%%1= relative (E/Eh% =Daylight factor)/2= Absolute (lux)
if nUnit==1;nTComp=6;else nTComp=12;end;%% components processed
nTCompDir=2; %direct components - no mc
aIllum1=zeros(nTComp,nTSky,nTAzX,nTDay,nTTime); % %MC 145
aIllum2=zeros(nTComp,nTSky,nTAzX,nTDay,nTTime); % MC 5221
aIllumDir=zeros(nTCompDir,nTSky,nTAzX,nTDay,nTTime); % Direct component
aEhd=zeros(nTSky,nTDay,nTTime); % external diffuse horizontal illuminance (no obstruction)
aEsn=zeros(nTSky,nTDay,nTTime); % normal solar illuminance (no obstruction)

% loop for 'when'
for iDay=[1:nTDay];for iTime=[1:nTTime]
 aWhen=[aDay(:,iDay);aTime(:,iTime)]; % [yyyy mm dd hh mm ss]
```

```
aSunData=fSunData(aWhen,aWhere);
%Generate standard skies & find illuminances(E):
for iSky=[1:nTSky]; for iAzX=[1:nTAzX]
 nAzX=aAzX(iAzX);
 nSky=aSky(iSky);
 sText=['Day ' fPut0(aDay(3,iDay),2) '/' fPut0(aDay(2,iDay),2)...
    '  Time ' fPut0(aTime(1,iTime),2) ':' fPut0(aTime(2,iTime),2)  ...
    '  Sky ' fPut0(nSky,2) '  Az ' num2str(nAzX) '°' ];
 set(nTFig,'String',{sTextBas;sText})

 nSunZon145=fSunZone(aSunData,aSkyZ);%% Find solar zone sky 145:
 nSunZon5221=fSunZone(aSunData,aSkyZ2);%% Find solar Zone sky 5221

aSkyLum=fKitLum(aSunData,nSky);%lum distribution of standard (cie sky)
if nSky==1
 aSkyLum=aSkyLum*nCoefKit145s1;     % adjust for geometrical approximation
elseif nSky==5
 aSkyLum=aSkyLum*nCoefKit145s5;     % adjust for geometrical approximation
else
 aSkyLum=aSkyLum*nCoefKit145;     % adjust for geometrical approximation
end

nIllumStanDif=sum(aSkyLum.*aSkyZ(:,3).*aSkyZ(:,9)); %Ehd (diffuse, sky)
aSkyLumN=aSkyLum./nIllumStanDif; %normalise luminances to Eh=1

%% Change Sun and Sky position in funciton of Azimuth nAzX - sky 145
aSkyLumN=fMovSky145(aSkyLumN,nAzX);
nSunZon145=fMovSun145(nSunZon145,nAzX);
%
aSkyLum5221=fKitLumSky5221(aSunData,nSky);%lum distrib (sky5221)
if nSky==1
 aSkyLum5221=aSkyLum5221*nCoefKit5221s1;     % adjust for geometrical approximation
elseif nSky==5
 aSkyLum5221=aSkyLum5221*nCoefKit5221s5;     % adjust for geometrical approximation
else
 aSkyLum5221=aSkyLum5221*nCoefKit5221;     % adjust for geometrical approximation
end
nIllumStanSol=sum(aSkyLum5221.*aSkyZ2(:,3).*aSkyZ2(:,9)); %Ehs (solar, direct)  /

aSkyLumN5221=aSkyLum5221./nIllumStanSol; %normalise luminances to Eh=1 / direct
%% Change Sun and Sky position in funciton of Azimuth nAzX - sky 5221
aSkyLumN5221=fMovSky5221(aSkyLumN5221,nAzX);%
nSunZon5221=fMovSun5221(nSunZon5221,nAzX);
%
if nTypeEhd==1
 nESky=fSkyLightIES(nUnit,nSky,aSunData(7)); %  Ehdif (IES)
else
 nESky=fSkyLight(nUnit,nSky,aSunData(7)); %  Ehdif (Empirical)
end
aEhd(iSky,iDay,iTime)=nESky;

% skylight components :
%%%% sky (for cie 145):
if ~isempty(aDC1)
 aIllum1(1,iSky,iAzX,iDay,iTime)=sum(aSkyLumN.*aDC1(:,1).*aSkyZ(:,9))*nESky;
 aIllum1(2,iSky,iAzX,iDay,iTime)=sum(aSkyLumN.*aDC1(:,2).*aSkyZ(:,9))*nESky;
end
%%%% sky (for s5221):
if ~isempty(aDC2)
 aIllum2(1,iSky,iAzX,iDay,iTime)=sum(aSkyLumN5221.*aDC2(:,1).*aSkyZ2(:,9))*nESky;
```

```
 aIllum2(2,iSky,iAzX,iDay,iTime)=sum(aSkyLumN5221.*aDC2(:,2).*aSkyZ2(:,9))*nESky;
end
%  sky (direct by sky2, no monte carlo) (sky 5221)
if ~isempty(aDCDirSky)
 aIllumDir(1,iSky,iAzX,iDay,iTime)=...
  sum(aSkyLumN5221.*aDCDirSky(:,1).*aSkyZ2(:,9))*nESky;
end
%%%% ground:
%% obs: there is no calculation for aDCGrdSky for sky 5221, then sky 145 is used
for iGr=1:nLenGrdZ
 aLGrd(iGr)=sum(aSkyLumN.*aDCGrdSky(iGr,:)'.*aSkyZ(:,9))*nESky*aGrdZ(iGr,6)/pi;
end
% sky 145
if ~isempty(aDC1)
 aIllum1(6,iSky,iAzX,iDay,iTime)=sum(aDCGrd1(:,1).*aGrdZ(:,5).*aLGrd');
 aIllum1(3,iSky,iAzX,iDay,iTime)=sum(aDCGrd1(:,2).*aGrdZ(:,5).*aLGrd');
end
% sky 5221
if ~isempty(aDC2)
 aIllum2(6,iSky,iAzX,iDay,iTime)=sum(aDCGrd2(:,1).*aGrdZ(:,5).*aLGrd');
 aIllum2(3,iSky,iAzX,iDay,iTime)=sum(aDCGrd2(:,2).*aGrdZ(:,5).*aLGrd');
end

%  ground (direct, no monte carlo ) (sky 145)
%aIllumDir(?,iSky,iAzX,iDay,iTime)=sum(aDCDirGrd(:,1).*aGrdZ(:,5).*aLGrd');

%%%% ext. surf:
%% obs: there is no calculation for aDCExtSky for sky 5221, then sky 145 is used
if lExt
 for iEx=1:nLenExt
  aLExt(iEx)=sum(aSkyLumN.*aDCExtSky(iEx,:)'.*aSkyZ(:,9))*aExtM(iEx,1)*nESky/pi;
 end
 % sky 145
 if ~isempty(aDC1)
  aIllum1(5,iSky,iAzX,iDay,iTime)=sum(aDCExt1(:,1).*aExtA(:,1).*aLExt');
  aIllum1(4,iSky,iAzX,iDay,iTime)=sum(aDCExt1(:,2).*aExtA(:,1).*aLExt');
 end
 % sky 5221
 if ~isempty(aDC2)
  aIllum2(5,iSky,iAzX,iDay,iTime)=sum(aDCExt2(:,1).*aExtA(:,1).*aLExt');
  aIllum2(4,iSky,iAzX,iDay,iTime)=sum(aDCExt2(:,2).*aExtA(:,1).*aLExt');
 end
 %  ext surf (direct, no monte carlo ) (sky 145)
 %aIllumDir(?,iSky,iAzX,iDay,iTime)=sum(aDCDirExt(:,1).*aExtA(:,1).*aLExt');
end
% sunlight components :
if ismember(nSky,aSkyWithSun) & nUnit~=1
 nESun=fEsn(aSunData,nSky); % solar normal illuminance
 aEsn(iSky,iDay,iTime)=nESun; %save in array
%%%% sky 145
if ~isempty(aDC1)
 aIllum1(7,iSky,iAzX,iDay,iTime)=aDC1(nSunZon145,1)*nESun;
 aIllum1(8,iSky,iAzX,iDay,iTime)=aDC1(nSunZon145,2)*nESun;
end
%%%% sky 5221
if ~isempty(aDC2)
 aIllum2(7,iSky,iAzX,iDay,iTime)=aDC2(nSunZon5221,1)*nESun;
 aIllum2(8,iSky,iAzX,iDay,iTime)=aDC2(nSunZon5221,2)*nESun;
end
%  sky (direct, no monte carlo) (sky5221)
```

```
if ~isempty(aDCDirSky)
 aIllumDir(2,iSky,iAzX,iDay,iTime)=aDCDirSky(nSunZon5221,1).*nESun;
end
%%%% ground:
%% obs: there is no calculation for aDCGrdSky for sky 5221, then sky 145 is used
aLGrdSun=aDCGrdSky(:,nSunZon145).*aGrdZ(:,6)*nESun/pi;
%%%% sky 145
if ~isempty(aDC1)
 aIllum1(12,iSky,iAzX,iDay,iTime)=sum(aDCGrd1(:,1).*aGrdZ(:,5).*aLGrdSun);
 aIllum1(9,iSky,iAzX,iDay,iTime)=sum(aDCGrd1(:,2).*aGrdZ(:,5).*aLGrdSun);
end
%%%% sky 5221
if ~isempty(aDC2)
 aIllum2(12,iSky,iAzX,iDay,iTime)=sum(aDCGrd2(:,1).*aGrdZ(:,5).*aLGrdSun);
 aIllum2(9,iSky,iAzX,iDay,iTime)=sum(aDCGrd2(:,2).*aGrdZ(:,5).*aLGrdSun);
end
%  (direct, no monte carlo) (sky145)
%   aIllumDir(?,iSky,iAzX,iDay,iTime)=sum(aDCDirGrd(:,1).*aGrdZ(:,5).*aLGrdSun);

%%%% ext. surf:
%% obs: there is no calculation for aDCExtSky for sky 5221, then sky 145 is used
if lExt
 aLExtSun=aDCExtSky(:,nSunZon145).*aExtM(:,1)*nESun/pi;
 %%%% sky 145
 if ~isempty(aDC1)
  aIllum1(11,iSky,iAzX,iDay,iTime)=sum(aDCExt1(:,1).*aExtA(:,1).*aLExtSun);
  aIllum1(10,iSky,iAzX,iDay,iTime)=sum(aDCExt1(:,2).*aExtA(:,1).*aLExtSun);
 end
 %%%% sky 5221
 if ~isempty(aDC2)
  aIllum2(11,iSky,iAzX,iDay,iTime)=sum(aDCExt2(:,1).*aExtA(:,1).*aLExtSun);
  aIllum2(10,iSky,iAzX,iDay,iTime)=sum(aDCExt2(:,2).*aExtA(:,1).*aLExtSun);
 end
 %  (direct, no monte carlo) (sky145)
%   aIllumDir(?,iSky,iAzX,iDay,iTime)=sum(aDCDirExt(:,1).*aExtA(:,1).*aLExtSun);
  end
 end
 end; end; %iSky iAzX
end; end; %iDay iTime

% create a summarised matrix 'alllum, with direct components from aIllumDir and
% others from aIllum1 (until decide about which sky division to be used)

aIllum=aIllum1;
aIllum(1,:,:,:,:)=aIllumDir(1,:,:,:,:); % direct sky comp
aIllum(7,:,:,:,:)=aIllumDir(2,:,:,:,:); % direct Sun component


sFile='bIllum';
sFile=[sFile '-r' sRoom]; % room number
sFile=[sFile '-g' num2str(nGrdType)]; % ground type
if isempty(aPt)
 sFile=[sFile '-pl' num2str(nPla) '-'] ;
else
 sFile=[sFile '-pt'];
 for iPt=1:3
  sFile=[sFile fDec2Str(aPt(iPt),2) '-'];
 end
end
sFile=[sFile 's']; % sky
```

```
for iSky=[1:nTSky]
  sFile=[sFile num2str(aSky(iSky)) '-'];
end
sFile=[sFile 'a']; % azimuth
for iAzX=[1:nTAzX]
  sFile=[sFile num2str(aAzX(iAzX)) '-'];
end
sExt='v01';
i=1;
cd(sOutputDir)
while exist([sFile sExt '.mat'])==2 %% avoid overwrite sFile
  i=i+1;  sExt=['v' fPut0(i,2)];
end
sFile=[sFile sExt '.mat'];


save(sFile,'aIllum','aIllum1','aIllum2','aIllumDir','aDCDirSky','aDC1','aDCGrd1',...
  'aDCExt1','aDC2','aDCGrd2','aDCExt2','aDCGrdSky','aDCExtSky','sRoom','nPla','aPt',...
  'aSky','aDay','aTime','aAzX','aEhd','aEsn','nTimes1','nTimes2','nTimes3');

cd(sInputDir)
sText=['Illuminances stored in file ' sFile];
set(nTFig,'String',{sText})
if nargin==0
  waitforbuttonpress
end
set(nTFig,'String','')
return
%%%%%%%%%%%%%%%%%%%%%%%%%%%%%%%%%%%%%%%%%%%%%%%%%%%%%%%%%%%%%%%%
%% end function aIllum1=fIllum(cDCFile,aSky,aDay,aTime)
%%%%%%%%%%%%%%%%%%%%%%%%%%%%%%%%%%%%%%%%%%%%%%%%%%%%%%%%%%%%%%%%
```

Appendix G - Validation graphs

G.1 Comparing illuminance from BRE-IDMP dataset with predicted by TropLux for 15 CIE standard skies

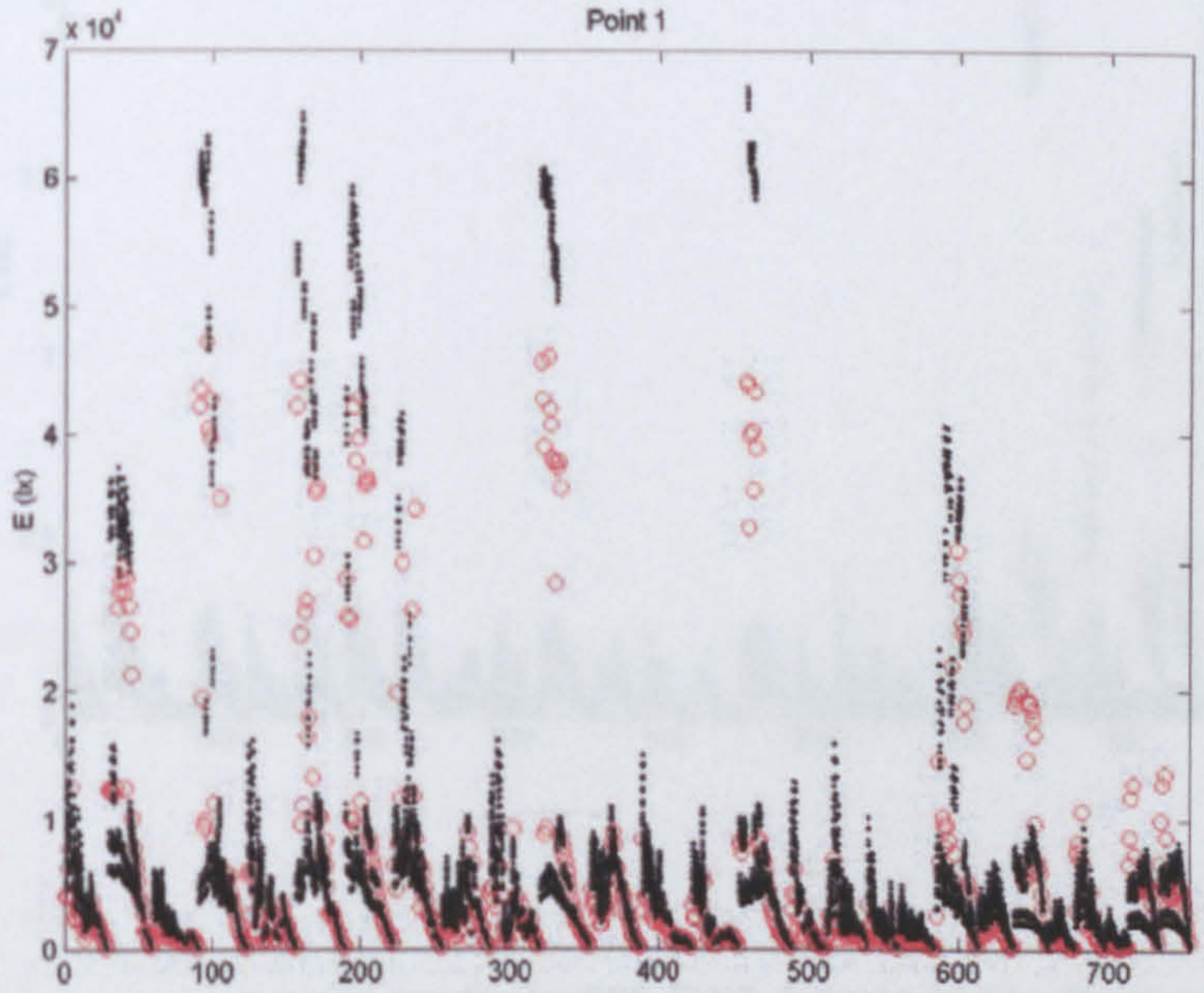

Figure G-1 - Comparing measured results by BRE-IDMP dataset and by TropLux with 15 CIE standard skies (Point 1)

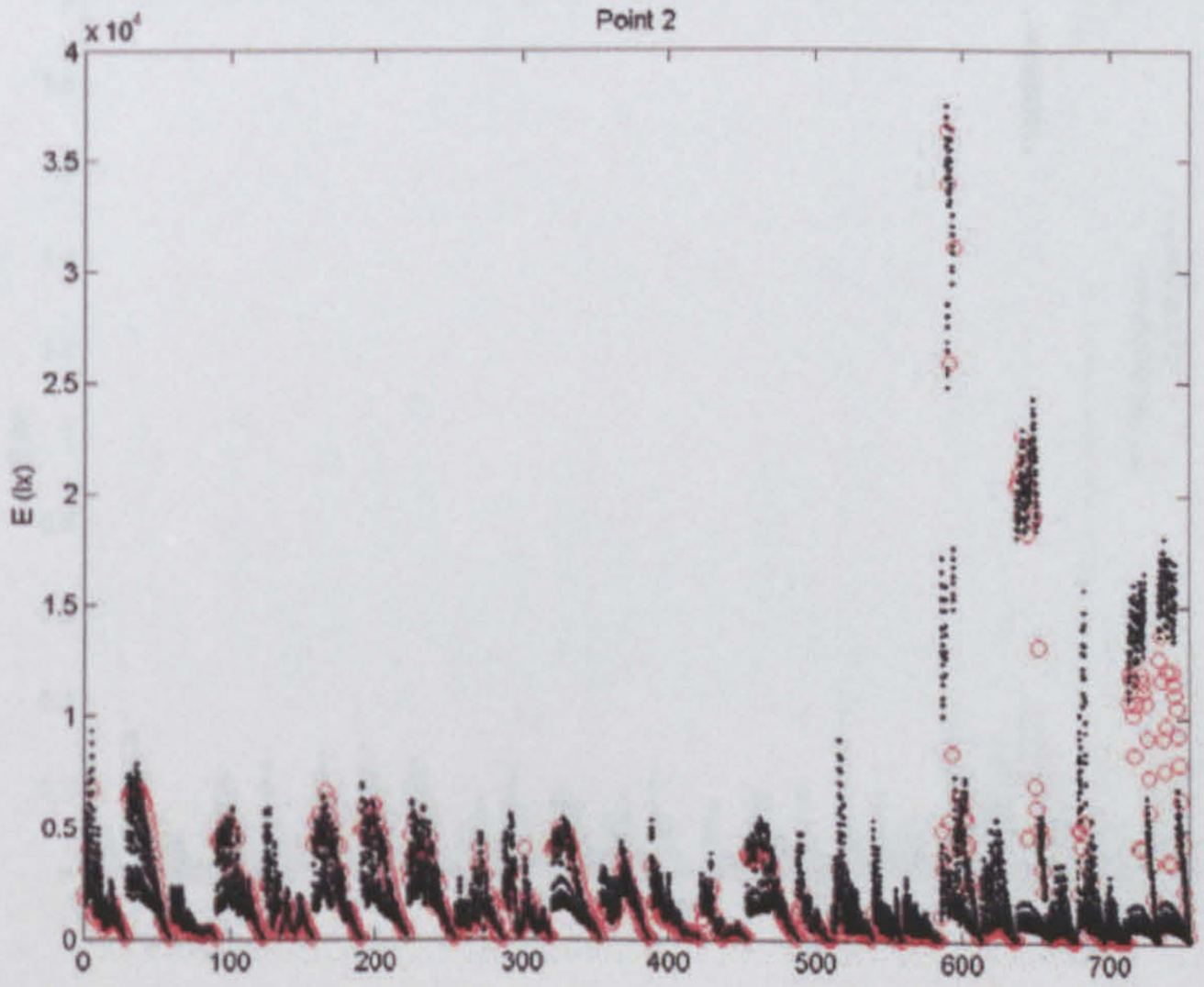

Figure G-2 - Comparing measured results by BRE-IDMP dataset and by TropLux with 15 CIE standard skies (Point 2)

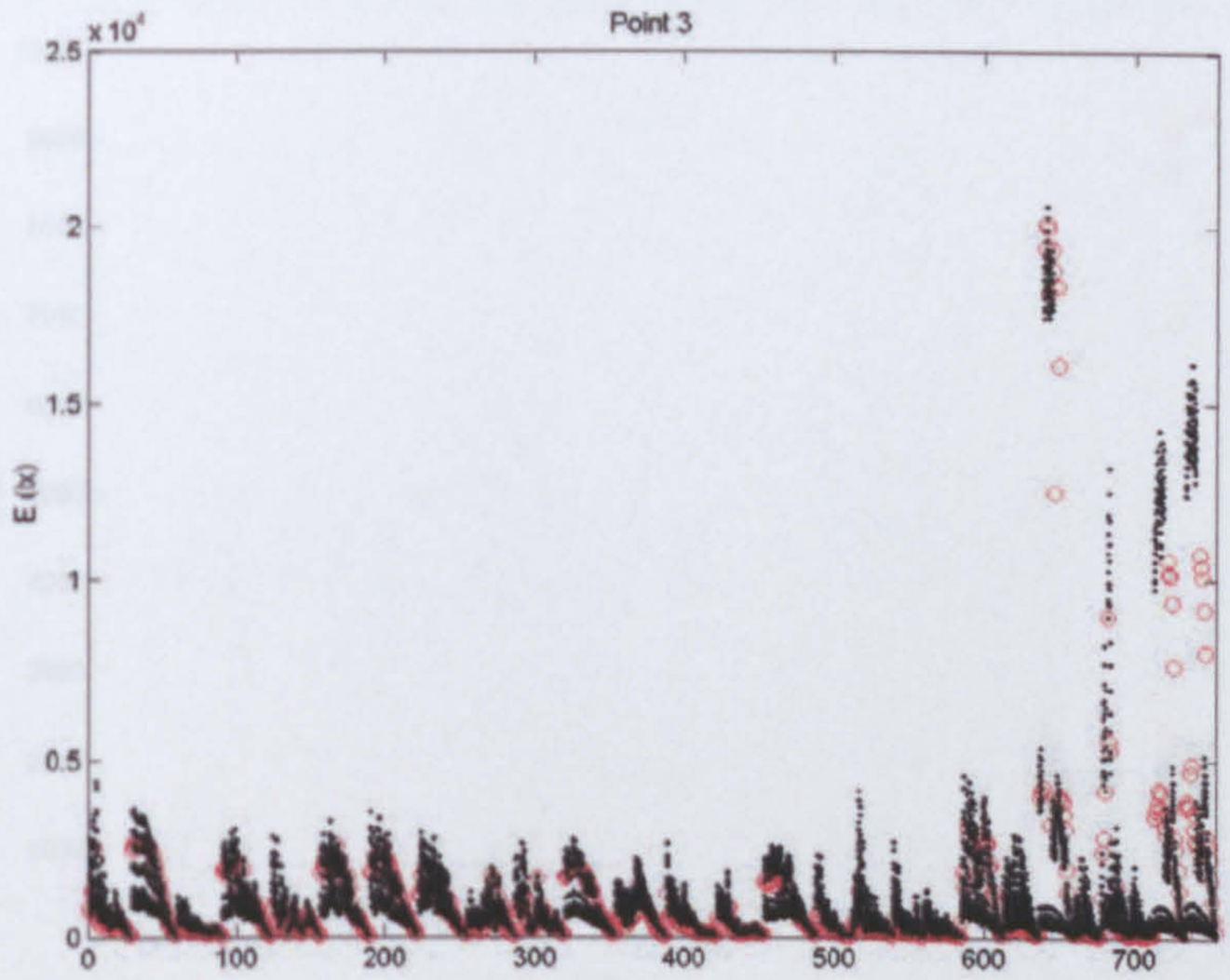

Figure G-3 - Comparing measured results by BRE-IDMP dataset and by TropLux with 15 CIE standard skies (Point 3)

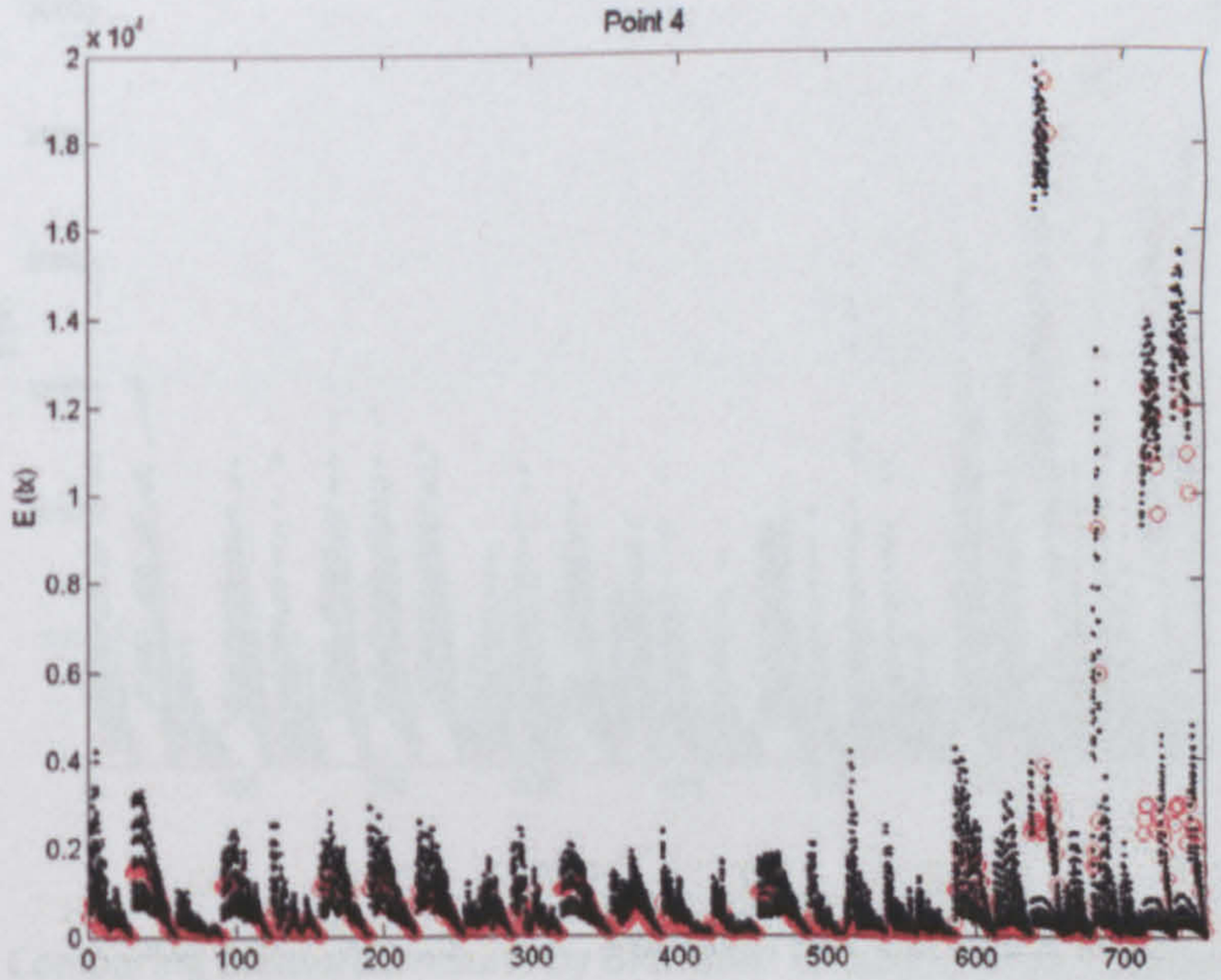

Figure G-4 - Comparing measured results by BRE-IDMP dataset and by TropLux with 15 CIE standard skies (Point 4)

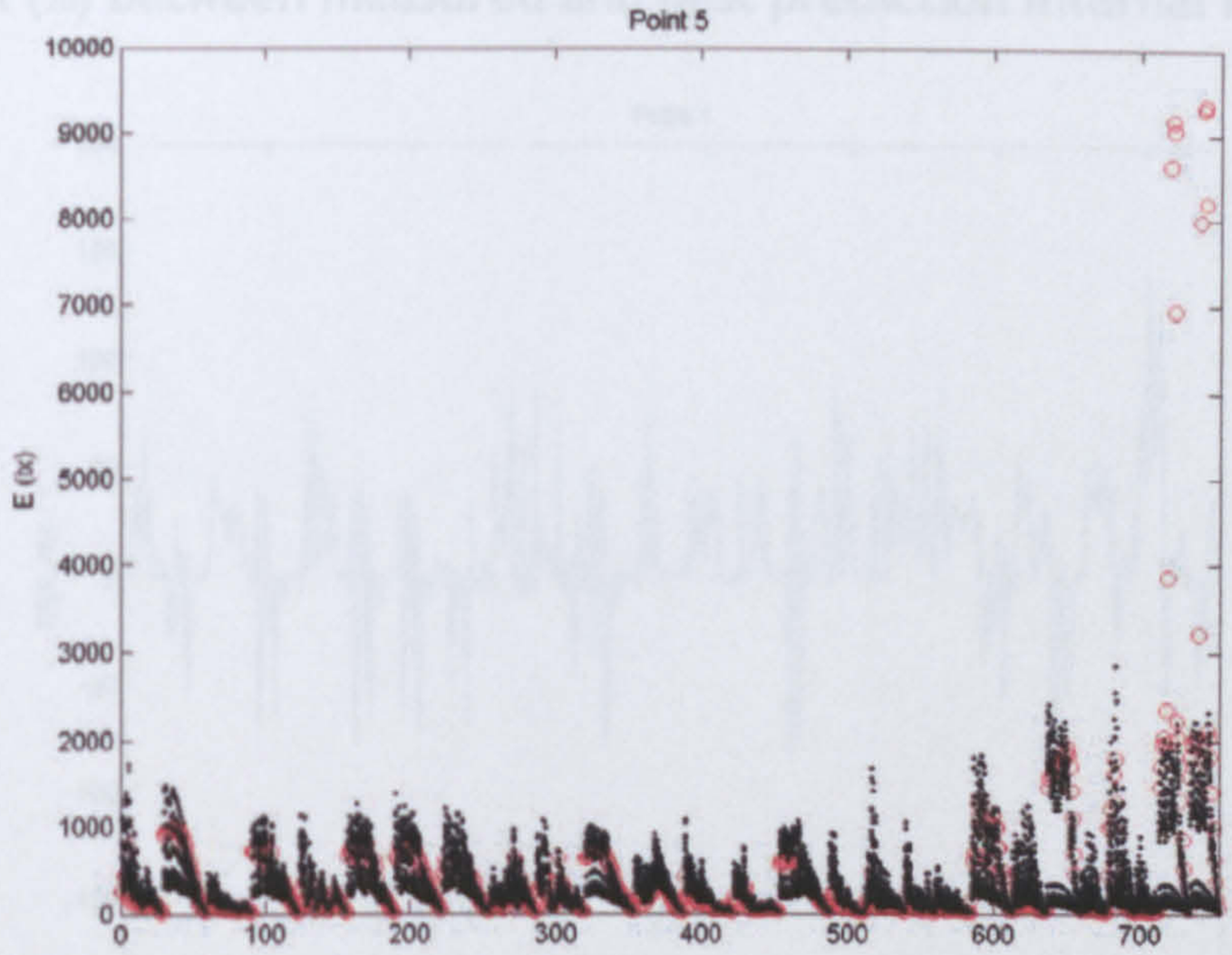

Figure G-5 - Comparing measured results by BRE-IDMP dataset and by TropLux with 15 CIE standard skies (Point 5)

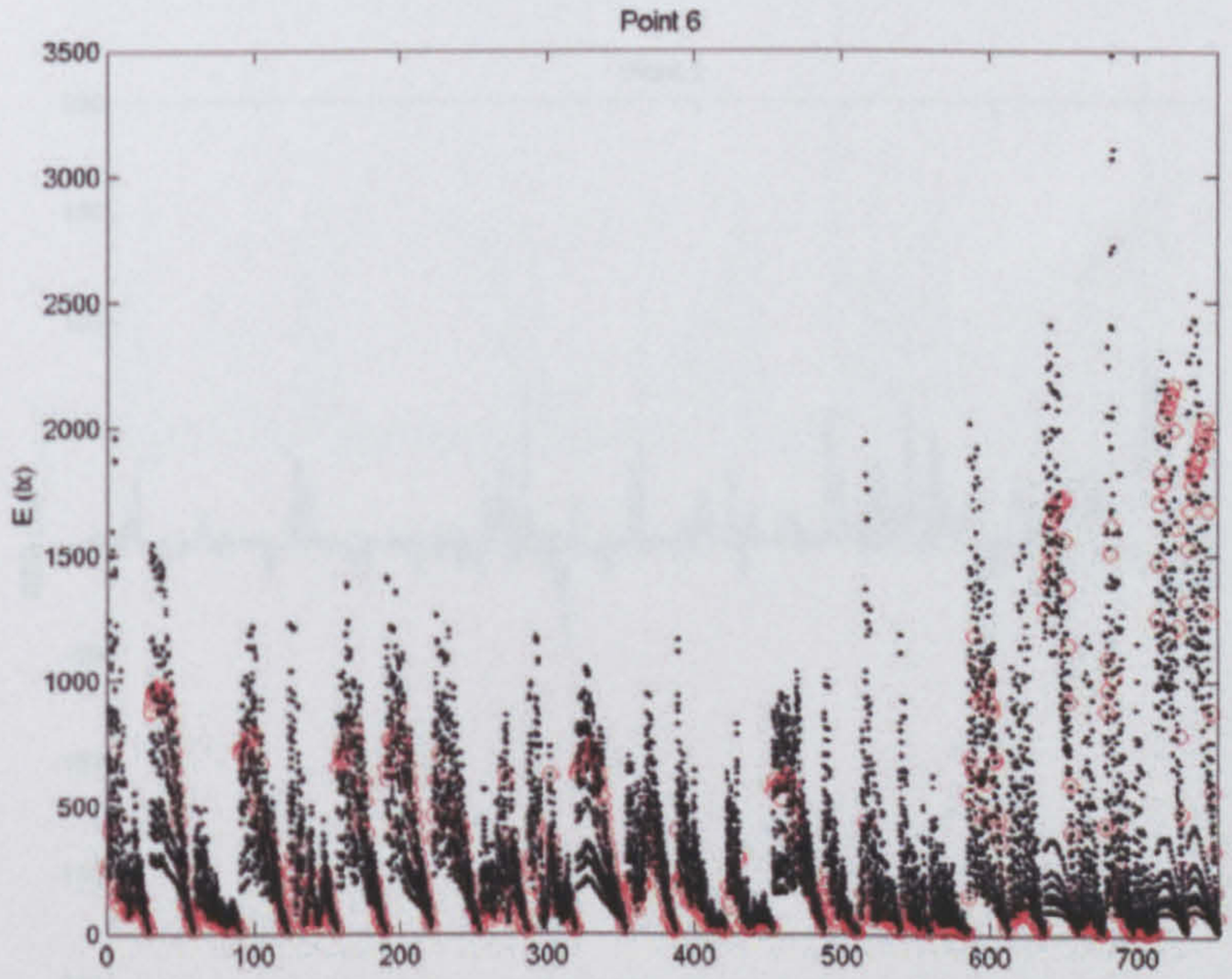

Figure G-6 - Comparing measured results by BRE-IDMP dataset and by TropLux with 15 CIE standard skies (Point 6)

G.2 RER (%) between measured and best prediction internal illuminance

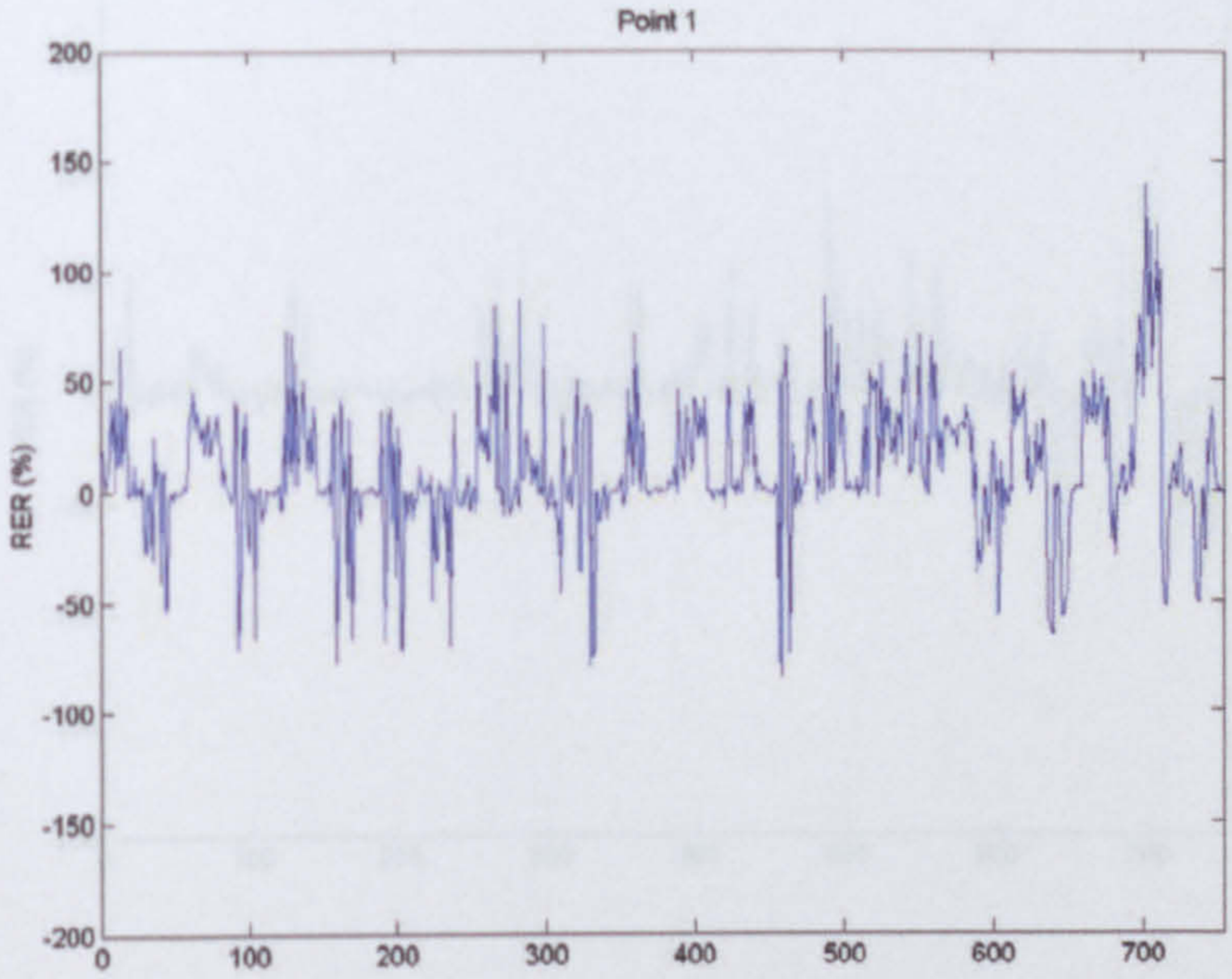

Figure G-7 - RER (%) between measured and best prediction internal illuminance (Point 1)

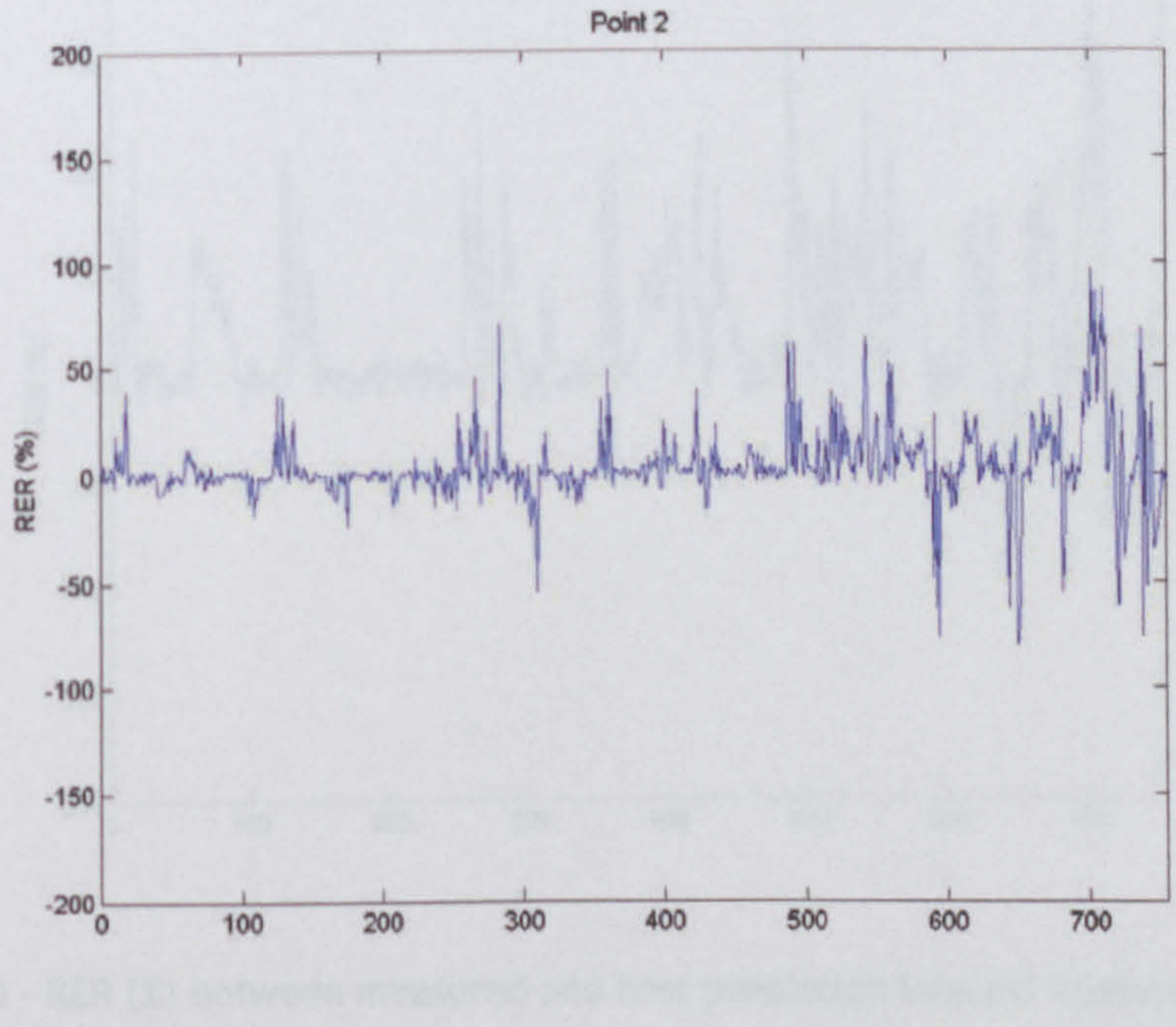

Figure G-8 - RER (%) between measured and best prediction internal illuminance (Point 2)

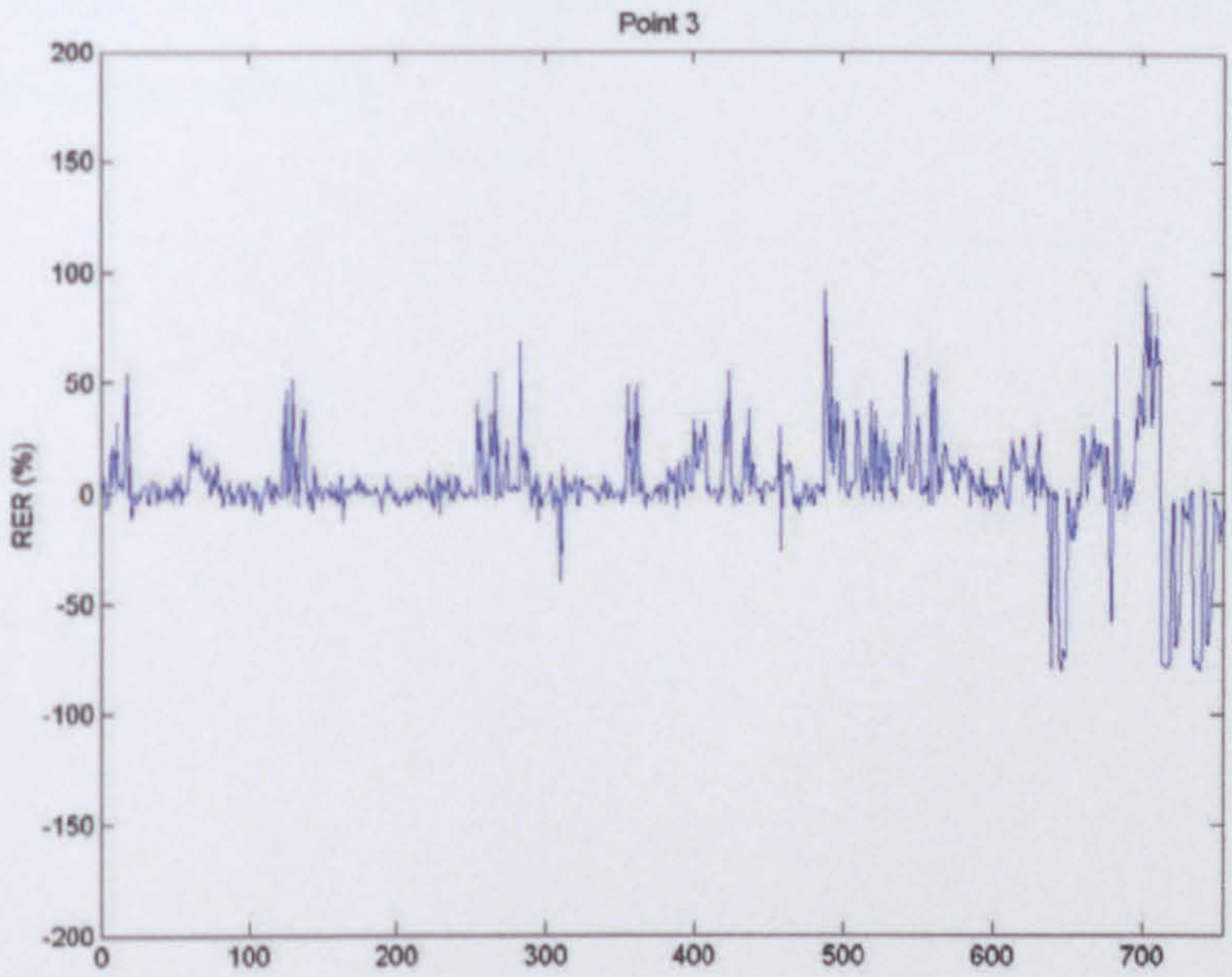

Figure G-9 - RER (%) between measured and best prediction internal illuminance (Point 3)

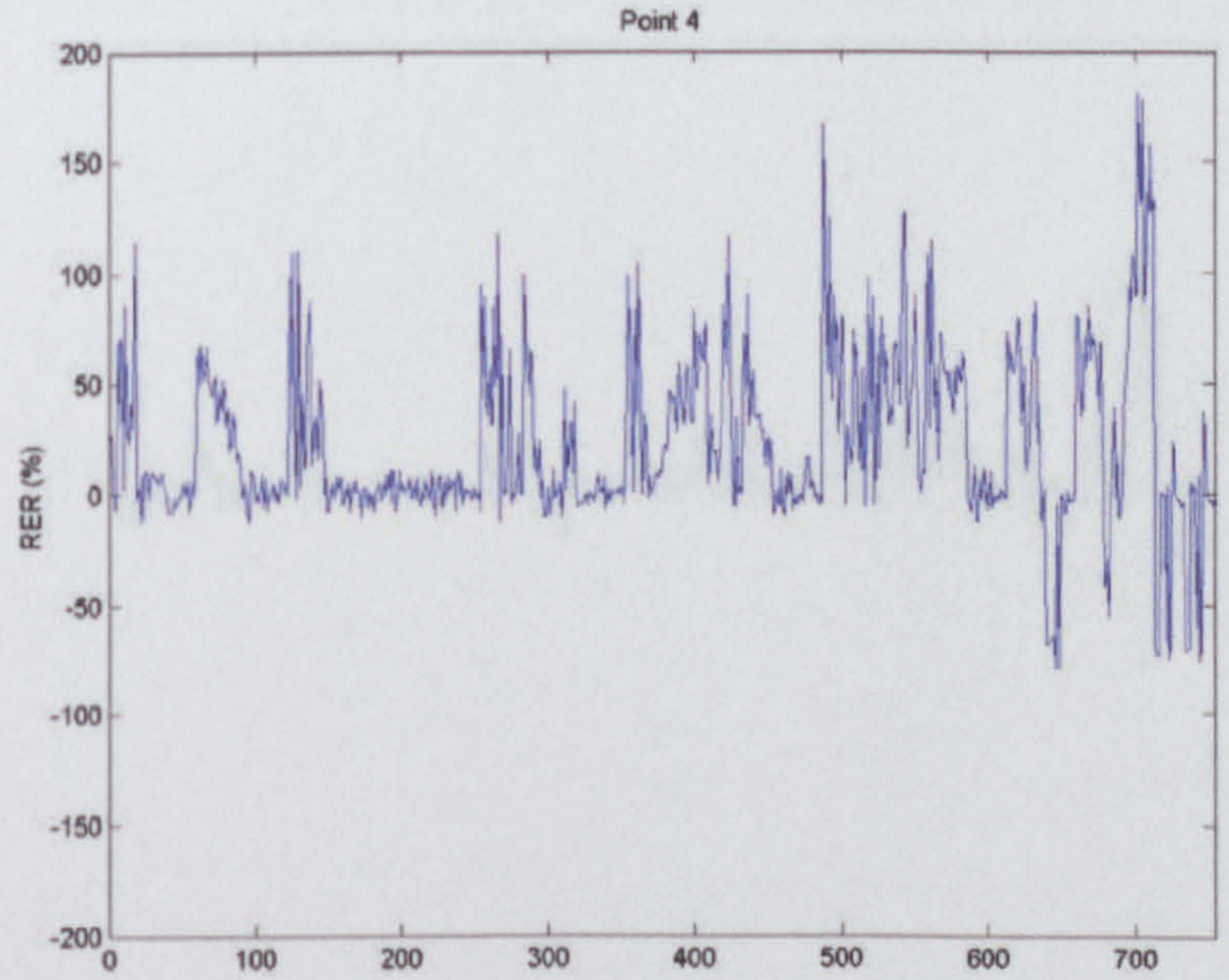

Figure G-10 - RER (%) between measured and best prediction internal illuminance (Point 4)

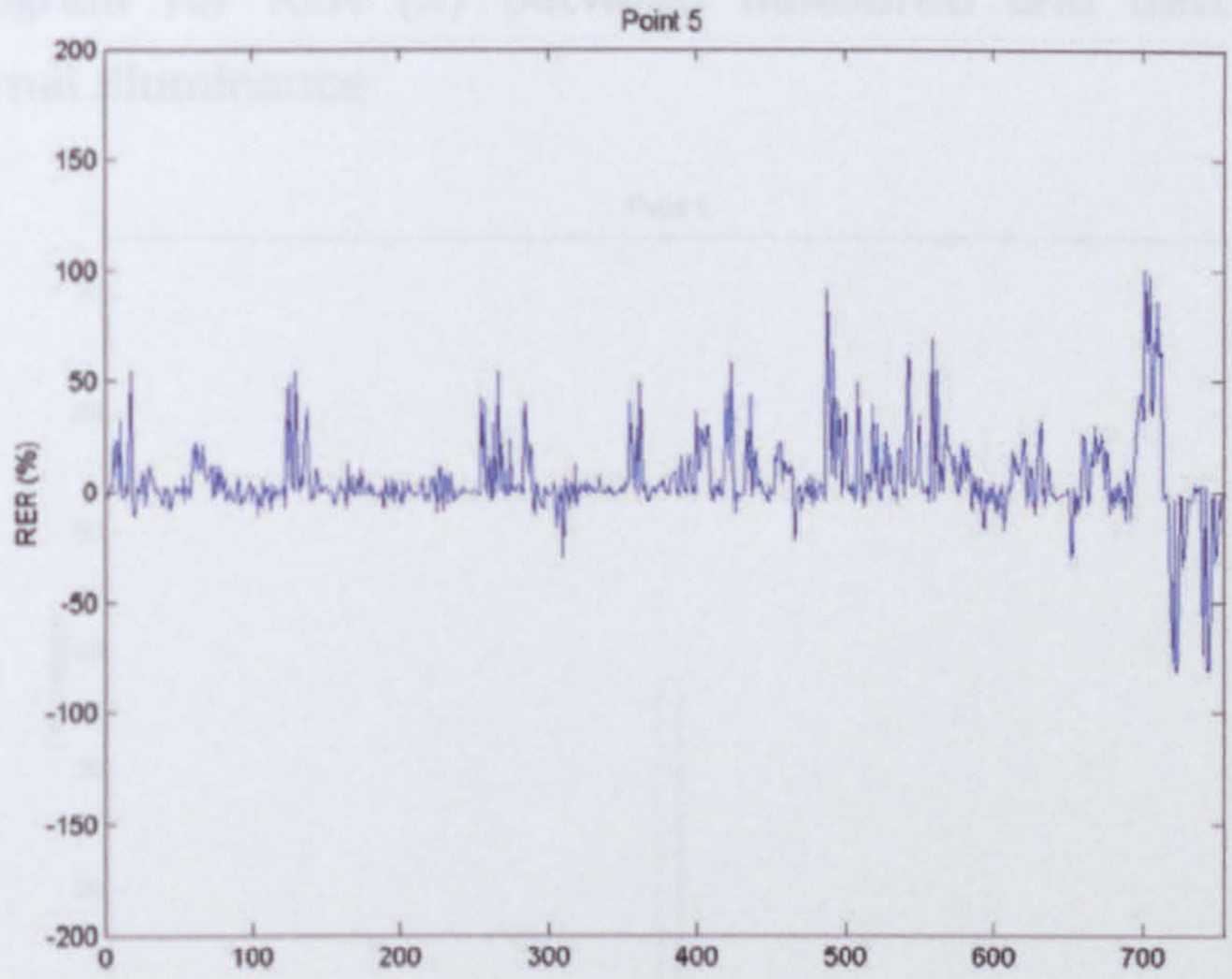

Figure G-11 - RER (%) between measured and best prediction internal illuminance (Point 5)

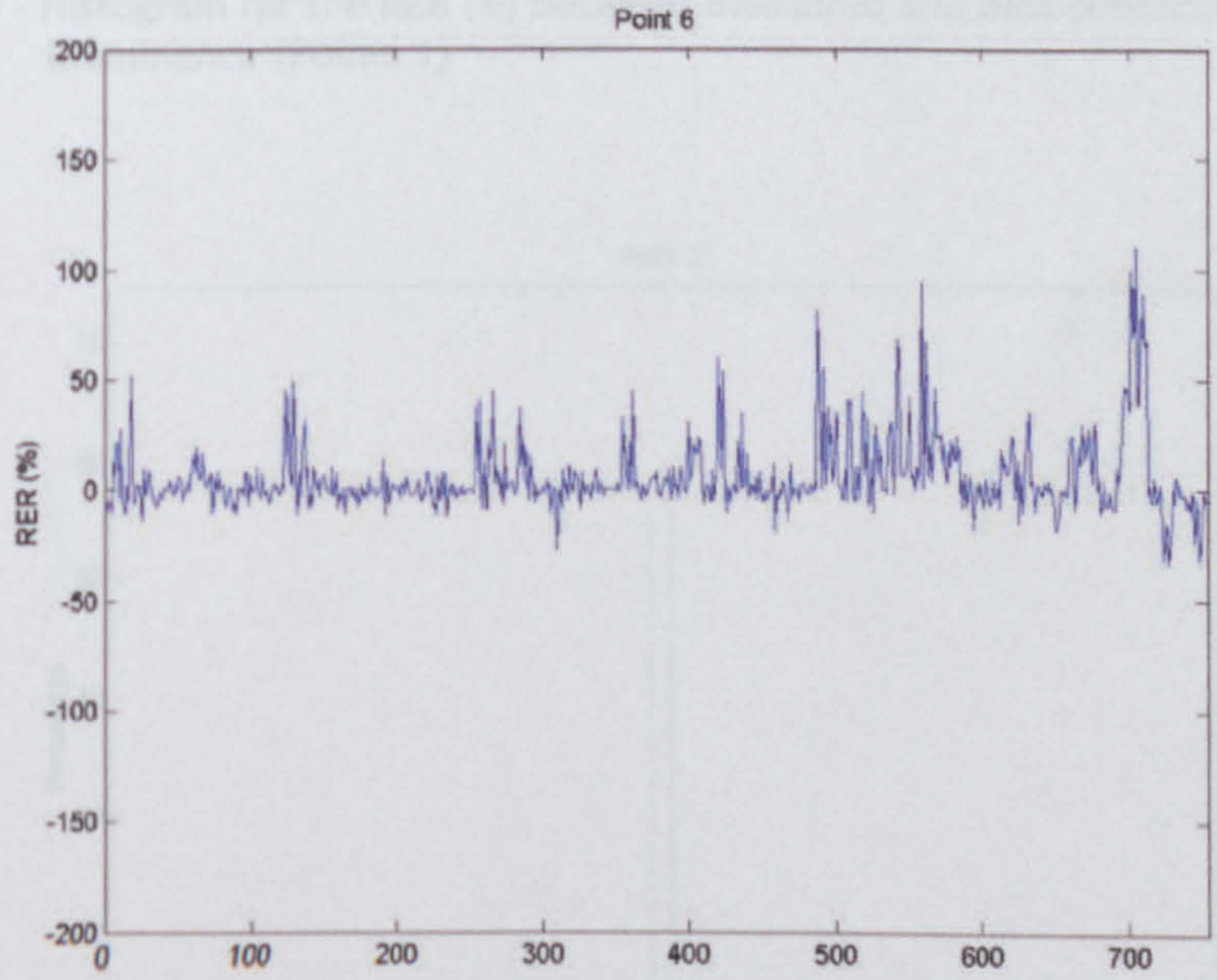

Figure G-12 - RER (%) between measured and best prediction internal illuminance (Point 6)

G.3 Histogram for RER (%) between measured and best prediction internal illuminance

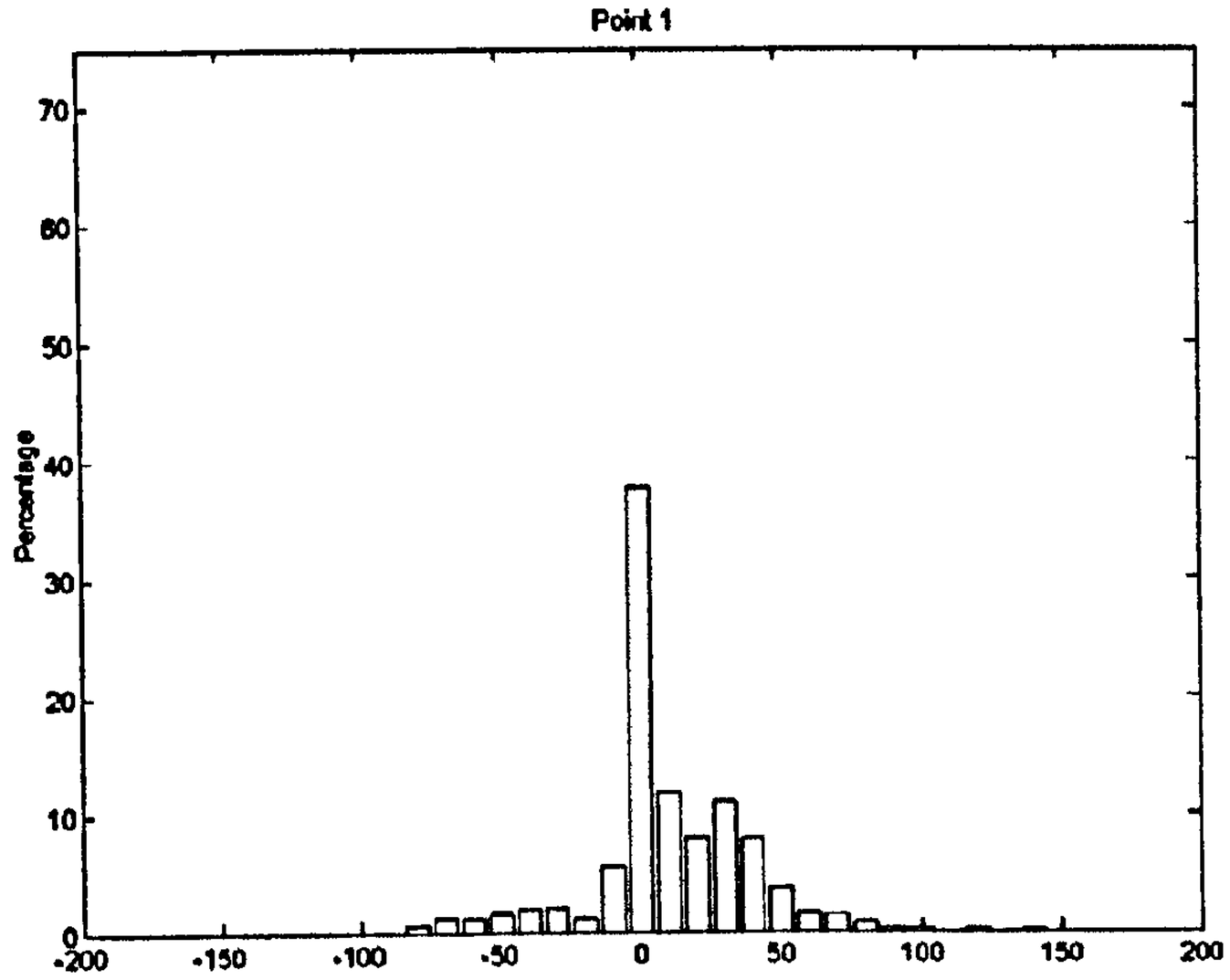

Figure G-13 - Histogram for the RER (%) between measured and best prediction internal illuminance (Points 1)

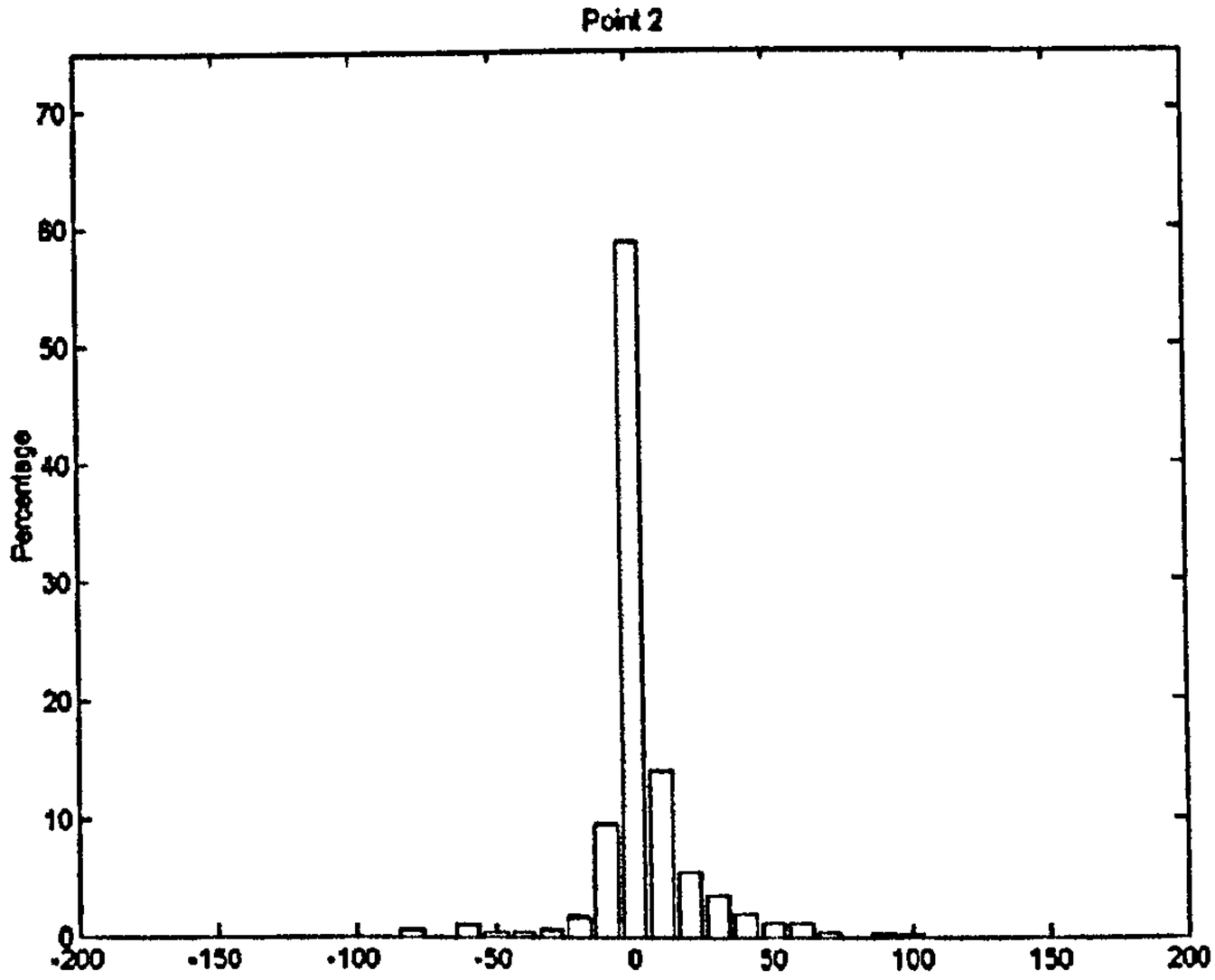

Figure G-14 - Histogram for the RER (%) between measured and best prediction internal illuminance (Point 2)

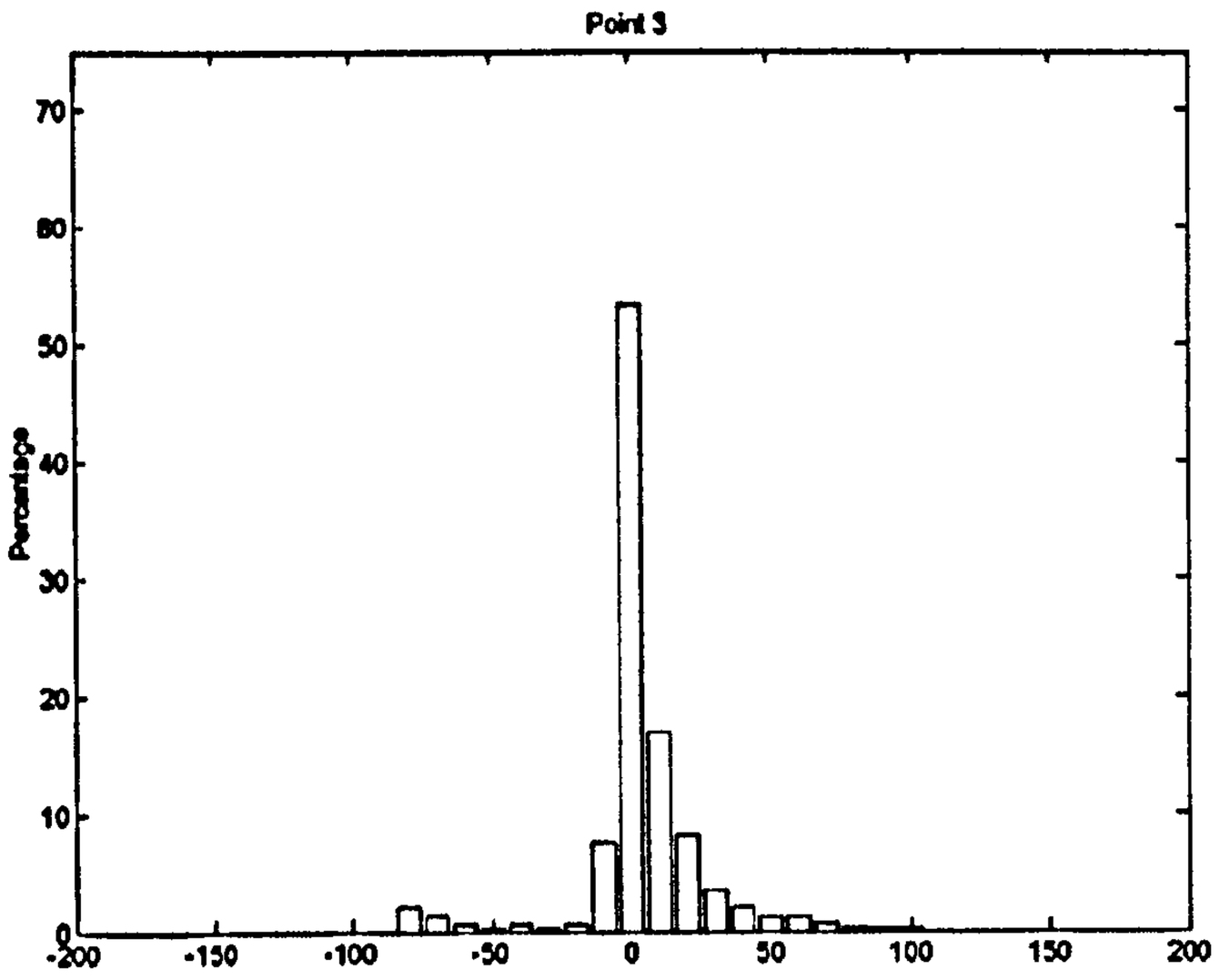

Figure G-15 - Histogram for the RER (%) between measured and best prediction internal illuminance (Point 3)

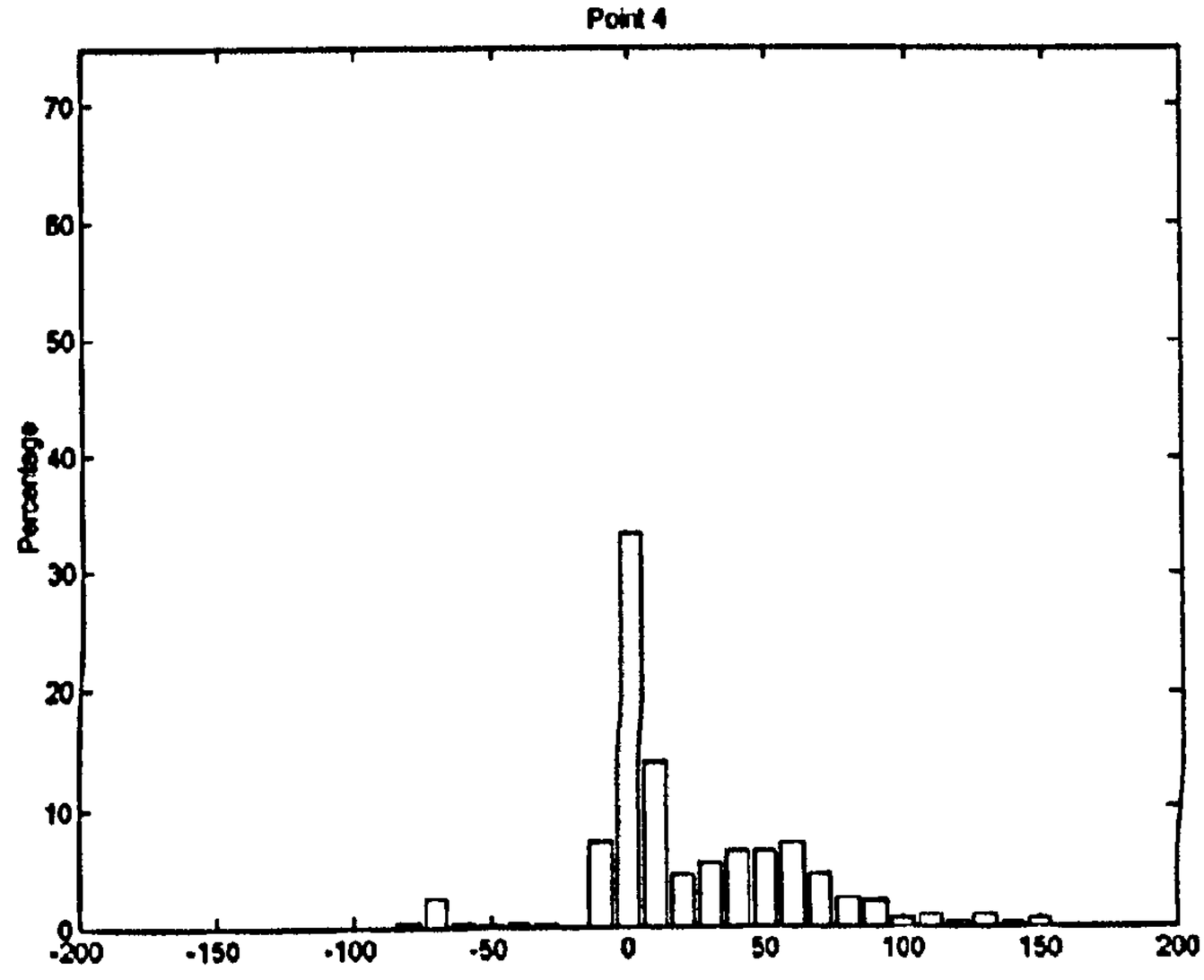

Figure G-16 - Histogram for the RER (%) between measured and best prediction internal illuminance (Point 4)

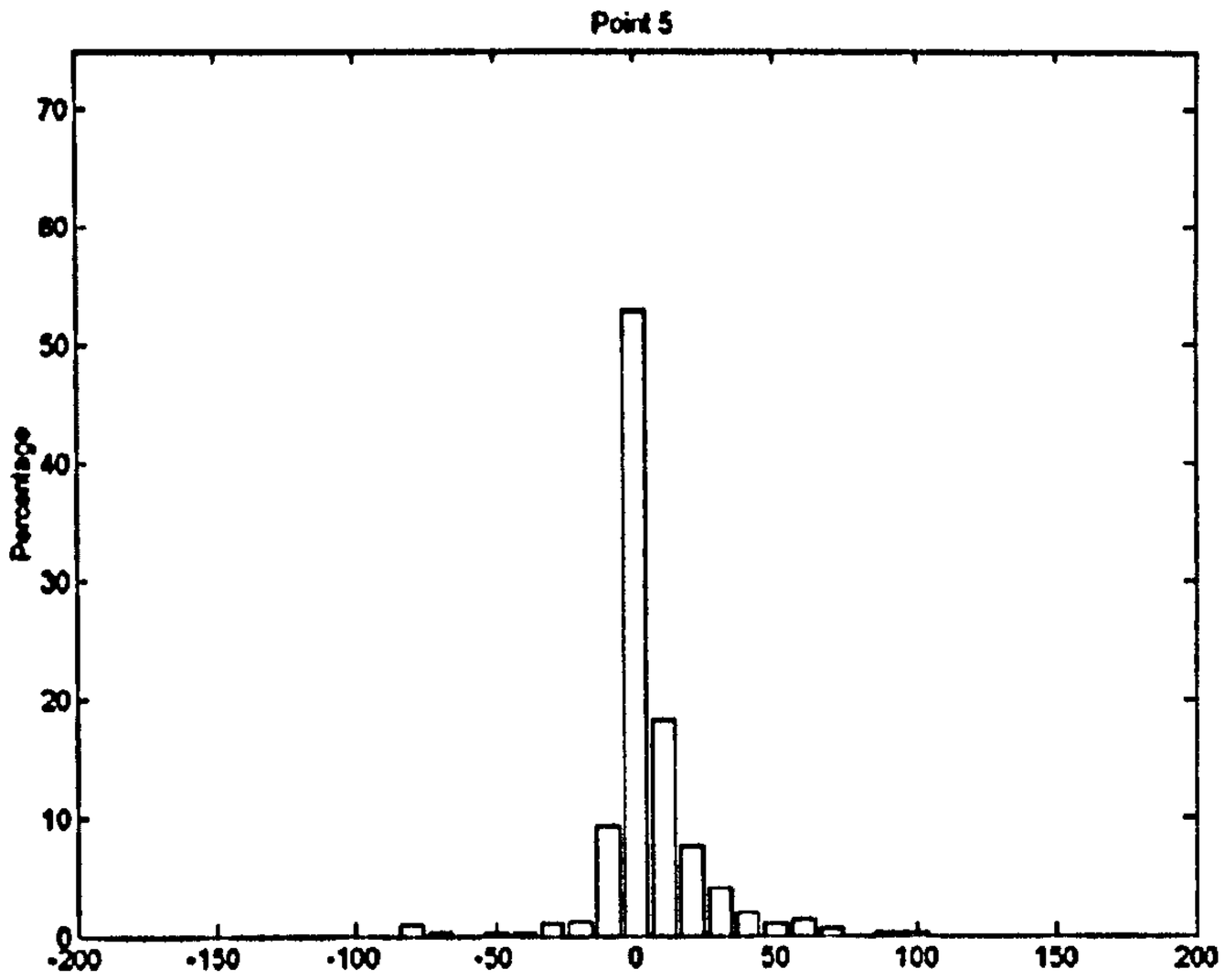

Figure G-17 - Histogram for the RER (%) between measured and best prediction internal illuminance (Point 5)

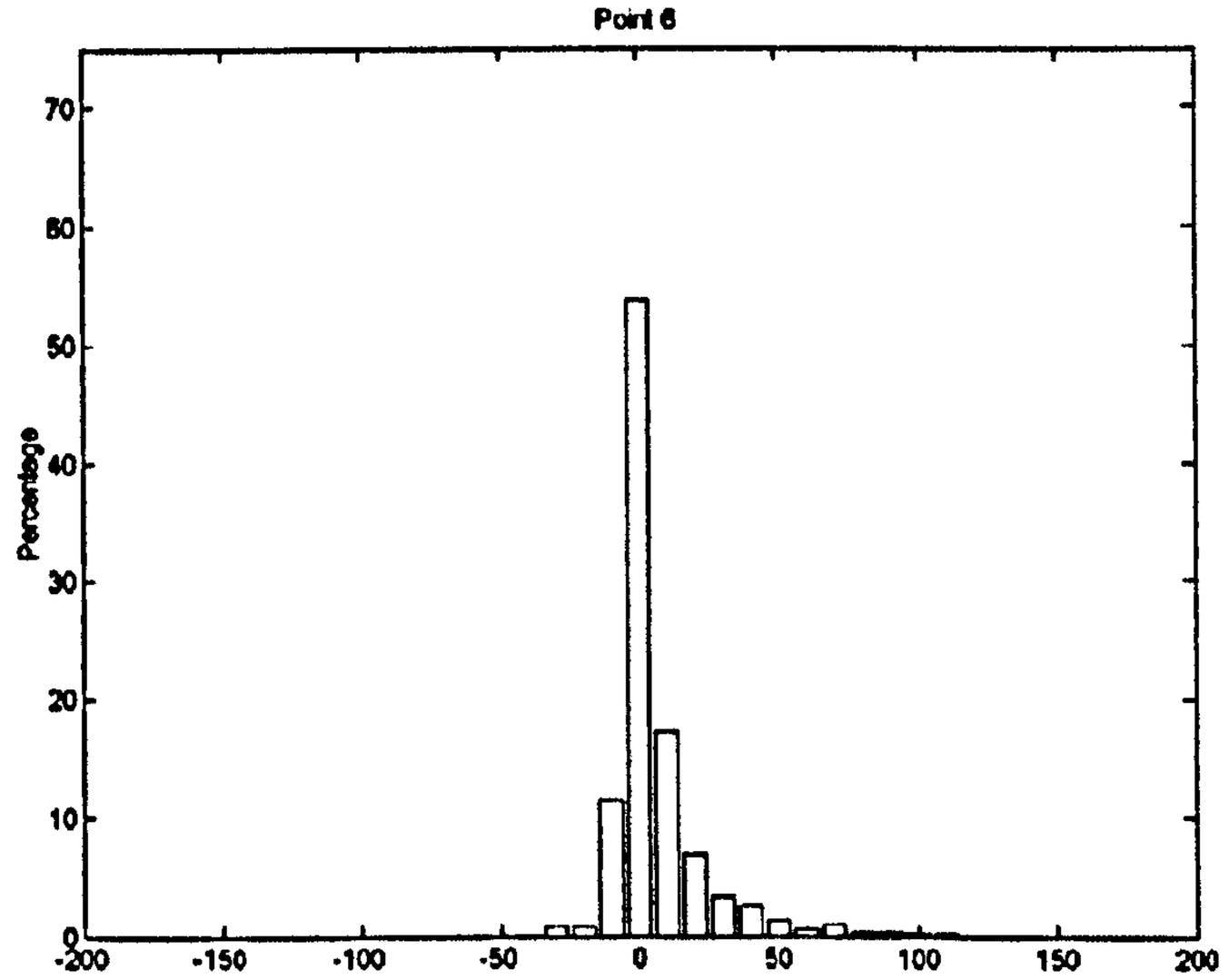

Figure G-18 - Histogram for the RER (%) between measured and best prediction internal illuminance (Point 6)

G.4 Correlation between measured and predicted illuminance

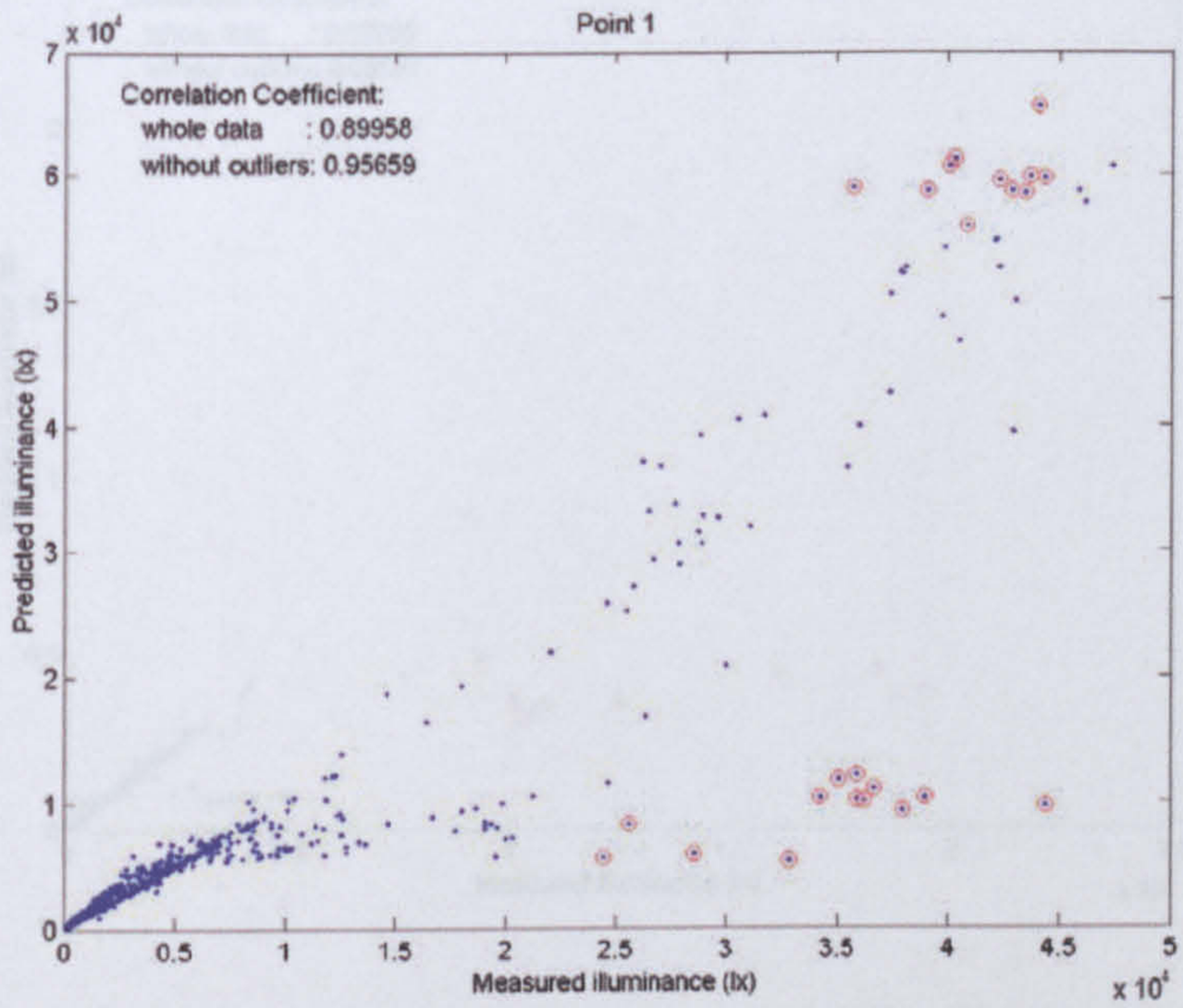

Figure G-19 - Correlation between measured and predicted illuminance. Outliers in red circle. (Point 1)

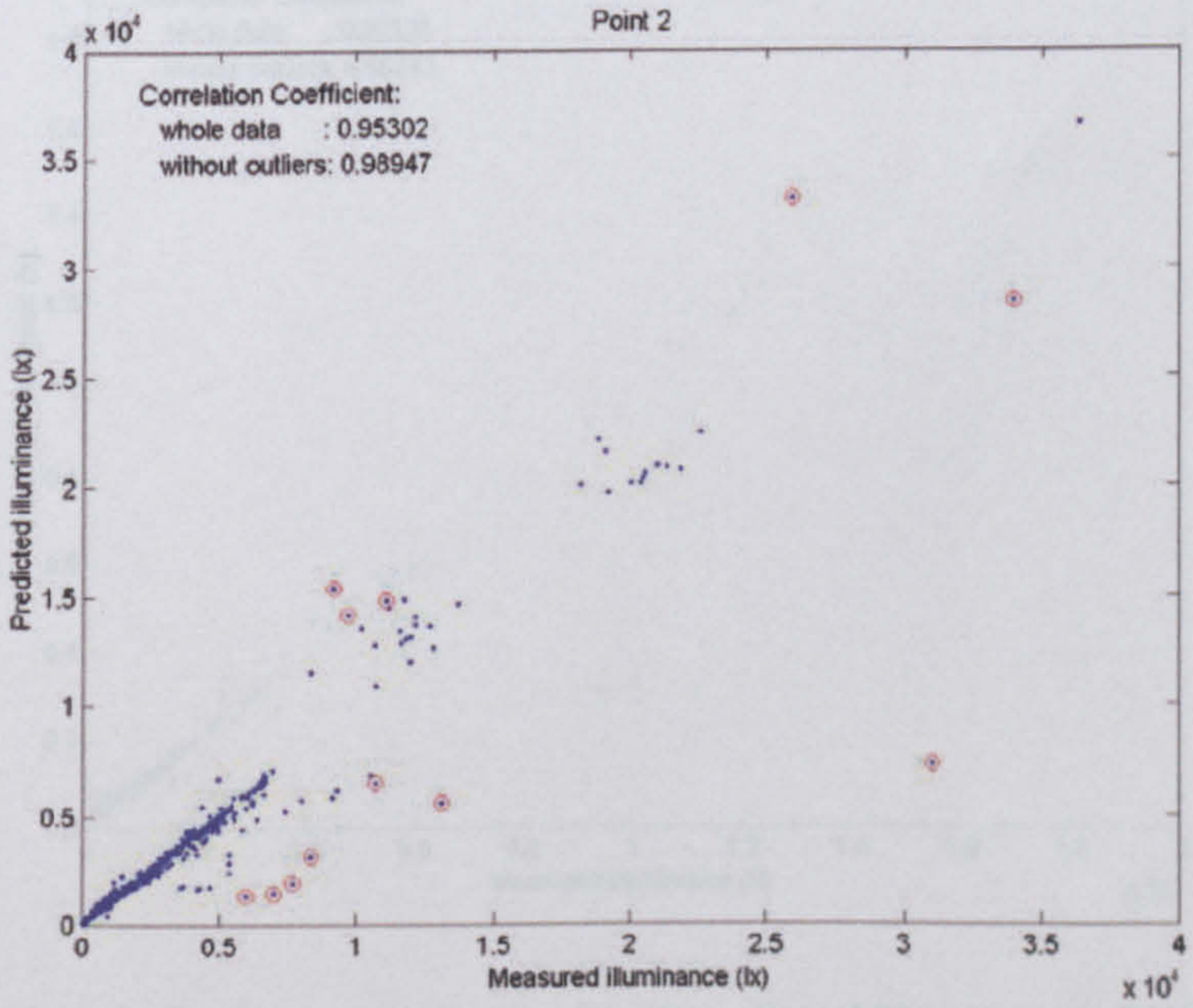

Figure G-20 - Correlation between measured and predicted illuminance. Outliers in red circle. (Point 2)

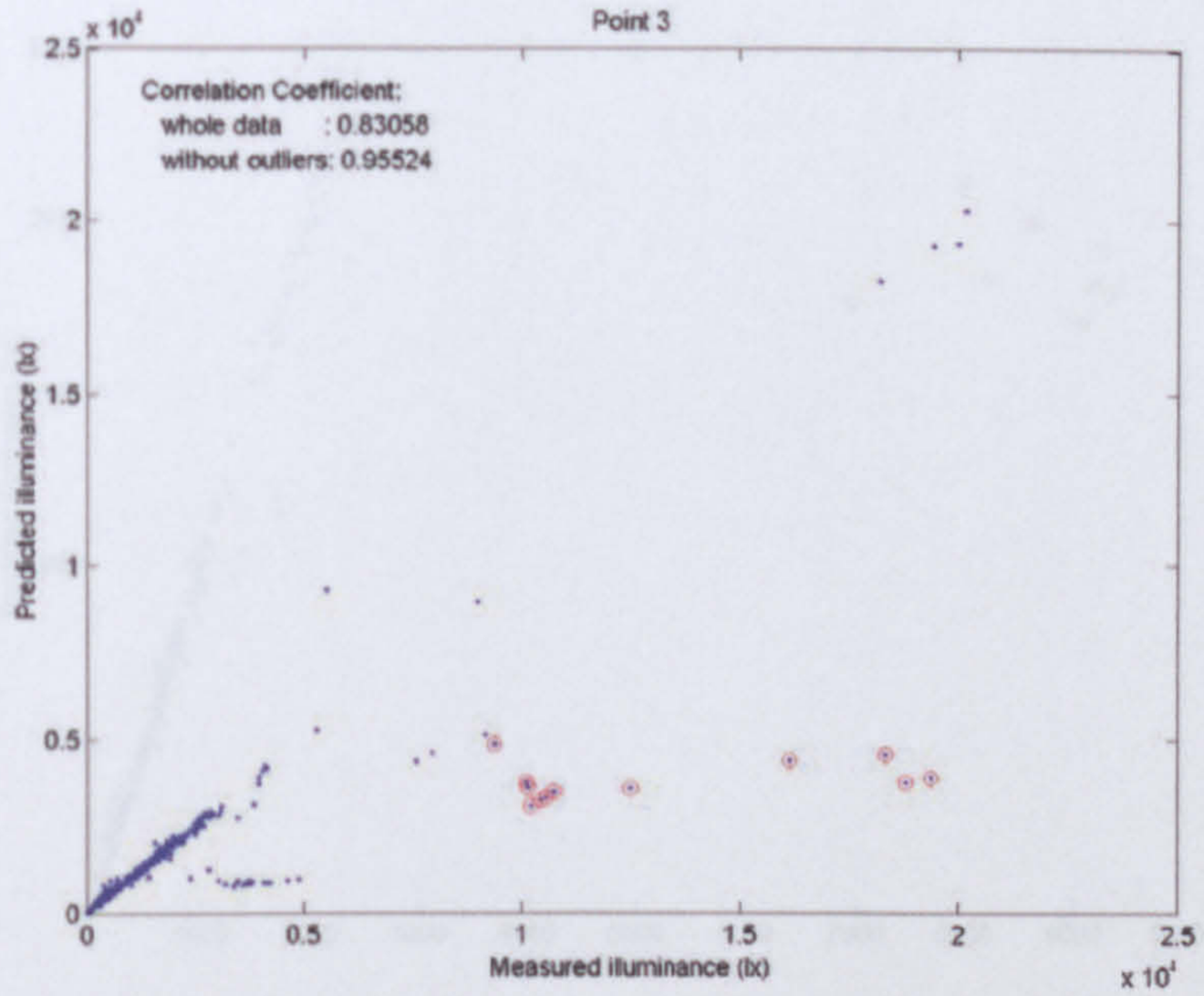

Figure G-21 - Correlation between measured and predicted illuminance. Outliers in red circle. (Point 3)

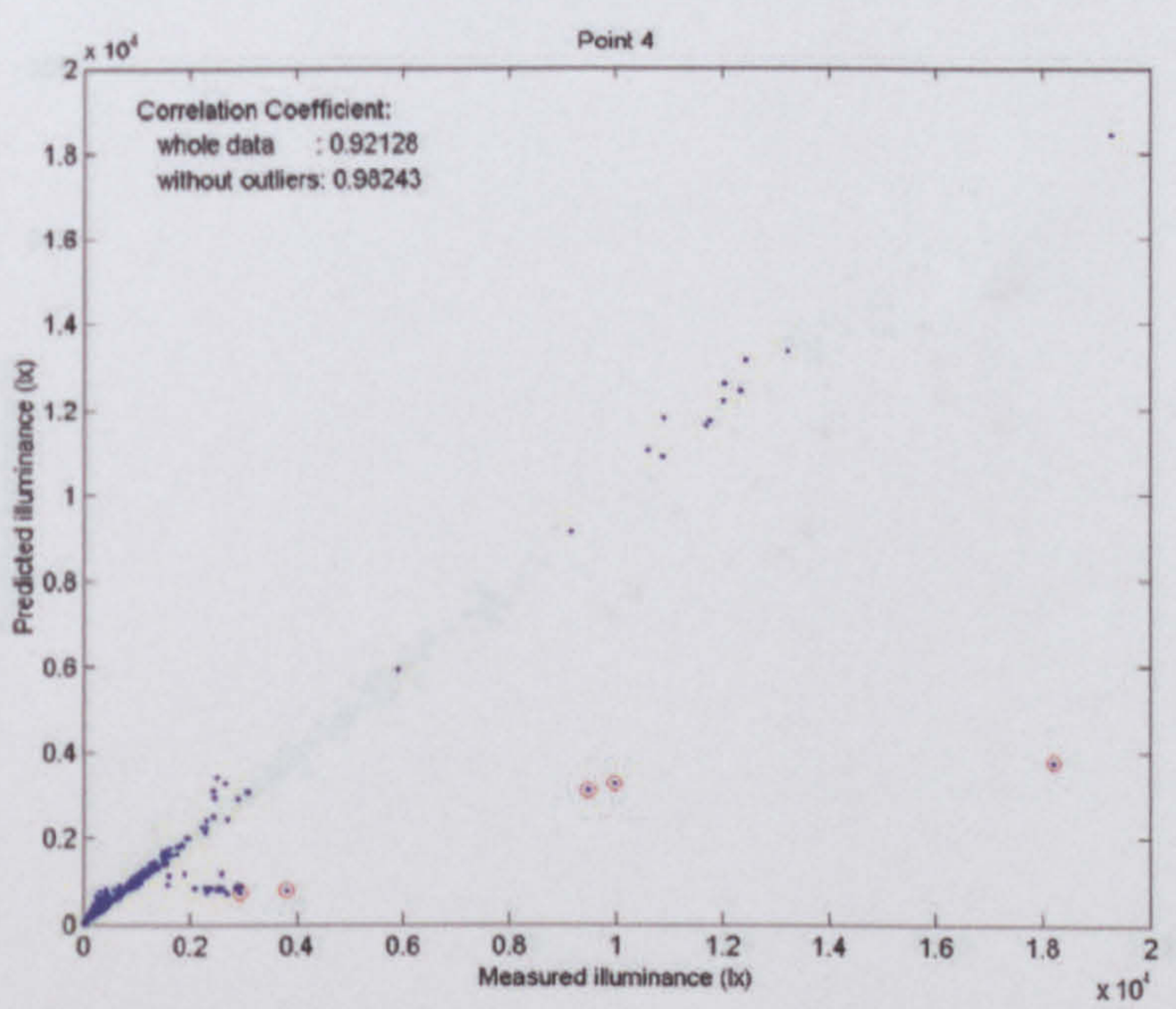

Figure G-22 - Correlation between measured and predicted illuminance. Outliers in red circle. (Point 4)

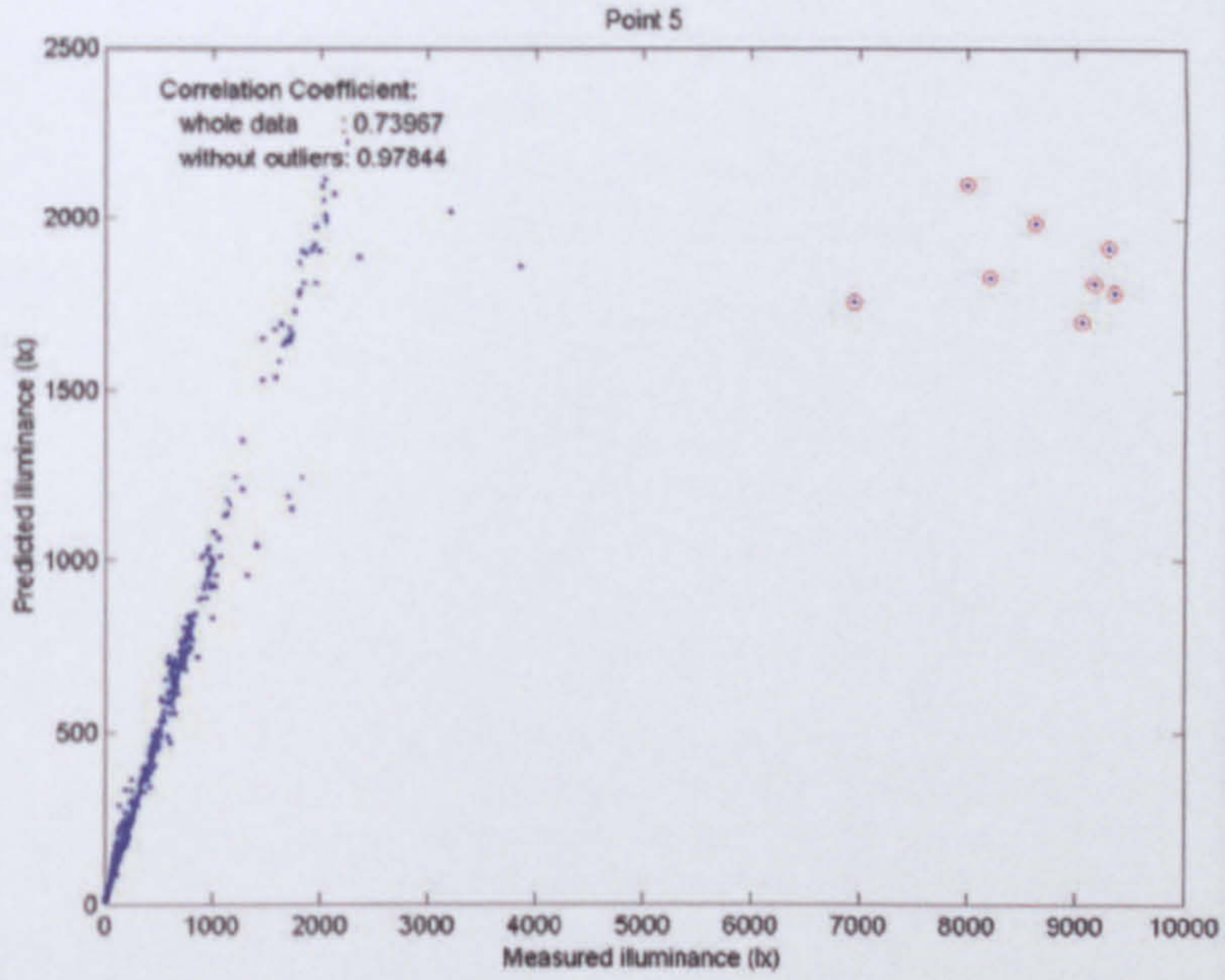

Figure G-23 - Correlation between measured and predicted illuminance. Outliers in red circle. (Point 5)

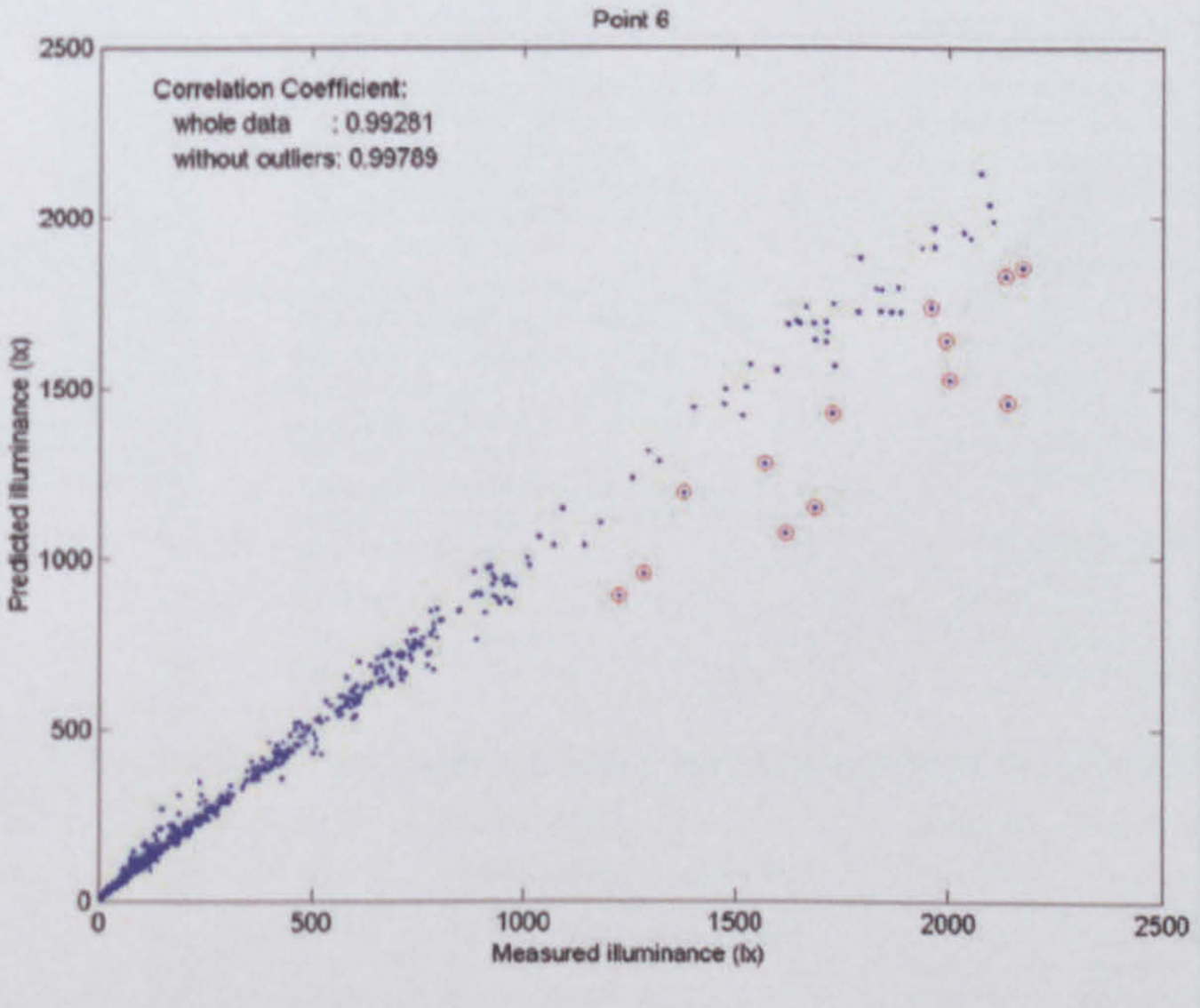

Figure G-24 - Correlation between measured and predicted illuminance. Outliers in red circle. (Point 6)

Appendix H - Published work

The influence of ground-reflected light in tropical daylighting

CONCLUSIONS

School classroom in Maceió - Brazil

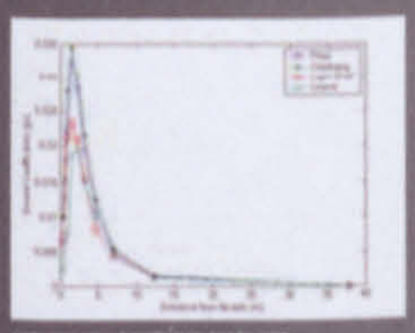

Daylighting ground coefficients (gc) by room positions in function of distance from window

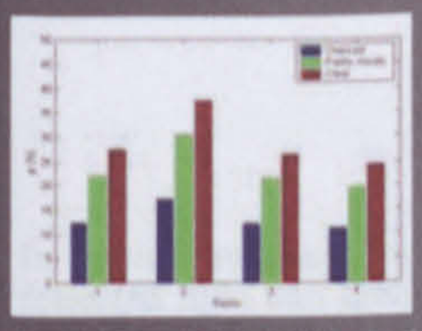

Contribution from ground-reflected light as a percentage of total daylight illuminance, at the test point of the reference room at working plane (fps) by window pattern and sky type

Light reflected from the ground can be a significant part of the total working-plane daylight in tropics.

In the examples analysed, it ranges from 10 to 40%.

There is a peak region where the ground can be more important to the internal daylighting. Designers can take the advantage of this point increasing reflectance in this area.

Rule of thumb: for a similar one-storey building, the boundaries of the peak region, A and B, can be found by the angles GSA=45° and GHB=70°, where G is the base of façade, S is the sill and H is the head of the window.

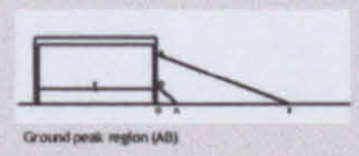

Ground peak region (AB)

Overhang has shown as the best shading device for improving ground reflected light, among the studied set.

There is no evidence of relation between sky type and shading device pattern to ground-reflected component.

AIMS

General Aim

To analyse the influence of daylight reflected on ground surfaces relating to internal daylighting performance in tropical region

Specific Aims

- How far from window's façade the ground can be important as a source of natural light;
- How a shading device's pattern can influence daylighting performance, relating to ground-reflected component;

METHOD

Reference room

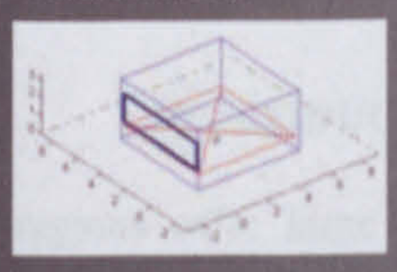

Shading Devices

Overhang (Room 1) Lightshelf (Room 2) Horizontal louvre (Room 4)

Ground subdivision

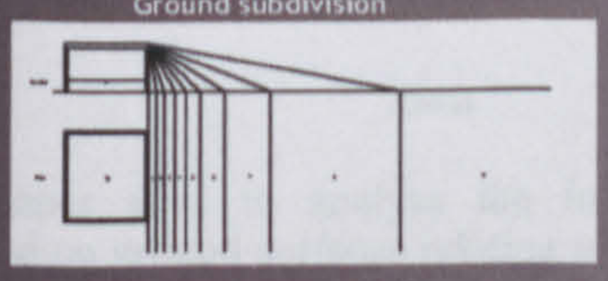

- Analysis is based on summer solstice, 22nd of December, midday.
- Shading devices have the same cut-off angle and not allow direct sunshine.
- The ground is split into 9 striped regions, parallel to window façade, defined by an angle with vertex in top façade, with 10° step.
- Illuminance levels are found for a single observation point in one reference room.
- The same room is tested for a plain window alone and with 3 different shading device patterns: overhang, lightshelf and louvre.
- The building is located at Maceió-Brazil, latitude 9°40'S and Longitude 35°42'W, window facing South.

Reflectances

Walls: 0.6 Ceiling: 0.7
Floor: 0.3 Ground: 0.2
Shading devices: 0.5

Computer simulation tool

- Results are based on computer simulation
- The software was developed in Matlab
- Uses backward ray tracing technique with Monte Carlo method and daylight coefficients
- Particular features:
  - Complex geometry
  - sky distribution configured by the user
  - ground subdivision
  - illuminance assessed by component (12 combinations are allowed)
  - skylight and sunlight contribution independently assessed

Programme screen with Run menu options

NEW CONCEPTS

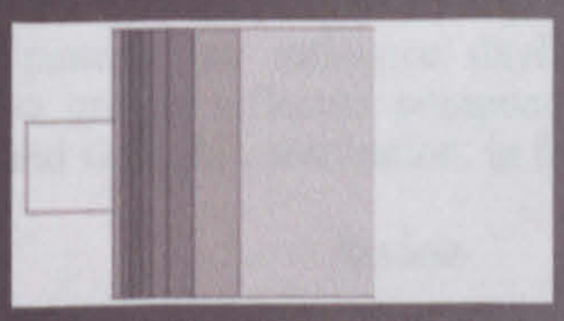

Ground coefficients (gc) by room position for a room with overhang

Ground coefficients (gc)

The concept of ground coefficients relates the illuminance (E) on a given surface, i, from a given patch, j, of ground and the ground patch luminance (L) and the subtended area in steradians (ω) of the ground patch, j, as described in equation below.

$$gc(i,j) = \frac{E(i)}{L(j)\,\omega(j)}$$

Ground reflected ratio (gr)

Some results in this work are given in the form of the ground-reflected ratio (gr). The ground-reflected component is related to the total internal illuminance for the same point or surface. This relation is expressed by the equation below.

$$gr = \frac{E_{gr}}{E_{in}} \times 100\%$$

SKY MODELS

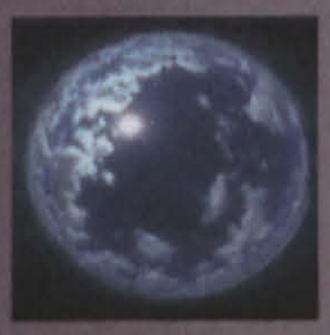

Partly Cloudy Sky in Maceió - Brazil

Three sky luminance distribution were chosen, based on a fieldwork and statistically related with the set of **CIE Sky** Luminance Models.

Best Choice:

- **Overcast** - CIE Sky 5 (Uniform Sky)
- **Partly Cloudy** - CIE Sky 10 (Partly cloudy with brighter circumsolar)
- **Clear** - CIE Sky 14 (Cloudless turbid with broader corona)

This research was supported by CAPES and the Federal University of Alagoas - UFAL - Brazil

Plea 2002 Toulouse - France

Ricardo C. Cabús - r.cabus@shef.ac.uk - University of Sheffield - School of Architecture - UK

Conference topic : design strategies

Keywords : daylighting, tropics, ground, ray tracing, Monte Carlo method

The influence of ground-reflected light in tropical daylighting

RICARDO C CABÚS

University of Sheffield
School of Architecture
The Arts Tower, Western Bank
Sheffield S10 2TN
England
rcabus@hotmail.com

Abstract

In tropical buildings the use of shading devices reduces the daylight entering a room from the sky. Ground-reflected light can then form a significant part of the daylight in a room. This paper analyses the ground-reflected component using a ray-tracing computer program based on the Monte Carlo method. The ground surface is divided into 9 strips parallel with the window facade of a reference room. Three sky types are analysed: overcast, partly cloudy and clear sky, taken into account sunlight and skylight contribution, for the last two. Illuminance is assessed for skylight and sunlight reflected by each ground patch and is related to global illuminance for the observation point. In addition, daylighting performance of three typical shading devices – overhang, light shelf and horizontal louvre – are compared with plain window. Results show that ground-reflected light can have a significant role in daylighting in tropical region. The work presents suggestions to improve daylighting performance using ground-reflected light.

Conference topic : design strategies

Keywords : daylighting, tropics, ground, ray tracing, Monte Carlo method

INTRODUCTION

Tropical regions offer large amounts of natural light. Direct sunlight must usually be screened from entering the window to prevent glare and thermal discomfort; but this also reduces the admittance of skylight. Sunlight reflected diffusely from external surfaces then becomes an important source of illumination, and the amount reflected by the ground surface can be significant.

Aims

This paper aims to analyse the influence of daylight reflected on ground surfaces relating to internal daylighting performance in tropical region. Three specific goals are investigated: how far from window's façade the ground can be important as a source of natural light; how a shading device's pattern can influence daylighting performance, relating to ground-reflected component; and what is the sunlight and skylight contribution, in function of sky type.

Review

During the mid of 20th Century, two papers, [1] and [2], point out the influence of ground as an important source of natural lighting for buildings located in regions where sun is often unobstructed. While [2] explore the point in a broad way, [1] indicate a method of attack on the subject, based on measurements using a model-scale and a heliodon to reproduce the relative motions of the earth and sun.

[3] also emphasises the importance of use the ground to reflect sunlight into buildings, mainly during summer and at low latitudes.

Afterwards, a study of [4] allows the assessment of the ground-reflected component in the mean illuminance on the working plane and on other room surfaces using a simplified method. It applies a split-flux technique and uses as data, solar normal illuminance and diffuse horizontal illuminance.

STUDY METHOD

This study observes the influence of ground-reflected light for buildings located in the tropical region, with particular reference to the impact of shading devices and ground distance to window façade.

In order to simplify the study, illuminance levels are found for a single observation point in one reference room. The same room is tested for a plain window alone and with 3 different shading device patterns: overhang, light shelf and louvre.

The building is assumed to be orientated East-West at Maceió-Brazil, latitude 9°40'S and Longitude 35°42'W, with the window facing south. Analysis is based on summer solstice, 22nd of December, midday.

The reference room

The reference room, as shown in Figure 1, is 6.00 x 6.00 m^2 and 3.00 m height. Those dimensions were chosen following previous studies done for daylighting and natural ventilation for the tropical climate (see [5] and [6]). Internal reflectances are as follow: walls 0.6, ceiling 0.7 and floor 0.3. Shading devices have reflectance equal to 0.5 for every surface. Windows are 6.00 x 1.50 m^2 and its sill is 1.00m

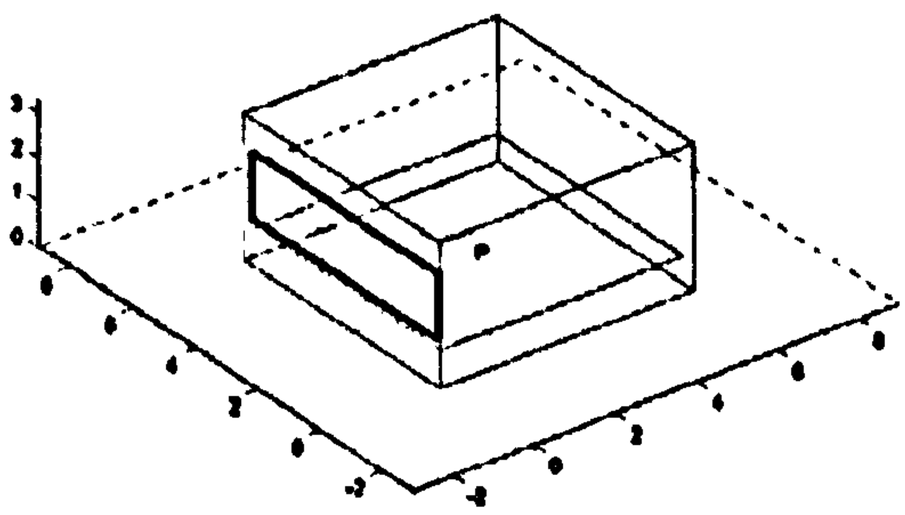

Figure 1. Reference room

height. Wall thickness is 0.15m, typical for light walls in the tropics.

The observation point (P) is located on the centre of the room – 3.00m from the window and others walls – and in the workplane, 0.75m height.

Shading devices, as seen in Figure 2, were designed protecting the workplane from direct sun, but allowing a maximum view of the sky.

The ground

The ground is split into 9 striped regions, parallel to window façade. Since the zone near the window façade is supposed to be more significant, the subdivision should be not even, but narrower near the window and wider as it goes far from façade. In this way the time spent in calculation is considerably decreased, without important loss in accuracy. Based on this assumption, the boundaries of each patch are related to an angle formed by imaginary planes from the roofline, on window façade wall, to the ground. The angles are defined each 10°, from 0°, on window façade to 90°, on the infinite (see Figure 3).

Table 1 shows the limits of each patch, as well as the midpoint and the width. The strip length is considered infinity.

In order to assess the influence of each patch, ground reflectance is set up to 0 for all strips, except the one to get results, which has reflectance equal to 0.2. After the independent calculation for every strip, results are concatenated.

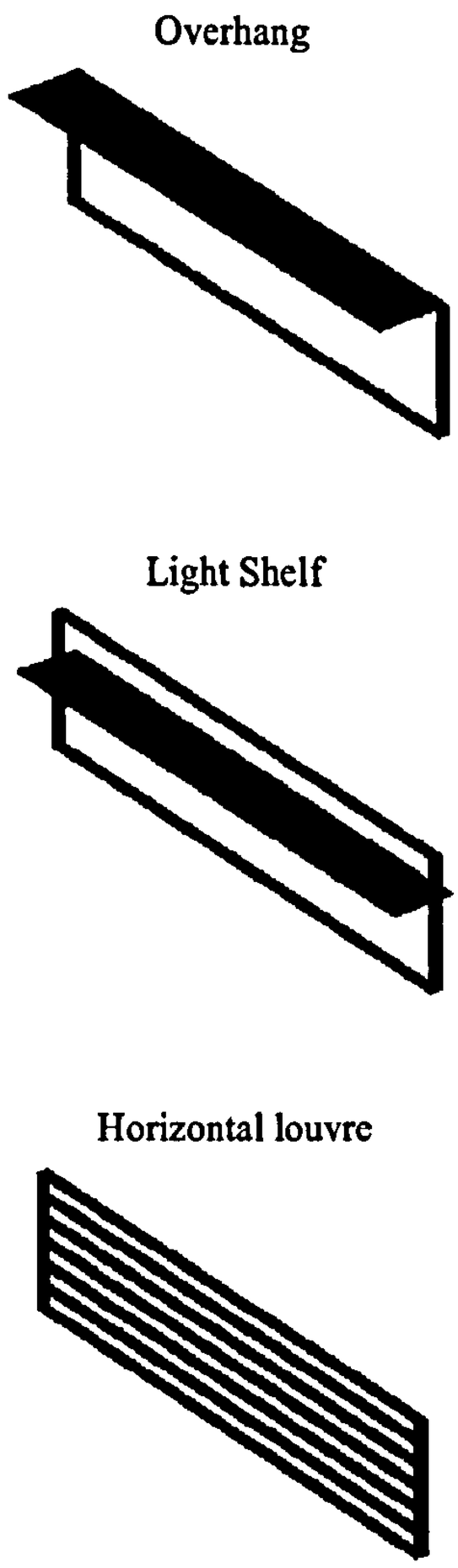

Figure 2. Shading Devices

The Simulation Model

All illuminance results are based on computer simulation.

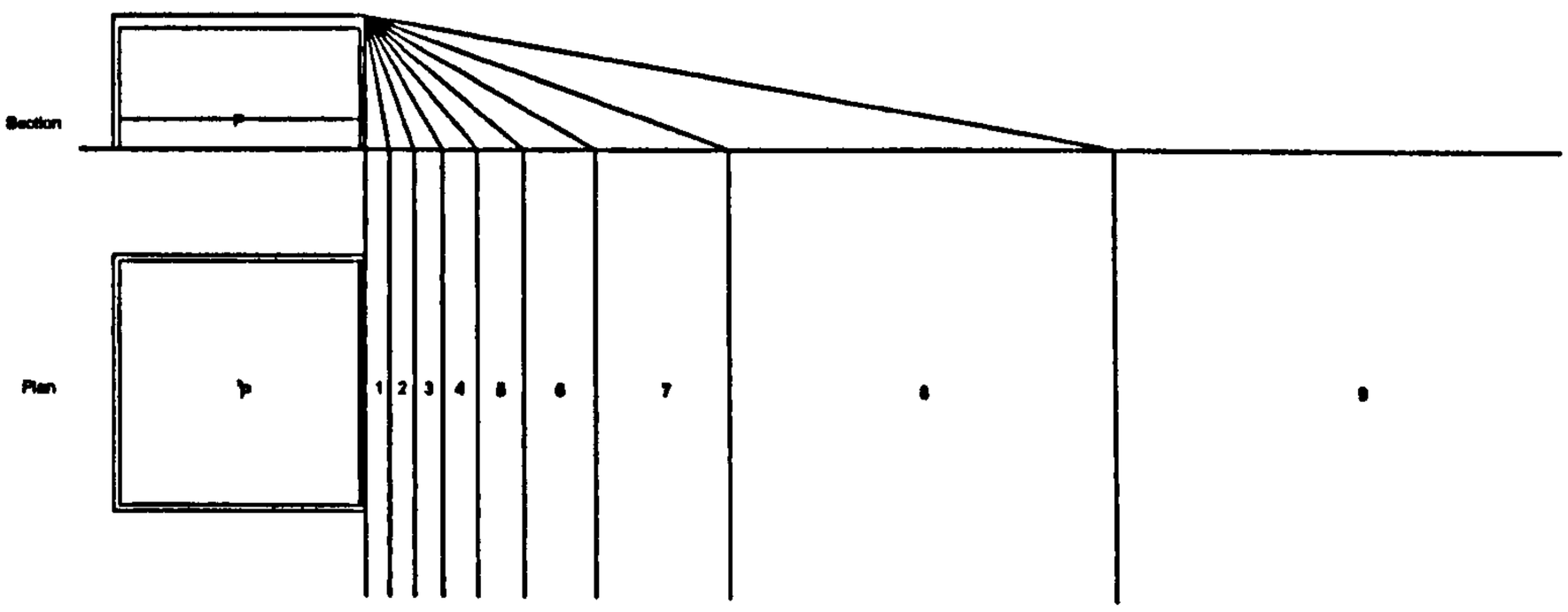

Figure 3. Ground patches and Reference Room – Section and Plan.

Table 1. Ground patch configuration

Patch	Distance from Window Façade (m) Limit 1	Mid	Limit 2	Patch width (m)
1	0.00	0.29	0.58	0.58
2	0.58	0.89	1.20	0.61
3	1.20	1.56	1.91	0.70
4	1.91	2.34	2.77	0.86
5	2.77	3.35	3.93	1.16
6	3.93	4.82	5.71	1.78
7	5.71	7.39	9.06	3.35
8	9.06	13.89	18.72	9.65
9	18.72	∞	∞	∞

The software was developed in Matlab® and uses ray tracing technique (see among others: [7]; [8]; [9]; [10]) with Monte Carlo Method (see among others: [11]; [12]; [13]; [14]) and daylight coefficients (see [15] and [16]).

Along with other features, the programme allows sky distribution configured by the user; ground subdivision; illuminance assessed by each component, for instance IRC, ERC, IRC (by ground) and direct, also reporting skylight and sunlight contribution independently.

The choice of sky distribution

Sky distributions were chosen based in a fieldwork carried out by the author on winter 2001 (South hemisphere). The complete study is described in another paper to be published. Briefly, sky luminance measurements were done on the site and outcomes were statistically compared with the 15 CIE Sky Luminance Models (see [17] and [18]). The best choice went to 3 sky distributions: an overcast sky, represented by CIE Sky number 5 (uniform sky); a partly cloudy sky, CIE Sky 10 (Partly cloudy, brighter circumsolar) and a clear sky, CIE Sky 14 (Cloudless turbid with broader solar corona). For this study, skis are renumbered respectively to sky 1, sky 2 and sky 3. For the last two, sunshine is also taken into account separately.

GROUND COEFFICIENTS

The concept of ground coefficients relates the illuminance (E) on a given surface, i, from a given patch, j, of ground and the ground patch luminance (L) and the subtended area in steradians (ω) of the ground patch, j, as described in equation (1).

$$gc(i,j) = \frac{E_i(j)}{L_j \omega_j} \qquad (1)$$

Note that the denominator expresses the direct normal illuminance on an unobstructed plane facing the ground patch.

The *gc* conception is similar to the daylight coefficients proposed by Tregenza [15], differing just on the source of light. There the luminous source is a sky patch, here the source is a ground patch. Consequently calculation can be done with the same methodology.

This concept deals with the geometry of building and ground and with the reflectance of surfaces. Ground coefficients are not dependent on sky distribution or sun position, however the ground luminance (L_{gr}) is.

GROUND-REFLECTED RATIO (gr)

Some results in this work are given in the form of the ground-reflected ratio (gr). In this way, the ground-reflected component is related to the total internal illuminance for the same point or surface. This relation is expressed by the equation (2)

$$gr = \frac{E_{gr}}{E_i} \times 100\% \qquad (2)$$

where E_i is the internal horizontal illuminance and E_{gr} is its ground-reflected component.

The advantage of using *gr*, instead of absolute illuminance values, is making possible to compare the influence of different variables, for instance sky type or latitude, using the same reference.

HOW FAR FROM WINDOW'S FAÇADE THE GROUND CAN BE IMPORTANT AS A SOURCE OF NATURAL LIGHT

The ground coefficients concept is used in order to assess the influence of ground distance to window's façade in its daylighting performance. It is calculated to every ground patch and results are plotted in Figure 4 for the four room patterns.

Independent of room pattern, it is possible to observe that there is a peak next to window façade which shows the most important ground region, regarding to its daylighting performance. For every pattern, *gc* is greater than 0.005 between 0.50m and 7.00m from façade. It means that if the direct normal illuminance generated by this patch is for instance 10,000 lux, the ground component will be 50 lux.

The influence of shading devices will be better analysed in the next section, however regarding ground location it is possible to note that difference between patterns can only be detected within the peak region. There, overhang appears as the best choice to take advantage of ground-reflected light.

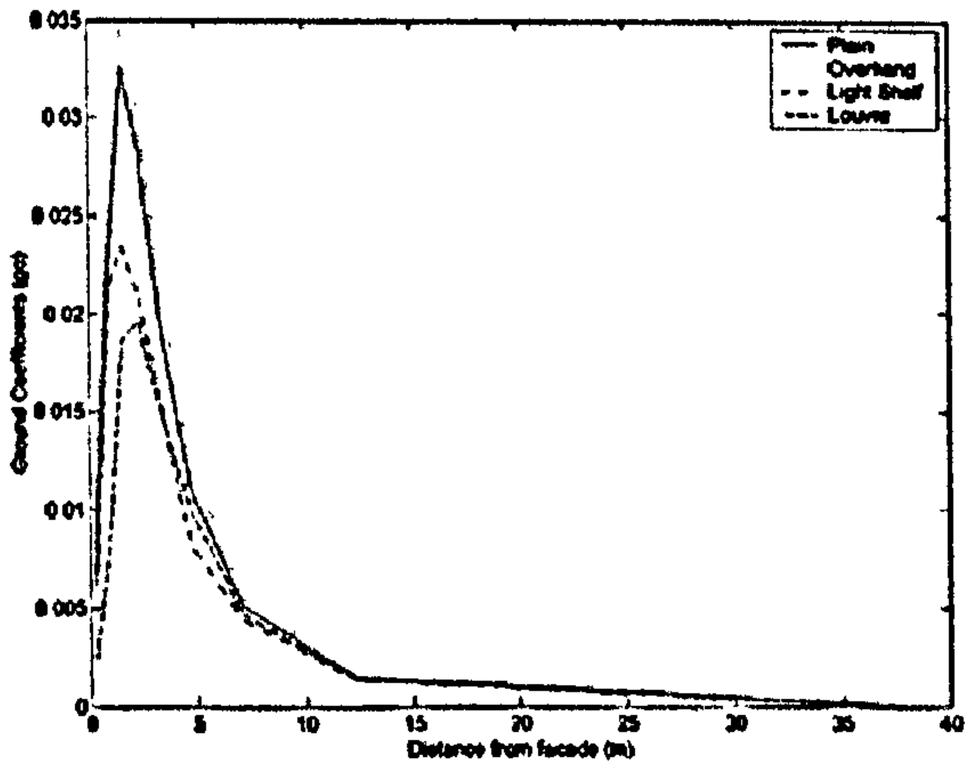

Figure 4. Comparing ground coefficients (gc) by room pattern in function of distance from window

HOW A SHADING DEVICE'S PATTERN CAN INFLUENCE DAYLIGHTING PERFORMANCE, RELATING TO GROUND-REFLECTED COMPONENT

The type of shading device can alter the influence of ground in internal daylighting performance. Comparing three different patterns: overhang (room 2), light shelf (room 3) and horizontal louvre (room 4), with a plain window (room 1), as shown in Figure 5, it is possible to observe that an overhang can increase the ground-reflected component relating to a plain window.

Concerning the other patterns, either light shelf or louvre produce only a slight reduction in the ground-reflected component, having the first a better performance.

It is worth noting that as regards the above points, there is no evidence of sky type influence altogether. Although, as discussed in next section, sky type can influence ground component, independent of window pattern.

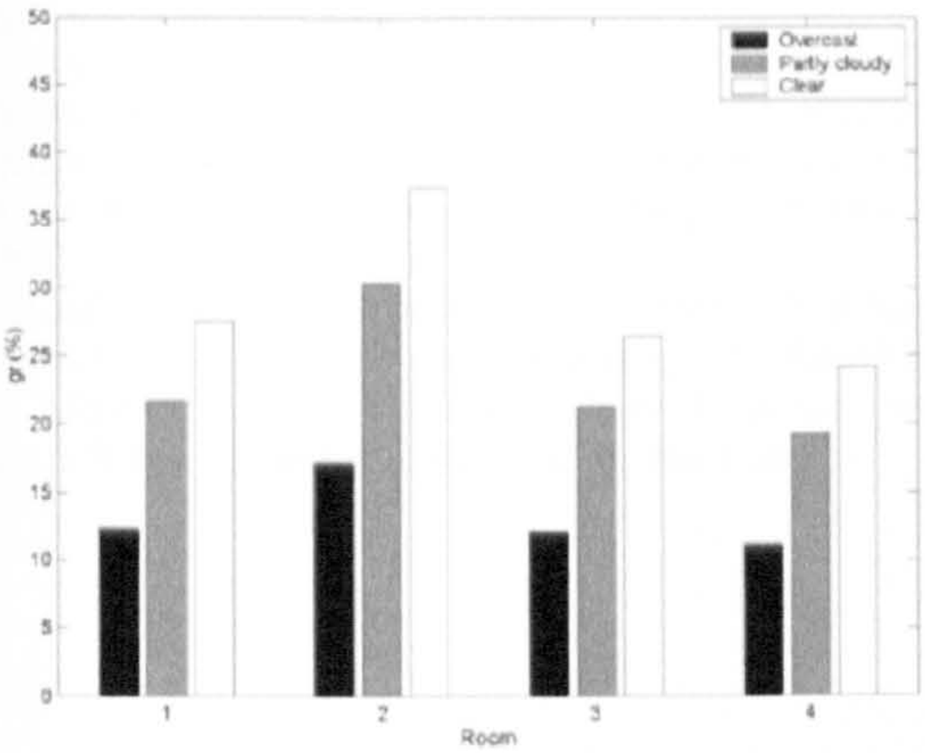

Figure 5. Illuminance from ground-reflected light as a percentage of total daylight illuminance, at the mid-point of the reference room at working-plane (*gr*) by window pattern and sky type

WHAT IS THE SUNLIGHT AND SKYLIGHT CONTRIBUTION, IN FUNCTION OF SKY TYPE

The relative influence of sunlight and skylight in the ground-reflected component varies with sky type.

Obviously, the overcast sky has no sunshine. For the studied patterns its *gr*, as shown in Figure 6, is within the interval from 12% to 18%. However, it is notable that *gr* due to skylight contribution in overcast sky is bigger than partly cloudy and clear skies. Although in absolute figures results show that skylight contribution for partly cloudy and clear skies is higher, due to bigger external horizontal illuminance.

In relation to partly cloudy skies it is possible to note that the sun and sky contribution is almost similar, with a minor difference pro sunlight, as can be seen in Figure 6, independent of window pattern.

For clear sky, even though its blue sky contributes less than a partly cloudy sky, its sunlight can supply about the double as its skylight, and consequently giving the best performance relating to ground-reflected component

It is also important to emphasise that previous analyses are valid independent of room pattern.

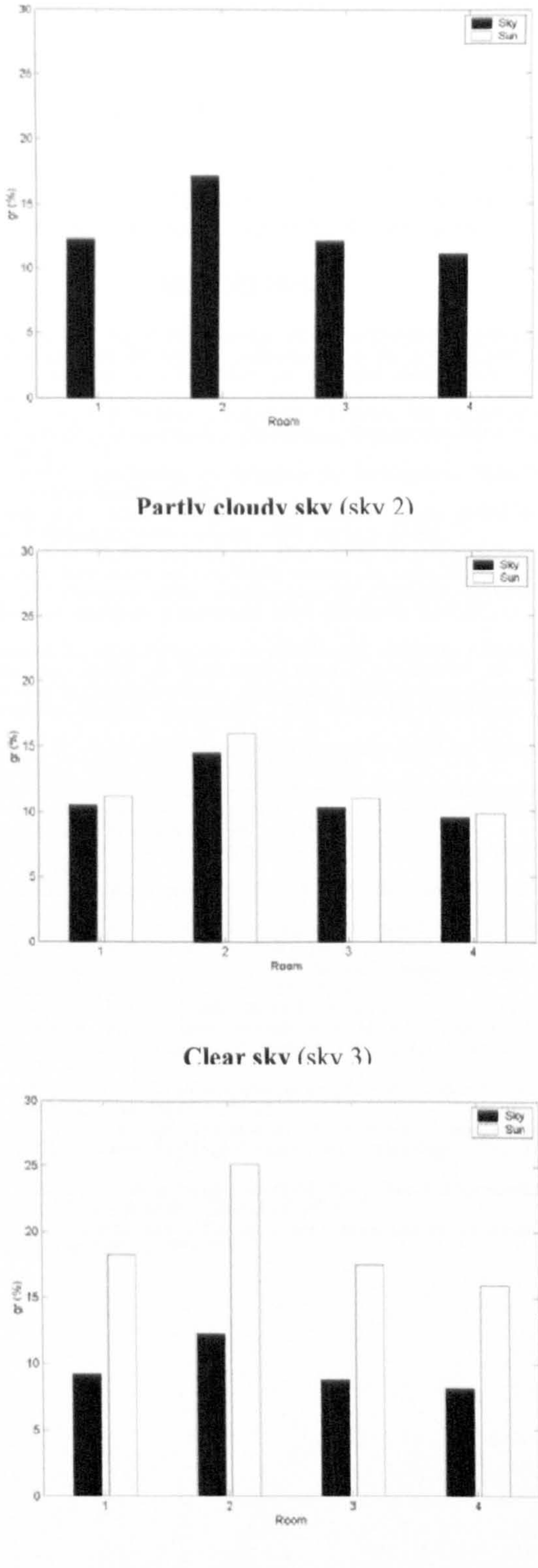

Figure 6. Illuminance from ground-reflected light as a percentage of total daylight illuminance, at the mid-point of the reference room at working-plane (gr) by window pattern and component

CONCLUSIONS

The work has shown that for this reference room the light reflected from the ground is a significant part of the total working-plane daylight. In the examples analysed, this value, denoted by *gr*, ranges from 10 to 40%. The highest values occur when there is sunshine on the ground. Diffusely reflected sunlight is clearly a significant source of illuminance in tropical buildings, but it can also be said that ground-reflected skylight should be taken into account, as its contribution is almost the same as the ground-reflected sunshine for partly cloudy skies.

It is up to the designer to weight up the importance of each kind of sky, in function of the building location. For instance, a hot-dry city designer may emphasise the clear sky characteristics, while a fellow in the humid-warm Brazilian northeastern coast may call more attention to the partly cloudy sky aspects.

Another point to arise is the ground distance to window façade. Results have revealed that there is a peak region where the ground can be more important to the internal daylighting. The designer can take the advantage of this point increasing reflectance in this area. This region is not dependent on the latitude, but in the material characteristics and geometry of building and surrounding. Figure 9 shows a section of the reference room with the peak region (AB) detached.

As a rule of thumb, for a similar one-storey building, the boundaries of the peak region, A and B, can be found by the angles GSA=45° and GHB=70°, where G is the base of façade, S is the sill and H is the head of the window.

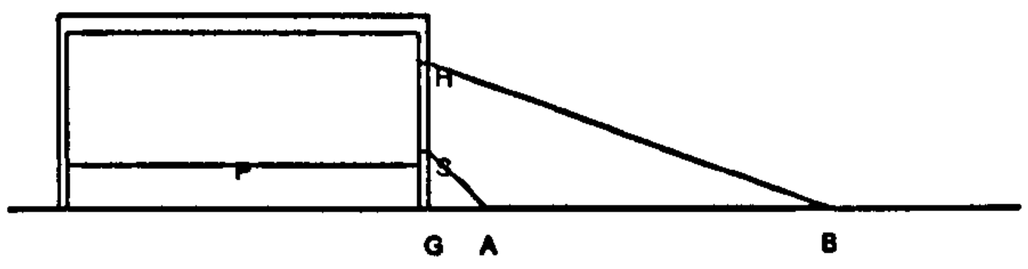

Figure 9. Peak region on the ground regarding ground-reflected component

Between the shading device patterns analysed, overhang has shown the best results for every sky type. Light shelf and horizontal louvre has achieved results near the plain window. But it is important to note that both can contribute to reduce glare and insolation, keeping the performance of a plain window, which has tendency to produce glare and thermal discomfort in tropics.

In addition, it is worth detaching that any changing in the shading device surfaces reflectance has a direct shifting in ground-reflected component. In this way the designer can increase or decrease its value in order to achieve his/her goal.

Since results were calculated for the room mid-point, it is expected that the ground-reflected ratio can be smaller near window, and greater in the rear of the room, due to the decreasing of direct sky component as the observation point (P) is far from the window.

In this study, all surfaces considered are perfect diffusers, and any specular reflection is not taken into account. Inter-reflection between the building and the ground was found to be insignificant with the geometry adopted for this example. Further work is examining the effects of façade orientation, latitude, time of day, day of year, observation point position, window size, room dimensions, and surface reflectance.

ACKNOWLEDGEMENT

I am thankful to Prof. Peter Tregenza for his valuable criticism, and to CAPES and the Federal University of Alagoas, for their financial support for this research.

REFERENCES

1. Hopkinson, R.G. and P. Petherbridge. *The natural lighting of buildings in sunny climates by sunlight reflected from the ground and from opposing facades.* in *Conference on Tropical Architecture.* 1953. London.
2. Griffith, J.W., O.F. Wenzler, and G.W. Conover, *The importance of ground reflection in daylighting.* Illuminating Engineering (New York), 1953. 48: p. 35-38.
3. Lam, W.M.C., *Sunlighting as formgiver for architecture.* 1986, New York: Van Nostrand Reinhold.
4. Tregenza, P.R., *Mean daylight illuminance in rooms facing sunlit streets.* Building and Environment, 1995. 30(1): p. 83-89.
5. Bittencourt, L., G. Bianna, and J.M. Cruz. *Efeito de protetores solares verticais e horizontais na ventilação natural de salas de aula do 2° grau.* in *I Encontro latino Americano e III Encontro Nacional de Conforto no Ambiente Construído.* 1995. Gramado: ANTAC. p. 383-388.
6. Bittencourt, L., *et al. Influência da localização, dimensão e forma das janelas nos níveis de iluminação natural produzidos por céus encobertos.* in *I Encontro latino Americano e III Encontro Nacional de Conforto no Ambiente Construído.* 1995. Gramado: ANTAC. p. 571-576.
7. Rogers, D.F., *Procedural elements for computer graphics.* Computer Science Serie. 1985, New York: McGraw-Hill.
8. Wallace, J.R., M.F. Cohen, and D.P. Greenberg, *A two-pass solution to the rendering equation: A synthesis of ray tracing and radiosity methods.* Computer Graphics, 1987. 21(4): p. 311-320.
9. Glassner, A.S., ed. *An introduction to ray tracing.* 1989, Academic Press: London.
10. Watt, A., *3D computer graphics.* 2nd ed. 1993, Wokingham: Addison-Wesley.
11. Tregenza, P., *The Monte Carlo method in lighting calculations.* Lighting Research & Technology, 1983. 15(4): p. 163-170.
12. Stanger, D., *Monte Carlo procedures in lighting design.* Journal of the Illuminating Engineering Society, 1984. 13(4): p. 368-371.
13. Kalos, M.H. and P.A. Whitlock, *Monte Carlo methods.* Vol. 1. 1986.
14. Haji-Sheikh, A., *Monte Carlo methods,* in *Handbook of numerical heat transfer,* W.J. Minkowycz, *et al.*, Editors. 1988, John Wiley & Sons: New York. p. 673-722.
15. Tregenza, P. and I.M. Waters, *Daylight coefficients.* Lighting Research & Technology, 1983. 15(2): p. 65-71.
16. Littlefair, P.J., *Daylight coefficients for practical computation of internal illuminances.* Lighting Research and Technology, 1992. 24(3): p. 127-135.
17. CIE - Comission Internationale de l'Eclairage, *Spatial Distribution of Daylight - CIE General Sky,* 2001, CIE TC 3-15.
18. Kittler, R., R. Perez, and S. Darula. *A new generation of sky standards.* in *Lux Europe.* 1997. p. 359-373.